

UNIVERSITY OF STRATHCLYDE  
Energy Studies Unit  
Glasgow

**PASSIVE SOLAR ENERGY  
AND BUILDINGS; INCLUDING  
SHADING AND CLIMATE  
OF SAUDI ARABIA**

**Nabeel Abdul-Rahman Joudah**

Thesis submitted for the award of the degree of  
**Doctor of Philosophy**  
**November 1992**

© Nabeel A. Joudah 1992

The copyright of this thesis belongs to the author under the terms of the United Kingdom Copyright Act as qualified by University of Strathclyde Regulation 3.49. Due acknowledgement must always be made of the use of any material contained in, or derived from, this thesis.



**In the Name Of Allah,  
Most Gracious, Most Merciful**

---

## Abstract

---

Climate is a major determinant in building design. There has been a long standing need by designers and architects, as well as engineers, in Saudi Arabia for easy access to hourly climatic data. Such data are essential for many passive and active solar applications, including the simulation of the energy performance of building designs. A major contribution of the present study lies in the development of a Reference Year representative of the climate in Saudi Arabia. This reference year compensates the scarcity and inadequate climatic data presently published in Saudi Arabia. It also provides substantial data base of climatic variable for use in simulation programs, not only for Saudi Arabia, but also for similar hot-arid regions.

The present study also bridges the gap, currently observed in literature and research, concerning the energy performance of internal shading devices. These devices, and in particular curtains and blinds, are quite common features in our living spaces. The effects such devices have on the energy balance of indoor spaces and the comfort of occupants, can be assessed by the simplified design tools developed in the present study.

The characteristics of two samples (a domestic curtain and a low-e coated blind) have been measured using outdoor test rooms at the "Passys" test site. Results have indicated that the blind is more effective than the domestic curtain. The blind can reduce the transmission coefficient of double glazed fenestration by 11%, and can reduce the solar heat gain factor by 34%. In comparison, the curtain reduces the fenestration heat transmission coefficient and solar heat gain factor by 8% and 29% respectively. Results from the simulation programs "ESP" and "Curtain" have been compared with measured parameters. The analysis have provided confidence in such tools.

This thesis has been structured to be of value to architects. The effort put forward in the layout and presentation of the thesis provide a readable and easy to understand research material. The reviews, results, and analysis covered in this thesis would be useful for further research.

---

## Acknowledgement

---

I would like to express my gratitude and thanks to my supervisor Dr. John Twidell (head of the Energy Studies Unit) for his consistent guidance and support during the study; to Dr. Paul Baker and Dr. Paul Strachan for their constructive support and advice during and after experimentation at the Passys test site; and to Dr. Joe Clarke (head of the Energy Simulation Research Unit) for his guidance with the ESP system.

I am very grateful to Mr John Hanson (technical manager) who supplied me with digital extracts of raw climatic data from the Photovoltaic Power Site of the Solar Village project near Riyadh. I also would like to acknowledge Mr Fahad Huraib (director of the HYSOLAR program sponsored by KACST) for granting me permission to use the climatic data.

I also gratefully acknowledge the supportive encouragement of all members of the Energy Studies Unit (secretarial staff, research staff, students and academic visitors).

Special thanks should go to my father Abdul-Rahman and to my brother Ameen for their moral and financial support throughout the period of the study. I also would like to thank all members of my family for their moral support and encouragement especially; my mother, whose prayers are always with me; my sisters; my parents in law and other family members; to my children; Zahra, Yasmin and Basma who suffered a lot; and last but not least, to my wife for her encouragement, support and extreme patience.

*Dedicated To  
Lallahoum, Zahra, Yasmin and Basma.*

---

# Table of Contents

---

<i>Abstract</i> .....	iv
<i>Acknowledgements</i> .....	v
<i>Table of Contents</i> .....	vi
<i>List of Figures</i> .....	xi
<i>List of Tables</i> .....	xvi
<b>1. INTRODUCTION</b> .....	<b>1</b>
1.1 Review .....	2
1.2 Summary of Objectives .....	6
1.3 Organisation of the Thesis .....	6
1.4 References .....	8
<b>2. CLIMATIC DATA AND ITS USE IN BUILDING DESIGN</b> .....	<b>9</b>
2.1 Introduction .....	10
2.2 Pre-design Analysis .....	11
2.2.1 The Mahoney Tables .....	11
2.3 Calculation of Building Heat Losses .....	14
2.3.1 Transmission Heat Loss: (steady-state) .....	14
2.3.2 Infiltration Heat Loss .....	18
2.4 Calculation of Building Heat Gains .....	19
2.4.1 Heat Gain Through Exterior Roofs and Walls: (sol-air method) .....	19
2.4.2 Heat Gain Through Fenestration .....	23
2.4.3 Estimation of Free Gains .....	25
2.5 Annual Heating and Cooling Requirements .....	26
2.5.1 Degree Days .....	26
2.5.2 Degree Day Method .....	27
2.5.3 Variable Degree Day Method .....	28
2.6 Conclusion .....	33
2.7 References .....	34
<b>3. DEVELOPMENT OF A CLIMATE REFERENCE YEAR FOR RIYADH (SAUDI ARABIA)</b> .....	<b>37</b>
3.1 Introduction .....	38
3.2 Background Information .....	41
3.2.1 Climate of Saudi Arabia .....	41
3.2.2 Riyadh Climate (an overview) .....	43

3.3	Riyadh Climate Reference Year .....	44
3.3.1	Data Processing .....	45
3.3.2	Results and Remarks .....	48
3.3.2.1	Temperature .....	48
3.3.2.2	Relative Humidity .....	49
3.3.2.3	Wind Speed and Direction .....	49
3.3.2.4	Insolation .....	51
3.4	Variation of Riyadh Climate Through the Day .....	53
3.4.1	Temperature Variation During the Day .....	53
3.4.1.1	Hourly Temperature Prediction Nomogram .....	54
3.4.2	Wind Speed Variations During the Day .....	54
3.4.3	Solar Irradiation Variations During the Day .....	56
3.5	Relationship Between Insolation and Sunshine Duration in Riyadh (Saudi Arabia) .....	58
3.5.1	Estimation of Monthly Mean Daily Global Insolation from Sunshine Data .....	59
3.5.2	Estimation of Monthly Mean Daily Diffuse Horizontal Insolation .....	61
3.6	Conclusion .....	62
3.7	References .....	63
4.	<i>GLAZING ENERGY PROCESSES AND SOLAR CONTROL DEVICES</i> .....	66
4.1	Introduction .....	67
4.2	Solar Characteristics of Glass .....	68
4.3	Heat Transfer at Glazing Surfaces .....	70
4.3.1	Radiative Heat Transfer at Internal Surfaces .....	71
4.3.2	Radiative Heat Transfer at External Surfaces .....	72
	<i>Estimation of ground and obstruction surface temperatures</i> .....	73
	<i>Sky temperature estimation</i> .....	73
4.3.3	Natural Convective Heat Transfer (Internal Surfaces) .....	75
4.3.4	Forced Convective Heat Transfer (External Surfaces) .....	77
4.4	Maximum Solar Heat Gain Through Glazing: (with application for Riyadh climate) .....	80
4.4.1	Inward-Flow Fraction of Absorbed Insolation .....	80
4.4.2	Calculation of Hourly Solar Heat Gain through a Reference Glazing in Riyadh, Saudi Arabia: (QREF program) .....	82
	<i>Results and Discussion</i> .....	84
4.5	Shading Design Tools .....	87
4.6	Efficiency of Shading Devices .....	89
4.6.1	Exterior Shading Devices .....	89
	<i>Sun Screens</i> .....	89
	<i>Exterior Shutters</i> .....	89
	<i>Exterior Roller Blinds</i> .....	90
	<i>Architectural Projections</i> .....	90
	<i>Awnings</i> .....	91
4.6.2	Internal Shading Devices .....	91
	<i>Internal Venetian Blinds</i> .....	91
	<i>Internal Roller Shades</i> .....	92

<i>Curtains</i> .....	92
<i>Insulating Shutters</i> .....	92
4.6.3 Planting and Shading .....	93
4.7 Solar Control Glazing .....	94
4.7.1 Heat–Absorbing Glass .....	94
4.7.2 Heat–Reflecting Glass .....	95
4.7.3 Photo–chromatic Glass .....	95
4.7.4 Applied Films .....	96
4.8 References .....	97
5. <i>SOLAR AND THERMAL CHARACTERISTICS OF INTERIOR SHADING DEVICES (Curtains)</i> .....	101
5.1 Introduction .....	102
5.2 Classification of Curtains .....	104
5.3 Thermophysical Properties of Curtain Fabrics .....	105
5.3.1 Specific Heat Capacity .....	105
5.3.2 Thermal Conductivity .....	106
5.4 Measurement of the Solar Properties of Flat Curtains .....	107
5.4.1 Experimental Setup .....	108
5.4.2 Accuracy of Measurements .....	110
5.4.3 Results and Conclusions .....	111
5.5 Geometric Configuration and Curtain Properties .....	112
5.5.1 Fullness vs. Solar Properties of Curtains .....	112
5.5.2 Geometric Configuration vs. U–value of Fenestration .....	113
5.6 Modeling the Hourly Heat Transfer Through Curtain– Shaded Windows (CURTAIN program) .....	115
5.6.1 Solar Angles and Incident Solar Radiation .....	116
5.6.2 Shortwave Transmission and Absorption .....	117
5.6.3 Inward Heat Flow by Convection and Radiation .....	120
5.7 Conclusion .....	124
5.8 References .....	125
6. <i>MEASUREMENT AND INSTRUMENTS</i> .....	127
6.1 Introduction .....	128
6.2 Temperature Measurement .....	129
6.2.1 Thermocouples .....	129
6.2.2 Resistance Thermometers .....	130
6.2.3 Remote Temperature Sensors (Infrared Radiometer) .....	131
6.3 Humidity Measurement .....	132
6.3.1 Psychrometers .....	132
6.3.2 Calculation of Relative Humidity .....	132
6.3.3 Hygrometers and Relative Humidity Indicators .....	133
6.4 Air Speed and Direction Measurements .....	134

6.4.1	Cup Anemometer and Windvane .....	134
6.4.2	Averaging of Wind Direction Data .....	135
6.5	Insolation Measurement .....	136
6.5.1	Radiation Sensors .....	136
	<i>Thermoelectric Sensors</i> .....	136
	<i>Photoelectric Sensors</i> .....	137
6.5.2	Pyranometers (Solarimeters) .....	137
	<i>Albedometers</i> .....	138
	<i>Shadow Ring</i> .....	138
6.5.3	Pyrheliometers .....	139
6.5.4	Infrared Radiometers .....	140
6.5.5	Ultraviolet Radiometers .....	140
	<i>Eppley Ultraviolet Radiometer</i> .....	141
6.5.6	Sunshine Recorders .....	141
	<i>Campbell–Stokes Sunshine Recorder</i> .....	141
6.6	Data Logging .....	142
6.6.1	Processing DT–Logger Data Output : (DTCLM Program) .....	142
6.7	References .....	145
7.	<i>TEST SITE EXPERIMENTS WITH A WINDOW BLIND</i> .....	147
7.1	Introduction .....	148
7.2	The PASSYS Test Site Facilities .....	149
7.2.1	The Passys Test Cell .....	149
7.2.2	South Walls (PSC) .....	150
7.2.3	Instrumentation and Data Acquisition .....	153
7.3	Test Methodology and Experimental Setup .....	154
7.3.1	Rational for Testing .....	154
7.3.2	Model for Averaged Test Cell Behaviour .....	155
7.3.3	Calibration of the Test Cells .....	157
7.3.4	Instrumentation and Monitoring Details .....	158
7.4	Analysis of Captured Data Sets .....	160
7.4.1	Steady–state Performance Characteristics of Test Cell 3 (with Blind) and Test Cell 4 (no Blind) .....	160
7.4.2	Effects of the Blind on the Thermal Performance of the Test cell in Typical Clear and Overcast Days .....	163
7.5	Comparison Between Measured and Simulated Results by “ESP” and “CURTAIN” Models .....	164
7.5.1	Input Variables to the Models .....	164
	<i>Fenestration &amp; climate definition for the “Curtain” Model</i> .....	164
	<i>Test Cell, TF–Wall &amp; the “Blind–Glazing” Definition in “ESP”</i> .....	164
	<i>Test Configuration &amp; Climate Definition in ESP</i> .....	165
7.5.2	Results and Discussion .....	166
	<i>Results for the Steady–state Period</i> .....	166
	<i>Results for the Period of Free Floating Mode</i> .....	166

<i>Results for Clear and Overcast Days</i> .....	168
7.6 Conclusions .....	172
7.7 References .....	173
8. <i>TEST SITE EXPERIMENTS WITH A DOMESTIC CURTAIN</i> .....	174
8.1 Introduction .....	175
8.2 Experimental Setup .....	176
8.3 Analysis of Captured Data Sets .....	177
8.3.1 Steady-state Performance Characteristics of the Passys Test Cell (With and Without Curtain) .....	179
8.3.2 Test Cell Parameters Identification: (MRQT program) .....	180
8.4 Comparison Between Measured and Simulated Results by "ESP" and "CURTAIN" Models .....	182
8.4.1 Input Variables to the Models .....	182
<i>Fenestration &amp; Climate Definition for the "Curtain" Model</i> .....	182
<i>Test Cell, Reference Wall &amp; the Curtain Definition in "ESP"</i> .....	182
<i>Test Configuration &amp; Climate Definition in ESP</i> .....	183
8.4.2 Results and Discussion .....	183
<i>Effects of the Curtain on the Test Cell Energy Balance</i> .....	183
<i>Comparative Analysis for Clear and Overcast Days</i> .....	184
8.5 Conclusions .....	189
8.6 References .....	190
9. <i>CONCLUSIONS</i> .....	191
<i>APPENDICES</i> .....	195
Appendix A: Climatic Data (Riyadh, Saudi Arabia) .....	196
Appendix B: Insolation Data (Riyadh, Saudi Arabia) .....	203
Appendix C: Sol-Air Temperature Data (Calculated) Riyadh, Saudi Arabia .....	210
Appendix D: Solar Heat Gain Flux Through Standard Glass (Riyadh, Saudi Arabia) .....	217
Appendix E: Computer Programs (Code Listing) .....	221
<i>QREF. BAS</i> .....	222
<i>CURTAIN. BAS</i> .....	224
<i>DTCLM. BAS</i> .....	228
Appendix F: Error Analysis and Instrumentation Data Sheets .....	234
Appendix G: "ESP" Input Data Files: for Energy Performance Simulation of the UK "Passys" Test Cells .....	249
<i>A Brief Description of the "ESP" Model</i> .....	249
<i>The Input Data Files</i> .....	250
Appendix H: Glossary .....	260
Appendix I: Contents of Supplementary Floppy Disk .....	263
Appendix J: Index .....	264

## List of Figures

<b>Figure 2.1</b>	The Bioclimatic chart. ....	11a
<b>Figure 2.2</b>	Heat flow through floor slab. ....	15
<b>Figure 2.3</b>	U-values for solid floors on soil. ....	17a
<b>Figure 2.4</b>	U-values for suspended timber floor above ground. ....	17a
<b>Figure 2.5</b>	Solar geometry. ....	20a
<b>Figure 2.6</b>	Sol-air temperature, at a horizontal roof in July (Riyadh climate) compared with external air temperature. ....	23a
<b>Figure 2.7</b>	Sol-air temperatures at horizontal roof and vertical walls. ....	23a
<b>Figure 2.8</b>	Mechanism of heat transfer through glass. ....	23
<b>Figure 2.9</b>	Formulae for the calculation of degree days, 15.5°C base, as defined and used by the UK Meteorological Offices. ....	26a
<b>Figure 2.10</b>	Diagram of the simple structure used in examples 2, 3 and 4. ....	28a
<b>Figure 2.11</b>	Monthly energy heating and cooling requirements for CASE #1 in Example 4. ....	31a
<b>Figure 2.12</b>	Monthly energy heating and cooling requirements for CASE #2 in Example 4. ....	31a
<b>Figure 2.13</b>	Annual heating and cooling energy requirements calculated by the Variable Degree Day method in example 4. ....	31
<b>Figure 2.14</b>	Comparison between annual heating/cooling energy requirements (example 4) calculated by the VDD and the DD methods. ....	32
<b>Figure 3.1</b>	Saudi Arabian Summer isotherm map. ....	41a
<b>Figure 3.2</b>	Saudi Arabian Winter isotherm map. ....	41a
<b>Figure 3.3</b>	Isohyetes of the average yearly precipitation. ....	42a
<b>Figure 3.4</b>	Saudi Arabian Isohel map. ....	42a
<b>Figure 3.5</b>	Saudi Arabian Iso-Radiation map. ....	42
<b>Figure 3.6</b>	Monthly percentages of valid hourly insolation raw data for the years 1984, 85 & 86. ....	45a
<b>Figure 3.7</b>	Monthly percentages of valid hourly temperature raw data. ....	45a
<b>Figure 3.8</b>	Monthly percentages of valid hourly wind speed raw data. ....	46a
<b>Figure 3.9</b>	Monthly means of actual and modified relative humidity (Riyadh CRY). ....	47a
<b>Figure 3.10</b>	Daily average, maximum and minimum dry bulb temperature (Riyadh CRY). ....	48a
<b>Figure 3.11</b>	Frequency distribution of hourly dry-bulb temperature (Riyadh CRY). ....	48a
<b>Figure 3.12</b>	Relative humidity – daily average, maximum and minimum. (Riyadh CRY). ....	49a
<b>Figure 3.13</b>	Frequency distribution of hourly relative humidity. (Riyadh CRY). ....	49a
<b>Figure 3.14</b>	Wind speed – daily average, maximum and minimum. (Riyadh CRY). ....	50a
<b>Figure 3.15</b>	Frequency distribution of hourly wind speed. (Riyadh CRY). ....	50a
<b>Figure 3.16</b>	Daily average wind directions in compass degrees. (Riyadh CRY). ....	50
<b>Figure 3.17</b>	Daily global, diffuse solar energy and calculated extraterrestrial radiation over Riyadh. ....	51a
<b>Figure 3.18</b>	Daily average and maximum global horizontal insolation. (Riyadh CRY). ....	52a
<b>Figure 3.19</b>	Daily average and maximum diffuse horizontal insolation. (Riyadh CRY). ....	52a
<b>Figure 3.20</b>	Frequency distribution of hourly global horizontal insolation (Riyadh CRY). ....	52
<b>Figure 3.21</b>	Frequency distribution of hourly diffuse horizontal insolation (Riyadh CRY). ....	52
<b>Figure 3.22</b>	Yearly mean of hourly insolation ( $G_h$ ) and temperature variations through the day. (Riyadh CRY). ....	53a
<b>Figure 3.23</b>	Nomogram for predicting diurnal temperature variations in Riyadh. ....	55a
<b>Figure 3.24</b>	Ratio of hourly to daily average wind speed. (Diurnal variation of wind speed in Riyadh). ....	55
<b>Figure 3.25</b>	Variation of global and diffuse insolation with time of day in Riyadh for the months January–April. ....	57
<b>Figure 3.26</b>	Variation of global and diffuse insolation with time of day in Riyadh for the months May–August. ....	58a
<b>Figure 3.27</b>	Monthly mean daily global insolation over the Solar Village. (measured & calculated values using monthly regression constants). ....	60a
<b>Figure 3.28</b>	A comparison between measured, and calculated daily global insolation over the Solar Village, (yearly regression constants). ....	60a

Figure 3.29	A comparison between measured & calculated daily global insolation over the Solar Village using the two sets of monthly constants of Table 3.11. ....	60
Figure 3.30	Monthly mean daily diffuse horizontal irradiation over the Solar Village. (measured & calculated values using yearly coefficients). ....	61a
Figure 3.31	A comparison between measured, and calculated daily diffuse insolation over the Solar Village (monthly regression coefficients). ....	61a
Figure 4.1	Solar spectral transmittance for typical architectural glass. ....	68a
Figure 4.2	Multiple reflection and transmission through a glass sheet of finite thickness. ....	69a
Figure 4.3	Clear and overcast sky temperatures as a function of outdoor air temperature. ....	74a
Figure 4.4	Non-clear sky temperature as a function of sky condition. ....	74a
Figure 4.5	Non-clear sky temperature with the external surface heat transfer coefficient as a function of sky condition. ....	75a
Figure 4.6	Convective heat transfer coefficients at internal vertical surfaces as a function of surface-air temperature difference. ....	77a
Figure 4.7	External surface heat transfer coefficients as a function of wind speed for windward and leeward surfaces. ....	79a
Figure 4.8	Schematic redistribution of absorbed insolation in a single glass for three possible temperature distributions. ....	80a
Figure 4.9	Flow chart of QREF.BAS program main routine. ....	82a
Figure 4.10	Flow chart of HTC Subroutine in QREF.BAS program. ....	83a
Figure 4.11	Flow chart of INSO Subroutine in QREF.BAS program. ....	84a
Figure 4.12	Flow chart of GLASS Subroutine in QREF.BAS program. ....	84a
Figure 4.13	Monthly means of daily solar heat gain through a 3mm reference glass of different orientations for summer & winter in Riyadh. ....	85a
Figure 4.14	Monthly means of hourly solar heat gain through a 3mm reference glass of different orientations (summer & winter). ....	85a
Figure 4.15	Hourly heat transfer coefficients at the internal surface of the reference glass for different orientations. ....	85
Figure 4.16	Hourly heat transfer coefficients at the external surface. ....	85
Figure 4.17	24h distribution of the reference glass U-value. ....	86a
Figure 4.18	Solar position in relation to building surfaces. (shadow angles). ....	87a
Figure 4.19	An example of graphical determination of solar radiation penetration through a window and a fixed shading device. ....	87a
Figure 4.20	Shading masks showing the shadows by vertical and horizontal shading elements. ....	87a
Figure 4.21	Shading design tools. (a) shading mask protractor. (b) sun chart for latitude 24°N. ....	88a
Figure 4.22	Various shading devices for a set performance ( $\theta_v = 60^\circ$ ). ....	88a
Figure 4.23	Sun penetration through a sun screen vs. sun altitude. ....	89a
Figure 4.24	A traditional external wooden sunscreen "Mashrabiya", common in the western region of Saudi Arabia. It is also known as "Roshan". ....	89a
Figure 4.25	Types of exterior shutters. ....	90a
Figure 4.26	Installation of an external roll blind. ....	90a
Figure 4.27	Types of awnings. ....	91a
Figure 4.28	Various types of internal blinds. ....	91a
Figure 4.29	Heat transfer mechanism through: (a) 6mm clear glass with internal light coloured blind; (b) double glazing with a blind inside the glazing air gap. ....	92a
Figure 4.30	Various types of roller shades. ....	92a
Figure 4.31	Curtain arrangements for energy efficiency. ....	92a
Figure 4.32	Various types of insulating shutters. ....	93a
Figure 4.33	Seasonal sun angle vs. the interference of trees and roof planting. ....	93a
Figure 4.34	Shade tree effectiveness vs. orientation. ....	93a
Figure 4.35	Shapes of trees as defined for "SHTREE" program. ....	93
Figure 4.36	Heat balance diagrams of (a) 6mm clear glass; (b) 6mm heat-absorbing glass; (c) heat-absorbing outer glass pane with 6mm clear glass. ....	94a
Figure 4.37	Heat balance diagrams of (a) 6mm heat reflecting glass; (b) heat-reflecting outer glass pane with 6mm "Kappafloat" inner glass. ....	95a
Figure 4.38	Schematic illustration of the polarization mechanism in photo-chromatic glass. ....	95a
Figure 5.1	Openness factor measuring instruments for (a) the visible solar spectrum (0.3–0.7 $\mu$ m) and (b) solar spectrum (0.4–1.15 $\mu$ m). ....	104a
Figure 5.2	Classification of curtain fabrics. ....	104a
Figure 5.3	Construction details of a black box to measure curtain solar properties. ....	108a
Figure 5.4	Shortwave radiation simulator. ....	108a
Figure 5.5	Experimental setup for the measurement of transmittance and reflectance of a curtain sample in a dark room. ....	108a

Figure 5.6	Test procedure to determine the transmittance of a curtain fabric. ....	109a
Figure 5.7	Test procedure (second step) to determine the reflectance of a curtain fabric. ....	109a
Figure 5.8	Test procedure to determine the reflectance of a curtain fabric using the net-radiometer. ....	110a
Figure 5.9	A Net-radiometer illustrated in vertical position. ....	110a
Figure 5.10	Transmittance and reflectance properties of a curtain sample (golden plain weave fabric) measured by the albedometer and the net-radiometer with two light sources. ....	111a
Figure 5.11	Plan and isometric diagrams showing the configuration of a folded curtain for the theoretical analysis of section 5.5.1. ....	112a
Figure 5.12	Apparent reflectivities ( $\rho^n_i$ ) for diffusely reflecting curtain fabrics under diffuse insolation. ....	112a
Figure 5.13	Apparent reflectivities ( $\rho^n_b$ ) for direct insolation in the diffusely reflecting cavity of folded curtains. ....	113a
Figure 5.14	Solar reflectance ( $\rho$ ) of flat curtain fabrics as a function of incident angle. ....	113a
Figure 5.15	Apparent absorptance and transmittance of light coloured curtains ( $\alpha = 0.26$ ; $\rho = 0.39$ ; $\tau = 0.35$ ) for 100% fullness and a horizontal shadow angle $\theta_b = 0^\circ$ vs. angle of incidence of solar radiation, for both theoretical and experimental determinations. ....	113a
Figure 5.16	Mean U-values of 4 fenestration assemblies. ....	114a
Figure 5.17	Sources of incident solar radiation and components of heat gain/loss through a curtain-shaded window. ....	115a
Figure 5.18	Component of transmitted, absorbed and reflected short wave flux (solar) incident upon: (a) single glazing with interior curtain, and (b) double glazing with interior curtain. ....	119a
Figure 5.19	An algorithm for computing the composite transmittance and absorptance of double glazing with interior curtain. ....	120a
Figure 5.20	Convective and longwave heat transfer components for a single glazing with a curtain. ....	122a
Figure 5.21	Convective and longwave heat transfer components for double glazing with a curtain. ....	122a
Figure 6.1	Tolerances of British and German specifications for 100 $\Omega$ thermometers. ....	130a
Figure 6.2	Construction of Platinum standard thermometers. ....	131a
Figure 6.3	Construction of platinum sondes. ....	131a
Figure 6.4	Whirling Hygrometer for direct readout of dry and wet bulb temperatures. ....	132a
Figure 6.5	Hair Hygrograph (human hair element). ....	133a
Figure 6.6	Cup anemometer for the measurement of wind speed. ....	134
Figure 6.7	Algorithms for averaging the wind direction suitable for computer programs. ....	135a
Figure 6.8	Example for averaging six wind directions. ....	135
Figure 6.9	Various arrangements of thermoelectric sensors. (a) thermocouple, (b) thermopile, (c) star-shape thermopile, (d) Moll thermopile. ....	137a
Figure 6.10	Typical structure of n-p junction solar cell. ....	137a
Figure 6.11	Spectral response of silicon solar cells. ....	137a
Figure 6.12	Cross-sectional diagram of Eppley precision spectral pyranometer. ....	138a
Figure 6.13	Albedometer based on two Kipp & Zonen solarimeters. ....	138a
Figure 6.14	Angular response of silicon solar cells with and without a plastic cover. ....	138a
Figure 6.15	(a) Shadow Ring installation for measurement of Diffuse Insolation. (b) Geometry of the Shadow Ring. ....	139a
Figure 6.16	Standard Cavity Radiometer, for calibrating pyrheliometers and pyranometers at the Solar Village, Riyadh, Saudi Arabia. ....	140a
Figure 6.17	Eppley Pyrheliometer (NIP) mounted on a Sun Follower II. ....	140a
Figure 6.18	Eppley Pyrgeometer for the measurement of infrared radiation (4–50 $\mu\text{m}$ ). ....	140a
Figure 6.19	A modified Net Radiometer for use as a Pyrriometer to measure the total horizontal insolation (0.3–80 $\mu\text{m}$ ). ....	141a
Figure 6.20	Schematic diagram of Eppley UV radiometer ( $\lambda = 0.29\text{--}0.39 \mu\text{m}$ ). ....	141a
Figure 6.21	Campbell-Stokes sunshine recorder. ....	141a
Figure 6.22	A flow-chart of the main routines in the data processing program (DTCLM .BAS) for use with DT-Logger output. ....	142a
Figure 7.1	Location of the Passys test sites by the end of phase 1 of the project. ....	149a
Figure 7.2	Sketch of the Passys test cell. ....	149a
Figure 7.3	Detailed drawings of the Passys test cell: (a) Plan, (b) Section. ....	150a
Figure 7.4	The UK Passys test site, Glasgow. (a) Site plan; (b) South view of the four test cells (1990). ....	151
Figure 7.5	Sunchart of the test site. ....	151
Figure 7.6	Reference wall construction. (elevation and sections). ....	152a
Figure 7.7	Timber-Frame wall construction. (elevation and sections). ....	152a
Figure 7.8	Test cell with the heating and cooling system (HCS). ....	153a
Figure 7.9	Conceptual diagram of the Parameter Identification methodology. ....	154a
Figure 7.10	Steady-state energy balance of the test cell. ....	154a

Figure 7.11	Thermal model of the test cell. ....	155a
Figure 7.12	Improvements in air tightness of the test cell. ....	158a
Figure 7.13	A sketch showing the type and location of some basic instruments listed in Table 7.10. ....	159a
Figure 7.14	(a) Double shield device for air temperature sensor; (b) Mounting and shielding of surface temperature sensor. ....	159
Figure 7.15	Ambient temperatures measured for the period of experiment. ....	160a
Figure 7.16	Wind speed and direction measured for the period of experiment. ....	160a
Figure 7.17	Measured global horizontal and diffuse horizontal insolation, (Jul. 29 <sup>th</sup> to Aug. 16 <sup>th</sup> ) ....	161a
Figure 7.18	Measured global vertical insolation, from July 29 <sup>th</sup> to August 16 <sup>th</sup> 1989. ....	161a
Figure 7.19	Regression curves for : (a) cell 3 fitted with glazing and the Passys blind, (b) test cell 4 fitted with glazing only. ....	161
Figure 7.20	A comparison between measured and calculated daily average heating requirements of cell 3; using (1) the correlation coefficients derived from the experiment results and (2) using results from MRQT program. ....	162a
Figure 7.21	A comparison between measured and calculated daily average heating requirements of cell 4; using (1) the correlation coefficients for cell 4 derived from the experiment, (2) MRQT output, and (3) the correlation coefficients derived from the calibration experiment. ....	162a
Figure 7.22	Variations of air temperature in cell 3 for clear and overcast days. ....	163a
Figure 7.23	Variations of air temperature in cell 4 for clear and overcast days. ....	163a
Figure 7.24	Hourly measured global vertical insolation and outdoor air temperature for clear and overcast days. ....	164a
Figure 7.25	Hourly heating requirements of cell 3 and cell 4 measured for clear and overcast days. ....	164a
Figure 7.26	Comparison between measured and two simulations of the heating requirement of cell 3 for the period of experiment. ....	166a
Figure 7.27	Comparison between measured and two simulations of th heating requirement of cell 4 for the period of experiment. ....	166a
Figure 7.28	Daily total energy balance at the air nodes of cells 3 & 4, calculated for the period from 210 to 220 Julian. ....	167a
Figure 7.29	A breakdown of the daily total energy balance at the air nodes of cells 3 & 4, due to convective exchanges with the timber–frame wall components. ....	167a
Figure 7.30	Instantaneous energy balance of cell 3 & 4 in free floating mode. ....	167
Figure 7.31	Measured and predicted ambient temperature of cell 3 and cell 4 for the free floating period of the blind experiment, (Aug.10 <sup>th</sup> to Aug.17 <sup>th</sup> 1989). ....	167
Figure 7.32	Measured and predicted heating requirement of cell 3 for clear and overcast days. ....	168a
Figure 7.33	Measured and predicted heating requirement of cell 4 for clear and overcast days. ....	168a
Figure 7.34	Shortwave radiation flux transmitted through the fenestration of cell 3 and cell 4. ....	169a
Figure 7.35	Combined convective–longwave heat flux through the fenestration of cell 3 and cell 4. ....	169a
Figure 7.36	Inward–flow fraction of absorbed insolation in the fenestration of cell 3 and cell 4 for clear and overcast days. ....	169
Figure 7.37	U–value of the fenestration in cell 3 and cell 4 for clear and overcast days. ....	169
Figure 7.38	Measured and predicted temperature of the Passys Blind in cell 3. ....	170a
Figure 7.39	Measured and predicted temperature of the inner glass panel in cell 3. ....	171a
Figure 7.40	Measured and predicted temperature of the inner glass panel in cell 4. ....	171a
Figure 7.41	Measured and predicted temperature of the outer glass panel in cell 3. ....	171
Figure 7.42	Measured and predicted temperature of the outer glass panel in cell 4. ....	171
Figure 8.1	Hourly ambient temperatures measured at the Passys test site for the period from 257 to 313 Julian (1989). ....	177a
Figure 8.2	Hourly ambient temperatures measured for the period from 332 to 361 Julian. ....	177a
Figure 8.3	Average daily insolation measured at the test site for the period 257–313 Julian. ....	178a
Figure 8.4	Average daily insolation measured for the period 332–361 Julian. ....	178a
Figure 8.5	Wind speed and direction measured for the period 257–313 Julian. ....	178
Figure 8.6	Wind speed and direction measured for the period 332–361 Julian. ....	178
Figure 8.7	Measured global vertical insolation, auxiliary heating of the cell, and the difference between the cell ambient and outdoor air temperatures. (257–313 Julian). ....	179a
Figure 8.8	Measured global vertical insolation, auxiliary heating, and temperature difference between the cell ambient and outdoor air temperatures. (332–361 Julian). ....	179a
Figure 8.9	Regression curves for cell 2 with and without curtain. ....	180a
Figure 8.10	A comparison between measured and calculated Heating of test cell 2 without curtain, using the regression coefficients derived from the calibration experiment. ....	181a
Figure 8.11	Comparison between measured and calculated Heating of test cell 2 with curtain. ....	181a
Figure 8.12	Measured and predicted average daily heating requirements of test cell 2 fitted with the curtain for the period from Nov.28 <sup>th</sup> to Dec.27 <sup>th</sup> 1989. ....	183a

<b>Figure 8.13</b>	Daily total energy balance at the air node of test cells 2 (with and without curtain), calculated by the "ESP" model for the period from 332 to 361 Julian. ....	184a
<b>Figure 8.14</b>	A breakdown of the daily total energy balances of the Reference-wall components. (from 332 to 361 Julian). ....	184a
<b>Figure 8.15</b>	Hourly measured global vertical insolation and outdoor air temperature for clear and overcast days from the curtain experiment. ....	184
<b>Figure 8.16</b>	Comparison between measured and predicted hourly heating requirements of test cell 2 (with the curtain installed) for clear and overcast days. ....	185a
<b>Figure 8.17</b>	Energy balance of test cell 2 (with and without curtain). ....	185a
<b>Figure 8.18</b>	Energy balance of the reference wall components (with and without curtain) Computed for a clear day (November 30th 1989). ....	186a
<b>Figure 8.19</b>	Energy balance of the reference wall components (with and without curtain) Computed for an overcast day (December 2nd 1989). ....	186a
<b>Figure 8.20</b>	Shortwave radiation flux (solar) transmitted through the fenestration of cell 2 (with and without curtain). Computed by the "Curtain" program for clear and overcast days. ....	186
<b>Figure 8.21</b>	Combined convective-longwave heat flux through the fenestration of test cell 2 (with and without curtain). Computed for clear and overcast days. ....	186
<b>Figure 8.22</b>	Inward-flow fraction ( $N_i$ ) of absorbed insolation in the fenestration (with and without curtain). Computed for clear and overcast days. ....	187a
<b>Figure 8.23</b>	U-value of the fenestration (with and without curtain). ....	187a
<b>Figure 8.24</b>	Measured and predicted temperature of the curtain, for clear and overcast days. ....	187
<b>Figure 8.25</b>	Measured and predicted temperature of the inner glass panel with curtain installed. ....	188a
<b>Figure 8.26</b>	Predicted temperature of the inner glass panel in cell 2 without curtain. ....	188a
<b>Figure 8.27</b>	Measured and predicted temperature of the outer glass panel with the curtain installed. ....	188
<b>Figure 8.28</b>	Predicted temperature of the outer glass panel in cell 2 without curtain. ....	188
<b>Figure F.1</b>	Normal probability curve of deviation of error (Standard Deviation). ....	235a
<b>Figure F.2</b>	State of the $\Delta T$ -logger with manual & computer instructions. ....	247
<b>Figure F.3</b>	HP data control system ....	248
<b>Figure F.4</b>	HP data aquisition system ....	248
<b>Figure G.1</b>	Program modules of the "ESP" software (series 6, 1990) ....	250a

## List of Tables

<b>Table 2.1</b>	Internal surface resistance, (typical values in $m^2 \text{ } ^\circ\text{C W}^{-1}$ ).	15a
<b>Table 2.2</b>	External surface resistance for different exposures to wind.	15a
<b>Table 2.3</b>	Overall resistance of unventilated cavities.	15a
<b>Table 2.4</b>	Thermophysical properties of selected building materials.	16a
<b>Table 2.5</b>	U-values for glazing without frames.	16
<b>Table 2.6</b>	U-values for typical windows (glass with frame).	16
<b>Table 2.7</b>	Air to air heat transfer coefficients of typical wall and roof constructions in Saudi Arabia.	17
<b>Table 2.8</b>	Recommended minimum rates of fresh-air supply to residential building zones for human habitation.	18a
<b>Table 2.9</b>	Solar gain factors and shading coefficients of window glazing.	24a
<b>Table 2.10</b>	Shading coefficients for glazing with shading devices.	24a
<b>Table 2.11</b>	Heat emission from human bodies.	25a
<b>Table 2.12</b>	Typical values of heat emission from domestic appliances.	25a
<b>Table 2.13</b>	Monthly total heating degree days for various base temperatures. (calculated for Riyadh, Saudi Arabia).	27a
<b>Table 2.14</b>	Monthly total cooling degree days for various base temperatures. (calculated for Riyadh, Saudi Arabia).	27a
<b>Table 2.15</b>	Monthly means of daily average solar heat gain through a 3mm clear glass. (calculated for Riyadh, Saudi Arabia).	29a
<b>Table 2.16</b>	Monthly means of daily average sol-air excess temperature at external roof and walls surfaces in Riyadh.	29a
<b>Table 3.1</b>	Climatic data requirements of energy models.	39a
<b>Table 3.2</b>	US Test Reference Year selection method.	39a
<b>Table 3.3</b>	Temperature and relative humidity ranges (summer & winter) for inland and coastal stations in Saudi Arabia.	41
<b>Table 3.4</b>	Meteorological data averaged over 20 years period (1961–1980) for Riyadh.	43a
<b>Table 3.5</b>	Monthly means of air and ground temperatures (Riyadh CRY).	48
<b>Table 3.6</b>	Mean monthly solar data (Riyadh CRY).	51a
<b>Table 3.7</b>	Hourly dry bulb temperature variations during the day (Riyadh CRY).	54a
<b>Table 3.8</b>	Percentages of hourly from daily total global horizontal insolation (Riyadh CRY).	56a
<b>Table 3.9</b>	Percentages of hourly from daily total diffuse horizontal insolation (Riyadh CRY).	57a
<b>Table 3.10</b>	Constant coefficients with their standard deviation errors for use in Equation 3.14.	59a
<b>Table 3.11</b>	Regression constants for: set 1 from data of Riyadh and set 2 from data of Al-Kharj.	59a
<b>Table 3.12</b>	Constant coefficients for estimating the diffuse horizontal insolation over Riyadh.	61
<b>Table 4.1</b>	Polynomial coefficients of transmittance and absorptance factors of a clear window glass (3mm), for use in Eq.4.11 to Eq.4.14.	69a
<b>Table 4.2</b>	Representative values of internal surface radiative heat transfer coefficients	72a
<b>Table 4.3</b>	Representative view factors of sky, exterior obstructions and ground for an external surface.	72a
<b>Table 4.4</b>	Empirical coefficients for Eq.4.49.	76a
<b>Table 4.5</b>	Empirical Coefficients and exponents for Eq.4.54.	78a
<b>Table 4.6</b>	Monthly means of the glazing external surface heat transfer coefficients for the climate of Riyadh, Saudi Arabia.	86a
<b>Table 4.7</b>	Solar control performance data for aluminium-coated polyester films on glass.	96a
<b>Table 5.1</b>	Density and Specific heat capacity of dry fibres.	105a
<b>Table 5.2</b>	Thermal conductivity of pads of fibre with a bulk density of $500 \text{ kg m}^{-3}$ .	106a
<b>Table 5.3</b>	Thermal conductivity of polymer fabrics in sheet form.	106a
<b>Table 5.4</b>	Representative Instruments that measure Thermophysical Properties of Textiles.	106a
<b>Table 5.5</b>	Solar characteristics of indoor window treatments.	107a
<b>Table 5.6</b>	Solar reflectance, transmittance and absorptance of three curtain fabrics.	111a
<b>Table 5.7</b>	U-values of fenestration for different fabric types and geometrical configurations.	114a
<b>Table 5.8</b>	Matrix form of the heat balance equations of single glazing with a curtain.	123a

<b>Table 5.9</b>	Matrix form of the heat balance equations of double glazing with a curtain. ....	123a
<b>Table 6.1</b>	Temperature measuring instruments. ....	129a
<b>Table 6.2</b>	Polynomial coefficients for type "T" thermocouples (for use in Eq.6.4). ....	130a
<b>Table 6.3</b>	Humidity measuring instruments. ....	132a
<b>Table 6.4</b>	Constants for use in Eq.6.7 at two ambient temperature ranges. ....	133a
<b>Table 6.5</b>	Air speed and direction measuring instruments. ....	134a
<b>Table 6.6</b>	Insolation measuring Instruments. ....	136a
<b>Table 6.7</b>	Classification of pyranometers. ....	137
<b>Table 6.8</b>	Classification of Pyrheliometers. ....	139a
<b>Table 7.1</b>	Measured values of shortwave absorptance and longwave emittance of the Passys test cell surfaces. ....	151a
<b>Table 7.2</b>	Thermophysical properties of the test cell materials. ....	151a
<b>Table 7.3</b>	Thermophysical properties of the materials used in the calibration wall. ....	152
<b>Table 7.4</b>	Thermophysical characteristics of the reference wall materials. ....	152
<b>Table 7.5</b>	Thermophysical characteristics of the TF-wall components. ....	152
<b>Table 7.6</b>	Solar characteristics of Versol aluminium-coated Passys blinds. ....	154a
<b>Table 7.7</b>	Heat loss coefficients and capacitances, calculated for the components of the Passys test cell, opaque calibration wall, reference wall, and the UK Timber-Frame wall. ....	156a
<b>Table 7.8</b>	Calculated heat transmission coefficients and capacitances of three Passys test cells. ....	156
<b>Table 7.9</b>	Steady-state characteristics of cells 3&4. (from calibration experiment) ....	158a
<b>Table 7.10</b>	Basic set of sensors used for the blind experiment and monitored at the UK Passys site. ....	159a
<b>Table 7.11</b>	Steady-state characteristics of cells 3&4. (from the Blind experiment) ....	161
<b>Table 7.12</b>	Matrix form of heat balance equations for the double glazing system in test cell 4. ....	165a
<b>Table 7.13</b>	Standard deviation and relative error percentages in the simulated temperatures of the fenestration layers in cell 3 and cell 4. ....	170a
<b>Table 8.1</b>	Steady-state characteristics of test cell 2. ....	180a
<b>Table 8.2</b>	Test cell parameters identified by the "MRQT" program. ....	181
<b>Table F.1</b>	Errors in measurements : Checklist. ....	235a
<b>Table F.2</b>	Probability of occurrence of errors or events according to the normal probability curve in Figure (F.1). ....	235a
<b>Table F.3</b>	Type "T" thermocouple reference table. ....	236
<b>Table F.4</b>	Resistance – temperature relationship. ....	237
<b>Table F.5</b>	Kipp & Zonen CM12 shadowing correction factors for uniform sky conditions. ....	245
<b>Table G.1</b>	Contents of a zone geometry file (*.GEO). ....	251a
<b>Table G.2</b>	Contents of a zone construction file (*.CON). ....	251a
<b>Table G.3</b>	Contents of a zone operation file (*.OPR). ....	251
<b>Table G.4</b>	Contents of a zone utilities file (*.UTL). ....	251
<b>Table G.5</b>	Contents of a blind/shutter file (*.BLN). ....	251
<b>Table G.6</b>	Contents of a zone transparent multi-layered construction file (*.TMC). ....	252a
<b>Table G.7</b>	Contents of the system configuration file (*.CFG). ....	252a
<b>Table G.8</b>	Contents of the configuration control file (*.CTL). ....	252a

# Chapter 1

# 1. INTRODUCTION

## 1.1 Review

---

This thesis considers low-energy buildings and the comfort of occupants. Certain general problems are investigated, and special application made for Saudi Arabia. The context of the study is the present day concern about the environment, including excessive use of fossil fuel systems threatening climate change; and the benefit of utilising renewable and solar technologies. There has been overlap with the European Commission sponsored project for Passive Solar Systems in Buildings (Passys), which includes the use of Test Rooms (Cells) and simulation modelling.

The thesis has been structured to be of value to architects. Terms like “environmentally friendly”, “energy efficient” have become household words for almost every aspect in our daily life. This public awareness warrants the need for architects to be the experts in energy matters in general and on climatic design in particular. Climatic design literally implies that after considering the existing climate, it is possible to design a building that negates adverse effects and accentuates the positive elements needed to maintain a comfortable dwelling. Three energy conservation strategies can be identified in the context of building design; *Basic*, *Vernacular*, and *Active*.

**Basic** means *no* building; doing without massive shelters, and living with the climate. It is life that is culturally rich and (maybe) materially poor. Often it implies making do with less. The nomad’s tent, for instance, or the shade of a tree need no imported or purchased energy.

**Vernacular** means building *with* the climate, as good vernacular architecture does. Thermal energy flows by natural means (passive), and local building materials are used. Nature’s own devices are used in buildings; exploiting for heating and cooling the thermal storage capacity of building materials, natural ventilation, orientation, building form, etc. The building is skillfully and purposefully used to modify the climate. Nowadays, vernacular architecture have been rediscovered for their energy-saving potential. We often refer to them as “passive buildings”. Refined calculations and systematic experiments have made passive building systems more predictable. The interior climate is the result of the building configuration as related to the exterior, and of the way people use the building.

**Active** means living and building *with great reliance on power-driven machines*. Man uses his ingenuity and nature’s resources to live where conditions would otherwise be unbearable, probably due to poor design. The energy to sustain these conditions is purchased and fed into the system. Central heating and air-conditioning are typical examples. Little use is made of the building envelope and fabric as a modifier of climate; instead, great reliance is placed on power-driven machines. In solar technology, active systems are used to collect solar energy for heating, cooling and mechanical work, the active part of the system being used to harvest energy. Such systems aim at high efficiency and are associated with high cost,

technology and rapid change. The availability of technology and cheap energy in the recent past has led to the indiscriminate use of air-conditioning where it was not climatologically warranted. It has been used as a corrective for environmentally poor building design.

In practice the neat division of strategies is neither necessary nor even desirable. The decision when to switch from one strategy to the other is influenced by culture, technology and cost. The strategies can also be divided into short, medium and long-term categories which are mostly related to the scale of investment.

In the hot arid region of Saudi Arabia, major cities like the capital Riyadh have experienced intensive development arising from two decades of economic expansion. There is growing evidence of problems associated with the so called "modern architecture" in sections of the city "alien" to local conditions. This awareness has led to renewed interest in traditional buildings with particular reference to the way in which their design and construction harmonise with climatic and social needs. Several authors have dealt with this subject. (e.g. see Kendel 1982, Mofti & Balto 1983, Joudah et. al. 1983, Kaizer 1984, Joudah 1985). Almost all the literature reviewed lack specific and detailed analysis of the energy performances of vernacular or contemporary buildings, and the focus of studies were in general and conceptual terms. As will be seen in the main text (chapter 3), other literature reviewed indicate that there is no easy access to accurate and long term climate data published for Saudi Arabia.

The key to successful energy efficient design is the ability to assess the effectiveness of various passive techniques at different stages in the design process. This requires the availability of real climatic data. For the earliest stage of building design the mean monthly and daily average data are sufficient for this stage and for assessing a sketch design in terms of seasonal/annual heating or cooling requirement. Such assessment can be performed with simple manual calculations, or through the use of personal computers with basic models. Littler (1982) gives a review of such programs. Calculation of heat transfer through building components is a well established engineering procedure in many literature among which are the fundamental handbooks of ASHRAE (1985) and the CIBS Guide (1980).

The simulation of the thermal state of a full scale building design requires sophisticated computer models. The program "ESP", available at the University of Strathclyde, is high in rank of such models. For these models, hourly values of climatic parameters are needed from a full reference year. Simple models like "Qref" and "Curtain", developed by the author in this thesis, also require hourly climatic data. The reference year should represent the climatic nature of the region in question. A number of countries have reference year data ready for commercial or research use.

Since accurate and long term climate data for Saudi Arabia are difficult to obtain it has been necessary to consider creating a Climate Reference Year (CRY) of data from little previous knowledge. As will be seen from the analysis conducted in this thesis, the resultant climate reference year is typical of a hot-arid climate. The CRY should prove extremely valuable for designers to simulate and analyse the energy performance of building components, not only for Saudi Arabian climate, but also for hot-arid regions in general.

In keeping with the formal language and spatial concepts of modern architecture, and with the development of new building materials, much is being made of large windows and large expanses of glass in building facades, irrespective of the local climate. This has resulted in the overheating of buildings owing to excessive heat gain even in temperate climates. It is also possible in modern buildings to restrict, or even to eliminate, access of daylight (e.g. in office buildings and department stores). In many cases, the problem consists in reducing to an acceptable level the intensity of solar heat gains transmitted through large window areas.

The problem of sun protection is, of course, far older than modern architecture. In the past, however, the size of the wall openings was small in relation to the building and it was sufficient to protect the interior by simple devices. In contrast, modern buildings with their large window areas call for special protection against the sun. An improvement to the overheating problem can be achieved through the use of shading devices. Shading devices can be applied either externally, internally or between double glazing. "Intelligent glazing" with varying solar optical properties can also provide some form of solar control without necessitating the reduction of glass area. The principal advantages and disadvantages of solar control devices are compared in this thesis. Internal shading devices are, in general, less effective than external shades in minimizing solar heat gains, but more effective in reducing heat losses through windows. The discussion will also show that, in reducing heat loss, if the internal device does not effectively trap air between itself and the window, the insulative value is minimal.

Proper selection of the type of glass and shading devices is important for reducing the heat gains or losses through glazed areas and thus the energy demands for maintaining indoor thermal environments at comfortable levels. To estimate the solar heat gain through different types of glass their spectral reflection, absorption and transmission characteristics for the entire range of wavelengths of solar spectrum are required. An evaluation of the expected performance of a planned shading device and its geometrical characteristics, prior to actual construction, is also essential for the satisfactory thermal performance of a building. The solar properties and the heat transfer mechanism at glazing surfaces are discussed in critical review of the various correlation techniques available in literature.

Curtains are probably the most used form of indoor shading devices. Evidence suggests that the average consumer has only a limited perception of the solar transmitting properties of interior shading devices and their potential for reducing solar heat gain or thermal losses (Braun 1981). Some of this failure in comprehension can be attributed to the diversity of available devices. Even after they have been reduced to specific categories such as curtains, roller shades, shutters, and blinds, there remains a profusion of materials and methods of construction within each group. Hence, most choices of a specific interior shading device are based upon perceived aesthetic properties, advice from an interior designer, or cost. After installation most users still have only a limited concept of how interior shading devices can or should be managed; most management is again predicated on factors other than energy conservation (e.g. privacy and glare control).

A survey of references that deal with the solar and thermal properties of curtains shows that only a few technical reports and journal articles have been published. It has been necessary, therefore, to produce a high standard review of the solar and thermal characteristics of curtains (textile fabrics). This should compensate for the lack of literature in this field and provide a useful basis for further research. The effects of curtain geometric configuration (i.e. folding, spacing between multi-layers of fabric, and between the fabric and the glazing) on the solar and thermal properties of the composite fenestration are discussed. Techniques for the measurement of curtain solar properties are also discussed, and results of tests, conducted by the author, on three domestic curtain types are presented. The "Curtain" program developed in this thesis provides architects and designers with a tool for modelling the energy performance of textile curtains installed onto single or double glazed windows under real climatic conditions.

In view of the above discussion, architects and designers should be able, (with the aid of models provided in this thesis), to assess the contributions that various passive solar techniques will make to energy savings and comfort levels in buildings. However, these models are theoretical and some form of validation is essential.

The availability of the "Passys" test site facilities at Strathclyde University campus provided the author with an opportunity to conduct the outdoor experiments discussed in this thesis, and to validate the theoretical models "ESP" and "Curtain". The Passys project is an European concerted action in the field of passive solar buildings initiated by the Commission of the European Communities as part of its Solar Energy R&D program, with the following objectives: (i) to develop reliable and affordable test procedures for Passive Solar Components in a buildings, (ii) to increase confidence in simulation models through validation, and (iii) to increase confidence in simplified design tools. The project operates with highly standardised test cells. The ESP simulation model has been chosen for validation and further development. Test cells and south wall components are located on test sites throughout the European Community so that their performances could be analysed in a range of climatic conditions. The Energy Studies Unit of Strathclyde University lead the UK consortium.

Description of the facilities is provided in the main text of chapter 7. Experiments were conducted on an energy efficient blind (pleated textile fabric, with aluminum coating on one side) supplied by the Passys group. Experiments were also conducted on a single domestic curtain, and results from both experiments are analysed.

## 1.2 Summary of Objectives

---

The Objectives can be summarised as follows:

- Develop a Climate Reference Year representative for Riyadh Saudi Arabia. It should comprise climatic parameters required by most building energy simulation programs. The CRY may also be useful for other hot-arid regions.
- Produce a high standard review of the solar and thermal characteristics of internal shading devices made of textile fabrics. This should compensate the lack of literature in this field and provide a useful base for further research.
- Develop simple design tools for modelling the energy performance of “blind” or “curtain” shaded fenestration under real climatic conditions. These should be verified experimentally.
- Conduct experiments to determine the thermal effects of a blind-shaded and a curtain-shaded fenestration installed in real building components. The study should give the performance characteristics of these components, and verify simulated results by the “ESP” and “Curtain” programs.

## 1.3 Organisation of the Thesis

---

The thesis has been organised into 9 chapters:

**Chapter 1** presents the general statement of the problem. It states the aims of this research and the organisation of the thesis.

**Chapter 2** focuses on the relationship between climatic data and buildings at different design stages. Various tools and simple mathematical models are reviewed. These will help architects and designers to determine the thermal characteristics of design principles and choices of materials to adapt buildings to a local climate. Examples are given to evaluate design alternatives and thermal performances of different solar control techniques under the climate of Saudi Arabia.

**Chapter 3** processes and compiles hourly climatic data for the years 1984 through to 1986 in a standard format (*Climate Reference Year*) for Riyadh, Saudi Arabia. The resultant Climate Reference Year is representative of hot-arid climatic regions, and can be used in computer simulation models (e.g. “ESP”). This chapter also analysis the climate in both qualitative and quantitative terms to assist designers and architects determine the comfort conditions most suited to this region. Variations of the climate through the year, month and day are discussed. Diurnal Nomograms for predicting hourly data from daily values are developed. Finally, based on the compiled Climate Reference Year, solar radiation prediction algorithms are derived which are often required in the absence of measured data. Daily meteorological data are tabulated in Appendix (A), and insolation data in Appendix (B). Note that the CRY is made available on a 5.25" computer floppy diskette in MSDOS format. (see Appendix I).

**Chapter 4** investigates different calculation procedures for the convective and radiative heat transfers at glazing surfaces (which can also apply to other building surfaces). Based on this, suitable procedures are adopted and incorporated in a computer program, developed by the author, to calculate the maximum solar heat gain flux through a clear window glass under the climate of Riyadh, Saudi Arabia. The output of this model is tabulated in Appendix (D). Code listing of the program is given in Appendix (E). A brief discussion of simplified design tools for solar control is presented, with emphasis on the sun and shading device angular relationship. The chapter concludes with a performance review of solar control glazing and different shading devices (external & internal).

**Chapter 5** provides the theoretical bases to determine the effectiveness of curtains in reducing heat gains and heat losses through windows. Classification, thermophysical properties of curtain fabrics, and the effect of geometric configuration on curtain properties are discussed. A computer model "Curtain.Bas" is developed. It computes the fenestration temperatures and energy flows associated with curtain-shaded single or double glazed windows exposed to real climatic conditions. This chapter also describes the laboratory experiments conducted by the author to measure the solar transmittance and reflectance of three domestic curtains. The discussion also highlights the accuracy of measurements made by two portable instruments.

**Chapter 6** is concerned with the knowledge of accuracy and use of instruments for both indoor and field measurements. It reviews various instruments to measure, temperature; relative humidity; wind speed and direction; and insolation. Special attention is given to the sensing mechanism and accuracy of instruments. Algorithms are provided for calculating temperature from measured voltage, and calculating relative humidity from measured dry bulb and wet bulb temperatures. In addition an accurate algorithm for averaging wind direction is proposed. This chapter also describes the computer model "Dtclm.Bas" developed by the author to process logged data. A quick and specific reference to the instruments used in the experimentation of this thesis is provided in Appendix (F) in the form of data sheets. This appendix also outlines the sources of error in measurements and consider the statistical methods of error analysis used in this thesis.

**Chapter 7** studies the thermal performance of a pleated metallised fabric blind with a low emissivity double glazed window from experiments conducted on the Passys test site. The main characteristics of this component are the heat transmission coefficient ( $\dot{U}$ ) and the solar aperture ( $\dot{A}$ ). The Passys facilities; i.e. the test cells, instrumentation, data acquisition and the south walls; are briefly described. Two test cells, one fitted with glazing and the Passys blind and the other with glazing only, have been used for side-by-side experiment to study the thermal performance of the blind-shaded window. Both cells had timber-frame walls with outer brick cladding. A steady-state test methodology for average cell behaviour is described; and solved by linear regression over the measured data. The Passys common test evaluation program "MRQT" is also used, and results compared. Results from this experiment are analysed over the whole period of experiment and for typical clear and overcast days. Comparison between measured and predicted results by the "ESP" and the "Curtain" models are also presented.

**Chapter 8** is concerned with experiments conducted at the Passys test site with a domestic curtain fitted on a double glazed window. Unlike the experiments conducted on chapter 7, one test cell was used. The test cell had a prefabricated sandwich concrete wall with rigid insulation (reference wall). Regression techniques and modelling are used to determine the solar and thermal performance characteristics of the “reference wall”, with and without the curtain. Results from this experiment are analysed over the whole period of experiment and for typical clear and overcast days. The effects of the curtain–shaded glazing on the test cell energy performance are discussed. Comparison between measured and predicted results by the “ESP” and the “Curtain” models are also presented, with emphasis on a clear and an overcast days.

**Chapter 9** concludes the thesis and suggests areas for further study.

## 1.4 References

---

ASHRAE (1985) *ASHRAE Handbook (Fundamentals)*. American Society of Heating, Refrigerating and Air–conditioning Engineers Inc. Atlanta, U.S.A.

Baker P., Clarke J., Guy A., Owens P., Pearson K., Strachan P. & Twidell J. (1992) “Passys II Final Report of the UK Consortium”, Draft report submitted to DG XII of the European Commission and the Energy Technology Support Unit, Jan. 1992.

Braun E. (1981) “Survey of Window–Treatment–Use Amongst Cities with Different Heating and Cooling Requirements”, MSc Thesis, Texas Tech University, Lubbock, Texas, USA.

CIBS (1980) “Thermal Properties of Building Structures”, Section A3, Chartered Institute of Building Services, London.

Joudah N. (1985) “Energy Conserving Architectural Design–indicators for the Hijaz Region in Saudi Arabia”, MArch thesis, Architecture & Energy Dept., University of Colorado at Denver, Colorado, U.S.A.

Joudah N., Salloum A., Al–Faisal A., Abo–Bakur H., & Benaghmouch B. (1983) “Housing for Under–Privileged Muslims”. BArch Terminal project, S.E.D., Eng. Dept., K.A.A.Univ., Jeddah, Saudi Arabia. Also the project was awarded the prize of the Royal Institute of Architects of Ireland, for the 7th International Competition for Students of Architecture; Union Internationale des Architects (UIA), rue Raynouad, 75016 Paris, 1984.

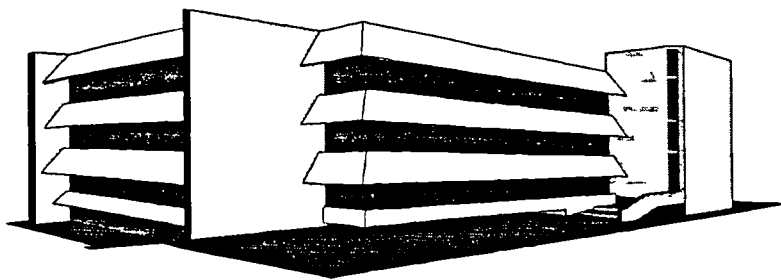
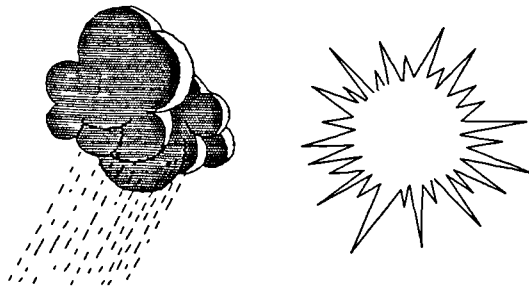
Kaizer T. (1984) *Shelter in Saudi Arabia*, Applied Science Publishers Ltd., London.

Kendel H. (1982) “Key Elements for the Design of Contemporary Buildings that Respect the Arab Muslim Cultural Heritage”, *Sym. Proc. of The Arab City*, Madina, Saudi Arabia.

Littler J. (1982) “Overview of Some Available Models for Passive Solar Design”, *Computer Aided Design*, 14, p 15.

Mofti F. & Balto S. (1983) “Lessons to be Learned from A Comparative Evaluation of the Traditional Towns of Riyadh and Jeddah in Saudi Arabia”, *Proc. of 2nd int. PLEA Conf.*, “Passive and Low Energy Architecture”, (ed.) Yannas S., Athens.

# Chapter 2



## 2. CLIMATIC DATA AND ITS USE IN BUILDING DESIGN

### 2.1 Introduction

---

Climate is a major determinant in building design. Many architects would consider climate, if at all, only in qualitative terms. Some would suggest that any quantitative analysis should be left to expert consultants. In the future it is possible that architects will be the experts on building energy matters in general and on climatic design in particular. Climatic design literally implies that after considering the existing climate, it is possible to design a building that negates adverse effects and accentuates the positive elements needed to maintain a comfortable dwelling.

Climatic data may be used at five levels of increasing complexity during the design process:

- In qualitative terms, for an initial appreciation
- For a pre-design analysis
- For assessing a sketch design in terms of annual / seasonal heating or cooling requirement, which may be repeated several times with modified designs
- Possibly in lieu of the above, using a simple simulation program to predict the thermal response of building design alternatives (Simple Design Tools)
- Full scale thermal simulation using fundamental heat transfer analysis, e.g. Environmental System Performance model (ESP).

The following chapter is related to the last level, by defining a Climate Reference Year for Riyadh, Saudi Arabia, (a hot-arid climate), which can be applied with the “ESP” program for an assessment of optimum designs in this climate. The other levels of climatic data usage in building design are the considerations of the present chapter.

A method to determine human requirements and basic design principles in relation to climate is presented as a tool for pre-design analysis. The design principles and choice of materials to adapt buildings to climate can be evaluated for their thermal characteristics by the different models discussed in this chapter.

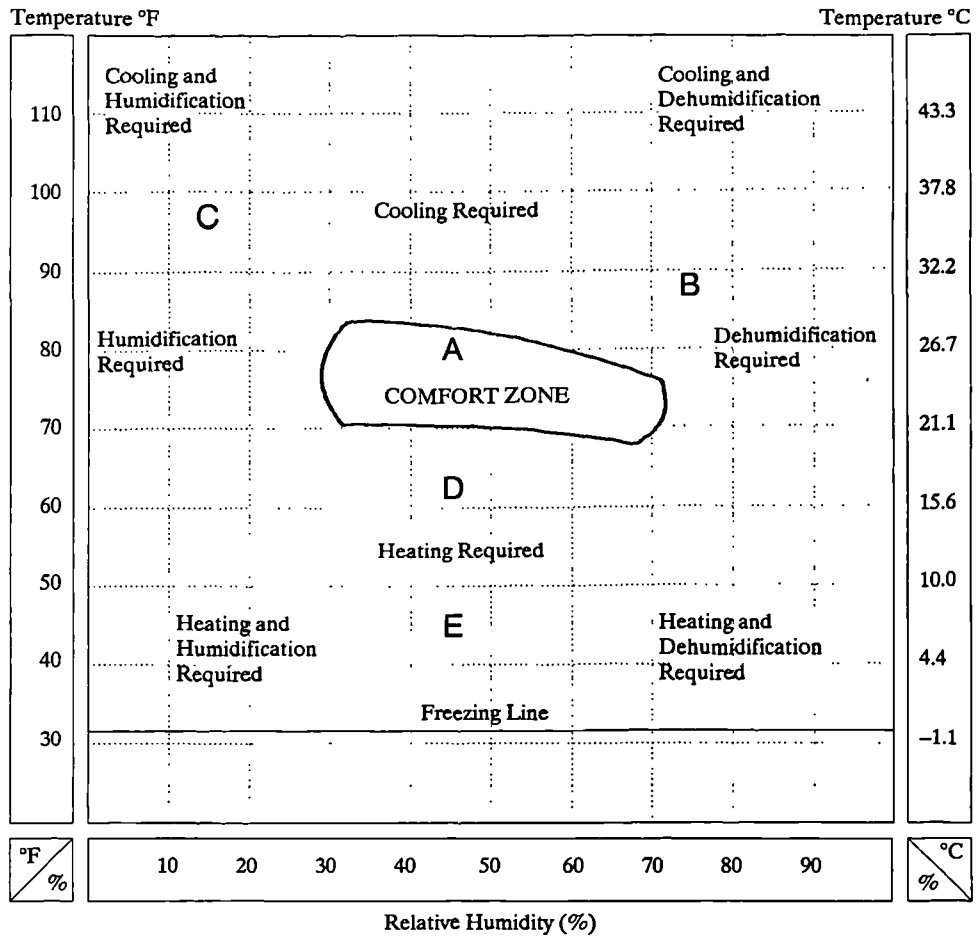


**Figure 2.1**

The Bioclimatic chart. It identifies the human comfort zone (A) in still air for a lightly clothed male. The two main coordinates are temperature and relative humidity with the varying degrees and causes for discomfort identified on the chart. In warm-humid conditions, excessive heat can be relieved with air movement (B), in hot-dry conditions comfort can be obtained by adding moisture and consequent evaporative cooling (C), in cool conditions comfort can be obtained by exposure to solar radiation (D), while in cold conditions additional heating is required (E). (reproduced from Bowen 1983).

## 2.2 Pre-design Analysis

---

In-depth analysis of climate is highly time consuming and requires much climatic information. This is not always available, and considering other factors in design (e.g. layout, spacing, construction, etc), climatic analysis may be underemphasised. To overcome this problem, various authors have developed simple tools that can be used to correlate climatic variables with human comfort and building at the pre-design stage (often called sketch design).

For example, the bioclimatic chart, Figure (2.1), developed by Olgyay (1963), identifies a human comfort zone. It also shows the corrective measures required when a combination of relative humidity and temperature falls outside the comfort zone (see the notes on Fig. 2.1). I have utilised the Olgyay's bioclimatic chart (Joudah 1985) in a procedure to develop design guidelines for the Hijaz climatic region in Saudi Arabia. (see also Joudah et. al. 1983 for applications in different climates).

Another method of analysing climate is the "Mahoney Tables" published in Koenigsberger et. al. 1971 & 1973. These are described and used for the climate of Riyadh in section 2.2.1 below. Other methods include those developed by Szokolay (1980) and by Evans (1980), which are both derived from the Mahoney tables.

### 2.2.1 The Mahoney Tables

The Mahoney tables provide a guide to design in relation to climate using readily available climatic data. By following a step by step procedure the designer is led from the climatic information to specifications for optimal conditions of layout, orientation, shape, and structure needed at the sketch design stage. To illustrate the use of Mahoney tables, a worked example (Example 1) is given for Riyadh, Saudi Arabia. The climatic data are obtained from Table 3.2. The analysis requires the use of five tables. To retain the orderly nature of the original work, the tables are numbered 1 to 5. A brief description of each table follows.

#### Air temperature (Table 1)

The values recorded in table (1) are the monthly mean maximum and minimum temperatures, the mean monthly range (difference between mean max. and min.). The "annual mean temperature" (AMT) is the average of the highest monthly mean maximum (Hi) and the lowest monthly mean minimum (Lo). The "annual mean range" (AMR) is the difference between (Hi) and (Lo).

EXAMPLE 1: Use of the Mahoney tables.

Location : Riyadh, Saudi Arabia

Lat. = 24°54'N Long. = 46°24'E Alt. = 564m

Table 1. TEMPERATURE

Temperature (°C)	J	F	M	A	M	J	J	A	S	O	N	D	Hi	AMT
Monthly mean max.	20	23	28	32	38	42	43	42	41	34	27	22	43	26
Monthly mean min.	8	10	14	19	24	26	27	22	22	18	14	9	8	35
Monthly mean range	12	13	14	13	14	16	16	20	19	16	13	13	Lo	AMR

Table 2. HUMIDITY, RAIN AND WIND

Relative humidity (%)	J	F	M	A	M	J	J	A	S	O	N	D		
Monthly mean max.	81	68	65	64	48	28	26	27	31	33	54	65		
Monthly mean min.	23	28	21	13	11	7	8	9	9	14	22	26		
Average	52	48	43	39	22	17	17	18	20	24	38	46		
Humidity group	3	2	2	2	1	1	1	1	1	1	2	2		
Rainfall (mm)	15	7	23	34	10	0	0	0	0	0	8	11	108	Total
Wind direction	Prevailing	SSE	SSE	SSE	SSE	N	NNW	N	NNE	Var	SE	SSE		

Table 3. DIAGNOSES

	J	F	M	A	M	J	J	A	S	O	N	D		
Humidity group	3	2	2	2	1	1	1	1	1	1	2	2		
Temperature (C°)														
Monthly mean max.	20	23	28	32	38	42	43	42	41	34	27	22		
Day comfort : Max.	29	31	31	31	34	34	34	34	34	34	31	31		
Min.	23	25	25	25	26	26	26	26	26	26	25	25		
Monthly mean min.	8	10	14	19	24	26	27	22	22	18	14	9		
Night comfort : Max.	23	24	24	24	25	25	25	25	25	25	24	24		
Min.	17	17	17	17	17	17	17	17	17	17	17	17		
Thermal stress														
Day	C	C	-	H	H	H	H	H	H	H	-	C		
Night	C	C	C	-	-	H	H	-	-	-	C	C		

Table 4. INDICATORS (one per tick)

	J	F	M	A	M	J	J	A	S	O	N	D	Totals
Humid													
H1 Air movement (essential)													
H2 Air movement (desirable)													
H3 Rain protection													
Arid													
A1 Thermal storage	√	√	√	√	√	√	√	√	√	√	√	√	12
A2 Outdoor sleeping				√	√	√	√	√	√	√			7
A3 Cold-season problems	√	√										√	3

**Humidity, rain and wind direction (Table 2)**

The monthly mean average relative humidities in this table are calculated from mean maximum and minimum values. The humidity group (HG) for each month are found from the following codes

Average Relative Humidity ( <i>R</i> )	Humidity Group (HG)
Below 30% .....	1
30 to 50% .....	2
50 to 70% .....	3
Above 70% .....	4

Also recorded in this table are the monthly total rainfall, the annual total rainfall and the prevailing wind direction in compass points for each month.

**Diagnosis of climatic stress (Table 3)**

Humidity group, monthly mean maximum and minimum temperatures are repeated in this table to assess day and night comfort ranges and thermal stresses. The day and night comfort limits are taken from the chart below, using the appropriate humidity group and relevant AMT (i.e. over 20°C). HG is the humidity group classification.

COMFORT LIMITS							
		AMT > 20°C		AMT 15–20°C		AMT < 15°C	
Average <i>R</i> (%)	HG	Day	Night	Day	Night	Day	Night
0–30	1	26–34	17–25	23–32	14–23	21–30	12–21
30–50	2	25–31	17–24	22–30	14–22	20–27	12–20
50–70	3	23–29	17–23	21–28	14–21	19–26	12–19
70–100	4	22–27	17–21	20–25	14–20	18–24	12–18

The symbols in the last two lines of this table represent symbols for day and night thermal stress rating. These are obtained by comparing the monthly mean maximum with the day comfort limits; and by comparing the monthly mean minimum with the night comfort limits, as:

Above comfort limits .....	H (Hot)
Within comfort limits .....	– (Comfort)
Below comfort limits .....	C (Cold)

**Indicators (Table 4)**

Certain groups of symptoms of climatic stress indicate the remedial action the designer can take. These are referred to (Koenigsberger et. al. 1971) as “indicators”. They tend to be associated with humid and arid conditions. One indicator by itself does not lead to a solution. Recommendations can be made only after adding the indicators for a whole year and completing this table.

EXAMPLE 1: Use of the Mahoney tables.  
 (continued) Location : Riyadh, Saudi Arabia  
 Lat. = 24°54'N Long. = 46°24'E Alt. = 564m

Table 5. SKETCH DESIGN RECOMMENDATIONS for Riyadh, Saudi Arabia

Indicator totals from table 4						Recommendations
Humid			Arid			
H1	H2	H3	A1	A2	A3	
0	0	0	12	7	3	
						<i>Layout</i>
						0-10
						11 or 12
						5-12
						0-4
						✓ 1. Buildings oriented on east-west axis to reduce exposure to sun
						✓ 2. Compact courtyard planning
						<i>Spacing</i>
						11 or 12
						2-10
						0 or 1
						✓ 3. Open spacing for breeze penetration
						✓ 4. As 3, but protect from cold/hot wind
						✓ 5. Compact planning
						<i>Air movement</i>
						3-12
						1 or 2
						0-5
						6-12
						2-12
						0
						0 or 1
						✓ 6. Rooms single banked. Permanent provision for air movement
						✓ 7. Double-banked rooms with temporary provision for air movement
						✓ 8. No air movement requirement
						<i>Openings</i>
						0 or 1
						0
						11 or 12
						0 or 1
						✓ 9. Large openings, 40-80% of N/S walls
						✓ 10. Very small openings, 10-20%
						✓ 11. Medium openings, 20-40%
						<i>Walls</i>
						0-2
						3-12
						✓ 12. Light walls; short time lag
						✓ 13. Heavy external and internal walls
						<i>Roofs</i>
						0-5
						6-12
						✓ 14. Light insulated roofs
						✓ 15. Heavy roofs; over 8 hours time lag
						<i>Outdoor sleeping</i>
						2-12
						✓ 16. Space for outdoor sleeping required
						<i>Rain protection</i>
						3-12
						× 17. Protection from heavy rain needed

The applicability of these indicators are listed below :

#### *Humid Indicators*

**H1** indicates that air movement is essential. It applies when high temperature (day thermal stress = H) is combined with high humidity (HG = 4) or when the high temperature (day thermal stress = H) is combined with moderate humidity (HG = 2 or 3) and a small diurnal range (i.e. less than 10°C);

**H2** indicates that air movement is desirable. It applies when temperatures within the comfort limits are combined with high humidity (HG = 4);

**H3** indicates that precautions against rain penetration are needed. Problems may arise even with low precipitation figures, but will be inevitable when rainfall exceeds 200mm per month.

#### *Arid Indicators*

**A1** indicates the need for thermal storage. It applies when a large diurnal range (10°C or more) coincides with moderate or low humidity (HG = 1, 2 or 3);

**A2** indicates the desirability of outdoor sleeping space. It needed when the night temperature is high (night thermal stress = H) and the humidity is low (HG = 1 or 2). It may be needed also when nights are comfortable outdoors but hot indoors as a result of heavy thermal storage (i.e. day = H, HG = 1 or 2 and when the diurnal range is above 10°C);

**A3** indicates winter or cool-season problems. These occur when the day temperature falls below the comfort limits (day thermal stress = C).

#### Recommendations (Table 5)

These are 17 in total and are grouped under eight subjects : layout; spacing; air movement; openings; walls; roofs; outdoor sleeping; and rain protection. The subjects are dealt with individually after transferring the indicator totals from table 4 to this table. Appropriate recommendations are found by examining the indicator columns. There can be only one recommendation per subject as one scans from left to right. A further alternative exist in a few cases, namely, recommendations 1 or 2, 6 or 7, and 7 or 8. In these cases, the choice of recommendation is made by proceeding with the scanning of indicator columns to the right and deciding according to the range of months given in the table. The above procedure is indicated on this table by the use of dashes and arrows.

It is important to note the logic behind the use of these tables. What is achieved by them is; 1- a record of some of the dominant climatic features of Riyadh, one by one, noting for each the period during which it is operative (Tables 1 to 4); 2- a set of general recommendations that may be appropriate for combinations of climatic features (Table 5). The architect decides how these recommendations may be applied in the design. At the end of the day, the over-all concept of the building design may be less than perfect. This does not invalidate the decisions arrived at through the use of Mahoney tables. It means merely that climatic design should not end with the completion of the sketch design stage.

## 2.3 Calculation of Building Heat Losses

An estimate of the heat losses of a building is vital for evaluating its thermal performance and for sizing heating systems. This is a well established engineering procedure in many literature among which are the invaluable British CIBS Guide (1980) and its US counterpart, the ASHRAE Handbook (1985). Calculating the heating load of a building involves estimating the maximum probable heat loss of each room or space to be heated for maintaining a selected indoor air temperature during periods of design outdoor weather conditions. Heat losses are mainly:

- Transmission losses or heat transferred through the confining walls, glass, ceiling, floor or other surfaces.
- Infiltration losses or energy required to warm outdoor air leaking in through cracks and gaps around doors and windows (due to pressure difference between the outside and inside) or through open doors and windows.

### 2.3.1 Transmission Heat Loss: (steady-state)

The transmission loss can be determined by the basic steady-state formula for the building components; walls, roofs, floors, windows and doors as

$$Q_{cl} = \sum (U A \Delta T) \quad \{2.1\}$$

where

- $Q_{cl}$  = total transmission heat loss of building components (W)  
 $U$  = thermal transmittance, of each component ( $W m^{-2} \cdot ^\circ C^{-1}$ )  
 $A$  = area of each component surface ( $m^2$ )  
 $\Delta T$  =  $T_i - T_o$   
 $T_i$  = inside air temperature ( $^\circ C$ )  
 $T_o$  = outside air temperature ( $^\circ C$ ). For floor losses this term would be the ground temperature in the case of solid floor in contact with the ground or ambient air temperature below suspended floors  
 $\Sigma$  = sum of all the parallel heat transfer through the components.

This equation is valid in situations where temperature does not change significantly with time. It is suitable when applied to buildings with little fenestration in winter conditions of low external temperature and little or no solar gain. There are important reservations about the value of a technique based on steady-state, one-dimensional heat flow to deal with the problems of, for example, corners in buildings, thermal energy storage in the building fabric and changes in the  $U$ -value, (e.g. due to moisture penetration).

However, this method has the great virtue of simplicity. The total error involved are not greater than, say, 20%. The  $U$ -value or thermal transmittance is give by

$$U = 1 / R \quad \{2.2\}$$

**Table 2.1** Internal surface resistance\*, ( $R_{si} = m^2 \text{ } ^\circ\text{C W}^{-1}$ ).

Building element	Direction of heat flow	Surface Emittance	
		$\epsilon = 0.9$	$\epsilon = 0.05$
Walls	Horizontal	0.12	0.30
Ceilings, roofs or floors	Upward	0.10	0.22
	Downward	0.14	0.55

**Notes**

Source : section A3 of the CIBS Guide (1980).

\* Resistances are for surfaces of the stated emissivity values facing an assumed black surface at  $\epsilon = 0.9$ . Surface temperature is assumed to be  $20^\circ\text{C}$ . Air speed at the surface is assumed to be not greater than 0.1 m/s

**Table 2.2** External surface resistance, ( $R_{so} = m^2 \text{ } ^\circ\text{C W}^{-1}$ ), for stated exposure.

Building element	Emissivity of surface	Exposures <sup>†</sup>		
		Sheltered	Normal	Severe
Wall	High ( $\epsilon = 0.9$ )	0.08	0.06	0.03
	Low ( $\epsilon = 0.05$ )	0.11	0.07	0.03
Roofs	High	0.07	0.04	0.02
	Low	0.09	0.05	0.02

**Notes**

Source : section A3 of the CIBS Guide (1980).

† Sheltered : up to 3rd floor buildings in urban centres;  
Normal exposure : most suburban and rural buildings, 4th–8th floor in urban centres;  
Severe exposure : buildings in coastal or hill sites, and for floors above those of normal exposure. (also see text for more information).

**Table 2.3** Overall Resistance of Unventilated Cavities, ( $m^2 \text{ } ^\circ\text{C W}^{-1}$ ).

Type of air cavity <sup>‡</sup>		Direction of heat flow		
Thickness	Surface emissivity	Horizontal	Upward	Downward
5mm	High	0.10	0.10	0.10
	Low	0.18	0.18	0.18
20mm or more	High	0.18	0.17	0.22
	Low	0.35	0.35	1.06
High emissivity plane and corrugated sheet in contact		0.09	0.09	0.11
Low emissivity multiple foil insulation with air space on one side		0.62	0.62	1.76

**Notes**

Source : section A3 of the CIBS Guide (1980).

‡ Emissivity ( $\epsilon$ ) : High = 0.9, Low = 0.05. Interpolation and extrapolation of resistance for other air space thickness is permissible.

where  $R$  is the sum of the series resistances of surfaces and layers of materials,  $m^2\text{C}(W^{-1})$ . More explicitly,

$$R = R_{si} + R_1 + R_2 + \dots + R_n + R_{so} \quad \{2.3\}$$

where

$R_{si}$  is the resistance of the inner surface (also known as inner air film resistance). It is the reciprocal of surface conductance ( $R_{si} = 1/h_i$ ), where the conductance of the inner surface is the combined radiative and convective heat transfer coefficients for still air, ( $h_i = h_{ri} + h_{vi}$ ). Details on the convective and radiative heat transfer coefficients at internal surfaces are discussed in chapter 4. (see section 4.3).

$R_{so}$  is the resistance of the outer surface or the outer air film resistance. This is calculated as above, [ $R_{so} = 1/h_o = 1/(h_{ro} + h_{vo})$ ]. Thus the convection part of surface conductance is strongly dependant on wind speed.

$R_1, \dots, R_n$  are the resistances of layers of materials (or air cavities). The thermal resistance of a layer of material is given by ( $R = x/k$ ) where ( $x$ ) is the layer thickness in  $m^2$ , and ( $k$ ) is the thermal conductivity in  $W(m^{\circ}C)^{-1}$ .

Internal surface resistances for building elements with high and low emissivities and for different directions of heat flow are provided in Table (2.1). The CIBS Guide (1980) gives external surface resistances for high and low emissivity walls and roofs (Table 2.2), as a function of building exposure to wind speed: Sheltered ( $0.7-1 m s^{-1}$ ); Normal exposure ( $2-3 m s^{-1}$ ); and Severe exposure ( $6-9 m s^{-1}$ ). The ASHRAE Handbook (1985) suggests the use of a summer surface resistance value of  $0.044 W m^{-2}\text{C}^{-1}$ , i.e. exposed to  $3.4 m/s$  wind speed, and a winter surface resistance value of  $0.03 W m^{-2}\text{C}^{-1}$ , (exposed to  $6.7 m s^{-1}$  wind), for all conditions of surface emittance and direction of heat flow. (see chapter 4 for specific surface heat transfer coefficients at glazing surfaces calculated for Riyadh climate).

Table (2.3) shows the resistances of a variety of air cavities. Typical thermal conductivities and other properties of common building materials are shown in Table (2.4). Table (2.5) gives  $U$ -values for different types of glazing; and  $U$ -values for typical windows (glazing with frames) are shown in Table (2.6).

For ground floors it is difficult to calculate heat losses accurately. Littler & Thomas (1984), stated that "It is not possible to calculate  $U$ -values for floors in the same way as for walls". The reason for this statement is as shown in Figure 2.2 (Markus & Morris 1980). The greater the length of the heat flow path the smaller is the rate of heat loss, hence the  $U$ -value to be used for the floor must be based upon the dimensions of the floor and the edge conditions.

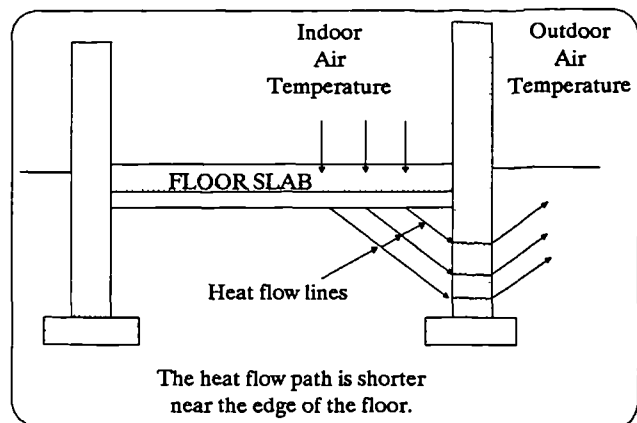


Figure 2.2 Heat flow through floor slab.

**Table 2.4** Thermophysical Properties of Selected Building Materials. †

Material	Conductivity $W (m \text{ } ^\circ C)^{-1}$	Density $kg m^{-3}$	Specific heat $J (kg \text{ } ^\circ C)^{-1}$	Emissivity (longwave)	Absorptivity (solar)
Asbestos sheet	0.36	700	1050	0.96	0.60
Asphalt mastic	1.15	2325	837	0.90	0.90
<i>BRICK</i>					
Outer leaf	0.84	1700	800	0.93	0.70
Inner leaf	0.62	1700	837	0.93	0.70
Insulating	0.27	700	837	0.93	0.70
<i>CONCRETE</i>					
Heavy	1.40	2100	653	0.90	0.65
Light	0.38	1200	653	0.90	0.65
Aerated block	0.24	750	1000	0.90	0.65
<i>INSULATION</i>					
Glass fibre quilt	0.04	12	840	0.90	0.65
Mineral fibre	0.04	105	1800	0.90	0.60
Polyurethane foam board	0.03	30	837	0.90	0.50
Polystyrene	0.03	25	1000	0.90	0.30
Urea formaldehyde foam	0.03	30	1764	0.90	0.50
<i>METAL</i>					
Aluminium	210.0	2700	880	0.22	0.20
Copper	200.0	8900	418	0.72	0.65
Steel	50.0	7800	502	0.12	0.20
<i>PLASTER</i>					
Dense	0.50	1300	1000	0.91	0.50
Light	0.16	600	1000	0.91	0.50
Gypsum board	0.16	950	840	0.91	0.50
<i>RENDERS &amp; SCREEDS</i>					
White cement render	0.50	1300	1000	0.91	0.40
Cast concrete	1.28	2100	1007	0.90	0.65
Granolithic	0.87	2085	837	0.90	0.65
<i>STONE</i>					
Sand stone	1.83	2200	712	0.90	0.60
Red granite	2.90	2650	900	0.90	0.55
White marble	2.77	2600	802	0.90	0.45
<i>TILES</i>					
Clay	0.85	1900	837	0.90	0.60
Concrete	1.10	2100	837	0.90	0.65
Slate	2.00	2700	753	0.85	0.85
Plastic	0.50	1050	837	0.90	0.40
Cork	0.08	530	1800	0.90	0.60
<i>WOOD</i>					
Block or Chip board	0.15	800	2093	0.90	0.65
Hard board	0.13	900	2000	0.91	0.70
Flooring	0.14	600	1210	0.91	0.65

**Notes**

Source : selected from the construction data base of ESP program data base (1987).

† The values in this table represent general design properties of dry material. The wide variety of materials available make it imperative that the manufacturer be consulted for more precise data.

**Table 2.5** U-values for glazing without frames\*, ( $\text{W m}^{-2}\text{°C}^{-1}$ ).

Construction	U-value for stated exposure		
	Sheltered	Normal	Severe
Single window glazing	5.0	5.6	6.7
Double window glazing with airspaces			
6mm	3.2	3.4	3.8
12mm	2.8	3.0	3.3
Triple window glazing with airspaces			
6mm	2.3	2.5	2.6
12mm	2.0	2.1	2.2
Roof glazing skylight	5.7	6.6	7.9

**Notes**

Source: section A3 of the CIBS Guide (1980).

\* In calculating the U-values, the thermal resistance of the glass has been ignored.

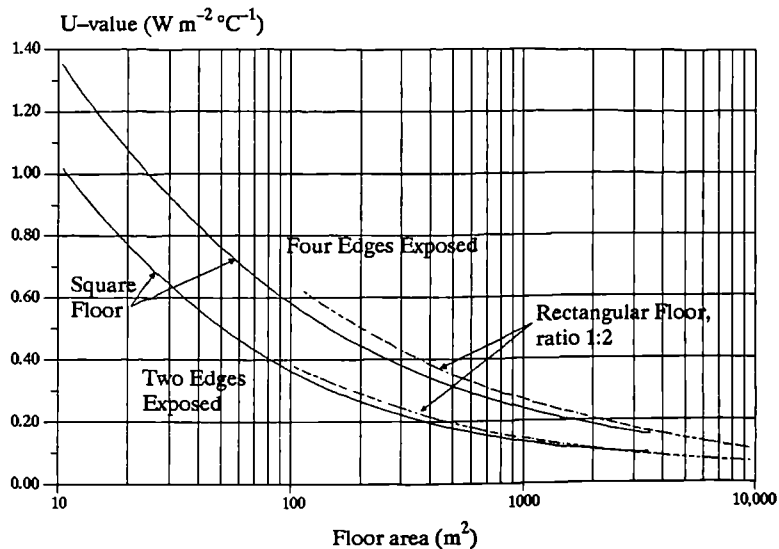
**Table 2.6** U-values for typical windows (glass with frame).

Window Type	† Fraction of area occupied by frame (%)	U-values for stated exposure ( $\text{W m}^{-2}\text{°C}^{-1}$ )		
		Sheltered	Normal	Severe
<b>SINGLE GLAZING</b>				
Wood frame	10	4.7	5.3	6.3
	20	4.5	5.0	5.9
	30	4.2	4.7	5.5
Aluminium frame	10	5.3	6.0	7.1
	20	5.6	6.4	7.5
	30	5.9	6.7	7.9
<b>DOUBLE GLAZING</b>				
Wood frame	10	2.8	3.0	3.2
	20	2.7	2.9	3.2
	30	2.7	2.9	3.1
Aluminium frame	10	3.3	3.6	4.1
	20	3.9	4.3	4.8
	30	4.4	4.9	5.6
Aluminium frame (with thermal break)	10	3.1	3.3	3.7
	20	3.4	3.7	4.0
	30	3.7	4.0	4.4

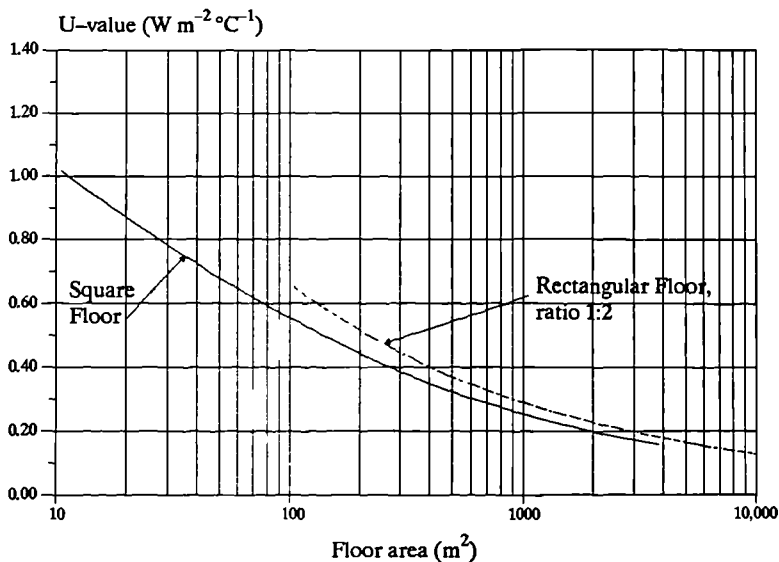
**Notes**

Source: section A3 of the CIBS Guide (1980).

† Where the proportion of the frame differs appreciably from the above values, particularly with wood or plastic, the U-value should be calculated. (metal members have a U-value similar to that of glass).



**Figure 2.3** U-values for solid floors on soil, (reproduced from Markus & Morris 1980).

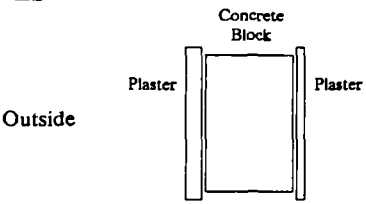
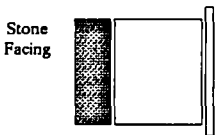
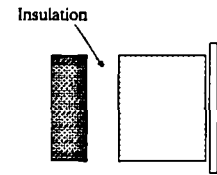
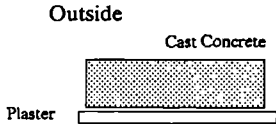
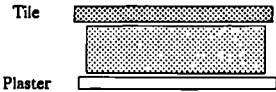


**Figure 2.4** U-values for suspended timber floor above ground, (reproduced from Markus & Morris 1980).

Little & Thomas (1984) give typical U-values for ground floors and the effect on U-value of increasing insulation. Figures (2.3 & 2.4) show the U-values of solid floors on soil and suspended timber floors respectively. They illustrate the influence that the edge conditions and floor area has upon the U-value. The ASHRAE Handbook (1985) discusses different procedures for ground loss calculations providing U-values for floors in relation to floor areas in one method and a theoretical loss coefficient related to perimeter exposure and length in another. However, all methods reviewed in the literature are subject to considerable uncertainty, and the U-values provided in Figures (2.3 & 2.4) should be adequate as long as the loss to ground is a small fraction of the total loss.

Table (2.7) gives U-values that I have calculated for several examples of typical wall, and roof constructions in Saudi Arabia, (based on personal experience with building practice in Saudi Arabia).

**Table 2.7** Air to air heat transfer coefficients of typical wall and roof constructions. †

Construction description		U ( $\text{W m}^{-2}\text{C}^{-1}$ )
<b>WALLS</b>		
	1 – solid concrete block, 100mm	3.6
	2 – hollow brick, 200mm	1.82
	3 – concrete block (2 core), 200mm	1.67
	4 – as (3) + “Riyadh stone” facing, 70mm	1.63
	5 – as (3) + “white marble” facing, 25mm	1.72
	6 – as (4) + 50mm cavity	1.26
	7 – as (5) + 50mm cavity	1.31
	8 – as (5) + 50mm insulation	0.55
<b>ROOFS</b>		
	9 – cast concrete, 150mm	2.46
		10 – as (9) + “Terrazzo” tiles, 25mm

† U-values are calculated for normal exposure. Riyadh stone is a type of sandstone, it is cut in different sizes and comes with a corrugated face. Diagrams are not to scale.

**Table 2.8** Recommended minimum rates of fresh-air supply † to residential building zones for human habitation.

Type of space	Recommended minimum rate of air supply
<b>Services</b>	
Bathroom and WCs . . . . .	2 air change h <sup>-1</sup>
Halls and passage . . . . .	1 air change h <sup>-1</sup>
Kitchen . . . . .	56 m <sup>3</sup> h <sup>-1</sup>
<b>Living rooms &amp; bedrooms</b>	
8.5 m <sup>3</sup> per person . . . . .	20.5 m <sup>3</sup> h <sup>-1</sup> per person
11.5 m <sup>3</sup> per person . . . . .	18.5 m <sup>3</sup> h <sup>-1</sup> per person
14 m <sup>3</sup> per person . . . . .	12 m <sup>3</sup> h <sup>-1</sup> per person

† see Burberry (1983) for recommended rates in other building types.

### 2.3.2 Infiltration Heat Loss

Heat loss caused by infiltration,  $Q_{vi}$ , is given by :

$$Q_{vi} = C_p \rho v (T_i - T_o) \quad \{2.4\}$$

where

$$\begin{aligned} C_p &= \text{specific heat of air} = 1000 \text{ (J kg}^{-1} \text{ }^\circ\text{C}^{-1}\text{)} \\ \rho &= \text{density of air} = 1.2 \text{ (kg m}^{-3}\text{)} \\ v &= \text{ventilation rate (m}^3 \text{ s}^{-1}\text{)} \end{aligned}$$

Infiltration loss can be estimated by using the crack length method as described in section A4 of the CIBS Guide (1976) and in chapter 22 of the ASHRAE Handbook (1985). In this method, the ventilation rate is a product of window or door crack length and air leakage for the wind velocity and type of window or door crack involved per meter of crack. Optionally, the infiltration loss can be based on an estimated number of air changes commonly used, rather than the length of window and door cracks. If we let  $V$  = volume of the space, and  $N$  = number of air changes per unit time (usually  $N$  per hour is used in building energy practice), then the ventilation rate  $v = VN / 3600 \text{ (m}^3 \text{ s}^{-1}\text{)}$ . Substituting in Eq.2.4 and using the values of  $C_p$  and  $\rho$  stated above, the infiltration loss will be :

$$Q_{vi} = 0.33 N V (T_i - T_o) \quad \{2.5\}$$

A certain amount of judgment is required when choosing an appropriate air change rate depending on construction quality of building, weather conditions, and room use. Warner (1976) gives empirical relations relating ventilation rates of different room functions to wind speed. The ASHRAE Handbook (1985) examines infiltration rates measured in two samples of unoccupied North American houses by Grimsrud, et. al. (1982) and by Grot & Clark (1979). Results showed a mean value of air changes per hour ( $N = 0.5 \text{ h}^{-1}$ ) for new constructions biased towards energy efficiency, and for old low-income houses an air change rate of  $0.9 \text{ h}^{-1}$  was the median. To allow for occupants influence on air change, a value between  $0.1$  and  $0.15 \text{ h}^{-1}$  added to the above values was suggested. Szokolay (1980), and Markus & Morris (1980) recommend an air change rate of  $1$  to  $1.5 \text{ h}^{-1}$  for domestic rooms, increasing up to  $6-10 \text{ h}^{-1}$  for lavatories and kitchens. Table (2.8) shows recommended rates of fresh air supply to buildings which can be used as a guide.

If the number of occupants in a room is known, the infiltration losses could be based on the requirement of each person for fresh air supply with regard to room function. In this case, Eq.2.5 becomes

$$Q_{vi} = n \cdot v \cdot 0.33 (T_i - T_o) \quad \{2.6\}$$

where

$$\begin{aligned} n &= \text{number of people in space.} \\ v &= \text{air change rate per person (m}^3 \text{ h}^{-1} \text{ per person).} \end{aligned}$$

## 2.4 Calculation of Building Heat Gains

Heat gain in a building occurs in the form of: (1) solar radiation through transparent surfaces, (2) heat conduction through exterior walls and roofs, (3) heat conduction through floors and interior partitions, (4) generated heat within the space by occupants, lighting and appliances (these can be referred to as free gains or casual gains), and (5) energy transfer as a result of ventilation and infiltration of outdoor air.

The latter can be calculated as described previously in section (2.3.2) using any of Eq.2.4 through to Eq.2.6 but with the temperature difference being ( $\Delta T = T_o - T_i$ ). Equation 2.1 can be used to calculate heat gains through floors and interior partitions assuming that they are not insulated and their thermal capacities are negligible. External walls and roofs are subject to solar radiation during the day, thus increasing the rate of heat flow. This effect should be accounted for in calculating heat gains through these building components. Simple steady-state calculation procedures for heat gain through exterior walls and roofs, through glazing, and free gains follows.

### 2.4.1 Heat Gain Through Exterior Roofs and Walls: (sol-air method)

The technique for calculating the steady-state heat gain through exterior walls and roofs is similar to that of transmission loss (i.e. based on the U-value of Eq.2.1). The difference is the introduction of the sol-air temperature concept to the steady-state equation. Thus

$$Q_{cg} = \sum [(U A) \cdot (T_e - T_i)] \quad \{2.7\}$$

where  $Q_{cg}$  is the conduction heat gain through external walls and roof (W); and  $T_e$  is the sol-air temperature at each external surface ( $^{\circ}\text{C}$ ).

Sol-air temperature is defined (ASHRAE 1985) as the temperature of the outdoor air that, in the absence of all radiation exchanges, gives the same rate of heat transfer through a building element as would exist with the actual combination of incident solar radiation, radiant energy exchange with the sky and outdoor surroundings and convective heat exchange with the outdoor air.

Sol-air temperature can be calculated for a surface from

$$T_e = T_o + [R_{so} (\alpha G - \epsilon G_i)] \quad \{2.8\}$$

where

- $T_e$  = sol-air temperature at the external surface ( $^{\circ}\text{C}$ )
- $T_o$  = outdoor air temperature ( $^{\circ}\text{C}$ )
- $R_{so}$  = external film or surface resistance, see Table 2.2, ( $\text{m}^2\text{C W}^{-1}$ )
- $\alpha$  = surface absorptivity for solar radiation (see Table 2.4)

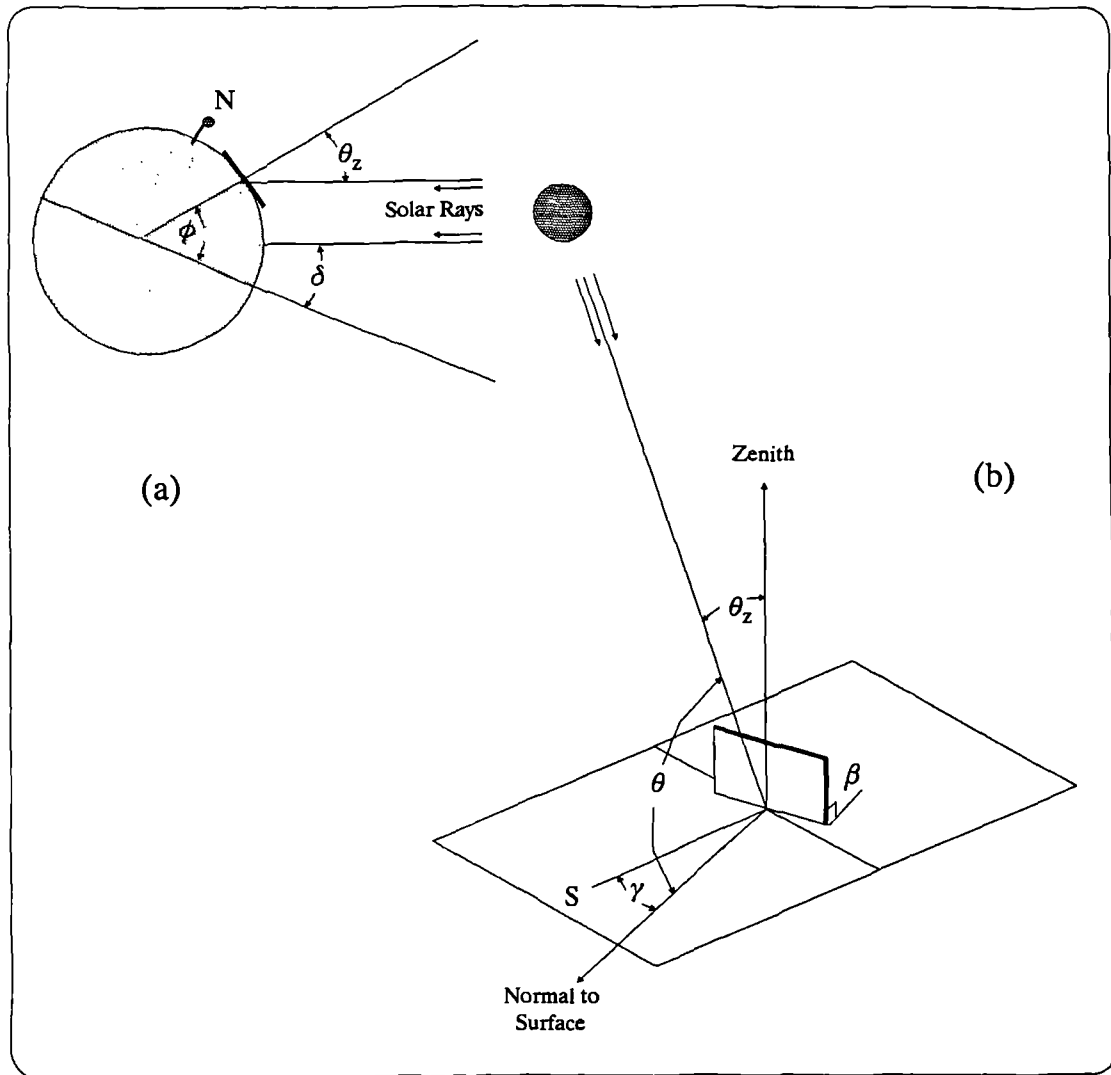


**Figure 2.5** Solar geometry. (a) Cross section of earth at solar noon, showing the relationship between latitude  $\phi$ , declination  $\delta$ , and the zenith angle  $\theta_z$ . (b) Angular relationship between a vertical surface and solar beam. The angle of incidence is denoted by  $\theta$ ,  $\beta$  is the surface slope, and  $\gamma$  is the surface azimuth angle.

- $G$  = global insolation incident on surface ( $\text{Wm}^{-2}$ ), this would be the global horizontal insolation  $G_h$  for flat roofs, but must be calculated for each wall orientation as discussed below
- $\epsilon$  = surface emissivity for longwave radiation (see Table 2.4)
- $G_l$  = longwave radiation balance between a black surface at  $T_o$  and the sky and surroundings ( $\text{Wm}^{-2}$ ), its calculation is discussed later in this section.

The global insolation incident on walls of any orientation used in Eq.2.8 has three potential components : direct beam, ground reflected, and sky diffuse (it is usual to disregard reflections from surrounding buildings). The direct component is simple to assess since it involves only angular operations on the horizontal direct insolation or the direct normal insolation, thus

$$G_{bv} = G_{bh} \cos(\theta) / \cos(\theta_z) \quad \{2.9\}$$

or

$$G_{bv} = G_{DN} \cos(\theta) \quad \{2.10\}$$

where

- $G_{bv}$  = direct insolation on a vertical surface of any orientation, ( $\text{Wm}^{-2}$ )
- $G_{bh}$  = direct insolation on the horizontal, ( $\text{Wm}^{-2}$ ), it is the difference between the global horizontal and diffuse horizontal insolation, ( $G_{bh} = G_h - G_{fh}$ )
- $G_{DN}$  = direct normal insolation ( $\text{Wm}^{-2}$ )
- $\theta_z$  = zenith angle, the angle between the beam from the sun and the vertical, ( $^\circ$ )
- $\theta$  = angle of incidence of beam radiation on the vertical surface, ( $^\circ$ )

Figure (2.5) shows the angular relationships between surfaces and the sun position. The angles of incidence of beam radiation on a horizontal surface (zenith angle  $\theta_z$ ) and on a vertical surface ( $\theta$ ), can be calculated from Equations (2.11 & 2.12) respectively

$$\cos(\theta_z) = \sin(\delta) \sin(\phi) + \cos(\delta) \cos(\phi) \cos(\omega) \quad \{2.11\}$$

$$\begin{aligned} \cos(\theta) = & \cos(\delta) \sin(\phi) \cos(\gamma) \cos(\omega) + \cos(\delta) \sin(\gamma) \sin(\omega) \\ & - \sin(\delta) \cos(\phi) \cos(\gamma) \end{aligned} \quad \{2.12\}$$

where

- $\delta$  = solar declination (i.e. the angular position of the sun at solar noon with respect to the plane of the equator), north positive ( $^\circ$ );
- $\phi$  = site latitude, north positive ( $^\circ$ );
- $\omega$  = hour angle ( $^\circ$ ), which is the angular expression of solar time (positive before noon and negative after);
- $\gamma$  = surface azimuth angle, that is, the deviation of the normal to the surface from the local meridian, the zero point being due south, east positive, and west negative.

The solar declination  $\delta$  can be found from the approximate equation of Cooper (1969) Eq.2.13, and the hour angle  $\omega$  from Eq.2.14,

$$\delta = 23.45 \sin[360 (284 + J) / 365] \quad \{2.13\}$$

$$\omega = 15 (12 - t_s) \quad \{2.14\}$$

where  $J$  is the year day number (Julian), and  $t_s$  is the local apparent time or solar time (does not necessarily coincide with local mean or clock time), and is given in hours by

$$t_s = t + E_t + (L_{std} - L_{loc}) / 15 \quad \{2.15\}$$

where  $t$  is the local mean time (h);  $L_{std}$  is the standard longitude for which the local time is based (e.g. 45°E for Saudi Arabia);  $L_{loc}$  is the longitude of the location in question; the denominator (1/15 h) represents a constant 4 minutes correction for every degree difference between the local and standard meridians; and  $E_t$  the equation of time (h), which makes allowance for the observed disturbances to the earth's rate of rotation, can be calculated from

$$E_t = [9.87 \sin(2e) - 7.53 \cos(e) - 1.5 \sin(e)] / 60 \quad \{2.16a\}$$

where  $e$  is a modulating function given by

$$e = 360 (J - 81) / 364 \quad \{2.16b\}$$

To determine the ground reflected component ( $G_{rv}$ ) of the total insolation incident on a vertical surface it is common to treat the ground as a diffuse reflector and so the combined horizontal direct and diffuse insolation is treated isotropically and reflected on to the surface as a function of a view factor between the surface and the ground equal to that from the surface to the sky, thus

$$G_{rv} = 0.5 (G_{bh} + G_{fh}) \rho_g \quad \{2.17\}$$

where  $G_{rv}$  is the ground reflected global insolation incident on a vertical surface ( $Wm^{-2}$ ); and  $\rho_g$  is the ground reflectivity (albedo).

The diffuse component  $G_{sv}$  of total insolation on a vertical surface ( $Wm^{-2}$ ) can be estimated from

$$G_{sv} = 0.5 G_{fh} \quad \{2.18\}$$

which is valid if we assume totally overcast sky conditions (i.e. fully isotropic sky). For desert locations like Riyadh (Saudi Arabia), Eq.2.18 is improper since clear sky conditions are dominant. Furthermore, it has been estimated that such an assumption leads to an underestimation of inclined surface intensities (Ma & Iqbal 1983). An alternative approach is to formulate an anisotropic model which account for the enhancement of diffuse insolation in the vicinity of the sun and at the horizon.

Based on the anisotropic models of Temps & Coulson (1977) and Klucher (1979), the sky diffuse insolation on a vertical surface can be expressed as :

$$G_{sv} = 0.5 G_{fh} [1 + F \sin^3(\beta/2)] [1 + F \cos^2(\theta) \sin^3(\theta_z)] \quad \{2.19a\}$$

where  $\beta = 90^\circ$  surface slope angle, and  $F$  is a modulating function given by

$$F = 1 - (G_{fh} / G_h)^2 \quad \{2.19b\}$$

thus, when the sky is completely overcast,  $F = 0$  and Eq.2.19a reduces to the isotropic sky case (Eq.2.18).

The global insolation incident on a vertical surface,  $G_v$  ( $Wm^{-2}$ ), is then found from

$$G_v = G_{bv} + G_{rv} + G_{sv} \quad \{2.20\}$$

The net longwave radiation from an extended flat black surface at temperature =  $\bar{T}_o$  parallel to an extended sky at  $\bar{T}_{sky}$  can be obtained from (Duffie & Beckman 1980):

$$G_l = \sigma (\bar{T}_o^4 - \bar{T}_{sky}^4) \quad \{2.21\}$$

where  $\sigma$  = Stefan-Boltzmann constant,  $\bar{T}_o$  is the absolute outdoor air temperature (K). Many relations for estimating the sky temperature,  $\bar{T}_{sky}$  (K), have been considered in chapter 4 (see section 4.3.2) and the Swinbank (1963) relation, Eq.2.22, is found to be more suitable for the climate of Riyadh

$$\bar{T}_{sky} = 0.0552 \bar{T}_o^{1.5} \quad \{2.22\}$$

Walls and roofs are considered as black surfaces, and it can be assumed that  $G_l$  for walls is zero, since heat gain from the ground to the wall is approximately the same as the loss from the wall to the sky (ASHRAE 1985). Thus Eq.2.8 can be written for walls as

$$T_{ev} = T_o + (R_{so} \alpha G_v) \quad \{2.23\}$$

where  $T_{ev}$  is the sol-air temperature for a wall ( $^\circ C$ ).

On the basis of the above algorithms (Eq.2.8 through to Eq.2.23), I have written a small basic program that produced the hourly sol-air temperatures for the horizontal (roof), and for vertical surfaces at 8 compass orientations (i.e. walls facing N, NE, E, SE, S, SW, W, and NW) for Riyadh (Saudi Arabia). The data input are the hourly global horizontal insolation, direct normal insolation, and outdoor air temperature, processed for Riyadh reference climate year (see section 3.3 & 3.4 of the next chapter). Ground surface albedo in Eq.2.17 was taken as ( $\rho = 0.2$ ). The following assumptions ( $\epsilon = 0.9, \alpha = 0.6, R_{so} = 0.04 m^2 \text{ } ^\circ C W^{-1}$ ), used in Eq.2.8, and ( $\alpha = 0.4, R_{so} = 0.06 m^2 \text{ } ^\circ C W^{-1}$ ) for Eq.2.23, were appropriate for typical light to medium coloured roofs and walls under normal exposure to wind speeds in Riyadh. Results are tabulated in Appendix (C) as monthly mean hourly sol-air temperature values for each month of the reference year.

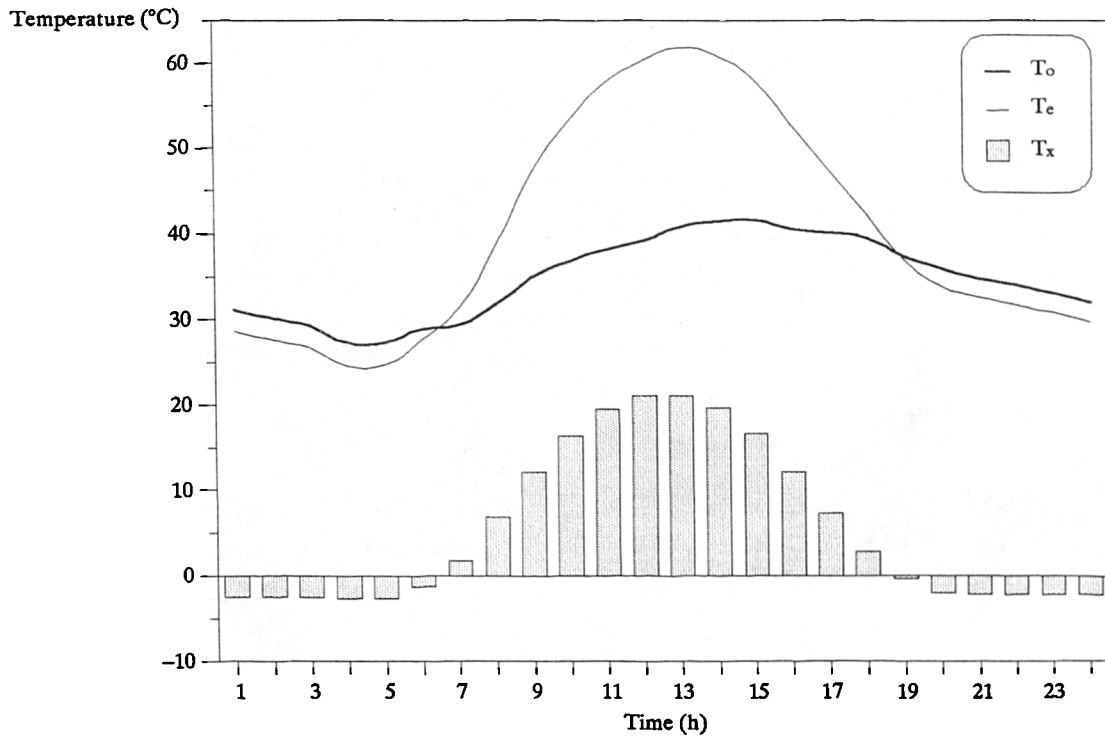


**Figure 2.6** Sol-air temperature ( $T_e$ ), at a horizontal roof in July (Riyadh climate) compared with external air temperature ( $T_o$ ). The negative values of the excess sol-air temperature  $T_x$  (which represent the second term in Eq.2.8) means longwave radiation losses to the sky dome at night.

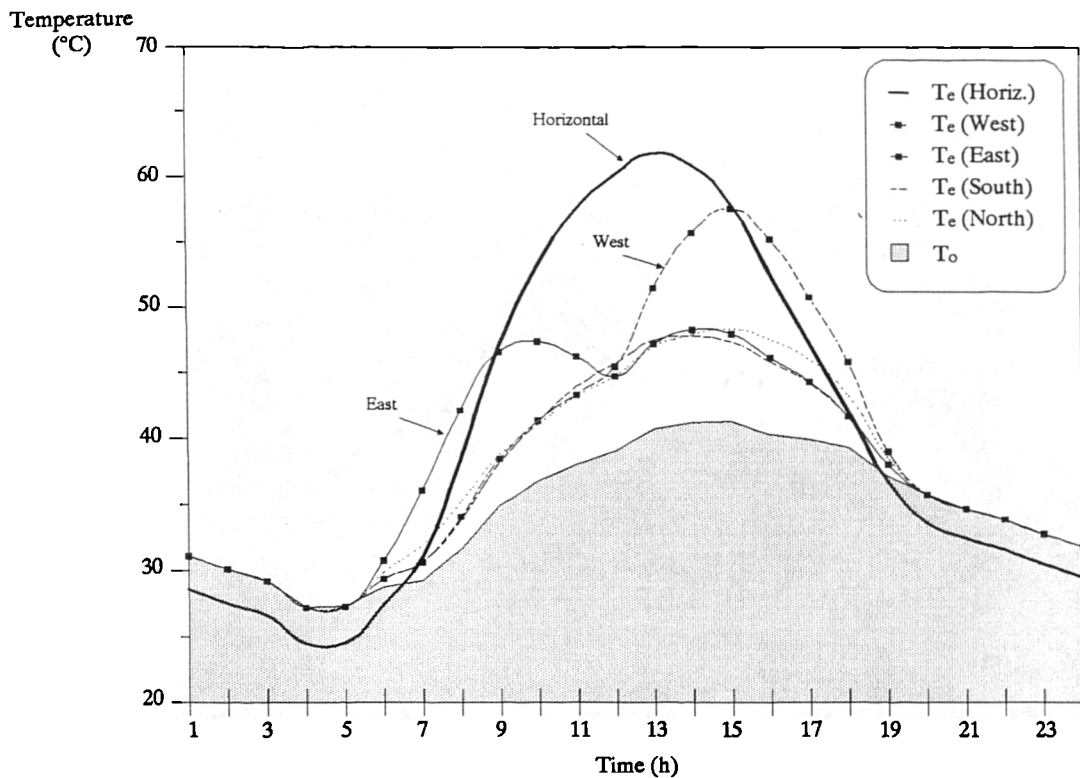


**Figure 2.7** Sol-air temperatures at horizontal roof and vertical walls (N, S, E & W orientations) in July (Riyadh climate) compared with external air temperature ( $T_o$ ).

It should be noted that the term  $[R_{so} (\alpha G - \epsilon G_i)]$  in Eq.2.8 can be negative when little or no radiation comes from the sky (see Figure 2.6). This allows for heat loss from the roof to the sky vault at night, (radiative cooling). Thus the time when the maximum value of the sol-air temperature occurs on a particular orientation (see Figure 2.7), may not be the same time as that for the maximum external air temperature. Figures (2.6 & 2.7) also indicate that roofs and west-facing walls have the highest potential for conduction heat gain through building fabric due to solar radiation in Riyadh's summer conditions.

## 2.4.2 Heat Gain Through Fenestration

Heat gain calculation through glass involves two separate steps : (1) the conduction gains (steady-state), which must be calculated on the basis of air temperature difference only (i.e. using Eq.2.1 with  $\Delta T = T_o - T_i$ ); (2) the solar gain which depends on the intensity of insolation on glazing area and the solar properties of the glass (i.e. transmission, reflection and absorption). The mechanism of heat gain through a clear glass is shown in Figure (2.8).

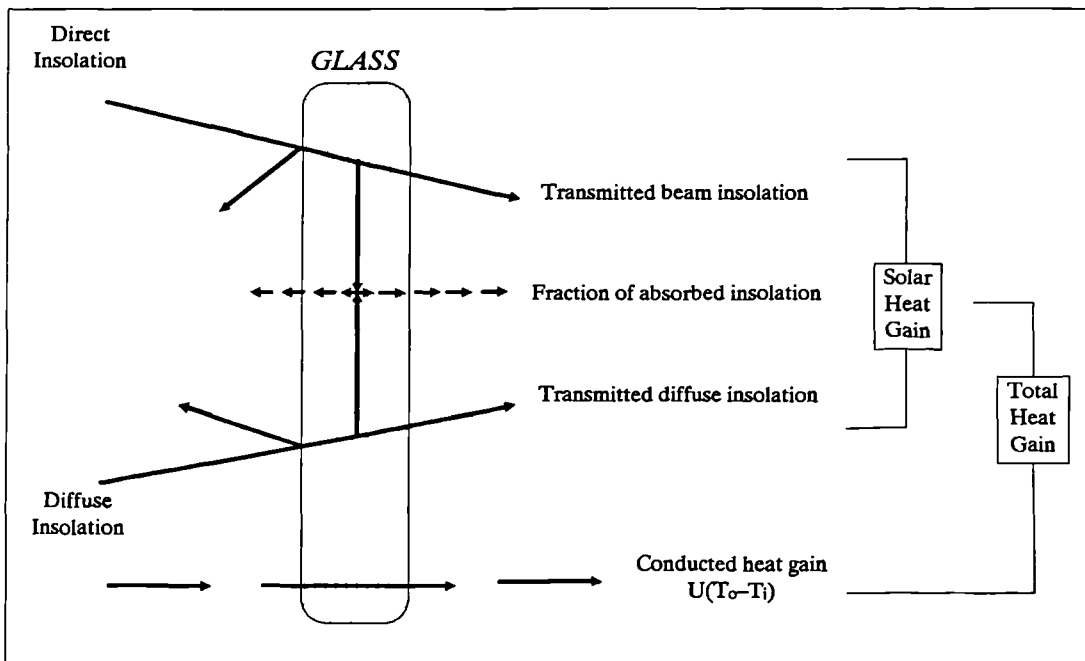


Figure 2.8 Mechanism of heat transfer through glass.

The solar heat gain through glass window includes a fraction of the absorbed energy by the glass pane that is retransmitted to interior space by convection and radiation, in addition to the solar transmittance, i.e.

$$Q_{sg} = A G_v [\tau + (N_i \cdot \alpha)] \quad \{2.24\}$$

where

$Q_{sg}$  = solar heat gain through glass (W)

$A$  = area of glass ( $m^2$ )

$G_v$  = global insolation incident on the window surface ( $W m^{-2}$ )

**Table 2.9** Solar gain factors and shading coefficients of window glazing. †

Type of glass	Solar gain factor ( $\Phi$ )							$\Phi_f$ Diffuse	S
	Solar beam angle of incidence								
	0°	20°	40°	60°	70°	80°	85°		
<b>Single</b>									
1 clear 4mm	0.84	0.84	0.84	0.77	0.64	0.41	0.22	0.78	0.96
2 clear 6mm	0.80	0.80	0.79	0.72	0.61	0.39	0.20	0.73	0.92
3 lightly heat absorbing 6mm	0.57	0.57	0.55	0.48	0.42	0.28	0.15	0.51	0.65
4 densely heat absorbing 6mm	0.43	0.43	0.40	0.36	0.32	0.23	0.13	0.38	0.49
5 lacquer-coated (gray)	0.61	0.61	0.59	0.53	0.45	0.30	0.16	0.55	0.70
6 heat reflecting (gold)	0.27	0.27	0.27	0.26	0.24	0.18	0.11	0.25	0.31
<b>Double</b>									
7 clear, 4mm + clear, 4mm	0.74	0.74	0.72	0.65	0.51	0.27	0.12	0.67	0.85
8 clear, 6mm + clear, 6mm	0.68	0.68	0.66	0.59	0.47	0.24	0.11	0.60	0.78
9 as (3) + clear, 4mm	0.45	0.45	0.42	0.36	0.29	0.16	0.08	0.38	0.51
10 as (3) + clear, 6mm	0.43	0.43	0.41	0.36	0.29	0.15	0.08	0.37	0.49
11 as (4) + clear, 6mm	0.29	0.29	0.27	0.23	0.18	0.11	0.08	0.24	0.33
12 as (6) + clear (sealed)	0.31	0.31	0.26	0.25	0.27	0.15	0.07	0.28	0.35

† Solar gain factors data from Szokolay (1980). Double glazing have a typical 12mm air space, and the first item designate outer layer. Shading coefficients (S) are calculated from dividing the normal solar transmittance of each glazing by 0.87 the normal transmittance of a 3mm clear glass.

**Table 2.10** Shading coefficients for glazing with shading devices. (after ASHRAE 1985). ‡

Type of glass	Type of shading (Internal)				
	Venetian Blinds †		Roller Shade		
	Medium	Light	Opaque		Translucent Light
			Dark	White	
<b>Single</b>					
clear glass	0.64	0.55	0.59	0.25	0.39
lightly heat absorbing	0.57	0.53	0.45	0.30	0.36
densely heat absorbing	0.54	0.52	0.40	0.28	0.32
heat reflecting (gold)	0.25	0.23			
<b>Double</b>					
clear + clear	0.57	0.51	0.60	0.25	0.37
heat absorbing + clear	0.39	0.36	0.40	0.22	0.30
heat reflecting + clear	0.27	0.26			

† shading coefficient values are for slate angle = 45°. If internal light coloured blinds are tightly closed, then S = 0.29 with single clear glass, and S = 0.25 with double clear glazing.

‡ The following information are taken from Lim et. al. (1979). An external canvas roller blind with single clear glass gives S = 0.14; a value of S = 0.25 is typical for canvas awning with single glass. In general, a completely shaded single clear glass by fixed type sun breakers have a shading coefficient S = 0.2.

- $\tau$  = glass transmittance at the angle of incidence  
 $\alpha$  = glass absorptance  
 $N_i$  = the fraction of absorbed energy that is transferred to interior space.

The value of  $N_i$  depends on the indoor and outdoor air temperatures and wind speed at either surface (see section 4.4.1 in chapter 4 for details). A value of 0.27–0.33 can be assumed (Lim et.al. 1979) although, under conditions of still air at the outside surface this value can be nearly 0.5. The term  $[\tau + (N_i \cdot \alpha)]$  in Eq.2.24 is usually published by glass manufacturers and authors as “total transmittance” or “solar gain factor”, which is dependant on the angle of incidence (e.g. see Pilkington Glass Ltd. 1988, Szokolay 1980, Lim et. al. 1979). Thus Eq.2.24 becomes

$$Q_{sg} = A G_v \Phi \quad \{2.25a\}$$

or

$$Q_{sg} = A [(G_{bv} \Phi) + (G_{fv} \Phi_f)] \quad \{2.25b\}$$

where  $\Phi$  is the solar gain factor for the angle of incident insolation which can be obtained for different types of glass from Table (2.9). If the beam ( $G_{bv}$ ) and diffuse insolation ( $G_{fv}$ ) are used, (Eq.2.25b), the angle of incidence for diffuse insolation is difficult to asses, thus the solar gain factors of diffuse insolation ( $\Phi_f$ ) in Table 2.9 may be used, assuming an incident angle of 55°.

For simplifying solar heat gain calculation and for comparing the effective solar control provided by different glazing systems and combinations of glazing and internal and external shading devices, the concept of “shading coefficient” has been introduced by American Society of Heating, Refrigeration and Air-conditioning Engineers (ASHRAE 1985). This is defined as the ratio of solar gain through a glazing system under a specific set of conditions to that of a reference glass (i.e. a 3mm clear glass with a normal incident transmissivity  $\approx 0.87$ ), under the same conditions, thus

$$S = \frac{\text{Solar heat gain flux (W m}^{-2}\text{) of fenestration}}{\text{Solar heat gain flux (W m}^{-2}\text{) of reference glass}} \quad \{2.26\}$$

From the above definition, the shading coefficient (S) is constant at all angles of incidence. Shading coefficients are provided in the last column of Table (2.9) for the glazing materials listed, and in Table (2.10) for glazing with indoor and outdoor shading devices, (more details about heat gain through curtain shaded windows are discussed in future chapters). Equation (2.26) can be written for solar heat gain through a fenestration as

$$Q_{sg} = A q_{ref} S \quad \{2.27\}$$

where A is the fenestration area ( $m^2$ );  $q_{ref}$  the maximum solar gain flux through a reference 3mm clear glass ( $W m^{-2}$ ) is provided in Appendix (D) for Riyadh as monthly mean hourly values, (see section 4.4.2 in chapter 4 for their determination).

**Table 2.11** Heat emission from human bodies (W), after Szokolay (1980). †

Degree of activity	Total ‡ W	Sensible & Latent emission (W) at temp. (°C)									
		15		20		22		24		26	
		S	L	S	L	S	L	S	L	S	L
Seated, at rest	115	100	15	90	25	80	35	75	40	65	50
Light work	140	110	30	100	40	90	50	80	60	70	70
Walking slowly	160	120	40	110	50	100	60	85	75	75	85
Light bench work	235	150	85	130	105	115	120	100	135	80	155
Medium work	265	160	105	140	125	125	140	105	160	90	175
Heavy work	440	220	220	190	250	165	275	135	305	105	335

**Notes**

† the above data are for a male body. 85% and 75% of those are reasonable estimates of the heat emission from female and children respectively. (ASHRAE 1985).

‡ values of total heat emission between 115–200 W are typical for household activities.

**Table 2.12** Typical values of heat emission from domestic appliances. (after ASHRAE 1985).

	Heat emission (kW)
<b>Gas appliances †</b>	
Stove, ring burners, per m <sup>2</sup> top surface	11.0
Range, 80*90*85 cm, top section	4.6
oven	3.6
<b>Electric appliances †</b>	
Range, 75*80*90 cm, top section	2.7
oven	1.2
Grill, 25*30 cm	1.2
Hair dryer, blower type	0.7
Typewriter	0.2

† all dimensions in cm (width, depth, height).

### 2.4.3 Estimation of Free Gains

Free gains refer collectively to internal heat gains from appliances, occupants and lighting, i.e.

$$Q_{ig} = Q_{ip} + Q_{il} + Q_{ia} \quad \{2.28\}$$

where  $Q_{ig}$  the internal free gain (W);  $Q_{ip}$  the heat gain from occupants;  $Q_{il}$  the heat gain from lighting; and  $Q_{ia}$  is the heat gain from appliances (including domestic hot water).

Free gains from occupants are usually approximated, since occupancy and occupant activities are varied and unpredictable. Some practical values of heat gain from occupants are given in Table (2.11) for different degrees of activity. Heat gain from occupants can be estimated from (Szokolay 1980)

$$Q_{ip} = n \cdot (H_{ps} + H_{pl}) \cdot u \quad \{2.29\}$$

where

- $n$  = number of people in space
- $H_{ps}$  = sensible heat emission from male body (W), female and children heat emission can be assumed as 85% and 75% respectively of that of a male body.
- $H_{pl}$  = latent heat emitted from body (W)
- $u$  = use factor = total hours of occupancy / 24h

Account for free gains from lighting fixtures (sensible heat only), can be estimated from

$$Q_{il} = \text{total supply power} \cdot u \cdot f \quad \{2.30\}$$

where ( $u$ ) the use factor = total hours of usage / 24h; ( $f$ ) is a special allowance factor = 1 for tungsten lamps, and varies from 1.18 to 1.3 for fluorescent lamps (ASHRAE 1985), which allow for the extra heat output of the control gear.

Internal heat gains from appliances are highly variable and depend on the major appliances in a house, efficiency of the individual units and usage patterns.

$$Q_{ia} = u \cdot H_e \quad \{2.31\}$$

where  $H_e$  is the heat emissions from appliances (W). Table 2.12 gives heat emission values of some appliances. The usage factor,  $u$ , may be very low for certain appliances.

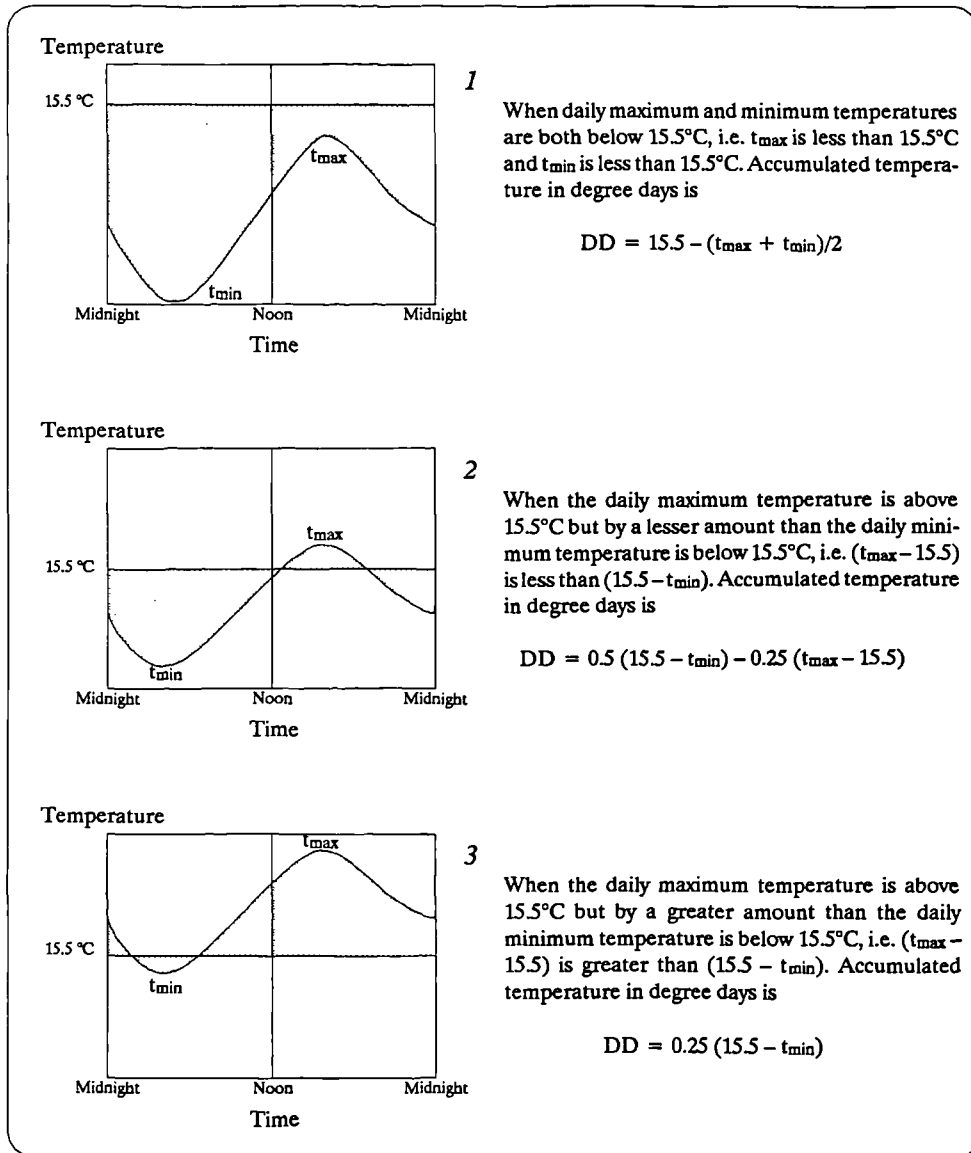


**Figure 2.9** Formulae for the calculation of degree days, 15.5°C base, as defined and used by UK Meteorological Offices. (reproduced from the Department of Energy, UK).

## 2.5 Annual Heating and Cooling Requirements

It is often necessary to estimate energy requirements and fuel consumption of HVAC systems for short or long term operation. Calculation methods vary in complexity. The sophistication of the calculation procedure can be inferred from the number of separate ambient conditions and/or time increments used in the calculation. Thus, a simple procedure may use only one measure, such as annual degree days, and will be appropriate only for simple systems and application. Accuracy can be improved by using more information, such as the number of hours anticipated under particular operating conditions. The most elaborate methods perform energy balance calculations hourly over a given analysis period, typically one year.

The methods discussed in this section are based on the “degree day” concept. They can be useful for the preparation of energy budget, but can also be used at the sketch design stage to compare the thermal performance of design alternatives (in a crude but quick way).

### 2.5.1 Degree Days

The number of degree days is a climatic indicator commonly used in calculations of heating requirement. This has been defined as the daily difference between an assumed base temperature ( $T_b$ ) and the 24-hours mean outside temperature ( $T_o$ ). This number can then be summed for any given period, e.g. a month or a year, or multiplied by 24 to give the degree hour number. The base temperature “generally accepted” in the UK publications is 15.5°C (Department of Energy UK.), although the IHVE guide (1970) suggests the use of a variable base for different building types. In the USA, the “well established base temperature for degree days” is 18.3°C (ASHRAE 1985), but degree days to selected bases are also published.

If the calculation of degree days is based on daily mean temperatures, then the difference ( $T_b - T_o$ ) can lead to serious errors. For example, the daily outside air temperature may vary between 23°C and 13°C, giving a mean of 18°C. For  $T_b = 18^\circ\text{C}$ , the degree day number will be taken as zero, whereas for about half of the day the temperature is below 18°C. If the calculation is based on monthly mean temperatures, the result will be grossly in error. Various authors developed different procedures to overcome this problem, one of which is provided in Figure (2.9).

An accurate procedure to calculate the degree days is by accumulating degree hours from weather tapes and averaging for each day as expressed by Eq.2.32 for heating degree days ( $DD_H$ ), and by Eq.2.33 for cooling degree days ( $DD_C$ ) :

$$DD_H = (24\text{h})^{-1} \cdot \sum_{j=1}^{24} (T_b - T_{oj}) \quad \text{if } T_{oj} < T_b \quad \{2.32\}$$

**Table 2.13** Monthly total heating degree days † (°C day) for the stated base temperatures. (Riyadh, Saudi Arabia).

Month	Heating DD								
	Base Temperature (°C)								
	10	12	14	16	18	20	22	24	26
Jan	21	44	76	117	167	222	281	342	404
Feb	6	15	32	57	91	132	181	234	289
Mar	0	2	6	16	34	61	98	143	194
Apr	0	0	0	0	3	12	30	59	95
May	0	0	0	0	0	1	2	9	22
Jun	0	0	0	0	0	0	0	1	5
Jul	0	0	0	0	0	0	0	0	0
Aug	0	0	0	0	0	0	0	0	2
Sep	0	0	0	0	0	0	1	5	14
Oct	0	0	0	2	6	13	27	47	75
Nov	0	1	3	10	28	55	92	137	190
Dec	15	36	68	111	163	219	279	340	402
Annual	42	98	185	313	491	716	991	1315	1692

† calculated by the author from Equation 2.32 using the hourly temperature data of Riyadh's climate reference year, (defined in chapter 3).

**Table 2.14** Monthly total cooling degree days † (°C day) for the stated base temperatures. (Riyadh, Saudi Arabia).

Month	Cooling DD								
	Base Temperature (°C)								
	10	12	14	16	18	20	22	24	26
Jan	113	74	44	23	11	4	1	0	0
Feb	165	119	79	48	26	12	4	1	0
Mar	309	249	191	139	95	60	35	17	7
Apr	412	352	292	232	174	124	83	50	27
May	615	553	491	429	367	305	246	190	141
Jun	663	603	544	484	424	364	304	244	188
Jul	766	704	642	580	518	456	394	333	271
Aug	722	660	598	536	474	412	350	289	229
Sep	627	567	507	447	387	328	268	212	161
Oct	491	429	367	307	249	195	146	104	70
Nov	294	234	176	124	81	48	25	10	3
Dec	110	68	38	19	9	3	1	0	0
Annual	5287	4613	3970	3369	2815	2310	1856	1450	1097

† calculated by the author from Equation 2.33 using the hourly temperature data of Riyadh's climate reference year.

$$DD_C = (24h)^{-1} \cdot \sum_{j=1}^{24} (T_{oj} - T_b) \quad \text{if } T_{oj} > T_b \quad \{2.33\}$$

where  $T_{oj}$  is the outside air temperature ( $^{\circ}\text{C}$ ) at  $j$  hours.

The above procedure is used to calculate the heating and cooling degree days, at base temperatures of 10 to 26 in  $2^{\circ}\text{C}$  intervals, for Riyadh (Saudi Arabia). The hourly temperature values used in the calculation are those compiled in section 3.3 of the next chapter. Results are presented in Tables (2.13 & 2.14) for heating and cooling degree days respectively.

## 2.5.2 Degree Day Method

The general equation of estimating the energy requirement for heating or cooling a building is :

$$E = UA \cdot DD \cdot 24h \quad \{2.34\}$$

where  $E$  is the energy required for the estimate period (Wh);  $UA$  is the building specific heat rate ( $\text{W }^{\circ}\text{C}^{-1}$ ), which includes  $UA_c$  values of the building components and  $UA_v$  of infiltration (see the examples bellow); and  $DD$  is the number of heating or cooling degree days for the estimate period.

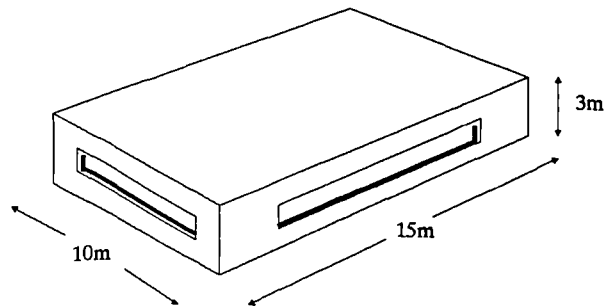
**Example 2 :** Consider the simple structure shown in Figure 2.10 (ignoring internal walls), 15•10m on plan and 3m high, with 20% windows of each wall surface. Calculate the annual heating and cooling energy requirement for this building in Riyadh.

**Solution :** For heating  $DD$  the base temperature is taken as  $18^{\circ}\text{C}$ , and  $21^{\circ}\text{C}$  for cooling  $DD$ , according to ASHRAE recommendation which allow for  $3^{\circ}\text{C}$  lift for solar and internal free gains. Thus from Tables 2.13 & 2.14, the annual heating degree days ( $DD_H = 491$ ) and the annual cooling degree days ( $DD_C = 2083$ ). The building  $UA$  value is :

	$\text{m}^2$	•	$\text{W m}^{-2}\text{ }^{\circ}\text{C}^{-1}$	=	$\text{W }^{\circ}\text{C}^{-1}$	
$UA_{\text{walls}}$	= 120	•	1.67	=	200	
$UA_{\text{windows}}$	= 30	•	5.6	=	168	
$UA_{\text{roof}}$	= 150	•	2.2	=	330	
$UA_{\text{floor}}$	= 150	•	0.56	=	84	
					<hr style="width: 50%; margin: 0 auto;"/>	
Total $UA_c$					$782 \text{ W }^{\circ}\text{C}^{-1}$	
For infiltration, assume an air change rate = $2 \text{ h}^{-1}$						
$UA_v$	= $450 \text{ m}^3 \cdot 0.33 \text{ Wh m}^{-3}\text{ }^{\circ}\text{C}^{-1} \cdot 2 \text{ h}^{-1}$					$= 297 \text{ W }^{\circ}\text{C}^{-1}$
					<hr style="width: 50%; margin: 0 auto;"/>	
Total building $UA$ value					$1079 \text{ W }^{\circ}\text{C}^{-1}$	

**Figure 2.10**

Diagram of the simple structure used in examples 2, 3 and 4. Case 1: defines an uninsulated building with single glazing fenestration, and Case 2: represents insulated construction with double glazed fenestration. A breakdown of the assumed 700W free gains is listed.



Component	Area (m <sup>2</sup> )	U-value W/(m <sup>2</sup> °C)	
		Case#1	Case#2
Wall: N or S	36	1.67	0.55
Wall: E or W	24	1.67	0.55
Roof	150	2.2	0.59
Floor	150	0.56	0.56
Window: N or S	9	5.6	3.0
Window: E or W	6	5.6	3.0

Free Gains	(Wh/day)
Occupants, 14 to 15 hours occupation. (two adults & two children, 65Wh/day per person)	260
Refrigerator (3.6kW), continuous 24h operation.	150
T.V. (80W), 8 hours operation per day.	25
Lighting (200W), 7 to 8 hours oper- ation per day.	60
Range (4kW), 1 hour use per day.	170
Miscellaneous.	35
<b>Total free gains</b>	<b>700</b>

substituting in Eq.2.34 and dividing by 1000, the annual heating energy requirement is

$$E_H = 1079 \cdot 491 \cdot 24 / 1000 = 12\,715 \text{ kWh}$$

and the annual cooling energy requirement is

$$E_C = 1079 \cdot 2083 \cdot 24 / 1000 = 53\,941 \text{ kWh}$$

Note that in this method solar and internal free gains are not considered, hence the base temperature chosen allow for about 3°C lift for these gains as standard. Therefore, the indoor temperature for the heating season will be 21°C and 24°C for the cooling season, which falls within the comfort limits for the climate of Riyadh. (see the comfort limits table in section 2.2.1). Based on the above assumptions and considering continuous plant operation, this method will give valid estimates (at least for a comparison of alternatives at the sketch design stage, as demonstrated by the next example).

**Example 3 :** Calculate the heating and cooling energy requirements of the construction in example 2 if walls have  $U = 0.55 \text{ W m}^{-2} \text{ }^\circ\text{C}^{-1}$  and  $U = 0.59 \text{ W m}^{-2} \text{ }^\circ\text{C}^{-1}$  for the roof, and the windows are fitted with double glazing ( $U = 3 \text{ W m}^{-2} \text{ }^\circ\text{C}^{-1}$ ).

**Solution :** The building specific heat flow rate is calculated as in example 2 and gives  $UA = 608 \text{ W }^\circ\text{C}^{-1}$  which is about 56% of the specific heat flow rate in example 2. Thus

$$E_H = 7\,165 \text{ kWh,}$$

$$E_C = 30\,395 \text{ kWh.}$$

which yield a 44% saving of cooling and heating consumptions due to the use of insulation and double glazing.

### 2.5.3 Variable Degree Day Method

The variable degree day method is a generalisation of the widely used degree day method. It retains the same concept, but counts degree days based on the “balance point temperature”, defined as the average outdoor temperature at which the building requires neither heating nor cooling (ASHRAE 1985). The steady-state heating and cooling requirements of a building can be expressed as

$$Q_H = UA (T_i - T_o) - Q_g \quad \{2.35\}$$

$$Q_C = UA (T_o - T_i) + Q_g \quad \{2.36\}$$

where  $Q_H$  and  $Q_C$  are the building heating and cooling requirements respectively (W); and  $Q_g =$  all space heat gains (W) that do not depend on indoor–outdoor temperature difference, i.e. internal free gains from occupants and appliances ( $Q_{\text{internal}}$ ); and solar gains

**Table 2.15** Monthly means of daily average solar heat gain through a 3mm clear glass †. (Riyadh, Saudi Arabia).

Month	Solar heat gain ( $\text{Wm}^{-2}$ )								
	Window orientation								Skylight Horiz.
	N	NW	W	SW	S	SE	E	NE	
Jan	60	60	92	130	138	100	71	61	134
Feb	57	68	118	150	147	116	90	64	171
Mar	61	81	123	134	115	113	102	73	195
Apr	67	93	118	110	82	102	108	86	199
May	94	127	145	122	91	122	142	124	253
Jun	89	133	149	112	77	112	143	126	275
Jul	92	137	155	121	85	116	140	122	269
Aug	84	126	157	136	94	125	137	111	254
Sep	63	94	141	145	116	136	130	88	234
Oct	57	70	116	145	153	143	114	70	192
Nov	50	53	91	134	158	127	87	54	146
Dec	45	46	81	121	134	96	63	46	115

† The values represent the 24h average of solar heat gain for each month. (Calculated by the author, see section 4.4.2 in chapter 4). For a common 4mm glass window, multiply the numbers by its shading coefficient (0.96). If external shading is used i.e. completely shaded window, then multiply by 0.2; or if internally shaded use the proper shading coefficient from table 2.10

**Table 2.16** Monthly means of daily average sol-air excess temperature † ( $^{\circ}\text{C}$ ) at external roof and walls surfaces in Riyadh, Saudi Arabia.

Month	Sol-air excess temp. ( $^{\circ}\text{C}$ )								
	Wall orientation								Flat roof Horiz.
	N	NW	W	SW	S	SE	E	NE	
Jan	1.5	1.6	2.4	3.3	3.5	2.7	1.9	1.5	0.6
Feb	1.5	2.0	3.1	4.0	4.0	3.1	2.4	1.7	1.8
Mar	1.7	2.4	3.3	3.7	3.4	3.1	2.7	2.0	2.6
Apr	1.9	2.6	3.1	3.0	2.5	2.8	2.9	2.4	2.8
May	2.7	3.5	3.9	3.4	2.6	3.4	3.8	3.4	4.7
Jun	2.7	3.6	4.0	3.2	2.1	3.1	3.8	3.4	5.5
Jul	2.7	3.7	4.2	3.4	2.4	3.2	3.7	3.4	5.5
Aug	2.4	3.5	4.1	3.7	2.8	3.4	3.6	3.0	5.0
Sep	1.7	2.6	3.7	3.9	3.5	3.7	3.4	2.4	4.2
Oct	1.5	1.9	3.0	3.8	4.1	3.7	2.9	1.8	2.7
Nov	1.3	1.4	2.4	3.5	4.1	3.3	2.2	1.4	1.2
Dec	1.2	1.3	2.2	3.2	3.5	2.6	1.7	1.2	0.2

† Sol-air excess temperature values are averaged from hourly calculations using the climatic data of Riyadh's reference year. (see 2.5.3 for more information).

transmitted through fenestration ( $Q_{solar}$ ), and conducted heat gains through external roof and walls due to sol-air temperature ( $Q_{sol-air}$ ),

$$Q_g = Q_{internal} + Q_{solar} + Q_{sol-air} \quad \{2.37\}$$

The solar gain through a window can be calculated from Eq.2.27, thus the total solar gain,  $Q_{solar}$  (W), through the building fenestration is

$$Q_{solar} = \sum_{i=1}^n (A_i q_i S) \quad \{2.38\}$$

where e.g.  $n = 5$  if fenestration exist on all building surfaces;  $A_i$  is the glazing area of surface  $i$ , ( $m^2$ );  $S$  is the shading coefficient of the glazing; and  $q_i$  ( $W m^{-2}$ ) is the total solar gain through a 3mm reference glass. Table 2.15 gives  $q_i$  as mean monthly values of the 24h daily averages calculated for Riyadh. (see Appendix from mean monthly hourly data).

The solar effect on the exterior of the building (roof and walls) can be treated as described in section 2.4.1, through the use of sol-air temperature, but only considering the “excess sol-air temperature” ( $T_x$ ) for each surface (i.e. the second term of Eq.2.7), hence DD calculation will consider the outdoor air temperature ( $T_o$ ). So, the excess sol-air temperature for a surface is

$$T_x = T_e - T_o \quad \{2.39\}$$

and the total conduction gain through a building fabric due to excess sol-air temperature  $Q_{sol-air}$  is :

$$Q_{sol-air} = \sum_{i=1}^n (A_i U_i T_{xi}) \quad \{2.40\}$$

where  $n = 5$  if all surfaces are sunlit, (i.e. not shaded by obstructing objects). Table 2.16 gives  $T_x$  for sunlit surfaces at different orientations for Riyadh climate, as mean monthly values of the 24h daily averages, calculated by the author.

The balance point temperature ( $T_b$ ) is determined by setting  $Q_H$  &  $Q_C = 0$  and solving Eq.2.35 & Eq.2.36 for  $T_b = T_o$  so

$$T_b = T_i - (Q_g / UA) \quad \{2.41\}$$

Once the balance temperature is determined, the energy requirement for heating or cooling can be calculated from:

$$E = 24h \cdot UA \cdot DD_{T_b} \quad \{2.42\}$$

where  $DD_{T_b}$  is the degree days calculated to the base temperature  $T_b$ .

There is some flexibility inherent in the variable degree day base concept since (E) can be calculated for periods as short as a week and as long as a season. If for example, the energy is calculated for a period less than a season, ( $E_i$ ), then the total seasonal requirement E becomes

$$E = \sum_{i=1}^m E_i \quad \{2.43\}$$

where e.g.  $m = 12$  if  $E_i$  is calculated on monthly bases.

**Example 4 :** Use the variable degree day method on monthly bases to solve the cases of examples 2 & 3 for the following conditions of solar control in each of the two cases; (A) unshaded windows; (B) windows with internal venetian blind (light colour); and (C) windows with external sun breakers. For this example, use the estimated 24h average free gains of 700W (listed in Fig.2.10); a heating setpoint temperature of 21°C and a cooling setpoint temperature of 24°C.

**Solution :** The shading coefficients of the fenestration types are first obtained from Tables 2.9 & 2.10. Thus, for the first case: (1A)  $S = 0.96$ ; (1B)  $S = 0.55$ ; (1C)  $S = 0.2$ , and for the second case: (2A)  $S = 0.85$ ; (2B)  $S = 0.51$ ; and (2C)  $S = 0.17$ . Solving for case 1A for the month of January : from Eq.2.38 and Eq.2.40, the solar gain ( $Q_{solar}$ ) and the sol-air gain ( $Q_{sol-air}$ ) are

$$Q_{solar} = S (A_{g1} q_1 + A_{g2} q_2 + A_{g3} q_3 + A_{g4} q_4) = 2563 \text{ W}$$

$$Q_{sol-air} = U_w (A_{w1} T_{x1} + A_{w2} T_{x2} + A_{w3} T_{x3} + A_{w4} T_{x4}) + (U_r A_r T_{xr}) = 671 \text{ W}$$

where the subscripts 1 to 4 & r represent surface orientations (N, E, W, S) and roof respectively; q is the reference solar heat gain (obtained from Table 2.15 for each surface orientation); the sol-air excess temperatures ( $T_x$ ) are obtained from Table 2.16.

From Eq.2.37 & Eq.2.41, the heating or cooling balance point temperature is

$$T_{b(\text{heating})} = T_{i(\text{heating})} - [(Q_{\text{internal}} + Q_{\text{solar}} + Q_{\text{sol-air}}) / UA] = 17.4^\circ\text{C}$$

$$T_{b(\text{cooling})} = T_{i(\text{cooling})} - [(Q_{\text{internal}} + Q_{\text{solar}} + Q_{\text{sol-air}}) / UA] = 20.4^\circ\text{C}$$

where  $T_{i(\text{heating})}$  is the heating setpoint temperature = 21°C and  $T_{i(\text{cooling})} = 24^\circ\text{C}$ ; UA is the specific heat flow rate = 1079 W/°C (as determined in example 2); and  $Q_{\text{internal}} = 700\text{W}$ . The heating and cooling degree days are then obtained from Tables 2.13 & 2.14 on the bases of the balance point temperatures determined above. Thus by interpolation  $DD_H = 142$  and  $DD_C = 3^\circ\text{C day}$ .

Finally, applying in Eq.2.42, the heating and cooling energy requirements ( $E_H$  &  $E_C$  respectively) for case 1A for January are

$$E_H = 24 \cdot 1079 \cdot 142 / 1000 = 3677 \text{ kWh}$$

$$E_C = 24 \cdot 1079 \cdot 3 / 1000 = 78 \text{ kWh}$$

**Figure 2.11**

Monthly energy heating and cooling requirements (MWh) for CASE #1 in Example 4.

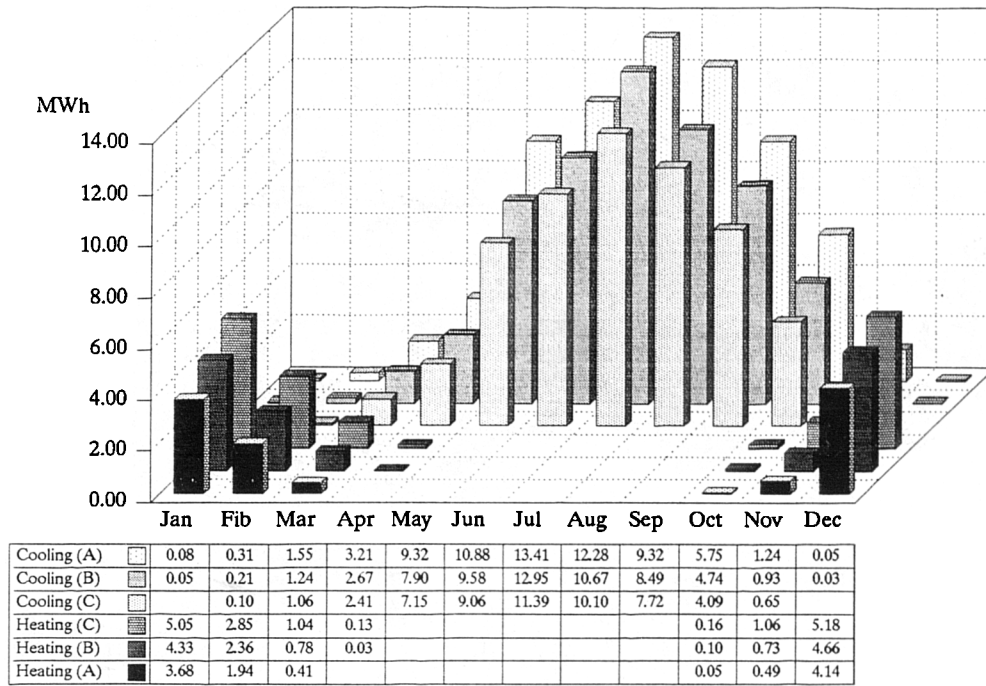
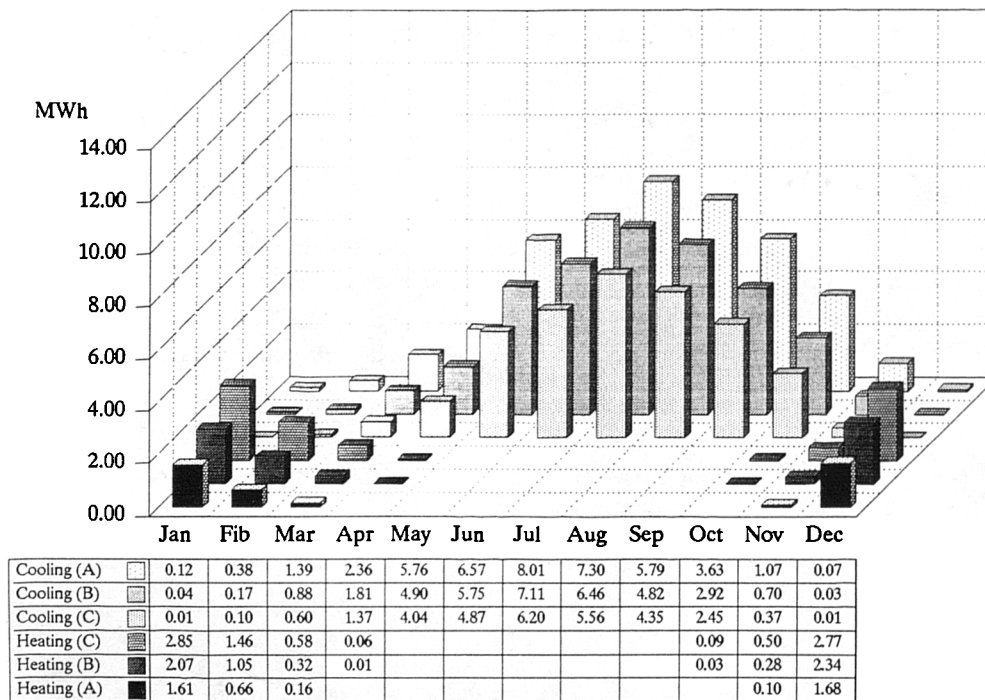


**Figure 2.12**

Monthly energy heating and cooling requirements (MWh) for CASE #2 in Example 4. (A) no shading, (B) internal shading and (C) external shading.



The above procedure is then repeated for each month, and each type of fenestration. Monthly energy heating and cooling requirements for case 1 and case 2 are shown in Figures 2.11 & 2.12 respectively. Annual heating and cooling requirements for both cases are shown in Figure 2.13.

The following conclusions can be drawn from the results:

- Compared to the building in case 1, the use of insulation and double glazing (i.e. case 2) can reduce the total annual heating and cooling energy requirements by 40% (no shading), 42% with internal shading and 45% with external shading. The reductions in cooling and heating requirements are shown individually as negative percentages in Figure (2.13).
- About 85% of the energy required for human comfort in the buildings of cases 1 & 2 is for cooling. Thus, from the two shading devices examined in this example, the external sunbreakers had the greatest impact on reducing the annual cooling requirement. (i.e. 20% and 29% reduction in cooling requirements by externally shading the windows in cases 1 & 2 respectively, compared with 12% and 16% reduction by the use of internal venetian blind).

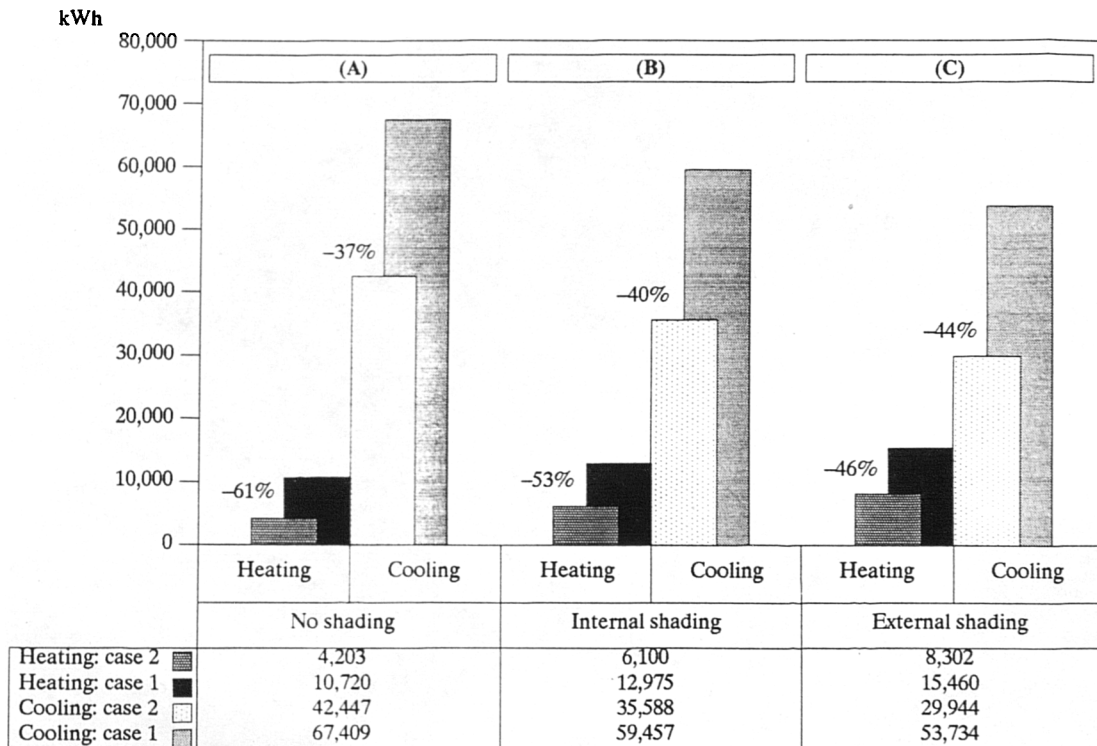


**Figure 2.13**

Annual heating and cooling energy requirements (kWh) calculated by the Variable Degree Day method (VDD) in example 4. The differences in annual heating/cooling energy requirements between the two cases are shown as negative percentages.

- Results from cases 1A & 2A in this example indicated higher cooling requirements and lower heating requirements than those calculated by the degree day method in examples 2 & 3. (see Figure 2.14). This is because the DD method uses standard base temperatures of 18°C for heating and 21°C for cooling, assuming 3°C to compensate for the solar and internal free heat gains, while the variable degree day method (VDD) calculates the base temperatures taking into account the actual gains.

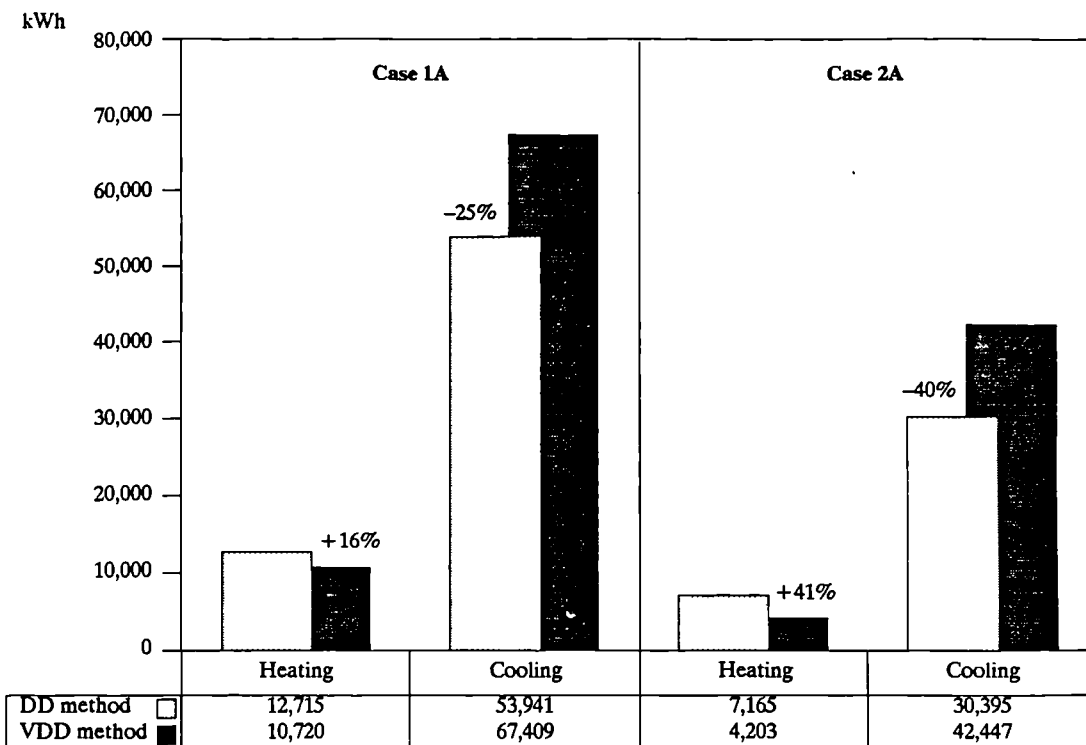


**Figure 2.14**

Comparison between the annual heating and cooling energy requirements (kWh) calculated by the Variable Degree Day method (VDD) in example 4 and by the Degree Day method in examples 2 & 3. The DD method underestimated cooling requirements by the negative percentages shown on the graph, and overestimated the heating requirements as shown by the positive percentages.

## 2.6 Conclusion

---

The data presented and the methods described in this chapter give a powerful tool to the architect for the production of better designs of energy efficient buildings. The systematic procedure of the “Mahoney Tables”, provides basic principles for adapting the design of a building to the human requirements and climatic conditions.

Design alternatives can be tested for annual energy requirements in a crude and simple way by either the degree day or the variable degree day methods. Thus the VDD method proved to be more flexible, i.e. shorter periods of estimation is possible with reasonable accuracy; effects of internal free gains can be investigated; it is also possible to evaluate the thermal performance of different solar control techniques.

The U-value technique based on the steady-state model is the simplest way of estimating the thermal performance of building components or the building as a whole. However, the sol-air model is more suitable to a climate such as Riyadh's, where the insolation gains are significant. Both models can be used with daily average or with hourly climatic data of, for example, a summer day and a winter day to determine the cooling and heating loads of a building. Results obtained with hourly calculations would be approximately valid for a building of negligible mass. For constructions with large thermal capacity (i.e. heavy mass), the best solution is to use a transient heat flow model. A comprehensive survey of various mathematical solutions to this problem is given by Givoni (1976).

The mathematical methods presented in this chapter can be performed by manual methods (but not expected to be so very often). At the other end of the scale, there are highly sophisticated computer programs available for the simulation of thermal performance of buildings, tracing the heat flow through its various paths from the inside to the outside or vice versa. These could well be used in the final design stages of a building. They can give either daily temperature profiles for unconditioned buildings or predict the long term (e.g. annual) heating or cooling requirement, thus the expected energy consumption of the building.

Calculations are often carried out for the whole year on an hourly basis. This requires hourly data of several climatic parameters for the whole year, which can only be handled in digital form and stored on “weather tapes”. Chapter 3 is aimed at defining a reference climate year, representative for Riyadh, for use in the Environmental Systems Performance (ESP) model. The reader may refer Appendix (G) and to Clarke (1985) for a description of the model ESP. This model is used in future chapters of this thesis.

## 2.7 References

---

ASHRAE (1985) ASHRAE Handbook (Fundamentals). American Society of Heating, Refrigerating and Air-conditioning Engineers Inc. Atlanta, U.S.A.

Barry R. & Chorley R. (1976) Atmosphere, Weather and Climate. Methuen & Co Ltd., London.

Bowen A. (1983) "Bioclimatic Comfort Analysis for 8 Cities in Saudi Arabia", Technical and lecture notes, School of Environmental Design (SED), King Abdul-Aziz University, Jeddah, Saudi Arabia.

Burberry P. (1983) Environment and Services. Batsford, London.

CIB (1982) "Prediction of the Thermal Performance and Energy Use in Buildings", *proc. of CIB W67, 3rd Int. Sym.*, "Energy conservation in the built environment", Vol. 2, Dublin.

CIBS (1976) "Air Infiltration", Section A4, Chartered Institute of Building Services, London.

CIBS (1980) "Thermal Properties of Building Structures", Section A3, Chartered Institute of Building Services, London.

Clarke J. (1985) Energy Simulation in Building Design. Adam Hilger Ltd., Bristol, UK.

Cooper P. (1969) "The Absorption of Solar Radiation in Solar Stills", *Solar Energy*, 12 (3).

Department of Energy (undated) Degree Days. Booklet (7), Department of Energy, Energy Efficiency Office, London.

Dickinson W. & Cheremisinoff P. (1980) Solar Energy Technology Handbook. Part (A), Engineering Fundamentals. Marcel Dekker Inc., New York.

Duffie J. & Beckman W. (1980) Solar Engineering of Thermal Processes. Wiley & Sons Inc., New York.

Evans M. (1980) Housing, Climate and Comfort. The Architectural Press, London.

ESP (1987) Environmental System Performance, A thermal simulation program developed by ABACUS, Univ. of Strathclyde. The program is continuously updated. (data obtained from the program data base).

Givoni B. (1976) Man, Climate and Architecture. Applied Science Publishers Ltd., London.

Grimsrud D., Sherman M. & Sonderegger R. (1982) "Calculating Infiltration : Implications for a construction quality standard." *Proc. of the ASHRAE-DOE Conf.* "The Thermal Performance of the Exterior Envelope of Buildings II.", Las Vegas, December 1982, p 422.

Grot R. & Clark R. (1979) "Air Leakage Characteristics and Weatherisation Techniques for Low-income Housing", *Proc. of the ASHRAE-DOE Conf. "The Thermal Performance of the Exterior Envelope of Buildings."*, Orlando, FL., December 1979, p 178.

IHVE Guide (1970) Institute of Heating and Ventilating Engineers. (now CIBSE), Section B.18, London.

Iqbal M. (1983) An Introduction to Solar Radiation. Academic Press, Canada.

Joudah N. (1985) "Energy Conserving Architectural Design—indicators for the Hijaz Region in Saudi Arabia", MArch thesis, Architecture & Energy Dept., University of Colorado at Denver, Colorado, U.S.A.

Joudah N., Salloum A., Al-Faisal A., Abo-Bakur H., & Benaghmouch B. (1983) "Housing For Under-Privileged Muslims". BArch Terminal project, S.E.D., Eng. Dept., K.A.A.Univ., Jeddah, Saudi Arabia. Also the project was awarded the prize of the Royal Institute of Architects of Ireland, for the 7th International Competition for Students of Architecture; Union Internationale des Architectes (UIA), rue Raynouuad, 75016 Paris, 1984.

Klucher T. (1979) "Evaluation of models to predict insolation on tilted surfaces", *Solar Energy*, 23 (2), pp 111-14.

Koenigsberger O., Mahoney C. & Evans M. (1971) Climate and House Design. United Nations, Department of Economic & Social Affairs, New York.

Koenigsberger O. & Szokolay S. (1973) Manual of Tropical Housing. Longman, London.

Lim B., Rao K., Tharmaratnam K. & Mattar A. (1979) Environmental Factors in the Design of Building Fenestration. Applied Science Publishers Ltd., London.

Littler J. (1982) "Overview of Some Available Models for Passive Solar Design", *Computer Aided Design*, 14, p 15.

Littler J. & Thomas R. (1984) Design With Energy : The conservation and use of energy in buildings. Cambridge University Press, U.K.

Ma C. & Iqbal M. (1983) "Statistical comparison of models for estimating solar radiation on inclined surfaces", *Solar Energy*, 31 (2), pp 313-17.

Markus T. & Morris E. (1980) Building, Climate and Energy. Pitman Publishing Ltd., London.

Olgay V. (1963) Design With Climate. Princeton University Press, Princeton, U.S.A.

Oliver J. (1973) Climate and Man's Environment : An introduction to applied climatology. John Wiley & Sons Inc., New York.

Oliver J. (1981) Climatology: Selected Applications. Edward Arnold Publishers, London.

Pilkington (1988) "Glass and Transmission Properties of Windows.", 7th Edition, Environmental Advisory Service, Pilkington Glass Ltd., England.

Swinbank W. (1963) "Longwave Radiation From Clear Skies", *Quart. J. Royal Meteorol. Soc.*, 89, pp 339-48.

Szokolay S. (1980) Environmental Science Handbook. The Construction Press, London.

Temps R. & Coulson K. (1977) "Solar Radiation Incident on Slopes of Different Orientations", *Solar Energy*, 19 (2), pp 179-84.

Warner P. (1976) "Natural Infiltration Rates and Their Magnitude In Houses : part 1- Preliminary Studies of Domestic Ventilation", Building Research Establishment, Garston, Watford, Herts.

# Chapter 3



### **3. DEVELOPMENT OF A CLIMATE REFERENCE YEAR FOR RIYADH (SAUDI ARABIA)**

#### **3.1 Introduction**

---

Accurate and long term climate data for Saudi Arabia is difficult to obtain. In published information about the Arabian peninsula, Schyfsma (1978) stated that "The number and distribution of weather observation stations in the area and the compiled data over the last years are far from adequate for the accurate analysis of regional climate data". Furthermore, Bowen (1983) expressed the difficulty of obtaining accurate and adequate data by stating "It is not centralised, and is uneven and unreliable". Therefore it has been necessary to consider creating a Climate Reference Year of data from little previous knowledge.

Fortunately the government of Saudi Arabia became interested in solar energy research through the Solar Village Program that made it possible for me to obtain three years (1984-86) of hourly values of reliable climatic information to accomplish this study.

For the earliest stage of building design all that is wanted is a qualitative appreciation of climate. This is best facilitated by graphic representation. The mean monthly and daily average data are sufficient for this stage and for assessing a sketch design in terms of long period (i.e. monthly, seasonal or annual) heating or cooling requirement as discussed in the previous chapter. Mean monthly meteorological information for the last decade can be obtained from published weather reports by the Department of Ministry of Defense and Aviation in Jeddah, and the Ministry of Agriculture and Water in Riyadh.

The simulation of the thermal characteristics of a full scale building design requires sophisticated computer models. For these models hourly values of climatic parameters are needed from a full reference year. Table (3.1) summarises the main climatic variables required for energy simulation modelling. The Climate Reference Year (CRY), also known as Test Reference Year (TRY), is a set of 8760 hours of weather data that may be used as representative in dynamic modelling. Paassen & Liem (1982) define the reference year as a 10 years, or more, average of climatic variables in order to include a reasonable range of climatic variations.

A number of countries have reference year data ready for commercial or research use, although the procedures used to establish them will vary by country (Clarke 1985). For example, in the USA (Stamper 1977) the procedure is to eliminate those years, in a period of record, containing months with extremely high or low mean temperatures until only one year, the TRY, remains. This is achieved by marking those months within the period which can be described, in terms of mean monthly temperature, as shown in Table (3.2). The procedure then continues by marking those months which can be described as the next-to-

**Table 3.1** Climatic data requirements of energy models. †

---

Dry bulb temperature  
 Wet bulb temperature  
 Dewpoint temperature  
 Ground surface temperature  
 Global (or direct) solar radiation  
 Diffuse solar radiation  
 Wind speed  
 Wind direction  
 Atmospheric pressure  
 Longwave radiation balance  
 Precipitation  
 Sunshine hours  
 Cloud cover and type

---

† Many weather observation centres collect these (and other) data at frequencies of one hour or greater. The type and number of climatic data varies with the requirements of different energy simulation models and some of the above list may be optional. (see section 3.3 for the ESP program requirements).

**Table 3.2** US "Test Reference Year" selection method. (after Clarke 1985).

---

hottest	July
coldest	January
hottest	August
coldest	February
hottest	June
coldest	December
hottest	September
coldest	March
warmest	May
coolest	November
warmest	October
coolest	April
coolest	July
mildest	January
coolest	August
mildest	February
coolest	June
mildest	December
coolest	September
mildest	March
coolest	May
warmest	November
coolest	October
warmest	April

---

hottest July, the next-to-coldest January and so on until one year remains without any marked months. The resulting reference year is considered useful for comparative studies, but not for the long term energy consumption.

In Japan, an alternative selection procedure is used (Saito & Matsuo 1974) based, not on the climatic variables, but on the cooling and heating loads calculated from the application of each climate year to a standardised design problem. These loads are computed hour-by-hour over a ten year period, for two different buildings and four different orientations. This gives eight different ten-year profiles. The procedure is then repeated for each individual year in the period of the record and the yearly profile considered “nearest” to the average of the ten-year profile (over all eight cases) is declared the test reference year.

The Danish selection procedure (Lund 1976, Anderson 1974) is based on rigorous statistical analysis applied to eleven years of climatic data. Test reference year selection is based on the daily mean dry bulb temperature, the daily maximum dry bulb temperature and the daily total of solar radiation according to three criteria:

- months with abnormal weather conditions are excluded at the outset;
- months with typical mean values (of the three parameters given above) are selected by comparing mean values for each month with the mean value for the same month calculated from the whole period data;
- months with typical variations of the three parameters are selected. This is done by comparing the deviation of the three parameters, from the previously selected monthly mean values, with the corresponding deviations for the whole period.

Each month is rank ordered according to these criteria and the reference year selected. A South African procedure involves the selection of typical hot days on the basis of either the daily maximum sol-air temperature or daily maximum dry bulb temperature occurring on 10, 5 and 2.5% of the days in the period considered. Typical cold days are selected on the basis of minimum temperatures. A study initiated by the UK Building Research Establishment and Meteorological Office proposed a similar method (IHVE 1973).

In the UK the Chartered Institute of Building Services has produced an “Example Year” based on a selection method proposed by Holmes and Hitchin (1978). Based on global and diffuse solar radiation, wind speed, dry bulb temperature and degree days, the method eliminates any year containing a monthly mean which varies by more than two standard deviations from the long term mean of this month.

It can be seen from the above review that there is no specific procedure to determine a climate reference year. However two conditions require to be met:

- The data should represent the conditions under which, at some time, the building will be required to function (winter design, winter typical, summer peak, long term average, and so on).
- The data should have some quantifiable severity measure which establishes their suitability for selection.

The former requirement is concerned with the availability of relevant, and site specific climatic data (10 years or more) and the latter requirement with the rank ordering of these available data according to severity criteria which include building-specific factors. Unfortunately it is not possible to apply any of the forementioned procedures to the data obtained for this study (three years of raw data). However, the definition of CRY by Paassen & Liem (1982) is the basis for the work produced in this chapter.

In the rest of this chapter both a qualitative and a quantitative analysis for the climate of the Riyadh region are developed. These are based on a collection of data over different periods from Riyadh meteorological station and the Solar Village Photovoltaic power site, 50km North of Riyadh. These may assist designers and architects to determine the comfort conditions most suited to this region.

The hourly data for the years 1984 through to 1986 are processed and compiled in a standard format (*Climate Reference Year*) for use in the computer simulation programs "ESP". Variations of the climate through the year, month and day are discussed. Diurnal Nomograms for predicting hourly data from daily values are developed. Finally, based on the compiled Solar Village data, solar radiation prediction algorithms are derived which often are required in the absence of measured data.

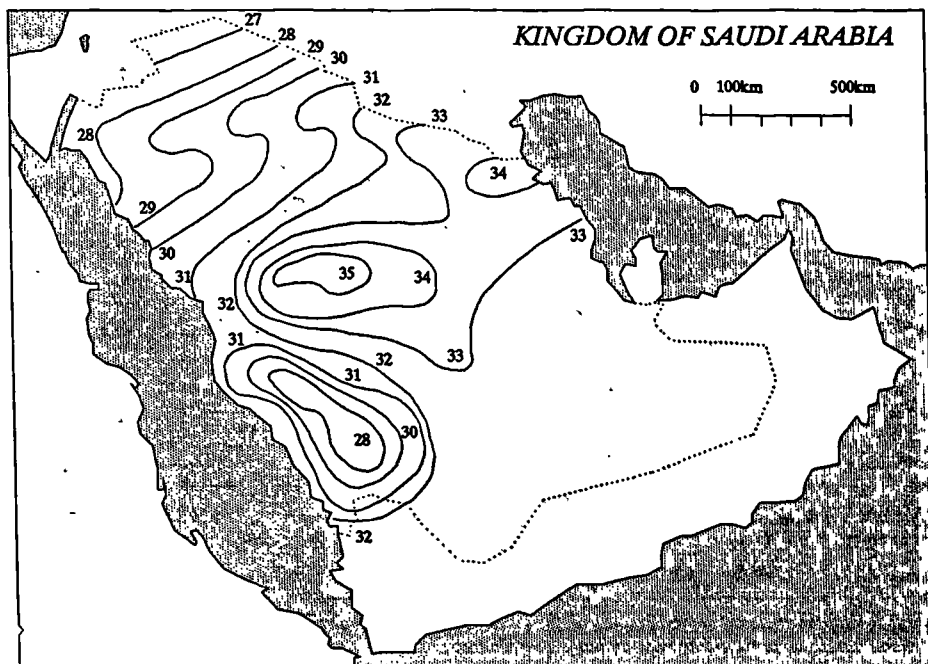


**Figure 3.1** Saudi Arabian *Summer isotherm* map. Mean monthly temperatures (°C), of June, July and August, for the period 1966–1974. (reproduced from Schyfsma 1978).

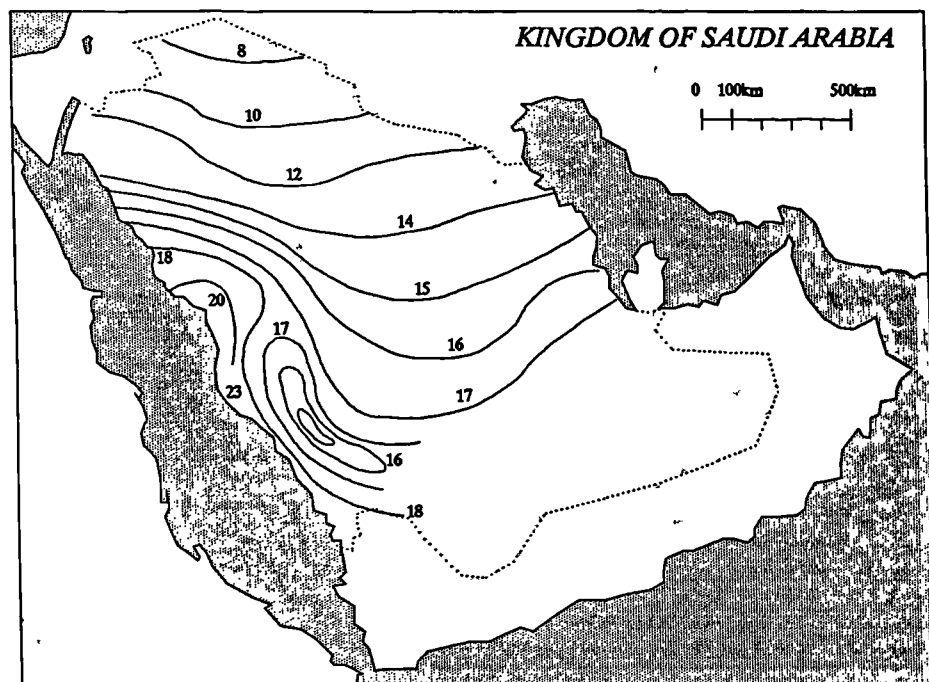


**Figure 3.2** Saudi Arabian *Winter isotherm* map. Mean monthly temperatures (°C), of January, February and December, for the period 1966–1974. (reproduced from Schyfsma 1978).

## 3.2 Background Information

Saudi Arabia is part of a great desert belt which stretches across North Africa and into Central Asia. During the summer months the climate is generally very hot and very dry with frequent dust and sand storms. The Red Sea and Arabian Gulf are two narrow water bodies which result in coastal climates that are hot and humid. Regional analysis of all Saudi Arabian climate patterns is not an easy task and is beyond the aims of this chapter. The following brief information may provide a picture of weather patterns of Saudi Arabia in general and Riyadh in particular.

### 3.2.1 Climate of Saudi Arabia

Saudi Arabia experiences significant changes from summer (June, July & August) to winter (December, January & February) temperatures, except along the Red Sea coast, where the difference is small and the relative humidity more evenly distributed throughout the year. Summer and winter isotherm maps are presented in Figures (3.1 & 3.2). The ranges of mean monthly temperatures and relative humidity averaged over 9 years from 21 stations in Saudi Arabia are presented in Table (3.3). Average rainfall is 100 to 1000 (mm) annually, with the Asir province in southwest Saudi Arabia receiving the largest amount as shown in Figure (3.3). Dust and sand storms are frequently encountered, and while these storms do not persist, there is constant windblown dust.

Until recently insolation data were lacking from meteorological publications except in the form of sunshine records. At present, monthly maps of solar radiation and hours of sunshine over Saudi Arabia are published (see SANCST 1983). Percentage possible sunshine varies from 72% of day time in coastal areas and up to 78% for inland. Figure (3.4) is a map of lines of constant sunshine (isohel) obtained from means of yearly total hours of sunshine over Saudi Arabia. The distribution of total annual global horizontal insolation over Saudi Arabia (see Fig. 3.5) shows that daily solar energy varies between 1800 to 2400 ( $\text{kWh m}^{-2} \text{y}^{-1}$ ) which is most encouraging from the solar energy utilization point of view.

Station	TEMPERATURE (°C)		RELATIVE HUMIDITY (%)	
	(Summer)	(Winter)	(Summer)	(Winter)
Inland	27.5–36.8	08.5–20.0	13–47	35–78
Arabian Gulf	30.6–36.8	11.0–22.2	37–63	65–73
Red Sea	27.9–33.5	18.6–26.9	58–64	60–74

**Table 3.3** Temperature and relative humidity ranges in summer (June, July & August) and winter (January, February & December) for inland and coastal stations in Saudi Arabia. (After Schyfsma, 1978)

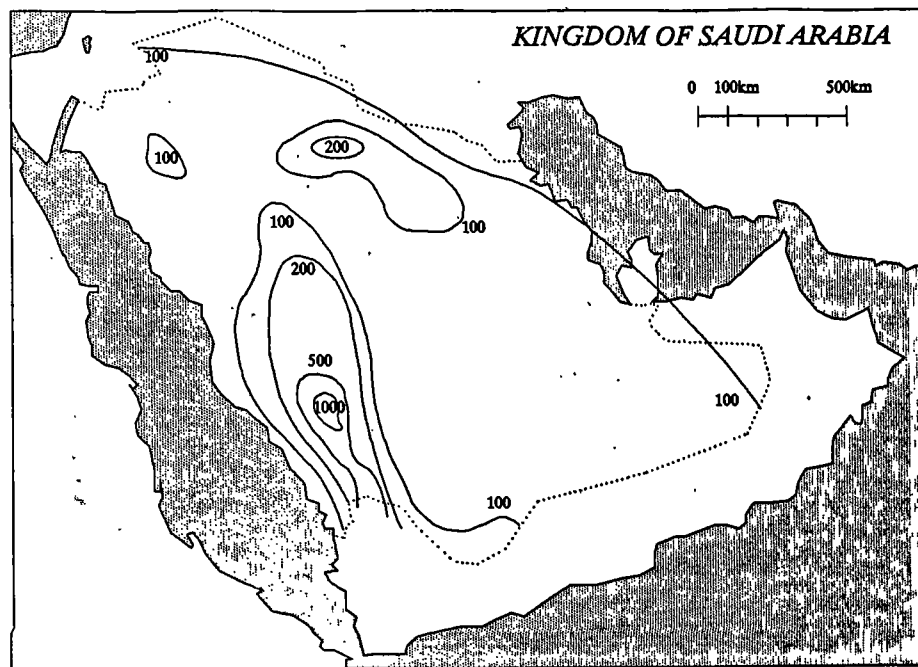


**Figure 3.3** Saudi Arabian *Isohyetes* map. Average yearly precipitation, in mm. (reproduced from Schyfsma 1978).

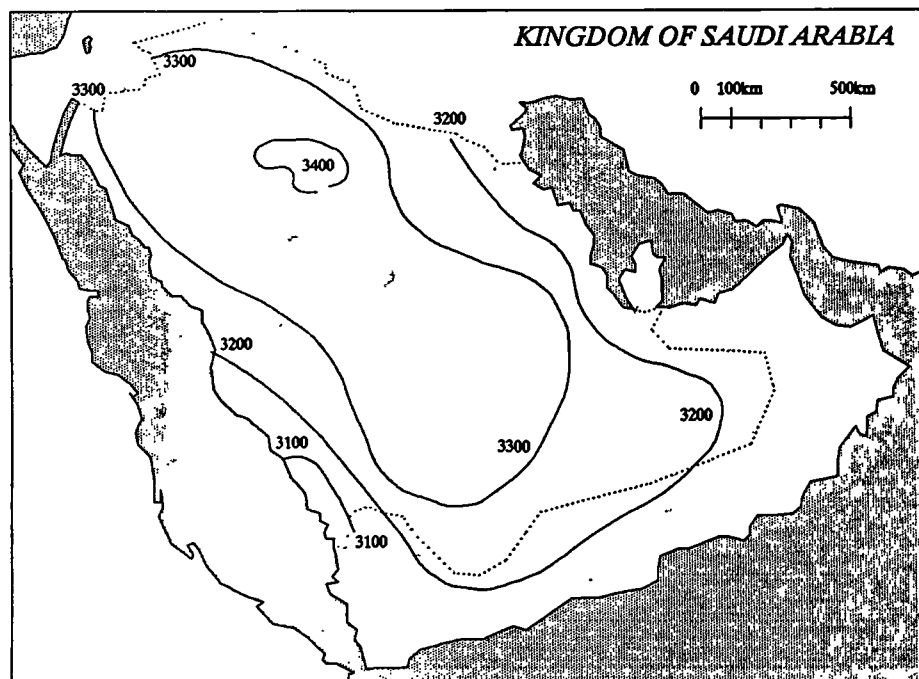


**Figure 3.4** Saudi Arabian *Isohel* map. Mean yearly sums of sunshine duration in hours. (reproduced from the "Saudi Arabian Solar Radiation Atlas", SANCST 1983). Maps of daily totals for each month can be obtained from the same reference.

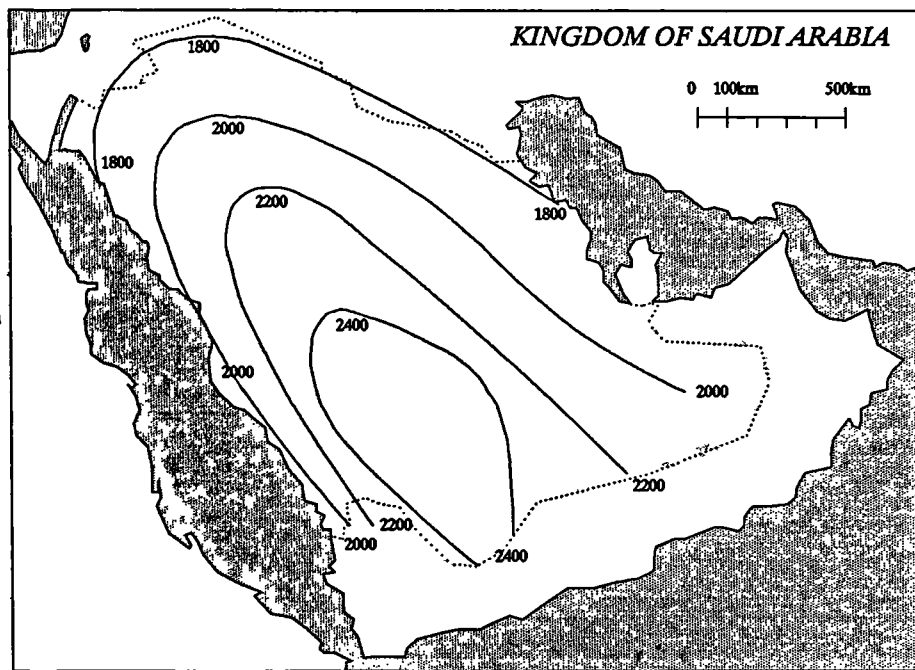


**Figure 3.5**

Saudi Arabian *Iso-Radiation* map. Mean yearly total global horizontal insolation in  $\text{kWh}/(\text{m}^2 \text{ y})$ . Reproduced from the "Saudi Arabian Solar Radiation Atlas", (SANCST 1983). Maps of daily totals for each month can be obtained from the same reference.

		CLIMATIC DATA (1961-80 RIYADH)											
Variables		Jan	Feb	Mar	Apr	May	Jun	Jul	Aug	Sep	Oct	Nov	Dec
<b>Temperature (°C)</b>													
Daily	Avg.	13.9	16.6	20.5	25.3	31.1	33.8	34.8	32.9	31.6	26.3	20.3	15.2
	Max.	20.1	23.1	28.0	32.3	38.4	41.6	42.5	42.3	41.4	34.3	27.1	21.9
	Min.	8.2	10.2	14.3	18.6	23.6	25.6	26.8	22.3	22.4	18.4	13.8	9.3
Extreme	Max.	30.0	34.8	38.0	42.0	45.6	48.8	46.7	46.3	44.0	41.1	34.2	31.0
	Min.	-2.0	0.0	5.0	9.8	15.8	19.0	21.8	21.4	17.0	11.0	5.0	-1.0
<b>Relative Humidity (%)</b>													
Daily	Avg.	52	44	36	33	22	14	14	14	15	21	38	45
	Max.	81	68	65	64	48	28	26	27	31	33	54	65
	Min.	23	28	21	13	11	7	8	9	9	14	22	26
<b>Wind</b>													
	Mean speed (m/s)	4	4	5	5	4	5	5	4	3	3	3	3
	Prevailing direction	SSE	SSE	SSE	SSE	SSE	N	NNW	N	NNE	VAR	SE	SSE
<b>Precipitation (mm)</b>													
	Monthly total	14.7	7.1	22.6	33.5	9.9	0.1	0.5	0.9	0.2	0.4	7.9	10.7
<b>Average number of days with :</b>													
	Precipitation (>0.1mm)	3.5	2.3	4.6	5.7	2.5	0.0	0.2	0.2	0.1	0.2	1.9	2.7
	Dust/sand storm	1.3	2.1	2.4	3.8	4.0	2.7	1.9	1.0	1.1	0.6	0.7	0.8
	Blowing dust	6.5	7.1	9.1	8.3	10.7	7.9	6.5	6.3	5.7	4.8	7.0	5.7
	Haze	8.6	6.5	10.7	10.3	11.3	10.9	10.9	9.3	9.3	9.9	9.9	10.8
		Jan	Feb	Mar	Apr	May	Jun	Jul	Aug	Sep	Oct	Nov	Dec

Table 3.4 Meteorological data averaged over 20 years period (1961-1980), for Riyadh. Lat = 24.43, Long = 46.43, Elevation = 611m. (from a summary sheet supplied by the Ministry of Defense and Aviation, Riyadh Met. Office, Saudi Arabia).

### 3.2.2 Riyadh Climate (an overview)

Riyadh can be categorised as in the hot arid climatic region. Analysis of compiled meteorological data over a 20 years period (1961–1980), (Ministry of Defense and Aviation), are presented in Table (3.4) from which the following points can be inferred:

- The summer stretches from April through to October with maximum hourly temperatures exceeding 40°C for most of the season. Temperature swings between maximum (day) and minimum (night) are typical of a desert climate in the range of 15 to 20°C. Daily average relative humidity values for the summer period are extremely low, from 14% to 22% except for the month of April (33%) where the maximum monthly rainfall occur.
- In winter months (December, January and February) the decrease of daily average temperatures from summer months is considerable; from 25.3–34.8°C for summer months to 13.9–16.6°C for the winter; i.e. from 20.1°C maximum in January to 26.8°C minimum in July. Daily average relative humidity for winter months ranges from 44% to 52%, and the temperature changes by about 12°C between day and night.
- The months of March and November experience moderate weather conditions with warm days (about 27–28°C max.) and cool nights (about 14°C min.).
- Wind speed throughout most of the year is calm, about 4 m s<sup>-1</sup>, increasing to about 5 to 6 m s<sup>-1</sup> in summer months. The average number of dust/sand storms amount to 22 days of the year. “Blowing dust” is more frequent, occurring for an average 86 days of the year. Prevailing wind direction is south to south–easterly most of the year, varying to north north–westerly from June to September.

### 3.3 Riyadh Climate Reference Year

---

The indoor climate and energy consumption of buildings are highly influenced by the outdoor climate. To simulate the dynamic behaviour of the energy balance of a building, at least hourly values of weather data obtained over a long period (10 years or more) are necessary (Paassen & Liem 1982). For this purpose long term weather data on tapes from meteorological stations are used. However the required computational time to perform one simulation using all such data is very long. An improvement to this situation is the use of a "Climate Reference Year". This is a set of 8760 hours of weather data that is representative of the long term weather data. The format and type of climatic variables in a reference year varies with the requirements of different simulation programs.

The prime objective of this section is to define hourly climatic variables for 365 days, to be used in the energy simulation program "ESP". The program requires 6 hourly climatic variables, namely:

- Global horizontal or Direct Normal insolation ( $\text{W m}^{-2}$ )
- Diffuse horizontal insolation ( $\text{W m}^{-2}$ )
- Ambient Dry Bulb Temperature ( $^{\circ}\text{C}$ )
- Relative Humidity (%)
- Wind Speed ( $\text{m s}^{-1}$ )
- Wind Direction (deg. North =  $0^{\circ}$ )

The program also requires mean monthly ground temperature values.

The data required to compile the reference year were obtained from the King Abdulaziz City for Science and Technology (KACST), Solar Projects Department. They represent extracts from the Data Acquisition Systems of the Photovoltaic Power Site (PVPS) in the Solar Village (Latitude =  $24.54^{\circ}\text{N}$ , Longitude =  $46.24^{\circ}$ ). These extracts were obtained in two formats:

- Floppy disks containing averaged hourly values, for the years 1984 and 1986 and 8 minute interval values for the year 1985, of direct normal insolation; global horizontal insolation; dry bulb temperature; and wind speed.
- Climatic data sheets (prepared by various departments in the project) in two sets: The first containing daily total, maximum and average values of insolation; including global insolation using various instruments, direct normal insolation, ultraviolet irradiation, infrared irradiation. The second set include daily average, maximum and minimum values of dry bulb temperature; relative humidity; wind speed; wind direction; ground temperature and daily sunshine hours. These data sheets were extremely useful in processing the hourly relative humidity and wind direction data.

The data of Table 3.4 were also used for validating the estimated relative humidity.

*Validity of Raw Insolation Data*

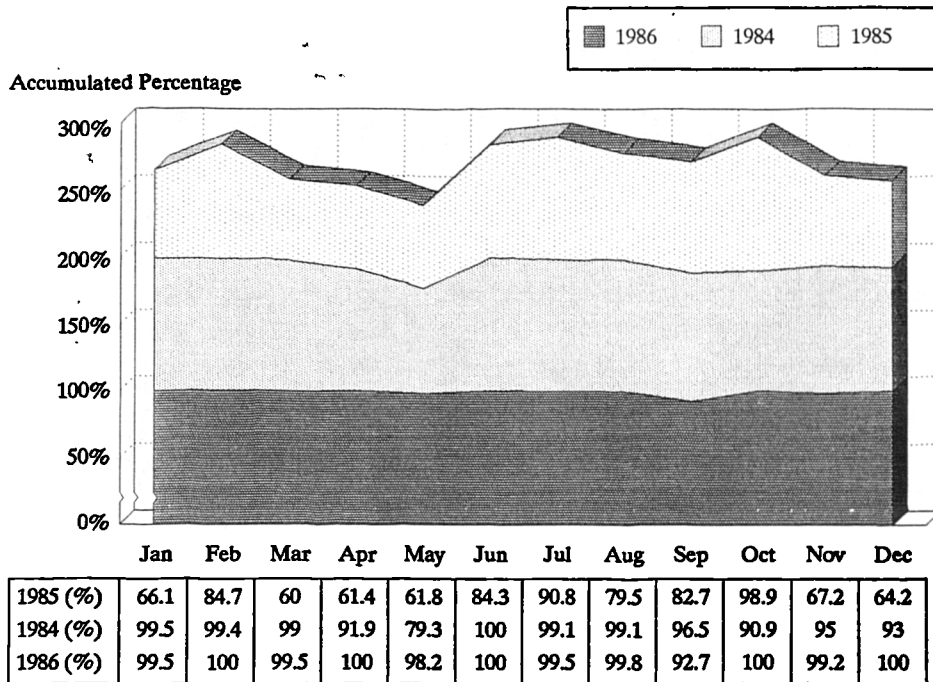


**Figure 3.6** Monthly percentages of valid hourly insolation data, obtained from KACST, for the years 1984, 85 & 86. (missing data are counted as invalid).

*Validity of Raw Temperature Data*

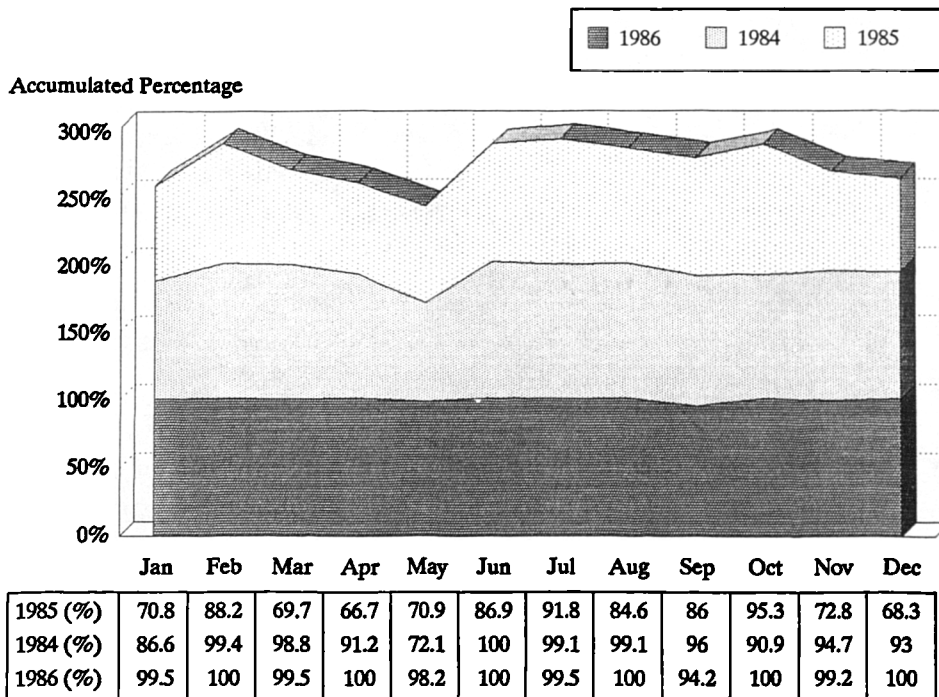


**Figure 3.7** Monthly percentages of valid hourly temperature data, obtained from KACST, for the years 1984, 85 & 86. (missing data are counted as invalid).

### 3.3.1 Data Processing

Processing the supplied raw data required the following steps:

- 1 – Data extraction, averaging and conversion
- 2 – Error corrections
- 3 – Missing data filling

Only the required climatic variables were extracted from the data supplied. In addition to missing data some of the values, on the original floppy disks were flagged with (-9999). These obviously represent erroneous data and hence are rejected. The percentages of valid raw data (insolation, temperature, and wind speed) for the three years are represented by the area graphs in Figures (3.6, 3.7, and 3.8). The data of 1986 is the most valid of the three years having only one missing day, compared with 3 days of missing data in 1984 and 32 days of missing data in 1985.

Steps 1 and 2 above were accomplished by developing and using GW-Basic™ simple programs. The missing data were filled manually by different techniques (discussed below for each climate variable) through the use of Lotus-123™ and Harvard Graphics™ programs.

#### Insolation Data Processing

The hourly global horizontal ( $G_h$ ) together with the direct normal ( $G_{DN}$ ) insolation were used to determine mathematically the hourly diffuse horizontal ( $G_{fh}$ ) data as follows:

$$G_{fh} = G_h - G_{bh} \quad \{3.1\}$$

$$G_{DN} = G_{bh} / \cos(\theta_z) \quad \{3.2\}$$

where  $G_{bh}$  is the direct component of the global insolation ( $W m^{-2}$ ); and ( $\theta_z$ ) the zenith angle for each hour is found from: (Duffie & Beckman 1980)

$$\cos(\theta_z) = \sin(\delta) \sin(\phi) + \cos(\delta) \cos(\phi) \cos(\omega) \quad \{3.3\}$$

where  $\phi$  = latitude angle (24.54°N); the declination angle ( $\delta$ ) is found from the commonly used approximation equation of Cooper (1969), Eq.(3.4); and the hour angle ( $\omega$ ) from Eq.(3.5).

$$\delta = 23.45^\circ \sin[360^\circ (284 + J) / 365] \quad \{3.4\}$$

$$\omega = 15^\circ h^{-1} (12h - t_s) \quad \{3.5\}$$

where  $J$  = Julian day from January 1st; and the solar time ( $t_s$ ) in hours, is calculated by:

$$t_s = t + E_t + (L_{std} - L_{loc}) / (15^\circ h^{-1}) \quad \{3.6\}$$

*Validity of Raw Wind Speed Data*

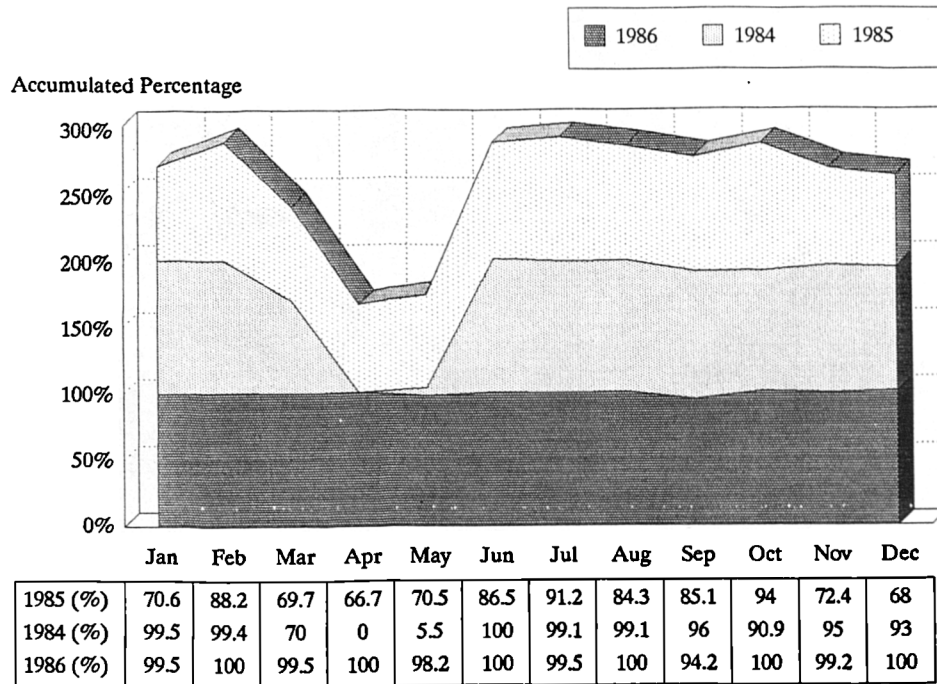


**Figure 3.8** Monthly percentages of valid hourly wind speed data, obtained from KACST, for the years 1984, 85 & 86. (missing data are counted as invalid).

where (t) is the local mean time (h);  $L_{std}$  is the standard longitude of Saudi Arabia = 45°E;  $L_{loc}$  is the local longitude of the Solar Village (Riyadh) = 46.24°E; and the equation of time ( $E_t$ ), in hours, is found from:

$$E_t = [9.87 \sin(2e) - 7.53 \cos(e) - 1.5 \sin(e)] / 60 \quad \{3.7a\}$$

where (e) is a modulating function given by:

$$e = 360^\circ (J - 81) / 364 \quad \{3.7b\}$$

The above procedure (developed in a conversion GW-Basic™ program) was valid for more than 98% of the calculations. Negative results of diffuse horizontal insolation were obtained mainly during the first and last hours of the day. This error may possibly be associated with one of the two measured values ( $G_h$  or  $G_{DN}$ ) and more likely with the latter due to the measuring instrument field of view (see section 6.5.3 in chapter 6). Therefore, a correction procedure was later introduced in the conversion program which replaced the value of ( $G_{DN}$ ) by ( $G_h$ ). This implies that overestimation occurred for those corrected ( $G_{fh}$ ) values, but since these are low values of insolation the error associated with the calculation procedure is insignificant.

Missing data were filled manually through either correlation to data of similar duration of sunshine or graphical visual interpolation. The data are then validated by calculating the total insolation for each day and comparing the result with that given on the supplementary data sheets.

### Temperature and Relative Humidity Data Processing

Erroneous temperature values (i.e. those flagged with -9999) throughout the years 1984 and 1986 numbered less than 1%. Average daily, maximum and minimum values from the supplied data sheets along with graphical interpolations gave a base for estimating the missing and invalid temperature values. The 32 days of missing data in 1985 were substituted by the corresponding days from the average of 1984 and 1986. In addition, 11% of the remaining erroneous hourly values were estimated through: (A) graphical interpolation for invalid values of less than 6 hours in a day; (B) substituted by the average of 1984 and 1986 corresponding values for more than 6 hours of invalid data in a day. Finally the estimated values were validated by comparing the 24h average of each day with those supplied in the data sheets.

Ground temperature data were given as average daily values in the supplementary data sheets for the years 1985 and 1986. No information was available on the type of instruments used for the measurements or at what depth beneath the ground surface the measurements were taken. However, the ESP program requires the annual variation in ground temperature, month-by-month, with no specific reference to what depth beneath the surface the measurements represent. Therefore the available two years data were averaged and the mean monthly values were calculated.

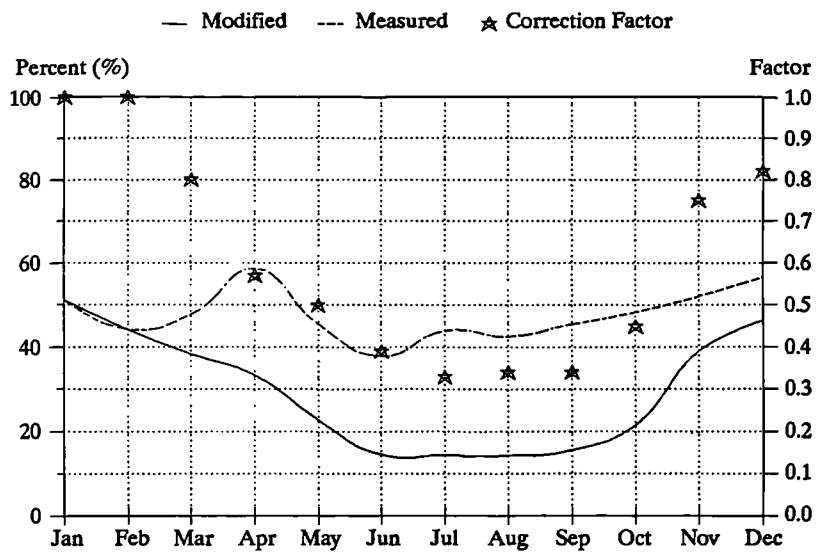


**Figure 3.9** Monthly means of measured and modified relative humidity. Correction factors (determined by Eq.3.11) were used in Eq.3.10 to produce the same monthly mean relative humidities as in Table (3.2).

Hourly values of relative humidity were calculated on the principle of their inverse relation with temperature. i.e. for each hour of the day:

$$T_j / T_a = R_a / R_j \quad \{3.8\}$$

$$R_j = (T_a / T_j) \cdot R_a \quad \{3.9\}$$

where  $T_a$  is the 24h average of ambient air temperature ( $^{\circ}\text{C}$ );  $R_a$  is the daily average relative humidity (%) supplied in the data sheets;  $T_j$  = ambient air temperature at hour  $j$ ; and  $R_j$  is the required relative humidity at the same hour. This procedure was found to be accurate for clear days where calculated maximum and minimum relative humidity values agreed with those supplied on data sheets. It should be noted that no average daily relative humidities were available for the year 1984, therefore, the relative humidity data for the reference year is an average of two years (1985 & 86).

Preliminary results from the above data processing indicated higher mean monthly relative humidities from April to December when compared with those given in Table (3.4). It was concluded that the measured relative humidity data (from data sheets), incorporated instrumental errors (Hansen, J. personal communication 1990). Therefore, the hourly values of relative humidity derived from Eq.3.9 were modified so that their monthly means agreed with the published data of Table (3.4). i.e.

$$R_{jm \text{ (new)}} = R_{jm} \cdot F_m \quad \{3.10\}$$

where  $R_{jm \text{ (new)}}$  is the new relative humidity value for the hour ( $j$ ) in the month ( $m$ );  $R_{jm}$  is the correspondent relative humidity value calculated by Eq.3.9; and  $F_m$  is a correction factor for the month ( $m$ ), determined by:

$$F_m = R_m / R_m^* \quad \{3.11\}$$

where  $R_m$  is the monthly mean of relative humidities calculated by Eq.3.9; and  $R_m^*$  is the monthly mean value for the month  $m$ , obtained from Table 3.4. The correction factors with mean monthly values of old relative humidity (i.e. based on Eq.3.9) and modified relative humidity (based on Eq.3.10) are plotted in Figure (3.9).

### Wind Speed and Wind Direction data processing

Wind speed data of 1986 were the most continuous of the three years with one missing day and less than 1% of missing hours of the year. The year 1985 had 32 days of missing data and 9% missing hours from the rest of the year. The year 1984 had two months missing data of wind speed. Missing data were filled manually through either: (A) substitution from corresponding data in the other years (e.g. the two months missing data in 1984 were substituted with the average values from the other two years for the same period); or (B) correlation to data of similar daily averages. Wind speed data were validated by comparing the 24h average of each day to those supplied in the data sheets.

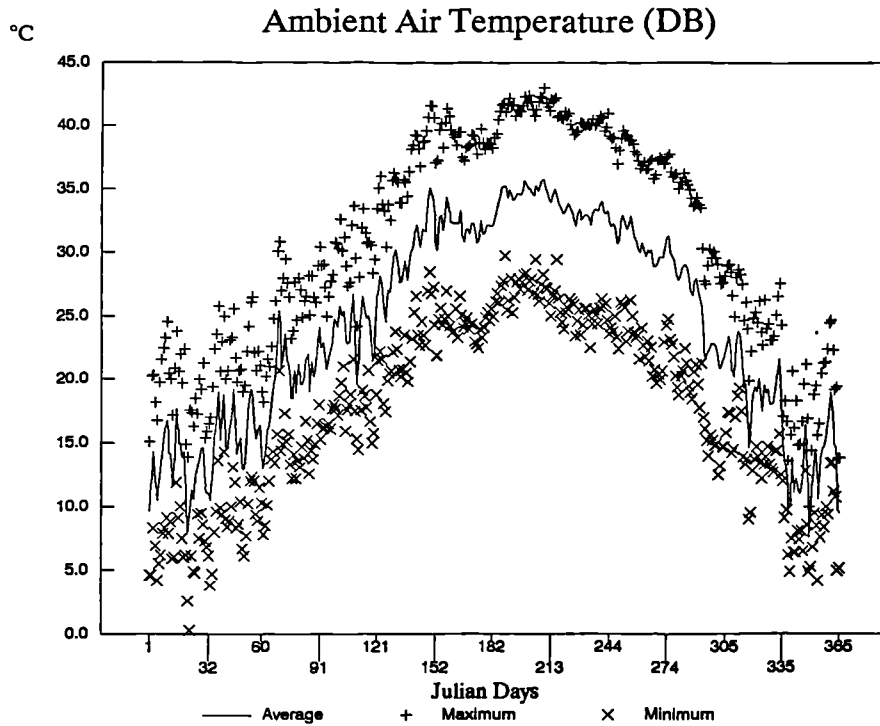
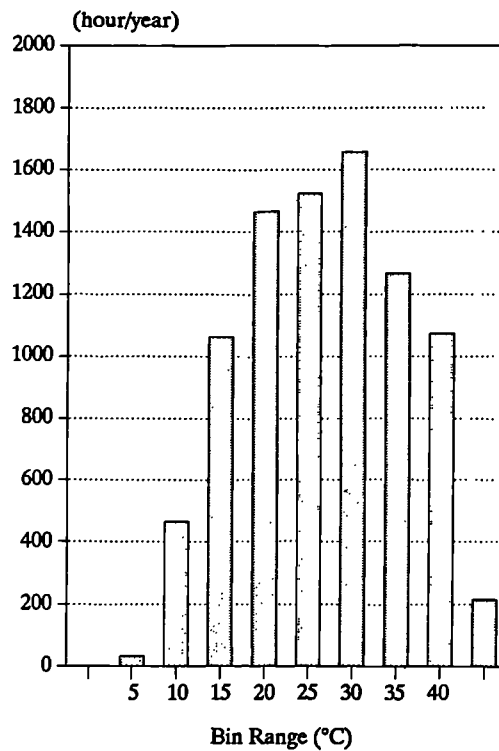


**Figure 3.10** Daily average, and maximum and minimum hourly dry bulb temperature values from Riyadh Climate Reference Year of this thesis.

**Figure 3.11** Frequency distribution of hourly dry-bulb temperature of the Riyadh Climate Reference Year (total of 8760 hours).



Daily prevailing wind direction for 1985 and 1986 (from the supplementary data sheets) were used systematically as hourly values of wind direction in the reference year. i.e. the odd hours in a day were filled with the prevailing wind direction of the corresponding day in 1985, and the even hours were filled with the wind direction of the corresponding day in 1986.

### 3.3.2 Results and Remarks Concerning the Riyadh “CRY”

The Climate Reference Year of Riyadh (hourly data) compiled as discussed above is available on computer floppy diskette in MS-DOS<sup>®</sup> format as well as in Unix<sup>®</sup> environment format. A copy of each is kept in the Energy Studies Unit (University of Strathclyde, Scotland). The 5.25" disk (360kB, MS-DOS format) supplied with this thesis contains the compiled CRY with additional insolation data, (see the list in Appendix I).

In this section daily average, maximum and minimum data of the reference climatic variables are presented graphically, along with statistical analysis emphasising some characteristics of the Riyadh climate. Daily meteorological data are tabulated in Appendix (A). The compiled insolation data with additional information useful for further research, i.e. daily infra-red (4–50  $\mu\text{m}$ ) and ultraviolet (0.29–0.39  $\mu\text{m}$ ) insolation, are presented in Appendix (B). (see chapter 6 for details on the measuring instruments of the climatic data of Riyadh). Characteristics of the Riyadh climate, based on the reference year data analysis, are emphasised in the following remarks for each climatic variable, (All data refer to hourly values, unless otherwise specified).

#### 3.3.2.1 Temperature

- Temperatures from 7°C minimum in winter to 42°C maximum in summer (Table 3.5) indicate the range over the whole year for design consideration. Daily average, maximum and minimum hourly temperatures are plotted in Figure (3.10). Frequency distribution of the reference year (8760 hours) over 5°C increments is illustrated in Figure (3.11).
- The difference between winter and summer temperatures is significant (e.g. from 18°C *maximum* in December to 27°C *minimum* in July).

Temp.	AMBIENT AND GROUND SURFACE TEMPERATURES (°C)												Year
	Jan	Feb	Mar	Apr	May	Jun	Jul	Aug	Sep	Oct	Nov	Dec	
<u>Ambient</u>													
avg.	13	16	20	24	30	34	35	33	31	26	20	13	24.6
max.	19	22	26	30	37	39	42	40	38	33	25	18	30.8
min.	7	10	14	18	23	24	27	25	23	18	14	8	17.6
<u>Ground</u>													
avg.	15	16	22	28	34	39	38	38	34	28	23	16	27.6

**Table 3.5** Monthly means of temperature data from the hourly Climate Reference Year. Ground temperatures are based on daily average data from 1985 & 1986.

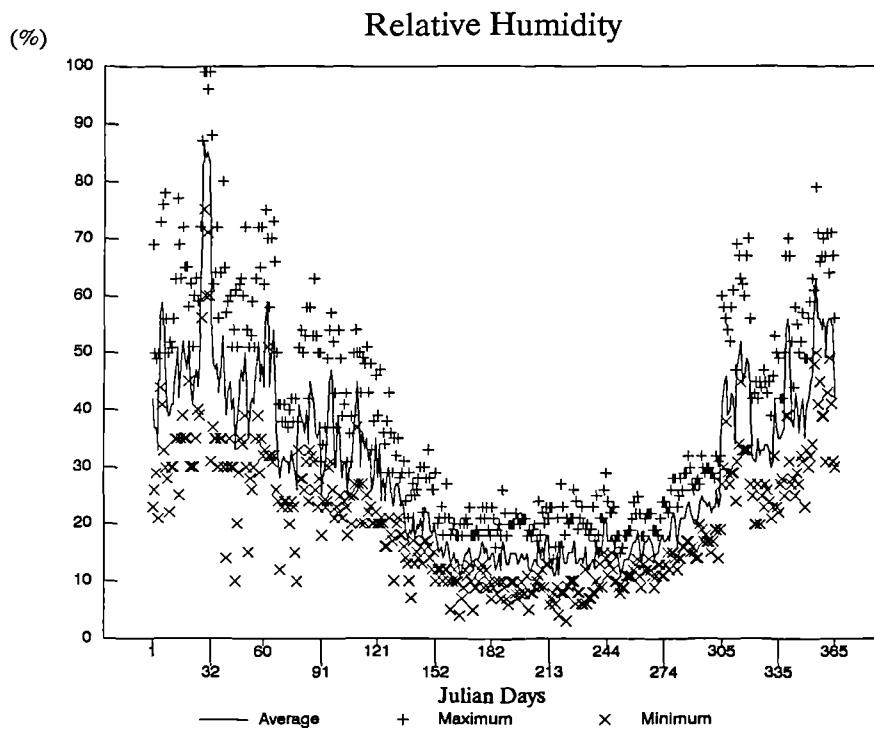
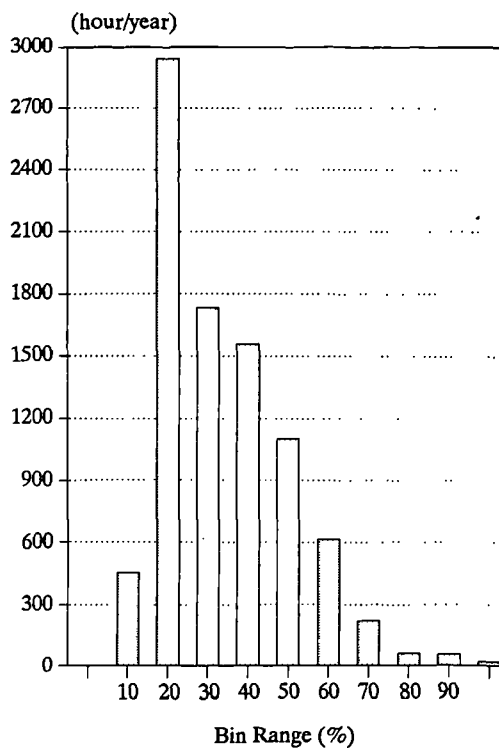


**Figure 3.12** Relative humidity (daily average, and hourly maximum and minimum) from the Climate Reference Year of Riyadh.

**Figure 3.13** Frequency distribution of the corrected hourly relative humidity of the Climate Reference Year of Riyadh (8760 hours).



- The daily temperature swings (i.e. the change between daytime maximum hourly and night time minimum values) are about  $13 \pm 2$  °C throughout the year. (see section 3.4 for more details).
- Daily average temperatures exceed 20°C over 66% of the year (242 days) of which 138 days are above 30°C.
- From daily hourly minimum values, temperatures are less than 15°C for 143 nights, 13 of which drop below 5°C.
- In terms of daily maximum hourly temperatures, 86% of the year (315 days) are above 25°C of which values for 86 days exceed 40°C.

### 3.3.2.2 Relative Humidity

- The hourly relative humidity values determined for this study involve a degree of uncertainty, hence 1- the estimation procedure relates relative humidity to one climatic parameter (temperature) in Eq.3.9; and 2- Eq.3.10 modifies the result to account for the difference in mean monthly values to that of the 20 years average data in Table 3.4. (see section 3.3.1). Unfortunately there was no other choice due to the lack of available hourly data from Saudi Arabia.
- The daily average, maximum and minimum hourly values of relative humidity (after modification) are shown in Figure (3.12).
- The daily average relative humidity is below 50% over most of the year (307 days). Minimum hourly values fall below 30% for 237 days, half of which are in the range of 0-20%.
- Daily maximum hourly values are within 40-70% for most of the year. Only 57 days exhibit daily maximum values above 70% in winter, but 89 summer days experience maximums of less than 40%. Hourly frequency distribution for the reference year over 10% intervals are shown in Figure (3.13).

### 3.3.2.3 Wind Speed and Direction

- Wind speed data (Fig.3.14) show no economical potential for wind energy application in Riyadh. The daily average values range from 2 to 5 ( $\text{m s}^{-1}$ ) with unpredictable frequency except that the highest values occur in summer months. Economically, oil is so cheap that alternatives are highly unlikely to be economic, unless external costs are included, or sites are very remote.

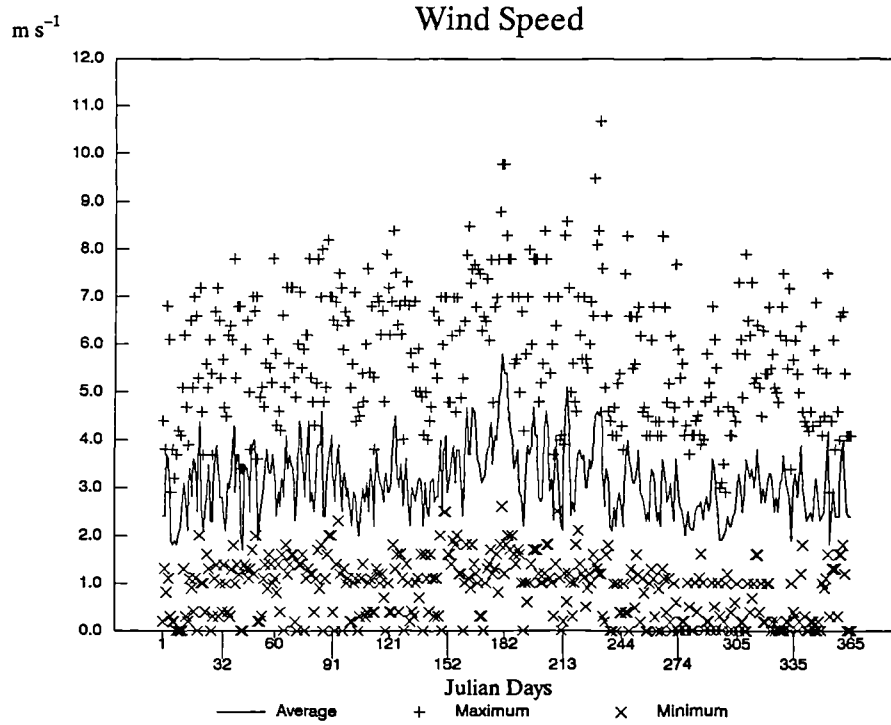
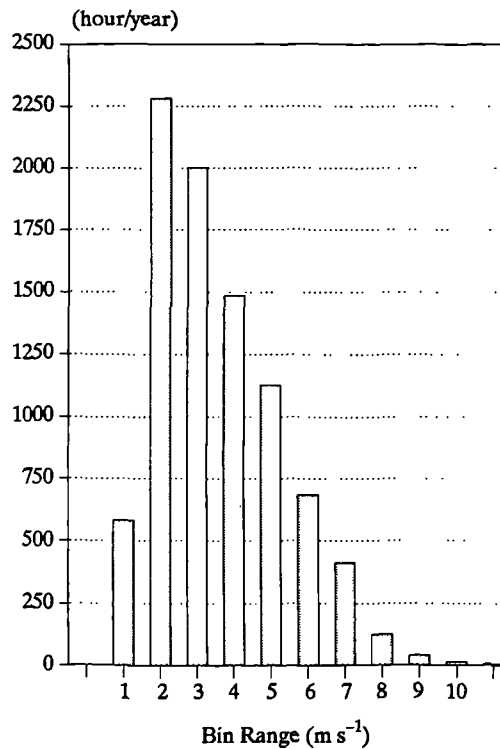


Figure 3.14 Wind speed (daily average, and hourly maximum and minimum) from Riyadh Climate Reference Year developed in this chapter.

Figure 3.15 Frequency distribution of hourly wind speed of the Climate Reference Year of Riyadh (8760 hours).



- The frequency distribution of wind speed shown in Figure (3.15) for the reference year (8760 hours) indicates that for about 78% of the year wind speed range from 2 to 5 ( $m s^{-1}$ ), most of which (63%) is within 2–3 ( $m s^{-1}$ ).
- The wind direction parameter is used in the ESP program and in the QREF.BAS program (developed in chapter 4) to assess external convection coefficients of surfaces under simulation. For that purpose the accuracy of the hourly wind direction values determined for this reference year are sufficient.
- Daily average data shown in Figure (3.16) indicate that prevailing wind direction is dominantly south oriented throughout the year ( $0^{\circ}$  is true north). The sector between  $135^{\circ}$ – $225^{\circ}$  degrees account for more than 52% of the reference year wind direction. Only 14% of the year’s wind direction values are within the range  $270^{\circ}$  to  $90^{\circ}$  degrees.

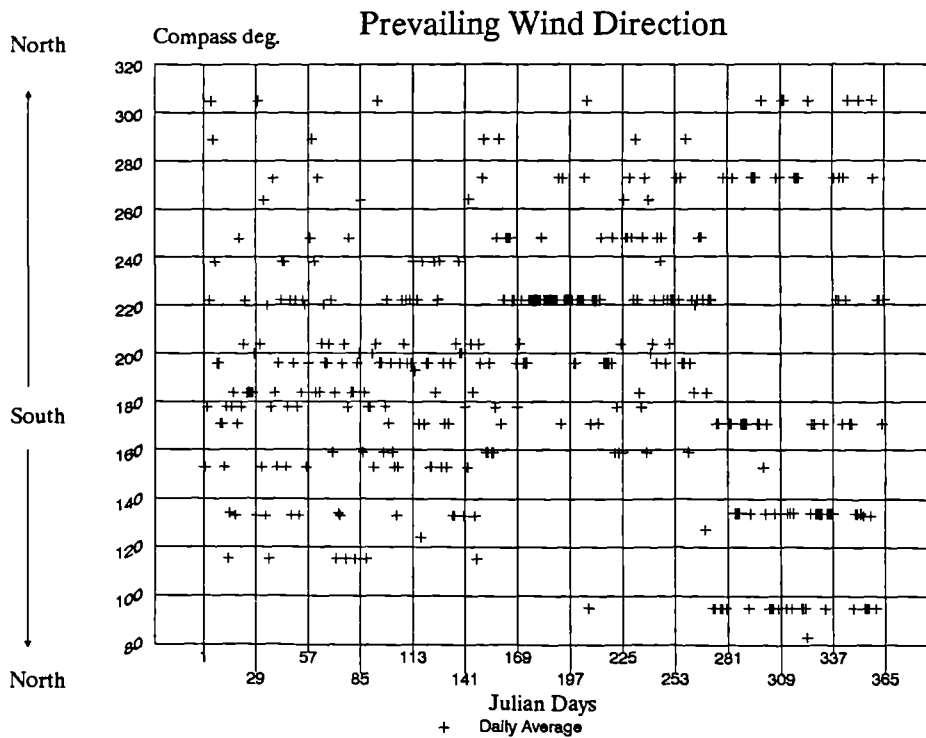


Figure 3.16

Daily average wind directions (compass degrees) from the Climate Reference Year of Riyadh.

**Table 3.6** Mean monthly solar data averaged from the hourly Climate Reference Year of Riyadh. Recorded sunshine hours are based on daily average data from 1985 and 1986. Maximum day lengths and extraterrestrial radiation are calculated from Eq.3.16 and Eq.3.17 respectively. (see section 3.5.1)

<i>INSOLATION DATA</i>												
	Jan	Feb	Mar	Apr	May	Jun	Jul	Aug	Sep	Oct	Nov	Dec
<b>Solar energy †</b>												
Extraterrestrial	6.72 (24.2)	7.82 (28.2)	9.18 (33.0)	10.32 (37.2)	10.92 (39.3)	11.10 (40.0)	10.98 (39.5)	10.49 (37.8)	9.54 (34.3)	8.20 (29.5)	6.95 (25.0)	6.36 (22.9)
Global horizontal	4.12 (14.8)	4.94 (17.8)	5.61 (20.2)	6.03 (21.7)	7.22 (26.0)	7.90 (28.4)	7.76 (27.9)	7.33 (26.4)	6.57 (23.7)	5.52 (19.9)	4.24 (15.3)	3.35 (12.1)
Diffuse horizontal	1.60 (5.8)	1.84 (6.6)	2.13 (7.7)	2.69 (9.7)	3.53 (12.7)	2.68 (9.6)	2.76 (9.9)	2.70 (9.7)	2.46 (8.9)	1.87 (6.7)	1.33 (4.8)	1.31 (4.7)
<b>Sunshine hours</b>												
Recorded sunshine	5.6	7.8	9.1	8.3	10.5	12.1	11.5	11.2	10.5	10.7	7.5	5.3
Maximum possible	10.7	11.2	11.9	12.6	13.2	13.5	13.4	12.8	12.1	11.4	10.8	10.5

† Solar energy in kWh/(m<sup>2</sup> day). Values in brackets are in MJ/(m<sup>2</sup> day).

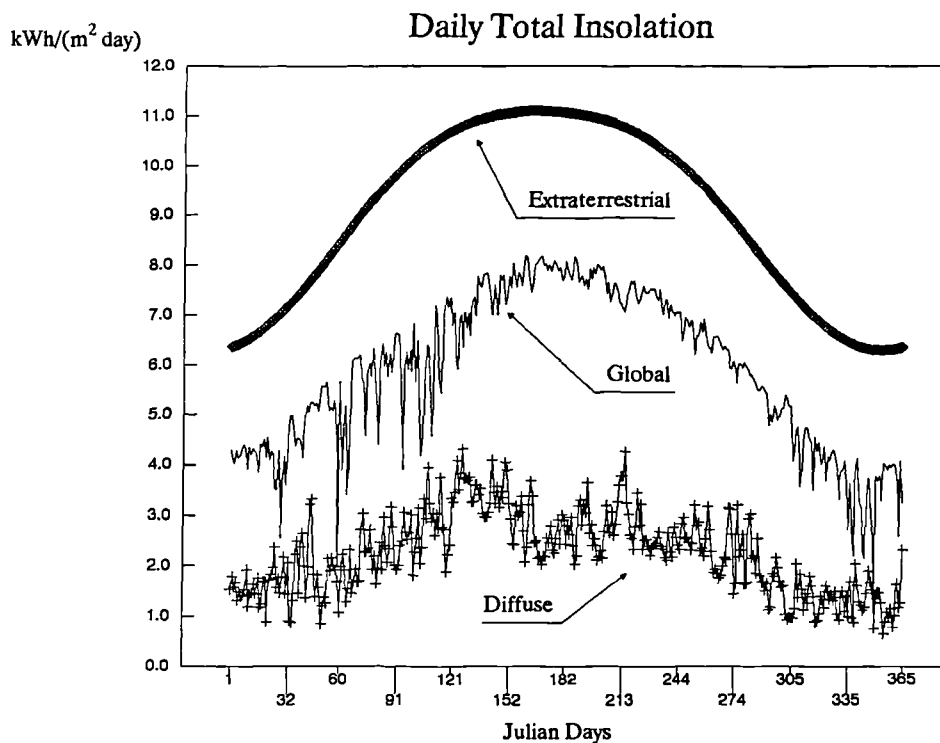


**Figure 3.17** Daily global and diffuse solar energy over Riyadh, kWh/(m<sup>2</sup> day), from the Climate Reference Year. Extraterrestrial radiation data are calculated from Eq.3.17 (see section 3.5.1).

### 3.3.2.4 Insolation

- Bright sunshine occurs for 76% of daylight time at Riyadh. The total horizontal solar energy received at ground level in Riyadh is about 64% of that above the atmosphere. A comparison between daily total extraterrestrial calculated by Eq.3.17 (see section 3.5.1), global and diffuse insolation is shown in Figure (3.17). These are also provided as mean monthly values in Table 3.6 along with day length and recorded sunshine hours. Correlation of global insolation and sunshine hours is considered later in section 3.5.1.
- The diffuse horizontal insolation is about 39% of global insolation on average through the year. Prediction of diffuse insolation over Riyadh from bright sunshine duration gives poor results (see section 3.5.2). For example in April (with 80% possible sunshine) the percentage of diffuse to global insolation is higher than that of May where possible sunshine is 66% (see Table 3.6).
- Daily global and diffuse horizontal insolation (averages over day lengths, and maximum hourly values) are presented in Figures 3.18 & 3.19 respectively. For over 65% of the reference year (238 days) the daily average global insolation ranges from 450 to 600  $\text{W m}^{-2}$ , and only 31 days experience values lower than 350  $\text{W m}^{-2}$ .
- In terms of daily maximum values, 266 days exhibit global insolation in the range of 700–900 ( $\text{W m}^{-2}$ ), and for more than half of the period (150 days), the maximum global exceed 800 ( $\text{W m}^{-2}$ ).
- The daily average diffuse horizontal insolation ranges from 150 to 250 ( $\text{W m}^{-2}$ ) for 214 days. Daily maximum values are above 300 ( $\text{W m}^{-2}$ ) for most of the reference year, with 48 days exceeding 400 ( $\text{W m}^{-2}$ ).
- Frequency distribution of global and diffuse insolation for all daylight hours of the reference year (4767 hours) are illustrated in Figures 3.20 & 3.21.
- In the light of the above discussion solar radiation provides a great potential for active solar energy applications in Riyadh. On the other hand it raises the question of caution in building design especially when dealing with fenestration, building orientation, roof structures, air conditioning, shading ...etc.

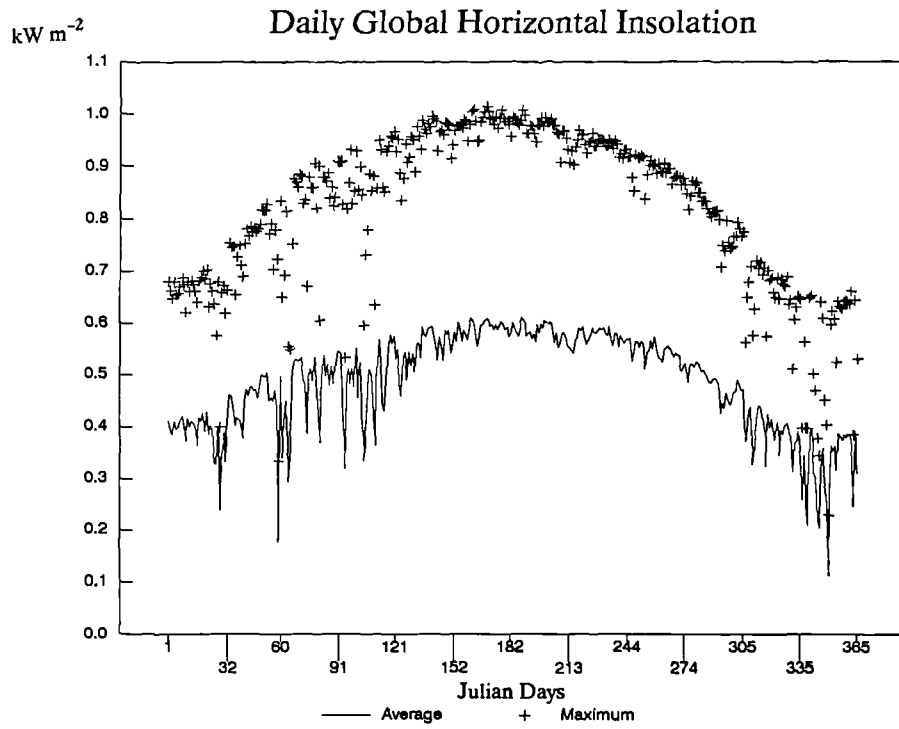


**Figure 3.18** Daily average and maximum global horizontal insolation from Riyadh Climate Reference Year. The average is calculated from sunrise to sunset.

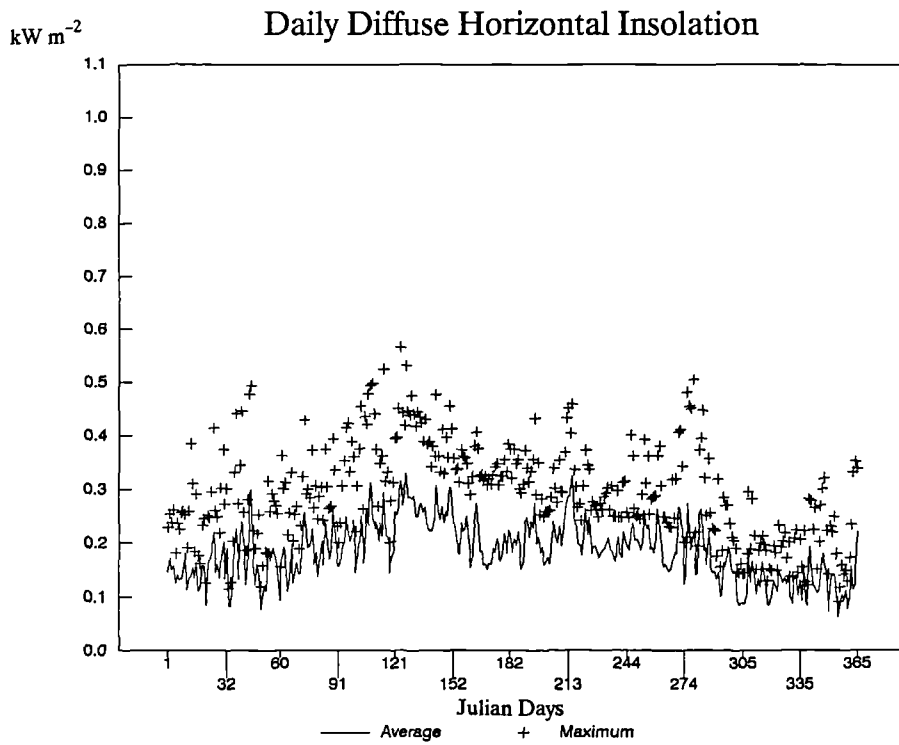


**Figure 3.19** Daily average and maximum diffuse horizontal insolation from Riyadh Climate Reference Year. The average is calculated from sunrise to sunset.

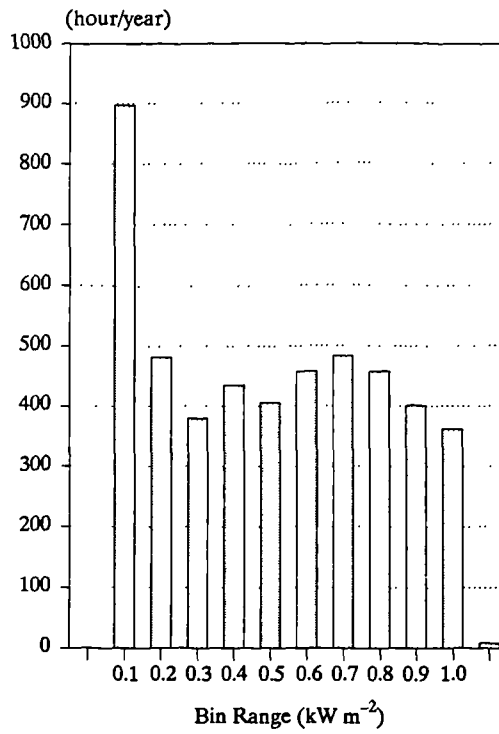


**Figure 3.20** Frequency distribution of hourly global horizontal insolation per year of daylight (4767 hours), from the reference climate year of Riyadh.

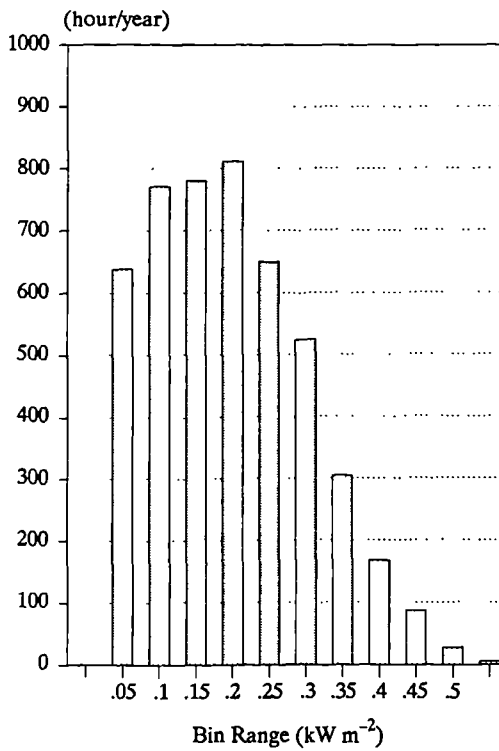


**Figure 3.21** Frequency distribution of hourly diffuse horizontal insolation per year of daylight (4767 hours), from the Climate Reference Year of Riyadh.

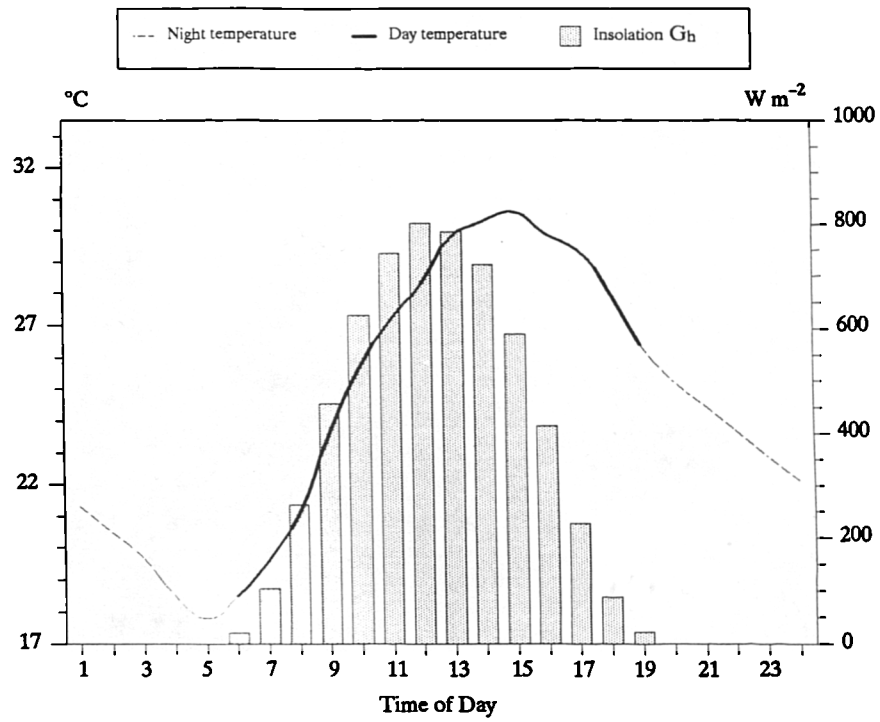


**Figure 3.22** Yearly mean of hourly insolation ( $G_h$ ) and temperature (Dry Bulb) variations through the day, (from the Climate Reference Year of Riyadh developed in section 3.3).

## **3.4 Variation of Riyadh Climate Through the Day**

---

In the previous section, variation of climate through the Climate Reference Year from month to month and from day to day were examined. The following analysis considers the diurnal variations of the Climate Reference Year parameters in an attempt to generalise diurnal nomograms for predicting hourly values.

### **3.4.1 Temperature Variation During the Day**

The Climate Reference Year has a quite large diurnal temperature range (12°C winter and 15°C summer temperature swings on average), with very little change in range from day to day. Therefore, the variations will follow a pattern (Fig.3.22).

The temperature drops to a minimum at about 5:00 hour and increases to a maximum at about 15:00 hour. The rate of temperature increase is rapid between 8:00 and 11:00 hours as the intensity of solar radiation increases. Between 15:00 and 19:00 hours the air temperature decreases by a small proportion of the increase (29%) which occurs between sunrise and the maximum, although the increase of insolation in the morning is matched by a corresponding decrease in the afternoon (see Figure 3.22).

The delay in peak of air temperature beyond midday is due to the heat transfer from the irradiated ground and the air and the thermal capacitance of the ground. This is a complex subject and the reader is referred to specialised literature for details (e.g. see Budyko 1963, Barry & Chorley 1976 and Oliver 1981).

Table (3.7) presents mean monthly air temperature variations through the day with their standard deviation (calculated from the Climate Reference Year data).

**Table 3.7** Hourly dry bulb temperature variations during the day for each month in the Climate Reference Year of Riyadh. The second row of values for each hour represent the standard deviations from the monthly means.

Hour	<i>DIURNAL TEMPERATURE VARIATIONS (°C)</i>												Year
	Jan	Feb	Mar	Apr	May	Jun	Jul	Aug	Sep	Oct	Nov	Dec	
01:00	10.5	13.2	17.3	20.7	26.2	28.4	31.1	29.6	27.0	22.7	17.5	11.2	21.3
	2.3	2.4	2.7	1.7	2.6	0.9	0.9	0.9	1.5	3.1	2.2	2.6	7.3
02:00	9.9	12.4	16.7	19.9	25.5	27.4	30.1	28.5	26.1	22.0	16.8	10.6	20.5
	2.2	2.4	2.7	1.6	2.5	0.9	1.0	1.0	1.5	3.2	2.1	2.7	7.2
03:00	9.1	11.7	16.0	19.2	24.5	26.5	29.2	27.4	25.1	21.0	16.3	10.1	19.7
	2.2	2.6	2.7	1.7	2.6	1.0	1.0	1.0	1.6	3.3	2.2	2.6	7.1
04:00	8.4	11.0	15.3	17.7	22.9	24.5	27.2	25.5	23.2	20.1	15.7	9.6	18.5
	2.3	2.6	2.7	1.7	2.7	1.1	1.2	1.3	1.8	3.2	2.2	2.6	6.6
05:00	7.0	9.6	14.1	17.7	22.8	24.5	27.3	25.4	23.1	18.5	14.5	8.5	17.8
	2.3	2.6	2.7	1.8	2.6	1.1	1.2	1.3	1.8	3.3	2.3	2.6	7.1
06:00	7.0	9.6	14.1	19.1	24.2	26.0	28.8	26.9	24.7	18.6	14.4	8.6	18.5
	2.3	2.5	2.5	1.8	2.6	1.1	1.1	1.2	1.8	3.3	2.3	2.7	7.7
07:00	8.4	11.1	15.5	19.6	25.1	26.9	29.3	27.4	25.0	20.0	15.9	9.9	19.6
	2.3	2.6	2.6	1.7	2.7	1.1	1.0	1.2	1.9	3.3	2.2	2.7	7.4
08:00	9.0	12.0	16.7	21.0	27.0	29.4	31.7	29.6	27.0	21.7	16.8	10.6	21.1
	2.4	2.5	2.7	1.7	2.8	1.1	1.1	1.0	1.8	3.6	2.4	2.8	8.0
09:00	11.0	13.9	18.7	22.9	29.3	32.1	34.9	33.3	30.9	25.2	18.6	12.0	23.6
	2.4	2.4	3.1	2.0	2.8	1.1	0.9	0.7	1.4	3.6	2.7	2.9	8.6
10:00	13.3	15.9	20.6	24.7	31.1	33.8	36.8	35.6	34.0	28.5	20.4	13.6	25.7
	2.5	2.4	3.2	2.2	2.8	1.3	1.1	0.7	0.9	3.7	2.8	3.0	8.7
11:00	15.2	17.4	22.0	26.2	32.7	35.1	38.1	36.9	35.4	30.0	21.8	14.8	27.2
	2.7	2.6	3.3	2.3	2.7	1.3	1.0	0.7	1.0	3.6	2.7	3.3	8.7
12:00	16.4	18.9	23.1	27.4	34.1	36.1	39.1	38.0	36.3	30.9	23.0	15.8	28.3
	2.8	2.6	3.2	2.3	2.6	1.2	1.0	0.8	0.9	3.5	2.6	3.5	8.6
13:00	17.9	20.5	24.5	28.8	35.7	38.0	40.8	39.6	37.3	32.1	24.4	17.0	29.8
	2.7	2.6	3.2	2.3	2.8	1.1	0.9	0.7	0.9	3.4	2.4	3.6	8.7
14:00	18.7	21.4	25.2	29.0	36.4	38.6	41.3	40.1	37.6	32.5	25.1	17.7	30.3
	2.8	2.6	3.3	2.5	2.8	1.0	0.8	0.7	1.0	3.4	2.3	3.5	8.6
15:00	19.2	21.9	25.6	29.2	36.6	38.9	41.4	40.3	37.7	32.5	25.4	18.0	30.6
	2.8	2.5	3.3	2.7	2.7	1.0	0.8	0.7	1.0	3.3	2.2	3.4	8.5
16:00	18.6	21.3	25.2	28.6	35.8	38.0	40.4	39.4	37.0	31.7	24.7	17.3	29.9
	2.8	2.4	3.3	2.7	3.0	0.9	0.7	0.7	1.0	3.3	2.2	3.2	8.4
17:00	18.0	20.9	24.7	28.3	35.1	37.6	40.0	39.0	36.5	31.0	24.0	16.7	29.4
	2.8	2.4	3.3	2.6	3.0	0.8	0.7	0.6	1.0	3.4	2.3	2.9	8.4
18:00	15.9	18.9	23.8	27.7	34.2	37.0	39.4	38.2	35.0	28.9	22.2	15.0	28.1
	2.6	2.3	3.3	2.4	2.9	0.8	0.7	0.6	1.5	3.3	2.2	2.7	8.7
19:00	14.7	17.7	22.0	25.8	32.1	34.8	37.2	36.1	33.1	27.6	21.1	14.0	26.4
	2.6	2.3	3.3	2.2	2.8	0.7	0.7	0.6	1.2	3.3	2.1	2.7	8.4
20:00	14.1	16.9	20.8	24.7	30.7	33.3	35.8	34.6	31.9	26.7	20.5	13.5	25.3
	2.4	2.3	3.1	2.2	2.8	0.7	0.8	0.7	1.2	3.3	2.2	2.6	8.0
21:00	13.3	16.3	20.2	23.8	29.9	32.4	34.7	33.6	30.9	25.8	19.9	12.9	24.5
	2.4	2.3	3.0	2.0	2.6	0.8	0.7	0.7	1.2	3.2	2.1	2.6	7.9
22:00	12.6	15.6	19.5	23.1	29.0	31.4	33.9	32.5	29.9	25.0	19.2	12.4	23.7
	2.3	2.2	2.9	2.0	2.6	0.7	0.7	0.8	1.2	3.2	2.2	2.6	7.7
23:00	12.0	14.7	18.9	22.4	28.1	30.4	32.9	31.4	29.0	24.1	18.6	11.9	22.9
	2.3	2.3	2.8	1.8	2.6	0.8	0.7	0.8	1.3	3.2	2.1	2.5	7.6
24:00	11.3	14.0	18.2	21.7	27.2	29.5	31.9	30.5	28.0	23.3	18.0	11.4	22.1
	2.2	2.3	2.8	1.8	2.5	0.8	0.7	0.9	1.4	3.2	2.2	2.5	7.5

### 3.4.1.1 Hourly Temperature Prediction Nomogram

From Table (3.7), the patterns of diurnal variations tend to be regular. Therefore, it is possible to predict with high probability the average hourly values, if the average daily maximum and minimum temperatures are known.

Based on a nomogram developed by C. Mahoney (Koenigsberger, et. al. 1971), a nomogram for predicting diurnal temperature variations was developed, for the Riyadh region. (see Figure 3.23)

The nomogram consists of two related graphs. The top half of the nomogram consist of a graph showing the proportional variation in air temperature during the day (noted by the letter [A] in Figure 3.23). The curve in this figure is constructed from the yearly values in Table (3.7). The lower half shows the actual variation in temperature (noted by [B]), which can be related to the proportional variation using the following simple procedure:

- 1- The mean daily maximum and mean daily minimum hourly temperatures for a given month are located on the upper and lower scales of of figure [B] and a diagonal line is drawn between the two points.
- 2- The temperature at a given hour can be found by locating the time of day on the time axis of figure [A], from the corresponding point on the proportional temperature curve the temperature can be found directly below the point on part [B] of the figure.

### 3.4.2 Wind Speed Variations During the Day

The diurnal variation of wind in the Riyadh region relate mostly to local temperature and radiation variations. When the ground is cooled by outgoing radiation at night, it will cool the layers of air immediately above the ground. This air, being cooler and denser than the upper air remains close to the ground, so that little or no vertical mixing of the air will take place.

By day when the sun heats the ground surface, the layer of air closest to the ground will become hotter than the upper air and will tend to rise. This vertical mixing, caused by convection currents, will cause eddies (very common in this region) and turbulence so that higher winds will be experienced randomly at ground level. Detailed studies on eddies can be found in literature (e.g. see Oliver 1981).

Wind speed variations during the day presented in Figure (3.24) relate to the yearly mean of hourly data. The general conclusions that can be drawn from wind speed diurnal analysis are as follows:

- Wind speeds are likely to be higher during the day than at night.

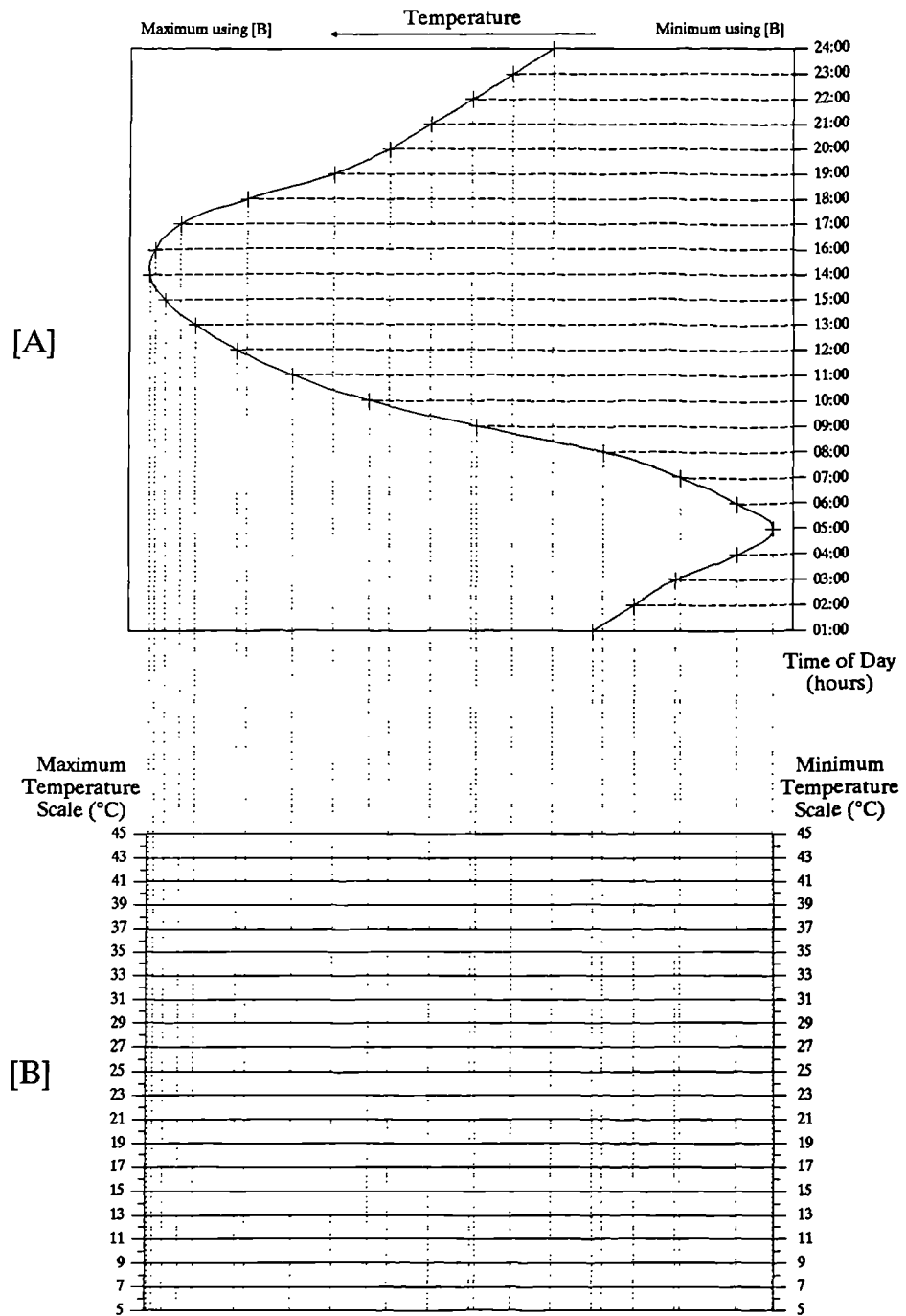


**Figure 3.23** Nomogram for predicting diurnal temperature variations in Riyadh. Graph [A] indicates the proportional variations in air temperature during the day. Graph [B] shows the actual variations in temperature which can be related to graph [A], (see section 3.4.1 for instructions).

- Wind speeds will decrease in the evening after sunset especially in clear sky conditions.
- Local thermal winds may replace regional winds at night when wind speeds would otherwise drop. These will not be as strong as the winds blown during the day.
- The maximum daily wind speeds that are experienced between 12:00 and 17:00 hours may be of sufficient speed to raise dust. This will form haze and will reduce the intensity of solar radiation in the afternoon. Haze and blowing dust conditions are more persistent in summer than winter.
- The curve on Figure 3.24 is the ratio of hourly to daily average wind speed. This can give a rough estimate of the hourly wind speed if the 24h daily average is known. Estimated hourly wind speeds using this graph would incorporate significant error. However if the monthly means of hourly values are to be estimated, the error will be in the range of 10–20%.

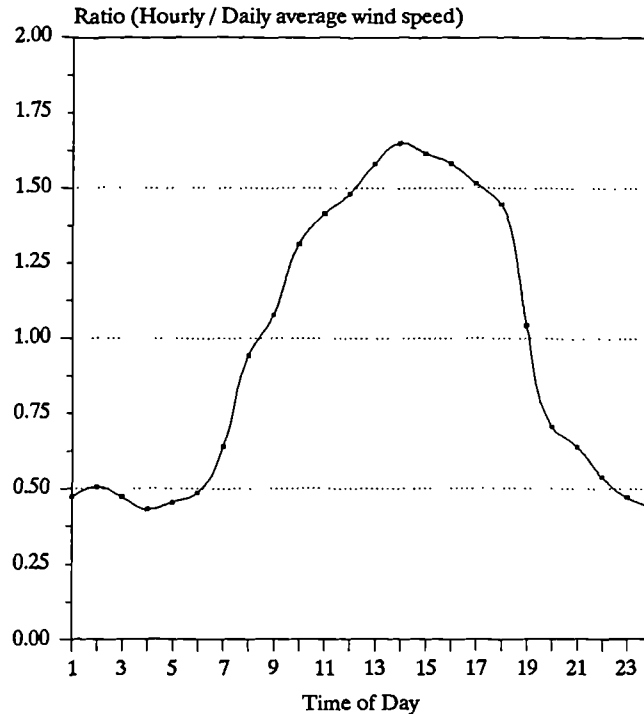


**Figure 3.24** Ratio of hourly to daily average wind speed. If the daily 24h average wind speed is known, multiplying it by the ratio corresponding to an hour on the time-axis gives the wind speed at that time.

<i>HOURLY GLOBAL INSOLATION PERCENTAGE FROM DAILY TOTAL (%)</i>												
<i>Time</i>	<i>Jan</i>	<i>Feb</i>	<i>Mar</i>	<i>Apr</i>	<i>May</i>	<i>Jun</i>	<i>Jul</i>	<i>Aug</i>	<i>Sep</i>	<i>Oct</i>	<i>Nov</i>	<i>Dec</i>
07:00	0.4	0.5	1.0	1.8	2.4	2.7	2.4	2.2	2.1	1.7	1.4	1.1
	0.1	0.1	0.3	0.6	0.3	0.1	0.3	0.2	0.2	0.3	0.5	0.5
08:00	2.4	2.8	3.7	4.6	5.3	5.4	5.1	5.0	5.1	4.9	4.1	3.2
	0.4	0.5	0.9	1.1	0.5	0.2	0.3	0.2	0.3	0.5	1.1	0.8
09:00	6.7	6.7	7.3	7.8	8.1	8.0	7.8	7.9	8.3	8.5	8.1	7.4
	0.9	1.0	1.3	1.5	0.7	0.2	0.3	0.2	0.3	0.5	1.3	1.7
10:00	10.7	10.4	10.6	10.6	10.4	10.1	10.0	10.3	11.0	11.5	11.6	11.5
	1.3	1.2	1.7	1.9	0.8	0.2	0.3	0.2	0.3	0.7	1.7	2.5
11:00	13.7	13.3	12.8	12.2	12.3	11.7	11.7	12.0	12.7	13.7	14.3	13.8
	1.7	1.8	2.1	2.3	0.5	0.2	0.3	0.2	0.3	0.9	1.5	3.8
12:00	15.2	14.7	14.0	13.2	13.0	12.4	12.5	12.8	13.5	14.5	15.4	15.6
	1.9	2.1	2.3	2.4	0.6	0.2	0.3	0.2	0.3	1.0	1.5	4.1
13:00	15.6	14.7	14.2	13.7	12.7	12.3	12.5	12.7	13.2	14.0	14.8	15.3
	1.6	2.3	2.0	1.8	1.0	0.3	0.4	0.2	0.4	0.9	1.3	3.6
14:00	14.1	13.7	12.9	12.3	11.6	11.4	11.6	11.8	11.8	12.3	12.8	13.5
	1.4	2.1	2.0	2.2	0.8	0.4	0.5	0.4	0.9	0.9	1.2	3.0
15:00	11.0	11.1	10.6	10.0	9.5	9.7	9.9	9.9	9.7	9.6	9.7	10.2
	1.2	1.9	1.7	2.2	1.1	0.4	0.4	0.5	0.7	0.7	0.9	2.4
16:00	7.1	7.6	7.6	7.1	7.1	7.5	7.6	7.5	6.9	6.2	5.7	6.0
	0.9	1.3	1.0	1.5	1.0	0.3	0.4	0.4	0.7	0.7	0.7	1.4
17:00	2.8	3.8	4.1	4.0	4.4	4.8	4.9	4.7	3.6	2.6	1.8	2.2
	0.6	0.7	0.6	1.0	0.7	0.3	0.4	0.4	0.6	0.6	0.3	1.3
18:00	0.4	0.7	1.2	2.0	2.1	2.4	2.5	2.1	1.2	0.7	0.4	0.3
	0.1	0.2	0.3	1.7	0.4	0.2	0.2	0.2	0.3	0.2	0.1	0.2

**Table 3.8** Percentages of hourly global horizontal insolation from daily total global insolation, ( $F_{j(\text{global})}$  calculated by Eq.3.12 and tabulated as mean monthly values). The standard deviations from the means are presented in the second row of each hour.

### 3.4.3 Solar Irradiation Variations During the Day

It is usually assumed that the solar energy received on the ground on a cloudless day are equal in the morning and in the afternoon. Away from urban or industrial pollution insolation may tend to be slightly higher in the afternoon than in the morning, since the relative humidities are lower, air temperatures are higher and cloud cover may be reduced (Evans, 1980). However above or near to urban and industrial complexes, increased aerosol in the afternoons reduces insolation (Raja 1992).

Analysis of the hourly global horizontal insolation from the Climate Reference Year indicate that morning insolation is higher than afternoon insolation for five months. The morning total insolation from 6:00–12:00 hours for the months (May and September through to December) is about 10 to 15% higher than the afternoon value (13:00–19:00 hours). The effect results from the higher diffuse radiation intensities experienced in the afternoon, and the large decrease in direct beam radiation. Dust particles in the atmosphere cause such phenomena which is apparent in summer months when relative humidities are extremely low and cloud cover is rare, so the effect of the dust is significant.

Diurnal variations of global and diffuse horizontal insolation for each month are presented in Figures (3.25 and 3.26). The curves on each graph represent the hourly solar intensity as a proportion of the 24h total.  $F_{j(\text{global})}$  is the fraction of the *daily global insolation*  $G_{h(\text{total})}$  and  $F_{j(\text{diffuse})}$  is the fraction of the *daily diffuse insolation*  $G_{fh(\text{total})}$ , averaged over each month. Thus for each hour in a day:

$$F_{j(\text{global})} = G_{hj} / G_{h(\text{total})} \quad \{3.12\}$$

$$F_{j(\text{diffuse})} = G_{fhj} / G_{fh(\text{total})} \quad \{3.13\}$$

where  $G_{hj}$  and  $G_{fhj}$  are the global horizontal and diffuse horizontal insolation for the hour  $j$  respectively. The percentages ( $F_{j(\text{global})}$  and  $F_{j(\text{diffuse})}$  for  $J = 7\text{am}$  to  $6\text{pm}$ ), with their corresponding standard deviations are provided in Tables (3.8 & 3.9) respectively.

With the knowledge of daily total global horizontal insolation it is possible to predict hourly values from the graphs or tables (i.e. by solving for  $G_{hj}$  in Eq.3.12) with good accuracy especially between the hours (9:00 to 17:00) where solar intensities are of significant magnitudes.

On the other hand, predicting hourly diffuse horizontal insolation by the use of Figures 3.25 & 3.26 or Table 3.9 may not be adequate (see standard deviation values in Table 3.9), and further correlation with other climatic conditions (i.e. diurnal variations of temperature and relative humidity, cloud cover, dust and pollution in the atmosphere) are recommended.

<i>HOURLY DIFFUSE INSOLATION PERCENTAGE FROM DAILY TOTAL (%)</i>												
<i>Time</i>	<i>Jan</i>	<i>Feb</i>	<i>Mar</i>	<i>Apr</i>	<i>May</i>	<i>Jun</i>	<i>Jul</i>	<i>Aug</i>	<i>Sep</i>	<i>Oct</i>	<i>Nov</i>	<i>Dec</i>
07:00	0.8	1.1	1.9	2.7	3.0	3.5	3.3	3.2	3.0	3.2	2.9	2.4
	0.2	0.3	0.5	0.7	0.5	0.9	0.5	0.7	0.6	0.8	0.7	1.2
08:00	3.0	3.4	4.4	5.0	5.6	4.7	4.9	5.0	5.2	7.1	5.9	5.1
	0.8	1.5	1.6	1.4	0.9	1.4	1.2	1.5	1.5	2.6	2.2	1.9
09:00	6.8	5.9	6.6	7.3	7.5	5.7	6.2	6.5	7.0	9.2	9.3	9.3
	2.0	3.0	2.3	2.6	0.9	1.7	1.7	2.1	2.2	4.8	3.2	4.1
10:00	9.7	8.7	8.4	8.6	9.3	6.7	7.2	8.0	8.6	10.5	10.2	11.4
	3.3	3.9	3.1	3.0	1.4	1.9	2.2	2.3	2.6	5.4	3.9	5.8
11:00	9.9	10.9	9.8	9.9	10.1	7.7	8.3	9.1	9.6	12.1	9.9	11.3
	3.0	4.9	3.3	3.0	1.9	2.2	2.4	2.4	2.4	6.7	4.5	6.1
12:00	11.3	12.1	10.8	11.8	10.7	8.6	9.1	9.8	10.9	10.1	10.0	11.7
	4.1	5.6	3.4	3.7	2.0	2.3	2.3	2.4	2.6	5.1	3.5	5.8
13:00	12.6	13.3	12.0	11.6	10.8	9.4	9.8	10.5	11.6	10.0	10.6	12.1
	4.6	5.7	3.6	3.3	2.3	2.2	2.2	2.2	2.5	4.2	3.2	5.9
14:00	14.4	13.1	12.3	11.1	10.9	10.8	10.7	11.1	11.6	10.3	11.3	12.2
	4.3	4.9	3.2	2.4	1.6	1.9	2.0	2.0	2.2	3.6	2.2	4.9
15:00	13.3	12.2	12.0	10.6	10.4	10.6	10.3	10.8	11.0	11.2	12.2	10.9
	2.8	3.8	3.1	1.9	1.1	1.7	1.7	1.8	1.9	2.4	1.8	3.4
16:00	11.1	10.4	10.6	8.9	8.8	12.6	11.0	9.6	9.4	10.1	10.8	9.0
	1.6	2.6	1.9	1.6	1.1	0.9	1.4	1.4	1.5	1.5	1.4	2.3
17:00	6.0	7.0	7.6	6.6	6.9	10	9.4	7.9	6.7	6.3	5.5	5.2
	1.0	1.2	1.2	1.2	0.8	0.5	0.5	1.0	0.9	1.2	0.9	3.2
18:00	1.1	1.9	3.0	4.3	3.9	5.6	5.7	5.0	3.1	2.1	1.3	0.7
	0.4	0.4	0.8	3.7	0.6	0.4	0.3	0.5	0.8	0.7	0.5	0.4

**Table 3.9** Percentages of hourly diffuse horizontal insolation from daily total diffuse insolation, ( $F_{j(\text{diffuse})}$  calculated by Eq.3.13 and tabulated as mean monthly values). The standard deviations from the means are presented in the second row of each hour.

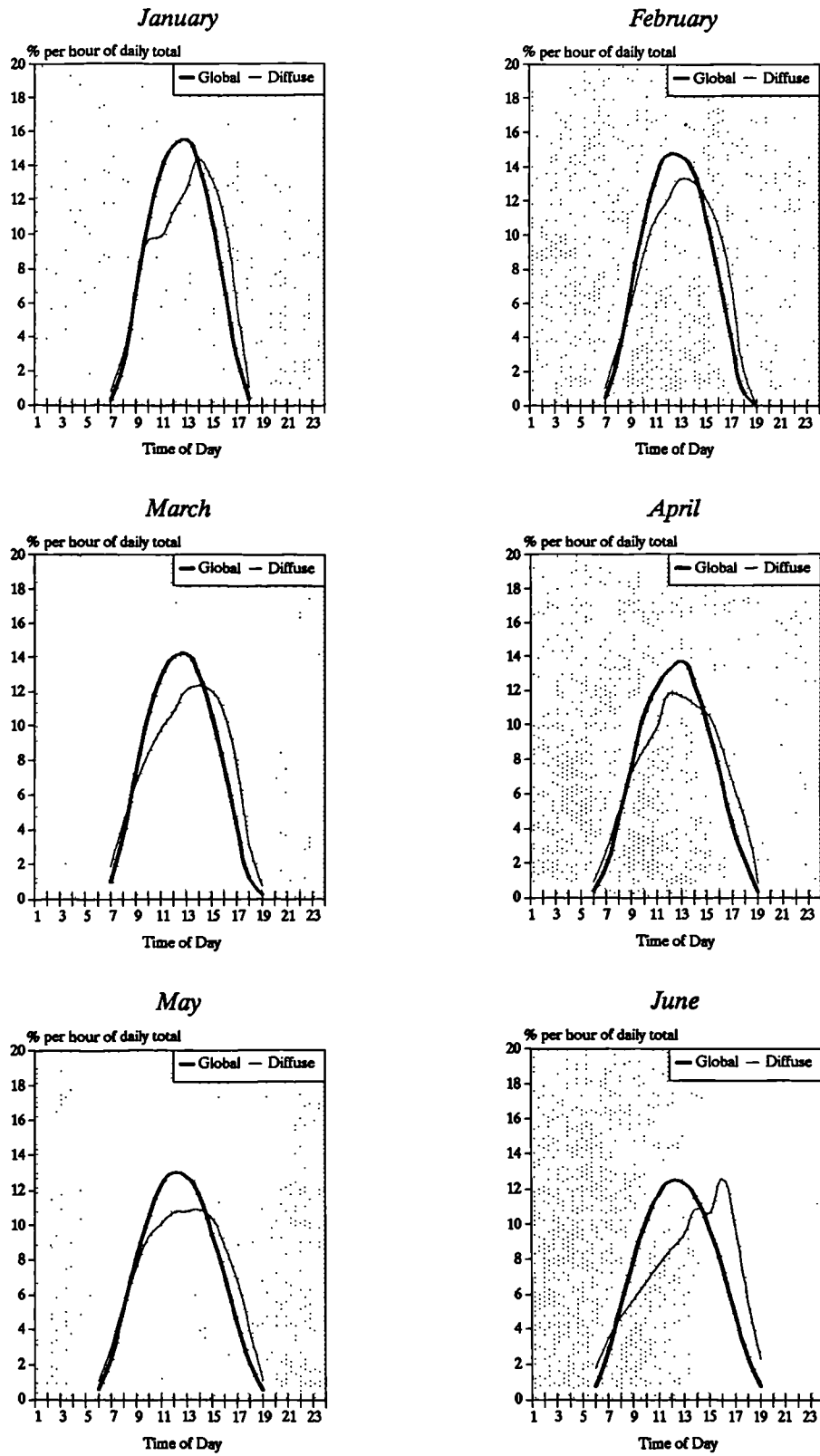
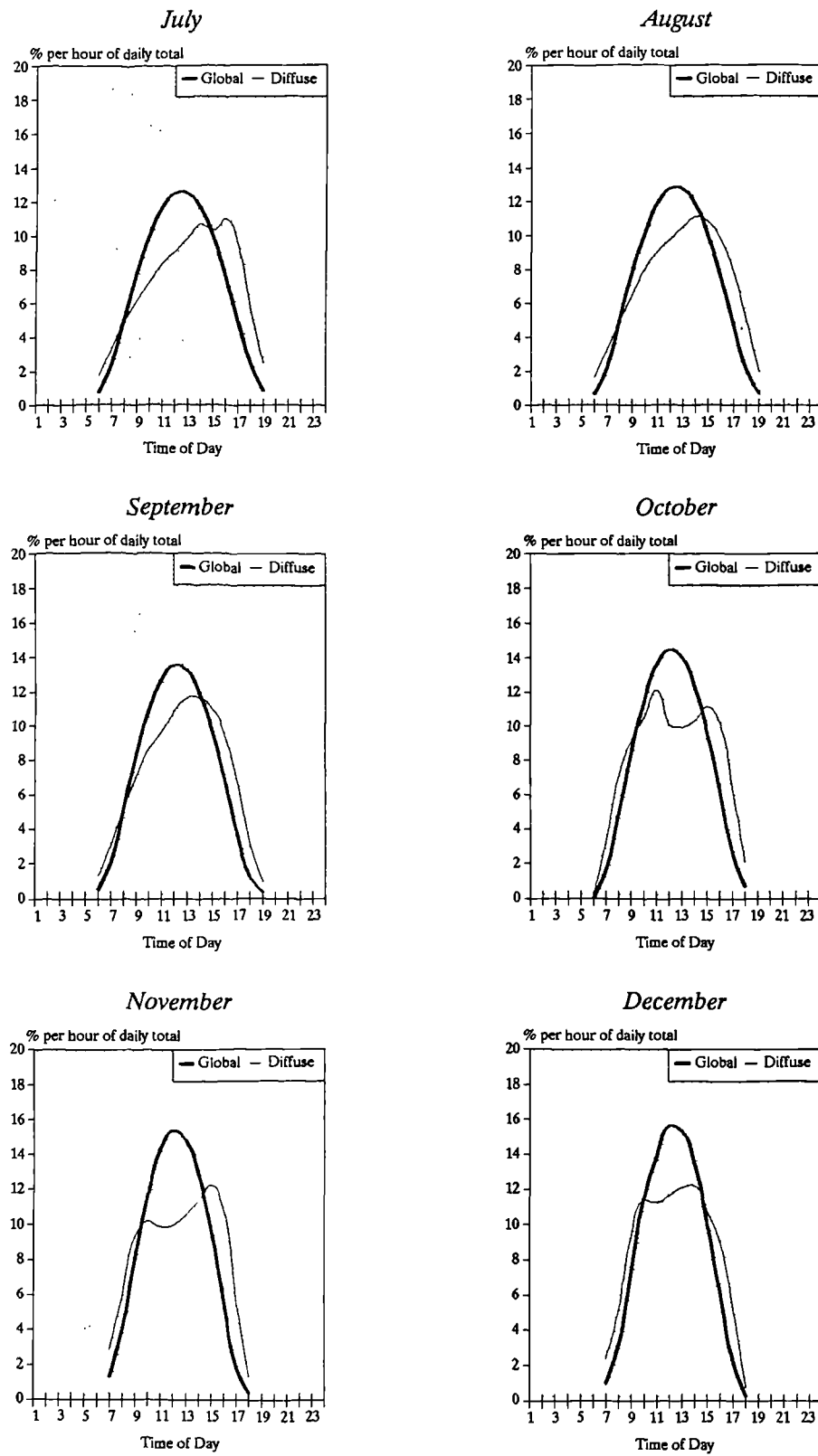


Figure 3.25

Variation of global and diffuse insolation with time of day in Riyadh for the months January–April. The curves on each graph represent the percentages  $F_j(\text{global})$  &  $F_j(\text{diffuse})$  discussed in section (3.4.3). Note the asymmetrical nature of the diffuse insolation about midday.



**Figure 3.26**

Variation of global and diffuse insolation with time of day in Riyadh for the months May–August. The curves on each graph represent the percentages  $F_j(\text{global})$  &  $F_j(\text{diffuse})$  discussed in section (3.4.3).

### 3.5 Relationship Between Insolation and Sunshine Duration in Riyadh

---

In applied solar energy studies it is useful to have simple methods for estimating the monthly mean daily amounts of solar radiation (i.e. global and diffuse insolation).

Several empirical formulae have been developed to calculate the global insolation using various meteorological parameters. Some of the parameters covered in the literature include (1) sunshine hours as in (Page 1961, Khogali et. al. 1983, Said 1985, Raja and Twidell, 1989); (2) precipitable water content, turbidity and surface albedo (Hoyt 1978); (3) relative humidity, sunshine duration and mean temperature (Reddy et. al. 1971); (4) number of rainy days, sunshine hours, latitude and location of place relative to the sea (Reddy 1971); (5) sunshine duration, relative humidity, maximum temperature, latitude and location (Sabbagh et. al 1977).

For estimating diffuse horizontal insolation, the empirical correlations put forward by Liu and Jordan (1960) and Page (1961) are the most widely used. Several new empirical equations using diffuse, global, extraterrestrial insolation and sunshine duration, have been proposed and applied to various locations (see Iqbal 1979; Lewis 1983; Castro-Diez et al. 1989 and Cappolino 1989). The Strathclyde University, Energy Studies Unit, PhD thesis by Raja (1992) considers this subject in great detail.

From the literature reviewed (regarding application to Saudi Arabia) Sabbagh et. al (1977) developed iso-radiation maps calculated by applying their proposed formula for the year 1973. The formation of their empirical equation is quite complicated and cannot be applied to the data of this research. However, the Angstrom regression equation provides the best estimation relation for global insolation (Lewis 1989). This relation was used by SANCST (now KACST) (1983) to produce the Solar Atlas for Saudi Arabia based on homogenized data over the period 1971-1980.

The following study examines the relationship between (1) global horizontal insolation and sunshine duration, (2) diffuse and global horizontal insolation, from average daily data for Riyadh over the period 1985-1986. The Angstrom type equation in the form of ( $Y = a + bX$ ) was applied to develop regression equations for the estimation of mean monthly global and diffuse insolation for the region.

	Jan	Feb	Mar	Apr	May	Jun	Jul	Aug	Sep	Oct	Nov	Dec	Year
Coeff., a	0.52	0.52	0.17	0.27	0.16	0.43	0.37	0.42	0.19	0.54	0.43	0.42	0.42
Std. Err	0.09	0.07	0.03	0.05	0.05	0.01	0.02	0.01	0.06	0.02	0.09	0.10	0.03
Coeff., b	0.15	0.15	0.57	0.43	0.62	0.30	0.38	0.31	0.56	0.17	0.23	0.26	0.29
Std. Err	0.06	0.04	0.03	0.03	0.06	0.03	0.04	0.04	0.08	0.06	0.07	0.06	0.06
Corr. R	0.67	0.72	0.97	0.92	0.90	0.91	0.87	0.81	0.76	0.69	0.76	0.73	0.82

**Table 3.10** Constant coefficients (a&b) with their standard deviation errors, for use in Equation 3.14. Values were determined from regression analysis over compiled climatic data (1985–1986) from the Solar Village, Saudi Arabia. (Lat. 24.54, Long. 46.24). See Fig.3.26.

	Jan	Feb	Mar	Apr	May	Jun	Jul	Aug	Sep	Oct	Nov	Dec	Year
<i>(set 1) RIYADH Data</i>													
Coeff., a	0.26	0.15	0.26	0.33	0.34	0.38	0.43	0.34	0.28	0.41	0.29	0.27	0.29
Coeff., b	0.45	0.64	0.51	0.32	0.33	0.29	0.24	0.29	0.31	0.33	0.49	0.50	0.41
<i>(set 2) AL-KHARJ</i>													
Coeff., a	0.37	0.34	0.39	0.29	0.29	0.41	0.36	0.27	0.37	0.24	0.40	0.24	0.32
Coeff., b	0.37	0.40	0.38	0.44	0.44	0.30	0.36	0.44	0.35	0.41	0.27	0.48	0.41

**Table 3.11** Regression constants (a&b) for: set 1 from data of Riyadh (Lat. 24.34, Long. 46.43), and set 2 from data of Al-Kharj (Lat. 24.10, Long. 47.24), based on 10 years of measured data. After SANCST (Saudi Arabian Solar Radiation Atlas, 1983). See also Fig.3.27.

### 3.5.1 Estimation of Monthly Mean Daily Global Insolation from Sunshine Data

The relationship between global insolation and sunshine period can be estimated in the usually accepted procedure using regression equations of the Angstrom type:

$$G_h = G_0 [a + b (n / N)] \quad \{3.14\}$$

where

$G_0$  is the average daily extraterrestrial insolation for the latitude of Riyadh ( $\text{Wh m}^{-2} \text{day}^{-1}$ )

$n$  is the mean daily period of observed bright sunshine (h)

$N$  is the mean daily period between sunrise and sunset (h)

$a$  and  $b$  are climatically determined regression constants.

Equation (3.3) can be solved for the sunrise hour angle ( $\omega_s$ ) when  $\theta_z = 90^\circ$ :

$$\cos(\omega_s) = -\tan(\phi) \tan(\delta) \quad \{3.15\}$$

It follows that the day length ( $N$ ) is given by: (Duffie 1980)

$$N = (2h/15) \cos^{-1}[-\tan(\phi) \tan(\delta)] \quad \{3.16\}$$

The extraterrestrial insolation is calculated by

$$G_0 = I \cdot (24/\pi) \cdot [(1 + 0.033 \cos(360 J/365)) \cdot (\cos(\phi) \cos(\delta) \sin(\omega_s) + (2\pi \omega_s/360) \sin(\phi) \sin(\delta))] \quad \{3.17\}$$

where  $I$  = solar constant ( $1353 \text{ W m}^{-2}$ ) at the mean solar–earth distance.

Calculated mean monthly daily extraterrestrial insolation, sunshine duration and measured sunshine hours are provided in Table 3.6. Regression analysis of daily ( $G_h/G_0$ ) and ( $n/N$ ) for each month yield the coefficients ( $a$  and  $b$ ) presented in Table (3.10). The yearly coefficients ( $a = 0.419$ ,  $b = 0.292$ ) with a correlation factor of ( $R = 0.82$ ) were obtained from regression over mean monthly daily values.

The monthly correlations ( $R > 0.8$ ) are best obtained for the months March–August with the rest,  $R$  being about 0.7. However, the percentage difference between calculated and measured global horizontal insolation (using the monthly values of  $a$  and  $b$ ) for the year 1986 is well within  $\pm 4\%$  (see Figure 3.27). Thus, applying the yearly coefficients produced differences varying from  $-8\%$  to  $+11\%$  (Fig.3.28).

Mean monthly daily global insolation for 1986 were also calculated from the regression coefficients ( $a$  and  $b$ ) of Table (3.11). These coefficients were obtained from the Saudi Arabian Solar Atlas (SANCST 1983) for two meteorological stations near the Solar Village (Riyadh and Al-Kharj).

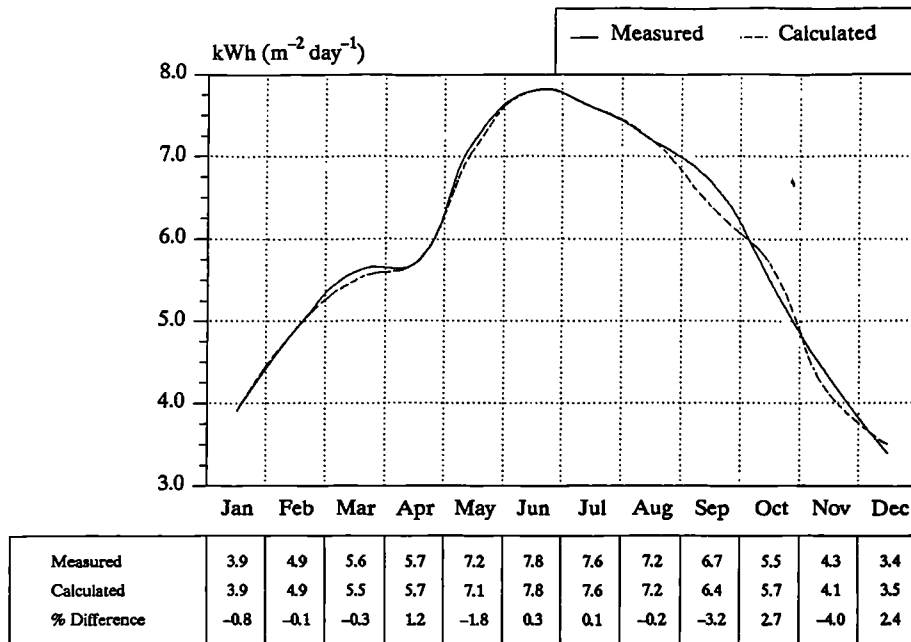


**Figure 3.27** Monthly mean daily global insolation over the Solar Village, for the year 1986. A comparison between measured, and calculated values using the monthly constants of Table 3.10 in Eq.(3.14).

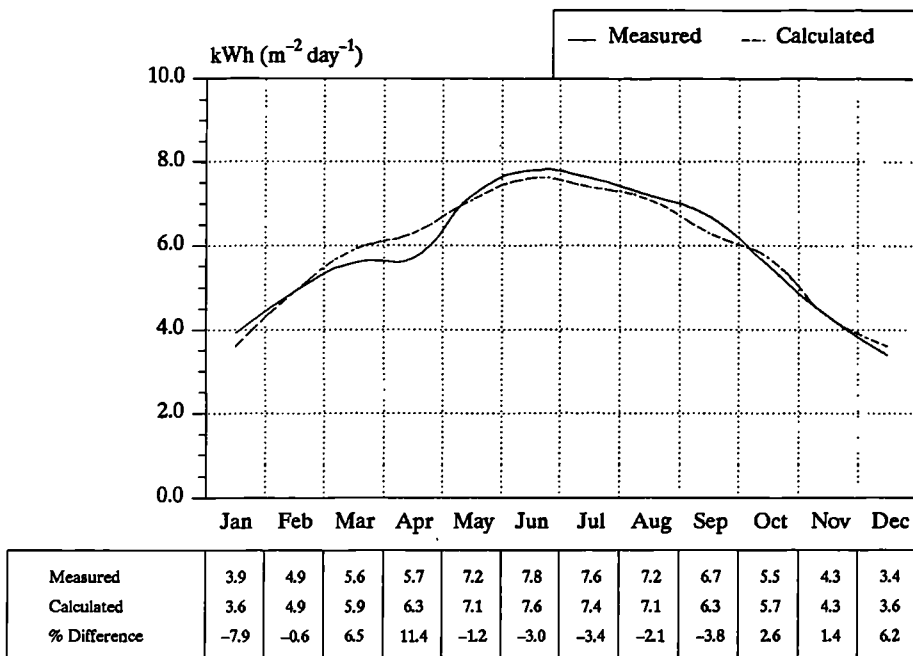


**Figure 3.28** A comparison between measured, and calculated monthly mean daily global insolation over the Solar Village, for the year (1986) using the yearly constants ( $a = 0.42$ ,  $b = 0.29$ ) in Eq.(3.14).

Although results indicate high percentage differences from measured values of 1986 (see Figure 3.29), the correlation of Al-Kharj data produced better estimates than Riyadh's.

Inter-comparison between the determined correlation values (a and b) and those published by SANCST is by no mean an indication of validity; hence no information could be obtained regarding the instruments used and reliability of the periods of records for the published data. Furthermore, independent analysis by Hansen (1989) showed that the Saudi Arabian Solar Atlas data were too general.

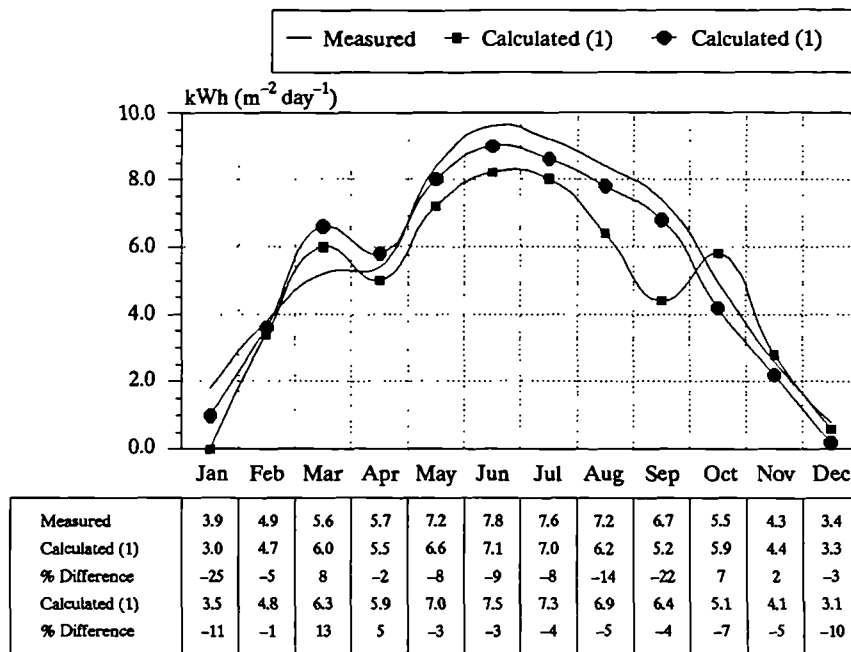


**Figure 3.29**

A comparison between measured, and calculated monthly mean daily global insolation over the Solar Village, for the year (1986) using the two sets of monthly constants of Table (3.11).

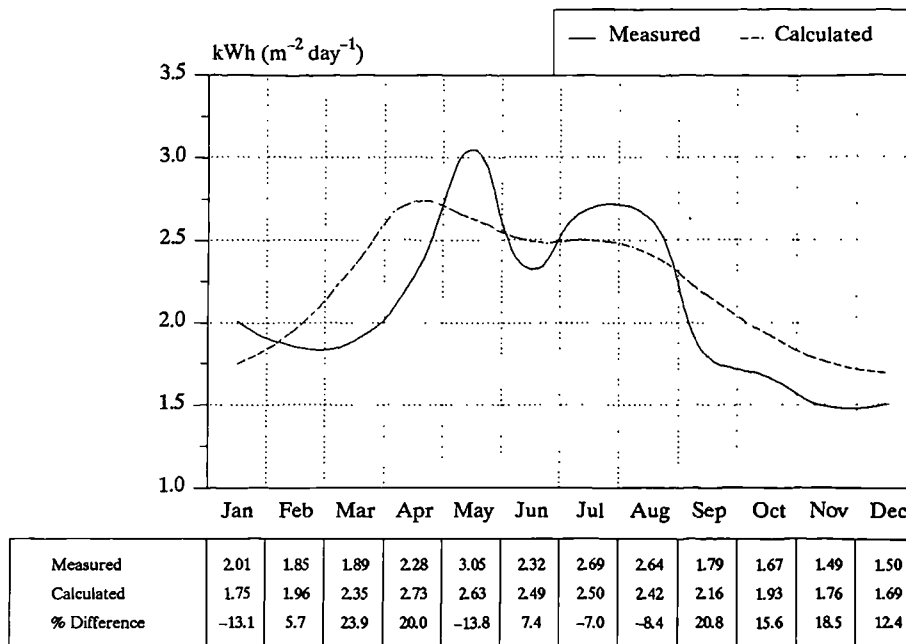


**Figure 3.30** Monthly mean daily diffuse horizontal irradiation over the Solar Village, for the year 1986. A comparison between measured, and calculated values using the yearly coefficients ( $c = 1.061$ ,  $d = -1.054$ ) in Eq. (3.18).

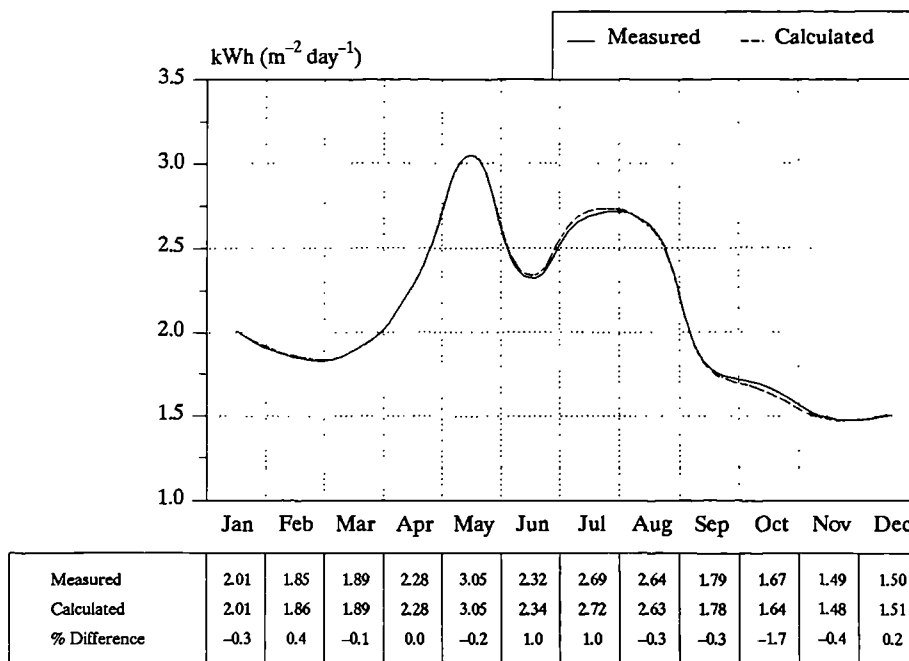


**Figure 3.31** A comparison between measured, and calculated monthly mean daily diffuse insolation over the Solar Village, for the year (1986) using monthly regression coefficients of Table 3.12 in Eq.(3.18).

### 3.5.2 Estimation of Monthly Mean Daily Diffuse Horizontal Insolation

Generally, two types of simple correlation are commonly used to estimate diffuse insolation ( $G_d$ ), (1) as a function of global and extraterrestrial insolation and (2) as a function of possible sunshine duration and extraterrestrial insolation. For the first type, Page (1978) has proposed the linear expression

$$G_{fh}/G_h = c + d (G_h/G_0) \quad \{3.18\}$$

where  $c$  and  $d$  are climatically determined regression constants.

In literature, the most common empirical correlation of the second type (Iqbal 1979) is:

$$G_{fh}/G_0 = c + d (n/N) \quad \{3.19\}$$

Preliminary analysis using Eq. 3.19 gave very poor correlation coefficients ( $R < 0.3$ ). The regression expression (Eq. 3.18) on the other hand produced far better correlation.

Regression analysis of daily ( $G_{fh}/G_h$ ) and ( $G_h/G_0$ ) for each month yielded the coefficients ( $c$  and  $d$ ) presented in Table (3.12). The yearly coefficients ( $c = 1.061$ ) and ( $d = -1.054$ ) with a correlation factor of ( $R = 0.77$ ) were obtained from regression over mean monthly daily values.

The percentage differences between calculated and measured mean monthly daily values (Fig. 3.30) were within  $-15\%$  and  $+20\%$ . The percentage differences by the use of monthly values of ( $c$  and  $d$ ) were within  $\pm 2\%$  (see Figure 3.31).

	Jan	Feb	Mar	Apr	May	Jun	Jul	Aug	Sep	Oct	Nov	Dec	Year
Coeff., $c$	1.18	1.76	1.12	1.24	1.29	2.23	2.16	2.12	2.79	2.20	1.96	1.10	1.06
Std. Err	0.11	0.21	0.10	0.08	0.04	0.04	0.04	0.06	0.06	0.12	0.09	0.15	0.05
Coeff., $d$	-1.10	-2.16	-1.22	-1.44	-1.30	-2.75	-2.58	-2.55	-3.61	-2.82	-2.61	-1.12	-1.05
Std. Err	0.16	0.50	0.12	0.12	0.12	0.37	0.23	0.49	0.57	0.68	0.35	0.17	0.28
Corr. R	0.78	0.65	0.87	0.92	0.89	0.81	0.89	0.69	0.77	0.61	0.81	0.77	0.77

**Table 3.12** Constant coefficients ( $c$  &  $d$ ) with their standard deviation errors, for use in Eq.(3.18). Values were determined from regression analysis over compiled climatic data (1985 & 1986) from the Solar Village, Saudi Arabia. (Lat. = 24.54, Long. = 46.24).

## 3.6 Conclusion

---

The main objective of defining a reference climate year for use in energy simulation programs has been accomplished. The uncertainties of different aspects in processing the climatic data were outlined. The results were presented mostly in graphical format which is easy to read. Daily meteorological data are tabulated in Appendix A, and insolation data in Appendix B.

The nature of the Riyadh climate and the availability of reliable data made it possible to develop procedures for predicting climatic variable (i.e. insolation and temperature) with a high degree of accuracy. Thus by discussing and presenting these studies, a better description of the region climate has been achieved.

The general conclusions describing the climate of this region (Riyadh), with reference to human comfort are as follows:

- The ambient air temperatures (in the shade) are considerably above indoor building comfort temperatures for most of the year (April through to October). During the months of December through to February the ambient temperature falls below comfort levels.
- Diurnal temperature changes (daily and seasonal variations) are typical of a desert climate, where the clearness of the sky contributes to such phenomena. In terms of building design, passive measures are needed to combat such variations (e.g. thermal mass of building fabric, insulation, surface properties, etc).
- Relative humidity is extremely low, and humidification is desirable for comfort.
- Wind speeds are generally low with the highest values being during the mid day time. In terms of building design and active solar applications (e.g. PV systems), the major concern associated with wind is the considerable amount of dust blown with it and hence the decrease in insolation and the covering of surfaces.
- Insolation received at this region is high, which is most encouraging from the point of view of solar capture application. On the other hand, shading and other cooling strategies are essential for human comfort (as for the individuals and their shelters).
- Diffuse insolation in the afternoons is greater than in the mornings. (see the asymmetrical nature of the diffuse radiation about noon in Figures 3.25 & 3.26). Blowing dust and the significant haze conditions in the afternoons contribute to this phenomena. Haze and dust storms are more persistent in summer than winter.

### 3.7 References

---

- Anderson B. (1974) "Meteorological Data for Design of Building and Installation", Report No. 89, Danish Building Research Institute, Holland.
- Angstrom A. (1924) "Solar and Terrestrial Radiation", *Q. J. R. Met. Soc.*, 50, pp 121-26.
- Barry R. & Chorley R. (1976) Atmosphere, Weather and Climate. Methuen & Co. Ltd., London.
- Bowen A. (1983) "Bioclimatic Comfort Analysis for 8 Cities in Saudi Arabia", Technical and lecture notes, School of Environmental Design, King Abdul-Aziz University, Jeddah, Saudi Arabia.
- Budyko M. (1963) Atlas of the Heat Budget of the Earth. Gidrometeorizdat, Mosko. (cited in Falconer P. & Peyinghaus W. (1975).
- Cappolino S. (1989) "A Simple Model For Computing Diffuse Solar Radiation", *Solar Energy*, 43 (6), pp 385-89
- Castro-diez Y., Alados-arboledas L. & Jimenez I. (1989) "A Model for Climatological Estimation of Global, Diffuse and Direct Solar Radiation on a Horizontal Surface", *Solar Energy*, 43 (5), pp 417-24.
- Clarke J. (1985) Energy Simulation in Building Design. Adam Hilger Ltd., Bristol, UK.
- Cooper P. (1969) "The Absorption of Solar Radiation in Solar Stills", *Solar Energy*, 12 (3).
- Duffie J. & Beckman W. (1980) Solar Engineering of Thermal Processes. Wiley, New York.
- Evans M. (1980) Housing, Climate and Comfort. The Architectural Press, London.
- Falconer P. & Peyinghaus W. (1975) "Radiative Balance in the Atmosphere as a Function of Season, Latitude and Height", *Arch. Meteorol. Geoph. Biokl., Ser. B* (23), pp 201-23.
- Hansen J. (1990) Private communication. (Address: 1 Allander Avenue, Bardowie, Glasgow G62 6EU, U.K.)
- Holmes M. & Hitchin E. (1978) "An Example Year for the Calculation of Energy Demand in Buildings", *J. Build. Serv. Eng.*, (January).

Hoyt D. (1978) "A Model for the Calculation of Solar Global Insolation", *Solar Energy*, 21, pp 27-35

IHVE (1973) "Some Fundamental Data Used by Building Services Engineers", Report, Working Group 6, Building Services Subcommittee of CACCI, London.

Iqbal M. (1979) "Correlation of Average Diffuse and Beam Radiation with Hours of Bright Sunshine", *Solar Energy*, 23 (2), pp 169-73.

KACST (1988) [King Abdulaziz City for Science and Technology]. Climatic Data For The Solar Village 1984-86: Digital extracts from the Data Acquisition Systems of the Photovoltaic Power Site (PVPS). HYSOLAR Program, Huraib F. (Director), Riyadh, Saudi Arabia.

KACST (undated) "The Solar Village". A brochure on one area of the SOLERAS program in Saudi Arabia, Al-Mutawa Press, Dammam, Saudi Arabia.

Koenigsberger O., Mahoney C. & Evans M. (1971) Climate and House Design. United Nation, Department of Economic & Social Affairs, New York.

Lewis G. (1983) "Diffuse Irradiation Over Zimbabwe", *Solar Energy*, 31, pp 125-28.

Lewis G. (1989) "The Utility of the Angstrom-type Equation for the Estimation of Global Irradiation", *Solar Energy*, 43 (5), pp 297-99.

Liu B. & Jordan R. (1960) "The Interrelationship and Characteristic Distribution of Direct, Diffuse and Total Solar Radiation", *Solar Energy*, 4 (3), pp 1-19.

Lund H. (1973) "Requirements and Recommendations for the Test Reference Year", *Proc. CIB Symp.* (cited in Clarke 1985).

Ministry of Defense and Aviation (1984) "Provisional Normals 1961-80", Tabulated data from Riyadh meteorological station # 40438, Saudi Arabia.

Oliver J. (1981) Climatology: Selected Applications. Edward Arnold Publishers, London.

Page J. (1961) "The Estimation of Monthly Mean Values of Daily Total Short-wave Radiation on Vertical and Inclined Surfaces from Sunshine Records for Latitudes 40N-40S", *Proc. of U.N. Conf. on New Sources of Energy*, Rome, Paper No. 35/5/98.

Page J. (1978) "Methods for the Estimation of Solar Energy on Vertical and Inclined Surfaces", Internal Report (BS-46), Department of Building Science, University of Sheffield, U.K.

Paassen A. & Liem S. (1982) "Short Series of Weather Data for Energy Analysis – Short Reference Year", Final report, contract # ESF-028-NL (RS), Delft, The Netherland.

Raja I. (1992) "Solar Radiation Assessment In Pakistan", PhD thesis, Energy Studies Unit, University of Strathclyde, Glasgow, U.K.

Raja I. & Twidell J. (1989) "Distribution of Global Insolation over Pakistan", *Solar Energy*, 43 (6), pp 355–57.

Reddy S. (1971) "An Empirical Method for the Estimation of Total Solar Radiation", *Solar Energy*, 13, pp 289–90.

Reddy S. (1971) "An Empirical Method for the Estimation of Net Radiation Intensity", *Solar Energy*, 13, pp 291–92.

Sabbagh J., Sayigh A. & El-Salam E. (1977) "Estimation of the Total Solar Radiation from Meteorological Data", *Solar Energy*, 19, pp 307–11

Said M. (1985) "Predicted and Measured Solar Radiation in Egypt", *Solar Energy*, 35 (2), pp 185–88.

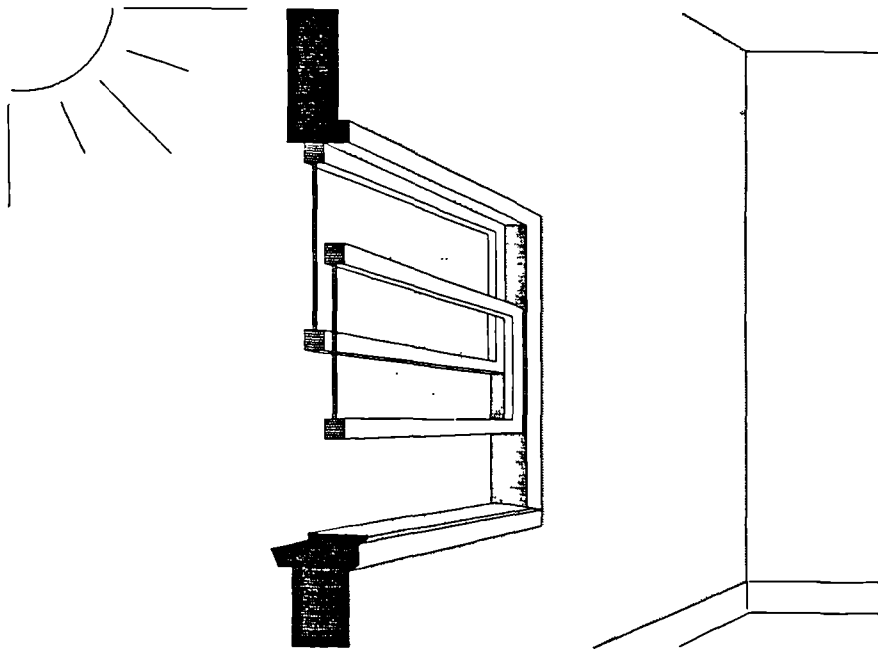
SANCST (1983) "Saudi Arabian Solar Radiation Atlas", The Saudi Arabian National Centre for Science and Technology, Riyadh, Saudi Arabia.

Schyfsma E. (1978) "General Information on the Arabian Peninsula: Climate". In Quaternary period in Saudi Arabia: Sedimentological, Hydrogeological, Hydrochemical, Geomorphological and Climatological Investigations in Central and Eastern Saudi Arabia. Sayari S., Zotl J. (Eds.), Springer-Verlag, Wien, Austria.

Saito H. & Matsuo Y. (1974) "Standard Weather Data for SHASE Computer Program", *Proc. 2nd symp.*, "Use of computers for environmental engineering related to buildings". (cited in Clarke 1985).

Stamper E. (1977) "Weather Data", *ASHRAE J.*, February, p.47

# Chapter 4



## 4. GLAZING ENERGY PROCESSES AND SOLAR CONTROL DEVICES

### 4.1 Introduction

---

One of the characteristics of modern architecture is the use of large expanses of glass in the building facades, irrespective of the climate. This has resulted in the overheating of buildings owing to excessive heat gain even in temperate climates. An effective improvement to the overheating problem can be achieved through the use of shading devices. Shading devices can be applied either externally, internally or between double glazing. They may be fixed, adjustable or retractable and of a variety of architectural shapes and geometrical configurations.

Recent advances in glass technology have succeeded in the production of special glasses with varying solar optical properties, (e.g. heat absorbing, heat reflecting and photo-chromatic glasses, and transparent films applied to glass surfaces). These developments can also provide some form of solar control of fenestration without necessitating the reduction of glass area.

However, proper selection of the type of glass and shading devices is important for reducing the heat gains or losses through glazed areas and thus the energy demands for maintaining indoor thermal environments at comfortable levels. To estimate the solar heat gain through different types of glass (as discussed in chapter 2) their spectral reflection, absorption and transmission characteristics for the entire range of wavelengths of solar spectrum are required.

This chapter discusses these properties of glass, and elaborates on the convective & radiative heat transfer at glazing surfaces (which can also apply to other building surfaces), before setting up a computer program to calculate the maximum solar heat flux gain through a clear window glass under the climate of Riyadh, Saudi Arabia. The output of this model is tabulated in Appendix (D) and its use was covered earlier in chapter 2.

Simplified design tools for solar control are widely available in many literature, among which is the pioneering book of Olgyay & Olgyay (1957). In this chapter, a brief discussion of their method is presented, with emphasis on the sun and shading device angular relationship. Finally, the chapter concludes with a performance review of solar control glazing and different shading devices (external & internal).

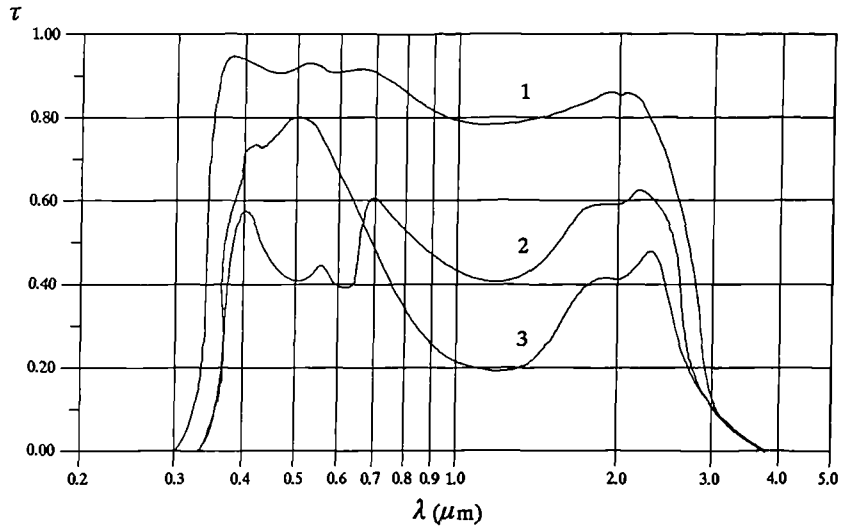


**Figure 4.1** Solar spectral transmittance for typical architectural glass. (reproduced from Brunello & Zecchin 1987).

- (1) Common window clear glass (3mm)
- (2) Grey heat absorbing glass (6mm)
- (3) Green heat absorbing glass (6mm)

## 4.2 Solar Characteristics of Glass

---

When a beam of solar radiation is incident on a glass surface, part is reflected, part is absorbed by the glass and the rest is transmitted. The relative proportions of these three components depend on the type of glass, thickness of the pane, the angle of incidence and the spectral composition of the radiation. The spectral transmittance depends on the chemical composition of the glass, tint and colour and special surface coatings.

In order to obtain the solar transmission and absorption characteristics of a specific glass, its *reflection*, *absorption* and *transmission* factors for monochromatic radiation must be determined for the full range of spectral bands of insolation. In general, measured data on the spectral transmission for normal incidence are available for most of the common types of architectural glass, (usually provided in technical literature of the product manufacturer). The spectral transmittance of clear and heat-absorbing glass is shown in Figure (4.1).

For monochromatic radiation, the variations with angle of incidence in solar reflectance and transmittance of a glass can be derived theoretically from the normal incidence transmittance data. Parmelee (1954), Mitalas & Stephenson (1962) and Petherbridge (1967) have dealt with this problem in more detail. (see also section 5.6.2 of the next chapter).

The present section briefly presents the monochromatic radiation relationships which have been utilised in a correlation procedure suitable for computer calculations as given by ASHRAE (1985) and adopted here for later use in section 4.4

The ratio of reflected to incident radiation for a single reflection at an air-glass interface is given by Fresnel's formula as

$$r = 0.5 \left[ \frac{\sin^2(\theta - \theta_r)}{\sin^2(\theta + \theta_r)} + \frac{\tan^2(\theta - \theta_r)}{\tan^2(\theta + \theta_r)} \right] \quad \{4.1\}$$

where  $\theta$  and  $\theta_r$  are the angles of incidence and refraction, respectively. The angle of refraction is obtained from Snell's law as

$$\sin(\theta_r) = \sin(\theta) / v \quad \{4.2\}$$

where  $v$  is the glass index of refraction ( $v = 1.526$  is a common assumption for glass). The part that is absorbed by the glass while the insolation beam is traversing through the glass depends on the product of the extinction coefficient of the glass,  $K$  ( $\text{cm}^{-1}$ ), and the path length  $L$  (cm). The fraction that is transmitted ( $T$ ) is given by Bouguer-Lambert's law as

$$T = e^{-KL} \quad \{4.3\}$$

For a glass sheet of thickness  $x$  the path length ( $L$ ) traversed through the glass is given by

$$L = x / \cos(\theta_r) \quad \{4.4\}$$

Figure 4.2 Multiple reflection and transmission through a thin glass sheet of finite thickness.

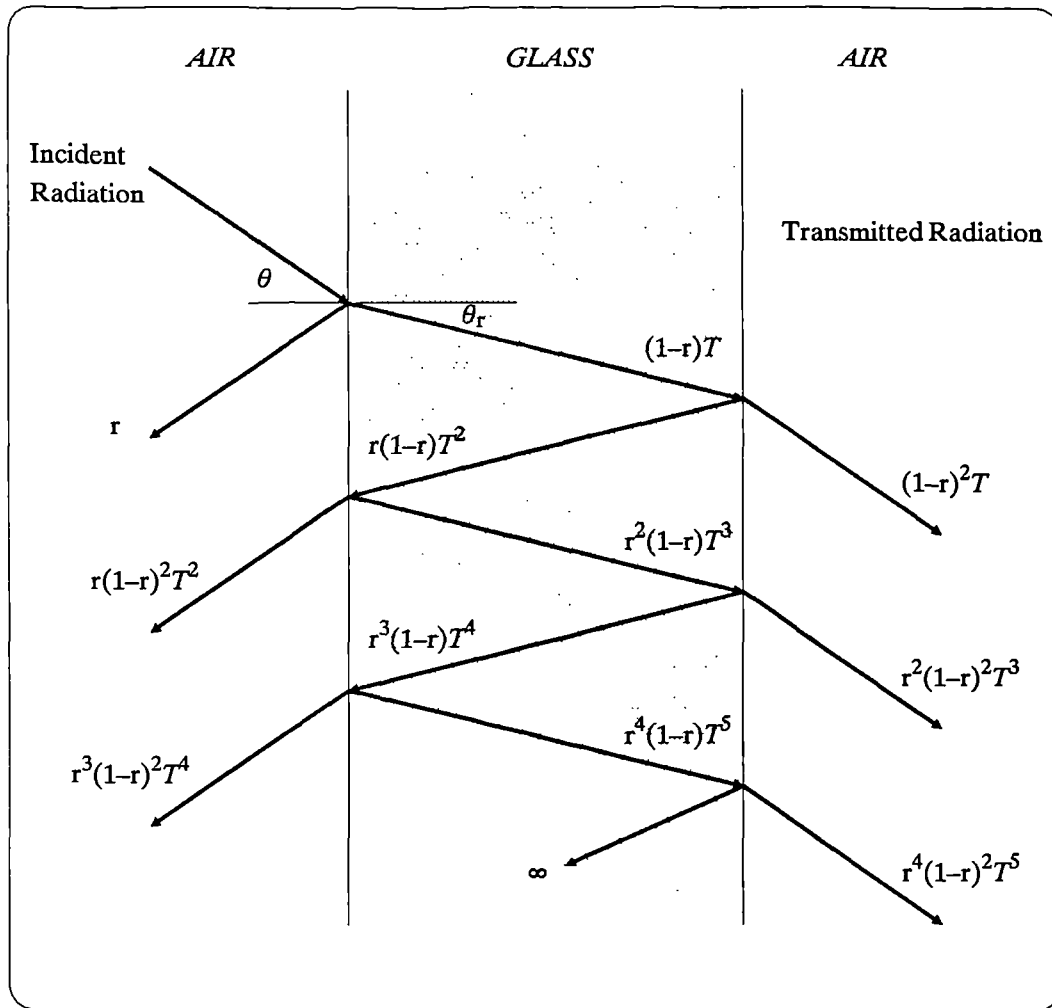


Table 4.1 Polynomial coefficients of transmittance and absorptance factors of a clear window glass (3mm), for use in Eq.4.11 through Eq.4.14. (after ASHRAE 1985).

j	$a_j$	$t_j$
0	0.01154	-0.00885
1	0.77674	2.71235
2	-3.94657	-0.62062
3	8.57881	-7.07329
4	-8.38135	9.75995
5	3.01188	-3.89922

For a glass sheet of finite thickness, multiple reflections will take place at each surface as illustrated in Figure (4.2). The net fraction of radiation finally transmitted after successive reflections is then obtained by the summation of an infinite series. Hence the expression for the total monochromatic transmissivity ( $\tau_\lambda$ ) and reflectivity ( $\rho_\lambda$ ) are given by Eq.4.5 & Eq.4.6 respectively; and from the fact that the sum of reflected, absorbed and transmitted components is unity, the absorptivity is obtained from Eq.4.7

$$\tau_\lambda = (1 - r)^2 T / (1 - r^2 T^2) \quad \{4.5\}$$

$$\rho_\lambda = [r + r(1 - r)^2 T^2] / (1 - r^2 T^2) \quad \{4.6\}$$

$$\alpha_\lambda = 1 - \rho_\lambda - \tau_\lambda \quad \{4.7\}$$

The foregoing is valid for monochromatic radiation if the extinction coefficient ( $K$ ) of a glass is known as a function of the wavelength of radiation. The overall transmissivity of glass for insolation is obtained by integration over the whole solar spectrum (effectively in the range of 0.3 to 2.8  $\mu\text{m}$ )

$$\tau = [ \sum (G_\lambda \tau_\lambda) \Delta\lambda ] / [ \sum (G_\lambda \Delta\lambda) ] \quad \{4.8\}$$

Thus the solar transmittance of a glass at a particular angle of incidence is the weighted mean of the spectral transmittance at this angle. Similarly, the solar reflectivity ( $\rho$ ) and absorptivity ( $\alpha$ ) are obtained by

$$\rho = [ \sum (G_\lambda \rho_\lambda) \Delta\lambda ] / [ \sum (G_\lambda \Delta\lambda) ] \quad \{4.9\}$$

$$\alpha = [ \sum (G_\lambda \alpha_\lambda) \Delta\lambda ] / [ \sum (G_\lambda \Delta\lambda) ] \quad \{4.10\}$$

From the above it can be seen that the calculation procedures are complex. Stephenson (1965) has modified the calculation procedure to be more suitable for computer machine calculations by computing the transmissivity and absorptivity for various angles of incidence ( $\theta = 0^\circ$  to  $90^\circ$ ) and expressing the results as polynomial functions of  $\cos(\theta)$ . For direct insolation the transmission and absorption equations become

$$\tau(\theta) = \sum t_j \cos^j(\theta) \quad \text{for } j = 0 \text{ to } 5 \quad \{4.11\}$$

$$\alpha(\theta) = \sum a_j \cos^j(\theta) \quad \text{for } j = 0 \text{ to } 5 \quad \{4.12\}$$

The polynomial coefficients for transmission ( $t_j$ ) and absorption ( $a_j$ ) for clear window glass are given in Table (4.1). The transmittance and absorptance for diffuse insolation is obtained by integrating the above expressions for angles of incidence of 0 to  $\pi/2$ . This assumes there is no directional symmetry to the diffuse radiation. These are thus obtained as

$$\tau_{(\text{diffuse})} = 2 \sum [ t_j / (j + 2) ] \quad \{4.13\}$$

$$\alpha_{(\text{diffuse})} = 2 \sum [ a_j / (j + 2) ] \quad \{4.14\}$$

### 4.3 Heat Transfer at Glazing Surfaces

---

The heat transfer from or to a glass surface involves a combination of radiation and convection. Assuming steady-state conditions, the total rate of heat transfer,  $Q$  (W) at a surface of area  $A_s$  ( $m^2$ ), is given by the expression

$$Q = h A_s (T_s - T_e) \quad \{4.15\}$$

where  $T_s$  is the mean surface temperature (K);  $T_e$  is the mean temperature of the surrounding environment; and  $h$ , the total surface heat transfer coefficient in  $W (m^{-2} K^{-1})$ , is the sum of radiative ( $h_r$ ) and convective ( $h_v$ ) heat transfer coefficients, i.e.

$$h = h_r + h_v \quad \{4.16\}$$

Equations 4.15 and 4.16 define the heat transfer coefficients which are non-linear functions of temperature. Standard values of internal and external surface heat transfer coefficients, for different surface properties and exposure to wind, can be obtained by inverting the values given in Tables 2.1 & 2.2 (see chapter 2). These values can be used to compare the thermal performance of different glazing systems. However, to compute the energy balance of a glazing system under, for example, the climate of Riyadh, these coefficients should be sensitive to changes in the external and internal environments.

Of the many environmental factors affecting the surface heat transfer coefficients, the most significant are:

- surface to air temperature difference,
- speed and direction of air flow across the external and internal surfaces,
- longwave radiation exchange between the surface of the fenestration and the surroundings.

There are more fundamental methods of separately calculating radiative and convective heat transfer from the basic laws of physics. Such methods are particularly important when large temperature differences occur. However for buildings, temperature differences greater than  $30^\circ C$  are unlikely to occur, so the simplified methods used generally and in this thesis for heat transfer are adequate.

The following discussion reviews the basic physical process and examines different numerical solutions of radiative and convective heat transfer coefficients. The discussion will be general, i.e. applying not only to internal and external glazing surfaces but also to other building surfaces (e.g. walls roofs and floors).

### 4.3.1 Radiative Heat Transfer at Internal Surfaces

The general equation for net radiation interchange between two surfaces 1 & 2 is given by (McAdams 1954) as

$$Q_r = f_{1-2} \sigma A_1 (T_1^4 - T_2^4) \quad \{4.17\}$$

where  $\sigma$  is the Stefan-Boltzmann constant, ( $\sigma = 5.67 \cdot 10^{-8} \text{ W m}^{-2} \text{ K}^{-1}$ );  $A_1$  is the surface area ( $\text{m}^2$ );  $T_1$  &  $T_2$  are the surfaces absolute temperatures (K); and  $f_{1-2}$  is an interchange factor involving the view factor and the emittance and absorptance of the surfaces. If the surface is a perfectly diffusing emitter and reflector, and if its emissivity is independent of temperature, then

$$f_{1-2} = [(1/F_{1-2}) + (1/\varepsilon_1) - 1 + (A_1/A_2) ((1/\varepsilon_2) - 1)]^{-1} \quad \{4.18\}$$

where  $\varepsilon$  is the hemispherical emissivity of a surface; and  $F_{1-2}$  is the geometric view factor, i.e. the fraction of radiation from surface 1 that is intercepted by surface 2. The calculation of  $F_{1-2}$  requires a complicated integration and different calculation procedures can be found in literature, e.g. Clarke (1985).

For a typical window glass (i.e. not coated with a low emissivity film) or a room surface radiating to the other room surfaces  $F_{1-2}$  is unity,  $\varepsilon_1 \cong \varepsilon_2$  and  $A_1 < A_2$  which allows the approximation

$$f_{1-2} = \varepsilon_1 \quad \{4.19\}$$

Measurements by Min et. al. (1956) at the ASHRAE Environment Laboratory found  $f_{1-2} = 0.876$  for the floor and  $f_{1-2} = 0.9$  for the ceiling, whilst  $\varepsilon_1$  and  $\varepsilon_2$  were both measured as 0.88 and using Eq.4.18 led to a calculated value for  $f_{1-2}$  of 0.85. On balance it would appear that for a typical room a value of  $f_{1-2}$  in the range 0.85 to 0.9 would be appropriate. It can also be noted that these measurements are consistent with the approximation in Eq.4.19 since most building materials (glass, mortar, wood, brick, etc) have an emissivity around the 0.9 value (see Table 2.4 in chapter 2).

Using the concept of linearised radiative heat transfer coefficient, Equation 4.17 can be expressed as

$$Q_{ri} = h_{ri} A_s (T_{si} - T_{ei}) \quad \{4.20\}$$

where  $T_{ei}$  is the mean temperature of the surrounding room surfaces (K);  $T_{si}$  is the temperature of the internal surface facing the room (K). From Eq.4.17 and Eq.4.20, the radiative heat transfer coefficient at internal surfaces,  $h_{ri}$ , is

$$h_{ri} = f_{si-ei} \sigma (T_{si}^2 + T_{ei}^2) (T_{si} + T_{ei}) \quad \{4.21\}$$

**Table 4.2** Representative values <sup>†</sup> of internal surface radiative heat transfer coefficients between an enclosure at  $T_{ei} = 20^\circ\text{C}$  and a glass surface at a given temperature,  $T_{si}$ .

$T_{si}$ °C	$h_{ri}$ $\text{W m}^{-2}\text{K}^{-1}$	$T_{si}-T_{ei}$ °C	$q_r$ $\text{W m}^{-2}$
50.0	5.99	30.0	179.7
40.0	5.69	20.0	113.8
30.0	5.41	10.0	54.1
25.0	5.28	5.0	26.4
21.0	5.17	1.0	5.2
20.1	5.14	0.1	0.5
19.0	5.12	-1.0	-5.1
15.0	5.01	-5.0	-25.1
10.0	4.89	-10.0	-48.9
0.0	4.64	-20.0	-92.8
-10.0	4.41	-30.0	-132.3

<sup>†</sup> Calculated by the author using Eq.4.21 with  $f_{1-2} = 0.9$ , i.e. assuming a black body enclosure and the surface emissivity is 0.9.

**Table 4.3** Representative values of sky and exterior obstructing and ground view factors for an external surface. (after Clarke 1985).

Location	$F_{so-sky}$	$F_{so-ext}$
1 City centre: surrounding buildings at same height, vertical surface	0.36	0.64
2 surrounding buildings higher, vertical surface	0.15	0.85
3 Urban site: vertical surface	0.41	0.59
4 Rural site vertical surface	0.45	0.55
5 Isolated vertical	0.50	0.50
6 Flat roof	1.00	0.00

In general  $h_{ri}$  depends strongly on temperature. However,  $T_{si}$  and  $T_{ei}$  in Eq.4.21 are absolute temperatures, so it is true that  $(T_{si} - T_{ei}) \ll T_{ei}, T_{si}$ . In this case Eq.4.21 can be simplified to

$$h_{ri} = 4\sigma f_{si-ei} T^3 \quad \{4.22\}$$

where  $T = 0.5(T_{ei} + T_{si})$  is the mean temperature. Representative values for  $h_{ri}$  for different surface temperatures are given in Table 4.2 in which the value of  $f_{si-ei}$  has been set at 0.9.

The detailed treatment of longwave radiation between the internal surfaces of a room is a complicated task which can only be handled in computer simulation models. Clarke (1985) provides detailed procedures of radiative heat exchange between surfaces as implemented in the "ESP" model. However, assumptions and approximations both for the physical processes involved and the numerical solution techniques inevitably lead to errors. Work is needed to quantify the differences between the predictions of models and precise analytical solutions. Nevertheless the steady-state solution of Eq.4.20 & 4.21 is reasonably adequate.

### 4.3.2 Radiative Heat Transfer at External Surfaces

The net longwave radiation exchange at an external building surface is given by the simultaneous difference between the emitted and received flux. If the surroundings are represented by some mean black body equivalent temperature,  $T_{eo}$ , then the net exchange per unit area,  $q_{ro}$  ( $W m^{-2}$ ), can be expressed by

$$q_{ro} = \varepsilon \sigma (T_{so}^4 - T_{eo}^4) \quad \{4.23\}$$

where  $\varepsilon$  is the surface emissivity; and the equivalent temperature  $T_{eo}$  is a function of sky, ground and obstruction surface temperatures and is given by

$$T_{eo}^4 = F_{so-sky} T_{sky}^4 + F_{so-ext} T_{ext}^4 \quad \{4.24\}$$

where  $F_{so-sky}$  is the sky view factor relative to the surface in question;  $F_{so-ext}$  is the view factor of ground and surrounding surfaces relative to the surface in question. Table 4.3 gives some representative values. Now Eq.4.23 can be expressed in the steady-state form of

$$q_{ro} = h_{ro} (T_{so} - T_{eo}) \quad \{4.25\}$$

which yields the external surface radiative heat transfer coefficient of

$$h_{ro} = \varepsilon \sigma (T_{so}^2 + T_{eo}^2) (T_{so} + T_{eo}) \quad \{4.26\}$$

The temperatures in Eq.4.24 may not be readily available, and estimation of these temperatures from known climatic data is therefore required.

### *Estimation of Ground and Obstruction Surface Temperatures*

According to Gay et. al. (1987), it is generally assumed that the temperature of ground and surrounding obstruction surfaces is the same as the outdoor air temperature near the ground (i.e  $T_{\text{ext}} = T_o$ ). Clarke (1985) on the other hand treats ground and obstruction surface temperatures separately. He assumes temperatures of obstruction surfaces are close to those of the corresponding surfaces (north face, south face, etc.) of the building being studied. For ground temperature estimation, one can use the concept of sol-air temperature as given by Eq.2.8 (see section 2.4.1 of chapter 2), so that

$$T_{\text{grd}} = T_o + [R_{\text{so}} (\alpha_{\text{grd}} G_h - q_{\text{net}})] \quad \{4.27\}$$

where  $T_o$  is the absolute air temperature (K);  $\alpha_{\text{grd}}$  is the ground absorptivity;  $G_h$  is the global horizontal insolation ( $\text{W m}^{-2}$ );  $R_{\text{so}}$  is the combined convective/radiative ground surface resistance ( $\text{m}^2 \text{K W}^{-1}$ ); and  $q_{\text{net}}$  is the net longwave radiation exchange between ground and sky ( $\text{W m}^{-2}$ ).

Application of this expression will require, firstly, that the longwave exchange term be evaluated. This in turn will require knowledge of the sky and surrounding building surface temperatures and, of course, the objective here is to calculate one surface of the other. It is possible to evaluate the longwave exchange term by:

$$q_{\text{net}} = \epsilon_{\text{grd}} \sigma (T_o^4 - T_{\text{sky}}^4) \quad \{4.28\}$$

where  $\epsilon_{\text{grd}}$  is the ground surface emissivity; and the ground surface temperature taken as the outdoor air temperature ( $T_o$ ) to allow the calculation to proceed.

### *Sky Temperature Estimation*

The sky temperature under non-cloudy conditions can be determined from

$$q_{\text{sky}} = 5.31 \cdot 10^{-13} T_o^6 \quad \{4.29\}$$

where  $q_{\text{sky}}$  is the longwave radiation flux ( $\text{W m}^{-2}$ ). This expression has been compared with measured data from different global locations (Swinbank 1963) and was found to be valid. If the assumption is made that the clear sky behaves as a black body ( $\epsilon = 1$ ), then

$$q_{\text{sky}} = \sigma T_{\text{sky}}^4 \quad \{4.30\}$$

and so

$$T_{\text{sky}} = 0.05532 T_o^{1.5} \quad \{4.31\}$$

Whillier (1967), on the other hand, simply subtracts 6°C from the air temperature so

$$T_{\text{sky}} = T_o - 6 \quad \{4.32\}$$

**Figure 4.3** Clear and overcast sky temperatures as a function of outdoor air temperature. Calculated by the author using: (A) Whillier relation, Eq.4.32; (B) Ineichen et. al. relation, Eq.4.38 with  $G_{fh}/G_h = 0$  for clear sky and  $G_{fh}/G_h = 1$  for overcast sky; (C) Cole relation, Eq.4.35 with  $C = 0$  for clear sky and  $C = 1$  for overcast sky.

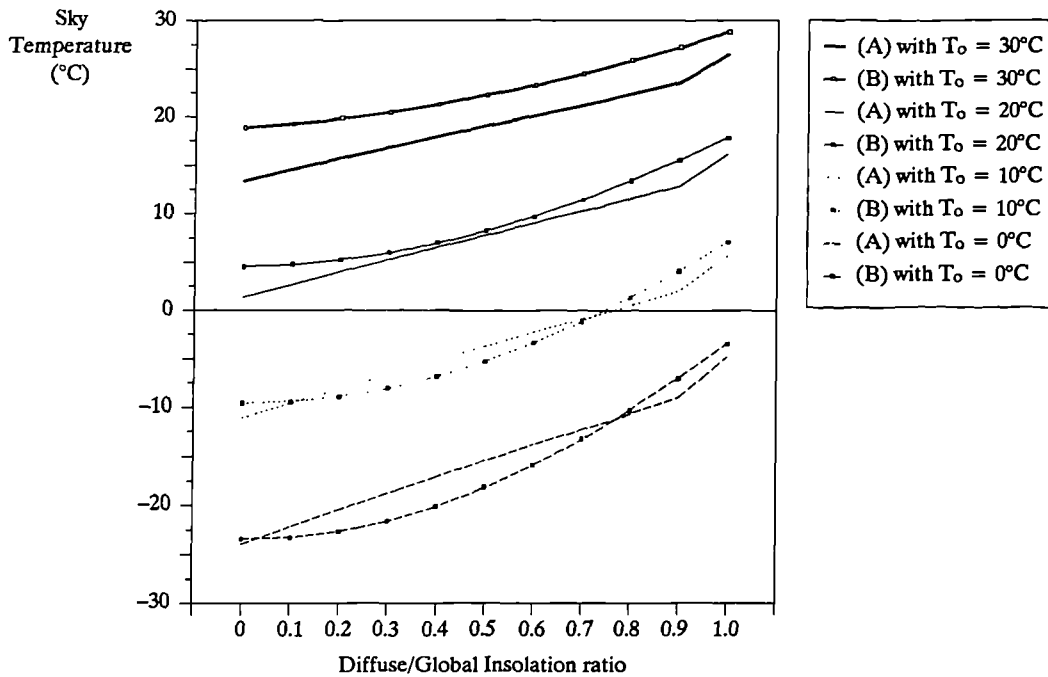
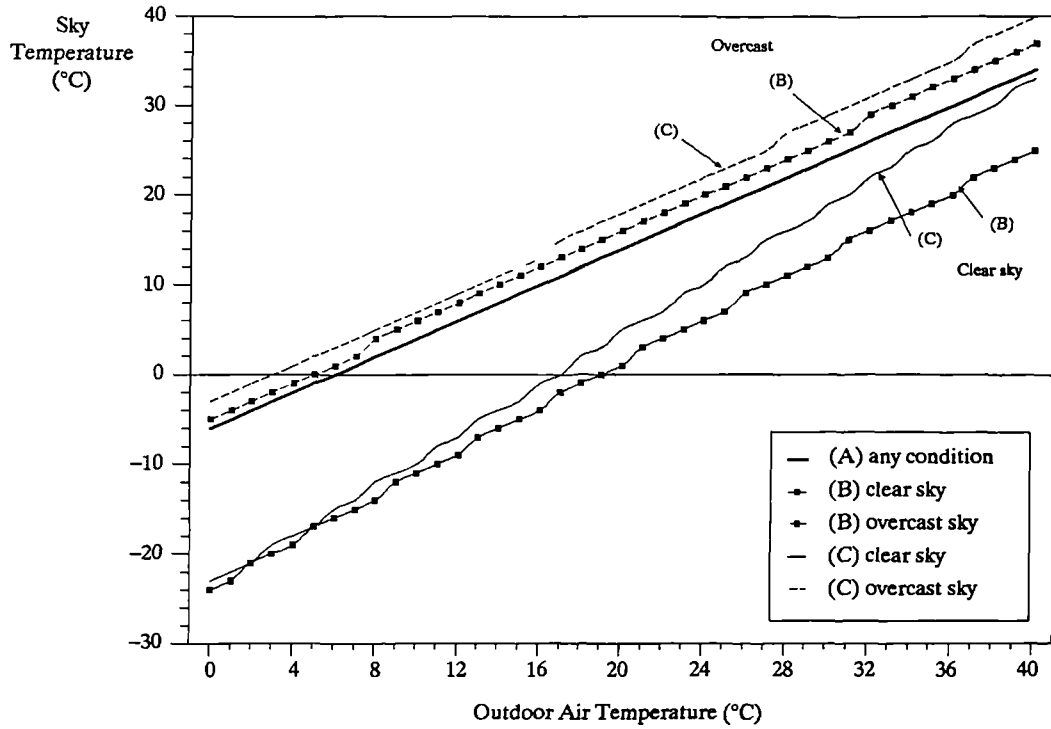


**Figure 4.4** Non-clear sky temperature as a function of sky condition, for outdoor air temperatures of 0, 10, 20 & 30°C. Calculated by the author using: (A) Eq.4.38; (B) Eq.4.35. Note that cloud cover factor in Eq.4.35 is taken as  $C = G_{fh}/G_h$ .

In the presence of clouds, the mean sky temperature increases and an alternative expression has been proposed (Cole 1976):

$$q'_{\text{sky}} = (1-C) q_{\text{sky}} + C \epsilon_c \sigma T_o^4 \quad \{4.33\}$$

where  $q'_{\text{sky}}$  is the cloudy sky longwave radiation flux ( $\text{W m}^{-2}$ );  $C$  is the cloud cover factor (0–1); and the emissivity of the cloudy sky ( $\epsilon_c$ ) is given by

$$\epsilon_c = (1-0.84C) [0.527 + 0.161 \cdot \exp(8.45 (1-273/T_o))] + 0.84C \quad \{4.34\}$$

thus, by substituting Eq.4.29 in Eq.4.33 and using Eq.4.30 the effective sky temperature under cloudy conditions becomes

$$T_{\text{sky}} = [9.3651 \cdot 10^{-6} (1-C) T_o^6 + \epsilon_c C T_o^4]^{0.25} \quad \{4.35\}$$

It is difficult to define a cloud cover factor for use in the above equations. Findings from different studies by Hoyt (1977) and Rangarajan et.al. (1984) show that ground observations of cloud cover ( $C$ ) have a systematic error because of projection problems and perspective errors inherent in eye estimates made from ground. The cloud cover factor may be derived from the simple relation  $C = (1 - n/N)$ , where  $n/N$  is the ratio of recorded to maximum possible duration of sunshine hours. However, cloud cover factors estimated from satellite photographs would be ideal for use in Equations 4.34 & 4.35.

Other relations that relate sky temperature to different meteorological variables have also been proposed in literature (e.g. see Brunt 1932; Bliss 1961; Unsworth & Monteith 1975). Ineichen et. al. (1984) in Geneva have made an attempt to correlate  $T_{\text{sky}}$  with two measured quantities: the air temperature and solar radiation. By plotting  $\Delta q = \sigma(T_o^4 - T_{\text{sky}}^4)$  versus a modulating factor  $(1 - G_{\text{fh}}/G_{\text{h}})$ , a good correlation was found with the following parameters:

$$\Delta q = 22 + 175 \cdot (1 - G_{\text{fh}}/G_{\text{h}}) \quad \text{if } (G_{\text{fh}}/G_{\text{h}}) > 0.9 \quad \{4.36\}$$

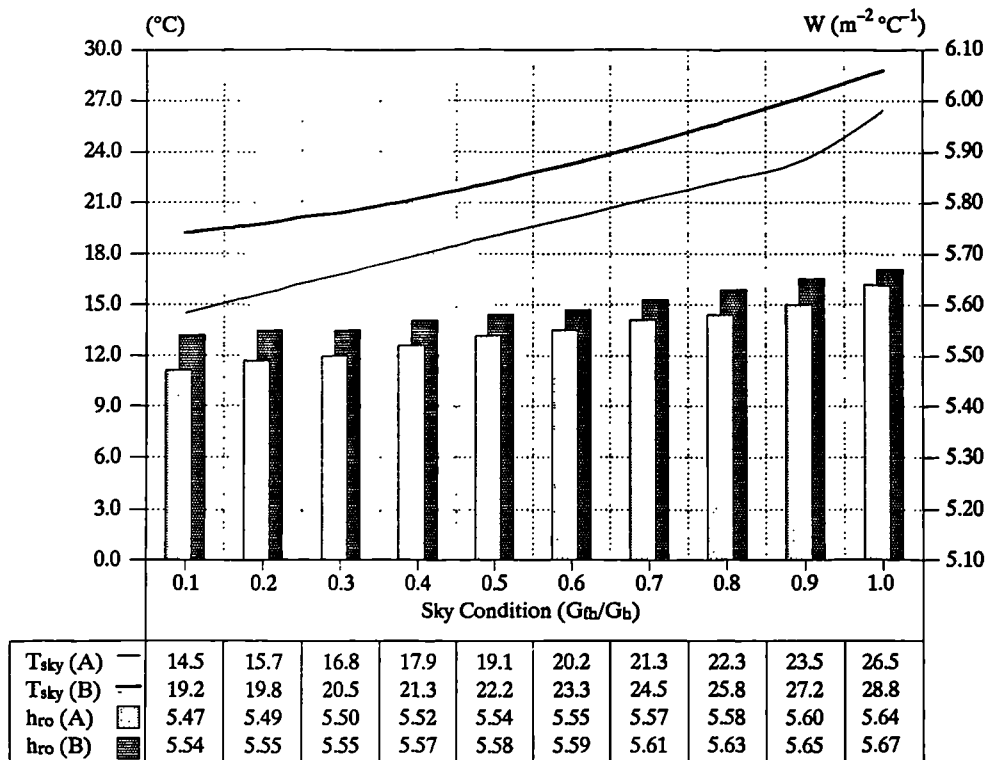
$$\Delta q = 34 + 63 \cdot (1 - G_{\text{fh}}/G_{\text{h}}) \quad \text{if } (G_{\text{fh}}/G_{\text{h}}) \leq 0.9 \quad \{4.37\}$$

where  $\Delta q$  is the net longwave radiation ( $\text{W m}^{-2}$ ) of an extended flat black surface at temperature  $T_o$  parallel to an extended sky at  $T_{\text{sky}}$ ;  $G_{\text{fh}}$  &  $G_{\text{h}}$  are the daily average diffuse and global horizontal insolation ( $\text{W m}^{-2}$ ) respectively. The sky temperature, of any sky condition, is then found from

$$T_{\text{sky}} = [T_o^4 - (\Delta q/\sigma)]^{0.25} \quad \{4.38\}$$

Figure (4.3) shows a comparison between the temperatures of clear and overcast skies, calculated by the relations discussed above, for the outdoor air temperature range of  $0^\circ\text{C}$  to  $40^\circ\text{C}$ . It is clear from this figure that the Whillier relation (Eq.4.32) is more suitable for overcast sky temperature estimates.

**Figure 4.5** Non-clear sky temperature and the external surface heat transfer coefficient as a function of sky condition, for outdoor air temperature of 30°C. Calculated by the author using: (A) Eq.4.38; (B) Eq.4.35 for sky temperature estimation, and results substituted in Eq.4.26 for  $h_{ro}$  calculation taking  $\epsilon = 0.9$  &  $T_{so} = T_o$ .



If we assume that the ratio of diffuse to global horizontal insolation is closely related to the cloud cover (i.e.  $C \approx G_{fh}/G_h$ ) then a comparison between Eq.4.35 & Eq.4.38 can be made for different cloud cover factors as shown in Figure (4.4).

Any of the above two relations can be used to estimate the temperature of clear and cloudy skies despite the difference of output, since the resulted errors in the calculation of the radiative heat transfer coefficients ( $h_{ro}$ ) in Eq.4.26 are negligible. i.e. an error in the order of 0.1–0.2 out of 4–6  $W (m^{-2} K^{-1})$ , (see Fig.4.5). Furthermore, the external radiative heat transfer coefficient is about 20–30% of the total external heat transfer coefficient for most applications in buildings, hence the error from sky temperature estimates is insignificant in the majority of situations.

### 4.3.3 Natural Convective Heat Transfer (Internal Surfaces)

Three dimensionless scale factors are of importance in the estimation of natural convection; 1– Nusselt number ( $Nu$ ); 2– Prandtl number ( $Pr$ ) and 3– Grashof number ( $Gr$ ). These can be obtained from the following equations respectively

$$Nu = h_v X / k \quad \{4.39\}$$

$$Pr = \nu / \kappa \quad \{4.40\}$$

$$Gr = g \beta X^3 \Delta T / \nu^2 \quad \{4.41\}$$

where

$h_v$	= natural convective surface heat transfer coefficient, ( $W m^{-2} K^{-1}$ )
$\nu$	= air kinematic viscosity ( $m^2 s^{-1}$ )
$X$	= a characteristic dimension (m)
$\kappa$	= air thermal diffusivity ( $m^2 s^{-1}$ )
$g$	= gravitational constant ( $m s^{-2}$ )
$\beta$	= coefficient of expansion ( $K^{-1}$ )
$\Delta T$	= temperature difference between surface and air (K)

Correlation of the above dimensionless scale factors is found, in literature, in the empirical form of either

$$Nu = c (Gr Pr)^n$$

or 
$$Nu = c A^n \quad \{4.42\}$$

where  $c$  &  $n$  are constants, and the product of Grashof and Prandtl numbers ( $Gr Pr$ ) is the Raleigh number ( $A$ ).

Most data correlations are obtained from experimental evaluation of the natural convection heat transfer from heated plates under experimental conditions. Twidell & Weir (1986) gives a summary of Equation 4.42 for a variety of experimental setups. Many other empirical formulations can be found in the literature (e.g. Jacob 1949; McAdams 1954 and Fujii & Imura 1970), with noticeable variations for typical conditions. This indicates that any of their

**Table 4.4** Empirical coefficients for Eq.4.49 from Alamdari & Hammond (1983).

Surface aspect	a	b	p	q	m
Vertical	1.5	1.23	1/4	1/3	6
Horizontal	1.4	1.63	1/4	1/3	6

empirical equations may only be accurate to  $\pm 10\%$  which is partly because formulas are approximations to the experimental conditions, and partly because the experimental data themselves usually contain both random and systematic errors.

In order to simplify the calculation of natural convective heat transfer for air at internal building surfaces ( $h_{vi}$ ), many authors have developed equations which give natural convection coefficients for surfaces as a function of surface–air temperature difference ( $\Delta T$ ), characteristic dimensions and the direction of heat flow. For example, Rogers & Mayhew (1967) have produced a theoretical solution of  $h_{vi}$  for vertical and horizontal surfaces, based on the Nusselt number correlations given by McAdams (1954), as follows:

For vertical surfaces, Equations (4.43 & 4.44) give  $h_{vi}$  for Laminar flow ( $A < 10^9$ ) and for Turbulent flow ( $A > 10^9$ ) respectively

$$h_{vi} = 1.42 (\Delta T/X)^{0.25} \quad \{4.43\}$$

$$h_{vi} = 1.31 (\Delta T)^{0.33} \quad \{4.44\}$$

and for a horizontal surface with heat flow upward, Equations (4.45 & 4.46) give  $h_{vi}$  under laminar and turbulent conditions respectively, while Eq.4.47 gives  $h_{vi}$  for stagnant flow (i.e. heat flow downward, like cold floor and hot ceiling)

$$h_{vi} = 1.32 (\Delta T/X)^{0.25} \quad \{4.45\}$$

$$h_{vi} = 1.52 (\Delta T)^{0.33} \quad \{4.46\}$$

$$h_{vi} = 0.59 (\Delta T/X)^{0.25} \quad \{4.47\}$$

where  $X$  in Eq.4.43 & Eq.4.44 is the height of the surface (m), and in Eq.4.45 to Eq.4.47 is found from the surface area ( $A$ ) and parameter ( $P$ ) by

$$X = 4A/P \quad \{4.48\}$$

Alamdari and Hammond (1983) have produced a general formula for both vertical and horizontal surfaces (with upward heat flow) valid over the range  $10^4 < A < 10^{12}$ , which represent most of the flow conditions found within buildings as

$$h_{vi} = [ [a(\Delta T/X)^p]^m + [b(\Delta T)^q]^m ]^{1/m} \quad \{4.49\}$$

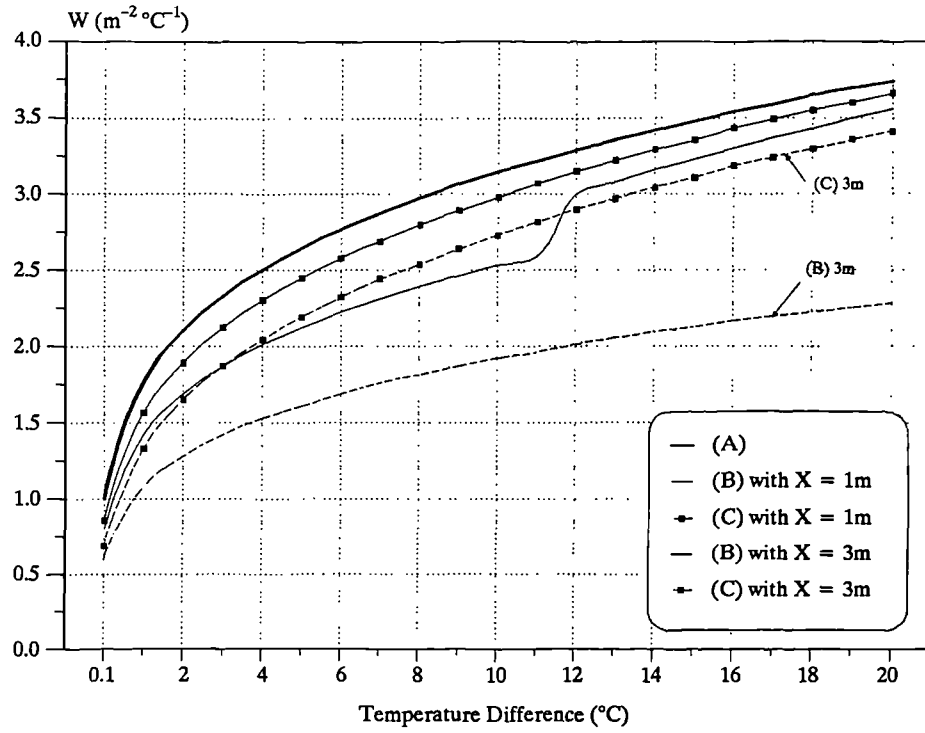
where  $a$ ,  $b$ ,  $p$ ,  $q$  &  $m$  are given in Table (4.4); and  $X$  represent height of surface (m), and for horizontal surfaces undergoing downward heat flow the heat transfer coefficient is given by

$$h_{vi} = 0.6 (\Delta T/X)^{0.2} \quad \{4.50\}$$

where the characteristic dimension  $X$  is found from Eq.4.48

To calculate  $h_{vi}$  at a vertical surface using Rogers & Mayhew formulas, we need first to define the air flow regime at that surface (laminar or turbulent) which is dependent on surface–air temperature difference ( $\Delta T$ ) and surface height ( $X$ ).

**Figure 4.6** Convective heat transfer coefficients at internal vertical surfaces as a function of surface-air temperature difference. Calculated by the author using: (A) the ASHRAE correlation, Eq.4.51; (B) Rogers & Mayhew correlation, Eq.4.43 & Eq.4.44; (C) Alamdari & Hammond, Eq.4.49. (X = surface height in meters).



For example, if we consider some vertical surfaces of the heights ( $X = 1, 1.5, 2, 3$  &  $4\text{m}$ ), using Eq.4.40 & Eq.4.41 with a reference air temperature of  $20^\circ\text{C}$  and  $\Delta T = 0.1$  to  $20^\circ\text{C}$ , yield the following conditions

laminar flow for  $X = 1\text{m}$  &  $\Delta T < 12^\circ\text{C}$   
 laminar flow for  $X = 1.5\text{m}$  &  $\Delta T < 4^\circ\text{C}$   
 laminar flow for  $X = 2\text{m}$  &  $\Delta T < 2^\circ\text{C}$   
 turbulent flow for  $X > 3\text{m}$

Accordingly,  $h_{vi}$  at vertical surfaces can be calculated using Eq.4.43 or Eq.4.44. By comparison, Alamdari & Hammond correlation (Eq.4.49) does not require the definition of the flow regimes at the vertical surfaces.

ASHRAE (1985), gives for  $h_{vi}$  with vertical surfaces a relation that is independent of the height, for surface temperatures of  $-10^\circ\text{C}$  up to  $55^\circ\text{C}$  and  $\Delta T$  of  $3^\circ\text{C}$  to  $30^\circ\text{C}$ , as:

$$h_{vi} = 1.77 (\Delta T)^{0.25} \quad \{4.51\}$$

Figure 4.6 gives heat transfer coefficient ( $h_{vi}$ ) as a function of  $\Delta T$  for surfaces of  $1\text{m}$  and  $3\text{m}$  high calculated using the correlations of Alamdari & Hammond, Rogers & Mayhew and ASHRAE.

It is difficult to determine what formula represents the best relation for detailed study of convective heat transfer coefficient at internal building surfaces, since each has its limitations. Knorr (1987), claims that many researchers use Equation 4.43 in computer calculations for determining building heat loads. However this formula is only valid for laminar convective flow, which may explain the recommendation, Knorr gave, for its use for small rooms of low heights.

The ASHRAE correlation (Eq.4.51) gives higher values of  $h_{vi}$  than the other correlations examined above (see Fig.4.6) and corresponds to turbulent flow only. The Alamdari & Hammond correlation (Eq.4.49), on the other hand, have the advantage of covering the full range of laminar, transitional and turbulent flows, and therefore avoid the need to determine which flow regime is in force. Hence they are suitable for use in computer programs that simulate the dynamic thermal performance of buildings.

### 4.3.4 Forced Convective Heat Transfer (External Surfaces)

When air motion is caused by some external force such as a fan or wind power, convection is termed forced. In this case another dimensionless scale factor is important, the Reynolds number ( $Re$ ), which strongly depend on air speed  $V$  ( $\text{m s}^{-1}$ ) and given by

$$Re = V X / \nu \quad \{4.52\}$$

**Table 4.5** Empirical Coefficients and exponents for Eq.4.54 from McAdams (1954).

Nature of surface	$V < 4.88 \text{ m s}^{-1}$			$4.88 \leq V < 4.88 \text{ m s}^{-1}$		
	a	b	n	a	b	n
Smooth	0.99	0.21	1	0	0.50	0.78
Rough	1.09	0.23	1	0	0.53	0.78

As with natural convection estimation, dimensional analysis techniques can be employed to determine some generalized expression. This is found to be similar to the empirical relation for natural convection with the Reynolds number replacing Grashof number giving

$$Nu = c Re^n Pr^m \quad \{4.53\}$$

with the coefficient  $c$  and the exponent terms  $n$  &  $m$  being assessed from experimental observations or theoretical considerations. For example, based on a copper plate experiment using a parallel flow of air at a reference temperature of 21.1°C, McAdams (1954) gives the following expression

$$h_{vo} = 5.678 [a + b (V / 0.3048)^n] \quad \{4.54\}$$

where  $h_{vo}$  is the forced convection heat transfer coefficient ( $W m^{-2} K^{-1}$ );  $V$  is the parallel air flow speed ( $m s^{-1}$ ); and  $a$ ,  $b$ , &  $n$  are empirical values given in Table (4.5). Equation 4.54 is found in many references relating the convective heat transfer coefficient ( $h_{vo}$ ) at external surfaces to wind speed ( $V$ ) as the simple expression of

$$h_{vo} = 5.7 + 3.8 V \quad \{4.55\}$$

The CIBS Guide (1976) gives a different expression for calculating external surface convective heat transfer coefficients, based on an early lab experiment by Jürges (1924), as

$$h_{vo} = 5.8 + 4.1 V \quad \{4.56\}$$

In any detailed calculation of forced heat transfer coefficients, two issues are of some importance; 1- the resolution of the prevailing wind direction into a surface, in the case of external surfaces, and 2- an assessment of system generated velocities (i.e., due to radiators near surfaces or fans and mechanical air ventilators) in the case of internal surfaces. The latter issue is difficult and cannot easily be obtained by calculation and it is necessary to determine the velocities by measurements. The former issue, wind direction resolution, is a simpler one.

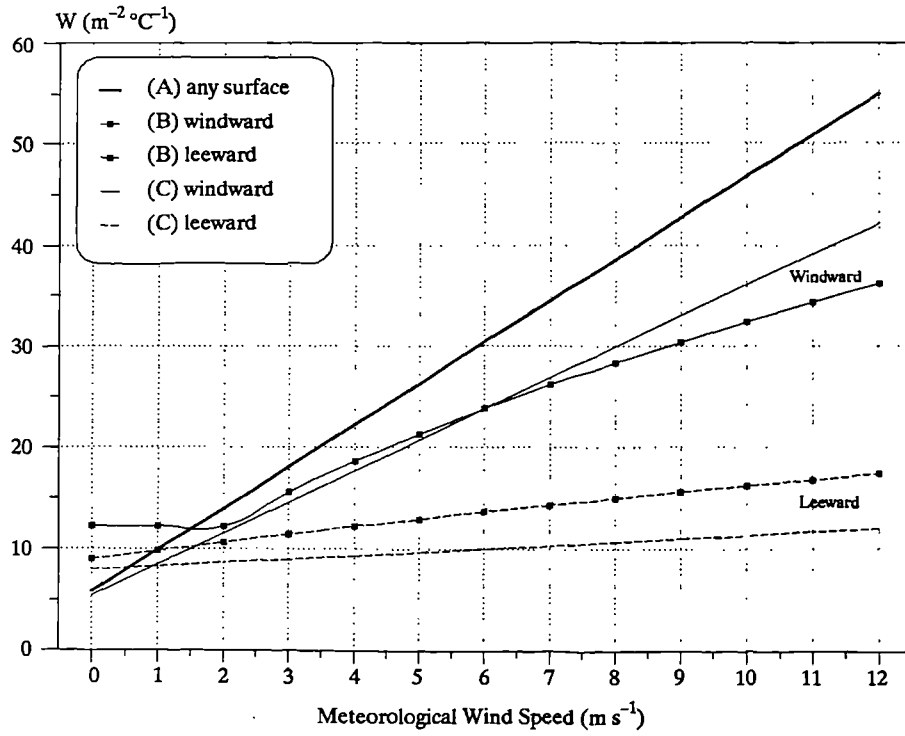
Based on experimental data, Ito et. al. (1972) have developed empirical relationships for the assessment of local wind speeds relative to external surfaces ( $V_s$ ), from the wind speed  $V_m$  (as provided by Meteorological stations). The wind direction relative to some building surface is given by

$$D_s = \gamma + 180^\circ - D_m$$

$$(if |D_s| > 180^\circ, D_s = 360^\circ - |D_s|) \quad \{4.57\}$$

where  $D_s$  is the wind direction relative to surface (deg.);  $\gamma$  the surface azimuth angle (the zero degree point being due south, east positive and west negative);  $D_m$  is the free stream wind direction (deg. from north, clockwise positive).

**Figure 4.7** External surface heat transfer coefficients as a function of wind speed, for windward and leeward surfaces. Calculated by the author using: (A) CIBS Guide correlation, Eq.4.56; (B) ASHRAE correlation, Eq.4.61; (C) Sharples correlation, Eq.4.64.



The surface wind speed ( $V_s$ ) is dependent on whether the surface is windward or leeward and on the magnitude of the wind speed. Its value is approximated by:

Windward (  $|D_s| < 90^\circ$  )

$$V_s = 0.25 V_m, \quad \text{for } V_m > 2 \text{ m s}^{-1} \quad \{4.58\}$$

$$V_s = 0.5, \quad \text{for } V_m < 2 \text{ m s}^{-1} \quad \{4.59\}$$

Leeward (  $|D_s| > 90^\circ$  )

$$V_s = 0.3 + 0.05 V_m \quad \{4.60\}$$

The work of Ito et. al. has gained international recognition. The ASHRAE Task Group (1975) has derived from Ito's work the following empirical formula:

$$h_{vo} = 18.6 V_s^{0.605} \quad \{4.61\}$$

Sharples (1984) carried out measurements on a 78m high building (18 story Art Tower at Sheffield university, U.K.), based on the same principles as the Ito experiments. Sharples derived relationships between  $h_{vo}$ , meteorological wind speed ( $V_m$ ), and the air speed near the wall surface ( $V_s$ ), which takes the form

Windward surface

$$V_s = 0.2 + 1.8 V_m \quad \{4.62\}$$

Leeward surface

$$V_s = 1.7 + 0.2 V_m \quad \{4.63\}$$

and for either surface

$$h_{vo} = 5.1 + 1.7 V_s \quad \{4.64\}$$

Figure 4.7 gives the external convective heat transfer coefficients ( $h_{vo}$ ) as a function of wind speed for windward and leeward surfaces, calculated using the correlations of ASHRAE (Eq.4.61), Sharples (Eq.4.64), and Equation (4.56) of the CIBS Guide.

The conclusion that can be drawn is that in order to carry out very detailed calculations of energy balance of building components (for example windows in different orientations) one must be aware that the values of  $h_{vo}$  derived by using any of the discussed correlations are based on few full scale experiments each with its own limitations and uncertainties. The ASHRAE correlation, however, is widely used in computer simulation models and will be adopted in this chapter.

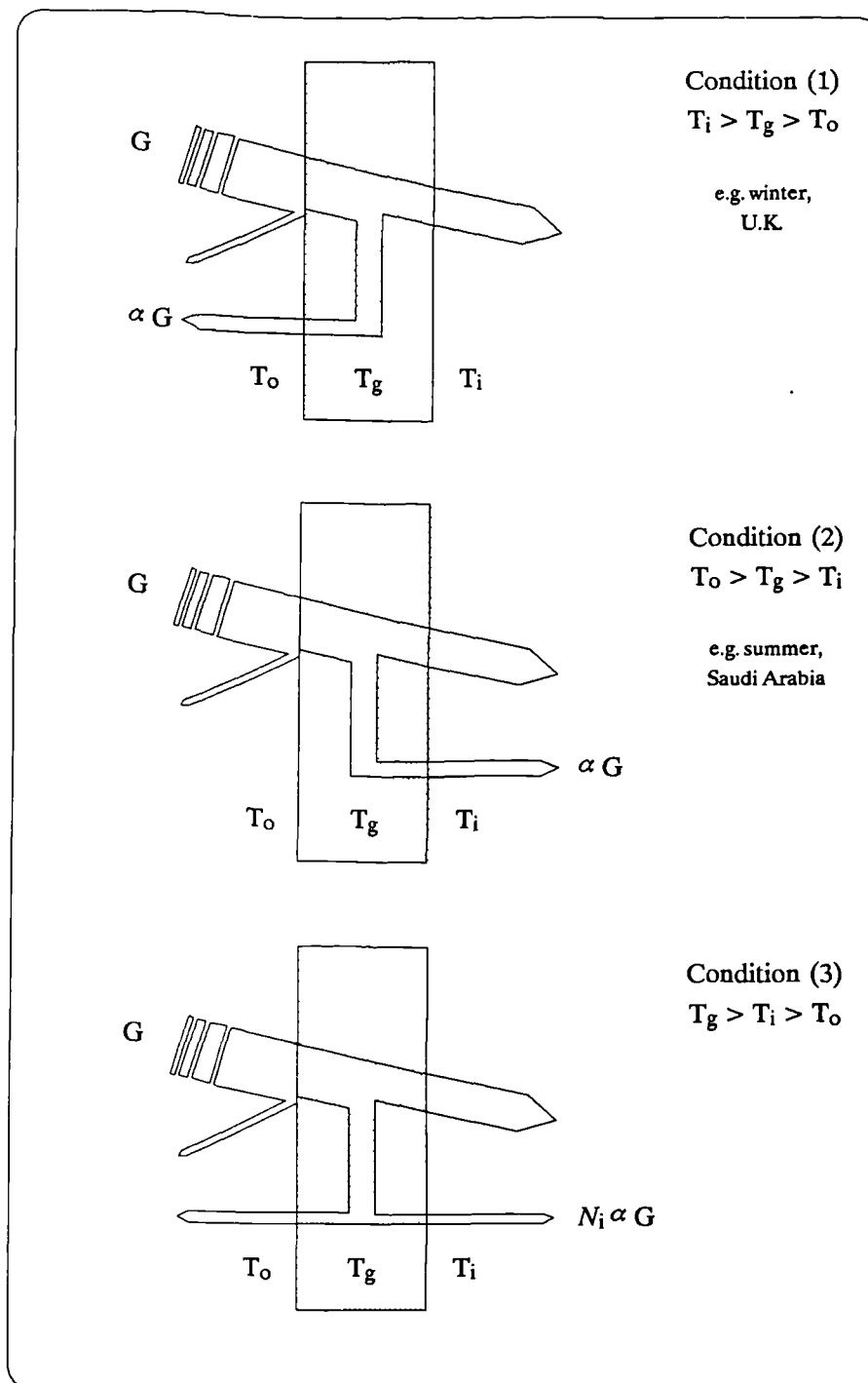


**Figure 4.8** Schematic redistribution of absorbed insolation in a single glass for three possible temperature distributions.

- (1) Cold, cloudy weather may produce this condition. The result is that the absorbed shortwave radiation does not produce a net convective/longwave heat flow into the enclosure.
- (2) Warm, cloudy weather may produce this condition. The result is that the absorbed shortwave energy produces a net convective/longwave heat flow into the enclosure from the internal surface of the glass.
- (3) High levels of solar radiation falling upon the glazing, together with a small difference of temperature between the internal and external air, will produce the condition of the glass being hotter than the air either side of it.

#### 4.4 Maximum Solar Heat Gain Through Glazing: (with application for Riyadh climate)

---

The concept of Shading Coefficient, introduced in chapter 2 (see section 2.4.2), allows for simple calculations of the solar heat gain through any type of fenestration as given by Eq.2.27. The calculation required knowledge of the solar heat gain flux through a reference glass,  $q_{ref}$  ( $W m^{-2}$ ). The reference glass, by definition, should admit the maximum possible solar heat gain. This is taken to be a clear glass of thickness 3mm with 0.86 solar transmittance, 0.08 reflectance and 0.06 absorptance at normal incidence and with 0.9 emissivity. Values of  $q_{ref}$  can be found in handbooks like ASHRAE (1985) for different window orientations and for latitudes of  $0^{\circ}N$  to  $64^{\circ}N$ . These values are based on theoretically determined insolation data and fixed surface heat transfer coefficients, hence insensitive to meteorological changes.

The objective of this section, therefore, is to compute hourly values of solar heat gain flux through the reference glass which are sensitive to variation in the climate of Riyadh, Saudi Arabia, (such variations include solar radiation incident on the glass, longwave radiation exchange between glass and surroundings, ambient air temperature, wind speed and direction). For this purpose, I have written a computer program (QREF.BAS) which can also be modified for use as a subroutine in a dynamic thermal model of energy analysis. The mathematical equations needed for this model have been covered in previous chapters of this thesis except for an important property of insulated glass which follows.

##### 4.4.1 Inward-Flow Fraction of Absorbed Insolation

With clear glass windows, the solar heat gain to the enclosure through the glazing consists mainly of transmitted shortwave radiation. The absorbed insolation will always raise the temperature of the glass, but the way the glass redistributes its absorbed energy flux depends on the prevailing internal and external climatic conditions.

Figure 4.8 presents schematically three possible ways that the absorbed insolation might be redistributed for a single glazed window. Under these circumstances the absorbed solar energy redistributes itself by dividing into an inward and outward flow. The fraction of the absorbed radiation flowing into the enclosure is denoted by ( $N_i$ ). It is only conditions 2 & 3 that produce a net inward flow of absorbed heat by convection and longwave radiation into the enclosure. However, the  $N_i$  concept may be applied to all three conditions by assuming, in condition 1, that the reduced heat loss through the glazing arises not from the warmer surface temperature, but from a fraction of the absorbed solar energy flowing inward.

To determine a value for  $N_i$  it is necessary to establish the energy balance of the glazing system. The energy balance of an insulated single glazing system can be written as

$$\alpha G = h_o (T_g - T_o) + h_i (T_g - T_i) \quad \{4.65\}$$

where  $T_o$ , and  $T_i$  are the external and internal air temperatures respectively ( $^{\circ}\text{C}$ );  $T_g$  is the glass temperature;  $h_o$  &  $h_i$  are the external and internal surface heat transfer coefficients respectively as defined by Eq.4.16  $\text{W (m}^{-2} \text{ }^{\circ}\text{C}^{-1}\text{)}$  for both convection and longwave radiation;  $G$  is the global insolation incident on the glass surface, ( $\text{W m}^{-2}$ ); and  $\alpha$  is the glass shortwave absorptivity at the same angle of incidence.

Equation 4.65 assumes negligible thermal resistance across the glass and negligible thermal storage within the glass, which is a normal practice for glazing energy process. Thus the glass external and internal surface temperatures are equal to  $T_g$ . Rearrangement of Eq.4.65 gives

$$T_g = (\alpha G + h_o T_o + h_i T_i) / (h_o + h_i) \quad \{4.66\}$$

The longwave and convective heat flow per unit area at the internal surface of the glass,  $q_{rci}$  ( $\text{W m}^{-2}$ ), is given by

$$q_{rci} = h_i (T_g - T_i) \quad \{4.67\}$$

and substituting for  $T_g$  in Eq.4.67 from Eq.4.66

$$q_{rci} = [(h_o h_i) / (h_o + h_i)] \cdot [T_o - T_i + (\alpha G / h_o)] \quad \{4.68\}$$

The  $U$ -value,  $\text{W (m}^{-2} \text{ }^{\circ}\text{C}^{-1}\text{)}$ , of a body of negligible internal resistance such as a 3mm glass sheet is given by the reciprocal of the sum of the two surface resistances:

$$U = [(1/h_o) + (1/h_i)]^{-1} = h_o h_i / (h_o + h_i) \quad \{4.69\}$$

Substituting Eq.4.69 into Eq.4.68 gives

$$q_{rci} = (U/h_o) \alpha G + U (T_o - T_i) \quad \{4.70\}$$

The total heat gain per unit area through the glass,  $\text{W m}^{-2}$ , is

$$q = \tau G + (U/h_o) \alpha G + U (T_o - T_i) \quad \{4.71\}$$

Which divides into an air-to-air conductance component,  $q_c$ , and a solar component,  $q_s$

$$q_c = U (T_o - T_i) \quad \{4.72\}$$

$$q_s = G [\tau + (U/h_o) \alpha] \quad \{4.73\}$$

Rewriting Eq.2.24 (see chapter 2) to give solar heat per unit area gives

$$q_s = G [\tau + N_i \alpha] \quad \{4.74\}$$

From Eq.4.73 & Eq.4.74, the inward-flowing fraction of absorbed insolation is a function of external and internal surface heat transfer coefficients

$$N_i = U/h_o = h_i / (h_i + h_o) \quad \{4.75\}$$

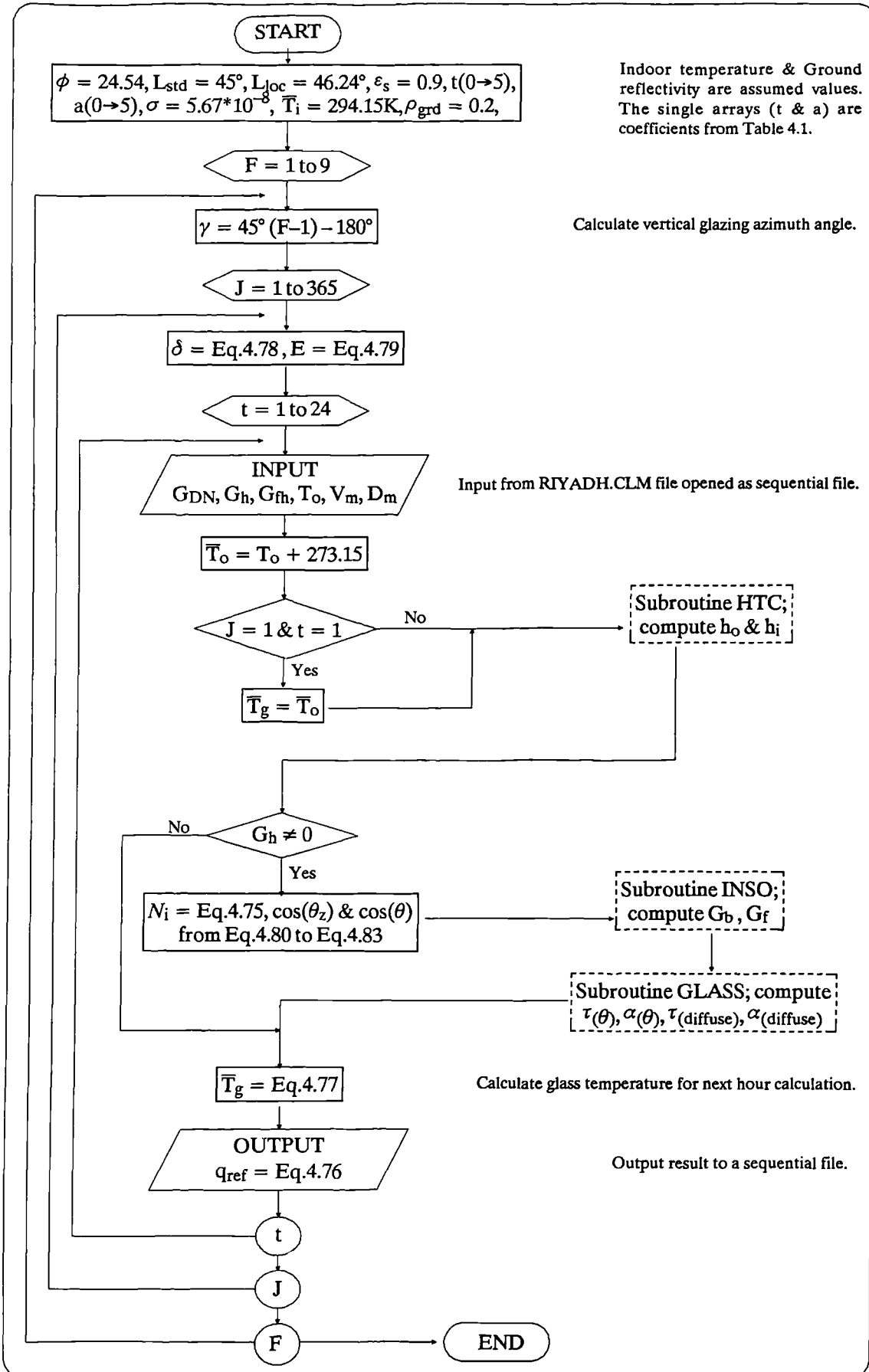


Figure 4.9 Flow chart of QREF.BAS program main routine.

#### 4.4.2 Calculation of Hourly Solar Heat Gain through a Reference Glazing in Riyadh, Saudi Arabia: (QREF program)

The solar heat gain flux through a 3mm reference window glass, at an angle of incidence  $\theta$  in  $\text{W m}^{-2}$ , is given by

$$q_{\text{ref}} = G_b [\tau(\theta) + N_i \alpha(\theta)] + G_f [\tau(\text{diffuse}) + N_i \alpha(\text{diffuse})] \quad \{4.76\}$$

where  $G_b$  &  $G_f$  are the direct and diffuse insolation incident on the glass surface respectively, ( $\text{W m}^{-2}$ ).

The computer model (QREF.BAS), developed and written in GW-Basic™ by the author, takes hourly climatic data from the Reference Climate Year file (Riyadh.Clm), and solves Eq.4.76 for a vertical glazing at 8 compass orientations and for a glazing in the horizontal position. The input climatic data are:– direct normal insolation, global horizontal insolation, diffuse horizontal insolation, air temperature, wind speed and wind direction. Flow charts of the program routines are given in Fig.4.9 through Fig.4.12. The program listing is provided in Appendix (E).

The program main routine (Fig.4.9) calculates the angles of incidence of solar radiation corresponding to the time of day, and controls the path to three subroutines (HTC, INSO and GLASS). From HTC subroutine output, the program computes the  $N_i$  value using Eq.4.75. The  $N_i$  value and the output of INSO & GLASS subroutines are then substituted in Eq.4.76 to compute the solar heat gain flux.

An initial estimate of the glass temperature is taken as the outdoor air temperature. The program then computes the glass temperature for the next hour calculation from

$$T_g = (G_b \alpha(\theta) + G_f \alpha(\text{diffuse})) + h_o T_o + h_i T_i / (h_o + h_i) \quad \{4.77\}$$

where the  $T_g$  &  $T_o$  are in Kelvin degrees, and the indoor air temperature at 21°C is constant,  $T_i = 294.15 \text{ K}$ . The solar angles are computed from Eq.4.78 through Eq.4.83. These equations have been discussed earlier in chapter 2 (see section 2.4.1).

$$\delta = 23.45 \sin[360 (284 + J) / 365] \quad \{4.78\}$$

$$E_t = [9.87 \sin(2e) - 7.53 \cos(e) - 1.5 \sin(e)] / 60 \quad \{4.79\}$$

$$e = 360 (J - 81) / 364$$

$$t_s = t + E_t + (L_{\text{std}} - L_{\text{loc}}) / 15 \quad \{4.80\}$$

$$\omega = 15 (12 - t_s) \quad \{4.81\}$$

$$\cos(\theta_z) = \sin(\delta) \sin(\phi) + \cos(\delta) \cos(\phi) \cos(\omega) \quad \{4.82\}$$

$$\cos(\theta) = \cos(\delta) \sin(\phi) \cos(\gamma) \cos(\omega) + \cos(\delta) \sin(\gamma) \sin(\omega) - \sin(\delta) \cos(\phi) \cos(\gamma) \quad \{4.83\}$$

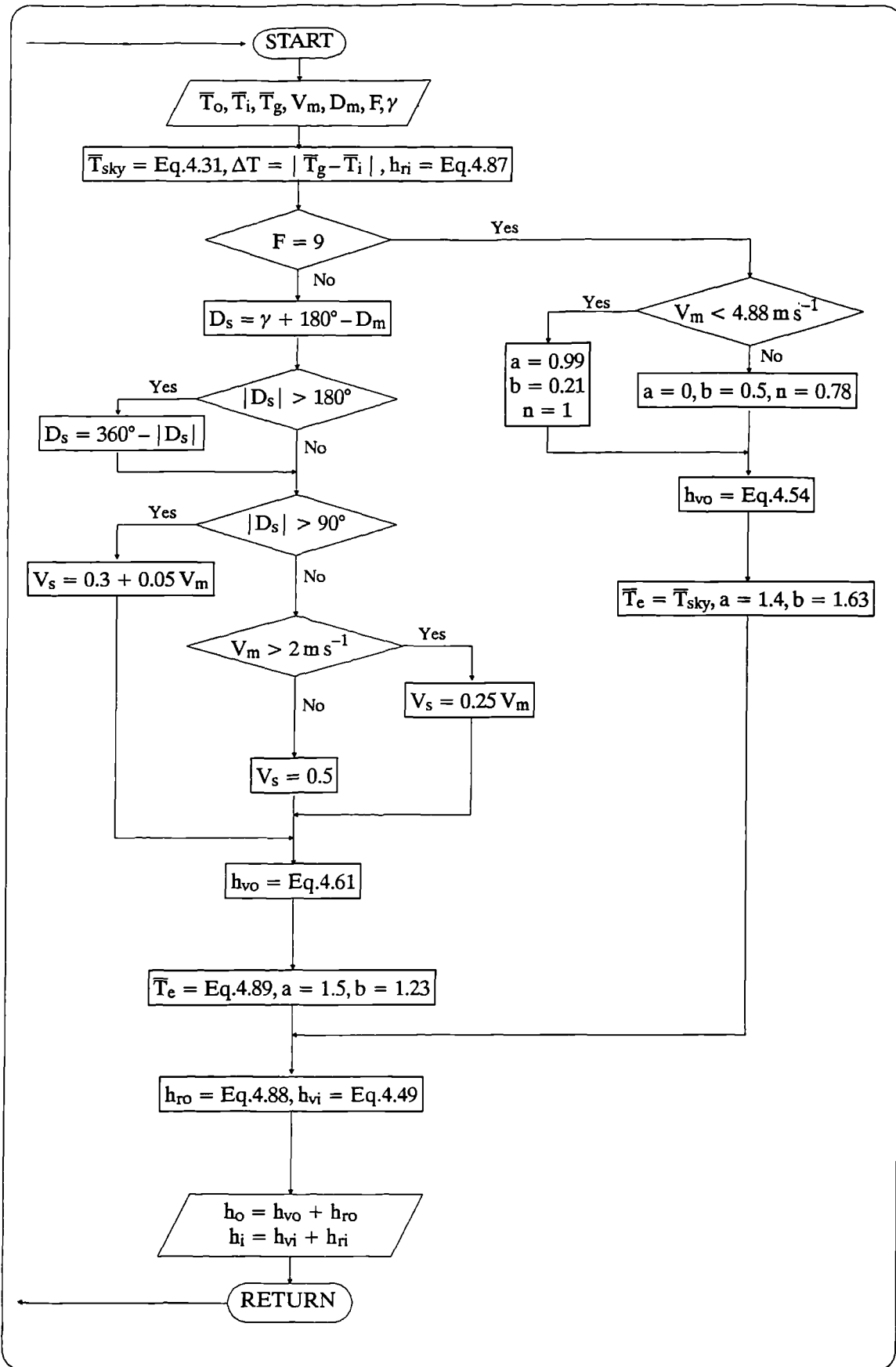


Figure 4.10 Flow chart of HTC Subroutine in QREF.BAS program.

where

- $\delta$  = solar declination, (°);
- $J$  = Julian day number (from January 1st);
- $E_t$  = the equation of time, (h);
- $e$  = a modulating function for use in Eq.4.79, (°);
- $t_s$  = the solar time, (h);
- $t$  = the local mean time, (h);
- $L_{std}$  = the standard longitude of Saudi Arabia = 45°East;
- $L_{loc}$  = the site longitude = 46.24°East;
- $\omega$  = hour angle, (°);
- $\phi$  = site latitude = 24.54°North;
- $\theta_z$  = zenith angle, the angle between the beam from the sun and the vertical, (°);
- $\theta$  = angle of incidence of beam radiation on the vertical glazing surface, (°);
- $\gamma$  = surface azimuth angle (due south = 0°, east positive and west negative)

The HTC subroutine (Fig.4.10) computes the glass internal and external surface heat transfer coefficient,  $W (m^{-2} K^{-1})$ , as follows

$$h_i = h_{ri} + h_{vi} \quad \{4.84\}$$

$$h_o = h_{ro} + h_{vo} \quad \{4.85\}$$

where  $h_{vo}$  for the vertical glass is computed from Eq.4.57 through Eq.4.61 which consider the wind speed and wind direction relative to the surface for each hour. In the case of a horizontal glazing Eq.4.54 is used with the constant coefficients taken from Table 4.5 for a smooth surface. The internal surface convective heat transfer coefficient,  $h_{vi}$ , is computed for each hour from Eq.4.49 with the constant coefficients taken from Table 4.4 for vertical or horizontal as applicable. The characteristic dimension in Eq.4.49 is taken as unity in either case,  $X = 1$ , and the temperature difference is

$$\Delta T = |T_g - T_i| \quad \{4.86\}$$

For computing the internal surface radiative heat transfer coefficient,  $h_{ri}$ , the glass is considered facing a black body at the same indoor air temperature  $T_i$  so

$$h_{ri} = \epsilon_g \sigma (T_g^2 + T_i^2) (T_g + T_i) \quad \{4.87\}$$

where the glass emissivity  $\epsilon_g = 0.9$ . Eq.4.87 is used for both vertical and horizontal glazing. The external surface radiative heat transfer coefficient,  $h_{ro}$ , is computed from

$$h_{ro} = \epsilon_g \sigma (T_g^2 + T_e^2) (T_g + T_e) \quad \{4.88\}$$

where the equivalent temperature  $T_e$  for the vertical glazing is

$$T_e = [0.5 (T_{sky}^4 + T_o^4)]^{0.25} \quad \{4.89\}$$

and for the horizontal glazing,  $T_e = T_{sky}$ .

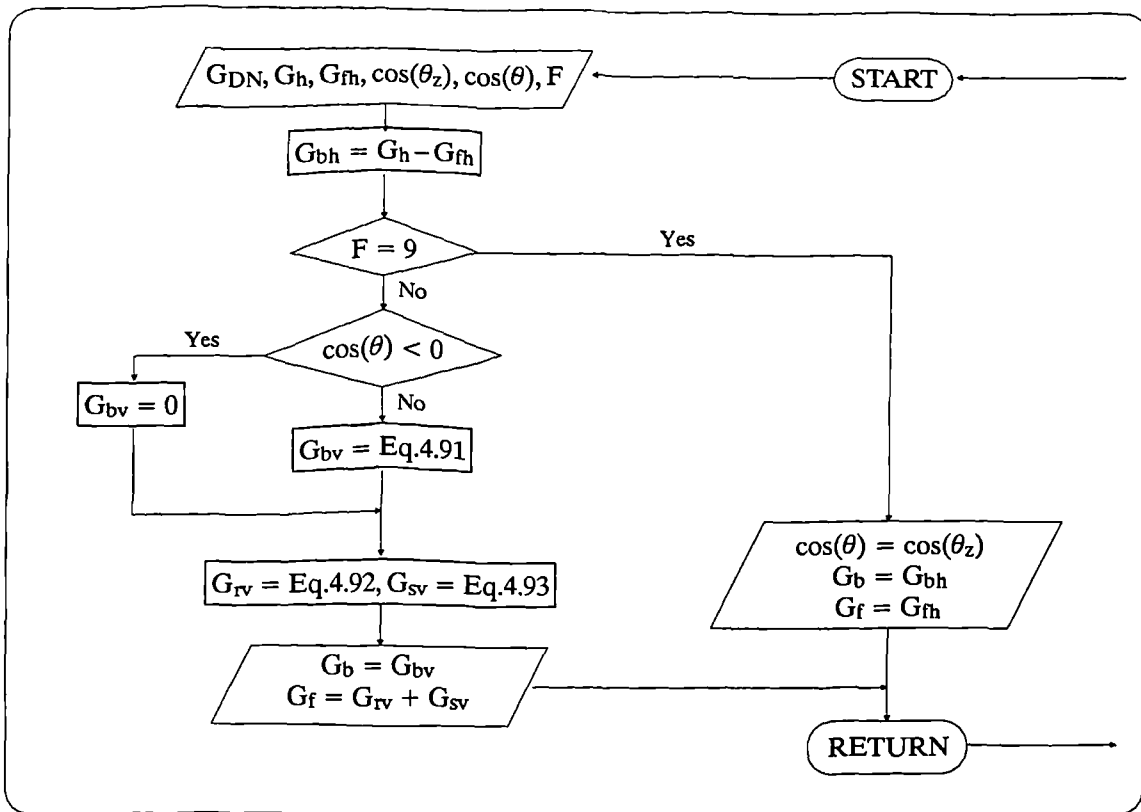


Figure 4.11 Flow chart of INSO Subroutine in QREF.BAS program.

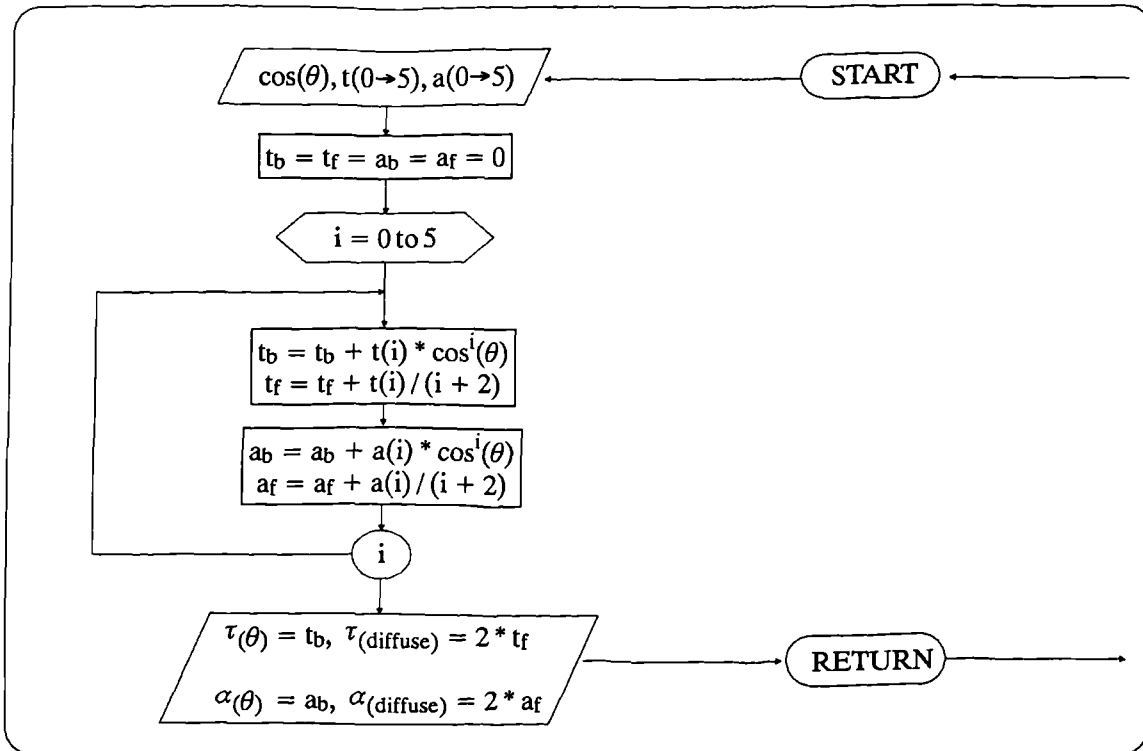


Figure 4.12 Flow chart of GLASS Subroutine in QREF.BAS program.

The sky temperature is computed from Eq.4.31. Equation 4.89 assumes a view factor between the glass surface and the sky equal to that from the surface to the ground, and that the temperature of ground is that of outdoor air.

The INSO subroutine (Fig.4.11) computes the direct and diffuse insolation,  $G_b$  &  $G_r$ , incident on the horizontal and vertical glazing from the following equations (note the subscripts h & v are for horizontal and vertical)

$$G_{bh} = G_h - G_{fh} \quad \{4.90\}$$

$$G_{bv} = G_{DN} \cos(\theta) \quad \{4.91\}$$

$$G_{rv} = 0.5 \rho_g G_h \quad \{4.92\}$$

$$G_{sv} = 0.5 G_{fh} [1 + F \sin^3(\beta/2)] [1 + F \cos^2(\theta) \sin^3(\theta_z)] \quad \{4.93\}$$

$$F = 1 - (G_{fh} / G_h)^2$$

$$G_{fv} = G_{rv} + G_{sv} \quad \{4.94\}$$

where  $\beta = 90^\circ$ , the glazing slope angle;  $F$  is a modulating function for use in Eq.(4.93);  $G_{rv}$  is the ground reflected global insolation on the vertical glazing ( $\text{W m}^{-2}$ ); and  $G_{sv}$  is the sky diffuse insolation on the vertical surface ( $\text{W m}^{-2}$ ). Equations 4.90 to 4.94 have been discussed earlier in chapter 2 (see section 2.4.1).

The GLASS subroutine (Fig.4.12) computes the glazing properties of absorption and transmission for both direct and diffuse insolation at the angle of incidence input from the main routine. Equations 4.11 through 4.14 are used for these calculations.

### *Results and Discussion*

The output of this program is tabulated in Appendix D as monthly means of hourly data. In general, about 2% of the solar heat gains are due to inward flow of absorbed insolation by convection and longwave radiation. Figure 4.13 shows the daily solar heat gain flux,  $\text{kWh (m}^{-2} \text{ day}^{-1})$ , through the horizontal and the vertical glazing at different orientations for July and December as representatives of summer and winter months. Figure 4.14 gives the hourly distribution of solar heat gains.

For vertical glazing, most of the solar heat gains are from diffuse insolation (see the percentages on Fig.4.13). This calls for caution in the sizing and location of windows and in selecting the type of external shading devices as means of solar heat gain control.

Figures 4.15 & 4.16 show the hourly distributions of internal and external surface heat transfer coefficients,  $h_i$  &  $h_o$ , respectively. Note that  $h_i$  is strongly temperature dependant, and almost independent of vertical glass orientation. The  $h_o$ , on the other hand, is dependant on the surface wind speed, hence dependent on surface orientation. (see Figure 3.24 in chapter 3, for the diurnal variations of wind speed in Riyadh).

**Figure 4.13**

Monthly means of Daily solar heat gain through a 3mm reference glass of stated orientations kWh(m<sup>-2</sup> day<sup>-1</sup>) for July & December months (as representative for summer & winter). Calculated by the author for Riyadh climate (see section 4.4.2).

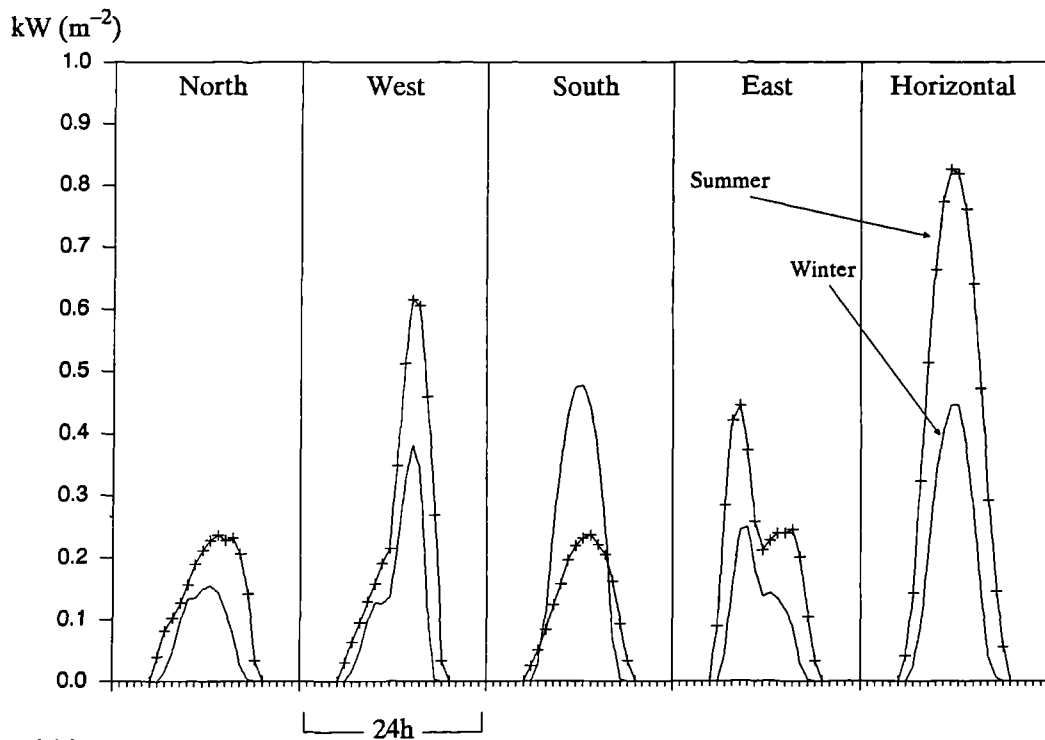
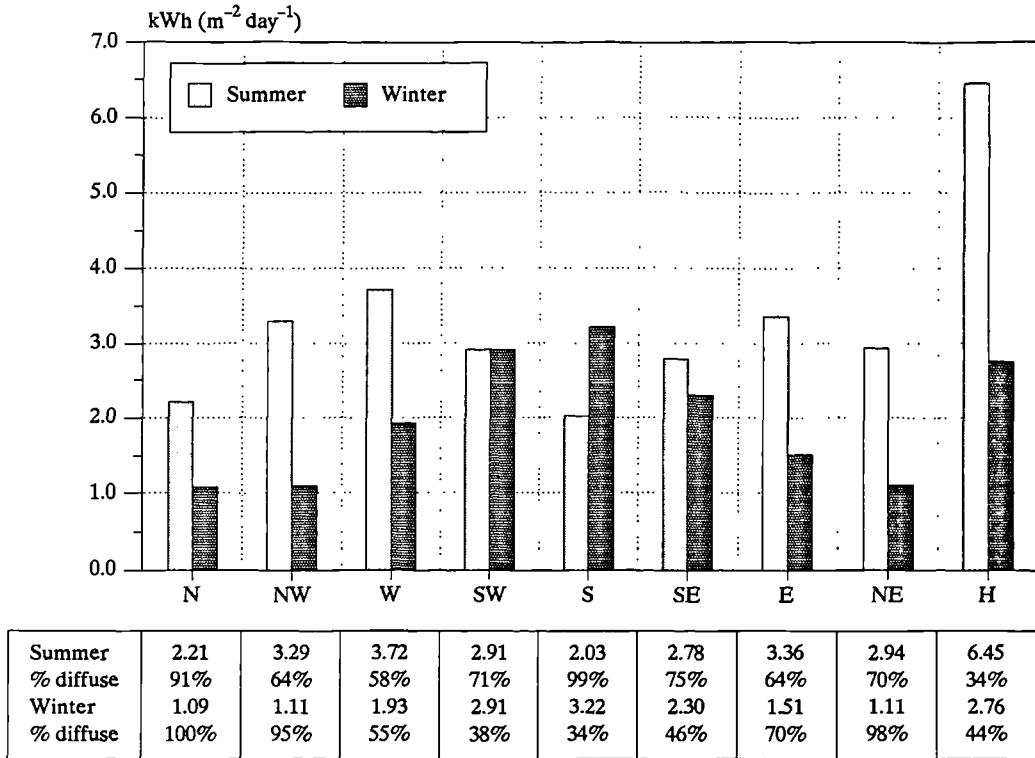


**Figure 4.14**

Monthly means of hourly solar heat gain through a 3mm reference glass of stated orientations (W m<sup>-2</sup>) for July & December months (summer & winter). Calculated by the author for Riyadh climate (see section 4.4.2).

**Figure 4.15**

Hourly heat transfer coefficients at the internal surface of the reference glass for the stated orientations,  $W (m^{-2} \text{ } ^\circ C^{-1})$ .

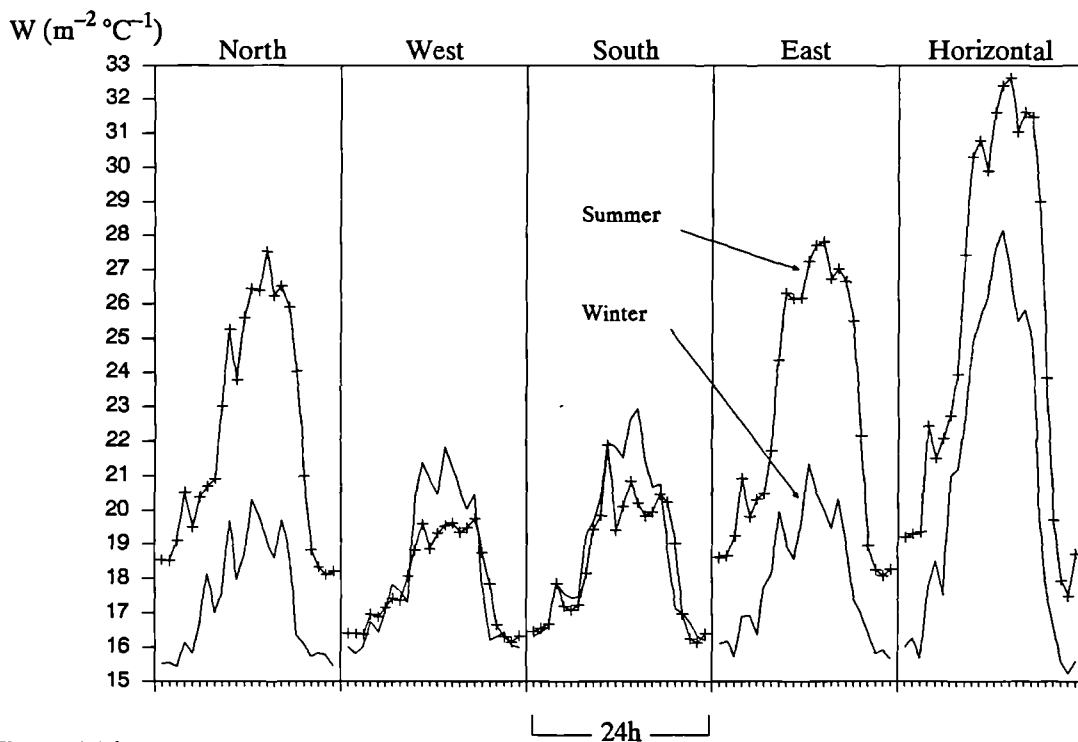
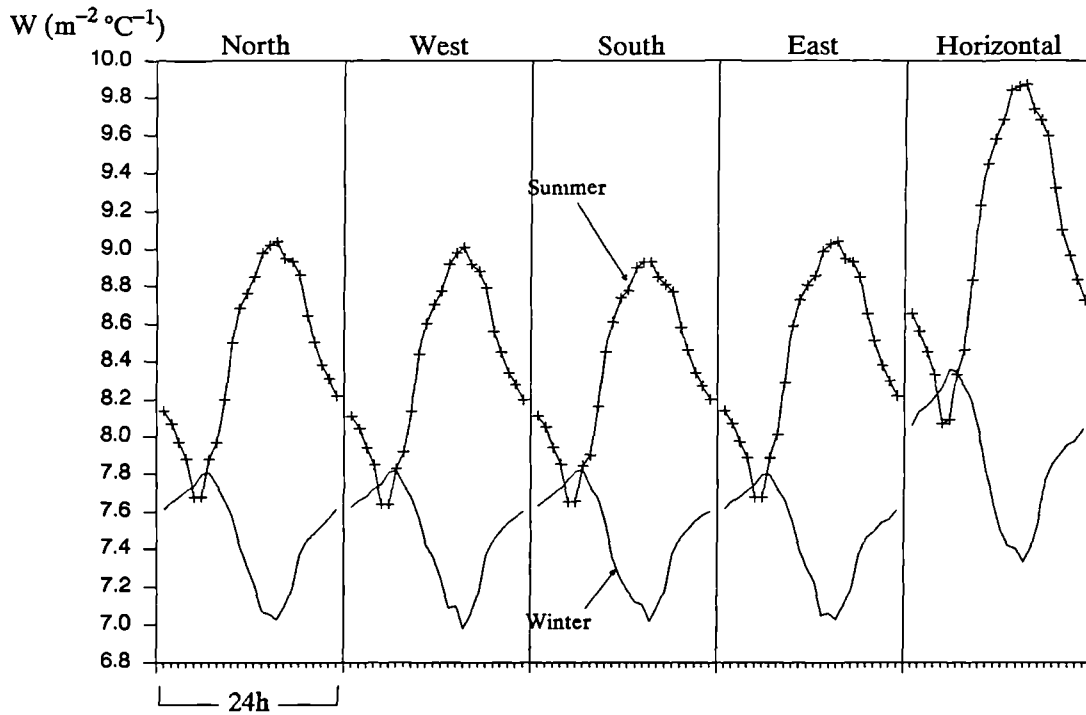


**Figure 4.16**

Hourly heat transfer coefficients at the external surface of the reference glass for the stated orientations,  $W (m^{-2} \text{ } ^\circ C^{-1})$ . Calculated using Riyadh climatic data (see section 4.4.2).

**Table 4.6** Monthly means of the glazing external surface heat transfer coefficients <sup>†</sup> for the climate of Riyadh, Saudi Arabia.

Month	Heat transfer coefficient $W(m^{-2} \cdot ^\circ C^{-1})$								
	Window orientation								Skylight Horiz.
	N	NW	W	SW	S	SE	E	NE	
Jan	16.3	16.6	17.8	19.2	19.6	19.5	18.2	16.8	20.9
Feb	16.8	16.9	18.1	19.5	20.5	20.3	19.0	17.7	22.3
Mar	16.9	17.5	18.6	20.6	21.2	20.7	19.6	17.6	23.2
Apr	16.8	17.0	18.1	19.8	20.5	20.4	19.3	17.5	21.9
May	17.4	17.6	18.8	20.3	21.2	21.0	19.7	18.2	23.0
Jun	23.4	22.1	18.1	17.6	17.7	19.1	23.2	23.5	25.9
Jul	22.2	19.9	17.9	18.0	18.5	21.0	22.8	22.7	25.3
Aug	22.2	21.7	18.1	17.6	17.5	18.1	21.9	22.2	24.2
Sep	20.5	20.5	20.4	18.0	17.8	17.7	17.9	20.3	22.5
Oct	16.8	17.4	18.4	19.3	19.5	18.9	17.9	16.9	20.3
Nov	17.6	17.7	18.4	19.4	20.2	20.1	19.3	18.3	22.2
Dec	17.3	17.9	18.2	18.7	19.0	18.4	17.9	17.5	21.0

<sup>†</sup> Calculated by the author from the HTC subroutine of QREF.BAS program (see section 4.4.2). Hourly data for July and December months are shown in Fig.4.11.

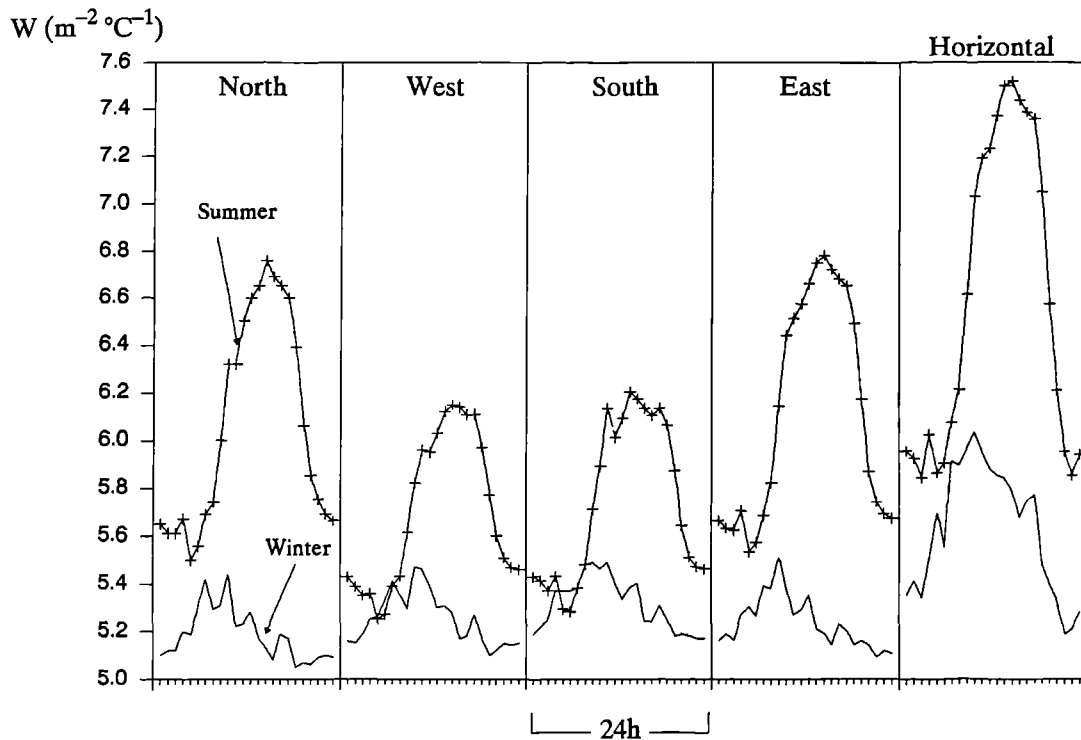
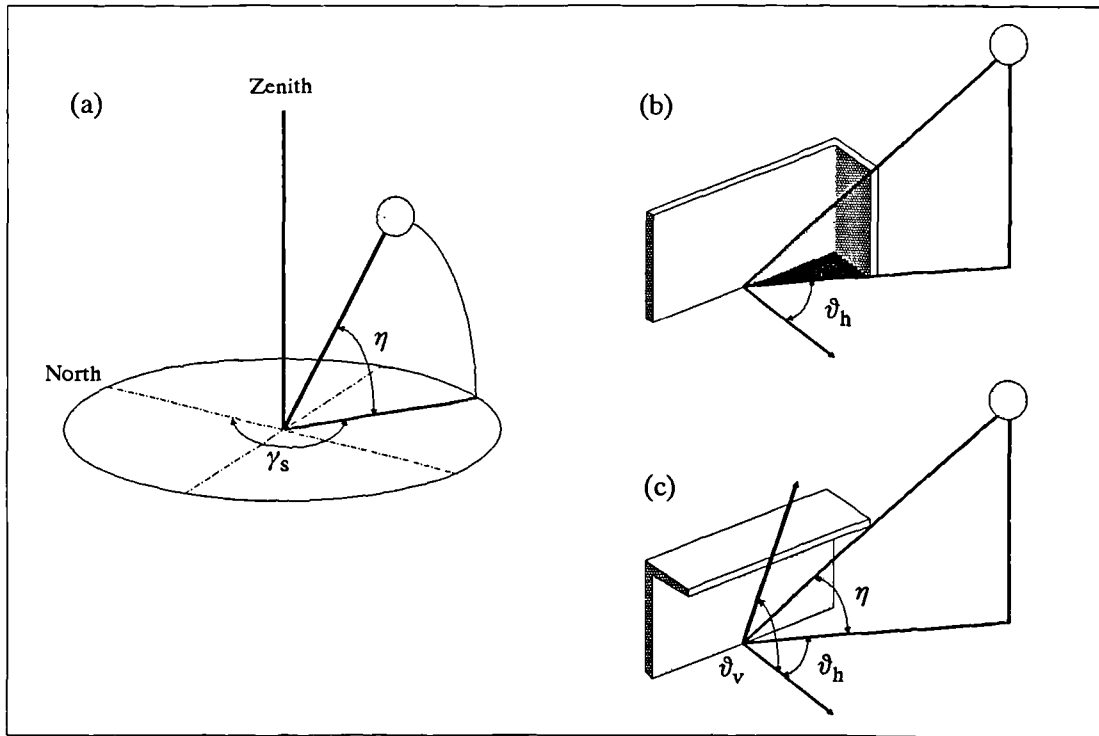


**Figure 4.17**

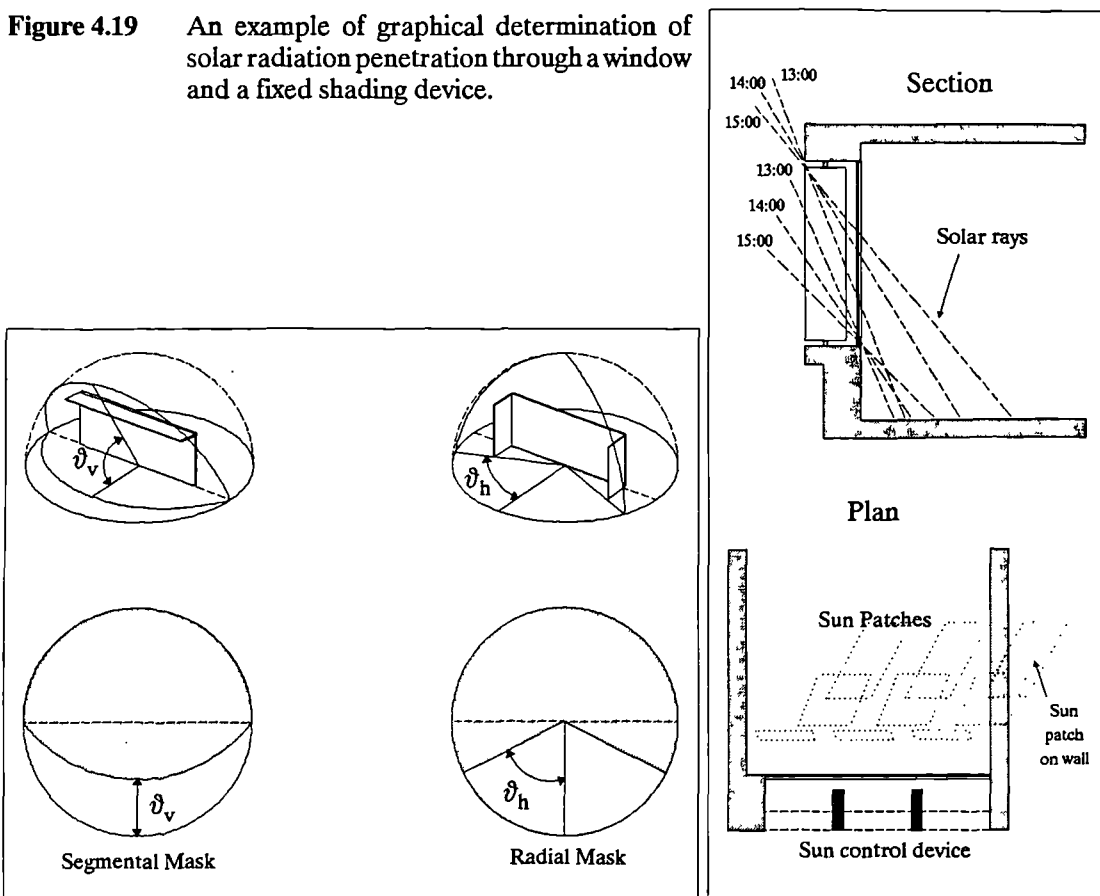
24h distribution of the reference glass U-value for the stated orientations,  $W (m^{-2} \cdot ^\circ C^{-1})$ . Calculated by the author for the climate of Riyadh using Eq.4.69.

Table 4.6 gives mean monthly values of external surface heat transfer coefficient,  $h_o$ , for the horizontal and the vertical glazing at 8 compass orientations. Figure 4.17 shows the hourly distribution of the glazing overall heat transfer coefficient, U value, for summer and winter. Note that  $h_o$  is the dominant factor in the U value, hence the overall heat transfer coefficient is strongly dependant on surface wind speed.

**Figure 4.18** Solar position in relation to building surfaces. (a) solar azimuth and altitude angles, (b) horizontal shadow angle and (c) vertical shadow angle.



**Figure 4.19** An example of graphical determination of solar radiation penetration through a window and a fixed shading device.



**Figure 4.20** Shading masks show the shadows by vertical and horizontal shading elements.

## 4.5 Shading Design Tools

An evaluation of the expected performance of a planned shading device and its geometrical characteristics, prior to actual construction, is essential for the satisfactory thermal performance of a building. Shading devices can be designed if the position of the sun relative to the building face is known, i.e. if the solar geometry is determined. The solar azimuth ( $\gamma_s$ ) and solar altitude ( $\eta$ ) angles specify the sun's position in relation to geographical coordinates, i.e. north taken as  $0^\circ$  azimuth and the horizontal taken as  $0^\circ$  altitude. These angles depend on the site latitude, solar declination and the local solar time, and can be determined from the following equations (Olgyay & Olgyay 1957) :

$$\sin(\eta) = \cos(\phi) \cos(\delta) \cos(\omega) + \sin(\phi) \sin(\delta) \quad \{4.95\}$$

$$\cos(\gamma_s) = [\sin(\eta) \sin(\phi) - \sin(\delta)] / \cos(\eta) \cos(\phi) \quad \{4.96\}$$

If the sun's position is to be specified in relation to a building or a window face, it can be done by further two angles; 1- the horizontal shadow angle ( $\vartheta_h$ ) given by Eq.4.97a or Eq.4.97b depending on the time of the day ( $t_s$ ), and 2- the vertical shadow angle ( $\vartheta_v$ ) which is the projection of the solar altitude angle onto a plane perpendicular to the building face (see Fig.4.18). When the sun is directly opposite to the building face, i.e. the solar azimuth equals the surface azimuth ( $\gamma_s = \gamma$ ), the solar altitude angle and the vertical shadow angle are identical, ( $\vartheta_v = \eta$ ). In all other cases, i.e. when the sun is to one side of the building's orientation, the vertical shadow angle is greater than the solar altitude,  $\vartheta_v > \eta$ . The relationship is expressed in Eq.4.98.

$$\vartheta_h = \gamma_s - \gamma \quad \text{if } t_s \leq 12 \quad \{4.97a\}$$

$$\vartheta_h = \gamma_s + \gamma \quad \text{if } t_s > 12 \quad \{4.97b\}$$

$$\tan(\vartheta_v) = \tan(\eta) / \cos(\vartheta_h) \quad \{4.98\}$$

Several methods exist for evaluating the performance of shading devices. One method is to determine the solar penetration through a fenestration by using the above equations and to plot sunlight patches on plan/section drawings (see Fig.4.19). It is also possible to construct a model and to test it under artificial or natural insolation conditions. Such techniques are discussed in detail in the literature (e.g. Aronin 1953 and Olgyay & Olgyay 1957).

A common method by which the design and examination of shading devices are determined was developed by Olgyay & Olgyay (1957). They pointed out that there are only two basic types of sun controls: vertical shading elements called fins, and horizontal shading elements called overhangs. The effect each will have on the window can be easily plotted as a shading mask (see Fig.4.20). By convention the reference point on the window is usually located at the bottom centre of the glass area. The shading mask simply shows the angle between the reference point and the edge of the fin or the overhang.

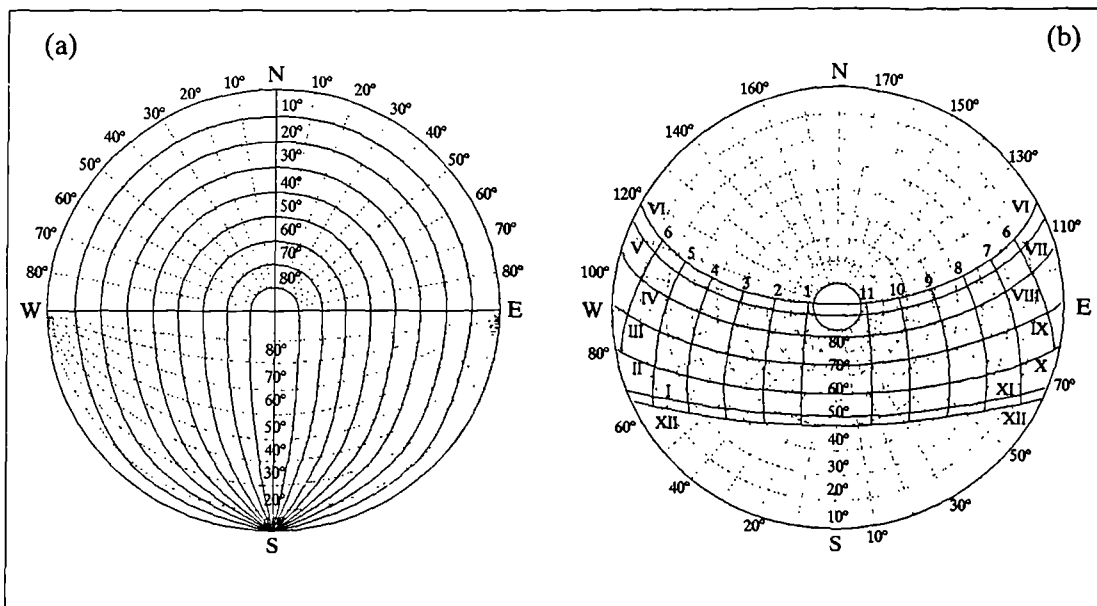


**Figure 4.21** Shading design tools. (a) The shading mask protractor to be overlaid on the sun chart. (b) Sun chart for latitude 24°N; it gives the solar azimuth and altitude angles for every time of day and every month (indicated by Roman Numerals I through XII). (reproduced from Givoni 1976).

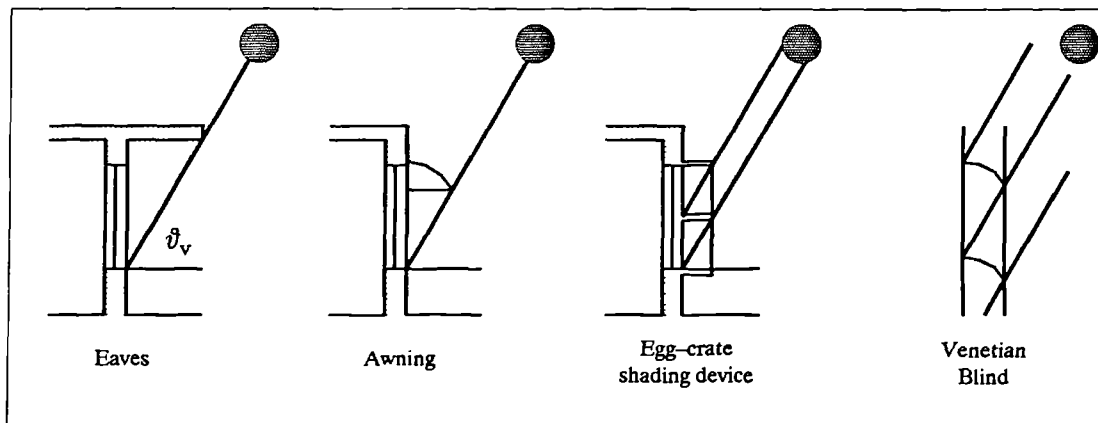


**Figure 4.22** Various shading devices for a set performance ( $\theta_v = 60^\circ$ ).

The shading effect of fins or any vertical edge that cast shadows is indicated by radial lines emanating from the reference point; these represents the horizontal shadow angles ( $\vartheta_h$ ). The shading effect of an overhang or any horizontal edge is indicated as a semi-circular segment showing the vertical shadow angle ( $\vartheta_v$ ).

The shading mask is independent of the orientation of the window or its latitude, since both fins and overhangs can be specified completely in terms of horizontal and vertical angles from the reference point. Therefore a shading mask protractor (Fig.4.21a) can be used as an overlay on the sun chart of any latitude and it can be rotated for a window facing in any direction. Figure 4.21b shows a sun chart for 24°N latitude.

The size and physical make-up of shading devices does not matter from the point of view of geometry. Figure (4.22) shows that many different devices can have the same performance. Thus, the designer may decide early in the design process the required shading performance, and still preserving the freedom for the selection of the actual device. However, the energy efficiency of a shading device is variable and depends on its position with respect to the glass and on its solar characteristics (i.e. reflectance and absorptance), as well as the ventilation conditions. The shading coefficient of a solar control device accounts for these factors. Thus if available, the shading coefficient is a good indicator for selecting a shading device.

Mathematical procedures for shading calculations suitable for computer application can be found in various literature such as, Budin & Budin (1982), Robert & Jones (1980), Yanda & Jones (1983), Barozzi & Grossa (1987). Computer models are also available which give the shading effects of complex objects in relation to buildings. For example, the "SHTREE" program developed by Sattler et. al. (1987) gives numerical and graphical results of the shading effects of trees in relation to buildings. The shading module in the "ESP" program, (*ESPshd*), gives graphical presentation of shading results and computes shading factors to be incorporated in the energy simulation of building zones. (see Clarke 1985).

**Figure 4.23** Sun penetration through a sun screen vs. sun altitude. (reproduced from Hastings & Crenshaw 1977).

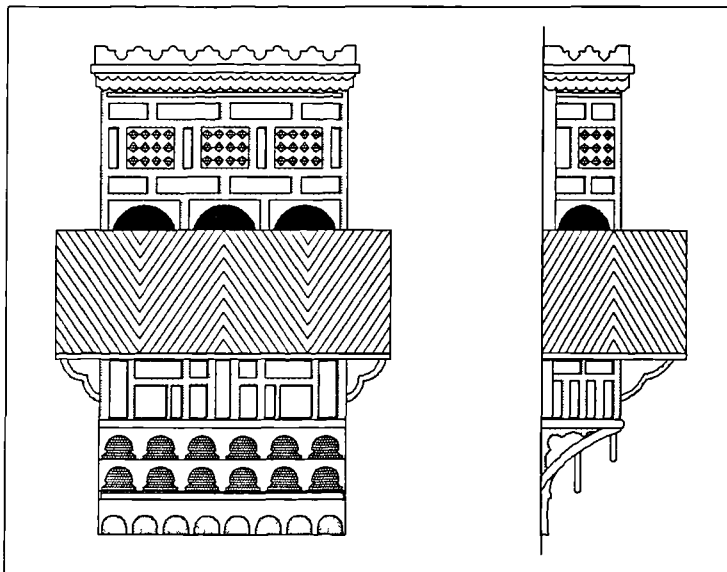
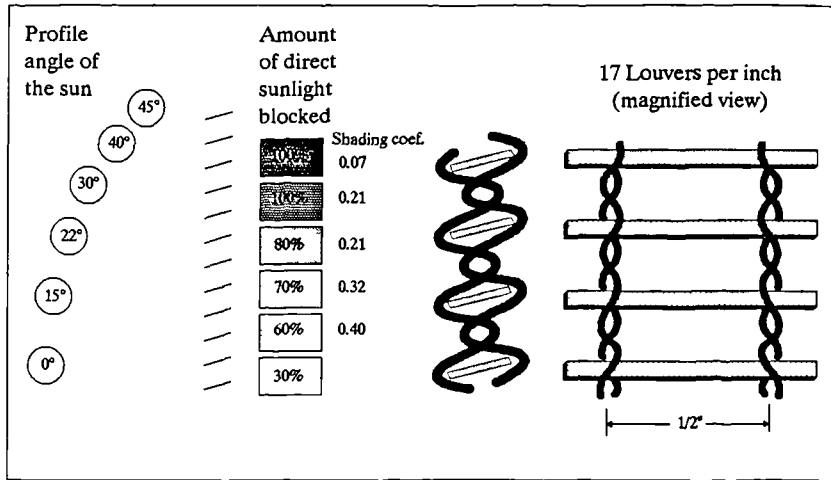


**Figure 4.24** A traditional external wooden sunscreen “Mashrabiya”, common in the western region of Saudi Arabia. It is also known as “Roshan”.

## 4.6 Efficiency of Shading Devices

---

The energy performance of a window can be greatly improved with external shading devices which are part of the window system or part of the wall or roof system. For example, shading can be effectively accomplished by louvered sun screens, blinds, awnings, or roof overhangs. Such devices often provide secondary energy benefits in addition to their primary function. For example, sun screens or external roll blinds, in addition to providing shade in the summer, reduce the heat transfer coefficient at the external surface of the glass (i.e. less exposure to wind speed and sky radiation), thus reducing winter heat losses. The principal advantage with external shades of all types is that the solar heat absorbed by them is dissipated in the open.

Interior shading devices include venetian blinds, vertical louvre systems, fabric blinds of various kinds and curtains. Because of their position they have advantages over the external devices in that they are protected against the weather and are easy to get at for control and maintenance. Such devices can reduce heat gain and heat loss through windows. Although internal shades can shield the occupants of a room against glare and against radiant solar heat, they are in general less effective than external shades for minimizing solar heat gains because a proportion of the heat they absorb is released to the room. In reducing heat loss, if the device does not effectively trap air between itself and the window, the insulative value is minimal. However, if it is installed to provide an air-tight enclosure and its material is selected with proper solar properties, an interior shading device can improve the energy performance of a window.

### 4.6.1 Exterior Shading Devices

#### *Sun Screens*

The effectiveness of a solar screen in shading a window depends on its geometry and reflectivity. The geometry determines the value of the sun altitude before the louvers block all direct insolation. The reflectivity of the louvers determines how much light penetrates indirectly by being reflected off the surface of the louvers, thus highly absorptive surfaces improve the effectiveness of a sun screen in terms of reducing solar heat gain through windows. Figure (4.23) is an example of the geometry and effectiveness of a sun screen. An external sun screen installed close to a single glazed window reduces the winter U value,  $W(m^{-2} \text{ } ^\circ C^{-1})$ , from 5.7 to 4.2 (ASHRAE 1985). Figure 4.24 shows a traditional sun screen “Mashrabiya” commonly used in the western region of Saudi Arabia.

#### *Exterior Shutters*

Figure (4.25) shows various types of exterior shutters. The wooden side-hinged type is the common external shading device to be found in traditional buildings in Saudi Arabia. Shutters have the merit of being simple in action and also giving extra security against burglary. The disadvantages of the traditional forms are that they may be difficult to maintain and control, and that their weight tends to limit their size.

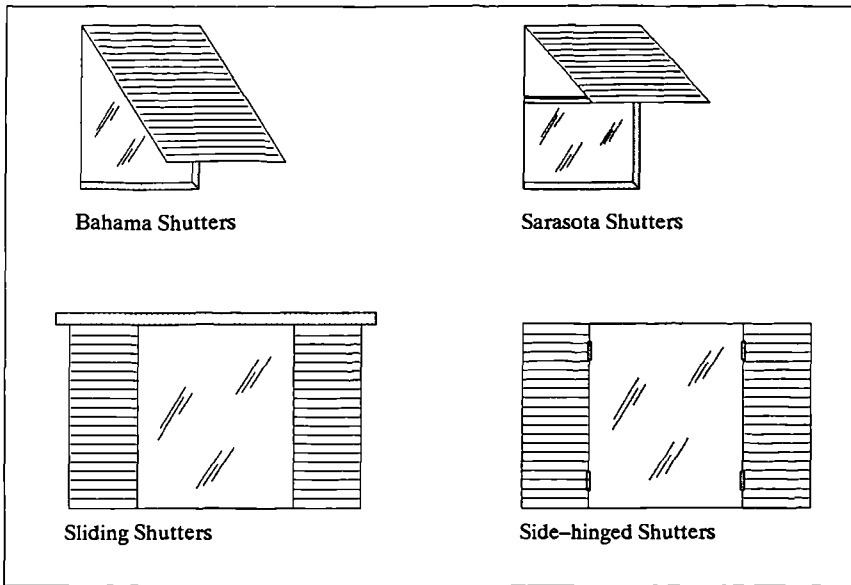


**Figure 4.25** Types of exterior shutters.

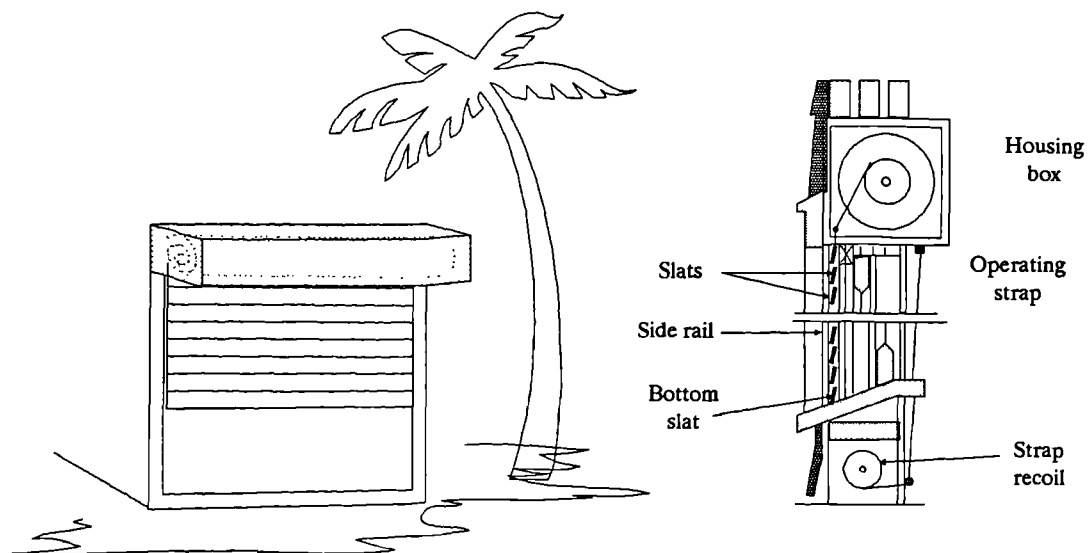


**Figure 4.26**

Installation of an external roll blind. (reproduced from Hastings & Crenshaw 1977).

An exterior shading device effectively blocking all direct sunlight can reduce solar heat gain through a window up to 80% (Lim et. al. 1979 and ASHRAE 1985). The shading performance of closed exterior shutters depends upon how well the heat absorbed by the shade itself is dissipated to the outside air. Operable louvers adjusted to block the sun but let air circulate improve the shutter's ability to reduce heat gains and if closed can be beneficial in reducing heat loss in winter. Light coloured shutters which reflect much of the solar radiation rather than absorb it are more effective than dark ones.

### *Exterior Roller Blinds*

A blind on a roller at the head of a window can be lowered to provide an opaque or semi-opaque barrier to the summer sun, blocking both direct and diffuse insolation. Roll blinds can be made from fabric coated both sides with PVC. Some roll blinds are made of horizontal slats, of aluminium or wood, wired together at an angle to exclude sun during most of the year. This type of blinds is flexible enough to be rolled, though it can be fixed to a rigid frame if desired (Fig.4.26).

Light coloured roll blinds are more effective than dark coloured ones in reducing solar heat gain through fenestration (Hastings & Crenshaw 1977). However, Beckett & Godfrey (1974) reported that dark coloured open-weave blinds of synthetic yarn are more effective in reducing solar heat gains than light coloured ones. One can infer from the latter statement that solar transmittance of the open-weave blind is high, therefore the higher absorption of solar radiation by the darker blind (which later dissipates in the open) is more significant than the solar radiation reflected.

Exterior roll blinds provide the most effective insulating air space of all external shading devices, because of the seal provided at the top and sides. Hastings & Crenshaw (1977) reported a reduction of the U-value of a single glazed window from 5.7 to 2.8  $\text{W}(\text{m}^{-2} \text{ } ^\circ\text{C}^{-1})$  with a roll blind in winter; and from 5.3 to 2.7  $\text{W}(\text{m}^{-2} \text{ } ^\circ\text{C}^{-1})$  in the summer.

### *Architectural Projections*

Horizontal or vertical plane(s) projecting out in front of or above a window can be designed to intercept direct insolation in summer and admit if not all the winter insolation. If the plane projects far enough from the building a single projection may be sufficient as in the case of roof overhangs and canopies or windows recessed deeply between vertical fins.

Alternatively, horizontal, vertical or egg-crate louvered systems fixed parallel to the plane of the window can give effective shading for a wide range of conditions depending on the setting of the blades. A practical difficulty with any closely spaced fixed louvre system is the question of access for maintenance, both to the louvre system itself and to the window behind. The way in which the window opens will also require consideration.

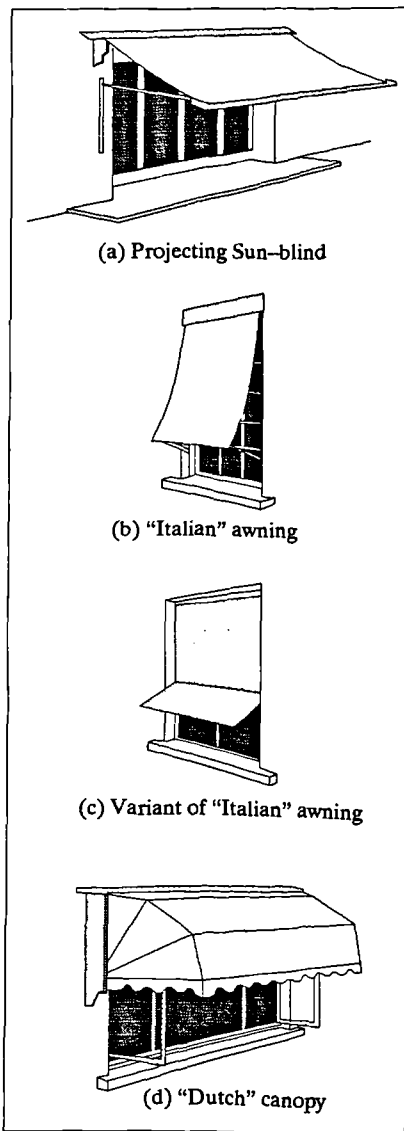


Figure 4.27 Types of awnings. (reproduced from Beckett & Godfrey 1974).

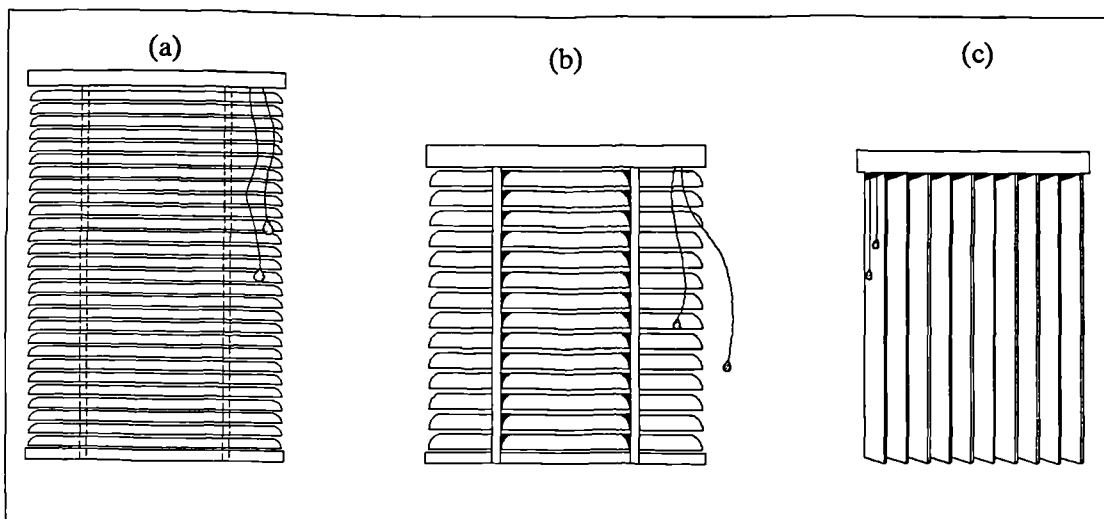


Figure 4.28 Various types of internal blinds. (a) classic miniblind, (b) venetian blind with wide tape and (c) vertical louver blind open and close as curtains and may rotate 180°. (reproduced from Nielson 1990).

East and west-facing windows can be effectively shaded by vertical projecting planes, south-facing windows are effectively shaded by horizontal projecting planes. The lower the latitude of a building location, the more important shading east and west-facing windows becomes and the less important shading south-facing windows becomes. This is due to the high altitude of the summer sun in lower latitude with the resulting decrease in direct insolation transmitted by the south-facing windows.

For shading effectiveness the colour of the inner surface(s) of the exterior projection should be dark to reduce insolation reflected off the projection and through the window. The insolation absorbed by this dark colour is then dissipated by radiation and convection. A separating gap between the shading device and the window is important to provide free circulation of the air to insure this heat dissipation. The use of horizontal louvered systems projecting outwards as canopies can give the same effect as solid projection with the benefits of being lighter in weight, less resistant to wind and admitting more diffuse daylight for better illumination.

### *Awnings*

Folding awnings often combine protection against sunlight with a decorative function, and the material being available in a large range of textile fabrics and aluminium slates. According to Beckett & Godfrey (1974), there are three types of awning – the ordinary projecting sun blind, the “Italian” type awning, and the “Dutch” type canopy. Figure (4.27) shows different types of awnings.

How well an awning shades a window is dependent on how opaque the material is to both direct and diffuse insolation. Light coloured awning materials are more effective than dark ones in reflecting solar radiation, thus reducing heat gains through windows. For example, a white canvas awning or a slatted, white aluminium awning reflects between 70% and 91% of insolation depending on how clean it is (dirt absorbs solar radiation). By comparison, a dark green canvas awning reflects only 21%, and a dark green plastic awning reflects 27% of solar radiation (Ozisik 1958).

## 4.6.2 Internal Shading Devices

### *Internal Venetian Blinds*

Venetian blinds can give very flexible control, both of direct sunlight and daylight admitted into a room. Venetian blinds are commonly made of aluminium alloy slates, although blinds made with plastic or fabric are also available. Beckett & Godfrey (1974) review various types of venetian blinds and include illustrations of usage and operating mechanisms ranging from manual operation to automatic control units activated by a photocell in response to changes in light intensity. An experimental study on the energy performance of a fabric blind is given in chapter 7. Figure 4.28 shows various types of internal blinds.

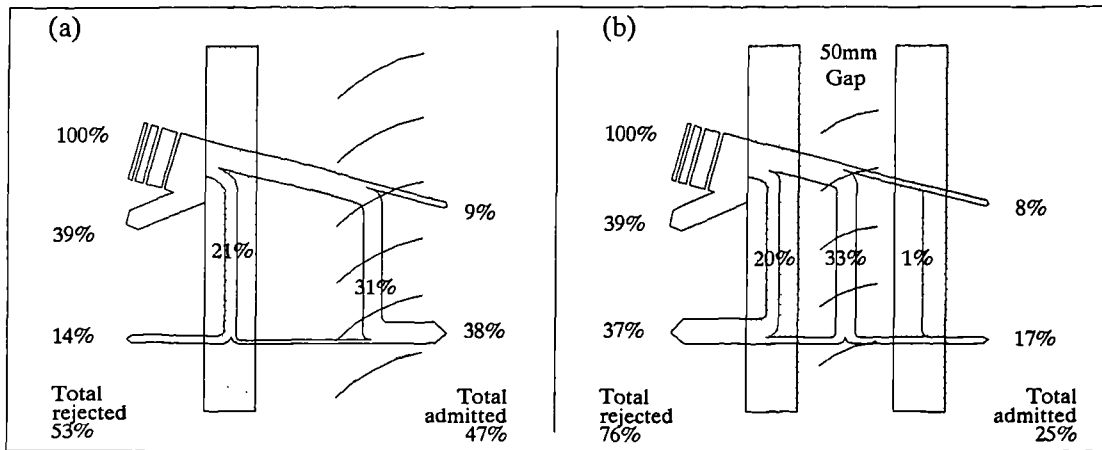


**Figure 4.29** Heat transfer mechanism. (a) through a 6mm clear glass with internal light coloured blind; and (b) through double glazing with a blind inside the glazing air gap, which reduces the total transmittance from 72% to 25%. (data from Pilkington 1988; see Table 2.10 in chapter 2 of this thesis for other examples).

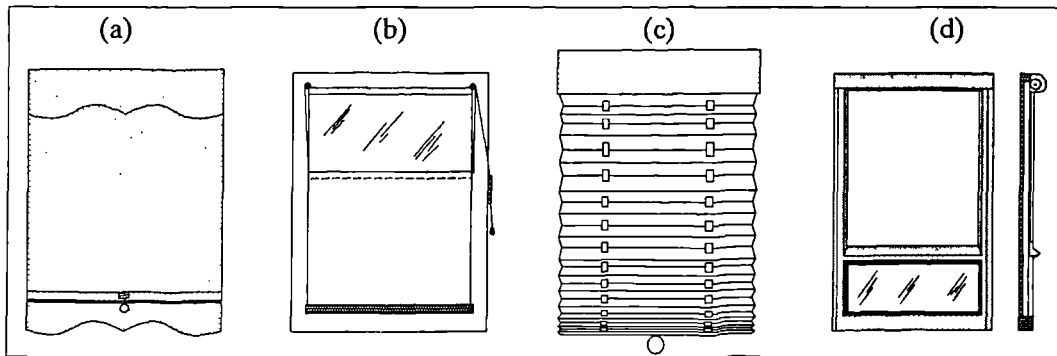


**Figure 4.30** Various types of roller shades. (a) common roller shade type; (b) roller shade that rolls up from the bottom with cord and pulley; (c) accordion shade usually made of stiffened polyester fabric drawn with a finger pull; (d) front and side views of a roller shade on a sealed track to increase its insulation effectiveness. (see Nielson 1990 for more examples).

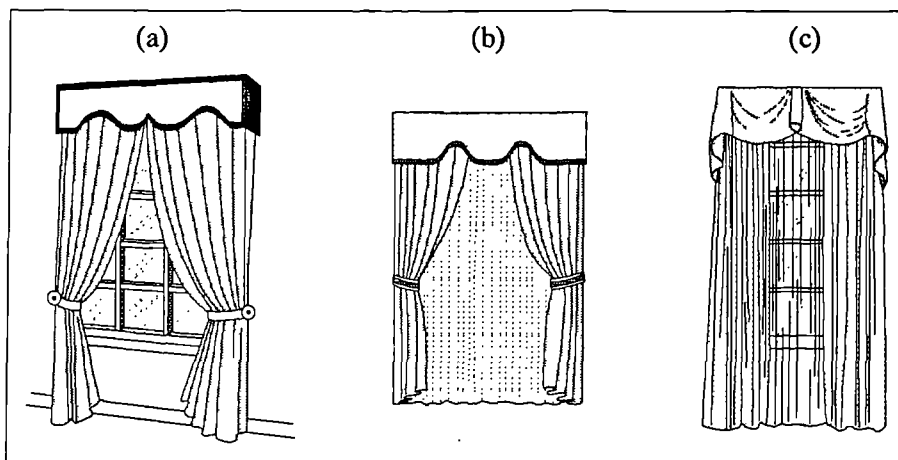


**Figure 4.31** Curtain arrangements for energy efficiency showing; (a) the use of upholstered cornice, made of hard material like plywood in this case, increases the curtain insulative property by trapping an air layer between the glazing and the curtain; (b) the insulative property of curtains is further improved by using liners, i.e. another fabric layer; (c) the cornice can also be made of fabric.

Slatted horizontal or vertical blinds can be tilted to provide maximum reflection of solar radiation, thus reducing heat gains through windows. For example, at a 45° tilt with insolation perpendicular to the slates, a medium coloured blind can reduce solar heat gain through a 4mm single glazed window by 36% and by 45% if a light coloured blind is used. Figure (4.29a) shows the mechanism of heat transfer through a 6mm clear glass with light coloured blind).

The effectiveness of medium and light coloured blinds in combination with various types of glass are given in Table 2.10 in terms of shading coefficients. (see section 2.4.2 of the second chapter). Where double glazed windows are used, installing a venetian blind between the glass panes can reduce the transmitted solar heat gain by 60% (see Fig.4.29b).

### *Internal Roller Shades*

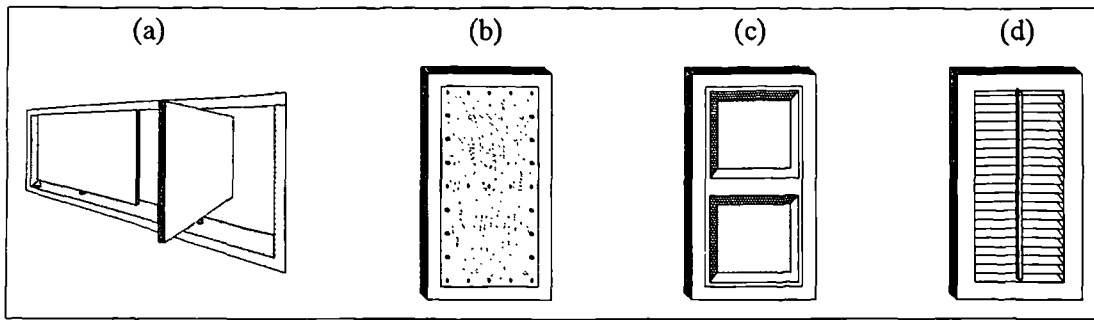
Although roller shades are less adaptable for dealing with direct sunlight than venetian blinds they have the merit of simplicity in operation and they are easy to maintain. They can be of opaque or translucent types. Figure 4.30 shows different types of roller shades. A roller shade can have a dark colour on one side which absorbs insolation and a white surface on the reverse side which reflects insolation. By simply reversing the shade from dark side facing out in winter to reflective side facing out in summer, the shade can perform as a solar collector or shading device varying with the season. According to ASHRAE (1985), a 13% reduction of the summer U-value of a roll shade with a moderately close fit to the window opening in the wall can be achieved. The effectiveness of opaque and translucent roller shades in combination with various types of glass are given in Table 2.10 in terms of shading coefficients. (see section 2.4.2 of the second chapter).

### *Curtains*

Heat loss and heat gain through a window can also be reduced using curtains. The next chapter is devoted to study the solar and thermal characteristics of fabric curtains, and in chapter 8, the thermal performance of domestic curtains is determined by test site experiments. In general, curtains are more effective in reducing solar heat gain than the reduction of heat loss through windows. However, efficiency of a curtain in reducing heat loss through windows can be improved by increasing its insulative value, using opaque or metallic lining fabrics as liners. It can also be improved by using upholstered cornices to reduce infiltration (see Fig.4.31). Curtains can also help to reduce the acoustic absorption, but the material must be of a heavy and dense weave if the contribution is to be significant.

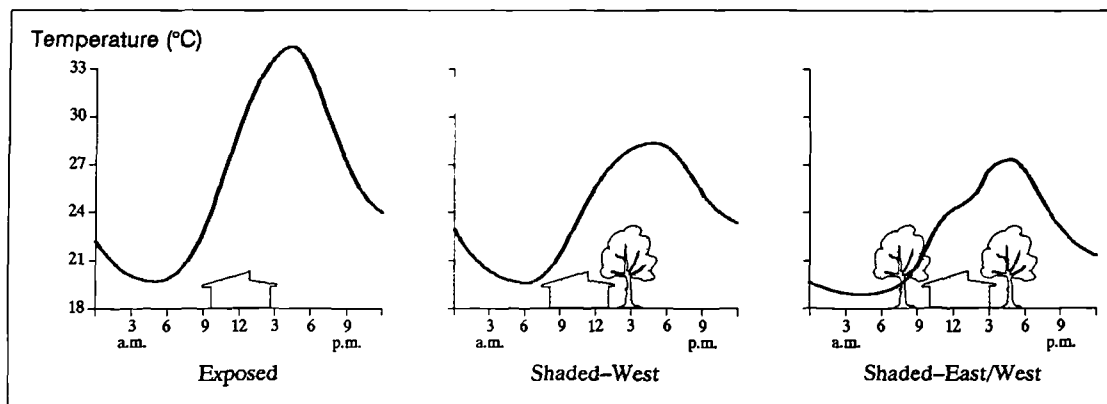
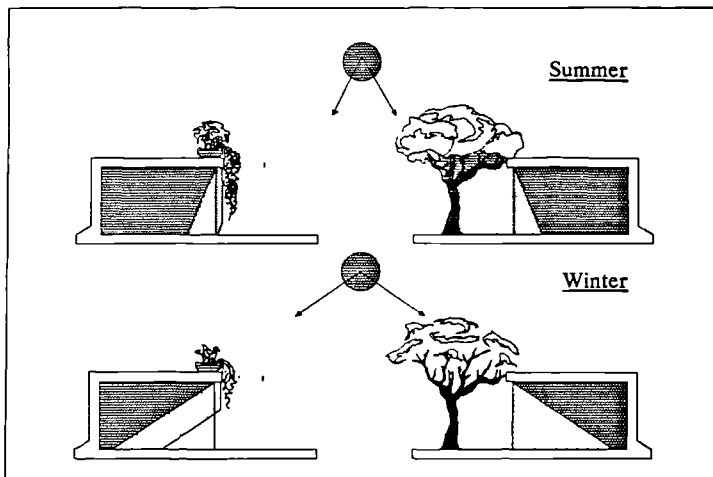
### *Insulating Shutters*

Figure 4.32 shows different types of insulating shutters. Hinged or removable opaque insulating shutters are the most effective devices in reducing heat loss through windows. Generally they are opaque and made of wood panels or rigid insulation material covered with decorative wood or fabric.



**Figure 4.32** Various types of insulating shutters; (a) pivoting shutters, which can be made of plain wood, or fabric-covered wood; (b) rustic riveted wood shutter; (c) raised-panel shutter made of wood or rigid insulation material; and (d) movable-louver shutter. (reproduced from Nielson 1990).

**Figure 4.33** Seasonal sun angle vs. the interference of trees and roof planting.



**Figure 4.34** Shade tree effectiveness vs. orientation. Temperature scale is in degrees Fahrenheit. (reproduced from Hastings & Crenshaw 1977).

The reduction of heat loss is proportional to the insulating value of the device measured as resistance to heat flow per unit thickness of material. If a gap between the insulating shutter and the glass exist with free circulation of air, the effectiveness of the panel in reducing heat loss will be drastically reduced. However, an air gap will improve the efficiency of a shutter if fitted tightly with no free circulation of air.

### 4.6.3 Planting and Shading

The planting of trees, bushes, or vines in appropriate places can adequately shade structures in many climates (Wright 1978). Evergreen trees, would provide permanent shading and reduce radiative heat loss to the night sky in winter. They could act as buffers, helping to block winter storms and summer sand storms. Deciduous trees provide shade in the summer, then lose their leaves and admit sunlight in winter. (see Fig.4.33).

Roof planting is also an effective way of providing shade to exterior building facades. Thus, in dry climates, irrigation of roof planting will do much to cool a structure through evaporation. Trees can act as evaporative coolers, lowering the temperature of air passing through the branches and thus modifying the microclimate. Figure 4.34 illustrates the effectiveness of a shade tree on the east or west side of a house in reducing the air temperature in the shaded area.

Trees are variable in shape, density of leaves, and interaction with the environment. This complexity make it difficult to quantify the shading efficiency of trees in shading buildings. An attempt to asses the shading effects of trees on a building facade at any times of day and year, at any location was done by Sattler et. al. (1987). They developed a computer program "SHTREE" which determines the shadow area and position of the shadows cast by a tree or a group of trees on a surface of any orientation. The program allows four different shapes of tree (spherical, cylindrical, upright cone or reversed cone) or any combination of these shapes to be used as shown in Figure 4.35.

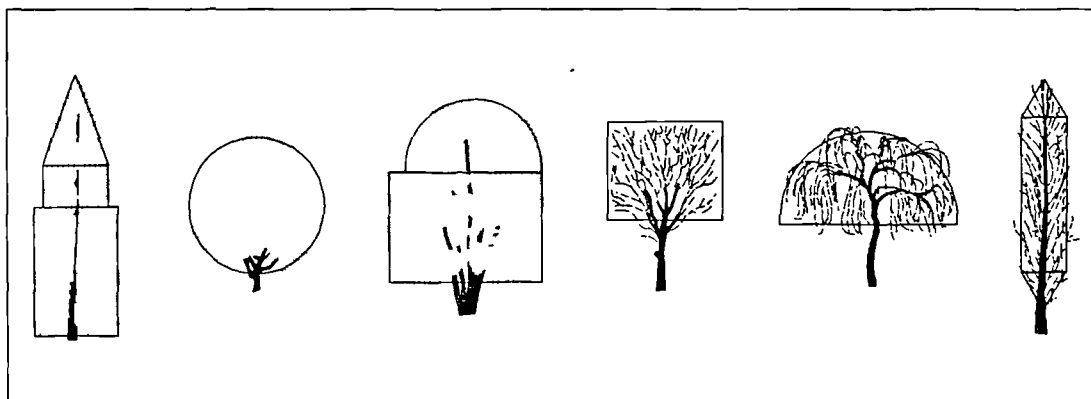
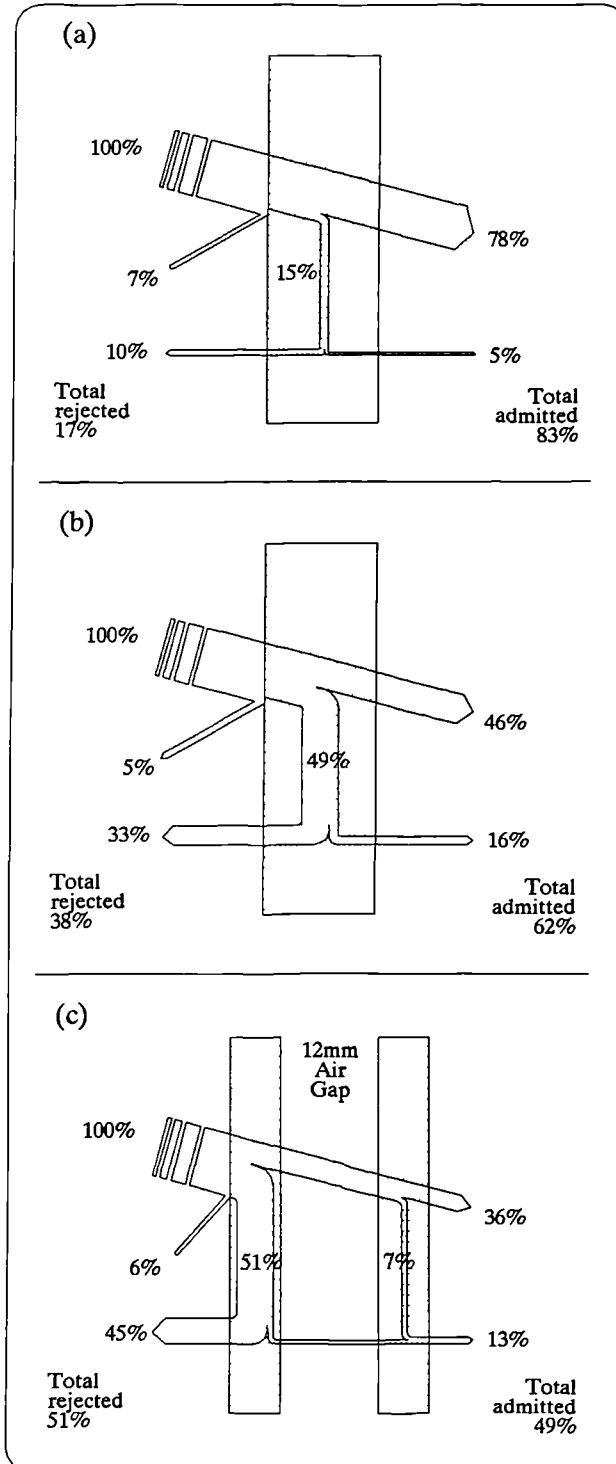


**Figure 4.35** Shapes of trees as defined for "SHTREE" program:– spherical, cylindrical, upright cone, reversed cone or any combination of these shapes. (reproduced from Sattler et. al. 1987)

**Figure 4.36** Heat balance diagrams of (a) 6mm clear glass; (b) 6mm heat-absorbing glass; (c) heat-absorbing outer glass pane with 6mm clear glass. (data from Pilkington 1988).



## 4.7 Solar Control Glazing

---

There have been notable European Commission programs for the development and use of several types of advanced glazing. The primary function of solar control glazing is to act as an efficient heat filter with little effect on the other functions of the windows such as view, provision of adequate daylight. The types of solar control glazing can be classified under the following broad categories:

- Heat-absorbing
- Heat-reflecting
- Photo-chromatic
- Applied films

### 4.7.1 Heat-Absorbing Glass

Adding a metallic oxide to the ingredients of glass during its manufacture gives it a tint and increases its absorptivity of visible and near infrared insolation. The greater absorptivity occurs in the near infrared band of the solar spectrum. The type and quantity of chemicals added to the glass ingredients determines the glass tint. For example, iron oxide imparts a bluish green colour. Nickel and cobalt oxides and selenium give a range of colours which include grey and bronze. (A.J. 1976, Lim et.al. 1979).

Heat-absorbing glass is also produced by a modified float process of glass manufacturing method called spectra float, in which a layer of metal ions is injected first under the surface of the glass ribbons as it is passed through the bath. This results in a bronze tinted layer just beneath one surface of the glass. Because of its single modified surface, the solar performance of the spectra float glass is affected by the actual thickness of the glass pane. Glass which absorbs non-selectively throughout the solar spectrum is called "neutral glass".

Heat balance diagrams for clear and heat-absorbing glasses are shown in Figures 4.36a & 4.36b, respectively. Note that the percentages given in these figures are for an example case and will vary as the sun angle varies. Performance data for some heat-absorbing glasses are given in Table 2.9 (see chapter 2). When heat-absorbing glass is used as the outer sheet of glass in double glazing, its performance is improved compared to its use as single glazing. (see Figure 4.36c).

One disadvantage of heat-absorbing glass is the partial dissipation of heat to the indoor; about 25–40% of the absorbed heat energy is retransferred to the interior by convection and radiation. Also the resulting increase in temperature of heat-absorbing glass exposed to direct insolation can cause discomfort to occupants near the window surface due to the longwave radiation emitted from the glass pane. It is possible for heat absorbing glass to break when exposed to direct insolation with closed curtains or shades. (Brunello & Zecchin 1987).

**Figure 4.37** Heat balance diagrams of (a) 6mm heat reflecting glass; (b) heat-reflecting outer glass pane with 6mm "Kappafloat" inner glass.

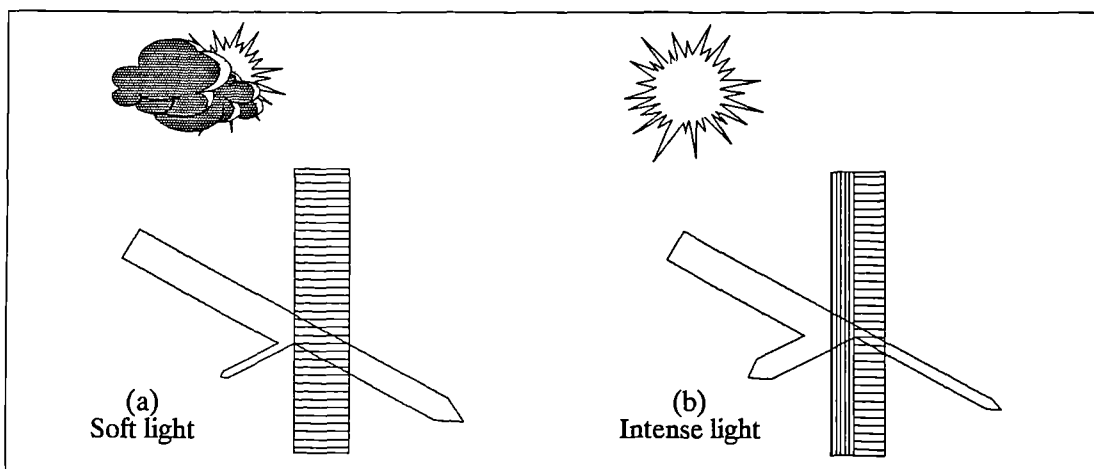
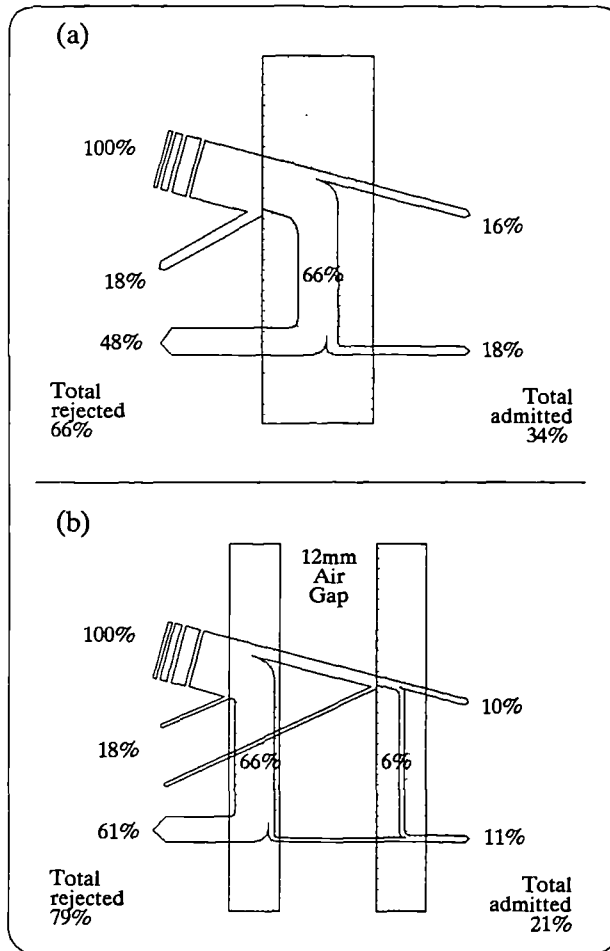


**Figure 4.38** Schematic illustration of the polarization mechanism in photo-chromatic glass; (a) matrix in parallel position so light is mostly transmitted; and (b) matrix in crossed position so light is filtered.

### 4.7.2 Heat-Reflecting Glass

Heat-reflecting glass is produced in an elaborate vacuum deposition technique which produces a microscopically thin layer of metal on one surface of clear float glasses. Metallic reflecting glass offers good reflecting performance in the infrared region of the solar spectrum.

Because of the fragile nature of the coating produced by vacuum deposition heat-reflecting glasses are made available either as double glazed units in which the coated surface is situated in a protected position on the inside surface of the outer pane, or as a laminated single glazed unit. The degree of solar heat control, light transmission and glare reduction is governed by the density of the metallic coating deposited on the glass. Gold, silver, bronze and azure are typical coating materials in heat-reflecting glass. These may provide aesthetic value to building's appearance. Reflective glazing appearance tend to be more effective in expanses, either as a series of windows in continuous band, or a single large area (Skolnik 1977).

The main advantage of heat-reflecting glass is the reduction of solar heat gain by reflecting most of the solar radiation. Units of the gold heat-reflecting glass are capable of rejecting as much as 78% of solar heat. However the azure type rejects about 67% of solar heat while transmitting 47% of visible light (Lim et. al. 1979).

Heat balance diagrams for heat-reflecting glass in a single and double glazing units are shown in Figures (4.37a & 4.37b). A drawback of heat-reflecting glass is the reduction of transmitted solar energy needed in the winter. It is also more costly than clear glass (also true for heat-absorbing glass).

### 4.7.3 Photo-chromatic Glass

This type of glass changes its transmittance property when exposed to light. This can be accomplished by a matrix of polarisation which filters light according to the positioning of chemical crystals, reducing light transmission when moved from parallel (clear) to crossed (dark) positioning as shown diagrammatically in Figure (4.38). Technical information on the active chemicals used in photo-chromatic glass and production procedures can be found in literature, e.g. see Smith (1967) & Lim et. al. (1979).

Visible transmittance of photo-chromatic glass lies in the range  $0.19 - 0.32\mu\text{m}$  during day time and  $0.59 - 0.71\mu\text{m}$  during night time (Lim et. al. 1979). From these figures it is clear that photo-chromatic glass is not promising for solar heat-control applications in buildings. It may find limited application where glare control is the prime consideration, and even this can be achieved by other types of glazing with a fraction of the cost.

**Table 4.7** Solar control performance data for aluminium-coated polyester films on glass (after Lim et. al. 1979).

Description	Shortwave <sup>†</sup> transmission (%)	Total transmission (%)	Shading coefficient —
<b>On 3-mm clear glass</b>			
medium-density coat	33	34	0.41
heavy-density coat	20	21	0.24
<b>On 6-mm heat absorbing glass</b>			
grey	13	33	0.38
bronze	16	33	0.38
<b>Ultraviolet inhibited polyester film</b>			
on 3-mm clear glass	75	81	0.93
medium-density reflective coat	30	37	0.42
heavy-density reflective coat	20	28	0.32
<b>Translucent tinted film</b>			
on 3-mm clear glass	11	25	0.29
on 6-mm glass	10	24	0.28
<b>Non-reflective translucent tinted film</b>			
on 3-mm clear glass	22	42	0.48
on 6-mm glass	20	39	0.45

† Transmittance data are for normal incident solar radiation.

#### 4.7.4 Applied Films

One of the techniques for control of solar heat gain through glass at a lower cost than reflecting glass, is to apply polyester-coated reflective films to clear glass panes. These films are constructed of a transparent polyester sheet film over which a controlled density of metallic vapour (e.g. aluminium) is deposited under vacuum. A further layer of polyester is superimposed to form a sandwich construction. This layer can be tinted (e.g. silver, gold, bronze, azure, and smoke grey) and ultra-violet inhibitors can also be incorporated to block the ultra-violet light transmission through the film to a very high degree.

Other types of film coatings are available which increase the glass reflectivity to room infrared heat while only minimally reduce insolation transmittance. The net effect of such “low-emissivity” films is a reduction in the U-value (overall heat transfer coefficient) of the window thus a reduction in heat loss (see experimental results in chapter 7 of this thesis).

Variation in the thickness of the film, the density of the metallic coating, the type of adhesive used and the colour tinting create a range of solar control reflective films with different solar-heat and light-transmission properties. Table 4.7 gives performance data for films applied to single and double glazing. (Lim et. al. 1979). As a rule, heaviest metal density films provide the greatest solar heat control (up to 75% reduction) and glare control (up to 82%). Medium and lighter density films give less solar heat and glare reduction but permit greater light transmission.

## 4.8 References

---

- Anon. (1976) "Window Glass Design Guide", *The Architects Journal*, January, P 1263.
- Alamdari F. & Hammond G. (1983) "Improved Data Correlations for Buoyancy-driven Convection in Rooms", Rep. SME/J/83/01 (Cranfield: Cranfield Institute of Technology, Applied Energy Group).
- Aronin J. (1953) Architecture and Climate. Reinhold Publishing Corp., New York.
- ASHRAE Task Group (1975) "Procedure for Determining Heating and Cooling Loads for Computerising Energy Calculations", ASHRAE Task Group Report, American Society of Heating, Refrigerating and Air-conditioning Engineers, New York.
- ASHRAE (1985) ASHRAE Handbook (Fundamentals). American Society of Heating, Refrigerating and Air-conditioning Engineers Inc., Atlanta, USA.
- Barozzi G. & Grossa R. (1987) "Shading Effect of Eggcrate Devices on Vertical Windows of Arbitrary Orientation", *Solar Energy*, 39 (4), pp 329-42.
- Beckett H. & Godfrey J. (1974) Windows: Performance, Design and Installation. Crosby Lockwood Staples in association with RIBA Publication Ltd., London.
- Bliss R. (1961) "Atmospheric Radiation Near the Surface of the Ground", *Solar Energy*, 5, p 103.
- Brunello P. & Zecchin R. (1987) "Solar Properties of Fenestration", In "Thermal and Solar Properties of Windows: Expert Guide", (eds.) Dijk H. & Knorr K., IEA, Energy Conservation in Buildings and Community Systems Program, Annex XII – Windows and Fenestration, Step 2. October 1987, Delft, Holland.
- Brunt D. (1932) "Notes on Radiation in the Atmosphere", *Quart. J. Roy. Meteorol. Soc.*, 58, pp 389-420.
- Budin R. & Budin L. (1982) "A Mathematical Model for Shading Calculations", *Solar Energy*, 29 (4), pp 339-49.
- CIBS Guide (1976) "Heat Transfer", Section C3, Chartered Institute of Building Services, London.
- Clarke J. (1985) Energy Simulation in Building Design. Adam Hilger Ltd. Bristol UK.

Cole R. (1976) "The Longwave Radiation Incident Upon the External Surface of Buildings", *Building Services Engineer*, **44**, pp 195–206.

Fujii T. & Imura H. (1970) "Natural Convection Heat Transfer from a Plate with Arbitrary Inclination", *J. Heat Mass Transf.*, **15**, pp 755–67.

Gay J., Morel N., Frank Th. & Puntener T (1987) "Thermal Radiative Heat Transfer", In "Thermal and Solar Properties of Windows: Expert Guide", (eds.) Dijk H. & Knorr K., IEA, Energy Conservation in Buildings and Community Systems Program, Annex XII – Windows and Fenestration, Step 2. October 1987, Delft, Holland.

Givoni B. (1976) Man, Climate and Architecture. Applied Science Publishers Ltd., London.

Hastings S. & Crenshaw R. (1977) Window Design Strategies To Conserve Energy. NBS Building Science Series 104, US Government Printing Office, Washington DC.

Holland L. (1964) The Properties of Glass Surfaces. Chapman and Hall, London.

Hoyt D. (1977) "Percent of Possible Sunshine and Total Cloud Cover", *Monthly Weather Review*, **105**, p 648

Ineichen P., Gremaud J., Guisan O. & Mermoud A. (1984) "Infrared Sky Radiation in Geneva", *Solar Energy*, **32** (4), pp 537–45.

Ito N., Kimura K. & Oka J. (1968) "A Field Experiment Study on the Convective Heat Transfer Coefficient on Exterior Surface of a Building", *ASHRAE Trans.*, **78**, pp 184–91.

Jakob M. (1949) Heat Transfer. John Wiley & Sons, New York.

Jürges W. (1924) "Der Wärmeübergang an einer ebenen Wand" (Heat transfer at a plane wall), *Beizh. z. Gesundh Ing.*, Series 1, No. 19. [cited in Schack A. (1965) Industrial Heat Transfer. Chapman and Hall, London].

Knorr K. (1987) "Convective/Conductive Heat Transfer", In "Thermal and Solar Properties of Windows : Expert Guide", (eds.) Dijk H. & Knorr K., IEA, Energy Conservation in Buildings and Community Systems Program, Annex XII – Windows and Fenestration, Step 2. October 1987, Delft, Holland.

Lim B., Rao K., Tharmaratnam K., & Mattar A. (1979) Environmental Factors in the Design of Building Fenestration. Applied Science Publishers Ltd., London.

McAdams W. (1954) Heat Transmission. McGraw–Hill, New York.

Min T., Schutrum L., Parmelee G. & Vouris J. (1956) "Natural Convection and Radiation in a Panel-Heated Room", *ASHRAE Trans.*, **62**, pp 337-58.

Mitalas G. & Stephenson D. (1962) "Absorption and Transmission of Thermal Radiation By Single and Double Glazed Windows", National Research Council, Canada, Division of Building Research, Research paper No. 173, Ottawa.

Nielson K. (1990) Window Treatments. Van Nostrand Reinhold, New York.

Olgyay A. & Olgyay V. (1957) Solar Control and Shading Devices. Princeton University Press, Princeton, NJ., USA.

Ozisk N. & Schutrum L. (1958) "Heat Gain Through Windows Shaded By Canvas Awnings", *ASHRAE Trans.*, **64**, P 472.

Parmelee G. (1945) "The Transmission of Solar Radiation Through Flat Glass Under Summer Conditions", *ASHVE Trans.*, **51**, pp 317-50.

Petherbridge P. (1967) "Transmission Characteristics of Window Glasses and Sun Controls", *Proc. CIE Conference "Sunlight in Buildings"*, Bouwcentrum, Rotterdam, 183-198. Also BRE Current Paper No. 72, October 1967.

Pilkington (1988) "Glass and Transmission Properties of Windows", 7th edition, Environmental Advisory Services, Pilkington Glass Ltd., England.

Rangarajan S., Swaminathan M. & Mani A. (1984) "Computation of Solar Radiation from Observations of Cloud Cover", *Solar Energy*, **32** (4), pp 553-56.

Robert E. & Jones R. (1980) "Effects of Overhang Shading of Windows Having Arbitrary Azimuth", *Solar Energy*, **24**, pp 305-12.

Rogers G. & Mayhew Y. (1967) Engineering Thermodynamics: Work and Heat Transfer. Longman, London.

Sattler M., Sharples S. & Page K. (1987) "The Shading of Buildings By Various Tree Shapes", *Solar Energy*, **38** (3), pp 187-201.

Sharples S. (1984) "Full-Scale Measurements of Convective Energy Losses from Exterior Building Surfaces", *Building and Environment*, **19** (1), pp 31-9.

Skolnik A. (1977) "Aesthetic Evaluation of Glass", *Progressive Architecture*, January, P 93.

Smith G. (1967) "Thermal Performance of Photochromatic Glass", *Building Research*, May-June, pp 24-9.

Stephenson D. (1965) "Equations for Solar Heat Gain Through Windows", *Solar Energy*, 9 (2), pp 81-6.

Swinbank W. (1963) "Longwave Radiation from Clear Skies", *Quart. J. Roy. Meteorol. Soc.*, 89, pp 339-48.

Twidell J. & Weir T. (1986) Renewable Energy Resources. E. & F.N Spon, London.

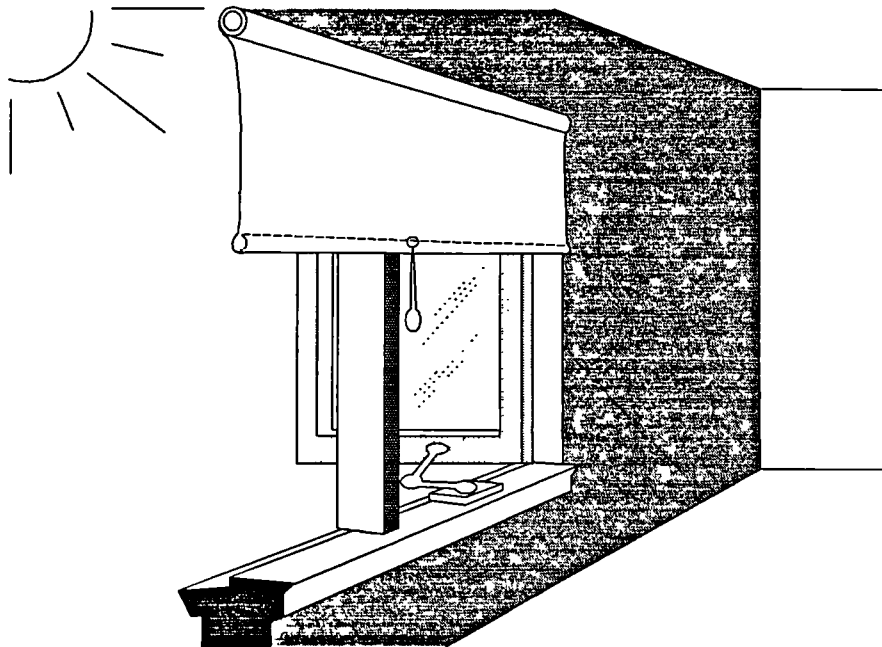
Unsworth M. & Monteith J. (1975) "Longwave Radiation at the Ground", *Quart. J. Roy. Meteorol. Soc.*, 101, pp 13-24.

Whillier A. (1967) "Design Factors Influencing Solar Collectors", *Low Temperature Engineering Applications of Solar Energy*, ASHRAE, NY.

Wright D. (1978) Natural Solar Architecture: A Passive Primer. Litton Educational Publishing Inc., New York.

Yanda R. Jones R. (1983) "Shading Effects of Finite Width Overhang on Windows Facing Toward the Equator", *Solar Energy*, 30 (2), pp 171-80.

# Chapter 5



## 5. SOLAR AND THERMAL CHARACTERISTICS OF INTERIOR SHADING DEVICES (Curtains)

### 5.1 Introduction

---

Interior shading devices can be categorised as:

- Curtains or Draperies (weaved fabrics)
- Roller Shades (fabrics or metallic coated fabrics)
- Blinds (vertical or horizontal metallic louvers or metallic coated weaved fabrics)
- Shutters (framed wooden louvers or panels of insulative fabric)

Domestic curtains, shades and blinds are not usually chosen for their optical or thermal properties. Most choices of interior shading devices are based upon perceived aesthetic properties and/or cost. After installation most users would have a limited concept of how internal shading devices can or should be managed; again most management is predicated on factors other than energy conservation (e.g. privacy and glare control). In addition to privacy, glare control, and aesthetic effects interior shading devices may provide, it is recognised that these devices can reduce summer heat gains and winter heat losses through fenestration. The first category (curtains) is the subject of this chapter, which focuses on the following:

- Classification of curtains
- Thermophysical properties of curtain fabrics
- Solar properties of curtains (measurement and results)
- The effect of geometric configuration on curtain properties
- Modelling the heat transfer through curtain-shaded windows.

A survey on references that deal with the solar and thermal properties of curtains shows that only a few technical reports and journal articles have been published. Early studies focused on heat gain and its relationship to the textile properties of absorption, transmission, reflection, openness of weave, and shading coefficient. For example, Ozisik & Schutrum (1960) determined the effectiveness of curtains in reducing solar heat gain through sunlit glass windows by testing curtains of different materials and colours in combination with regular and heat absorbing glasses. They concluded that heat gain through a single glass with a curtain could be obtained by multiplying the incident solar radiation on the glass by a solar heat transfer factor and that the solar reflectance of the curtain primarily determined the solar heat gain at the window. In principle the solar heat transfer factor referred by Ozisik & Schutrum is similar to the glazing solar gain factors discussed in chapter 2. (see section 2.4.2 and Table 2.9).

Yellott (1965) stressed the importance of the “openness” of curtains (open area between the yarn of fibers in a fabric) in determining the amount of solar heat transmitted through a curtain. He concluded that solar reflectance determines the curtain shading coefficients for tightly-woven fabrics having very low openness factors, whereas solar transmission controls shading properties for fabrics having equal reflectance.

Dix & Lavan (1974) conducted studies to measure the effectiveness of curtains and other indoor shading devices on the coefficient of thermal transmission, U-value, under winter and summer conditions. With the aid of two environmentally controlled chambers and thermistors located near a test window, they determined that a medium coloured drapery with a white plastic backing reduced conductive heat loss in the winter by 6-7%, and conductive and radiant (solar) heat gains in the summer by 33%. Because shades inside casements were more effective than curtains in reducing heat loss under winter conditions, they concluded that the ability of the materials to block air flow was more important than other properties of the material used. In the textile industry, the bulk of literature deals with the chemical and physical properties of fibres. However a few references give some thermophysical properties in terms of the thermal insulation ability of fabrics. These references are reviewed in section 5.3 of this chapter.

In terms of measuring the solar properties of a curtain fabric, Moore & Pennington (1967) conducted their study for the purpose of standardizing methods of measuring solar transmittance and reflectance, and of reporting the results of such measurements. A recent study by Woodson et. al. (1983), based on the recommendations of Moore & Pennington, presented the measured solar optical properties of some commercially available interior window treatments in the USA. The work of (i) Moore and Pennington, and (ii) Woodson et. al. was enlightening and provided the background for much of the experimental study conducted in section 5.4 of this chapter.

Other studies considered the effect of geometric configuration on the solar and thermal properties of curtains. For example, Farber et. al. (1963) developed a procedure to calculate the apparent solar properties of a folded curtain, from the properties of the flat fabric. Epps et. al. (1986) conducted experimental studies to examine the effect of geometric configuration on the thermal transmittance of edge-sealed curtains. The findings of both references are discussed later in section 5.5.

Regarding the heat transfer through shaded glazing, three models were reviewed. The first by Pennington et. al. (1964), which predicts the total heat gain through a double glazed window with curtains as a function of the transmissivity, reflectivity, and absorptivity, of individual barriers, amounts of direct and diffuse insolation incident upon the window surface, and the outdoor-indoor temperature differential. The second by Sharples (1980) is a quasi steady-state procedure to compute the hourly heat transfer through shuttered windows under real climatic conditions. And the third model by Hassani and Brundrett (1986) computes the night time heat transfer through double glazing with internal thermal curtain. The mathematical procedure by Pennington et. al. was adopted for the computer program “CURTAIN.BAS” developed in section 5.6 of this chapter.

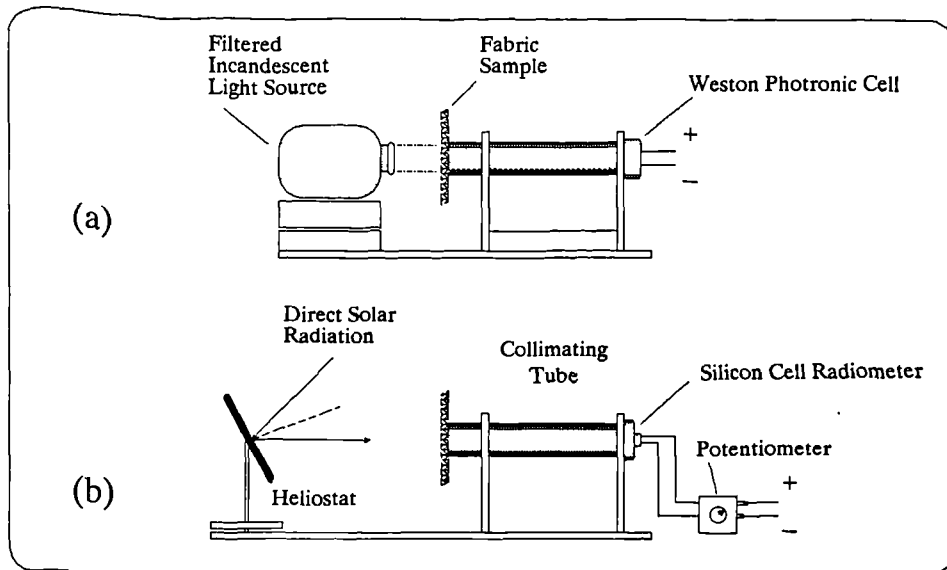


**Figure 5.1** Openness factor measuring instruments, (a) arrangement for the visible solar spectrum (0.3–0.7 $\mu\text{m}$ ) using a photo cell; and (b) arrangement for solar spectrum (0.4–1.15 $\mu\text{m}$ ) using a silicon cell. (reproduced from Yellott 1965).

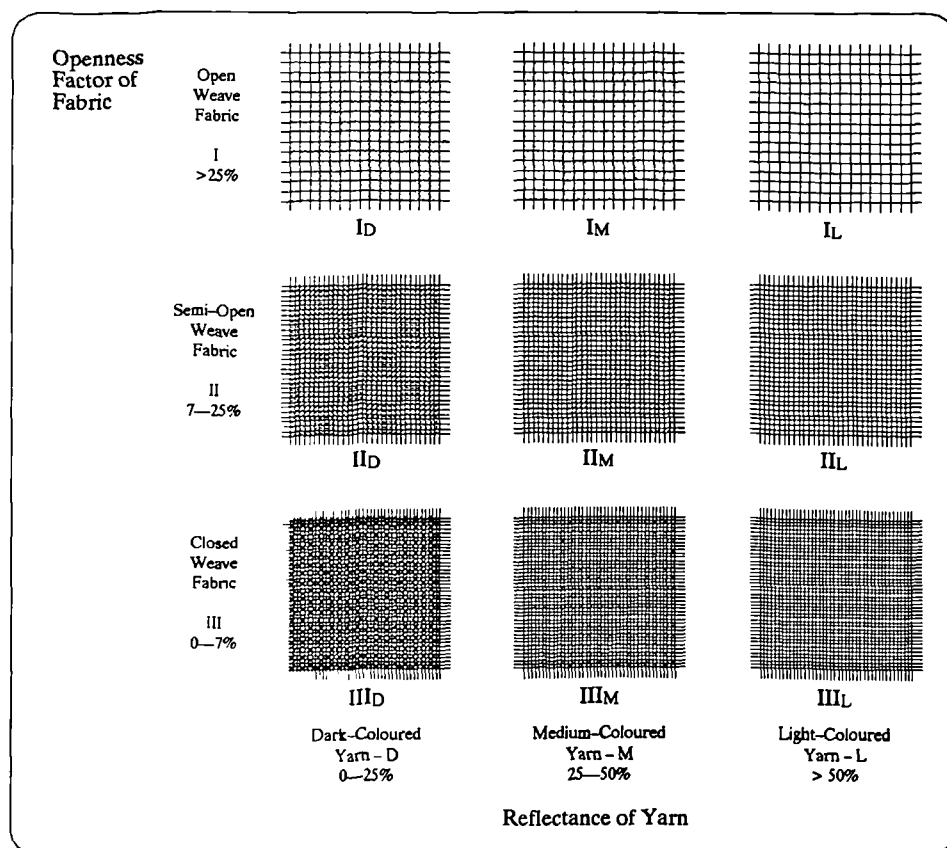


**Figure 5.2** Classification of curtain fabrics (after ASHRAE 1985).

**Note 1.** Designators IM, IIIL indicate open weave, medium coloured yarn, and close weave light coloured yarn, and so forth.

**Note 2.** Classes may be approximated by eye. With **Closed** fabrics, no objects are visible through the material, and large light or dark areas may show. **Semi-open** fabrics do not permit details to be seen, and large objects are clearly defined. **Open** fabrics allow details to be seen, and the general view is relatively clear with no confusion of vision. Light, medium, and dark fabrics may be identified by eye; keep in mind it is the yarn colour or shade of light or dark which is being observed.

## 5.2 Classification of Curtains

---

Fabric type, colour, and finish are the basic factors which classify curtains for a householder. From an energy point of view, other properties are needed. ASHRAE (1985) classifies curtains by weave as open, semi-open and closed, and by colour as dark, medium and light.

While curtains may be described in this manner, these terms do not indicate the true solar properties of the fabric which determine the solar heat gain through it. The solar heat gain (as far as the curtain is concerned) is a function of various properties including *transmittance*, *absorptance* and *reflectance* of the curtain in place across the window. These properties are discussed in depth later in this chapter (see section 5.4).

Colour may not be directly related to the curtain reflectance (i.e. ability to reflect the solar energy impinging on the fabric). A dark, glossy material may be more reflective than a light dull one. Solar reflectance, rather than colour, is one of the properties which indicates ability to reduce solar heat gain through curtain fabrics. If a close correlation existed between openness and transmittance, then openness could be used to indicate the solar heat transmittance through a fabric. Openness of a flat fabric, if properly determined would provide a basis for determining the radiant energy passing between fibres. It would provide no basis for determining the energy passing through the fibres themselves which is dependent on the type of material of which the fabric is made, its thickness and other characteristics.

Yellott (1965) suggested that curtain fabrics can be rated in terms of both the reflectance of the yarns and their openness factor ( $\phi$ ); and for fabrics of approximately equal reflectance, the transmittance is the controlling property. Thus

$$\rho_{(\text{yarn})} = \rho_{(\text{total})} / (1 - \phi) \quad \{5.1\}$$

Openness factor can be measured using the instruments and configurations illustrated in Figure (5.1). It may also be estimated by inspection, since the human eye can readily distinguish between tightly woven fabrics which permit less direct solar radiation through the fibres than loosely woven fabrics (Keyes 1967). Net for example has about 50% openness; a view from outside will be clearly visible. A fabric about 11% open is in the semi-open range; only general outlines can be seen through it. Nothing can be seen through a closed fabric, although it still has a few small openings. The principle of classifying curtains by their yarn reflectance and openness factor is illustrated in Fig.(5.2).

**Table 5.1** Density and Specific heat capacity of dry fibres.  
(after Morton & Hearle 1975)

Fibre	Specific heat (J kg <sup>-1</sup> °C <sup>-1</sup> )	Density kg m <sup>-3</sup>
Cotton	1210	1350–1550
Viscose Rayon	1260	1520
Wool	1360	1300
Silk	1380	1340
Nylon	1430–1510	1140
Terylene and other Polyester fibres	1340	1390

### 5.3 Thermophysical Properties of Curtain Fabrics

In the textile industry, the bulk of literature deals with the chemical and physical properties of fibres. However a few investigate the thermophysical property in terms of the thermal insulation ability of fabrics or “warmth”. Various investigators use varying terminology in defining thermal insulation and warmth properties. For example Hardy (1949) defines thermal conduction in classical physics terminology as

$$Q = k A \Delta T / x \quad \{5.2\}$$

where  $Q$  is the quantity of heat conducted (W);  $k$  is the thermal conductivity of the fabric ( $\text{W m}^{-1} \text{ }^\circ\text{C}^{-1}$ );  $A$  is the area of surface ( $\text{m}^2$ );  $x$  the thickness of fabric (m); and  $\Delta T$  is the temperature difference between warm and cool surfaces ( $^\circ\text{C}$ ). Marsh (1931) suggests the term Thermal Insulation Value (TIV), which is the percent saving in heat loss from a heated surface to covering it with a fabric thus

$$\text{TIV} = 100 (Q_u - Q_c) / Q_u \quad \{5.3\}$$

where  $Q_u$  is the heat loss from the uncovered surface; and  $Q_c$  is the heat loss from the covered surface. Rees (1946) suggests the word “TOG” as a unit of measure of thermal resistance. He defines it as (one-tenth of) the ratio of the temperature differential causing heat to flow to the actual heat flow in watts per square meter, i.e.

$$10 \text{ tog} = 1 (\text{m}^2 \text{ }^\circ\text{K W}^{-1}) \quad \{5.4\}$$

Other investigators use terms based on human physiological and psychological factors definable in terms of body comfort. For example Gagge et. al. (1941) use the term “Clo” as a unit of insulation which is defined as “a unit of insulation necessary to maintain comfort and a mean skin temperature of 92°F (33°C) in a room at 70°F (21°C) with air movement not over 10 feet per minute ( $0.05 \text{ m s}^{-1}$ ), humidity not over 50%, with a metabolism of 50 calories per square meter per hour ( $0.058 \text{ W m}^{-2}$ )”.

For dynamic analysis of the energy flow through a curtain fabric, the thermal conductivity,  $k$  ( $\text{W m}^{-1} \text{ }^\circ\text{C}^{-1}$ ), and the specific heat capacity,  $C_p$  ( $\text{J kg}^{-1} \text{ }^\circ\text{C}^{-1}$ ), are required. The latter is readily available in literature, from direct measurements, and data are presented below. There are no records of direct measurements of thermal conductivity, and what is published are estimated data.

#### 5.3.1 Specific Heat Capacity

Various workers have measured the specific heat of dry fibres at room temperature, and some typical values of specific heat capacity and density are given in Table 5.1 (Morton & Hearle 1975). This table demonstrates that the heat capacity of most fibers is in the same range, and hence have little bearing on the heat insulation properties of textile structures.

**Table 5.2** Thermal conductivity of pads of fibre with a bulk density of 500 ( $\text{kg m}^{-3}$ ).

Fibre	$k^\dagger$ $\text{W (m}^\circ\text{C)}^{-1}$
Cotton	0.071
Wool	0.054
Silk	0.050

$\dagger$  Data from Baxter (1946). Note that still air has a thermal conductivity of  $0.025 \text{ W/(m}^\circ\text{C)}$ .

**Table 5.3** Thermal conductivity,  $k$  ( $\text{W m}^{-1}^\circ\text{C}^{-1}$ ), of polymer fabrics measured in sheet form.

	$k^\ddagger$ $\text{W (m}^\circ\text{C)}^{-1}$
Polyvinyl chloride (PVC)	0.16
Cellulose acetate	0.23
Nylon	0.25
polyester	0.14
polyethylene	0.34
polypropylene	0.12

$\ddagger$  Data from Morton & Hearle (1975).

**Table 5.4** Representative Instruments that measure Thermophysical Properties of Textiles. (after Vigo & Nowacki 1979).

Instrument	Measuring Technique	Properties Measured	Other Properties Measured or Controlled
Guarded hot plate	Equilibrium temp.	Resistance	Convection, radiation
Reeves warmth tester	Equilibrium temp.	Resistance	None
Chamois-covered copper cylinder	Equilibrium temp.	Resistance	None
Togmeter	Heat flow disks	Resistance	Convection, radiation, temperature
Fiber heat sink	Equilibrium temp.	Conductivity	Radiation, convection, emissivity
Warmth tester	Equilibrium temp.	Resistance	Air velocity, convection, radiation
Cenco-Fitch	Rate of heating	Conductivity	Convection
Heat transfer apparatus	Heat flux	Conductivity	Convection, radiation
Thermal moisture tester	Rate of heat and moisture transfer	Thermal efficiency	Relative humidity, temperature
Adiabatic calorimeter	Temperature/heat input	Specific heat	Heat of fusion of absorbed water, temperature.

Extensive studies have been done on the variation of specific heat with temperature, but these variations are insignificant in the temperatures encountered in residential buildings. However the increase of moisture content in curtain fabrics will increase the specific heat. The reader may refer to Morton & Hearle (1975) and Kaswell (1977) for further details.

### 5.3.2 Thermal Conductivity

Unfortunately little data are available on the thermal conductivity of fibres themselves because it is an accepted fact that the thermal insulation of a textile fabric is substantially independent of this inherent property. Rather it is a function of the state of aggregation of the fibers in the textile structure and therefore the trapped still air within the fabric. Cassie (1946) states that the heat insulation of a fabric comes from the air entrapped in it; and he further states that “ In general, the conductivity of the wool fiber is ten times that of air; silk is fifteen times that of air; plant fibers thirty times; synthetic fibers are more like plant fibers than protein”.

However, an estimate of relative values of thermal conductivity can be obtained by comparing the results of measurements of thermal conductance of pads of different fibres packed to the same density (Baxter 1946). Some values are given in Table (5.2). The protein fibres have a lower conductivity than the cellulosic fibres. Experiments can also be made with materials in the solid form. Table (5.3) gives values for the thermal conductivity of some solid polymers tested in sheet form.

A detailed study of instrumentation for the measurement of total thermal conductance or resistance of textiles can be found in Vigo & Nowacki (1979). The instruments can be classified on the bases of the state of heat flow involved : (a) constant temperature, (b) rate of cooling or warming, and (c) heat flow meters or disks. Table 5.4 lists representative instruments and the conditions and parameters with which the thermal properties of textiles are measured. Many experimental studies demonstrated that thermal conductance primarily depends on fabric thickness and air present in the material; however, the conductivity of air accounts for the greater part of the conductivity values observed. (Kaswell 1977)

The lack of thermal conductivity data can be attributed to various factors, such as the diversity of available curtain fabrics; the variability of the amount of air trapped in a fabric; the common mixing of different fibres in textiles, and the change of fabric structure, e.g. due to washing and dry cleaning. The values given in Tables 5.2 and 5.3 may only be used as rough estimates of the curtain thermal conductivity.

**Table 5.5** Solar characteristics of indoor window treatments. †

WINDOW TREATMENTS Fabrication/Finish/Colour	SOLAR CHARACTERISTICS (%)		
	$\rho$	$\tau$	$\alpha$
<i>Lined Drapery</i>			
Satin / – / Goldenrod	66	15	19
Lining: Plain / Opaque / White			
Satin / – / Dark brown	57	2	41
Lining: Plain / Opaque / White			
Satin / – / White	68	18	14
Lining: Plain / Opaque / White			
Mali / – / Beige with brown accents	47	34	19
Lining: Plain / Translucent / Beige			
<i>Unlined Satin Drapery</i>			
Brocade / Acrylic foam back / Beige	70	8	21
Brocade / Acrylic foam back / Beige	67	10	24
Modified Satin / Acrylic foam back / Beige	73	17	10
Modified Satin / Acrylic foam back / Green	75	9	16
Modified Satin / – / Variegated brown	51	30	19
<i>Unlined Casement Drapery</i>			
Mali / – / Beige	41	54	5
Mali / – / Variegated brown	54	29	16
Mali / – / Beige	37	56	7
Mali / – / Beige	42	36	23
<i>Shirred Curtains</i>			
Plain (nixon) / – / Beige	27	65	8
Plain (nixon) / – / White	29	66	5
Plain (marquissette) / – / White	14	76	10
<i>Pleated Curtains</i>			
Plain (nixon) / – / Beige	37	27	37
<i>Venetian Blinds</i>			
2-inch Slats / Steel / White	55	4	41
1-inch Slats / Aluminium / White	57	2	41
<i>Vertical Blinds</i>			
3 1/2-inch Film / PVC / White	70	1	28
3 1/2-inch Plain weave / – / White	58	31	11
<i>Translucent Roller Shade</i>			
Open plain weave / Vinyl coated fibre glass / White	43	48	9
Plain weave / Vinyl coated cotton / Beige	65	19	16
Perforated film / Aluminium backed / Silver	71	21	8
<i>Opaque Roller Shade</i>			
Plain weave / Vinyl coated cotton embossed / Beige	66	0	34
Plain weave / Vinyl coated layer / White	74	0	26
Plain weave / Laminated embossed / White	75	0	26
Film / Vinyl coated embossed / White	67	15	18
<i>Roll-up Shade</i>			
Modified plain weave / Vinyl tube yarns / Beige	53	33	14
<i>Drapery Liner</i>			
Plain weave / Acrylic coated / White	66	18	16
Plain weave / Acrylic coated / White	70	17	13
<i>Wooden Shutters</i>			
Wood (louvers closed) / – / Beige	63	0	37
<i>Wooden Shutter Frame with Fabric</i>			
Wood / – / Beige; Fabric: Ninon / – / White			
width: 3-times frame opening, Shirred	35	62	4
Wood / – / Beige; Fabric: Ninon / – / White			
width: 6-times frame opening, Shirred	51	32	17

† The solar reflectance, transmittance and absorptance were measured experimentally by Woodson et. al. (1983). See Table 5.6 for curtain solar properties measured by the author for this thesis. Definition of terms used above are given in the Glossary section of this thesis (see Appendix H).

## 5.4 Measurement of the Solar Properties of Flat Curtains

The solar properties of a curtain fabric are the transmittance, reflectance and absorptance fractions of incident solar radiation. To be specific in the discussion of measurement of curtain solar transmittance and reflectance, the following definitions apply:

- Transmittance ( $\tau$ ) : the ratio A/B where A is the total insolation passing through the curtain fabric, and B is the total insolation impinging uniformly on the material.
- Reflectance ( $\rho$ ) : the ratio C/D where C is the total insolation reflected onto the sensing element by a uniformly insolated curtain fabric subtending the entire hemispherical field of view of the sensing element surface, and D is the total insolation impinging uniformly on the sensing element surface when held facing the incident solar radiation.
- Absorptance ( $\alpha$ ) : this quantity is obtained by subtracting the values of transmittance plus reflectance from unity.

In these definitions it is assumed that the sensing element used for measurement is sensitive throughout the solar range of wavelengths, and that the sensor is held parallel to the plane of the curtain fabric, and that the sensor is so small that the effect of its shadow for the reflectance measurements is negligible.

Moore & Pennington (1967) conducted a study for the purpose of standardizing methods of measuring solar transmittance and reflectance and of reporting the results of such measurements. The study included a comparison of property measurements made with an artificial light source and solar radiation, and an investigation of reliable instruments for solar-optical property determination. The reader may refer to the above reference for detailed discussion on the instruments investigated and recommendations for their use. The following are some of the conclusions drawn from their study regarding instrumentation:

- Five instruments for determining the transmittance and reflectance of shading devices were investigated. Three of these, the *selenium cell*, the *silicon cell* and the *pyrheliometer* are portable and relatively inexpensive, while the *spectrophotometer* and *solar calorimeter* are non-portable and costly.
- The silicon cell pyranometer used outdoors in sunlight, is capable of giving the most reliable transmittance and reflectance readings per money investment in instruments.

Based on the recommendations of the above reference, Woodson et. al. (1983) have conducted an experimental study of solar optical properties for thirty-four different interior window treatments (draperies, curtains, roller shades, blinds and shutters). Table 5.5 lists the solar properties ( $\tau$ ,  $\rho$  and  $\alpha$ ) of window treatments measured in their study.

The following describes the laboratory experiments conducted by the author to measure the solar transmittance and reflectance of three domestic curtains: (1) golden plain weave fabric with stripes embossed (65% polyester, 35% cotton); (2) light-cream Dralon brocade fabric (82% acrylic, 18% nylon); and (3) green velveteen fabric (base cloth tufted from one side,

**Figure 5.3** Construction of the black box.

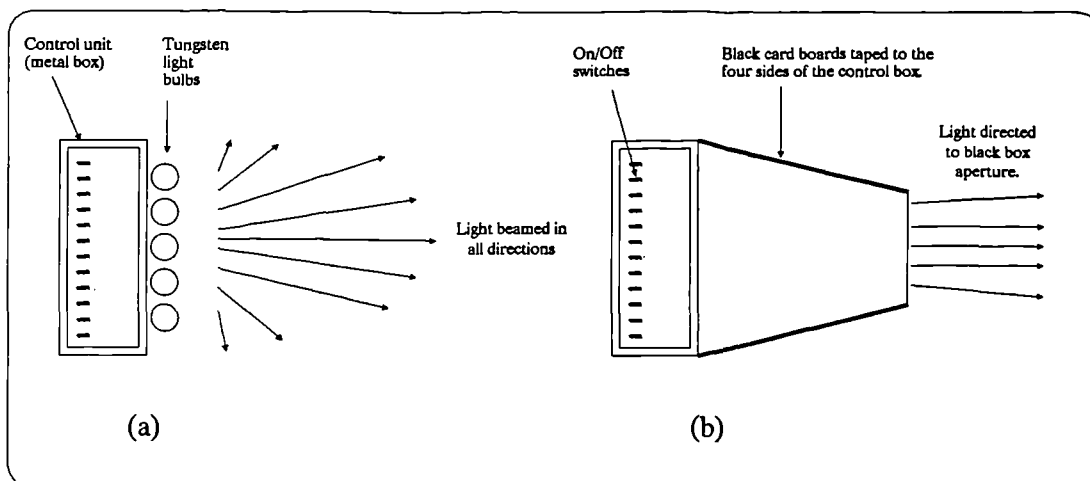
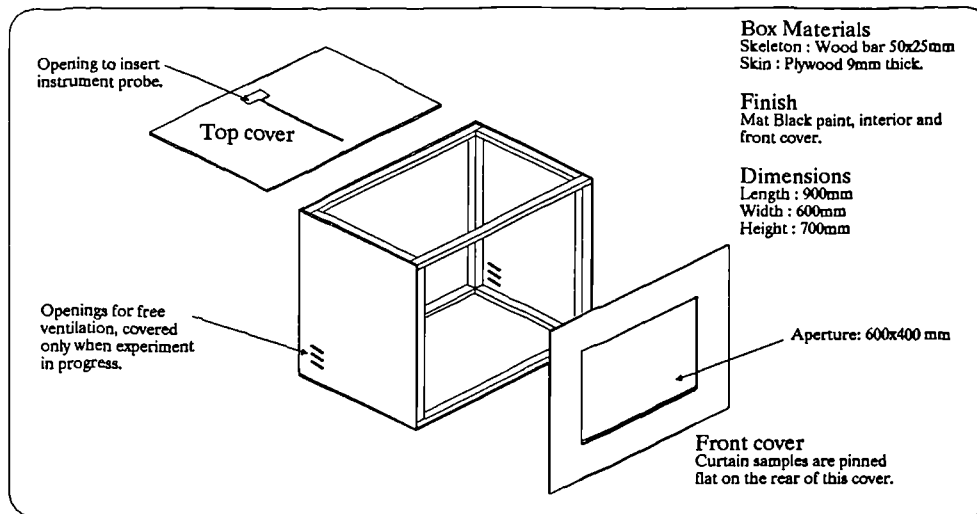


**Figure 5.4** Shortwave radiation simulator; (a) the unit beam light in all directions within a hemispherical field; (b) a treatment to direct light to the front side of the black box.

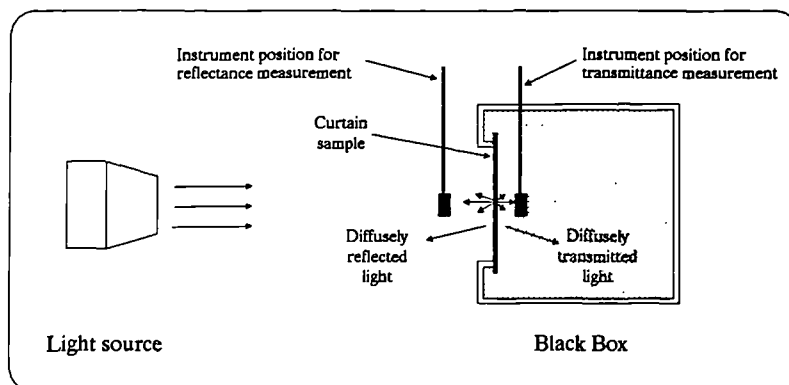


**Figure 5.5** Experimental setup for the measurement of transmittance and reflectance of a curtain sample in a dark room. See Figures 5.6, 5.7 and 5.8 for more details.

approx. 2mm thick). The discussion also highlights the accuracy of measurements made by two portable instruments.

### 5.4.1 Experimental Setup

The experiments were conducted in a dark room with the following setup:

- A wooden box (0.9 x 0.6 x 0.7m) was constructed for testing the three curtain samples under artificial light. Figure 5.3 shows a schematic representation of the box construction. The aperture (0.6 x 0.4m) in the front side of the box and the wooden frame mounted on the inner side of it, provided the support to test each curtain sample in a flat position. The holes at the sides of the box ensured free movement of air, thus removing any heat buildup inside the box. The opening in the top side of the box ensured flexibility of locating the measuring instrument.
- In measuring transmittance, it is important that the area around and behind the curtain sample be masked with a non-reflective material, otherwise, diffuse radiation from these sectors will increase the instrument reading beyond that given by the transmitted radiation alone. A solution to this problem was to paint the interior surfaces of the box with a mat black paint. The front side of the box was also painted black so that reflectance measurement are not influenced by any radiation other than that reflected by the curtain surface.
- Two light sources were used: a controllable array of 60W & 100W tungsten light bulbs totaling 1040 W; and a slide projector with 500W light bulb. The light from the lamp array was beamed to the black box aperture as shown in Figure (5.4).
- Two instruments were used for this study: (1) a Net-radiometer model DRN/301, and an Albedometer model DRA/2 from Didcot Instrument Co. Ltd. (see the next chapter and data sheets DS9 & DS11 in Appendix F for a full description of these instruments). The net-radiometer gives a single output, difference between the incident radiation on each sensor, and sensitive to wavelengths in the 0.3 to 80 $\mu$ m range. The albedometer gives two outputs, the incident radiation on each sensor, and sensitive in the 0.4–0.9 $\mu$ m range. Thus the albedometer was used as a radiometer taking only one sensor output for the experiments conducted here. Readings from these instruments were obtained via a digital voltmeter.

Experiments using the net-radiometer were only conducted for the first curtain sample, once with the lamp array and another with the slide projector as the light source. The albedo meter was used also with the lamp array and the slide projector for measuring the transmittance and reflectance of all three curtain samples. The test procedure is simple and straight forward (Fig.5.5). Basically the light source is beamed to the box aperture and readings from the

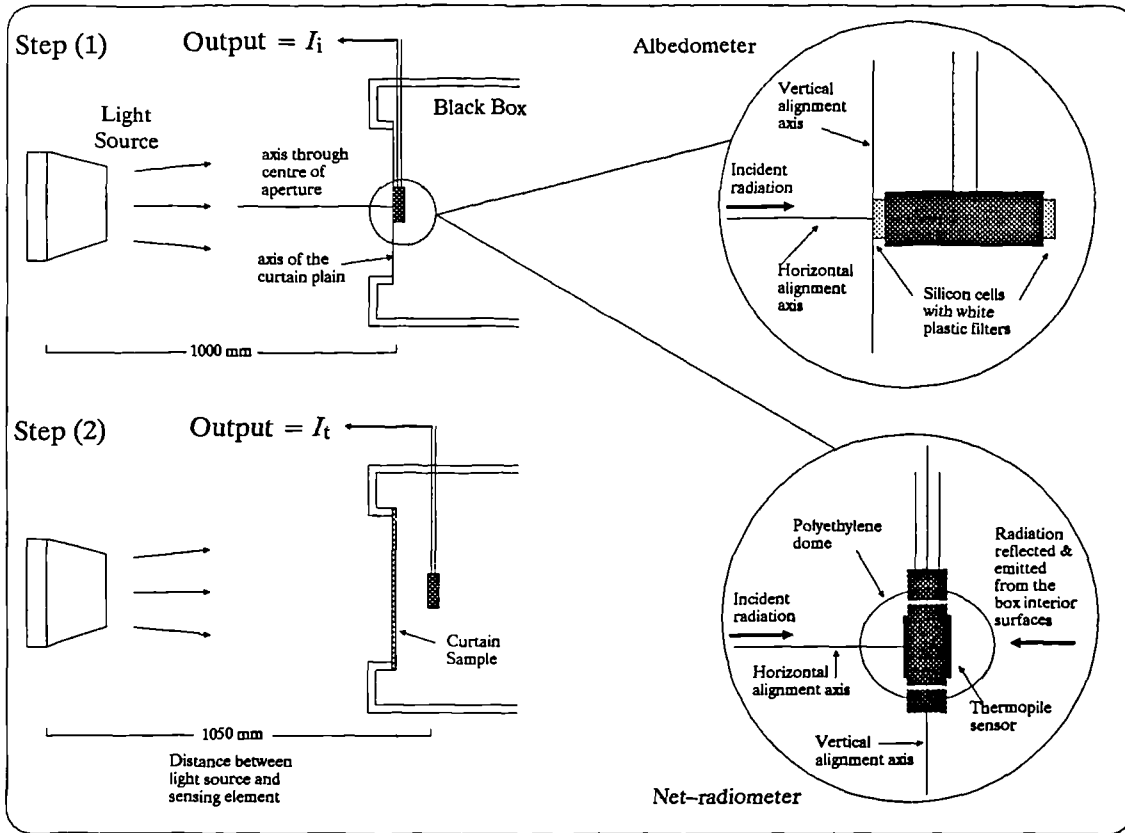


**Figure 5.6** Test procedure to determine the transmittance of a curtain fabric. Enlarged diagrams show the alignment of the instrument used.

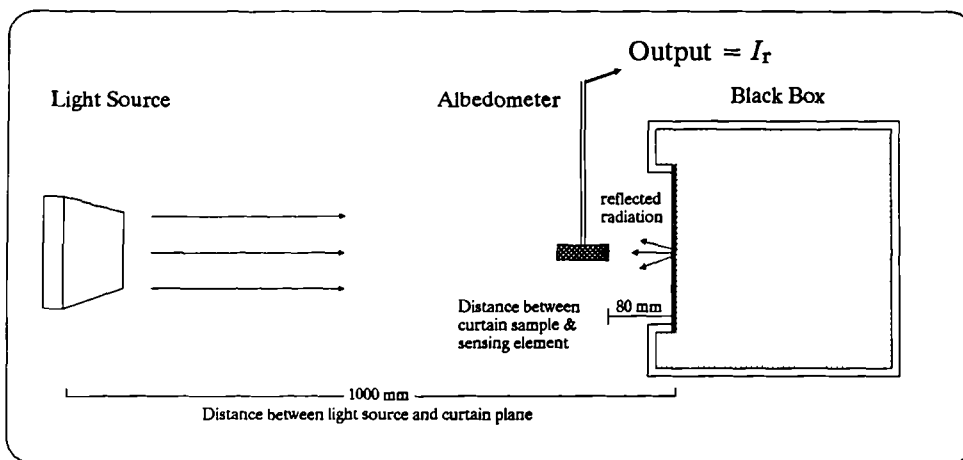


**Figure 5.7** Test procedure (second step) to determine the reflectance of a curtain fabric. Note that the first step is typical to that of Figure 5.6. (see text for details).

instruments, located as shown in Figure 5.5, are taken once with no curtain fitted and once with the curtain sample in place.

For the measurement of transmittance, using either the net-radiometer or the albedometer; the first step is to take a reading of incident light,  $I_i$  (mV), with the sensing element positioned on the same axis of the curtain plane (so that it sees the same light pattern seen by the face of the curtain sample). In the second step the curtain is fitted and a reading,  $I_t$  (mV), taken with the sensor held 5cm behind the sample. Diagrams showing the alignment of the sensing elements in relation to the light source and the curtain position are shown in Figure (5.6) for both instruments used. The transmittance value of the curtain sample ( $\tau$ ) is then obtained from

$$\tau = I_t / I_i \quad \{5.5\}$$

Note that the radiation reflected or emitted from the interior surfaces of the box to the sensing element are insignificant due to nature of these surfaces (rough wood surfaces painted mat black) and the low level of radiation intensity from the source light. Therefore Eq.5.5 is applicable for outputs obtained from tests by the albedometer and the net-radiometer.

Using the albedometer for the measurement of curtain reflectance (Fig.5.7); first a reading of incident light,  $I_i$  (mV), is taken with the sensing element positioned on the same axis of the curtain plane (with no curtain fitted, as conducted in the first step of the transmittance measurement). Next the curtain is fitted and the measuring sensor, outside the box, is held parallel to and facing the curtain surface. While the sensor is moved slowly away from the surface, the output voltage will be seen to slowly rise, then level off at a distance of about 8cm. The reflected radiation reading,  $I_r$  (mV), is taken at this position. If the sensor is moved further away from the surface, the output voltage will be observed to start to decrease. These variations in the output voltage arise because the measuring sensor sees not just a narrow angle in front of itself, but an entire hemispherical solid angle. The reflectance value of the curtain sample ( $\rho$ ) is then obtained from the relation

$$\rho = I_r / I_i \quad \{5.6\}$$

As mentioned earlier, the reading obtained by a net-radiometer is the difference between the radiation intensities received by its two sensing elements (thermopiles). Therefore the curtain reflectance measured with this instrument is quite complex (see Figure 5.8). The first step, similar to the albedometer measurement, gives a reading of incident radiation as received by the the curtain surface,  $I_i$  (mV). For the second step, also as conducted with the albedometer, the net-radiometer output at a distance  $x$  from the curtain surface,  $I_{netx}$  (mV), can be written as

$$I_{netx} = I_{ix} - (\rho I_i) \quad \{5.7\}$$

where  $I_i$  is the incident radiation at the curtain surface which is reflected to the sensor facing it by the factor  $\rho$ ; and  $I_{ix}$  is the incident radiation received by the sensing element facing the light source and at a distance  $x = 15\text{cm}$  from the curtain surface.

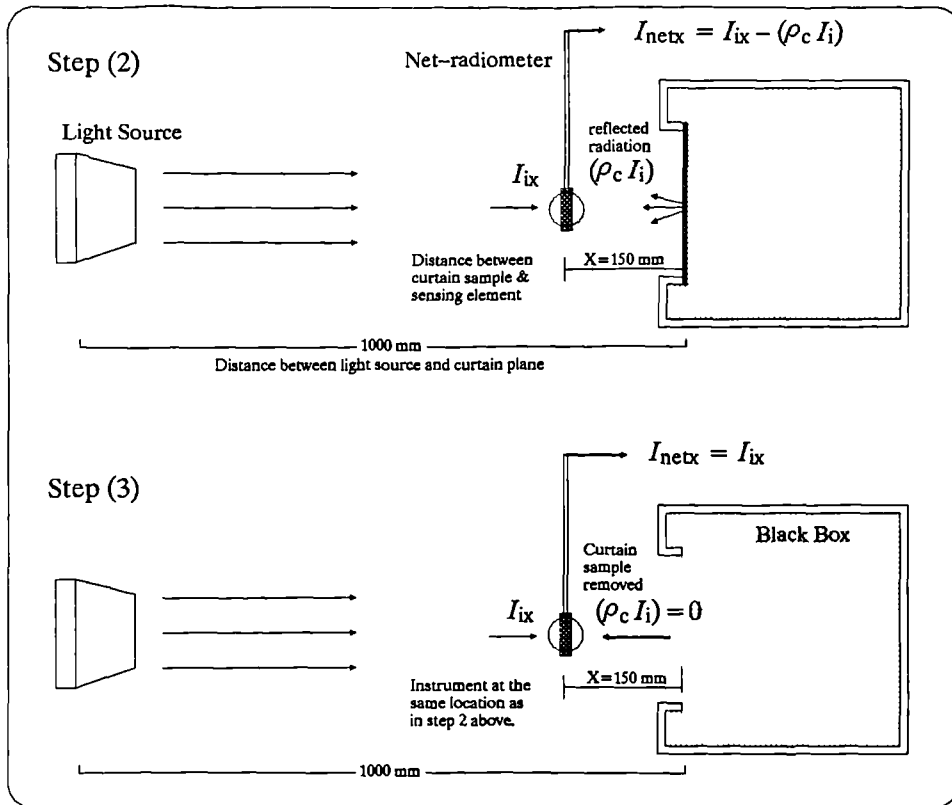


**Figure 5.8** Test procedure to determine the reflectance of a curtain fabric using the net-radiometer. Note that the first step is typical to that of Figure 5.6. (see text for details).

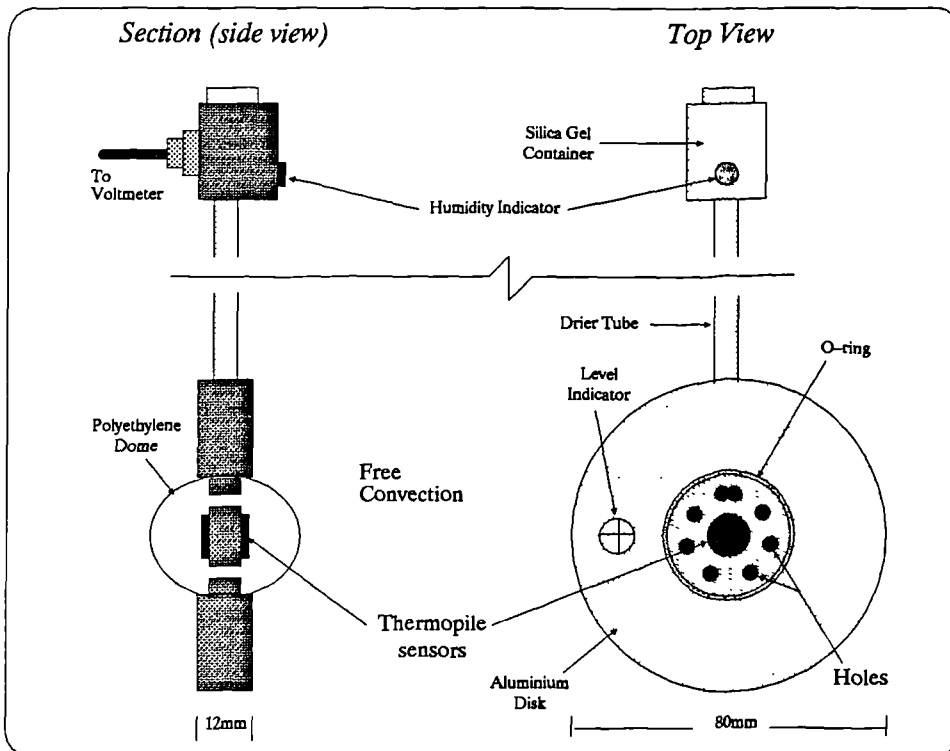


**Figure 5.9** A Net-radiometer illustrated in vertical position. The holes allow free air movement between the silica gel container and the thermopile sensors. This will cause noise in the instrument output, particularly in measuring low radiation levels.

If the curtain is then removed the reading from the net-radiometer gives the incident radiation  $I_{ix}$ ; i.e. taking into account that the sensor facing away from the light source receives no radiation from the black surfaces of the box or from the surroundings of the dark room. Now Eq.5.7 can be rearranged to give the curtain reflectance from the three observed readings

$$\rho = (I_{ix} - I_{netx}) / I_i \quad \{5.8\}$$

The absorptance of a curtain sample is calculated by

$$\alpha = 1 - (\tau + \rho) \quad \{5.9\}$$

## 5.4.2 Accuracy of Measurements

The net-radiometer is thought to be ideal for measuring the shortwave and longwave transmittance and reflectance of a curtain. However tests using this instrument did not give reproducible results for the same set of conditions; and unstable output readings from the instrument were observed.

The noise in the instrument output may possibly be associated with the presence of holes in the aluminium base of the instrument sensor. When the net-radiometer is used vertically, convection current occur across both surfaces of the instrument sensor, (see Figure 5.9), hence the output is unstable. After consultation with the manufacturers the following conclusions are derived

- The holes in the instrument head serve two purposes, (a) to ensure free movement of air as the silicon gel dries out all moisture from the sensor head; and (b) to ensure equilibrium of air temperature under both domes.
- The instrument can only be used in a horizontal position. If used vertically, convection currents occur at the thermopile surfaces of the instrument which will give unpredictable results.
- At low radiation intensities, the instrument has a  $\pm 5\%$  margin of error; and a response time of 15 seconds to 90% of change. These figures given by the manufacturer are for the instrument in the horizontal position. At least  $\pm 30\%$  margin of error would be expected if the instrument is used in the vertical position.
- According to the manufacturer, if the domes are removed and a constant flow of air across the two sensors from the side is provided, the instrument can give reliable results in a position other than the horizontal. However, the instrument would require recalibration under these conditions.

The albedometer on the other hand gave steady and reproducible results. It has the advantage of being smaller in size (2cm diameter compared to 8.5cm diameter of the net-radiometer head). Thus the shadow cast by the instrument on the curtain surface would have a lesser effect on reflectance measurement.

**Table 5.6** Solar reflectance, transmittance and absorptance of three curtain fabrics.<sup>†</sup>

Fabric type / Colour	$\rho$	$\tau$	$\alpha$
Plain weave with stripes embossed / Gold	36	25	39
Dralon brocade / Light Cream	49	33	18
Velveteen on base cloth <sup>‡</sup> / Green	47	05	48

† The properties are measured with the silicon cell albedometer using the tungsten lamp array to simulate solar radiation.

‡ The reflectance of the velvet surface is 30% while the value given above is for the base cloth side. Transmittance is the same through either side.

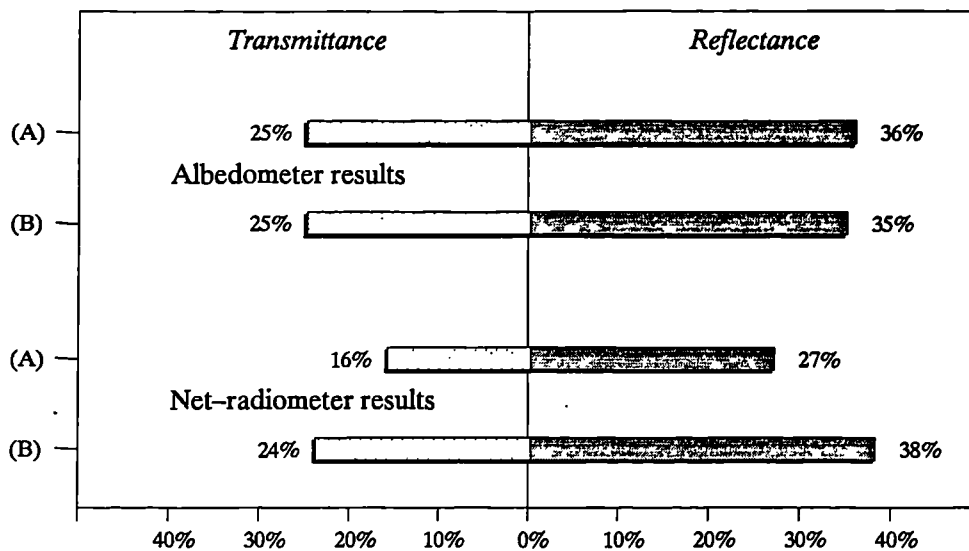


**Figure 5.10** Transmittance and reflectance properties of a curtain sample (golden plain weave fabric) as measured by the albedometer and the net-radiometer with two light sources: (A) Tungsten lamp array; (B) Slide projector.

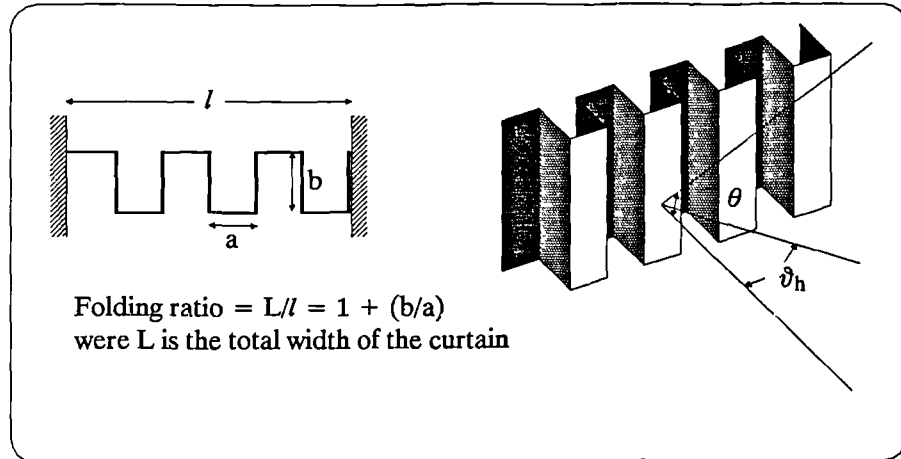
### 5.4.3 Results and Conclusions

Table 5.5 gives the shortwave reflectance, transmittance and absorptance of the three curtain samples. These are measured using the albedometer with the lamp array; and represent the most reproducible results from all experiments conducted, hence the most accurate.

Results from tests on the three curtain sample conducted with the albedometer and the slide projector agreed with those using the lamp array. However, variations in the transmittance and reflectance of the first curtain sample (golden plain weave fabric) were observed when the net-radiometer was used (see Figure 5.10). Note that the net-radiometer results are averages of tests conducted at various intervals of time.

The conclusions that can be drawn from this study are:

- In comparing the two measuring instruments, it become obvious that the greatest differences in results will be due to differences in the instruments response to the radiation wavelengths.
- The net-radiometer is found to be unsuitable for use in laboratory experiments to measure the transmittance and reflectance of a curtain fabric. The instrument is restricted for use outdoors in the horizontal position.
- Similar to Moore & Pennington (1967) and Woodson et. al. (1983) findings, the measurements of curtain transmittance conducted above are less complex than that of measuring reflectance and values obtained are reproducible.
- The problem with reflectance measurement arise from several interacting variables, most of which arise because of the instrument field of view being an entire hemispherical solid angle.
- Among the variables that affect reflectance readings are: (1) the amount of background surrounding and beyond the sample as seen by the sensing element; (2) the relative intensity of longwave radiation from the background as compared to that of the sample; (3) the size of the shadow cast upon the sample by the instrument; (4) the distance from the sensing element to the reflecting surface; and (5) the nature of the background behind the sample.
- The net-radiometer when used with the slide projector (as the radiation source) provided results that are relatively close to those obtained by the albedometer. However it is important to take frequent readings as heat buildup inside the box and in the dark room itself adds to the irregularity of the instrument output.



**Figure 5.11** Plan and isometric diagrams showing the configuration of a folded curtain for the theoretical analysis of section 5.5.1.

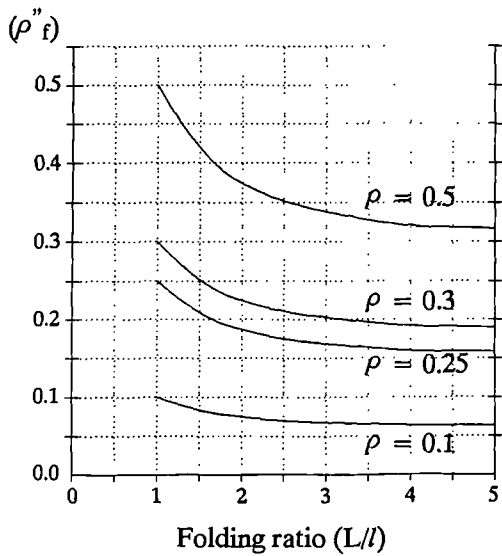


**Figure 5.12** Apparent reflectivities ( $\rho''_f$ ) for diffusely reflecting curtain fabrics under diffuse insolation.  $\rho$  = flat material reflectance. (reproduced from Farber et. al. 1963). Note that reflectance decreases with increase in folds.

## 5.5 Geometric Configuration and Curtain Properties

---

It is seen from the previous section that the solar properties of flat curtains can be measured with  $\pm 5\%$  accuracy for reflectance and better than 1% for transmittance, and values of such properties were given in Tables (5.5 & 5.6). The analysis of curtain-shaded fenestration, however, should consider folded curtains as used rather than flat material. The following review discusses the effect of “fullness” on (1) solar properties of curtains (i.e. transmittance and reflectance); and (2) the overall heat transfer coefficient (U-value) of the shaded fenestration. The effect on the thermal performance of the shaded fenestration of spacing between (i) the curtain and the glass surface and (ii) two layers of curtain fabrics are also discussed.

The term “fullness” implies a width of curtain material greater than that of the window opening (i.e. folding ratio  $L/l > 1$ ), and calculated by

$$\text{Fullness} = (L/l) - 1 \quad \{5.10\}$$

where  $l$  is the window width and  $L$  is the curtain width. Thus a 100% fullness curtain has twice the width of the window, and a flat curtain has a 0% fullness.

### 5.5.1 Fullness vs. Solar Properties of Curtains

In practice curtains hang in random configurations. The inconsistency of the folding configuration of curtains make it difficult to obtain perfectly reproducible measurements. Moore & Pennington (1967) developed and used a special device to measure the folded curtain solar properties. No details about the device were given except that it rotates a sensor in circles parallel to the folded curtain surface; and they concluded that, as with the flat material experiments, the transmittance values were the most reproducible.

However, if the properties of the flat materials used for curtains are known, the apparent properties of folded curtains can be determined mathematically. In the theoretical analysis of solar heat gain through shaded glass, Farber et. al. (1963) conducted their study on three curtains. Their analysis was made for the diffuse and direct incident radiation with simple configurations, adapting modeling procedures from an earlier study by Sparrow and Johnson (1962). The assumptions made in Farber’s study were that (a) the configuration shown in Figure (5.11) could be used as an approximation and (b) the curtain material is perfectly diffuse in reflection and transmission.

This implies that the analysis is only valid for the tightly woven fabrics. Nevertheless, the study provided useful information and graphs that can be used to correlate flat curtain properties to geometrical configurations. Figure 5.12 plots computed apparent reflectivities ( $\rho''_t$ ) under diffuse insolation for various flat material reflectivities as a function of the folding ratio ( $L/l$ ).

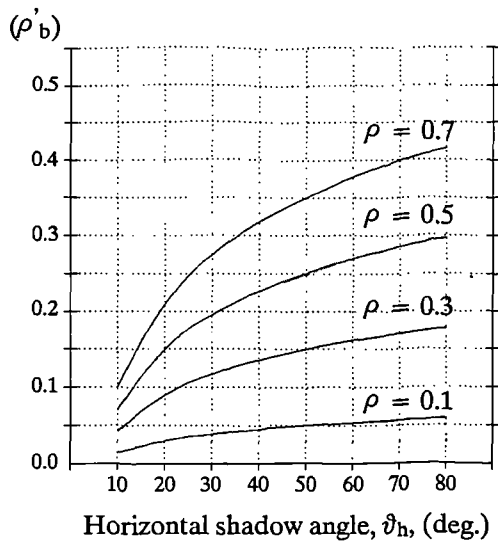


**Figure 5.13**  
Apparent reflectivities ( $\rho'_b$ ) for direct insolation in diffusely reflecting cavity of the folded curtain.  $\rho$  = flat material reflectance,  $L/l \geq 2$ . (reproduced from Farber et. al. 1963).

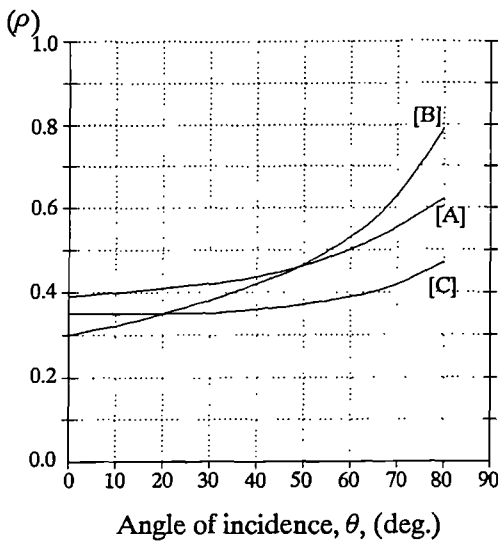


**Figure 5.14**  
Solar reflectance ( $\rho$ ) of flat curtain fabrics as a function of incident angle. Type [A] is a light coloured curtain with normal incident properties of  $\tau = 0.35$ ,  $\alpha = 0.26$ ; type [B] a medium coloured curtain with  $\tau = 0.23$ ,  $\alpha = 0.47$ ; and type [C] is a dark coloured curtain with  $\tau = 0.14$ ,  $\alpha = 0.51$ . (reproduced from Farber et. al. 1963).

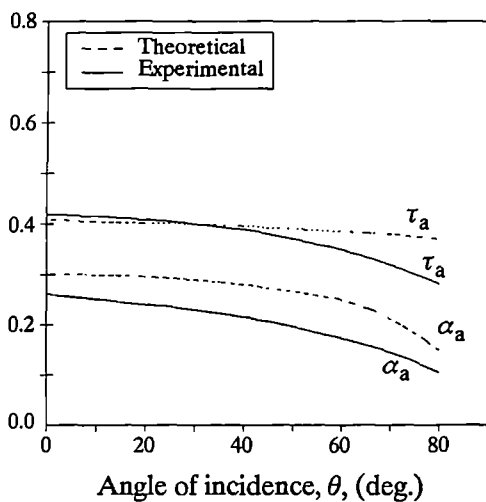


**Figure 5.15**  
Apparent absorptance and transmittance of light coloured curtains ( $\alpha = 0.26$ ;  $\rho = 0.39$ ;  $\tau = 0.35$ ) for 100% fullness and a horizontal shadow angle  $\vartheta_h = 0^\circ$  vs. angle of incidence of solar radiation, for both theoretical and experimental determinations. (reproduced from Farber et. al. 1963).

It is seen from figure 5.12 that  $\rho''_f$  decreases significantly if  $(1 < L/l < 2.5)$  and an increase in the amount of fullness above 100% will not significantly influence the reflectance.

Figure 5.13 plots computed apparent reflectivities under direct insolation as a function of horizontal shadow angle. The values in Figure 5.13 apply for the cavity portion of folded curtain. Figure 5.14 shows the solar reflectance of three types of curtain fabric as a function of incident angle. Figures 5.13 & 5.14 could be used to find the apparent reflectivity of folded curtain fabric in the following procedure:

(i) obtain  $\rho$  from Figure 5.14, (ii) use this value in Figure 5.13. to determine the apparent reflectivity of the cavity part of the curtain ( $\rho'_b$ ), (iii) calculate the apparent reflectivity for direct insolation ( $\rho''_b$ ) from

$$\rho''_b = 0.5 (\rho'_b + \rho) \quad \{5.11\}$$

From the ratio of direct to total incident insolation

$$\xi = G_b / (G_b + G_f) \quad \{5.12\}$$

the apparent reflectivity for the folded curtain is then found from

$$\rho_a = \xi \rho''_b + (1 - \xi) \rho''_f \quad \{5.13\}$$

Assuming that the apparent transmissivity ( $\tau_a$ ) varies due to the same factors as the apparent reflectivity ( $\rho_a$ ), Farber et. al. obtained the following expression

$$\tau_a = \tau [ (1 - \rho_a) / (1 - \rho) ] \quad \{5.14\}$$

and the apparent absorptivity ( $\alpha_a$ ) can be determined from

$$\alpha_a = 1 - \rho_a - \tau_a \quad \{5.15\}$$

In validating the above mathematical procedure, Pennington et. al. (1964), conducted experiments and compared the theoretical and experimental values as shown in Figure (5.15) for the light coloured curtain. This figure shows the inability to obtain an accurate mathematical expression for curtain folding as seen by the variations in the curves. However, in the absence of experimental data, the above theoretical procedure may be used for a rough estimate of the folded curtain solar properties.

## 5.5.2 Geometric Configuration vs. U-value of Fenestration

The insulation of a glazing system can be improved, i.e. reduced U-value, by the use of curtains. The reduction in the U-value results principally from adding a semi-closed air space to the barrier. This implies that edge-sealed curtains are more efficient than loosely fitted ones, and multiple layers of fabric are more effective than single fabric curtains.

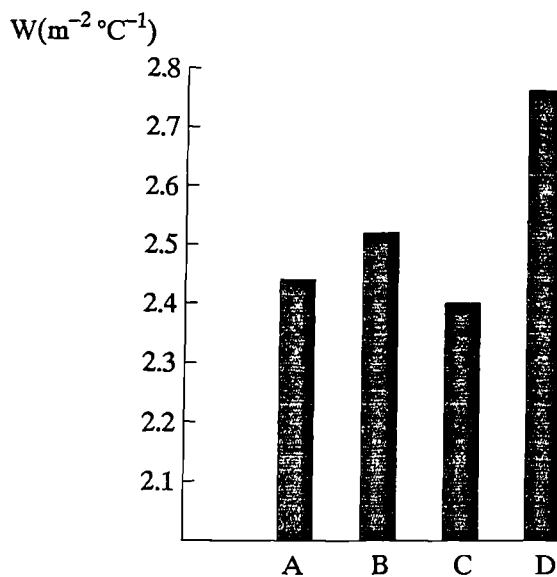
**Table 5.7** U-values of fenestration (glass + lining + curtain) for the stated fabric types and geometrical configuration, ( $W (m^{-2} \circ C^{-1})$ ). (after Epps et. al. 1986).

Configuration <sup>†</sup>			Fabric <sup>‡</sup>			
CF	LF	SP	A	B	C	D
50	0	0	2.227	2.315	2.213	2.652
50	0	1/4	2.276	2.365	2.239	2.565
50	0	1/2	2.293	2.291	2.237	2.549
50	50	0	2.705	2.801	2.476	2.872
50	50	1/4	2.531	2.474	2.405	2.859
50	50	1/2	2.436	2.477	2.425	2.820
100	0	0	2.289	2.291	2.278	2.624
100	0	1/4	2.257	2.418	2.261	2.598
100	0	1/2	2.296	2.237	2.376	2.573
100	100	0	2.722	2.917	2.728	2.905
100	100	1/4	2.609	2.793	2.663	2.970
100	100	1/2	2.528	2.756	2.438	2.771

**Notes**

† The geometric configuration of a fenestration assembly in this study is designated by three parameters:  
 CF = curtain fullness, (%)  
 LF = lining fullness, (%)  
 SP = spatial separation between lining fabric and curtain fabric, (inches)

‡ The curtain fabrics, (A) cotton class III, (B) rayon class II, (C) polyester class III, and (D) polyester class I, are combined with a class III cotton lining fabric. (see section 6.2 for details on the classification of curtain fabrics).

**Figure 5.16**

Mean U-values of the fenestration assemblies measured by Epps et. al (1986). The letters A to D designate fabric types (see section 5.5.2).

In the “normal double curtain arrangement” behind single glazing, according to ASHRAE (1985), it is estimated that a U-value of  $3.23 \text{ (W m}^{-2} \text{ }^\circ\text{C}^{-1}\text{)}$  will be achieved. This implies a reduction of about 40% in comparison with unshaded single glass. (Normal arrangement here refers to a double curtain with a light open weave fabric on the window side of the double curtain and a heavy close weave fabric on the room side).

Prior to the experimental work of Epps et. al. (1986) it was believed that insulation increases as the fullness of a curtain increases. However, their results show that a flat fabric provides greater insulation. The folding of a curtain increases its surface area, thus increasing its openness factor. This increases air permeability through the fabric, and in turn the U-value increases.

The laboratory experiments of Epps et. al. determined the thermal transmittance, U-value, of a double curtain shaded window for various configurations of curtain fullness, lining fullness, and spacing between lining and curtain fabrics. Figure (5.16) shows the mean U-value of the fenestration using four fabric types: (a) tightly woven 100% cotton; (b) semi-open weave 100% rayon; (c) tightly woven 100% polyester; and (d) open-weave 100% polyester. All the curtains were lined with tightly woven 100% cotton print cloth. The measured U-values of fenestration assemblies are listed in Table (5.7).

Although the findings of Epps et. al. can be useful for designing energy efficient curtains, the experimental arrangements (that of tightly sealed double-layered curtains, and uniform curtain folding) would limit the applications to typical window curtain configurations.

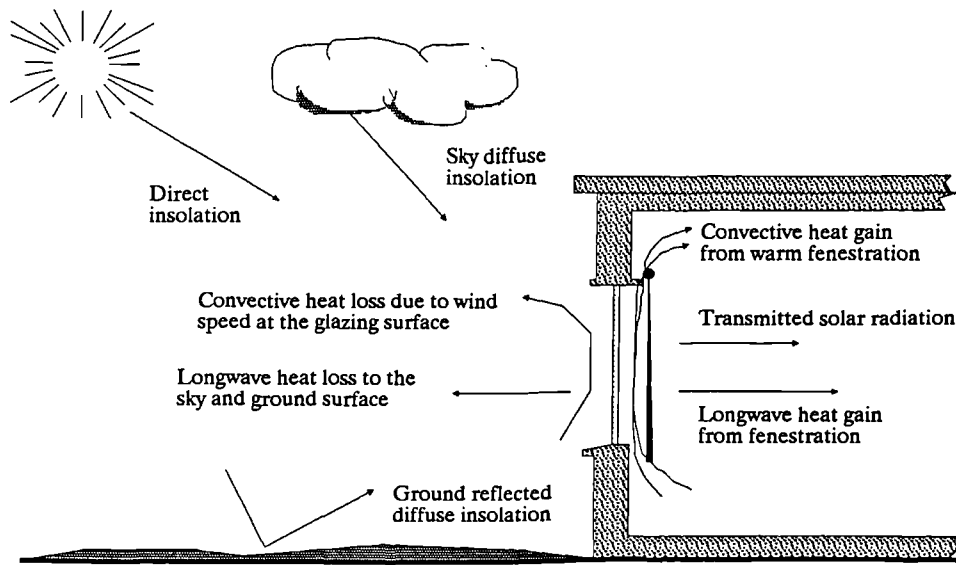


**Figure 5.17** Sources of incident solar radiation and components of heat gain/loss through a curtain-shaded window.

## 5.6 Modeling the Hourly Heat Transfer Through Curtain-Shaded Windows (CURTAIN program)

The aim of this section is to develop a mathematical model that calculates the instantaneous rate of heat gain or loss through curtain shaded windows under real climatic conditions. The proposed model is based on an earlier study by Farber et. al. (1963). In their model, Farber et. al. assume constant external and internal heat transfer coefficients at each surface of a curtain shaded double glazed window, and calculate the total heat gain through the fenestration at a particular angle of incidence. The input variables to their model are the solar properties of each of the fenestration layers.

The total heat gain through a curtain shaded window is illustrated schematically in Figure (5.17) and can be expressed as:

$$q_{tsw} = G_{bv} \tau_{gs(b)} + G_{fv} \tau_{gs(f)} \quad \{5.16\}$$

$$q_{rci} = N_{igs} [G_{bv} \alpha_{gs(b)} + G_{fv} \alpha_{gs(f)}] + U (T_o - T_i) \quad \{5.17\}$$

where

- $q_{tsw}$  = transmitted shortwave flux through the fenestration  $W m^{-2}$
- $q_{rci}$  = heat flow inward by radiation and convection from the fenestration  $W m^{-2}$
- $N_{igs}$  = inward-flowing fraction of absorbed insolation
- $G_{bv}$  = direct solar irradiation incident on the fenestration surface  $W m^{-2}$
- $G_{fv}$  = diffuse solar irradiation  $W m^{-2}$
- $\tau_{gs(b)}$  = fenestration transmittance for direct insolation
- $\tau_{gs(f)}$  = fenestration transmittance for diffuse insolation
- $\alpha_{gs(b)}$  = fenestration absorptance for direct insolation
- $\alpha_{gs(f)}$  = fenestration absorptance for diffuse insolation
- $U$  = air to air heat transfer coefficient of the fenestration  $W(m^{-2}C^{-1})$
- $T_o$  = outdoor air temperature  $^{\circ}C$
- $T_i$  = indoor air temperature  $^{\circ}C$

The following discussion describes the computer model (CURTAIN.BAS), written by the author in GW-Basic, which treats curtain shaded windows of single or double glazing under real climatic conditions. A code listing of the program is given in Appendix (E). The input variables to CURTAIN program consist of three parts; (i) site information: latitude, longitude difference and ground reflectivity; (ii) hourly climatic variables: global horizontal insolation, diffuse horizontal insolation, wind speed, wind direction, outdoor and indoor air temperatures; and (iii) fenestration properties: solar transmittance and reflectance of each layer at normal incidence, emissivity of each surface for each layer. The program output is saved in a result library file (ASCII format).

Equation 5.16 may be the dominant factor of total heat gain through fenestration. The transmitted shortwave flux undergoes a complex process of reflection and absorption by the room internal surfaces and, depending on the properties of these surfaces, may be released to the room air node at a later stage. The value of  $t$  is the net transmittance of all the radiation that is subsequently absorbed in the room. To simplify the model, the transmitted insolation is given separately in Eq.5.16 from Eq.5.17 for further processing by the user. Equation 5.17

on the other hand is a direct gain or loss to the air node which is a function of the variables discussed in section 5.6.3. Section 5.6.1 lists the algorithms used to compute solar angles and solar radiation incident on the fenestration. Section 5.6.2 discusses the procedure for calculating the fenestration solar properties at various angles of incidence.

## 5.6.1 Solar Angles and Incident Solar Radiation

The program computes the solar angles from Eq.5.18 through Eq.5.23. The direct and diffuse insolation,  $G_{bv}$  &  $G_{fv}$ , incident on the vertical glazing are computed from Eq.5.24 through Eq.5.28. Note that Eq.5.18 through Eq.5.28 have been discussed earlier in chapter 2 (see section 2.4.1).

$$\delta = 23.45 \sin[360 (284 + J) / 365] \quad \{5.18\}$$

$$E_t = [9.87 \sin(2e) - 7.53 \cos(e) - 1.5 \sin(e)] / 60 \quad \{5.19\}$$

$$e = 360 (J - 81) / 364$$

$$t_s = t + E_t + (L_{std} - L_{loc})/15 \quad \{5.20\}$$

$$\omega = 15 (12 - t_s) \quad \{5.21\}$$

$$\cos(\theta_z) = \sin(\delta) \sin(\phi) + \cos(\delta) \cos(\phi) \cos(\omega) \quad \{5.22\}$$

$$\cos(\theta) = \cos(\delta) \sin(\phi) \cos(\gamma) \cos(\omega) + \cos(\delta) \sin(\gamma) \sin(\omega) - \sin(\delta) \cos(\phi) \cos(\gamma) \quad \{5.23\}$$

$$G_{bh} = G_h - G_{fh} \quad \{5.24\}$$

$$G_{bv} = G_{bh} \cos(\theta) / \cos(\theta_z) \quad \{5.25\}$$

$$G_{rv} = 0.5 \rho_{grd} G_h \quad \{5.26\}$$

$$G_{sv} = 0.5 G_{fh} [1 + F \sin^3(\beta/2)] [1 + F \cos^2(\theta) \sin^3(\theta_z)] \quad \{5.27\}$$

$$F = 1 - (G_{fh} / G_h)^2$$

$$G_{fv} = G_{rv} + G_{sv} \quad \{5.28\}$$

where

- $\delta$  = solar declination, (°);
- $J$  = Julian day number (from January 1st);
- $E_t$  = the equation of time, (h);
- $e$  = a modulating function for use in Eq.5.19, (°);
- $t_s$  = the solar time, (h);
- $t$  = the local mean time, (h);
- $L_{std}$  = the standard longitude (°);
- $L_{loc}$  = the site longitude (°);
- $\omega$  = hour angle, (°);
- $\phi$  = site latitude;
- $\theta_z$  = zenith angle, the angle between the beam from the sun and the vertical, (°);
- $\theta$  = angle of incidence of beam radiation on the vertical glazing surface, (°);
- $\beta$  = the glazing slope angle, = 90°;
- $F$  = a modulating function for use in Eq.(5.27);
- $G_{rv}$  = the ground reflected global insolation on the vertical glazing ( $W m^{-2}$ );
- $G_{sv}$  = the sky diffuse insolation on the vertical surface ( $W m^{-2}$ ).

## 5.6.2 Shortwave Transmission and Absorption

For the solution of Eq.5.16 & Eq.5.17, it is necessary to know the properties of absorptance and transmittance of each layer of the fenestration. These properties, at normal incidence, for different glass types are provided in Table 2.9 in chapter 2 and in Tables 5.5 and 5.6 of this chapter for curtains.

The variations with angle of incidence in solar transmittance and absorptance of glass can be derived using the correlation procedure described in the previous chapter (see section 4.2). However, the polynomial coefficients required can only be found in literature for a limited number of glazing types (e.g. Kusuda 1976, gives polynomial coefficients for 8 types of glass categorised by their KL product values, where K is the glass absorption coefficient and L the thickness of the glass). The KL value of a glass is not readily available. Glass normal transmittance, on the other hand, is the figure usually quoted by glass manufacturers and readily available in literature.

Petherbridge (1967) have introduced the concept of “equivalent normal-incidence KL” which can be calculated from the normal incidence transmittance. Petherbridge then assumes that this equivalent KL value stays constant over all angles of incidence and applies it to the monochromatic Fresnel equations to obtain the solar transmittance and absorptance for the glass at any angle of incidence. This concept is adopted for the CURTAIN program, and the relevant equations are discussed below. Note that the following apply to the direct component of solar radiation, determined from Eq.5.23, at incident angle =  $\theta$  for the hour in question. For the diffuse component it is difficult to assess an angle of incidence. Since direct insolation is the dominant factor for incident angles less than  $70^\circ$ ; therefore, the diffuse component can be treated as the direct component in most cases.

The monochromatic radiation may be resolved into two components; one component with the plane of variation parallel to the glass and the other perpendicular to the glass. The specular reflectance of the glass-air interface varies with the direction of polarisation by Fresnel's equations:

$$r_{p||} = \sin^2(\theta - \theta_r) / \sin^2(\theta + \theta_r) \quad \{5.29\}$$

$$r_{pd} = \tan^2(\theta - \theta_r) / \tan^2(\theta + \theta_r) \quad \{5.30\}$$

where  $r_{p||}$  is the reflectivity for the parallel polarisation;  $r_{pd}$  is the reflectivity for the perpendicular polarisation;  $\theta$  and  $\theta_r$  are the angles of incidence and refraction respectively. The angle of refraction is obtained from Snell's law as

$$\sin(\theta_r) = \sin(\theta) / v \quad \{5.31\}$$

where  $v$  is the glass index of refraction ( $v = 1.526$  is assumed for glass). At normal incidence  $r_{p||}$  and  $r_{pd}$  are equal and given by

$$r_{p||} = r_{pd} = [(v - 1) / (v + 1)]^2 \quad \{5.32\}$$

After passing through the glass the fraction of the incident energy,  $T$ , remaining is given by Bouger–Lambert’s law as

$$T = \exp[-KL / \cos(\theta_r)]$$

and so, from Eq.5.31,

$$T = \exp[-KL / (1 - \sin^2(\theta)/v^2)^{0.5}] \quad \{5.33\}$$

The transmittance and absorptance of the glass,  $\tau_x$  and  $\alpha_x$ , respectively are found from:

$$\tau_x = (1 - r_x)^2 T / (1 - r_x^2 T^2) \quad \{5.34\}$$

$$\alpha_x = 1 - \tau_x - (1 - r_x)^2 T / (1 - r_x T) \quad \{5.35\}$$

The x subscript signifies that each component must be evaluated separately for the parallel and perpendicular directions of polarisation. The overall solar transmittance or absorptance is then found from the average of the parallel and perpendicular values, and solar reflectance is obtained by subtracting transmittance and absorptance components from unity, thus

$$\tau = (\tau_{p||} + \tau_{pd})/2 \quad \{5.36\}$$

$$\alpha = (\alpha_{p||} + \alpha_{pd})/2 \quad \{5.37\}$$

$$\rho = 1 - \tau - \alpha \quad \{5.38\}$$

The equivalent KL value is calculated by considering the normal incidence condition of Eq.5.32, so Eq.5.34 reduces to

$$\tau_o = [(1 - r)^2 \exp(-KL)] / [1 - r^2 \exp(-2KL)] \quad \{5.39\}$$

where  $\tau_o$  is the transmittance at normal incidence for monochromatic radiation. In Petherbridge’s method this is assumed equivalent to  $\tau_{ou}$ , the solar transmittance at normal incidence input by the user. Substituting and rearranging Eq.5.39 gives

$$\tau_{ou} \exp(2KL) - (1 - r)^2 \exp(KL) - \tau_{ou} r^2 = 0 \quad \{5.40\}$$

Let  $Y = \exp(KL)$

$$\therefore \tau_{ou} Y^2 - (1 - r)^2 Y - \tau_{ou} r^2 = 0 \quad \{5.41\}$$

$$\therefore Y = ((1 - r)^2 \pm [(1 - r)^4 + 4 \tau_{ou}^2 r^2]^{0.5}) / (2 \tau_{ou}) \quad \{5.42\}$$

Only the positive root of the square root term is applicable since this term must always be greater than  $(1 - r)^2$ . The equivalent normal–incidence KL value is then found from

$$KL = \ln(Y) \quad \{5.43\}$$

According to Sharples (1980), the variation of solar transmittance with angle of incidence derived from the constant equivalent KL value technique and the more rigorous weighted–mean variable KL method show excellent agreement for clear and lightly heat absorbing glasses up to  $(KL = 1.6)$ . The Petherbridge method as adopted in this thesis tends to decrease in accuracy as the KL value increases.

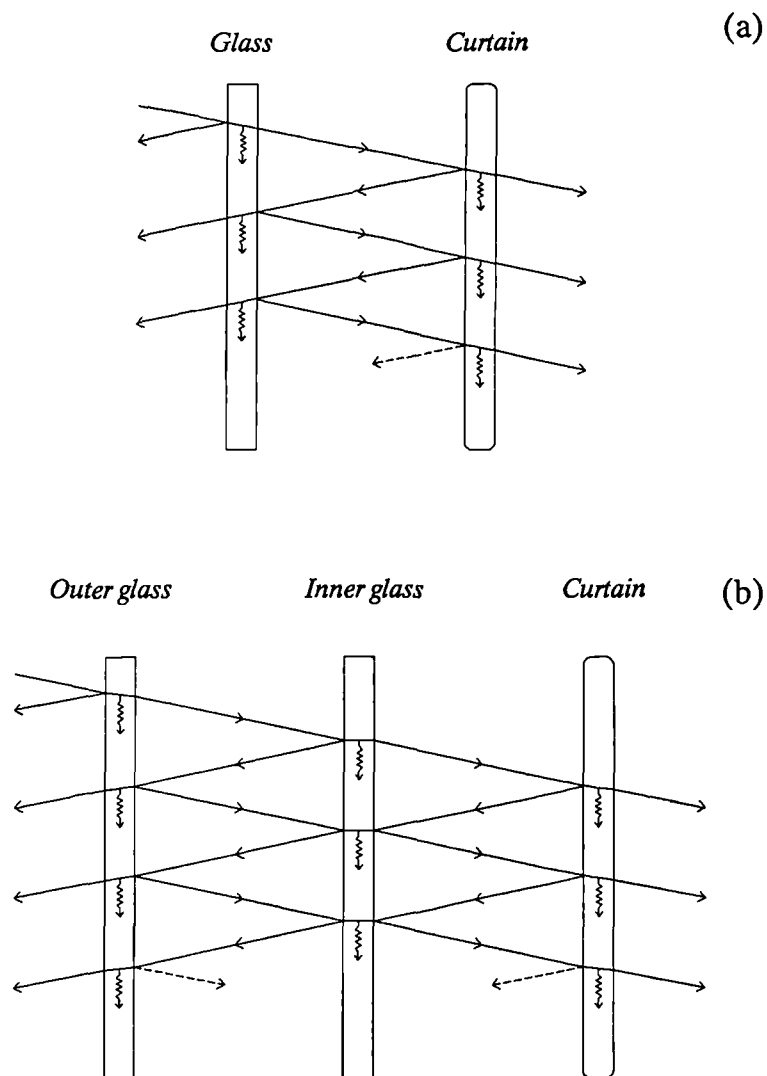


**Figure 5.18** Component of transmitted, absorbed and reflected short wave flux (solar beam) incident upon: (a) single glazing with interior curtain, and (b) double glazing with interior curtain.

The variations with angle of incidence in solar transmittance and absorptance of a curtain fabric can only be determined experimentally. Therefore, the user-input solar transmittance and absorptance of the curtain are assumed constant for incident angles calculated by the CURTAIN program.

Now, knowing the individual properties of the fenestration layers, the program determines the absorptance, reflectance and transmittance of the composite fenestration. Figure (5.18a) illustrates the multiple absorption, reflection and transmission of insolation flux for curtain shaded single glass. The infinite processes shown in this figure are convergent geometric series, hence the composite fenestration properties are calculated from

$$\tau_{gs} = \tau_g \tau_s / (1 - \rho_g \rho_s) \quad \{5.44\}$$

$$\rho_{gs} = \rho_g + [\rho_s \tau_g^2 / (1 - \rho_g \rho_s)] \quad \{5.45\}$$

$$\alpha'_g = \alpha_g + [\alpha_g \tau_g \rho_s / (1 - \rho_g \rho_s)] \quad \{5.46\}$$

$$\alpha'_s = \tau_g \alpha_s / (1 - \rho_g \rho_s) \quad \{5.47\}$$

Figure 5.18b illustrates the multiple absorption, reflection and transmission of insolation flux for curtain shaded double glazing. The infinite process is not convergent. Farber et. al. (1963) state that the composite fenestration properties can be approximated by considering the major component and one or two reflected components of energy flux. The result of their analysis yields:

$$\tau_{gs} = \tau_{go} \tau_{gi} \tau_s (1 + \rho_s \rho_{gi}) \quad \{5.48\}$$

$$\rho_{gs} = \rho_{go} + \tau_{go}^2 (\rho_{gi} + \tau_{gi}^2 \rho_s) \quad \{5.49\}$$

$$\alpha'_{go} = \alpha_{go} [1 + \tau_{go} (\rho_{gi} + \tau_{gi}^2 \rho_s)] \quad \{5.50\}$$

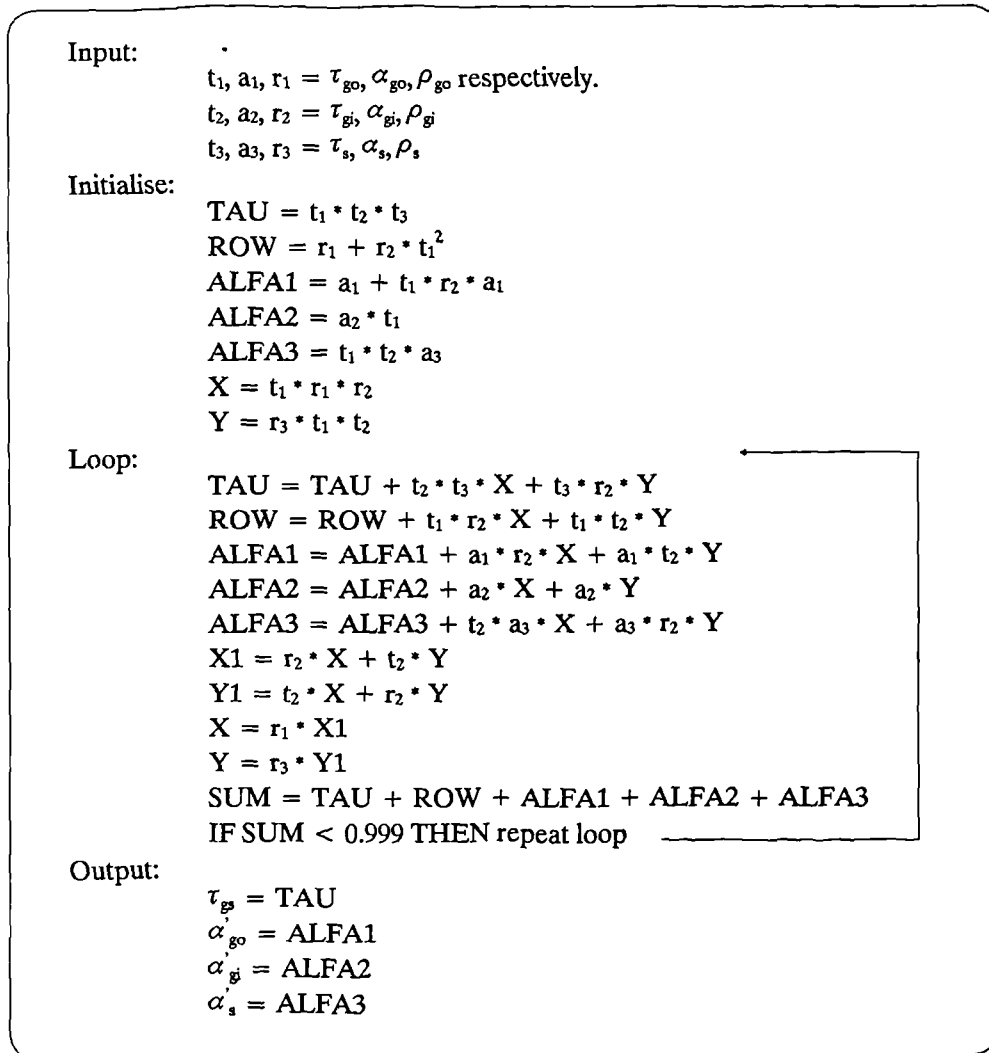
$$\alpha'_{gi} = \alpha_{gi} [\tau_{go} (1 + \tau_{gi} \rho_s)] \quad \{5.51\}$$

$$\alpha'_s = \alpha_s [\tau_{go} \tau_{gi} (1 + \rho_s \rho_{gi})] \quad \{5.52\}$$

where  $\tau, \rho, \alpha$  are the solar transmittance, reflectance and absorptance of each layer with the subscripts (go, gi, and s) denoting properties of external glass, internal glass and the curtain shade respectively; and  $\alpha'$  is the pseudo-solar absorptivity of each fenestration layer, taking into account inter-reflections of the composite fenestration.

Equations 5.48 through 5.52 result in values of about 90–93% accuracy. An alternative to these is to compute the transmittance, reflectance and absorptance values in series with maximum iteration to achieve significant variance at say the 0.001 level, (see the algorithm shown in Fig.5.19). This algorithm, used in the CURTAIN program, gives more accuracy but at the expense of computational time.

**Figure 5.19** An algorithm for computing the composite transmittance and absorptance of double glazing with interior curtain (written by the author).



### 5.6.3 Inward Heat Flow by Convection and Radiation

The heat transfer phenomena in the two curtain fenestration types handled by the program (single glazing with curtain and double glazing with curtain) are illustrated in Figure 5.20 and Figure 5.21 respectively. By writing the basic heat transfer relationships for each of the quantities shown in these figures, and by taking heat balances at each layer of glass and the curtain, sufficient equations can be obtained so that the convection and long wave radiation heat gain can be expressed as a function of the heat transfer coefficients of the surfaces, absorptivity of the individual barriers, incident solar radiation, and the inside and outside air temperatures, i.e.

$$q_{rci} = f(h_0, h_1, h_2, h_3, h_4, h_5, h_6, \alpha'_{go}, \alpha'_{gi}, \alpha'_s, h_a, G_{bv}, G_{fv}, T_o, T_a, T_i)$$

where  $h_0$  is the outer glass external surface heat transfer coefficient;  $h_1$  the radiative coefficient between glass panes (for double glazing only);  $h_3$  &  $h_6$  are radiative heat transfer coefficients;  $h_2, h_4$  &  $h_5$  are convective heat transfer coefficients  $W(m^{-2} \text{ } ^\circ C^{-1})$  as indicated on Fig.5.20 & Fig.5.21; and  $h_a$  is a constant coefficient  $W(m^{-2} \text{ } ^\circ C^{-1})$  that represents infiltration heat transfer from the room air temperature node to the air space temperature node between curtain and glass ( $T_a$ ).

The infiltration coefficient is one of three values ( $2.4, 4.8,$  and  $9.6 W m^{-2} \text{ } ^\circ C^{-1}$ ) corresponding to user specification of the curtain fitting, i.e. (1) a sealed curtain; (2) normal fitting; and (3) loosely fitted curtain. These are estimated from

$$h_a = C_p \rho_{air} u a \quad \{5.53\}$$

where

- $C_p$  = specific heat capacity of air =  $1000 (J kg^{-1} \text{ } ^\circ C^{-1})$
- $\rho_{air}$  = density of air =  $1.2 (kg m^{-3})$
- $u$  = air speed for natural convection,  $\approx 0.04 m s^{-1}$  (ASHRAE 1985)
- $a$  = an estimated opening area at the bottom or top of curtain per square meter of glass. The dimensionless ratio,  $a$ , in Eq.5.53 is taken nominally as 0.05, 0.1, and 0.2 for sealed, normal and loosely fitted curtains respectively.

The external surface heat transfer coefficient,  $h_0$ , is computed for each hour using the ASHRAE method discussed in the previous chapter (see section 4.3.4). Relevant equations are listed below:

$$D_s = \gamma + 180^\circ - D_m \quad \{5.54a\}$$

$$D_s = 360^\circ - |D_s|, \quad \text{if } |D_s| > 180^\circ \quad \{5.54b\}$$

$$V_s = 0.25 V_m, \quad \text{if } |D_s| < 90^\circ \text{ \& } V_m > 2 m s^{-1} \quad \{5.55a\}$$

$$V_s = 0.5, \quad \text{if } |D_s| < 90^\circ \text{ \& } V_m < 2 m s^{-1} \quad \{5.55b\}$$

$$V_s = 0.3 + 0.05 V_m, \quad \text{if } |D_s| > 90^\circ \quad \{5.55c\}$$

$$T_{sky} = 0.05532 T_o^{1.5} \quad \{5.56\}$$

$$T_e = [0.5 (T_{sky}^4 + T_o^4)]^{0.25} \quad \{5.57\}$$

$$h_0 = 18.6 V_s^{0.605} + \epsilon_{go} \sigma (T_{go}^2 + T_e^2) (T_{go} + T_e) \quad \{5.58\}$$

where  $D_s$  is the wind direction relative to the window surface;  $\gamma$  the surface azimuth angle (the zero degree point being due south, east positive and west negative);  $D_m$  is the free stream wind direction (deg. from north, clockwise positive);  $V_m$  and  $V_s$  are the meteorological wind speed and the wind speed relevant to the window surface respectively ( $\text{m s}^{-1}$ );  $\sigma$  is the Stefan–Boltzmann constant;  $\epsilon_{go}$  is the hemispherical surface emissivity of the external glass;  $T_{go}$  is the external glass temperature in Kelvin; and the equivalent temperature  $T_e$  (K) accounts for equal window view factors to the sky at temperature  $T_{sky}$  and to the ground at outdoor air temperature  $T_o$ .

The radiative heat transfer coefficient between the curtain and room surfaces,  $h_6$ , is computed hourly as given from

$$h_6 = \epsilon_s \sigma (T_s^2 + T_i^2) (T_s + T_i) \quad \{5.59\}$$

where  $\epsilon_s$  is the emissivity of the curtain surface facing the room;  $T_s$  the curtain temperature (K); and the room surfaces are assumed as a black body at indoor air temperature  $T_i$ . The remaining heat transfer coefficients are computed, as applicable, for each hour by:

$$h_r = \sigma (T_1^2 + T_2^2) (T_1 + T_2) / [(1/\epsilon_1) + (1/\epsilon_2) - 1] \quad \{5.60\}$$

$$h_v = [(1.5 \Delta T^{0.25})^6 + (1.23 \Delta T^{0.33})^6]^{1/6} \quad \{5.61\}$$

where  $h_r$  is the radiative coefficient for heat transfer between two surfaces in the fenestration (applicable for  $h_1$  &  $h_3$ ); the subscripts 1 & 2 signify properties for the two radiative surfaces in question;  $h_v$  is the convective coefficient for heat transfer between a surface and internal air node (applicable for  $h_2$ ,  $h_4$  &  $h_5$ ); and  $\Delta T$  is the absolute surface–air temperature difference ( $^{\circ}\text{C}$ ). Note that the reciprocal of the denominator in Eq.5.60 represents the interchange factor given in Eq.4.21 (see section 4.3.1 of the previous chapter), for two closely spaced parallel planes. (see also Twidell and Weir 1986). Eq.5.61 represents the Alamdari & Hammond correlation discussed in section 4.3.3 of the previous chapter.

An initial estimate of the unknown node temperatures shown in Figures 5.20 & 5.21 (i.e  $T_g$ ,  $T_{go}$ ,  $T_{gi}$ ,  $T_a$  &  $T_s$ ) is derived from the following simple algorithm:

$$T_j = T_{j-1} - (T_o - T_i) / (n-1), \quad \text{for } j = 1 \text{ to } n-2 \quad \{5.62\}$$

where  $n$  is the total number of nodes in the fenestration;  $T_j$  is the temperature at node  $j$ . The program then computes the unknown temperatures for the next hours by solving the heat balance equations of the fenestration.

Now, for a fenestration of single glazing with curtain, the heat transfer and heat balance equations that apply to the quantities illustrated in Figure 5.20 are :-

$$q_0 = h_0 (T_g - T_o) \quad \{5.63\}$$

$$q_2 = h_2 (T_g - T_a) \quad \{5.64\}$$

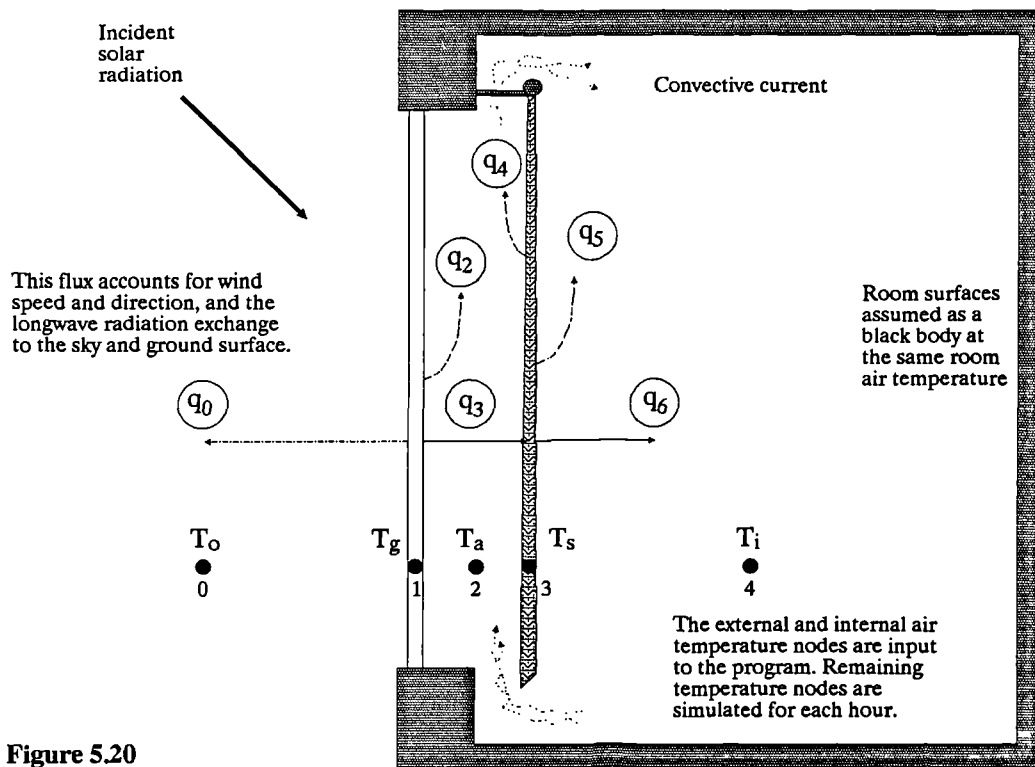


Figure 5.20

Convective and longwave heat transfer components for a single glazing window with a curtain.

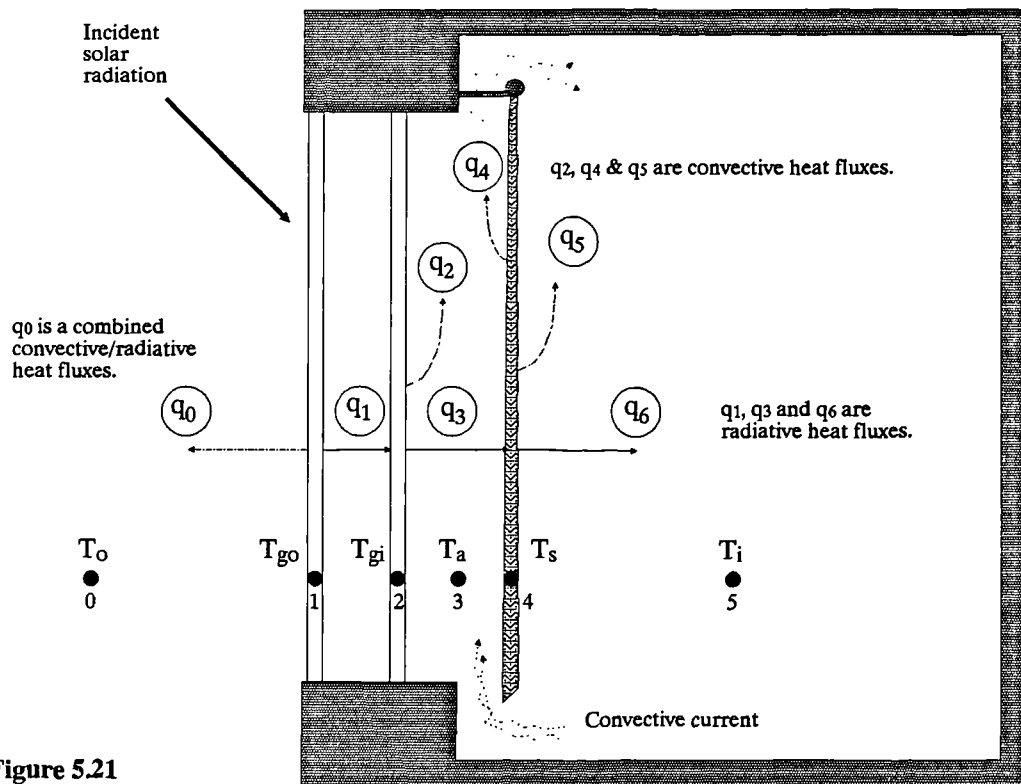


Figure 5.21

Convective and longwave heat transfer components for a double glazing window with a curtain.

$$q_3 = h_3 (T_g - T_s) \quad \{5.65\}$$

$$q_4 = h_4 (T_s - T_a) \quad \{5.66\}$$

$$q_5 = h_5 (T_s - T_i) \quad \{5.67\}$$

$$q_6 = h_6 (T_s - T_i) \quad \{5.68\}$$

$$q_{rci} + q_0 = G_v (\alpha'_g + \alpha'_s) \quad \{5.69\}$$

$$q_0 + q_2 + q_3 = G_v \alpha'_g \quad \{5.70\}$$

$$q_3 + G_v \alpha'_s = q_4 + q_5 + q_6 \quad \{5.72\}$$

$$q_2 + q_4 = h_a (T_a - T_i) \quad \{5.73\}$$

where  $G_v$  is the total incident solar radiation, i.e. the sum of direct and diffuse components of solar radiation incident upon the fenestration, ( $G_v = G_{bv} + G_{fv}$ ).

Substituting Eq.5.63 to Eq.5.68 into Equations (5.69 to 5.73), yields:-

$$q_{rci} + h_0 T_{go} = T_o h_0 + G_v (\alpha'_{go} + \alpha'_s) \quad \{5.74\}$$

$$T_g (h_0 + h_2 + h_3) - T_a h_2 - T_s h_3 = T_o h_0 + G_v \alpha'_g \quad \{5.75\}$$

$$-T_g h_3 - T_a h_4 + T_s (h_3 + h_4 + h_5 + h_6) = G_v \alpha'_s + T_i (h_5 + h_6) \quad \{5.76\}$$

$$T_s h_4 + T_{gi} h_2 - T_a (h_2 + h_4 + h_a) = -h_a T_i \quad \{5.77\}$$

The determinant of four equations (5.74 to 5.77) and four unknowns ( $T_g$ ,  $T_a$ ,  $T_s$  and  $q_{rci}$ ) is solved in a matrix algebra as:- (see Table 5.8)

$$[A] \cdot [X] = [C] \quad \{5.78\}$$

where

[A] is a two dimensional matrix of coefficients

[X] is the vector of the five unknowns

[C] is the right hand side constant vector

For a fenestration of double glazing with curtain, the heat transfer and heat balance equations that apply to the quantities illustrated in Fig.5.21 are as follows:-

$$q_0 = h_0 (T_{go} - T_o) \quad \{5.79\}$$

$$q_1 = h_1 (T_{go} - T_{gi}) \quad \{5.80\}$$

$$q_2 = h_2 (T_{gi} - T_a) \quad \{5.81\}$$

$$q_3 = h_3 (T_{gi} - T_s) \quad \{5.82\}$$

$$q_4 = h_4 (T_s - T_a) \quad \{5.83\}$$

$$q_5 = h_5 (T_s - T_i) \quad \{5.84\}$$

$$q_6 = h_6 (T_s - T_i) \quad \{5.85\}$$

$$q_{rci} + q_0 = G_v (\alpha'_{go} + \alpha'_{gi} + \alpha'_s) \quad \{5.86\}$$

$$q_0 + q_1 = G_v \alpha'_{go} \quad \{5.87\}$$

**Table 5.8** Matrix form of the heat balance equations of single glazing with a curtain.

$$\begin{bmatrix}
 1 & h_0 & 0 & 0 \\
 0 & h_0 + h_2 + h_3 & -h_2 & -h_3 \\
 0 & -h_3 & -h_4 & h_3 + h_4 + h_5 + h_6 \\
 0 & h_2 & -h_2 - h_4 - h_a & h_4
 \end{bmatrix}
 \begin{bmatrix}
 q_{rci} \\
 T_g \\
 T_a \\
 T_s
 \end{bmatrix}
 =
 \begin{bmatrix}
 G_v(\alpha'_g + \alpha'_s) + h_o T_o \\
 G_v \alpha'_g + h_o T_o \\
 G_v \alpha'_s + T_i(h_5 + h_6) \\
 -h_a T_i
 \end{bmatrix}$$

**Table 5.9** Matrix form of the heat balance equations of double glazing with a curtain.

$$\begin{bmatrix}
 1 & h_0 & 0 & 0 & 0 \\
 0 & h_0 + h_1 & -h_1 & 0 & 0 \\
 0 & -h_1 & h_1 + h_2 + h_3 & -h_2 & -h_3 \\
 0 & 0 & -h_3 & -h_4 & h_3 + h_4 + h_5 + h_6 \\
 0 & 0 & h_2 & -h_2 - h_4 - h_a & h_4
 \end{bmatrix}
 \begin{bmatrix}
 q_{rci} \\
 T_{go} \\
 T_{gi} \\
 T_a \\
 T_s
 \end{bmatrix}
 =
 \begin{bmatrix}
 G_v(\alpha'_{go} + \alpha'_{gi} + \alpha'_s) + h_o T_o \\
 G_v \alpha'_{go} + h_o T_o \\
 G_v \alpha'_{gi} \\
 G_v \alpha'_s + T_i(h_5 + h_6) \\
 -h_a T_i
 \end{bmatrix}$$

$$q_1 + G_v \alpha'_{gi} = q_2 + q_3 \quad \{5.88\}$$

$$q_3 + G_v \alpha'_s = q_4 + q_5 + q_6 \quad \{5.89\}$$

$$q_2 + q_4 = h_a (T_a - T_i) \quad \{5.90\}$$

Substituting Eq.5.79 to Eq.5.85 into Equations (5.86 to 5.90), and rearranging yields the matrix form of five determinant equations and five unknowns ( $T_{go}$ ,  $T_{gi}$ ,  $T_a$ ,  $T_s$  &  $q_{rci}$ ) as shown in Table 5.9.

To solve for the vector [X] in Eq.5.78, we will obtain

$$[X] = [A]^{-1} \cdot [C] \quad \{5.91\}$$

and this is solved in the CURTAIN program using the Gauss-Jordan method.

The  $N_{igs}$  term of Eq.5.14 can be obtained by setting  $G_v = 1$ , and  $T_o = T_i = 1$  in the matrix constant vector [C]. The U value is calculated by setting  $G_v = 0$ , and  $T_o = 2$  and  $T_i = 1$ .

## 5.7 Conclusion

---

Various properties associated with the curtain fabric and the curtain–glass fenestration have been discussed in this chapter. Of prime importance are the solar properties (curtain reflectance, transmittance and absorptance) which significantly influence the solar heat gain through fenestration. The thermophysical properties which, if available, may influence the conductive heat transfer through, tightly woven and considerably thick, curtain fabrics.

A method for indoor measurement of solar reflectance and transmittance of flat curtain fabrics has been described and results from tests on three curtain fabrics reported. From the experiments conducted, using two different instruments, the silicon cell radiometer proved more reliable than the net–radiometer in measuring the solar properties of a curtain.

In practice curtains hang in random configurations. From the study of geometric configuration effects on curtain properties, the following conclusions can be drawn:

- Fullness of a curtain alters the solar transmittance and reflectance of the fabric.
- The apparent solar properties of a folded curtain may be estimated from the flat fabric properties using the procedure discussed in section 5.5.1. However, for better results experimental determination is recommended.
- Insulation efficiency of a curtain fenestration decreases as the fullness increases. Thus a flat curtain provides less heat loss than a folded one.
- The use of a lining with a curtain (two layers of fabric) improves the insulative efficiency of the fenestration.
- Insulation of fenestration can also be improved by reducing the space between curtain fabrics and the glass surface.

The CURTAIN program developed in this chapter computes the fenestration temperatures and energy flows associated with curtain shaded single or double glazed fenestration exposed to real climatic conditions. The curtain fenestration may have any orientation and location within the northern hemisphere. A listing of the program is given in Appendix (E). Note that the program is validated by the experiments conducted in chapters 7 & 8, and good agreement between measured and computed fenestration temperatures was obtained.

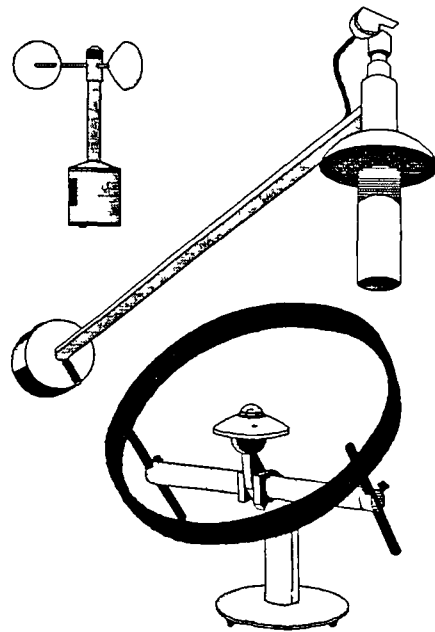
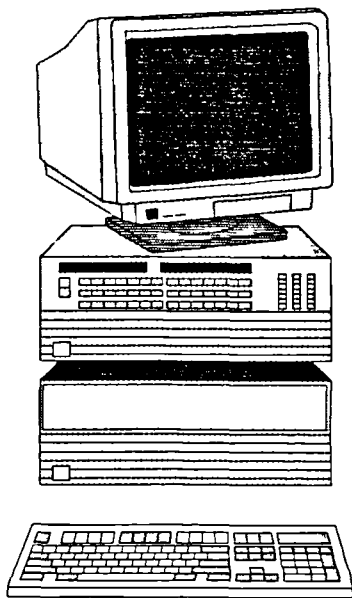
## 5.8 References

---

- ASHRAE (1985) ASHRAE Handbook (Fundamentals). American Society of Heating, Refrigerating and Air-conditioning Engineers Inc., Atlanta, USA.
- Baxter S. (1946) "The Thermal Conductivity of Textiles", *Proc. Phys. Soc.*, **58**, p 105.
- Cassie A. (1946) "Natural Fibres vs. Man Made Fibres", *J. Text. Inst.*, **37**, p 556
- Dix R. & Lavan Z. (1974) "Window Shades and Energy Conservation", Illinois Institute of Technology, Chicago, USA.
- Epps H., Goswami B. & Hassenboekler C. (1986) "Effect of Geometric Configuration and Surface Area on the Thermal Transmittance of Edge-sealed Draperies", *ASHRAE Trans.*, **92** (2A), pp 95-110.
- Farber E., Smith W., Pennington C. & Reed J. (1963) "Theoretical Analysis of Solar Heat Gain through Insulating Glass with Inside Shading", *ASHRAE J.*, August, pp 79-90.
- Gagge A., Burton A. & Bazett H. (1941) "A Practical System of Units for the Description of the Heat Exchange of Man with His Environment", *Science*, **94**, p 428.
- Grasso M. & Anderson J. (1986) "On-Site Evaluation of An Insulating Window Shade in Actual Use", *ASHRAE Trans.*, **92** (1A), pp 420-29.
- Hardy J. (1949) "Heat transfer", In Physiology of Heat Regulation and the Science of Clothing. (ed.) Newburgh L., W. B. Saunders Co., Philadelphia.
- Hassani A. & Brundret E. (1986) "An Experimental and Analytical Evaluation of the Insulative Properties of Double Glazing and Thick Curtains", *Solar Energy*, **37** (6), pp 437-44.
- Helcke G. & Peckham R. (1982) "Semi-Reflecting Roller Blinds for Windows: A Performance Simulation Using Real Weather Data for Locations in England, Denmark and Switzerland", *Int. J. Ambient Energy*, **3** (3), pp 153-62.
- Jordan R. & Threlkeld J. (1959) "Determination of the Effectiveness of Window Shading Materials on the Reduction of Solar Radiation Heat Gain", *ASHRAE J.*, June, pp 45-9.
- Kaswell E. (1977) "Textile Fibers, Yarn, and Fabrics: A Comparative Survey of their Behaviour with Special Reference to Wool", University Microfilms Print, University of Strathclyde, Glasgow.
- Kusuda T. (1976) "NBSLD: The Computer Program for Heating and Cooling Loads in Buildings", NBS Building Science Series 69, U.S. Government Printing Office, Washington DC.

- Keyes M. (1967) "Analysis and Rating of Drapery Materials Used for Indoor Shading", *ASHRAE Trans.*, **73**, pp 115-24.
- Marsh M. (1931) "The Thermal Insulating Properties of Fabrics", *J. Text. Inst.*, **22**, T245.
- Moore G. & Pennington C. (1967) "Measurement and Application of Solar Properties of Drapery Shading Materials", *ASHRAE Trans.*, **73**, pp VIII.3.1-3.15.
- Morton W. & Hearle J. (1975) Physical Properties of Textile Fibres. The Textile Institute and Heinemann Ltd., London.
- Nielson K. (1990) Window Treatments. Van Nostrand Reinhold, New York.
- Ozisik N. & Schutrum L. (1960) "Solar Heat Gain Factors for Windows with Drapes", *ASHRAE Trans.*, **66**, pp 228-39.
- Petherbridge P. (1967) "Transmission Characteristics of Window Glasses and Sun Controls", *Proc. of the CIE Conf.*, "Sunlight in Buildings", Bouwcentrum, Rotterdam, pp 183-98.
- Pennington C., Smith W., Farber E. & Reed J. (1964) "Experimental Analysis of Solar Heat Gain through Insulating Glass with Indoor Shading", *ASHRAE J.*, February, pp27-39.
- Rees W. (1946) "The Protective Value of Clothing", *J. Text. Inst.*, **37**, P132.
- Sharples S. (1980) "Modelling the Short Wave, Longwave and Convective Heat Transfer at Glazing Surfaces for the Detailed Computation of the Thermal Performance of Unshuttered and Shuttered Windows", Rep. BS 54, Sep.1980, Dept. of Building Science, Faculty of Architectural Studies, University of Sheffield.
- Tortora P. (1987) Understanding Textiles. Macmillan Publishing Company, New York.
- Twidell J. & Weir T. (1986) Renewable Energy Resources. E. & F.N Spon, London.
- Vigo T. & Nowacki L. (1979) Energy Conservation in Textile and Polymer Processing. American Chemical Society, Washington DC.
- Woodson E., Horridge P., Khan S. & Tock R. (1983) "Solar Optical Properties of Accepted Interior Window Treatments", *ASHRAE J.*, **25** (8), pp 40-5.
- Yellott J. (1964) "Selective Reflectance: A New Approach to Solar Heat Control", *ASHRAE J.*, January, pp 87-106.
- Yellott J. (1965) "Drapery Fabrics and their Effectiveness in Solar Control", *ASHRAE Trans.*, **71**, pp 260-71.

# Chapter 6



## 6. MEASUREMENT AND INSTRUMENTS

### 6.1 Introduction

---

Both the climatic data analysis and the practical part of this research required a knowledge of the accuracy and use of instruments for both indoor and field measurement. This chapter reviews various instruments to measure, temperature; relative humidity; wind speed and direction; and insolation, with emphasis on:

- instruments used in the Solar Village (Riyadh, Saudi Arabia) that produced the data analysed in chapter 3, and
- instruments used in the UK “Passys” test site where the experiments discussed in the next two chapters were conducted.

Special attention is given to the sensing mechanism, accuracy, and characteristics of the instruments. Algorithms are provided for calculating temperature from measured voltage, and calculating relative humidity from measured dry and wet bulb temperatures. In addition an accurate algorithm for averaging wind direction is proposed.

This chapter also describes the computer model “DTCLM.Bas” developed by the author to process logged data. The mathematical relationships discussed are implemented in this model. Code listing of the program is given in Appendix (E).

A quick and specific reference to the instruments used in the experimentation of this thesis is provided in Appendix (F) in the form of data sheets. These include : manufacturer or supplier address in the UK; description with illustrations; output type; range; accuracy; and performance evaluation of each instrument. Appendix (F) also outlines the sources of error in measurements and consider the statistical methods of error analysis used in this thesis. Definitions and terminology associated with the instruments, and with error and accuracy are included in the glossary (Appendix H).

**Table 6.1** Temperature Measuring Instruments.  
(data from ASHRAE 1985 and manufacturers literature).

Type	Application	Range (°C)	Precision (°C)	Limitations
<b>1. Glass-stem thermometers:</b>				
Mercury-glass	Temperature of gases and liquids by contact	-39/300	Less than 0.6 to 5.6	In gases, accuracy affected by radiation.
Alcohol-glass		-70/38		
<b>2. Gas thermometer</b>	Primary standard	-273/540	Less than 0.006	Requires considerable skill to use.
<b>3. Resistance thermometers:</b>				
Platinum-resistance	Precision; remote readings; temp. of fluids or solids by contact	-195/980	Less than 0.01 to 2.7	High cost; accuracy affected by radiation in gases.
Nickel-resistance	Remote readings; temp. by contact	-100/150	0.2	Accuracy affected by radiation in gases.
Thermistors		315	0.06	
<b>4. Thermocouples:</b>				
Pt-Pt-Rh thermocouple (type S or R)	Standard for thermocouples	1650	0.06 to 2.8	High cost.
Chrome-alumel (type K)	General testing of high temp; remote rapid readings by direct contact	1200	"	Less accurate than above
Iron-constantan (type J)		850	"	Subject to oxidation.
Copper-constantan (type T)	Same as above, especially suited for low temp	400	"	
Chrome-constantan (type E)				
<b>5. Bimetallic thermometers</b>	For approximate temp.	-18/540	0.6	Unsuitable for remote use; unreliable.
<b>6. Optical pyrometers</b>	For intensity of narrow spectral band of high temp radiation (remote)	815+	8.3	
<b>7. Radiation pyrometers</b>	For intensity of total high temp radiation (remote)	Any range		
<b>8. Melting and boiling points of materials</b>	Standards	All range	Extremely precise	For laboratory use only.

## 6.2 Temperature Measurement

---

Instruments for measuring temperatures are listed in Table (6.1). The following discussion refers mainly to the temperature sensors used in this research. Note that the temperature of a material or surface is difficult to measure if the temperature sensor is being irradiated, e.g. by sunshine.

### 6.2.1 Thermocouples

When two wires of dissimilar metals are joined by soldering, welding or twisting, they form a thermocouple junction. An electromotive force (EMF) that depends on the wire materials and the junction temperature, exists between the wires. When the wires are joined at two points, a thermocouple circuit is formed. By keeping one junction at a constant temperature, usually 0°C, a voltage is generated (due to EMF difference of the two junctions) which is a nonlinear function of temperature. In practice many thermocouples are used with electronically controlled reference temperatures. Data sheet DS1 (see Appendix F) includes a table of temperature as a function of voltage for type “T” thermocouple. A mathematical relationship between temperature and EMF can be used instead of tables. It is of the polynomial form (ASHRAE 1985):

$$T = a_0 + (a_1 E) + (a_2 E^2) + (a_3 E^3) + (a_4 E^4) \quad \{6.1\}$$

where T is the temperature (°C); E is the voltage ( $\mu\text{V}$ ); and  $a_0$  to  $a_4$  are constants which depend on the range of temperature, and accuracy of the relationship. Sets of these constants for various types of thermocouples can be obtained from the NBS Monograph 125 (Powell, 1973).

Polynomial coefficients for type-T thermocouple, (for use in Eq.6.1), are listed in Table (6.2). These constants represent two ranges of temperature (-200 to 0°C & 0 to 400°C), and two accuracy ranges. (i.e. for quadratic and cubic approximation in Eq.6.1). The specifications of a type-T thermocouple used in this research are discussed in data sheet DS1 (see Appendix F. Further characteristics of thermocouples in general are as follows:

- By using thermocouples, temperatures can be measured at remote points, and within thin materials, narrow spaces or otherwise inaccessible locations.
- The thermocouple is useful in determining surface temperatures. It can be attached to a surface either permanently (e.g. soldering, brazing) or temporarily (e.g. taped, glued). However protection measures against radiation are needed if the surface is irradiated, e.g. in sunshine. (see section 7.3.4 of the next chapter)
- Small thermocouples respond more promptly to temperature changes and are less affected by radiation than large ones. For use in heated air or gases, thermocouples are often protected against chemical attack by shields.

**Table 6.2** Polynomial coefficients for type “T” thermocouples for use in Eq.6.1. (data from ASHRAE 1985 chp.13).

Temperature Range (°C)	$a_1$	$a_2$	$a_3$	$a_4$	Error Range (°C)
-200 to 0	$2.3837090 \times 10^{-2}$	$-2.987883 \times 10^{-6}$	$-7.1945810 \times 10^{-10}$	$-1.0041943 \times 10^{-13}$	-0.3 to 0.3
0 to 200	$2.5661297 \times 10^{-2}$	$-6.1954869 \times 10^{-7}$	$2.2181644 \times 10^{-11}$	$-3.5500900 \times 10^{-16}$	-0.15 to 0.17
-200 to 0	$2.8388396 \times 10^{-2}$	$1.1561610 \times 10^{-6}$	$4.3380483 \times 10^{-10}$		-1.0 to 0.8
0 to 200	$2.5074243 \times 10^{-2}$	$-4.4920686 \times 10^{-7}$	$7.9942544 \times 10^{-12}$		-0.6 to 0.7

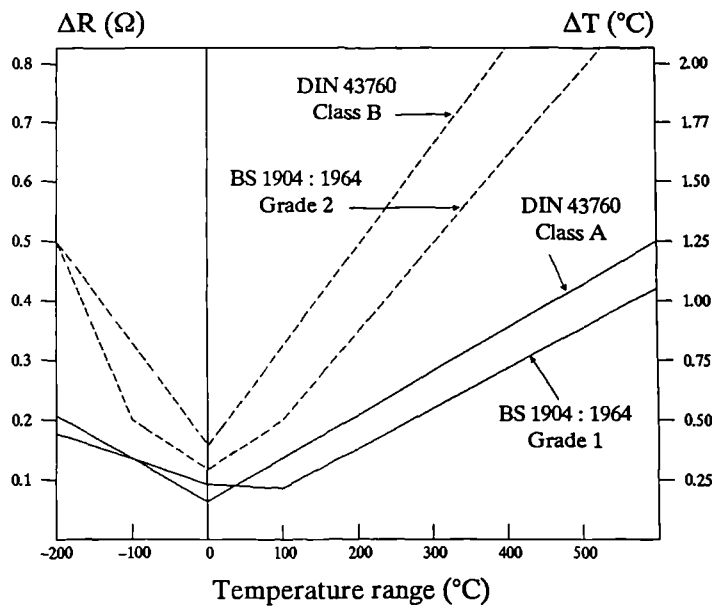


**Figure 6.1** Tolerances of British and German Specifications for 100Ω Thermometers. (reproduced from Labfacility Ltd.)

- Thermocouples in series, with every alternate junction maintained at a common temperature, produce an EMF that, when divided by the number of couples, gives the average EMF corresponding to the temperature difference between two sets of junctions. This series arrangement of thermocouples, often called “thermopile”, can be extremely sensitive in detecting very small temperature changes and differences. Thermopiles are used in some solar radiation sensors, (see section 6.5.1 and Fig.6.9).
- Thermocouple characteristics often depart from standard values of temperature–EMF relationship, therefore, calibration against a reference thermometer is necessary to achieve higher accuracies.

## 6.2.2 Resistance Thermometers

The resistance thermometer depends on the change of electric resistance of a sensing element with temperature change. For temperature measurement, only metals which characteristics remain unaltered in the temperature range to be measured can be used. Furthermore, the resistance should be reproducible as a function of temperature, and not altered by external influences (e.g. pressure, humidity, corrosion). Platinum fulfills all these requirements better than any other metal (see list in Table 6.1). Purer platinum sensors ensure long term stability and good reproducibility.

The commonly used type of these thermometers is a platinum resistance thermometer (PT100) which has a resistance of 100Ω at 0°C. The tolerances of British (BS 1904) and German (DIN 43760) specifications for this sensor are presented in Figure (6.1). The resistance of a PT100 as a function of temperature can be calculated from the following polynomial relations (Hattem 1987):

For temperature range 0°C to 850°C

$$R_T = R_0 (1 + b_1 T + b_2 T^2) \quad \{6.2\}$$

For temperature range –200°C to 0°C

$$R_T = R_0 [1 + b_1 T + b_2 T^2 + b_3 (T-100) T^3] \quad \{6.3\}$$

where

$R_T$	= resistance at temperature T °C
$R_0$	= resistance at temperature 0°C
T	= temperature °C
$b_1$	= $3.90784 \times 10^{-3} \text{ } ^\circ\text{C}^{-1}$
$b_2$	= $-0.578408 \times 10^{-3} \text{ } ^\circ\text{C}^{-1}$
$b_3$	= $-4.481924 \times 10^{-12} \text{ } ^\circ\text{C}^{-4}$

Two types of platinum resistance sensors (used in ambient air temperature and surface temperature measurement) are discussed in data sheets DS2 (see Appendix F).

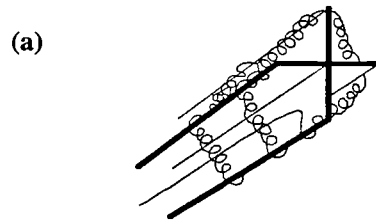


**Figure 6.2**

Construction of Platinum Standard Thermometers. (a) Meyers construction, and (b) Bird-cage construction. These constructions minimise the strain on the wires. (reproduced from Hattem 1987).

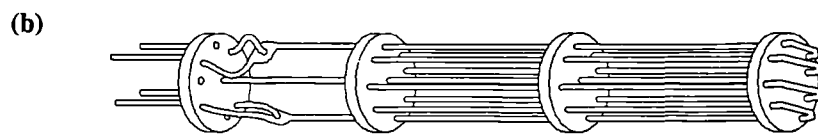
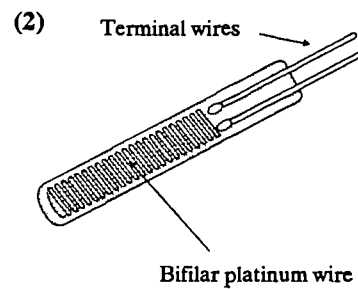
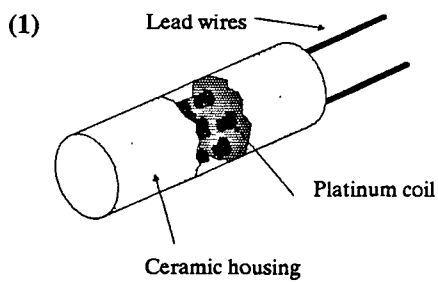


**Figure 6.3**

Construction of platinum sondes (1) Ceramic support, and (2) Glass support. (reproduced from Hattem 1987).



Data sheet DS3 (see Appendix F) describes an RM-Young aspirated thermometer for outdoor temperature measurements. Further characteristics of resistance thermometers are outlined below:

- Platinum resistance thermometers use is largely similar to that of thermocouples, although readings tend to be unstable above 510°C (ASHRAE 1985).
- Unlike the basic thermocouple, the resistance thermometer does not require a cold junction, and can be simply scaled for more accurate measurements; but because of its construction, it is more costly.
- Construction of PT thermometers for laboratory standards are made in two ways as shown in Figure (6.2). Platinum temperature sondes, which are more practical, can be made in several ways, e.g. ceramic cylinder support, glass support and thin film detectors (Fig.6.3). Hattem (1987) discusses some calibration methods for platinum sondes over different temperature ranges.
- PT thermometers are available in two, three and four wire elements. Two lead temperature elements are not recommended (ASHRAE 1985), since they do not permit correction for lead resistance. At least three leads to each resistor are necessary to obtain consistent readings.

### 6.2.3 Remote Temperature Sensors (Infrared Radiometer)

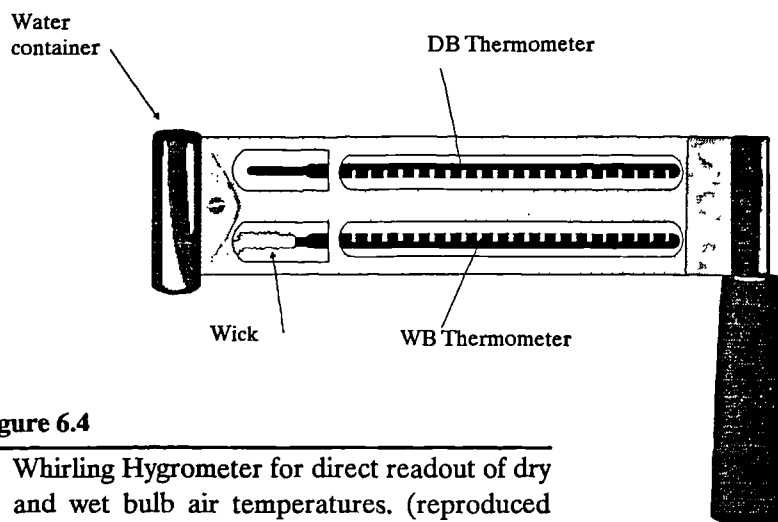
Infrared radiometers that permit non contact measurement of surface temperature are commercially available. The radiant energy from the observed object is focused by an optical system onto an infrared detector that sends an output signal, proportional to the incident radiation, to a meter or display unit.

It is important to recognise that this type of radiometer only measures the energy level of the radiation incident on the detector, and this incident radiation includes radiation emitted by the object and radiation reflected from the surface of the object. An accurate measurement of surface temperature, therefore, requires knowledge of the longwave emissivity of the object and the radiant field surrounding the object.

A full description and the characteristics of a non-contact infrared digital thermometer, used in experimentation to measure curtains and blind surface temperatures, are provided in data sheet DS4 in Appendix F.

**Table 6.3** Humidity Measuring Instruments. (data from ASHRAE 1985)

Type	Application	Range	Precision	Limitations
<i>Psychrometer</i>	Room of building, outside air, air ducts.	0 to 260°C	0.3 to 3% R	Should be used in air stream about $5 \text{ ms}^{-1}$ ; small diameter wet bulbs may be used at lower velocities; difficult to use at sub-freezing temperatures.
<i>Dew Point :-</i> Condensation type	Automated systems in industrial processes & meteorological observations.	-120 to 100°C dp	0.1 to 1.1°C dp	Expensive, some difficulty with supercooling effect.
Fogtype	Wide range, method for sampling.	-60°C to 50°C dp	1.1°C dp	Manual, series of readings needed for measurement.
Salt-phase transition	Meteorological & lab measurements; simple to use.	0 to 100°C dp	0.6 to 1.1°C dp	Not usable below approximately 15% R; susceptible to some atmospheric contaminants.
<i>Mechanical:-</i>	Control & measurement where air motion is slight.	0 to 100% R -40 to 65°C dp	3% R	Frequent calibration required when used at extremes of range; hair has considerable lag, low sensitivity, and is adversely affected by temperature above 52°C and R below 20%.
<i>Electrical Conductivity</i>	Measurement & control.	-40 to 65°C dp	1.5 to 3% R	Susceptible to damage by air contaminants; some to water; require frequent calibration checks.
<i>Electrolytic</i>	Measurement.	-75 to -2°C dp	5% of scale range	Ordinarily limited to low humidity.
<i>Gravimetric</i>	Measurement, standard.		0.1 to 2%	Special equipment & extreme care required for high accuracy.

**Figure 6.4**

Whirling Hygrometer for direct readout of dry and wet bulb air temperatures. (reproduced from Casella & Co. Ltd.)

## 6.3 Humidity Measurement

Instruments for measuring humidity and comments on each are listed in Table (6.3). The principal instruments for measuring relative humidity are described.

### 6.3.1 Psychrometers

Any instrument capable of measuring the humidity or the psychrometric state of air is a hygrometer. A psychrometer is a particular kind of hygrometers consisting of two identical sensors, one is dry but the bulb of the other is enclosed in a wick or sock. The wick is wetted with water and ventilated with air moving at a sufficient rate, usually  $3.5 \text{ (m s}^{-1}\text{)}$  or more, relative to the instrument (ASHRAE 1985). The difference between dry and wet bulb temperatures gives a non-linear measurement of relative humidity (see section 6.3.2).

Figure (6.4) show a sling psychrometer (also referred to as whirling hygrometer). It operates manually by whirling the device through air, then visually reading the two framed mercury-filled thermometers. In the aspirated psychrometers, the thermometers remain stationary, and a small fan or blower is used to move the air across the thermometers bulbs. Other temperature sensors, such as thermocouples and resistance thermometers are used. A Vector aspirated psychrometer (using PT sensor) is described in data sheet DS5 (see Appendix F). Large errors may result from improper use of psychrometers, and care must be taken to avoid them, particularly where strong radiation and large temperature differential exist.

### 6.3.2 Calculation of Relative Humidity

Charts and tables are available showing the relationship between temperatures and relative humidity (see IHVE guide 1970 and ASHRAE Fundamentals 1985). The following mathematical relations, adopted from ASHRAE Fundamentals, were used in the “DTCLM” Basic model, (see section 6.6.2), to calculate relative humidities from measured dry and wet bulb temperatures as follows:

First the saturation pressure over ice for the temperature range  $-100^\circ\text{C}$  to  $0^\circ\text{C}$  or over liquid water for the temperature range  $0^\circ\text{C}$  to  $200^\circ\text{C}$  is required

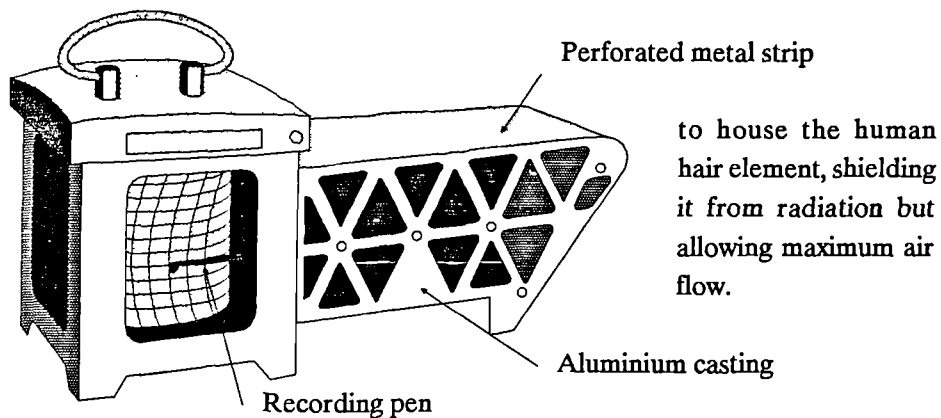
$$\ln(P_{ws}) = (c_1/T) + c_2 + c_3 T + c_4 T^2 + c_5 T^3 + c_6 \ln(T) \quad \{6.4\}$$

where  $P_{ws}$  the saturation vapour pressure at a given temperature  $T$ , (Pa);  $\bar{T}$  is the absolute temperature (K); and  $c_1$  to  $c_6$  are constants given in Table (6.4) for the two temperature ranges. The humidity ratio ( $W$ ), defined as the ratio of the mass of water vapour to the mass of dry air contained in a moist air sample, is then calculated from

$$W = [(d_1 + d_2 \bar{T}^*) W_s^* - (T - \bar{T}^*)] / [d_1 + d_3 T - d_4 \bar{T}^*] \quad \{6.5\}$$

**Table 6.4** Constants for use in Eq.6.4 at two ambient temperature ranges.

	$-100^{\circ}\text{C} < T < 0^{\circ}\text{C}$	$0^{\circ}\text{C} \leq T < 200^{\circ}\text{C}$
$c_1 =$	-5674.5359	-5800.2206
$c_2 =$	6.3925247	1.3914993
$c_3 =$	$-0.9677843 \cdot 10^{-2}$	-0.04860239
$c_4 =$	$0.62215701 \cdot 10^{-6}$	$0.41764768 \cdot 10^{-4}$
$c_5 =$	$0.20747825 \cdot 10^{-8}$	$-0.14452093 \cdot 10^{-7}$
$c_6 =$	$0.9484024 \cdot 10^{-12}$	0

**Figure 6.5**

Hair Hygrograph (human hair element). The relative humidity is recorded on a daily, weekly or monthly chart wrapped round a drum rotated by a spring-driven clock. (reproduced from Casella).

where  $T$  and  $T^*$  are the dry bulb and wet bulb temperatures respectively ( $^{\circ}\text{C}$ );  $d_1$  to  $d_4$  are constants with the values ( $d_1 = 2501$ ;  $d_2 = 2.381$ ;  $d_3 = 1.805$ ; and  $d_4 = 4.186$ ); and  $W_s^*$  is the saturated air humidity ratio at wet bulb temperature calculated from

$$W_s^* = 0.62198 [P_{ws}^* / (P - P_{ws}^*)] \quad \{6.6\}$$

where  $P$  the total barometric pressure of moist air (assumed to be 101.325 kPa); and  $P_{ws}^*$  is the saturated vapour pressure at wet bulb temperature (Pa).

The degree of saturation ( $\psi$ ) is thus obtained from:

$$\psi = W / W_s \quad \{6.7\}$$

where ( $W_s$ ), the saturated air humidity ratio at dry bulb temperature, is calculated using  $P_{ws}$  in Eq.6.6. The relative humidity ( $R$ ) at dry bulb temperature  $T$  is given by

$$R = \psi / [1 - (1-\psi) (P_{ws} / P)] \quad \{6.8\}$$

In temperatures below  $0^{\circ}\text{C}$ , the water on the wick may freeze. Since the wet bulb temperature is different for ice and water, its state must be known and the proper constants should be used for Eq.6.4 or a proper chart should be used.

### 6.3.3 Hygrometers and Relative Humidity Indicators

Dew Point Hygrometers and Mechanical Hygrometers are usually direct readout instruments only. Electrical hygrometers, that use resistance or capacitance transducers, can provide an electrical output for data logging purposes. Electrical hygrometers are very sensitive to humidity change with accuracy of  $\pm 2\%$  in the range of 20% to 80% relative humidity, but diminishing accuracy at higher humidities. Excessive humidities affect the property of sensing elements in electric hygrometers, thus periodical calibration, against standard instruments or by exposure to an atmosphere maintained at a known humidity and temperature, is required.

Many organic materials change in dimension with changes in humidity; this action is used in many simple and effective humidity indicators and recorders. Commonly used organic materials are human hair, nylon, dacron, animal membrane, animal horn, wood and paper. However, no organic material has been found to consistently reproduce its action over an extended period of time (ASHRAE 1985). Responses can be affected by exposure to extremes of humidity. Figure (6.5) show a hair hygrometer. Humidity reading is obtained from the alteration in length of a human hair, transmitted to a recording pen by a magnifying linkage. Such devices require initial calibration and frequent recalibration (experience with using two hair hygrometers).

**Table 6.5** Air Speed and Direction Measuring Instruments.  
(data from ASHRAE 1985 & Vector Instr.)

Type	Application	Range (m/s)	Precision	Limitations
<i>SPEED</i>				
1. <i>Smoke puff or airborne solid tracer</i>	Low air velocities in rooms; highly directional	0.025–0.25	10 – 20%	Awkward to use but valuable in tracing air movement.
2. <i>Deflecting vane anemometer</i>	Air velocities in rooms, at outlets, etc; directional	0.15–120	5%	Not well suited for duct readings; needs periodic check calibration.
3. <i>Revolving vane anemometer</i>	Moderate air velocities in ducts and rooms; somewhat directional	0.5–15	5 – 20%	Extremely subject to errors with variations in velocities with space or time; easily damaged; needs periodic calibration.
4. <i>Pitot tube.</i>	Standard instrument for measurement of duct air speeds.	0.9–50	1 – 5%	Accuracy falls off at low end of range.
5. <i>Impact tube &amp; side-wall static tap</i>	High speeds, small tubes and where air direction may be variable.	0.6–50	1 – 5%	Accuracy depends on constancy of static pressure across stream section.
6. <i>Heated thermocouple</i>	Air speeds in ducts, velocity distributions.	0.5–10	3 – 20%	Accuracy of some types not good at lower end of range; steady state measurements only.
7. <i>Hot-wire anemometer</i>	(a) Low speeds; directional and non-directional available (b) High air speeds.	0.005–5 up to 300	1 – 20% 1 – 10%	Require accurate calibration at frequent intervals ; complex and costly.
8. <i>Cup anemometer</i>	Standard instrument for the measurement of wind speeds; available in analogue and pulse output types; nondirectional only.	0.15–75	2%	Needs yearly calibration; nonlinearity increases outside the (10 to 55 m s <sup>-1</sup> ) range.
<i>DIRECTION</i>				
9. <i>Wind vane</i>	Wind direction; commonly operates by reed-switches; potentiometer type available.	0° to 360°	1 to 5%	Needs alignment to North except for self-referencing windvanes; averaging output samples is required for better accuracy.

## 6.4 Air Speed and Direction Measurements

Instruments for measuring air velocity and comments on each are listed in Table (6.5). Most of these instruments measure air speeds in rooms and ducts (see ASHRAE 1985. Chp 13, for details). The following discussion describes wind speed and direction measuring instruments used in this research as part of weather monitoring at the PASSYS test site in Glasgow (see chapter 7), and examines proposals for the averaging of wind direction data.

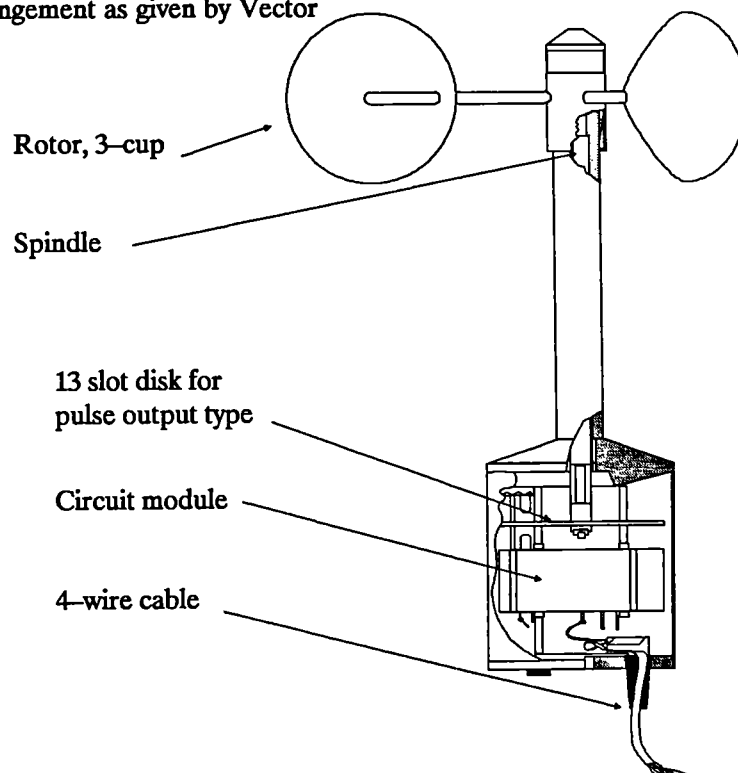
### 6.4.1 Cup Anemometer and Windvane

The cup-type anemometer is almost universally used for measuring wind speeds. It consists of three or four hemispherical cups mounted radially from a vertical shaft (Fig.6.6). Wind from any direction causes the cups and shaft to rotate. The rotation is transferred by a gear mechanism to a counter. Halliday (1988) discusses cup anemometer's characteristics and calibration in depth.

The output of this instrument is usually linear with respect to wind speed (Voltage output), but it is possible to produce pulse output in some versions by amplification of the sensor signals. Two versions of Vector cup anemometers are discussed in data sheet DS6 (see Appendix F). For the measurement of wind direction in compass degrees, a potentiometer windvane was used. The characteristics of this device are provided in data sheet DS7 of Appendix F.

**Figure 6.6**

Cup anemometer for the measurement of wind speed. General arrangement as given by Vector Instruments (1987).



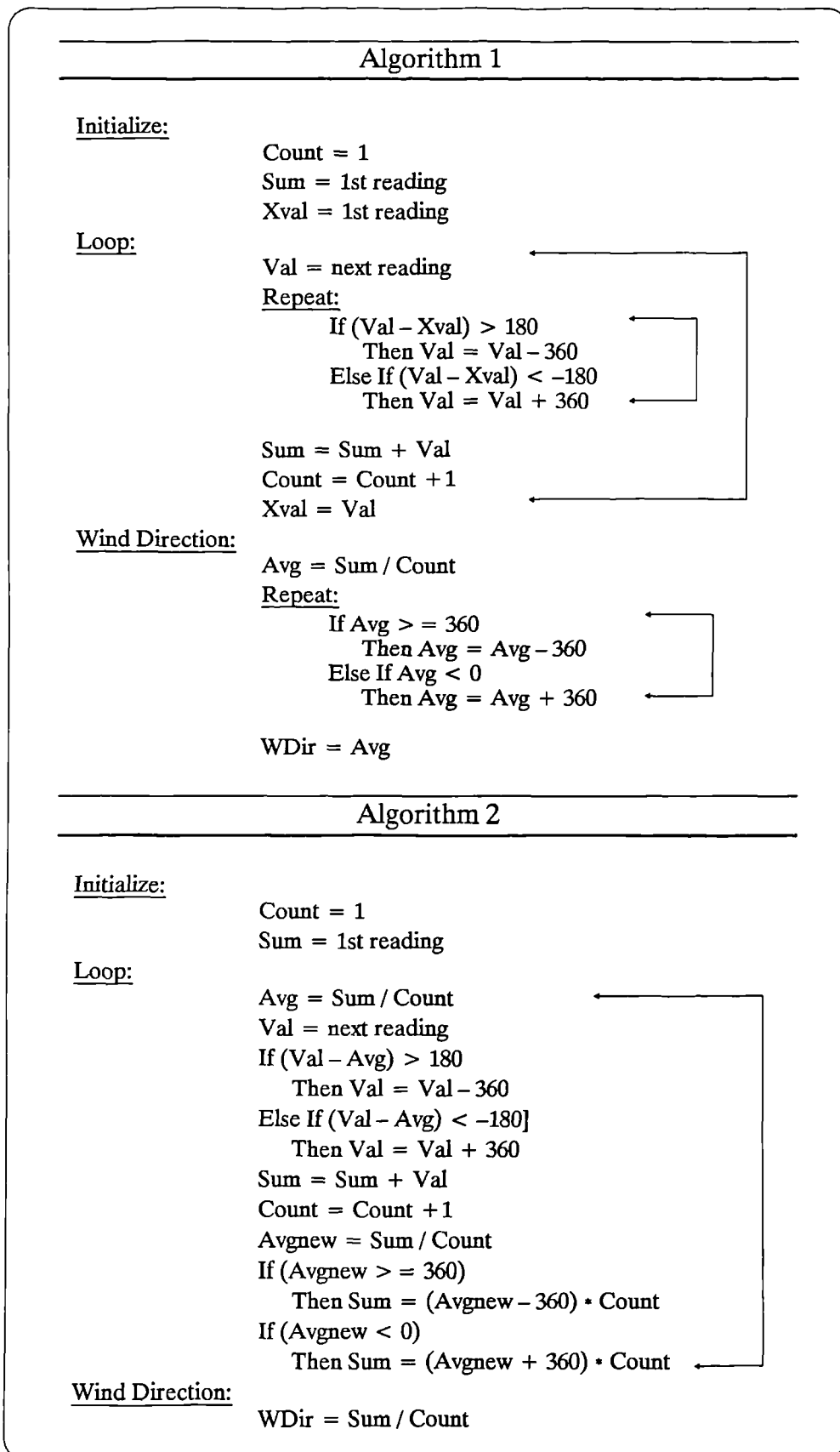


**Figure 6.7** Algorithms for averaging the wind direction suitable for computer programs. The second algorithm is applied in DTCLM program, (see Appendix E for code listing).

## 6.4.2 Averaging of Wind Direction Data

Care is needed when averaging wind direction data because of the discontinuity at 0/360. All directions are measured in the range 0°–360°, so directions of 10° and 350° would give an average of 180° rather than 0° or 360°. Assuming that directions do not change rapidly with respect to short sampling intervals, Halliday et.al. (1986) suggested a scheme to account for discontinuity in averaging wind direction as shown in algorithm 1 of Figure (6.7).

For instance, using algorithm 1 to average successive readings of 20°, 20°, 20°, 280°, 170°, and 60°, (see Figure 6.8), gives a 275° average wind direction. However, the true average of wind direction in this example is obviously about 35°, where four of the six readings prevail. This can be achieved using the procedure in algorithm 2 (see Fig.6.7).

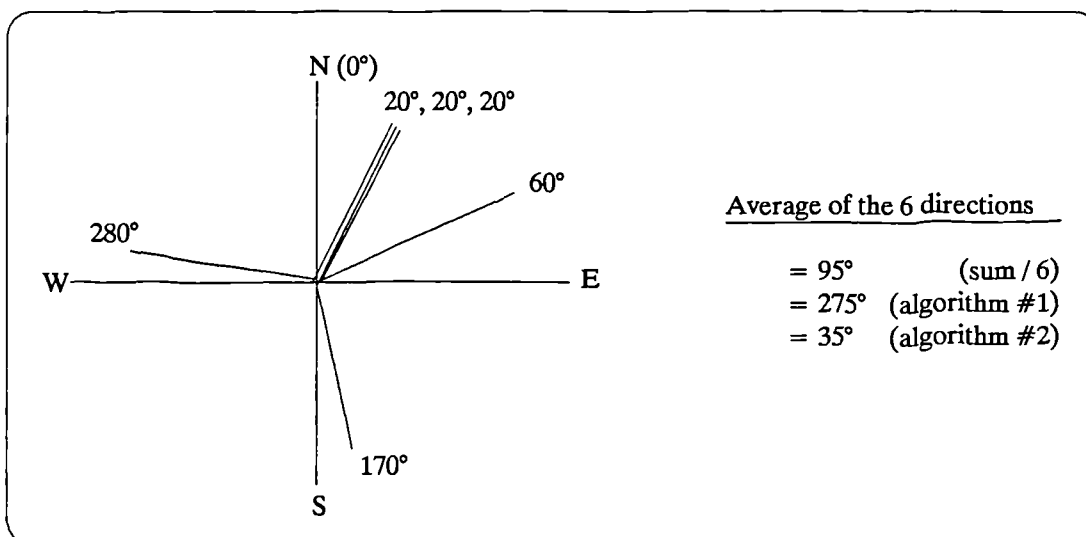


Figure 6.8 Example for averaging six wind directions.

Both algorithms produce equal results unless successive readings differ by 180° or more. Algorithm (1) uses the last value for defining whether to adjust the current value by  $\pm 360^\circ$ . Algorithm (2) uses the average of readings to date for comparison with the current value. “DTCLM” program, developed by the author, include a BASIC code of algorithm 2, (see Appendix E).

Algorithm (2) is more suitable in the presence of widely fluctuating wind direction readings. It will only give a better measure of prevailing wind direction if a stable pattern has not been established, otherwise it gives no advantage as compared with algorithm (1).

**Table 6.6** Insolation measuring Instruments.  
(data from Manufacturer's literature, Coulson 1975, and Twidell & Weir 1986).

Instrument	Sensor type	Range	Application & Features
<i>Pyrheliometers:</i> [WMO Standard] : Absolute Cavity Radiometer (Eppley)	Thermopile	–	Measures direct normal insolation (absolute, i.e. against electrical heating); used mainly to calibrate other pyrheliometers and pyranometers.
[WMO 1st class] : Normal Incident Pyrheliometer (Eppley NIP)	Thermopile	0.3–2.8 $\mu\text{m}$	Measures direct normal insolation; quartz aperture with an angle of 5.7°; comes with a rotatable disk which accommodates filters; it follows the sun by a tracking mechanism.
Linke Feussner pyrheliometer (Kipp & Zonen Actinometer)	Moll thermopile	0.3–2.8 $\mu\text{m}$	46-junction thermopile; 10.2° aperture angle; provision for using five different filters.
[WMO 2nd class] : Moll Gorczynski Pyrheliometer (Kipp & Zonen)	Moll thermopile	0.3–2.8 $\mu\text{m}$	Early type of pyrheliometers with 80-junction thermopile; not in production.
<i>Pyranometers:</i> [WMO 1st class] : Solarimeter (Kipp & Zonen CM-11)	Moll thermopile	0.3–2.8 $\mu\text{m}$	Measures global insolation; sensor is mounted under two glass domes; most popular in Europe; high accuracy.
Precision Spectral Pyranometer (Eppley PSP)	Thermopile	0.3–2.8 $\mu\text{m}$	The sensor is the hot junction while the instrument body acts as the cold junction; the outer glass dome can be replaced with lower wavelength cutoff filters.
[WMO 2nd class] : Black & white pyranometer (Eppley 8-48)	Thermopile	0.3–2.8 $\mu\text{m}$	Sensor is covered with a ground-glass dome; less accurate than PSP model.
[WMO 3rd class] : Bimetallic strip pyranograph	Blackened bimetallic strip	0.3–2.8 $\mu\text{m}$	Built-in chart recorder; purely mechanical; recommended for daily total measurements only; about 10% accuracy; requires frequent calibration.
<i>Albedometer</i> (Kipp & Zonen)	Thermopile	0.3–2.8 $\mu\text{m}$	Measures solar radiation balance or albedo over surfaces of different nature; consists of two identical solarimeters attached back to back.
<i>Solar Cells</i>	Silicon PV cell	0.4–1.1 $\mu\text{m}$	Measures global insolation; non-uniform spectral response, needs plastic diffusers to improve cell's cosine response; low cost.
<i>UV Radiometer</i> (Eppley)	Photocell	0.29–0.39 $\mu\text{m}$	Measures near ultraviolet radiation; filters available for narrower part of the near ultraviolet region.
<i>Infrared Radiometers:</i> Net Radiometer (Dicot)	Thermopile	0.3–80 $\mu\text{m}$	Measures earth-sky radiation balance; the sensors are covered with polyethylene domes; must be in a horizontal position; by shielding the lower sensor it can be used to measure sky IR radiation.
Pyrgeometer (Eppley)	Thermopile	4–50 $\mu\text{m}$	Measures infrared radiation; sensor covered with silicon dome with interference filter.
<i>Sunshine Recorder</i> Campbell-Stokes	Calibrated chart	All	Measures sunshine hours; variable threshold level of radiation; simple and widely used.
<i>Satellite photo</i>	Photo	% cloud	Can be used for general forecasting, needs radio receiver and special plotters.

## 6.5 Insolation Measurement

---

There are two types of instruments for measuring the sun's radiation; (i) Pyrheliometer to measure direct normal insolation; and (ii) Pyranometer to measure global insolation, usually on a horizontal surface. Modification of some elements in those instruments enables the measurement of specific optical ranges (e.g. to study atmospheric turbidity), the measurement of ultraviolet radiation, infrared radiation, surface albedo. This section will discuss the common types of solar instrument, with emphasis on those used in this research. Solar instruments are listed with comments in Table (6.6).

### 6.5.1 Radiation Sensors

Sensing elements (detectors) of the various insolation instruments can be classified as: calorimetric, thermomechanical, thermoelectric, or photoelectric. Some of the calorimetric sensor instruments serve as primary standards for calibration. Thermomechanical type instruments are of less quality compared with other types. Specialised publications such as, Coulson (1975); Reid, et. al. (1978); Dickinson & Cheremisinoff (1980) treat this subject in depth.

Thermoelectric and photoelectric sensors form the basic sensory mechanism of solar instruments used in this research. A brief description of these two types follows.

#### *Thermoelectric Sensors*

It is mentioned earlier (section 6.2.1) that thermocouple junctions connected in series (thermopile) is highly sensitive to temperature changes (i.e. produce higher EMF than a single thermocouple). This principle is applied in radiometry by exposing one junction to the incident radiation (hot junction) while the other is shielded from it (cold junction) as shown in Figures (6.9a & 6.9b).

In a number of insolation instruments, the thermopile is arranged in a star-shaped flat grid (Fig.6.9c). Hot junctions are coated with black paint, and cold junctions are painted white to shield them from solar radiation.

In order to obtain stable conditions (usually called zero drift) it is necessary to maintain cold junctions at constant temperature (electronic cold junction compensation is now possible to high accuracy). To achieve this objective, Moll (1923) devised a thermopile in which the cold junctions are thermally attached to, but electrically insulated from, a thick brass plate (Fig.6.9d). The large heat capacity of the brass absorbs small temperature variations caused by air currents.

**Figure 6.9**

Various arrangements of thermoelectric sensors. (a) a standard thermocouple, (b) thermocouple junctions connected in series to increase EMF, this arrangement is called a "thermopile". (c) star-shape thermopile used in some second class pyranometers (e.g. Eppley "black & white" pyranometer. (d) Moll thermopile, used in first class Kipp & Zonen solarimeters. (reproduced from Iqbal 1983).

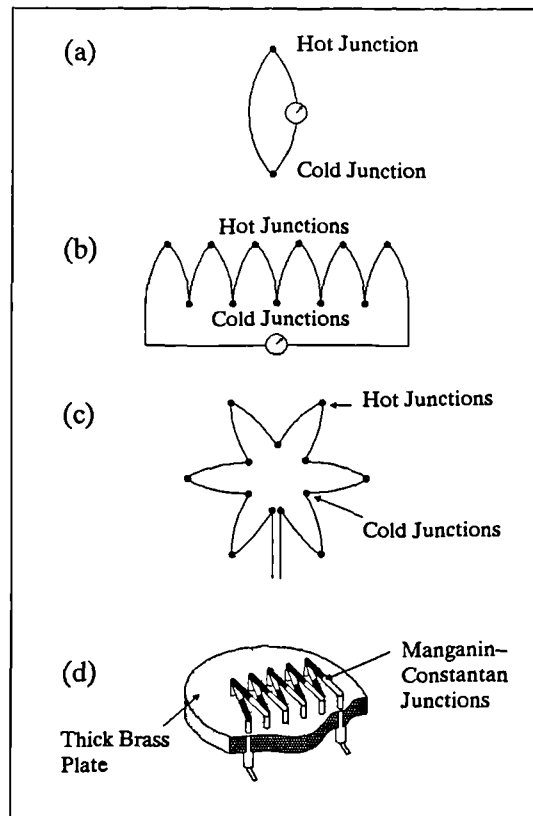


**Figure 6.10**

Typical structure of n-p junction solar cell. BSF: back surface field. (reproduced from Twidell and Weir 1986).

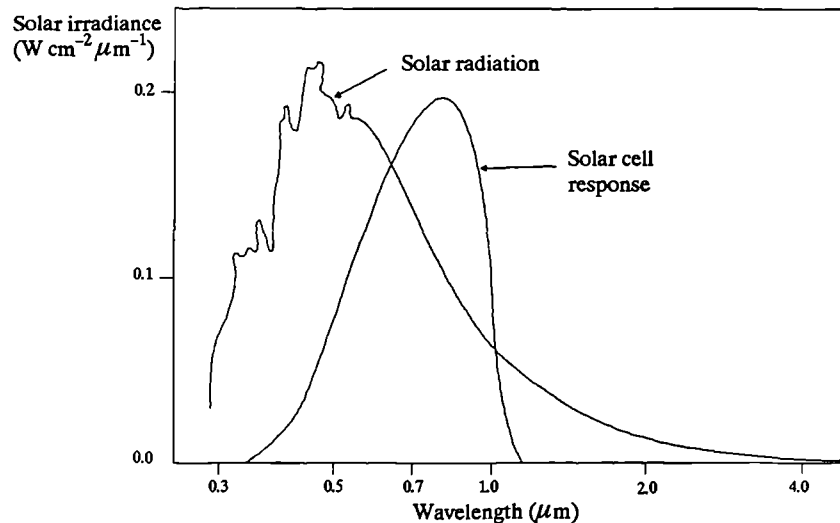
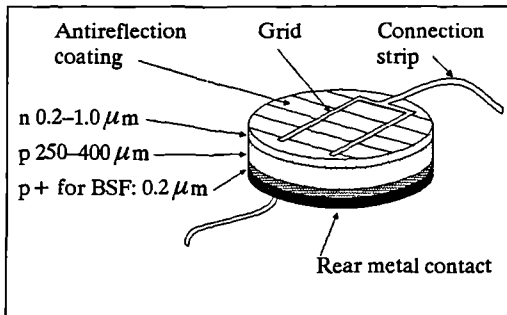


**Figure 6.11** Spectral response of silicon solar cells compared with the spectral distribution of solar radiation. (reproduced from Coulson 1975)

### Photoelectric Sensors

The great advantage of photoelectric detectors is that the sensor is activated by discrete events of photons striking the material, and not by a change of temperature because of absorption of the solar radiation, as in thermoelectric detectors. Among the photoelectric detectors, photovoltaic based instruments are commonly used in the field of solar radiation measurement (Iqbal 1983). The majority of photovoltaic cells (solar cell) are silicon semiconductor junction devices (Fig.6.10). The properties and characteristics of silicon solar cells are well described in Twidell & Weir (1986).

A disadvantage of silicon cell devices is their spectral response which is strong only in the visible and near-infrared portions of the solar spectrum as shown in Figure (6.11). However, their advantages are low cost and fast response time for instantaneous measurements.

### 6.5.2 Pyranometers (Solarimeters)

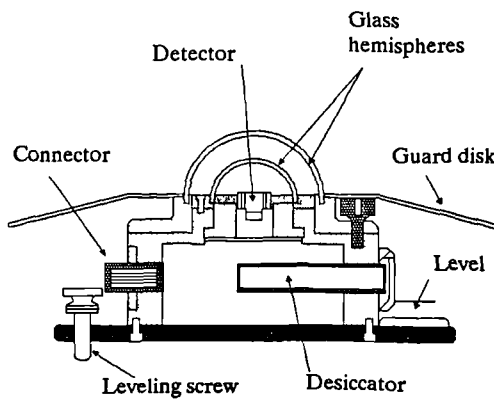
The world meteorological organization, (WMO 1971) has defined three classes of pyranometers on the bases of their accuracy and overall system performance. The bases of classification are given in Table (6.7).

**Table 6.7** Classification of pyranometers. (World Meteorological Organisation 1971)

	First Class	Second Class	Third Class
Sensitivity ( $W/m^2$ )	$\pm 1$	$\pm 5$	$\pm 10$
Stability (% change per year)	$\pm 1$	$\pm 2$	$\pm 5$
Temperature (maximum error due to changes of ambient temperature, in %)	$\pm 1$	$\pm 2$	$\pm 5$
Selectivity (maximum error due to departure from assumed spectral response, in %)	$\pm 1$	$\pm 2$	$\pm 5$
Linearity (maximum error due to nonlinearity not accounted for, in %)	$\pm 1$	$\pm 2$	$\pm 3$
Time constant (maximum, in seconds)	25	60	240
Cosine response (deviation from that assumed, taken at sun elevation $10^\circ$ on clear day, in %)	$\pm 3$	$\pm 5-7$	$\pm 10$
Azimuth response (deviation from that assumed, taken on clear day, in %)	$\pm 3$	$\pm 5-7$	$\pm 10$

**Figure 6.12**

Cross-sectional diagram of Eppley precision spectral pyranometer. It is used for global insolation measurement ( $0.3\text{--}2.8\ \mu\text{m}$ ). (reproduced from Eppley Laboratories).

**Figure 6.13**

Albedometer based on two Kipp & Zonen solarimeters. This instrument can be used for the measurements of either short wave radiation balance, global insolation ( $0.3\text{--}2.8\ \mu\text{m}$ ), or surfaces albedo. (reproduced from DIDCOT Instrument Co. Ltd.)

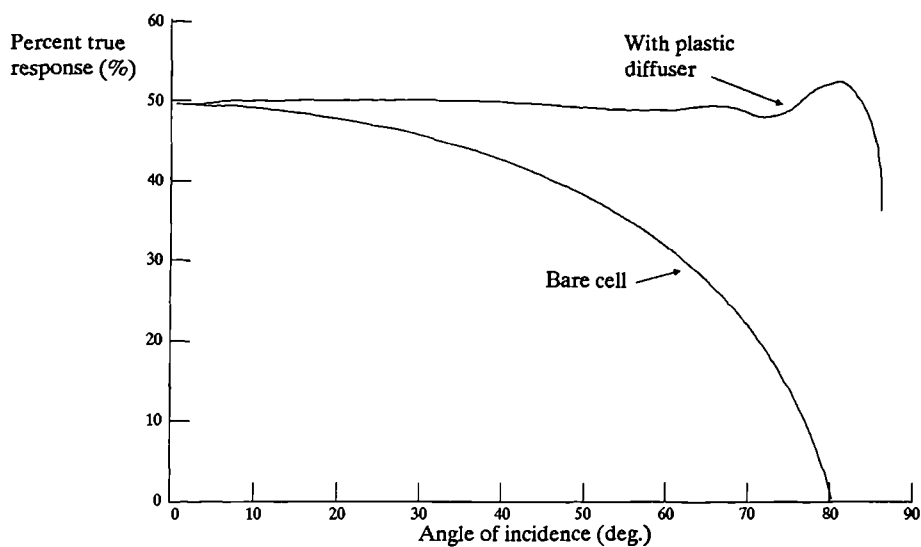
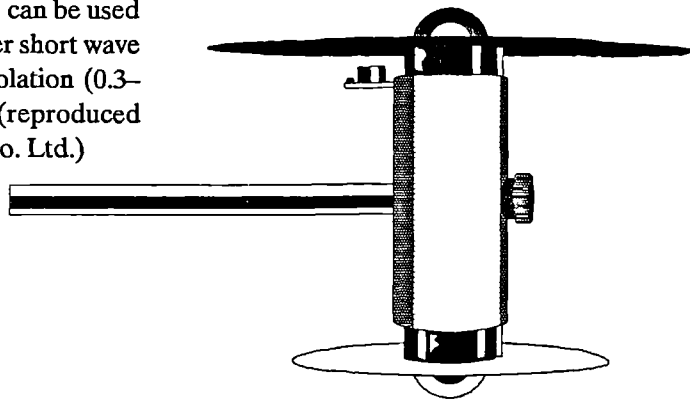


**Figure 6.14** Angular response of silicon solar cells with and without a plastic diffusing cover. (reproduced from Coulson 1975)

A pyranometer (Fig.6.12) is an instrument for measuring the global (direct and diffuse) insolation from one hemisphere, i.e. a solid angle of  $180^\circ$ . Data sheet DS8 in Appendix (F) describes a Kipp & Zonen Moll-thermopile based solarimeter (pyranometer) used in this research. Descriptions of different pyranometers with historical background and calibration procedures are well covered by Coulson (1975) and Anson (1980). The following discussion examines the use of pyranometers as albedometers and in the measurement of diffuse insolation.

### *Albedometers*

The albedometer consists of two identical pyranometers (see Figure 6.13), one measures the incident solar radiation ( $G$ ), the other the radiation reflected by a surface ( $G_r$ ). There are two modes of operating. (i) With the pyranometers connected in series opposite to each other, the shortwave balance is measured ( $\lambda = 0.3\text{--}2.8\ \mu\text{m}$  with thermopile sensors or  $\lambda = 0.4\text{--}1.1\ \mu\text{m}$  with silicon cells). (ii) When the output of the pyranometers is recorded separately, incident and reflected radiation can be used to calculate the surface albedo ( $\rho$ ) as

$$\rho = G_r / G \quad \{6.9\}$$

A Didcot albedometer with silicon cell sensor covered with plastic diffuser is described in data sheet DS9 (see Appendix F). The plastic diffuser improves the response of the silicon solar cell with the angle of incident radiation (cosine response), as shown by the upper curve of Figure (6.14).

### *Shadow Ring*

A pyranometer can measure diffuse insolation alone if the sensor is shaded from the sun with a disc. A fixed shadow ring is commonly used for this purpose, but this itself shields some of the diffuse insolation and requires corrections to the data. The shadow ring should satisfy the following requirements which can be verified from Figure (6.15a)

- The axis of the circular shadow ring must be always parallel with the polar-axis. In consequence the angle between ring axis and horizontal equals the latitude of the observation site.
- The shadow ring should be able to shift along the ring axis following the sun's declination.
- The pyranometer should be placed with the centre of its sensor on the ring axis.

The above features are embodied in the construction of a Kipp & Zonen shadow ring described in data sheet DS10 (see Appendix F).

**Figure 6.15** (a) Shadow Ring installation for measurement of Diffuse Insolation.  
 (b) Geometry of the Shadow Ring. (notation for use in Eq.6.12–6.14).

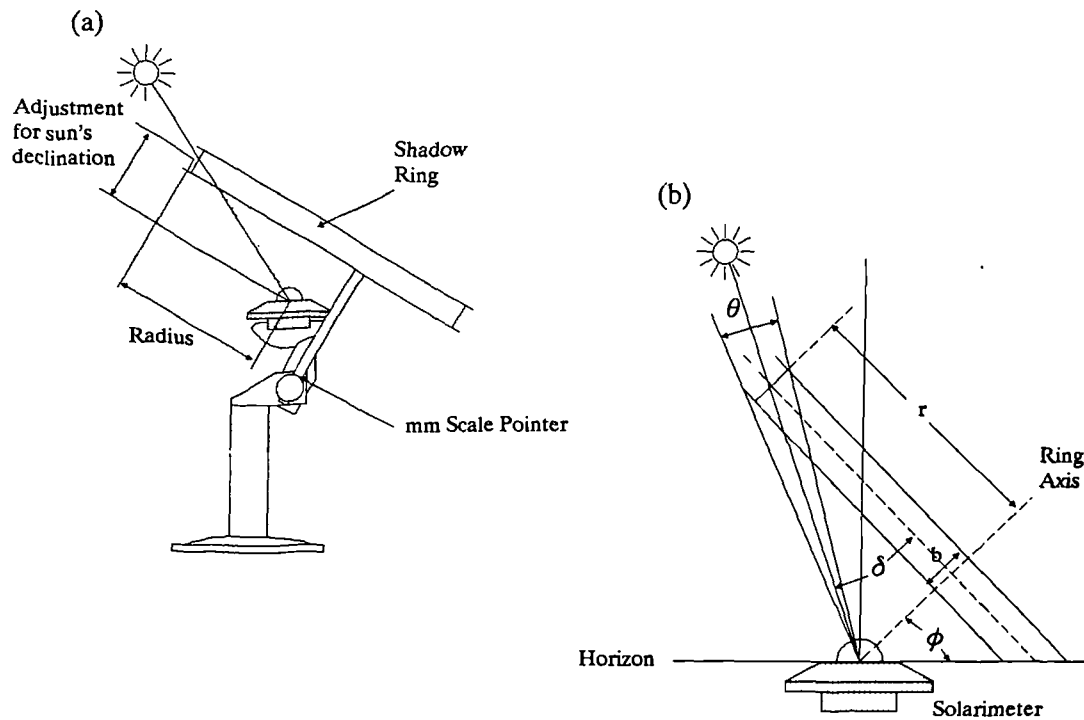


**Table 6.8** Classification of Pyrheliometers. (World Meteorological Organisation 1971)

	Standard	First Class	Second Class
Sensitivity ( $\text{W m}^{-2}$ )	$\pm 2.0$	$\pm 4.0$	$\pm 5.0$
Stability (% change per year)	$\pm 0.2$	$\pm 1.0$	$\pm 2.0$
Temperature (maximum error due to changes of ambient temperature, in %)	$\pm 0.2$	$\pm 1.0$	$\pm 2.0$
Selectivity (maximum error due to departure from assumed spectral response, in %)	$\pm 1.0$	$\pm 1.0$	$\pm 2.0$
Linearity (maximum error due to nonlinearity not accounted for, in %)	$\pm 0.5$	$\pm 1.0$	$\pm 2.0$
Time constant (maximum, in seconds)	25.0	25.0	60.0

Correction of pyranometer data for the sky radiation which is intercepted by the shadow ring ( $G_{sr}$ ) can be approached theoretically

$$G_f = F \cdot G_f' \quad \{6.10\}$$

where

- $G_f'$  = corrected diffuse insolation ( $W m^{-2}$ );
- $G_f$  = diffuse insolation data from the pyranometer ( $W m^{-2}$ ); and
- $F$  = a correction factor calculated as given by

$$F = 1 / (1 - G_{sr}) \quad \{6.11\}$$

The intercepted part of sky radiation by the shadow ring ( $G_{sr}$ ) can be calculated by (Kipp & Zonen 1987)

$$G_{sr} = 2\theta \cos^3(\delta) [(\pi \omega / 180) \sin(\phi) \sin(\delta) + \sin(\omega) \cos(\phi) \cos(\delta)] / \pi \quad \{6.12\}$$

where

- $\delta$  = sun declination angle ( $^\circ$ );
- $\phi$  = latitude of the observation site;
- $\omega$  = sunrise hour angle ( $^\circ$ ) which is computed from

$$\omega = -\tan(\phi) \tan(\delta) \quad \{6.13\}$$

and  $\theta$  the view angle of the ring (radians) or

$$\theta = b / r \quad \{6.14\}$$

where  $b$  is the shadow ring width and  $r$  is the radius (see also Figure 6.15b). Substituting Eq.6.14 in Eq.6.13 would provide the same relation proposed by Drummond (1956) for Eppley Shadow Band.

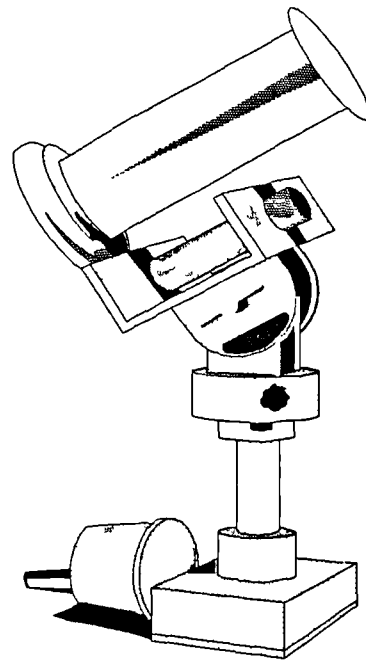
### 6.5.3 Pyrheliometers

The World Meteorological Organization (1971) has defined three classes of pyrheliometers on the bases of their accuracy and overall system performance. The bases of classification are given in Table (6.8).

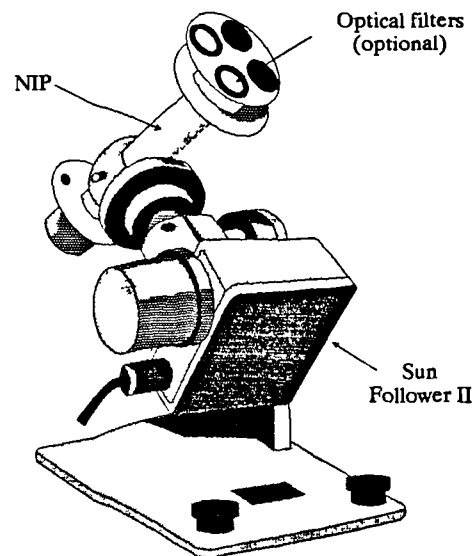
A pyrheliometer is an instrument for measuring the intensity of direct insolation at normal incidence (i.e. pointing directly at and measuring the radiant beam plus a small portion of the diffuse component through a circular cone angle of about  $5.5^\circ$ ). Only the reference standard pyrheliometer gives an absolute reading (Twidell & Weir 1986). In this instrument, the solar beam falls on an absorbing surface, whose temperature rise is measured and compared with the temperature rise in an identical (shaded) absorber heated electrically.

**Figure 6.16**

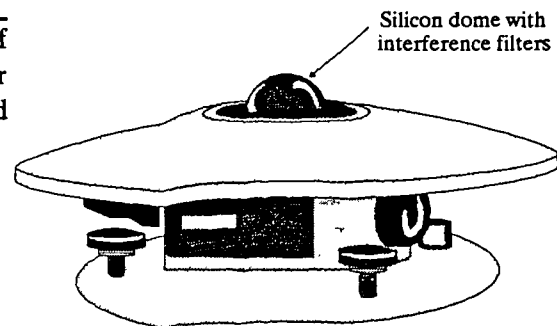
Standard Cavity Radiometer, for calibrating pyrheliometers and pyranometers at the Solar Village, Riyadh, Saudi Arabia. (reproduced from KACST 1985).

**Figure 6.17**

Eppley Pyrheliometer (NIP) mounted on a Sun Follower II, for the measurement of direct normal insolation ( $0.3\text{--}2.8\ \mu\text{m}$ ) at the Solar Village, Riyadh, Saudi Arabia. (reproduced from KACST 1985).

**Figure 6.18**

Eppley Pyrgeometer for the measurement of infrared radiation ( $4\text{--}50\ \mu\text{m}$ ), at the Solar Village, Riyadh, Saudi Arabia. (reproduced from Eppley Laboratories).



An example of standard pyrheliometers is the Eppley "standard cavity radiometer" (see Figure 6.16), used in the Solar Village at Riyadh, Saudi Arabia (see chapter 3) for calibrating pyrheliometers and pyranometers.

Direct normal insolation data in Appendix (B), are measured with a first class instrument Pyrheliometer (Fig.6.17). It operates on the thermopile effect and so is similar to pyranometers in this respect. Problems with these instruments include the fraction of sky radiation measured due to the aperture angle and the precise tracking of the sun. The use of correction factors is not only involved but somewhat unreliable, according to Coulson (1975).

### 6.5.4 Infrared Radiometers

Infrared radiometers are of two general types: instruments that are "solar blind" (i.e. capable of measuring spectral intensity  $\lambda > 4 \mu\text{m}$ ), and instruments that measure the total radiation received throughout broad wavelength regions. Coulson (1975) gives a comprehensive treatment of contemporary and historical infrared instruments. Infrared radiation ( $\lambda = 4$  to  $50 \mu\text{m}$ ) data tabulated in Appendix (B), are measured with an Eppley pyrgeometer (Fig.6.18). This instrument is in the solar blind category, and is rather like a pyranometer, but the thermopile sensor is covered by a silicon dome with interference filter in place of the glass domes in a pyranometer.

Pyrradiometers and net pyrradiometers are from the second category of infrared radiometers. A pyrradiometer measures the total radiation (solar and infrared) on a horizontal surface in one direction. A net pyrradiometer (also referred to as net radiometer) measures the difference of total radiation between the upward and downward directions. The net radiometer can be used as a pyrradiometer by shielding the lower sensor monitoring its temperature as shown in (Fig.6.19).

A Didcot net radiometer is described in data sheet DS11 (see Appendix F). This instrument is restricted for use in the horizontal position. Errors due to convection currents over the instrument sensors were experienced when used in vertical position, (see section 5.4.2 of the previous chapter).

### 6.5.5 Ultraviolet Radiometers

There are, in general, three main classes of detectors for measuring ultraviolet radiation, namely, physical, chemical, and biological. Many instruments for measuring solar ultraviolet radiation are based on physical principles. Definitions and examples of each class instruments are discussed in Coulson (1975). Appendix (B) includes data of near ultraviolet solar radiation ( $\lambda = 0.29$  to  $0.39 \mu\text{m}$ ) over Riyadh (Saudi Arabia). A brief description of the instrument used follows.

**Figure 6.19** A modified Net Radiometer for use as a Pyrradiometer to measure the total horizontal insolation, (reproduced from Anson 1980). The spectral range of the measured radiation flux depends on the spherical dome material of the instrument. The common material in use is polyethylene which transmits radiation in the spectral range of  $0.3 \mu\text{m}$  to  $80 \mu\text{m}$ .

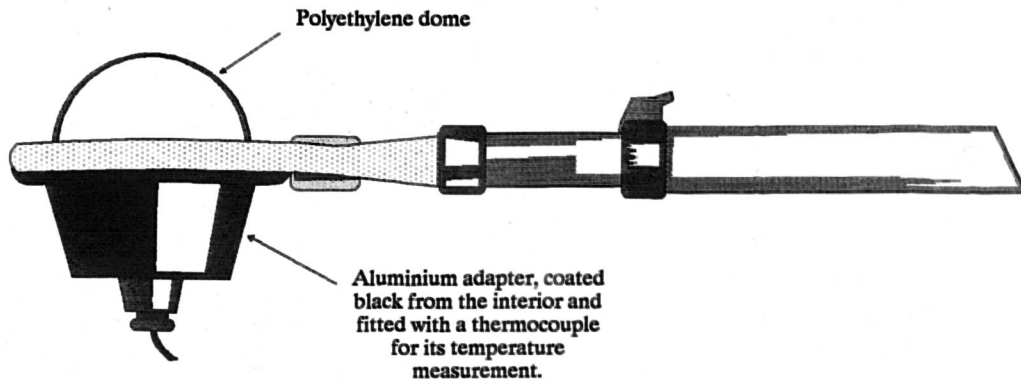


**Figure 6.20**

Schematic diagram of Eppley UV radiometer (used at the Solar Village for measuring ultraviolet insolation,  $\lambda = 0.29\text{--}0.39 \mu\text{m}$ ). (reproduced from Drummond & Wade 1969).

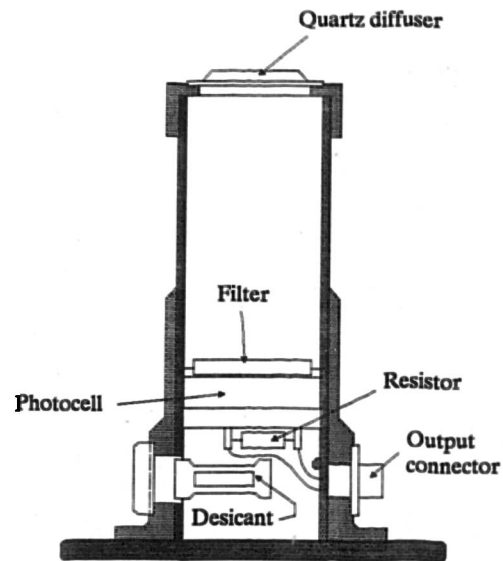
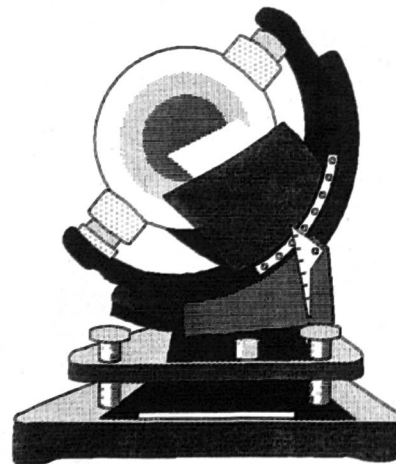


**Figure 6.21**

Campbell-Stokes Sunshine Recorder. (reproduced from Casella).



### *Eppley Ultraviolet Radiometer*

This instrument is designed for continuous measurements of the global flux in the near ultraviolet region ( $\lambda = 0.29$  to  $0.39 \mu\text{m}$ ). The sensor is a Wiston selenium barrier-layer photoelectric cell with a sealed-in quartz window mounted inside a blackened tube beneath an interference filter and translucent quartz diffusing disk. The configuration of the device as given by Drummond & Wade (1969), can be seen from Figure (6.20).

## 6.5.6 Sunshine Recorders

Two main types of sunshine duration instruments in use (Anson 1980) are

- The focusing type, includes the classic and most widespread Campbell–Stokes recorder.
- The photovoltaic type, includes the Foster sunshine recorder (not commercially available).

These instruments are sensitive only to direct beam solar radiation when it is above some imprecise threshold, usually when a visible shadow is produced. The actual value of this threshold varies amongst instruments of the same general type, as well as varying between the two functional types of instruments (focusing and photovoltaic types). The new standard for sunshine duration (defined by the Commission for Instruments and Methods of Observation of the WMO in 1981) is the time during which a threshold of  $120 \text{ W}(\text{m}^{-2})$  is exceeded, using a standard pyrheliometer pointed at the solar disk, (Iqbal 1983).

### *Campbell–Stokes Sunshine Recorder*

In the Campbell–Stokes recorder, direct solar rays passing through the glass sphere (Fig.6.21) are focused on a calibrated chart. As the sun moves through the sky a brown line is burned into the paper when the insolation is above the threshold level. When the insolation is below the threshold level, the burned line is interrupted by an unburned length. Number of bright sunshine hours is then determined by measuring the length of burned segments for the day.

This instrument is subject to errors that result from personnel reading the charts. A major problem with this instrument is the effect of humidity on the card and its ability to establish a fixed threshold level of insolation. Threshold may vary from  $280 \text{ W}(\text{m}^{-2})$  in very humid conditions down to  $70 \text{ W}(\text{m}^{-2})$  in very dry climates.

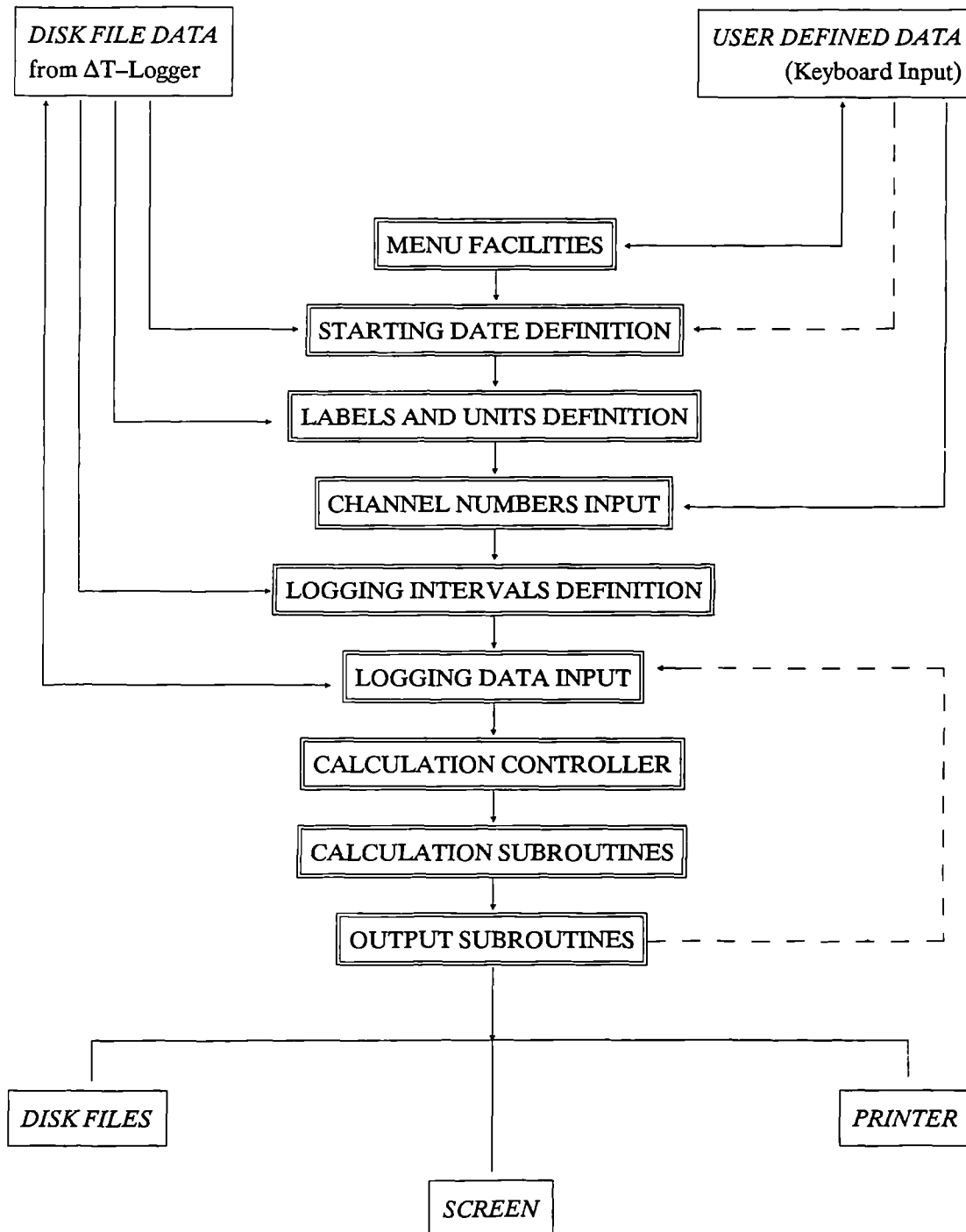


**Figure 6.22**

A flow-chart of the main routines in the data processing program (DTCLM.Bas) for use with ΔT-Logger output. (see Appendix E for program listing).

## 6.6 Data Logging

---

Technological advances have made transducer output measurement possible with self-balancing recorders and computer-compatible data logging systems. Transmission of information from transducer (instrument) to recording system (logger) is often accomplished simply and may only require connection of a pair of wires. In some cases, the effect of distance of an instrument relative to a logger requires special consideration. For example, long cable connection may cause spurious signals and noise; in some cases the resistance of leads must be considered, and if significant, must be accounted for by computation or by balancing (e.g. resistance thermometers).

Recording equipments may use electrical or mechanical means and each could be converted to the other. Readout equipment, chart recorder and tape recorder are types of logging systems which present or store data in either analog or digital forms. Digital tape (or floppy disk) recording systems (loggers) are usually designed to meet the user's needs. A wide selection of channels and number of inputs is available. Loggers can be adapted to permit sampling, by scanning at fixed time intervals, determined by a clock in the system or in response to a special command, e.g. when the phenomenon being measured reaches a certain level.

For the experimentation of this research, two data logging systems were used, a Delta-T ( $\Delta T$ ) Logger and a Hewlett Packard Data Acquisition System (HP-DAS). Descriptions of these are provided in Appendix F (see data sheets DS 12 & DS 13 respectively).  $\Delta T$ -Logger can convert readings to engineering units and perform simple data processing, but the averaging of samples will not account for out-of-range or error data, discontinuity of  $0/360^\circ$  in wind direction averaging, and the complexity of relative humidity calculation. Therefore, I have developed a simple program to process  $\Delta T$ -Logger output properly, and to prepare climate files for use in "ESP" program.

### 6.6.1 Processing DT-Logger Data Output : (DTCLM Program)

The "DTCLM.Bas" program analyses and processes data that are input from a specified sequential disk file. In particular, it computes defined values of meteorological or/and thermal conditions from raw data obtained by a  $\Delta T$ -Logger. This program was developed by the author in the process of learning Basic language modeling. It serves my experimental and analytical work, but may help other  $\Delta T$ -Logger users. A listing of the program is provided in Appendix (E). Figure (6.22) shows a flow-chart of the program main routines. The contents of each routine are briefly described bellow.

#### *Menu Facilities*

Main Menu, (program lines 3730 to 3850) prompt and control the following sub-menus :-

Help : summary of the program function and operation. (program lines 3860 to 4120).

System I/O : for hardware operating system. Double disk or hard disk PC, mainly to define the output port if requested. (program lines 4130 to 4280).

Save & Display Options : a default screen display format or/and save results on disk file(s). (program lines 4290 to 4370).

Save Format Options : save results on [.DAF] file (tabulated format), or/and save meteorological data on [.ESP] file for later use in ESP software. (program lines 4380 to 4580).

Run : provide a check list, Get variables, and start program execution. (program lines 4590 to 4750).

### *Starting Date Definition*

The starting and finishing logging dates (day-month-hour), are read from the data file by this routine. It optionally allows the user to alter these values for a shorter period of analysis. (program lines 330-400 & 1240-1400).

### *Labels & Units Definition*

This section inputs from the data file all strings which represent labels and units of logging channels, and assigns integer numbers in sequence to indicate channel numbers (program lines 420-460 & 1420-1540). Information is stored in an array for later redisplay.

### *Channel Numbers Input for Correlation with Computing Procedures*

This routine inputs user-defined integers that correspond with channel numbers required for each calculation subroutine. (program lines 1560 to 1980). A redisplay of channel numbers and their labels helps the user to obtain those integer values. These are stored in a two dimensional array for use in the calculation controller routine.

### *Data Logging Intervals*

This routine reads from the data file values of logging dates, then computes the logging intervals per hour. (program lines 2000 to 2070).

### *Logging Data Input (hour by hour)*

Sequentially this routine reads from the data file (one hour \* intervals) logged data for all channels, and stores values in an array, (program lines 680 to 850). This routine starts input from defined starting date, and discards invalid or out-of-range values.

### *Calculation Controller Routine*

The main program has variable calculation procedures. The channel numbers input by the user may only correspond to few calculation procedures, therefore, this routine (program lines 870 to 900) is set to control the path of the program to the required calculation procedures.

### *Calculation Subroutines*

There are 21 calculation subroutines to obtain certain functions (program lines 2090 to 3290). They can be summarised as :

- One procedure for wind direction based on algorithm 2 discussed in section (6.4.2);
- two, for wind speed from pulse counting, ( $\text{Speed} = \# \text{pulses}/10$ ) and from voltage output ( $\text{Speed} = \text{mV} * \text{CF}$ ), where CF is the calibration factor;
- one, for dry-bulb and relative humidity (see section 6.3.2);
- five, for different insolation results by multiplying (mV) output by the calibration factor of each instrument, supplied by manufacturer.
- four, for indoor average temperature in PASSYS test cells (average of 7 readings in each cell);
- four, for indoor average temperature in service rooms; and
- four, for heating load periods in the test cells by the sum of number of samples where ON switch value ( $> 20$ ) is reached. (this value is a scanning command assigned for an auxiliary channel when heating is switched ON).

### *Output Subroutines*

The program contains three results output routines; (1) a screen display of 19 variables comprising meteorological data and indoor thermal data, (program lines 3300 to 3410), (2) special format to save 6 meteorological data on a disk file for use with the *ESPclm* program, (program lines 3530 to 3610), and (3) ASCII tabulated format for all results on a disk file (program lines 3430 to 3510). Activating one, two or the three routines is a user-defined option.

## 6.7 References

---

Ambrosius E., Fellows R. & Brickman A. (1966) Mechanical Measurements and Instrumentation. Ronald Press, New York.

Anson D. (1980) "Instrumentation for Solar Radiation Measurements", In: Solar Energy Technology Handbook. Part A: Engineering Fundamentals. Dickinson W. & Cheremisinoff P. (Eds). Marcel Dekker Inc., New York.

ASHRAE (1985) ASHRAE Handbook (Fundamentals). American Society of Heating, Refrigerating and Air-Conditioning Engineers Inc., Atlanta, USA.

Barford, N. (1967) Experimental Measurements: Precision, Error, and Truth. Addison-Wesley Pub., London.

Coulson K. (1975) Solar and Terrestrial Radiation. Academic Press, New York.

Dickinson W. & Cheremisinoff P. (1980) Solar Energy Technology Handbook. Part (A), Engineering Fundamentals. Marcel Dekker Inc., New York.

Drummond A. (1956) "On the Measurement of Sky Radiation", *Arch. Meteorol. Geophys. Bioclimatol. Ser.*, B7, pp 3-4.

Drummond A. & Wade H. (1969) "Instrumentation for the Measurement of Solar Ultraviolet Radiation", In: The Biological Effects of Ultraviolet Radiation. Urbach F. (edt), Pergamon, Oxford.

Halliday J. (1988) "Wind Meteorology and the Integration of Electricity Generated by Wind Turbines", PhD thesis, University of Strathclyde, Glasgow, U.K.

Hattem van D. (1987) "Use and Calibration of Platinum Resistance Temperature Detectors for Passive Test Cells", Internal PASSYS report, CEC, Joint Research Centre, Ispra, Italy.

Iqbal M. (1983) An Introduction to Solar Radiation. Academic Press, Canada.

KACST (1985) "Photovoltaic Research Test Facility", King Abdul-Aziz City for Science and Technology., Brochure printed by NCFEI, Ministry of Finance and National Economy, Riyadh, Saudi Arabia.

Le Baron B. (1980) "Correction for Diffuse Irradiance Measured with Shadow Bands", *Solar Energy*, 25 (1), pp 1-13

Lunde P. (1980) Solar Thermal Engineering. (Space Heating and Hot Water Systems). John Wiley & Sons, New York.

Moll W. (1923) "A Thermopile for Measuring Radiation", *Proc. Phys. Soc. London, Ser., B.35*, pp 257-60

Norris D. (1973) "Calibration of Pyranometers", *Solar Energy*, **14** (2), pp 99-108

Norris D. (1974) "Calibration of Pyranometers in Inclined and Inverted Positions", *Solar Energy*, **16** (1), pp 53-5

Powell R. (1973) "Thermocouple Reference Tables Based on the IPTS-68 NBS Monograph 125", National Bureau of Standards.

Reid M., Berdahl C. & Kendahl J. (1978) "Calibration Standards and Field Instruments for Precision Measurement of Insolation", *Solar Energy*, **20** (4), pp 357-58

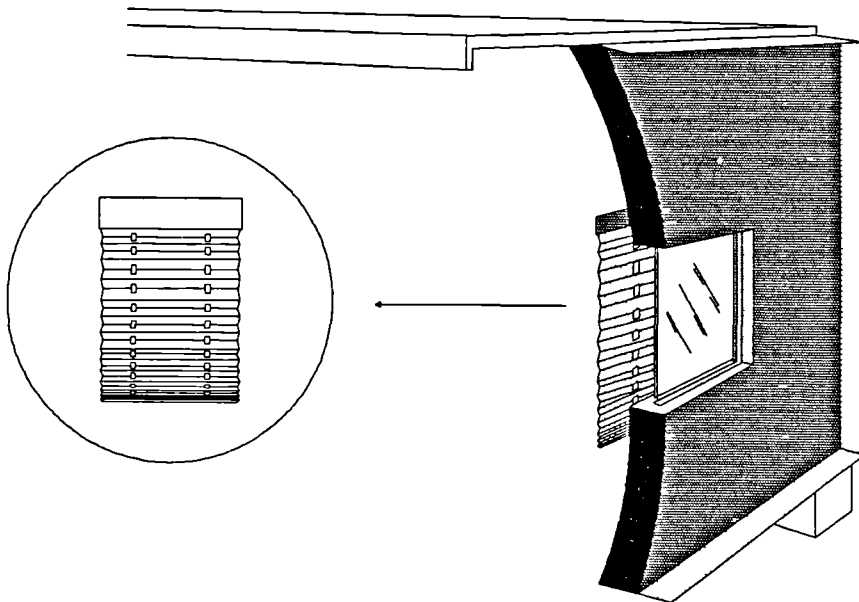
Schenck H. (1968) Theories of Engineering Experimentation. McGraw-Hill, New York.

Tuve G. and Domholdt L. (1966) Engineering Experimentation. McGraw-Hill, New York.

Twidell J. and Weir T. (1986) Renewable Energy Resources. E. & F.N Spon, London.

World Meteorological Organisation (1971) "Measurement of Radiation and Sunshine", In: Guide to Meteorological Instruments and Observing Practices. 4th ed, WMO, No. 8, T.P. 3, Geneva, Switzerland.

# Chapter 7



## 7. TEST SITE EXPERIMENTS WITH A WINDOW BLIND

### 7.1 Introduction

---

For the widespread use of passive solar techniques in buildings (e.g. glazing type and size, shading devices, sunspaces, trombe walls, use of insulation in walls, etc.), designers must be able to assess the contribution that different passive solar components (PSC's) will make to energy savings and comfort levels. These should be determined experimentally but the time and cost involved give opportunities to simulation models and simple design tools. Such design tools have been discussed previously. For example, chapter 2 of this thesis examined the basic design tools for the assessment of energy performance of building components as a whole. Chapters 4 and 5 on the other hand have dealt specifically with building fenestration and a simple model was developed, "CURTAIN.Bas" program. However, such design tools are theoretical and some form of empirical validation is required.

The main objective of the work of this chapter was to study experimentally the thermal performance of a pleated metalised fabric blind with a low emissivity double glazing window. The main characteristics of this component are the heat transmission coefficient ( $\dot{U}$ ) and the solar heat gain factor or solar aperture ( $\dot{A}$ ). The use of an outdoor highly insulated test cell (room) has potential for providing these thermal performance measures in real climates. Although more accurate methods exist for the laboratory assessment of  $\dot{U}$ -value (e.g. hot-boxes), no wholly satisfactory equivalents are currently available for solar aperture. In addition, the use of an outdoor facility enables the influence of climatic effects, other than temperature and solar radiation, to be assessed.

The availability of "Passys" test site facilities at Strathclyde University campus made it possible to conduct the experiments discussed in this and the following chapter. These facilities; i.e. test cells, instrumentation, data acquisition and the south wall PSC's; are described in the next section.

Due to a tight time schedule, of the Passys project, experiments conducted by the author are limited and of a shorter period than planned. Two test cells have been used for side-by-side experiment to study the thermal performance of the blind. The UK test methodology which is based on a steady-state energy balance technique was adopted for this study. The Passys common test evaluation program "MRQT" was also used, and results compared.

Results from this experiment are analysed over the whole period of experiment and for typical clear and overcast days. Comparison between measured and predicted results by "ESP" and "CURTAIN" models are also presented.

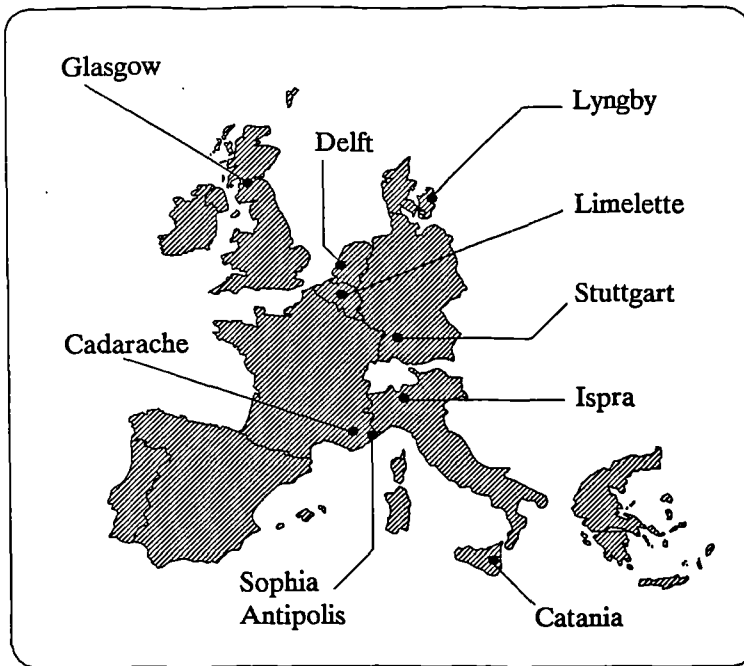


**Figure 7.1** Location of the PASSYS test sites by the end of phase one of the project (1990). Three new test sites at Portugal, Spain and Greece have been developed for the second phase of Passys project.

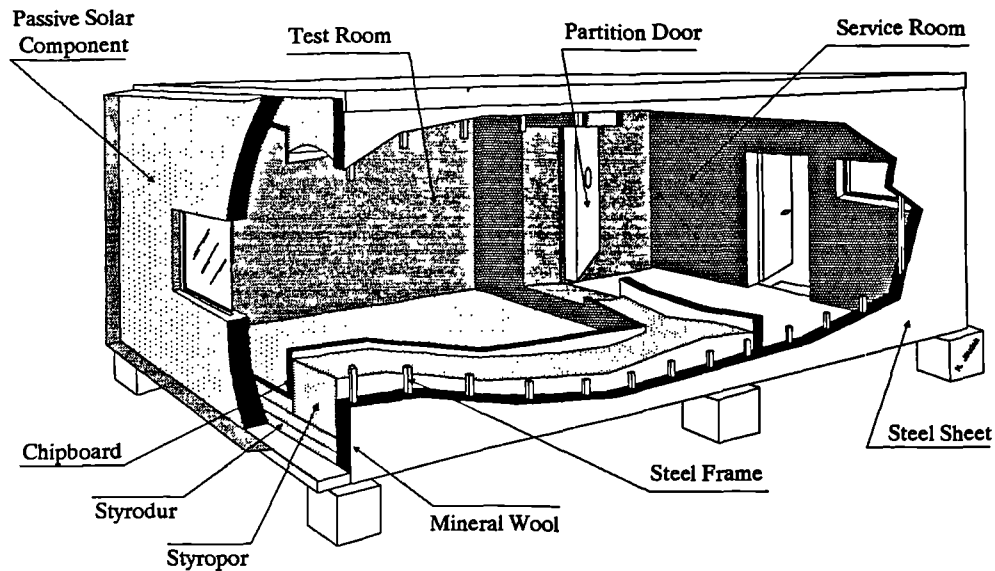


**Figure 7.2** Sketch of the PASSYS test cell.

## 7.2 The PASSYS Test Site Facilities

---

The Passys project is an European concerted action in the field of passive solar building construction which has been initiated by the the Commission of the European Communities (CEC) as part of its Solar Energy R&D programme, with the following objectives:

- To develop reliable and affordable test procedures for PSC's in a building system.
- To increase confidence in simulation models through validation and further refinement.
- To increase confidence in simplified design tools (SDT) through the activity of development and validation.

The project operates with highly standardised test cells. The ESP simulation model has been chosen for validation and development. Test cells and south wall components are located on test sites throughout the European Community so that their performances could be analysed in a range of climatic conditions. At the end of the first phase of the Passys programme, test cells were installed at nine sites in seven countries (Fig.7.1). Research activities of the Passys project were organised into five sub-groups addressing *test methodology, simulation model validation, simplified design tools development, instrumentation and passive solar components definition.*

The Energy Studies Unit (ESU) of Strathclyde University lead the UK consortium of the – University of Strathclyde (ESU and the Energy Simulation Research Unit ESRU); Building Research Establishment (BRE); Pilkington Glass Ltd.; and the Energy Technology Support Unit (ETSU) of the Department of Energy.

### 7.2.1 The Passys Test Cell

The key to the CEC Project Passys is the standard test cell. The rationale behind the cell is to provide a highly standardised facility for testing passive solar/south wall components operating in a realistic but readily controllable and configurable manner. The cell (Fig.7.2) is prefabricated with a rugged steel structural frame packed with mineral wool insulation. The outer skin of the cell is coated with chipboard and shielded with stainless steel. The inner cell construction is of expanded polystyrene foam, protected at the interior surfaces by chipboard covered with galvanised steel.

Detailed drawings are shown in Figures (7.3a & 7.3b). Internally the cell has two zones, a service room and a test room, divided by a well insulated partition containing a sealed door. The test room door is made of plastic coated steel sheets filled with 140 mm polyurethane foam insulation. The entrance door and the window in the service room north wall are standard components.

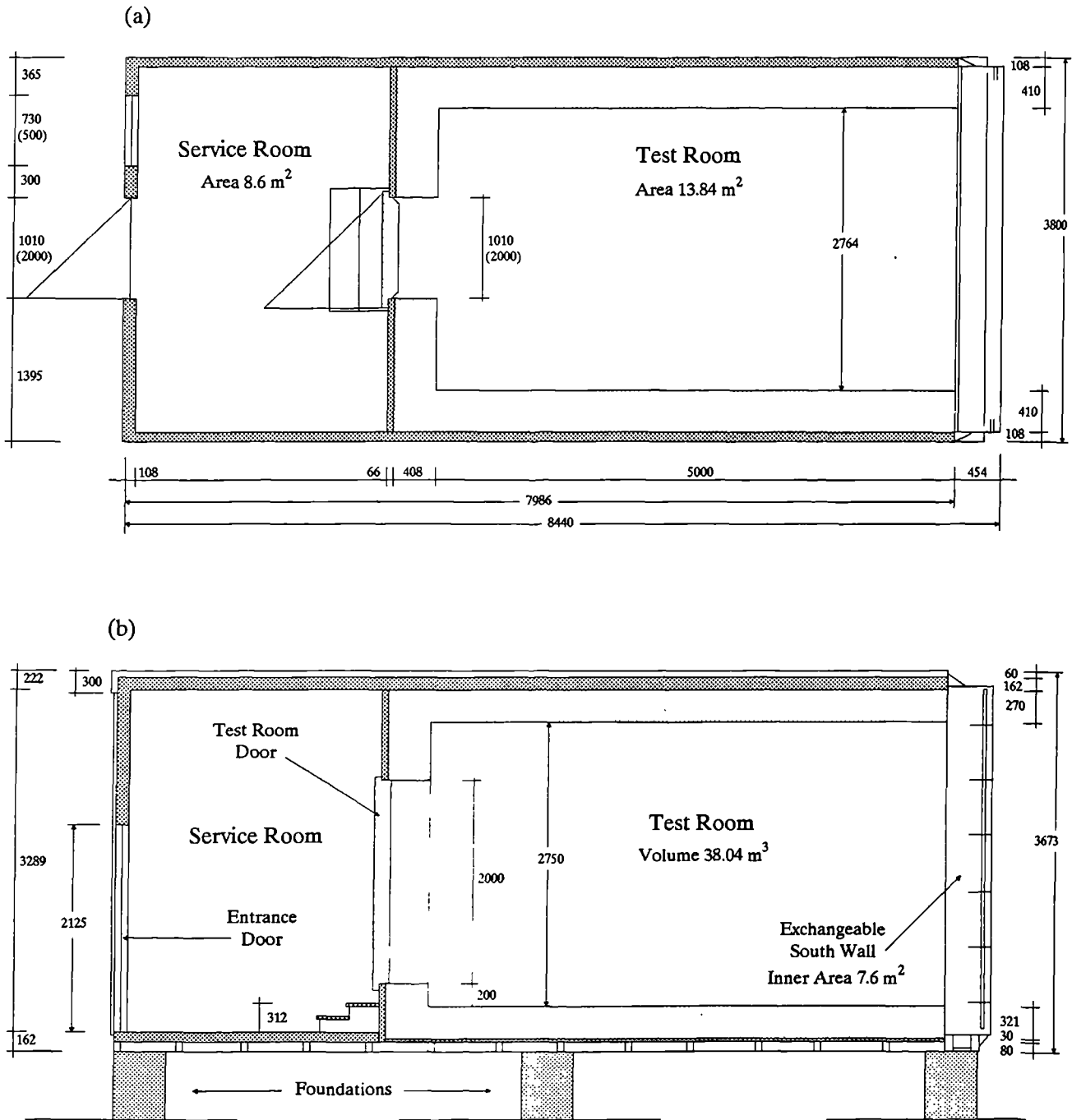


**Figure 7.3**

Detailed drawings of the PASSYS test cell: (a) Plan, (b) Section. All dimensions in mm.

The test cell south wall is of exchangeable components that can be built into a galvanised steel frame which bolts onto the cell. The frame size allows the testing of realistically sized building components with dimensions of height 3.6m, width 3.3m and thickness up to 0.4m. The provision exists to add on, for example, a conservatory as was done on the UK site.

Table 7.1 gives measured values of the absorptance and emittance of the test cell surfaces. The emittance values of the roof surface show scattered results. The highest values are found on dirty, the lowest on clean spots. Table 7.2 gives the thermophysical properties of the test cell materials according to DIN 4108 as well as measured data. The constructional overall heat transfer coefficients of the test cell are:  $U \leq 0.1 \text{ W (m}^{-2} \text{ K}^{-1})$  for the test room and  $\leq 0.4 \text{ W (m}^{-2} \text{ K}^{-1})$  for the service room.

The UK consortium has four test cells, situated at Strathclyde University in central Glasgow, at latitude 55.54 °N, longitude 4.15 °W, and an elevation of 36m (see site plan in Figure 7.4). Figure 7.5 shows a sunchart of the site indicating the shading of the south wall of the test cells by obstacles as a function of the season and day time.

## 7.2.2 South Walls (PSC)

The south wall frame, made of galvanised steel, can be equipped with different south wall components. Within the European context of Passys two common south wall components were provided:

- A well insulated, so called “calibration wall”, previously referred to as the adiabatic wall, with thermal and geometrical characteristics as given in Table 7.3. This wall is used to determine the basic cell parameters of heat transmission coefficient, solar aperture and infiltration. It is also used as a base reference component in comparative experiments.
- A concrete “reference wall”, also called Gibat wall, which incorporates a window with 1.2 m<sup>2</sup> of double glazing with wooden frame. Table 7.4 gives the thermal characteristics of the wall components. Detailed drawings are given in Figure 7.6.

As the first example of another component, two timber-frame walls (TF-wall) with an outer brick cladding have been constructed in the UK (for test cells 3 & 4). The complete structure of the wall is configurable for different sized windows and patio doors. Figure 7.7 shows detailed drawings of the TF-wall. Table 7.5 gives the thermal characteristics of the wall components. Single, double, low-e coated double and advanced triple glazing components were tested with the TF-walls. A single glazed sun space, attached to the TF-wall, was also tested.

**Table 7.1** Measured values of shortwave absorptance and longwave emittance of the test cell surfaces. (after Wouters & Vandaele 1990).

Material	Location	Shortwave Absorptance	Longwave Emittance
Refined steel (outside)	Lab : Brand New	—	0.164
	Test Cell : <i>Side Walls</i>	0.38 – 0.41 avg 0.40	0.23 – 0.25 avg 0.25
	<i>Roof</i> (clean and dirty spots)	0.38 – 0.48 avg 0.45	0.14 – 0.69 † avg 0.25
Galvanised steel blue painted (inside)	Lab : Brand New	0.84	0.87
	Test Cell : <i>Floor</i>		0.89
	<i>Interior Walls</i>		0.87

† The highest values of roof surface emittance are found on dirty, and the lowest on clean spots.

**Table 7.2** Thermophysical properties of the test cell materials. (data from Wouters & Vandaele 1990).

Material	Type	Conductivity $W (m K)^{-1}$	Density $kg m^{-3}$	Specific heat $J (kg K)^{-1}$
Chipboard	Kauramin V100	0.130 0.100 <sup>‡</sup>	800	2093
Mineral wool	Rockwool	0.040 0.038 <sup>‡</sup>	105	1800
Rigid foam	Styropor PS30	0.040 0.035 <sup>‡</sup>	33	850
Steel sheet	stainless	15	7800	502
Steel sheet	galvanised	50	7800	502
Plywood	waterproof	0.130 0.108 <sup>‡</sup>	560	2500
Flooring	PVC	0.850	2000	837
Extruded rigid foam	Styrodur 40	0.029 0.026 <sup>‡</sup>	40	850

‡ Measured data.

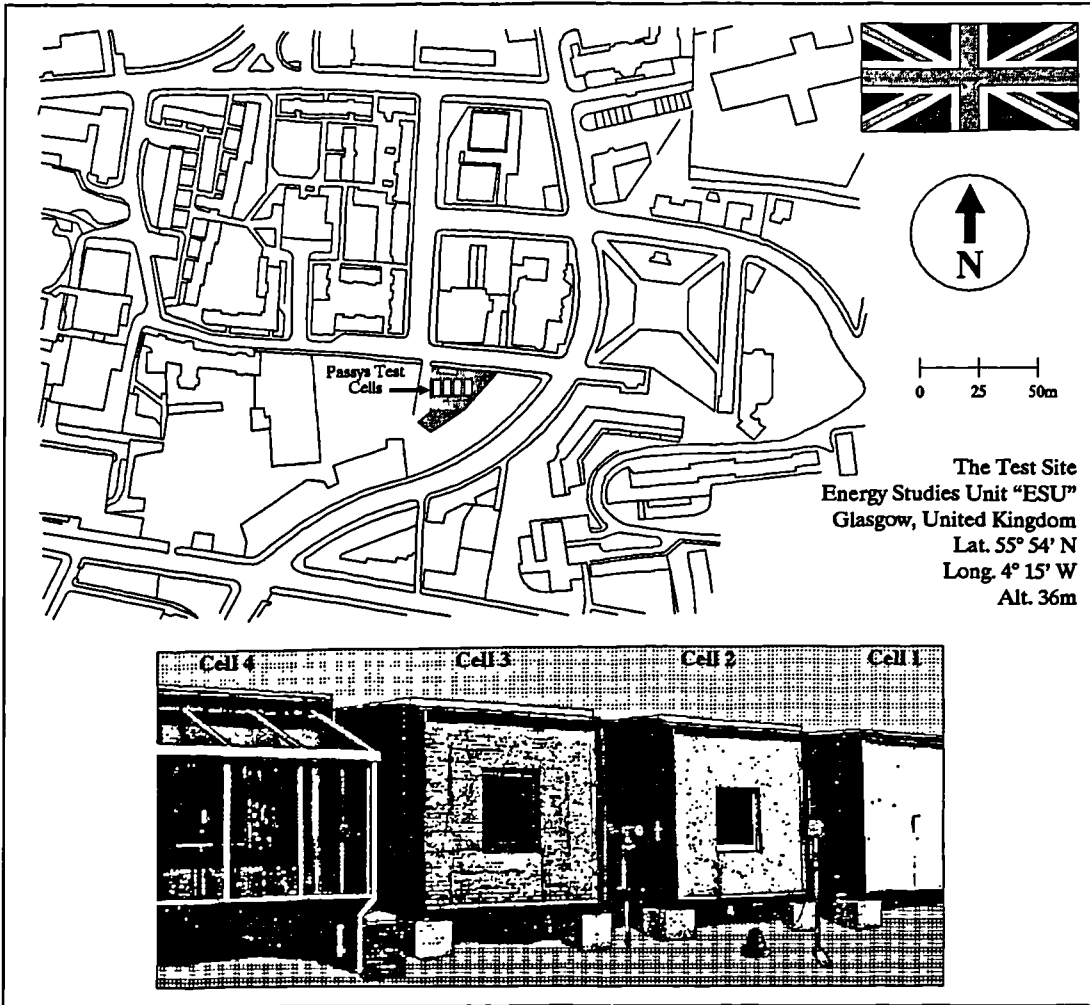


**Figure 7.4** The PASSYS test site, at the corner of Rottenrow street (east/west) and High street (north/south), Glasgow. (a) Site plan; (b) South view of the four test cells (1990).

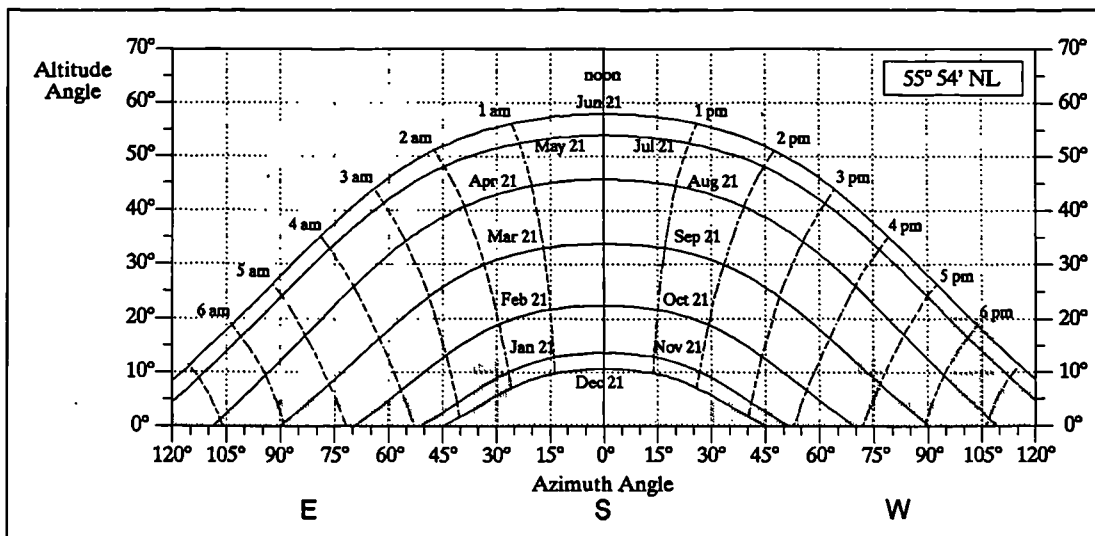


**Figure 7.5** Sunchart of the test site. It indicates the shading of the south wall of the test cells by obstructing surfaces as a function of the season and day time.

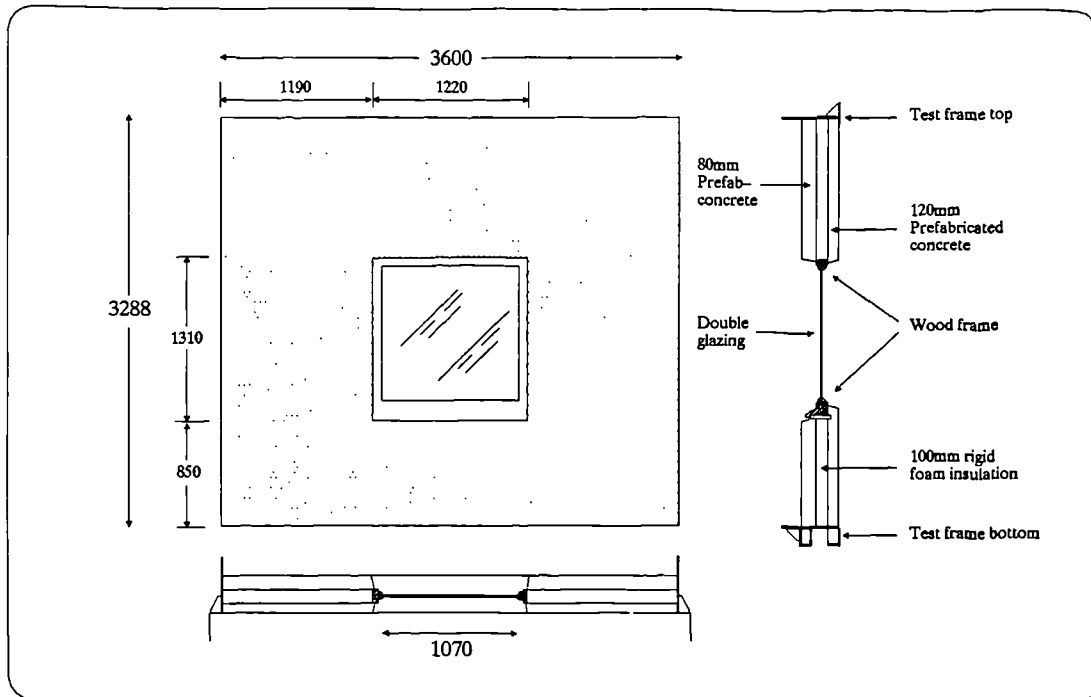


**Figure 7.6** Reference wall construction. (elevation, vertical and horizontal sections). All dimensions in mm.

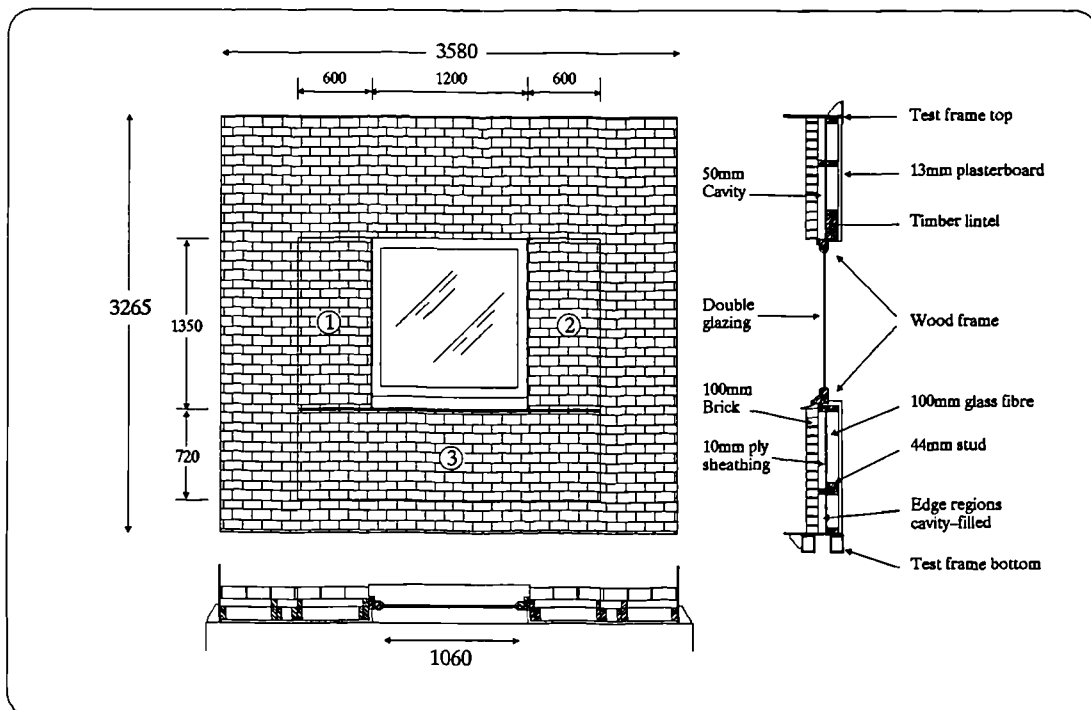


**Figure 7.7** Timber-Frame wall construction. (elevation, vertical and horizontal sections). All dimensions in mm. The wall is configurable for different sized windows and patio door by changing the panels numbered 1, 2 and/or 3.

**Table 7.3** Thermophysical properties of the materials used in the calibration wall. (after Wouters & Vandaele 1990).

Material	Type	Conductivity $W (mK)^{-1}$	Density $kg m^{-3}$	Specific heat $J (kg K)^{-1}$	Thickness mm
Chipboard	Kauramin V100/E	0.13	800	2093	8
Rigid foam	Styropor PS30SE	0.04	33	850	400
Plywood		0.11	620	2500	8

**Table 7.4** Thermophysical characteristics of the reference wall materials. (after Wouters & Vandaele 1990).

Material	Type	Conductivity $W (mK)^{-1}$	Density $kg m^{-3}$	Specific heat $J (kg K)^{-1}$	Thickness mm
Concrete		1.75	2400	880	120
Rigid foam	Styrofoam	0.03	30	1200	100
Concrete		1.75	2400	880	80
Window frame	exotic wood <sup>†</sup>	0.16	800	2093	50
Glazing	clear + clear <sup>‡</sup>	1.05	3500	837	4/12/4

<sup>†</sup> Data for the wooden frame (not included in the reference) are obtained from ESP primitive construction database

<sup>‡</sup> Double 4mm glass window with 12mm air gap. Properties are needed only if defined in ESP construction file as TMC.

**Table 7.5** Thermophysical characteristics of the TF-wall components. <sup>†</sup> (data from Guy 1991 and ESP primitive construction database).

Material	Type	Conductivity $W (mK)^{-1}$	Density $kg m^{-3}$	Specific heat $J (kg K)^{-1}$	Thickness mm
Plasterboard	over polythene vapour barrier	0.16 (0.22)	950	840	12
Wood studs	(timbre frame)	0.16 (0.11)	560	2500	100
Fibre glass	Frametherm	0.04	13 (13.6)	840	100
Plywood		0.15	560	2500	10
Cavity					50
Brick	Ibstock cored rustic	0.84 (0.65)	1700 (1810)	800	100
Window frame		0.16	800	2093	50
Glazing	clear + low-e <sup>‡</sup>	1.05	3500	837	6/12/6

<sup>†</sup> Data in brackets () are measured values, performed by Pilkington Glass Ltd.

<sup>‡</sup> The inner pane of the double glazing unit is coated with low emissivity layer. Other glass combinations are available at the test site. (see section 7.2.2)

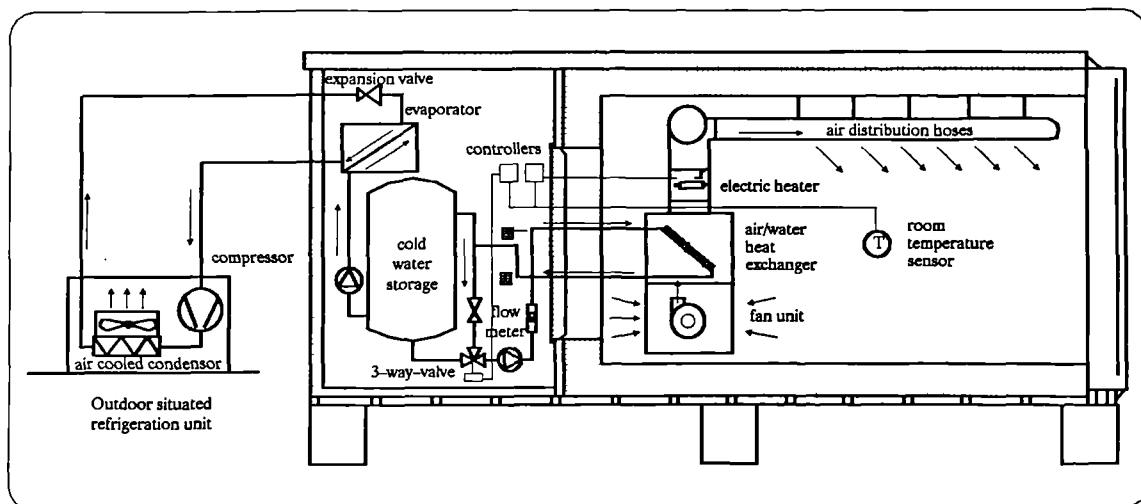


Figure 7.8 Schematic view of the test cell with the heating and cooling system (HCS).

### 7.2.3 Instrumentation and Data Acquisition

Each site in Europe has a common base set of sensors with each test cell and at each site for climate monitoring. The previous chapter gave full details on some of the instruments used in the Passys project. The following parameters are measured at the UK site (see the data sheets in Appendix F for instruments details) :

- inside air temperature at 7 positions in the test cell and one sensor in the service room,
- surface temperatures. One sensor per internal surface painted blue. Also one sensor per external surface, shielded with stainless steel on stainless steel skin or painted to match surface,
- external air temperature (1) aspirated/shielded sensor south of the test cells, (2) shielded sensor north of the test cells, and (3) shielded sensors underneath each cell,
- ground temperature near surface in shaded and exposed positions,
- heat flux through south wall,
- electrical power to test room (heaters, fans, etc),
- global horizontal, global vertical and diffuse horizontal insolation,
- wind speed and direction at 10m reference height, and wind speed and direction at 1m above cell 2, and wind speed under cell 2,
- relative humidity, calculated from measured dry and wet-bulb temperatures as given in section 6.3.2 of the previous chapter (see also the "DTCLM.Bas" program code listing for a Basic interpretation of the calculation procedure).
- pressurisation and infiltration measurements are carried out periodically.

The data acquisition system (DAS) essentially comprises a Hewlett-Packard A600 computer, HP3852 mainframe acquisition unit with a 5.5 digit voltmeter and two HP3853 extenders, and a 40MB hard disc and 60MB tape facility (see Data sheet DS13 in Appendix F for more details). The DAS system is operated by a software, which allows the possibility of measuring 300 channels (voltages or resistances) with an acquisition interval of 1 minute for all channels. Raw data are stored in compressed binary format each day on the hard disk, and automatically backed up on tape. The software enables the operator of the DAS to select specific channels from the stored data, and convert from binary to ASCII format, for transfer to a PC environment. The UK site also uses a Delta-T logger for additional measurements, e.g. pulse-counting for integrated power measurements using kWh meters. (see data sheet DS12 in Appendix F for more details).

Two cells were equipped with a heating/cooling system (HCS). The system (see Fig.7.8) is designed to control the test room temperature and to fulfill the demands of different climates and south wall components. It is a water based unit providing a high internal air flow rate via a fan-cooled heat exchanger. A sophisticated air distribution system is incorporated in order not to disturb the natural air speed distribution within the cell. Potentially, provided adequate control of the HCS from the data acquisition system can be maintained, heating and cooling cycles which simulate the loading of real building may be imposed on the Passys test cells.

**Table 7.6** Solar characteristics of Versol aluminium-coated blinds<sup>†</sup>. (after Knorr 1986).

Type of fabric	Code	$\rho$	$\tau$	$\alpha$	$\epsilon_{\text{alu}}$	$\epsilon_{\text{fab}}$
Transparent	33	0.32	0.45	0.23	0.29	0.55
Semi-transparent ‡	316	0.53	0.16	0.31	0.30	0.76
Semi-opaque	312	0.56	0.07	0.37	0.36	0.83
Opaque	975	0.63	0.04	0.33	0.30	0.85

† Data measured by TNO Institute of Applied Physics in the Netherland. The subscripts (alu) and (fab) indicate the hemispherical emissivities of metalised and fabric sides of the blind respectively.

‡ The semi-transparent type is supplied by Passys and used for the experimental work in this chapter.

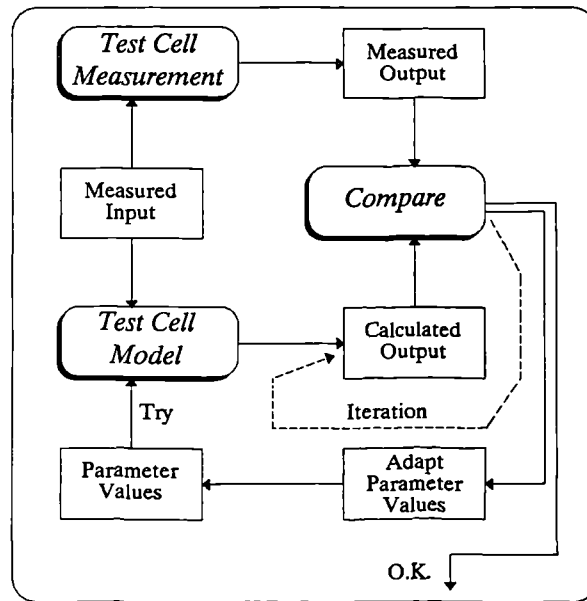


**Figure 7.9** Conceptual diagram of the *Parameter Identification* methodology.

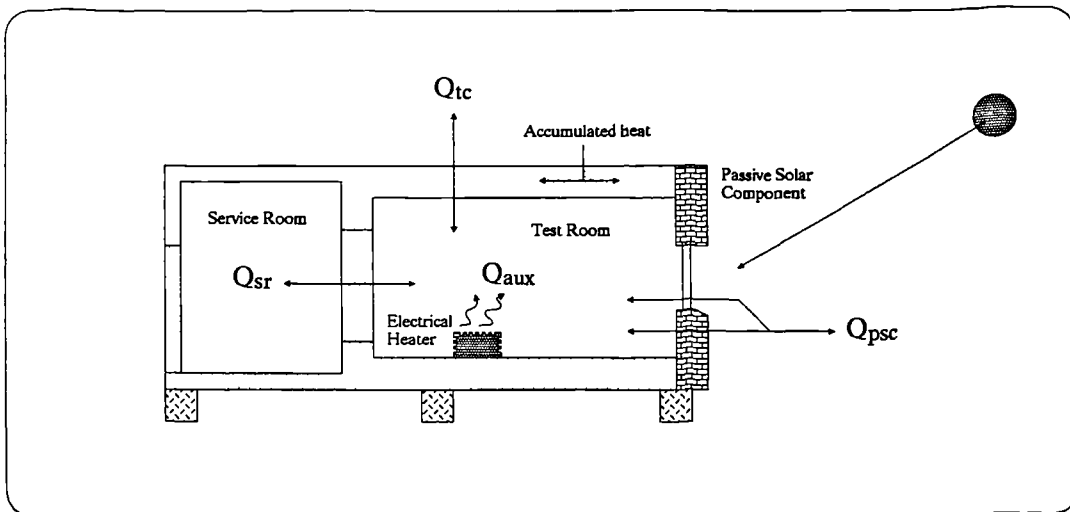


**Figure 7.10** Steady-state energy balance of the test cell.

## 7.3 Test Methodology and Experimental Setup

Two test cells (No.3 & 4 on the UK site) have been used for a side-by-side experiment to study the energy performance of the standard Passys window blind. Various “energy effective” blinds are commercially available from Versol company, Enschede, the Netherlands. Table (7.6) lists the solar properties of these models from which the semi-transparent model is used in this experiment. At the time of conducting this experiment, all the Passys test methodologies were under development. Thus, in line with the UK methodology, a steady-state approach was adopted. (see section 7.3.2).

A large number of test methodologies were considered by the Passys groups. These ranged from *steady-state integrated absolute methods*, where two cells are subjected to identical external and internal conditions, to *parameter identification techniques*, where the experiment is so arranged as to enable a determination of the parameters of a selected dynamic model of the cell. Comparison of the different test methodologies eventually led to the choice of *parameter identification* as the common approach for the Passys groups. This methodology, facilitated in the form of two linked programs (MRQT and LUMPA), was developed by the Dutch subgroup. The program works on creating a non-linear nodal model, then an iteration technique is applied, as illustrated in Figure 7.9, with initially assumed parameter values the result of the model is compared with the measured result. Depending on the discrepancy the parameter values are adjusted and the calculation is repeated to obtain a better result. This iterative process continues until the deviation is considered acceptably low. A detailed description of the method principles is given by Cools et. al. (1988) and van Dijk (1990). The parameter identification method was also used on the Blind experiment results.

### 7.3.1 Rational for Testing

The adopted test method should provide the basic steady-state performance properties of the measured blind-glazing system, including (i) heat transmission coefficient ( $U$ )  $W\ C^{-1}$  and (ii) solar heat gain factor or solar aperture ( $\hat{A}$ )  $m^2$ . The test methodology applied, should also be able to determine the performance characteristics of the test cell itself.

Using auxiliary energy from an electric heater, to maintain a steady internal air temperature, it is possible to maintain steady-state conditions within the test cell. Figure (7.10) shows the steady-state energy balance of the test cell. By choosing a suitable averaging periods of measured data the thermal capacitance effects become negligible. Thus, the steady-state energy balance of the test cell when averaged can be written as

$$Q_{aux} = Q_{psc} + Q_{sr} + Q_{cell} \quad \{7.1\}$$

where  $Q$  is the average rate of heat flow (W), and the subscripts :- ‘aux’ refers to the auxiliary energy supplied to the cell, ‘psc’ refers to that flowing into/through the passive solar component (PSC), ‘sr’ refers to that flowing to the service room (north) wall from the cell, and ‘cell’ refers to the energy flowing into the other walls of the test cell.

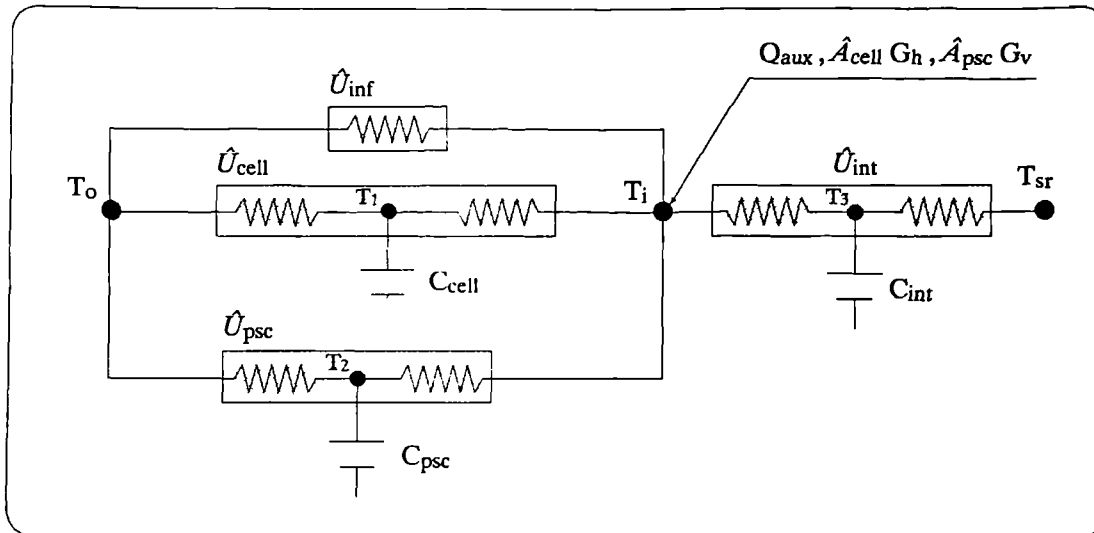


**Figure 7.11** Thermal model of the Passys test cell.

$\dot{U}$  is the heat transmission coefficient,  $\hat{A}$  is the solar aperture, and  $C$  is the effective capacitance with subscripts (cell, psc, int, and inf) representing the test room components (roof, floor and side walls combined), south wall, infiltration, and intermediate north wall respectively. The outdoor air temperature, test room and service room ambient temperatures, Global horizontal and vertical insolation, and auxiliary heat ( $T_o$ ,  $T_i$ ,  $T_{sr}$ ,  $G_h$ ,  $G_v$ , and  $Q_{aux}$  respectively) are measured parameters.  $T_1$ ,  $T_2$  and  $T_3$  are temperature nodes in cell structure, south wall structure and intermediate north wall structure.

A comparison between the energy performances of two identical test cells, one fitted with the blind and the other without, is sufficient to determine the blind steady-state characteristics providing that:

- The two test cells are matched.
- The test cells are sealed to minimise air infiltration to negligible amounts.
- Instrumentation is carefully calibrated to reduce possible systematic errors.
- Measurements are made over a sufficiently long period to reduce possible random errors.
- In terms of data analysis, a suitable integration time is selected to “average-out” transient effects of accumulated energy within the test cell components. (all such effects are therefore assumed to be linear with change in temperature).

The cells had been calibrated and were matched to within a few percent (see section 7.3.3). Discrepancies between the cell’s behaviour would most certainly reduce the accuracy of the blind performance characteristics determined by comparative experiments. However, calibration experiments on test cells fitted with the opaque walls allow for the cell’s performance properties to be determined. Thus in subsequent measurements on real PSC’s (i.e. the blind shaded glazing in the south wall), the derived cell properties can be used to correct for cell behaviour in calculating the PSC performance parameters.

The experiment duration should be long, so that satisfactory confidence limits on the results for the performance characteristics ( $\hat{U}$  and  $\hat{A}$ ) can be derived from the data obtained over the period. The period can only be decided from error analysis on results from several experiments of varying durations. Initial calibration experiments conducted by the UK group indicated that a period of 3–4 weeks produces errors in calculated results which are of similar magnitude as the measurement error contributions. On that bases and also to fit in with the Passys time schedule, a month duration was selected for the blind experiment.

The steady-state approach would be to average the variables of interest over a sufficiently long representative time period. A representative averaging period of 24 hours was chosen in order to maximise the number of available data points from the averaging procedure, whilst reducing net residual effects due to cell thermal capacity influences during that period. The justification of this period is that it includes the instantaneous transmitted solar radiation effects through the PSC, and diurnal cyclic influences of climate.

### 7.3.2 Model for Averaged Test Cell Behaviour

Figure 7.11 shows a nodal diagram of the thermal behaviour of the Passys test cell. Table 7.7 gives the theoretical heat transmission coefficients,  $\hat{U}$  ( $W\ ^\circ C^{-1}$ ), and capacitances,  $C$  ( $J\ ^\circ C^{-1}$ ), of all the test cell components, calculated by the author from known thermophysical properties listed in the same table. (see the notes on Table 7.7 for calculation procedures). The expected heat transmission coefficients and capacitances of cells fitted with (1) opaque calibration wall, (2) reference wall and (3) the TF-wall, are summarised in Table (7.8).

**Table 7.7** Heat loss coefficients  $\dagger$ ,  $\hat{U}$  ( $\text{W } ^\circ\text{C}^{-1}$ ), and capacitances  $\ddagger$ ,  $C$  ( $\text{J } ^\circ\text{C}^{-1}$ ), calculated by the author for the Passys test cell components, opaque calibration wall, reference wall (Gibat), and the Timber-Frame wall.

	k W/(m °C)	$\rho$ kg/m <sup>3</sup>	$C_p$ J/(kg °C)	x m	$C_i$ J/°C	C J/°C	$\hat{U}$ W/°C
Roof (A = 13.84 m <sup>2</sup> )	50	7800	502	0.0015	81288	21465	1.544
	0.15	800	2093	0.026	602516		
	0.04	105	1800	0.08	209261		
	0.15	800	2093	0.013	301258		
	0.04	33	850	0.26	100935		
	0.15	800	2093	0.008	185390		
	50	7800	502	0.002	108384		
Side-wall (A = 13.75 m <sup>2</sup> )	50	7800	502	0.0015	80759	22186	1.110
	0.15	800	2093	0.013	299299		
	0.04	105	1800	0.08	207900		
	0.15	800	2093	0.013	299299		
	0.04	33	850	0.4	154275		
	0.15	800	2093	0.008	184184		
	50	7800	502	0.002	107679		
Floor (A = 13.84 m <sup>2</sup> )	0.15	560	2500	0.03	581280	45862	1.531
	0.035	33	850	0.3	116464		
	0.15	800	2093	0.019	440300		
	50	7800	502	0.002	108384		
North-wall (A = 5.58 m <sup>2</sup> )	0.15	800	2093	0.013	121461	10822	0.487
	0.04	105	1800	0.04	42185		
	0.15	800	2093	0.013	121461		
	0.04	33	850	0.4	62608		
	0.15	800	2093	0.008	74745		
	50	7800	502	0.002	43698		
Door (A = 2.02 m <sup>2</sup> )	0.04	33	850	0.2	11332	11332	2.424 <sup>¶</sup>
Opaque Calibration wall (A = 7.6 m <sup>2</sup> )	0.15	800	2093	0.008	101804	31875	0.739
	0.04	33	850	0.4	85272		
	0.15	800	2093	0.008	101804		
TF-wall (A = 4.04 m <sup>2</sup> )	0.65	1810	800	0.1	584731	3816	1.212
	0.15	560	2500	0.01	56535		
	0.04	13.6	840	0.1	4613		
	0.16	950	840	0.012	38670		
TF-studs (A = 1.94 m <sup>2</sup> )	0.65	1810	800	0.1	280564	9859	1.313
	0.15	560	2500	0.01	27126		
	0.11	600	1210	0.1	140670		
	0.16	950	840	0.012	18554		
Window glazing (A = 1.14 m <sup>2</sup> )	1.05	3500	837	0.006	19936	16	2.16 <sup>Ⓜ</sup>
	1.2	1000	1000	0.012	16		
	1.05	3500	837	0.006	19936		
Frame (A = 0.49 m <sup>2</sup> )	0.16	800	2093	0.05	41023	41023	0.955
Gibat-wall (A = 6.04 m <sup>2</sup> )	1.75	2400	880	0.08	1 · 10 <sup>6</sup>	20998	2.162
	0.04	30	1200	0.1	21744		
	1.75	2400	880	0.12	2 · 10 <sup>6</sup>		
Window glazing (A = 1.13 m <sup>2</sup> )	1.05	3500	837	0.004	13241	16	3.39 <sup>Ⓜ</sup>
	1.2	1000	1000	0.012	16		
	1.05	3500	837	0.004	13241		
Frame (A = 0.43 m <sup>2</sup> )	0.16	800	2093	0.05	36000	36000	0.873

#### Notes

For each component: A = area,  $\hat{U}$  = heat loss coefficient, C = effective thermal capacity, k = thermal conductivity,  $\rho$  = density,  $C_p$  = specific heat capacity, x = thickness,  $C_i$  = thermal capacity of element i in the component. (units are given above)

<sup>†</sup> The heat loss coefficient is calculated by  $\hat{U} = A / [R_{so} + R_{si} + \sum (x/k)_i]$ , for i = 1 to number of elements in the component.  $R_{si}$  and  $R_{so}$  are respectively the resistance of internal and external surfaces of the component. These are obtained from Table 2.1 and Table 2.2 (see chapter 2) for normal exposure to wind speed and appropriate direction of heat flow.

<sup>‡</sup> The effective thermal capacitance of a component is calculated by  $C = (\sum C_i^{-1})^{-1}$ , for i = 1 to number of elements in the component, and for each element,  $C_i = A \rho C_p x$ .

<sup>Ⓜ</sup> Heat loss coefficient for glazing is calculated by  $\hat{U} = U A$ . The glazing U-values 1.9 and 3 ( $\text{W m}^{-2} \text{ } ^\circ\text{C}^{-1}$ ) were used for the glazing of the TF-wall and Gibat-wall respectively.

<sup>¶</sup> A U-value of 1.2 ( $\text{W m}^{-2} \text{ } ^\circ\text{C}^{-1}$ ) was used in calculating the heat loss coefficient of the door in the intermediate wall (North) to allow for thermal bridging of the door frame.

Now if the capacitances,  $C_{\text{cell}}$ ,  $C_{\text{psc}}$  and  $C_{\text{int}}$ , (see Fig.7.11) are lumped in a single effective capacitance for the test cell,  $C$ , at a mean temperature,  $T_m$ , then the governing heat balance equation for the model is given by

$$Q_{\text{aux}} = (\hat{U}_{\text{cell}} + \hat{U}_{\text{psc}} + \hat{U}_{\text{inf}}) (T_i - T_o) + \hat{U}_{\text{int}} (T_i - T_{\text{sr}}) - \hat{A}_{\text{cell}} G_h - \hat{A}_{\text{psc}} G_v + C \partial T_m / \partial t \quad \{7.2\}$$

where each term in the equation is averaged over 24 hours; and the parameters ( $Q_{\text{aux}}$  the auxiliary power requirement,  $T_o$  the outdoor air temperature,  $T_i$  &  $T_{\text{sr}}$  the test cell and service room ambient temperatures,  $G_h$  the global horizontal insolation, and  $G_v$  the global vertical insolation incident on the passive solar component) are measured values;  $\hat{A}_{\text{cell}}$  is the cell solar aperture referred to  $G_h$  because the roof of the cell is most affected by solar radiation;  $\hat{A}_{\text{psc}}$  is the solar aperture of the passive solar component;  $\hat{U}_{\text{int}}$  is the cell-to-service room heat transmission coefficient;  $\hat{U}_{\text{cell}}$  &  $\hat{U}_{\text{psc}}$  are the cell-to-external heat transmission coefficients through the cell structure and passive solar component respectively; and  $\hat{U}_{\text{inf}}$  is the cell-to-external heat transmission coefficient by infiltration.

Infiltration losses can be calculated using the “air change per hour” concept,  $N \text{ h}^{-1}$ , given in section 2.3.2 of chapter 2 (see Eq.2.5). Thus, for the test cell,  $\hat{U}_{\text{inf}}$  is

$$\hat{U}_{\text{inf}} = C_{p(\text{air})} \rho_{\text{air}} V N = 12.68 (\text{Wh } ^\circ\text{C}^{-1}) N (\text{h}^{-1}) \quad \{7.3\}$$

where  $V$  is the volume of the test cell =  $38.04\text{m}^3$ . Number of air change per hour ( $N$ ) can only be determined by laborious experiments, e.g. tracer gas decay technique and pressurization tests. Such experiments were conducted by the UK Passys group on cells fitted with the adiabatic wall (see section 7.3.3 and Figure 7.12). The results of these tests showed an air change rate of  $N < 0.002 \text{ h}^{-1}$ , for average wind speeds of  $2.5 \text{ m s}^{-1}$  (Baker 1989). So from Eq.7.3 the infiltration transmission coefficient is ( $\hat{U}_{\text{inf}} < 0.02 \text{ W } ^\circ\text{C}^{-1}$ ), that is much less than 1% of the overall heat transmission coefficient of the test cell. Therefore, air infiltration losses are negligible and  $\hat{U}_{\text{inf}}$  can be omitted from Eq.7.2.

The term  $C \partial T_m / \partial t$  in Eq.7.2 represents the change in energy stored in the thermal capacitance of the cell mass over 24 hours. Typically ( $\partial T_m / \partial t$ ) is less than  $\pm 0.1^\circ\text{C}$  over 24h for a structure such as the test cell. However, if we assume this term to be as high as  $\pm 1^\circ\text{C}$  over 24h, so, from Table 7.8,  $C (\partial T_m / \partial t)$  would be about  $\pm 0.16 \text{ MJ}$  over 24h, i.e.  $\pm 1.9 \text{ W}$ . This quantity is negligible compared with other terms in the equation, i.e. in the magnitude of less than 1% of the auxiliary heat input to the cell.

	Cell-1	Cell-2	Cell-3
Heat transmission coefficient $\hat{U}$ , ( $\text{W } ^\circ\text{C}^{-1}$ )			
Cell-to-service room $\hat{U}_{\text{int}}$	2.91	2.91	2.91
Cell-to-external $\hat{U}_{\text{tc}}$	6.1	12.5	11.6
Capacitance of the cells ( $\text{MJ } ^\circ\text{C}^{-1}$ )	0.1549	0.1679	0.1800

**Table 7.8** Calculated heat transmission coefficients and capacitances of three Passys test cells. (Summary from Table 7.7).

Thus Eq.7.2 reduces to

$$Q_{aux} = \hat{U}_{tc} \Delta T + \hat{U}_{int} \Delta T_{int} - \hat{A}_{cell} G_h - \hat{A}_{psc} G_v \quad \{7.4\}$$

where the overall test cell heat transmission coefficient  $\hat{U}_{tc} = \hat{U}_{cell} + \hat{U}_{psc}$ ,  $\Delta T = T_i - T_o$ , and  $\Delta T_{int} = T_i - T_{sr}$ . Equation 7.4 apply for experiments with both opaque calibration wall (OCW) and passive solar component (PSC).

For tests with the opaque calibration wall, the solar aperture of opaque calibration wall is assumed  $\hat{A}_{psc} = \hat{A}_{ocw} = 0$ ; and  $\hat{U}_{psc} = \hat{U}_{ocw}$  obtained from an embedded TNO heat flux meter measurements. Thus the basic equation for analysis becomes:

$$(Q_{aux} / \Delta T) = \hat{U}_{tc} + \hat{U}_{int} (\Delta T_{int} / \Delta T) - \hat{A}_{cell} (G_h / \Delta T) \quad \{7.5\}$$

Equation 7.5 is solved by linear regression for  $\hat{U}_{tc}$ ,  $\hat{U}_{int}$  and  $\hat{A}_{cell}$ . The cell heat transmission coefficient excluding the opaque calibration wall,  $\hat{U}_{cell}$ , is simply

$$\hat{U}_{cell} = \hat{U}_{tc} - \hat{U}_{ocw} \quad \{7.6\}$$

For tests with passive solar components, the influence of the service room in Eq. 7.4 can be reduced by maintaining the service room at the same temperature as the cell, and by applying a small correction term to the cell auxiliary heat input for any temperature difference that may occur. Correction is also applied for  $\hat{A}_{cell}$ , obtained from solving Eq.7.5. Thus

$$Q_{aux}^* = Q_{aux} - (\hat{U}_{int} \Delta T_{int} - \hat{A}_{cell} G_h) \quad \{7.7\}$$

where  $Q_{aux}^*$  is the corrected auxiliary heat input. The regression equation becomes:

$$(Q_{aux}^* / \Delta T) = \hat{U}_{tc} - \hat{A}_{psc} (G_v / \Delta T) \quad \{7.8\}$$

and

$$\hat{U}_{psc} = \hat{U}_{tc} - \hat{U}_{cell} \quad \{7.9\}$$

The regression analyses, multivariate for cell calibrations and linear for PSC tests, yield estimates of the required parameters together with their associated random errors due to the models (standard errors).

### 7.3.3 Calibration of the Test Cells

After installation of the necessary sensors and instrumentation in the four test cells, the main tasks for the UK Passys group were to

- (1) Calibrate the test cells to determine essential cell-to-external component properties and cell-to-service room properties (i.e. heat transmission coefficients and solar apertures), and ensuring that the cell performances are identical.
- (2) Ensure that ventilation exchange contributions in the calibration measurements were negligible, so that in subsequent tests on PSC's, any ventilation loss inherent to the PSC could be more readily identified.

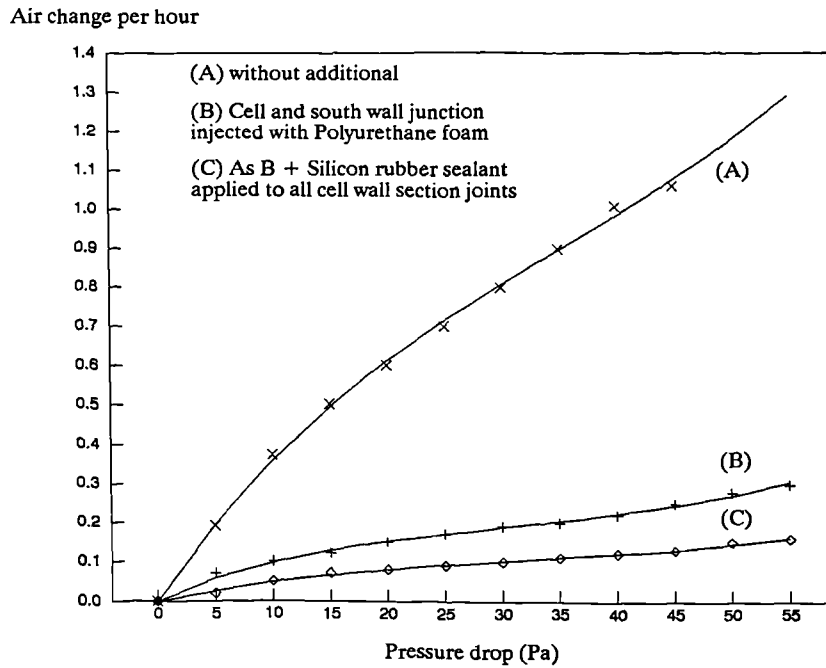


**Figure 7.12** Improvements in air tightness of the Passys test cell fitted with the opaque calibration wall. (data from Baker 1990)

**Table 7.9** Steady-state characteristics of cells 3&4. (after Baker 1989)<sup>†</sup>

	Cell 3 no Blind	Cell 4 no Blind
Heat loss coefficient, $\dot{U}_{tc}$ ( $W\ ^\circ C^{-1}$ )	12.24	12.41
Standard error	0.28	0.29
Solar aperture, $\hat{A}_{pcs}$ ( $m^2$ )	0.68	0.65
Standard error	0.11	0.12

<sup>†</sup> Based on calibration experiment conducted in Nov. and Dec. 1988. Both cells were fitted with low emissivity coated double glazing window in the UK timber frame wall.

The latter was a difficulty, given that the south walls had to be removable. Great care was therefore taken in sealing the cells. Figure (7.12) depicts the results of pressurisation tests on one of the cells fitted with an opaque calibration wall, showing the improvements made in reducing air leakage, firstly by injecting polyurethane foam into the junction of the cell and south wall, and secondly, by applying a silicon rubber sealant to all cell wall section joints.

For the first task, pairs of the cells have been fitted in turn with the opaque calibration walls and their performance compared by monitoring auxiliary heat requirements to maintain a constant temperature of 30°C, and by measuring the rate of temperature decay in the absence of auxiliary heating. The measured heat transmission coefficients ( $\text{W } ^\circ\text{C}^{-1}$ ) were  $\dot{U}_{ocw} = 0.6$ ,  $\dot{U}_{int} = 2.9$ , and  $\dot{U}_{cell} = 7.2$ ; with  $\hat{A}_{cell} = 0.07 \text{ m}^2$ , referred to global horizontal insolation. (calculated by Eq.7.5 & Eq.7.6). Comparison of cells in terms of the loss coefficients indicate that their performance lies within a tolerance of better than  $\pm 5\%$ . (Strachan et. al. 1988). This implies that the cell heat transmission coefficient lie in the range of 6.8–7.6  $\text{W } ^\circ\text{C}^{-1}$ , which is above the theoretical value of 6.1  $\text{W } ^\circ\text{C}^{-1}$  (see Table 7.8). The difference may be due to thermal bridging effects not included in the theoretical value.

A calibration test on cells 3 & 4, fitted with identical low emissivity double glazed windows in timber-frame walls, was conducted in November and December 1988. Results from this experiment (see Table 7.9) indicate the the heat transmission coefficients of the cells lie within a tolerance of better than 2%. (Baker 1989).

### 7.3.4 Instrumentation and Monitoring Details

Each of test cells 3&4 was fitted with a low emissivity, double-glazed window in the TF-wall. Window frame edges and top vents were sealed to further improve the air tightness of the the cell. The Passys blind was fitted flat onto the inside of the window of cell 3. The blind was kept on throughout the duration of the experiment (from July 28th to August 16th 1989).

The test rooms were maintained at a constant temperature using electric fan heaters (1kW setting) controlled by domestic thermostats (30°C setpoint). The rate of heat input to each cell was monitored for the first two weeks. The heaters were then switched off for the remaining period of the experiment to study the cell thermal behaviour in free floating mode. The service rooms were kept at constant temperature (30°C setpoint), using the original wall heaters provided with each test cell.

The sensors used for this experiment are listed in Table (7.10) and shown schematically in Figure (7.13). Note that the data sheets of Appendix F give more details on each sensor (i.e. description, mounting & connections, output range, accuracy and performance in general). All PRT sensors are Grade 1 (with the exception of the surface thin film PRT's which are grade 2) and their calibration has been checked at two temperatures in a stirred water bath using the HP data acquisition system. All temperatures were within 0.2°C of a reference precision PRT. Four-wire measurements were made on all PRT's.

**Table 7.10** Basic set of sensors used for the blind experiment and monitored at the UK Passys site. For more details on each instrument refer to the data sheets in Appendix (F). Data sheet numbers designated here in square brackets [DS#]. (The sketch below shows the type and location of some basic instruments).

DESIGNATION	SENSOR TYPE AND LOCATION
<i>Weather Station Sensors</i>	
0ATE01	External air temperature (shielded and ventilated PRT), 2m above ground, 0.5m in front of cell 3. [DS3]
0ATE03	Wet bulb temperature (shielded and ventilated PRT), 2m above ground.
0ATE04	Dry bulb temperature (shielded and ventilated PRT), position as for 0ATE03. [DS5]
0ADE01	Wind direction (signal voltage), 10m high on mast, requires a reference voltage. [DS7]
0AVE01	Wind speed (analogue output), 10m high on mast. [DS6]
0GHE01	Global horizontal solarimeter, on top of cell 3. [DS8]
0DHE01	Diffuse horizontal solarimeter with shadow ring, on top of cell 3. [DS10]
0GVE01	Global vertical solarimeter, position in vertical position as for 0ATE01.
<i>Air Temperature in Test Rooms (i designate cell number, 3 or 4)</i>	
iATI01	Air temperature (shielded PRT), 15cm above floor in the middle of the floor. [DS2]
iATI02	15cm bellow ceiling in the middle of the ceiling.
iATI03	15cm from east wall in the middle of the wall.
iATI04	15cm from west wall in the middle of the wall.
iATI05	Middle of the room, 1.38m high and 2.5m from south wall.
iATI06	0.6m from south wall, 1.38m above floor.
iATI07	0.6m from north wall, 1.38m high.
<i>Surface Temperature</i>	
iSTEG1	External surface temperature of window glazing (shielded thin film PRT), centre of panel. [DS2]
iSTIG1	Internal surface temperature of window glazing, position opposite to iSTEG1.
iSTIB1	Internal surface temperature of blind (non-contact IR digital thermometer), 3m from blind to measure a target diameter of 60mm on the centre of the blind surface. [DS4]

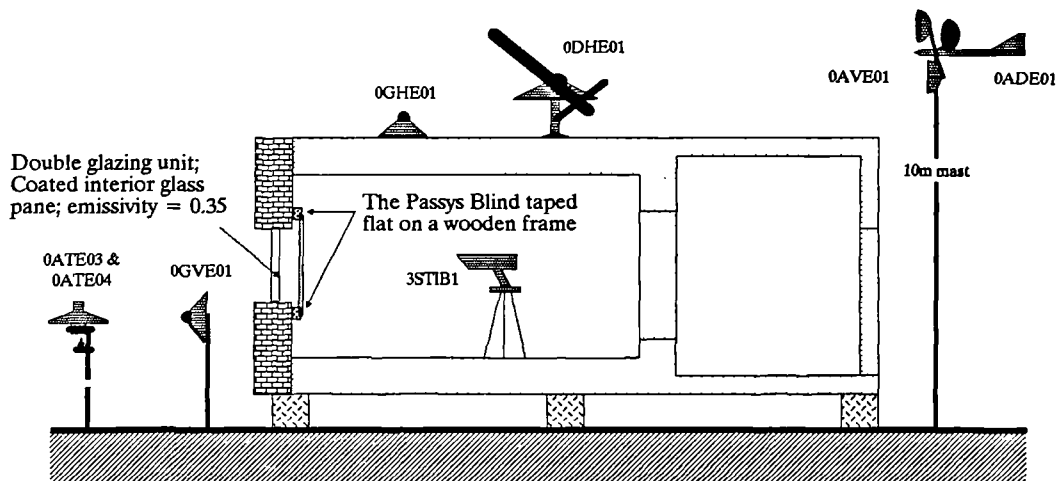


**Figure 7.13** A sketch showing the type and location of some basic instruments listed above.

Air temperature sensors were double shielded from possible incoming radiation as shown in Fig.7.14a. Mounting and shielding of the glass surface temperature sensors is shown in Figure (7.14b).

Due to the nature of the blind textile fabric, it was difficult to use a conventional thin film PRT for the measurement of the blind surface temperature. Therefore, a non-contact IR thermometer, available at the ESU, was used. Note that this instrument provides easy and precise way of measuring surface temperatures, but at a price tag of £400 + , other options need to be investigated.

The auxiliary heat input to the test rooms was measured by pulsed output from kWh-meters using a Delta-T logger. Power meters were calibrated against a nominal standard meter. The power meter in cell 3 has a calibration factor of 0.320 W/count and a calibration of 0.064 W/count for the power meter in cell 4. Service rooms were heated by the original wall mounted heaters (2kW). The accuracy of auxiliary heat measurements is estimated to be within 3%. The HP Data Acquisition System was used for logging data from all temperature sensors at nominal 5 minute intervals; and from the weather station at 1 minute intervals. Hourly averages calculated for all data.

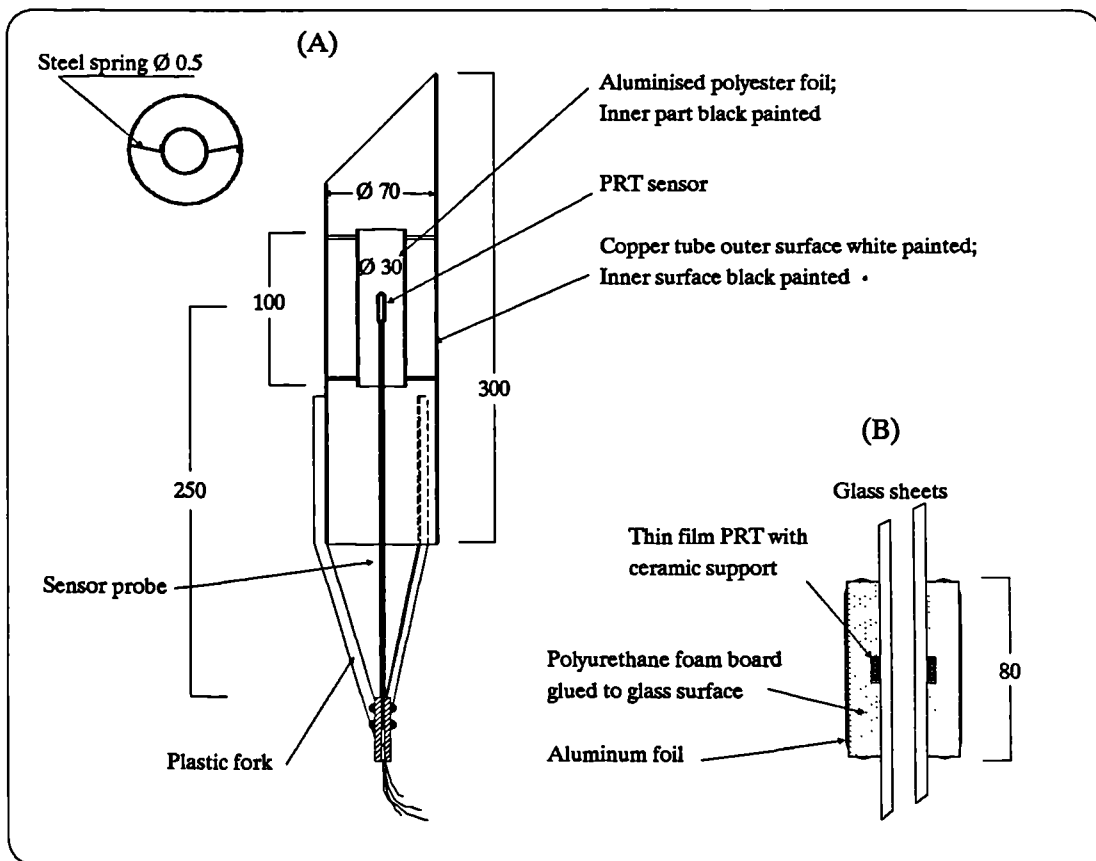


**Figure 7.14** (A) Double shield device for air temperature sensor; made by Specitec, France. (B) Mounting and shielding of surface temperature sensor; made by the author. The surface PRT films are glued to glass surfaces by a conductive paste. Dimensions in mm.

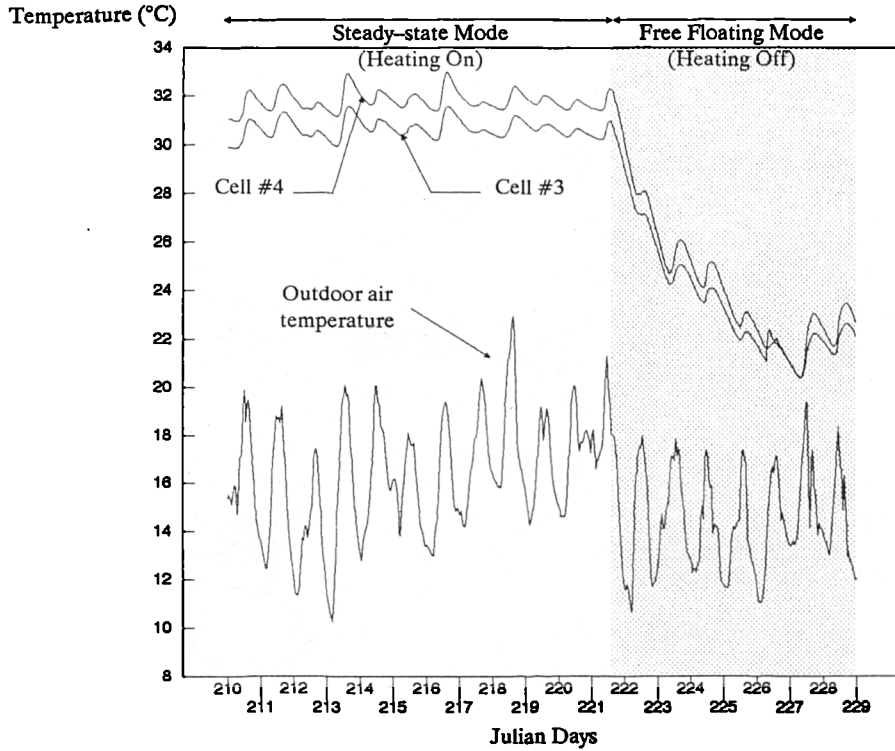


**Figure 7.15** Ambient temperatures measured for the period of experiment. Test cell temperature is taken as the average of air temperatures at 7 locations in the test room (see Table 7.10).

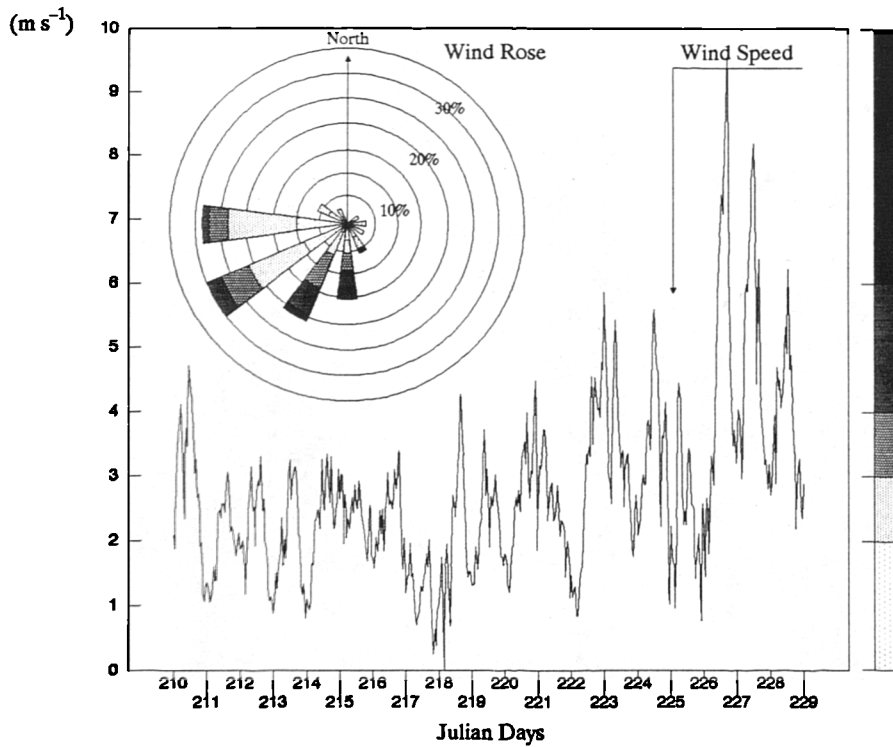


**Figure 7.16** Wind speed and direction measured at the test site for the period of experiment.

## 7.4 Analysis of Captured Data Sets

The captured data sets encountered some erroneous values of glazing surface temperatures, in cell 3, for the first day of the experiment only (209 Julian). Thus the valid data for comparative analysis are from July 29th to August 16th 1989. Figure 7.15 shows the hourly outdoor air temperature and the ambient temperatures of cells 3 and cell 4. The ambient temperature of each cell is an average of seven readings taken at various positions within the cell as given in Table 7.10. Note that due to systematic errors in the thermostats used, the effective setpoint temperatures of cells 3 & 4 were found to be 30.6°C and 31.7°C respectively.

Hourly wind speed and wind direction rose for the period of experiment are shown in Figure 7.16. The average wind speed for the whole period was 2.78 m s<sup>-1</sup> and 2.2 m s<sup>-1</sup> average wind speed was recorded for the steady-state period of the experiment (heating on). The wind direction was dominantly west south-west oriented. 82% of the recorded wind directions lie in the range of 195° to 285°, 70% of which have corresponding wind speeds in the range of 0 to 4 m s<sup>-1</sup>. Global and diffuse horizontal insolation data are shown in Figure 7.17, averaged over 24h, and Figure 7.18 shows the daily average vertical global insolation.

The following subsections analyse the performance characteristics of the blind in two ways: (i) The steady-state overall performance of cell 3 fitted with the blind compared with cell 4 without blind; (ii) Analysis of the fenestration effects on the energy balance of the test cells for typical clear and overcast days.

### 7.4.1 Steady-state Performance Characteristics of Test Cell 3 (with Blind) and Test Cell 4 (no Blind)

The steady state model discussed in section 7.3.2 has been used to derive the performance characteristics of the cells, namely the heat transmission coefficients,  $\hat{U}_{tc3}$  and  $\hat{U}_{tc4}$  (W °C<sup>-1</sup>) and solar apertures,  $\hat{A}_{psc3}$  and  $\hat{A}_{psc4}$  (m<sup>-2</sup>) referred to  $G_v$ . The steady-state energy balance for each cell is given in the linear relation between the measured response of the test cell ( $Q_{aux}/\Delta T$ ) and the climatic correlation ( $G_v/\Delta T$ ) as given by Eq.7.8, Thus

$$(Q_{aux3}/\Delta T_3) = \hat{U}_{tc3} - \hat{A}_{psc3} (G_v/\Delta T_3) \quad \{7.10\}$$

$$(Q_{aux4}/\Delta T_{tc4}) = \hat{U}_{tc4} - \hat{A}_{psc4} (G_v/\Delta T_4) \quad \{7.11\}$$

where  $Q_{aux3}$  &  $Q_{aux4}$  the auxiliary heat input to the cells 3 & 4 are modified for any difference in temperature between the test rooms and the service rooms, using Eq.7.7. Note that the parameters of Eq.7.10 and Eq.7.11 are 24h averages. The linear correlations of Eq.7.10 & Eq.7.11 were solved using Lotus-123<sup>®</sup> software. Regression analysis over 12 average daily values (the steady-state period of the experiment) were performed. The data were then assorted, by excluding the data with maximum residual, and a second regression was performed on the remaining values. The results are listed in Table (7.11) and plotted in Figure 7.19 for both cells.

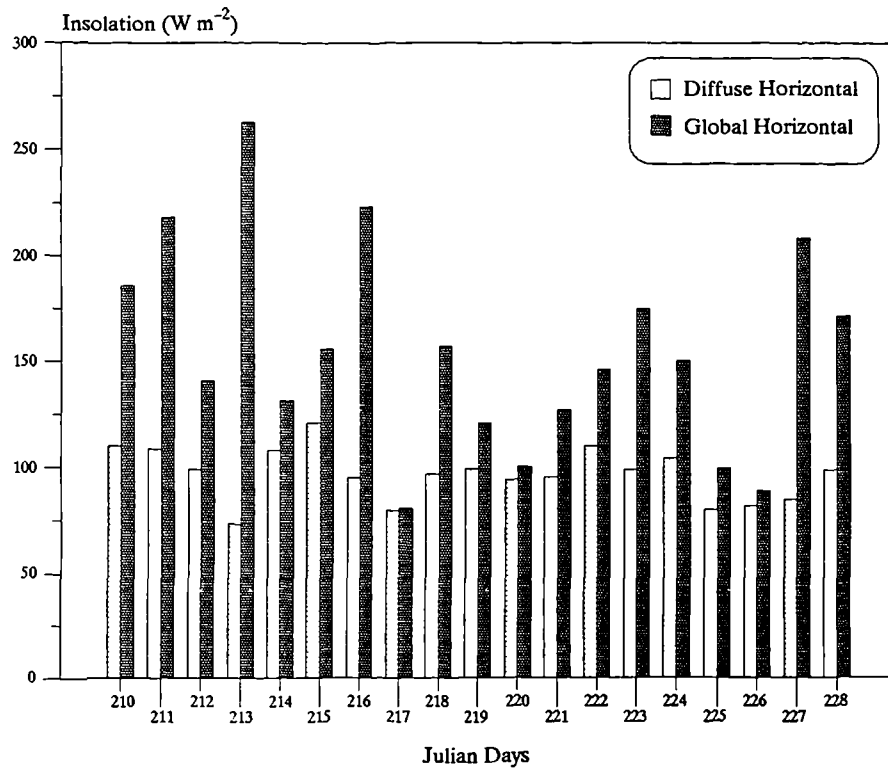


**Figure 7.17** Measured global horizontal and diffuse horizontal insolation ( $W m^{-2}$ ), for the period from July 29<sup>th</sup> to August 16<sup>th</sup> 1989.

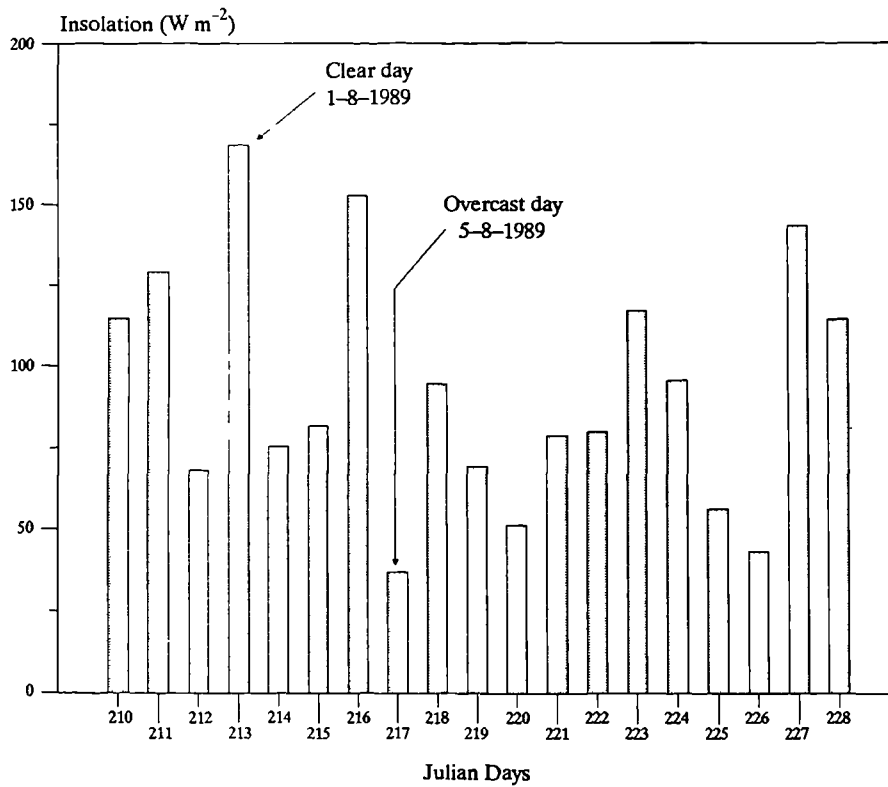


**Figure 7.18** Measured global vertical insolation ( $W m^{-2}$ ), for the period from July 29<sup>th</sup> to August 16<sup>th</sup> 1989.

**Table 7.11** Steady-state characteristics of cells 3&4 † from the “blind” experiment.

	Cell 3 with Blind	Cell4 no Blind
Heat loss coefficient, $\hat{U}_{tc}$ ( $W^{\circ}C^{-1}$ )	9.45	10.68
Standard error	0.80	0.70
Solar aperture, $\hat{A}_{psc}$ ( $m^2$ )	0.33	0.50
Standard error	0.06	0.06
Correlation R value	0.87	0.94

† Both cells were fitted with low emissivity coated double glazing window in the UK timber frame wall, and cell 3 had the Passys Blind fitted.

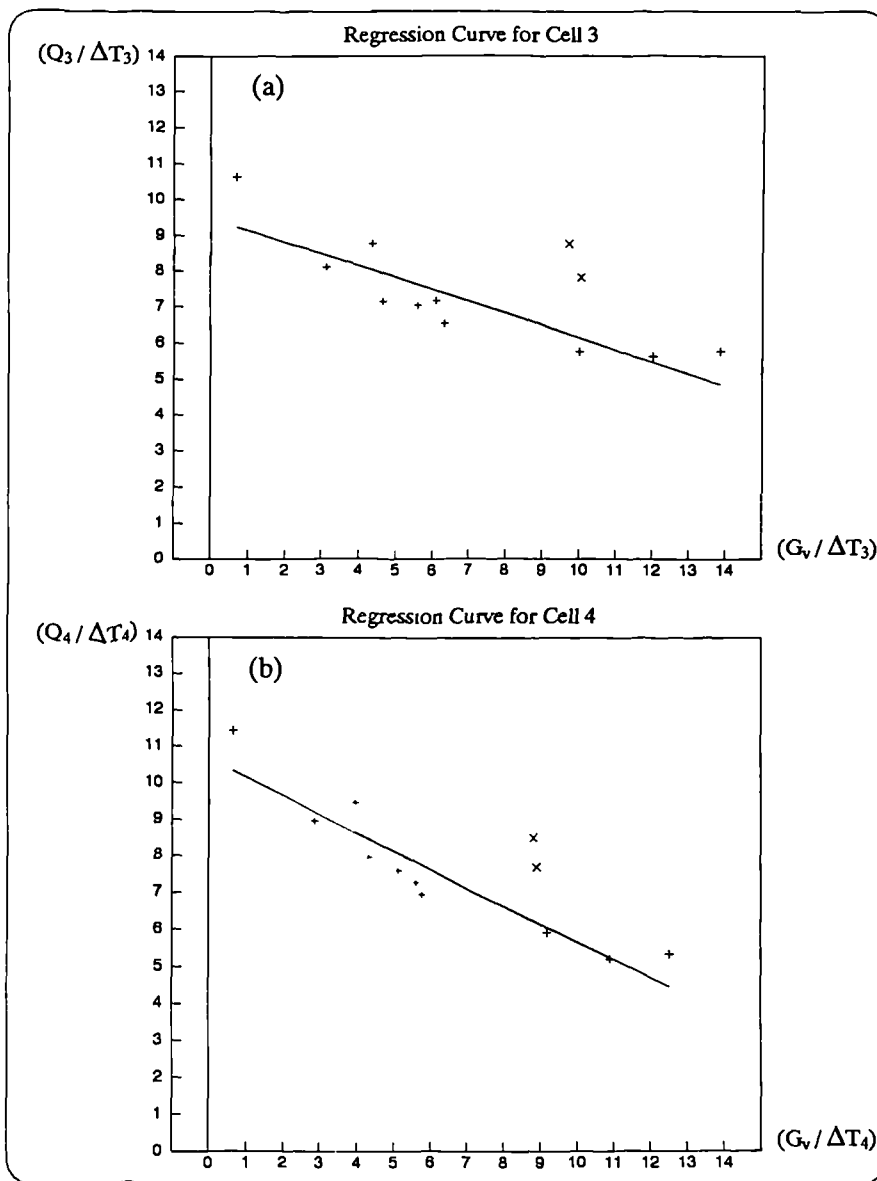


**Figure 7.19** Regression curves for (a) cell 3 fitted with glazing and the Passys blind, and (b) cell 4 fitted with glazing only. The two average daily parameters marked “x” have large residual values and correspond to days 210 and 218 Julian.

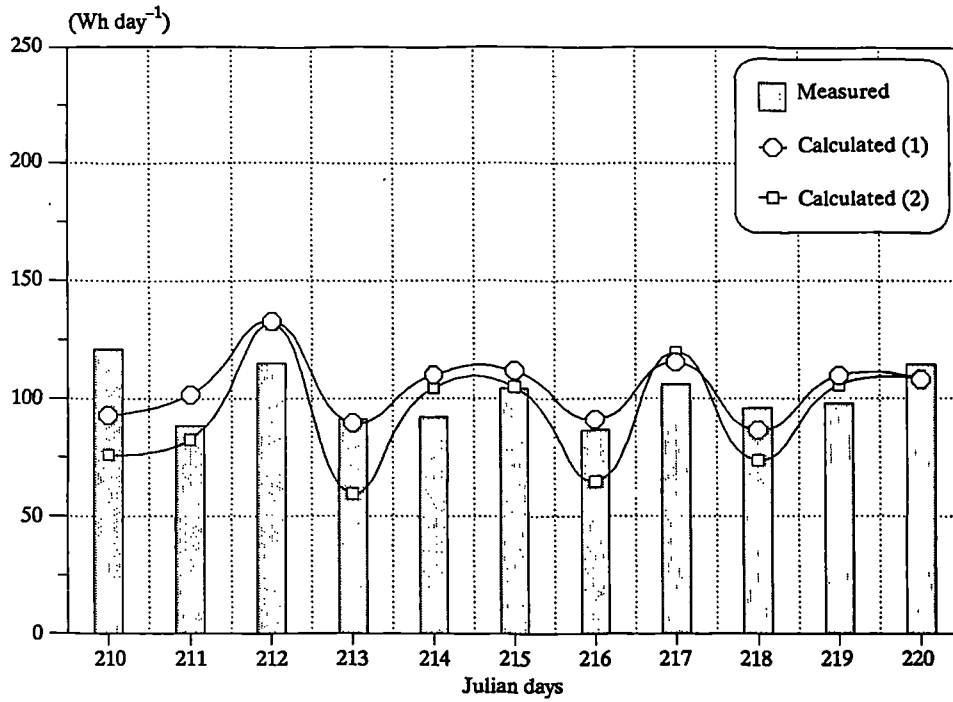


**Figure 7.20** Daily average heating requirements of *cell 3*. A comparison between measured and calculated values using (1) the correlation coefficients  $\hat{U}_{tc}$  &  $\hat{A}_v$  derived from the experiment results (see Table 7.11) and (2) using results from MRQT program ( $\hat{U}_{tc} = 10.53$  &  $\hat{A}_v = 0.61$ ).

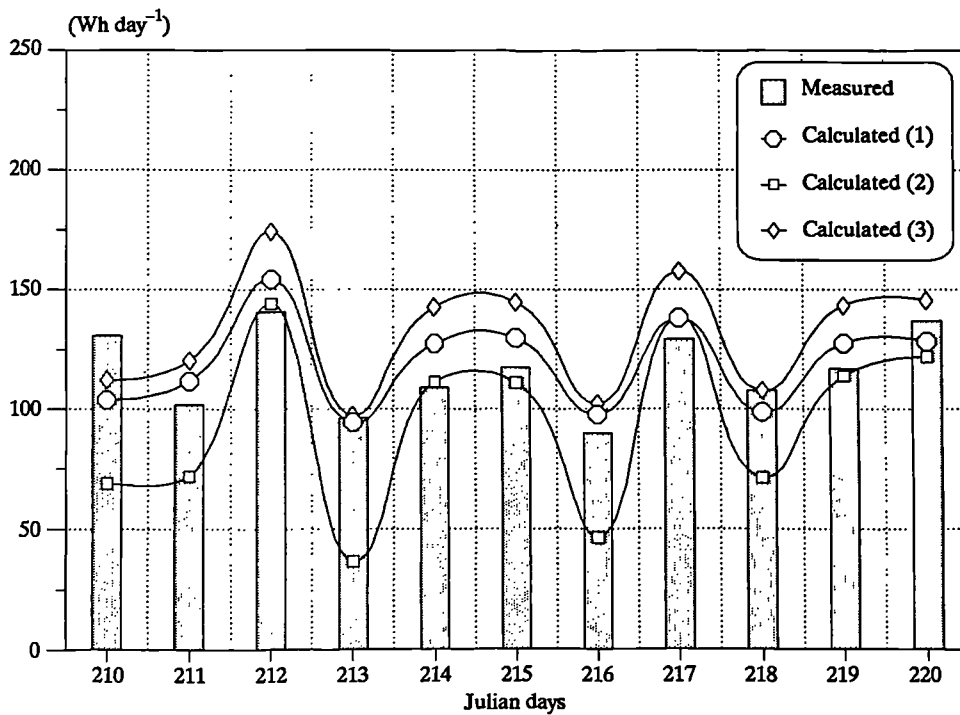


**Figure 7.21** Daily average heating requirements of *cell 4*. A comparison between measured and calculated values using (1) the correlation coefficients for cell 4 in Table 7.11, (2) MRQT output ( $\hat{U}_{tc} = 11.91$  &  $\hat{A}_v = 0.96$ ), and (3) using the correlation coefficients derived from the calibration experiment (see Table 7.9).

The results of Table 7.11 show that the heat transmission coefficient and solar aperture of cell 3, fitted with the blind, are respectively 11.5% and 34% less than those of cell 4, without blind. Note that  $\hat{U}_{tc4}$  and  $\hat{A}_{psc4}$  differ from those given Table 7.9 (from the calibration tests on cell 4 with the same PSC). The difference could be due to air infiltration losses through window frame edges and its ventilation vent on the previous calibration experiment.

The heat transmission coefficients and solar apertures of both cells were also determined using the Passys recommended program “MRQT”, and results have shown very high solar aperture values ( $\hat{U}_3 = 10.53$ ,  $\hat{U}_4 = 11.91$ ,  $\hat{A}_3 = 0.61$ , and  $\hat{A}_4 = 0.96$ ). The reductions of heat transmission coefficient and solar aperture due to the blind were 11.6% and 36.4% respectively, which are close to the reduction percentages of the regression analysis.

Figure 7.20 shows a comparison between the measured and calculated auxiliary heating requirement of cell 3 using the correlation coefficients ( $\hat{U}_3$  &  $\hat{A}_3$ ) given in Table 7.11 and coefficients from the “MRQT” program. The average heating requirement of test cell 3, for the whole period, calculated using the “MRQT” coefficients was 7% lower than the measured auxiliary heating. Average auxiliary heating of cell 3 calculated by regression coefficients was 3% higher than the measured. From the daily auxiliary heating of cell 3, calculated by the experiment regression coefficients and by the “MRQT”, the standard error percentages were found to be 12% and 20.7% respectively.

Figure 7.21 shows a comparison between measured and calculated heating requirement of cell 4. The average auxiliary heating of cell 4 calculated by the regression coefficients of this experiment was 2.7% higher than the measured, compared with 13% higher and 19% lower heating as calculated by the calibration experiment coefficients (see Table 7.9) and the “MRQT” coefficients respectively. The standard error percentages in calculated auxiliary heating of cell 4 by the coefficients of the blind experiment, calibration experiment, and MRQT were 10.5%, 12% and 26% respectively.

The total heating measured in cell 3 for the whole period analysed was less than that of cell 4 by 12.8%. In comparison, the regression coefficients of this experiment and the “MRQT” coefficients give calculated values of cell 3 heating which are 12.3% and 0.5% lower than cell 4 respectively. Thus it is apparent that the steady – state performance properties (i.e correlation coefficients  $\hat{U}$  and  $\hat{A}$  in Table 7.11) derived from the blind experiment produce better estimates of auxiliary heating than those derived by the “MRQT” program.

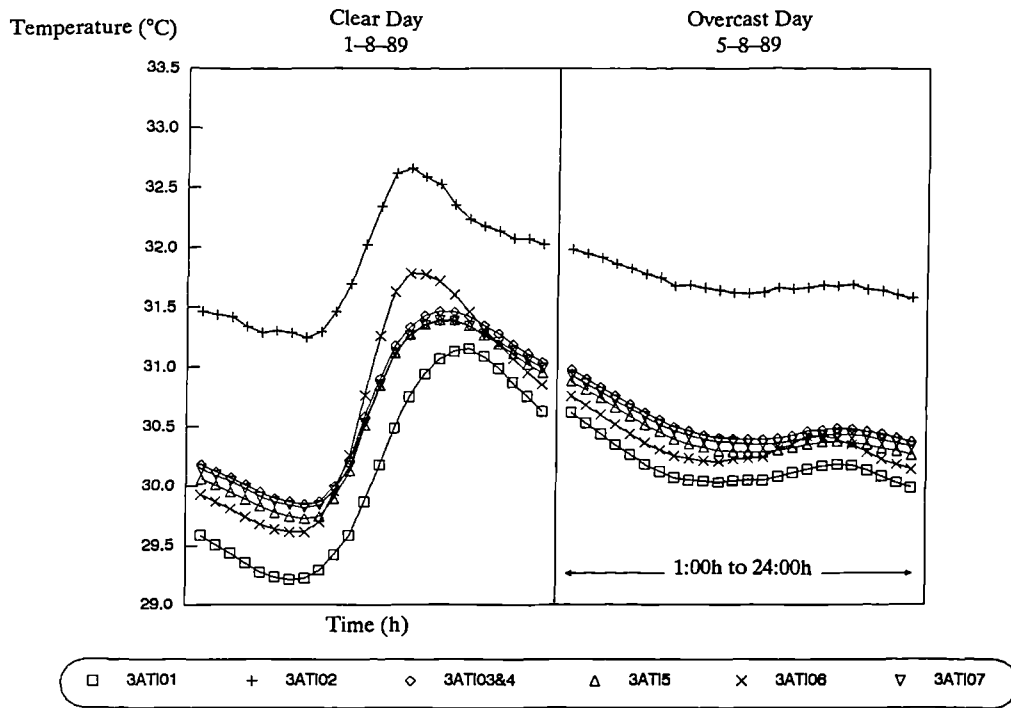


Figure 7.22 Variations of air temperature in cell 3 for a clear and overcast days (i.e. Julian days 213 and 217 respectively).

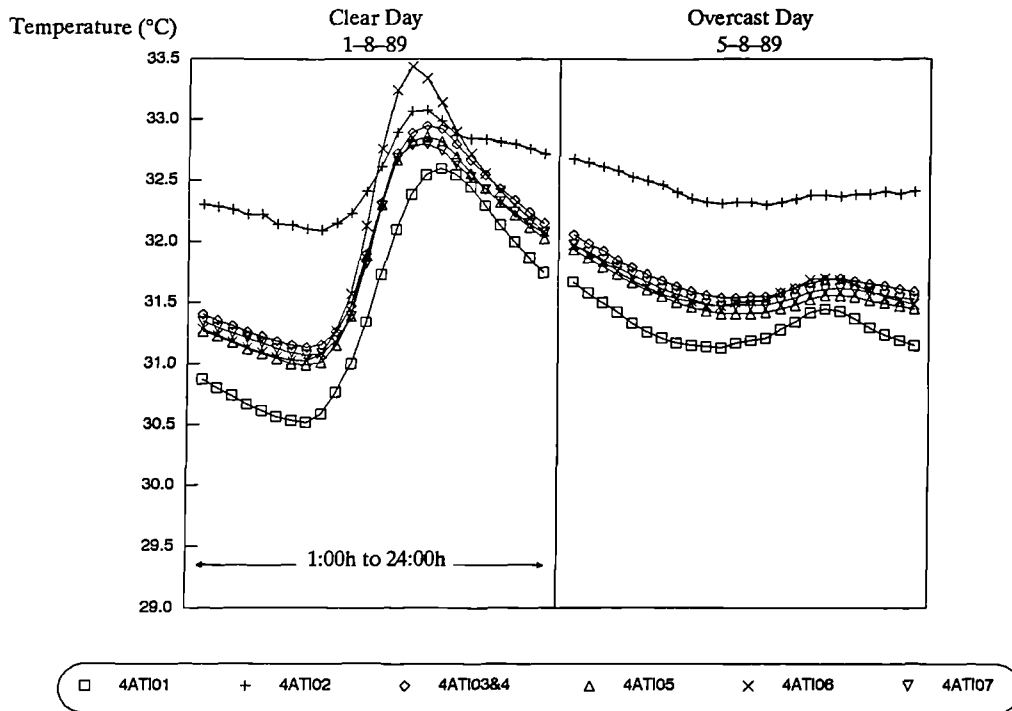


Figure 7.23 Variations of air temperature in cell 4 for a clear and overcast days (i.e. Julian days 213 and 217 respectively).

## 7.4.2 Effects of the Blind on the Thermal Performance of the Test cell in Typical Clear and Overcast Days

Two days were chosen for the analysis based on the solar data (Fig.7.17 & Fig.7.18), day 213 Julian and day 217 Julian. Figures 7.22 and 7.23 show the ambient temperature distribution for both days inside test cells 3 and test cell 4 respectively. The stratification of temperature within each test cell was apparent by the differences in temperature sensor readings at various locations within the cell despite the sky conditions. Such phenomenon should be taken into consideration in locating a thermostat for instance.

Figures 7.22 and 7.23 also show that the temperatures nearest to the windows (i.e. 3ATI06 & 4ATI06) are highly influenced by insolation intensity during the day. Hourly global vertical insolation for the clear and overcast days are shown in Figure 7.24. This figure also shows the hourly outdoor air temperature variations for both days.

To establish better direct comparison between the thermal performance of the passive solar components, auxiliary heat values of cell 4 were modified to allow for the (1.1 °C) difference in set point temperature. The following equation was used:

$$Q_{4new} = Q_4 \cdot (\Delta T_4 - 1.1^\circ\text{C}) / \Delta T_4 \quad \{7.12\}$$

Auxiliary heat differences of the two cells for both days are plotted in Figure 7.25.

From Fig.7.25, the effect of the blind on the energy balance of the test cell is apparent. In overcast conditions test cell 3 (with blind) required 6% and 16% less auxiliary heating for day and night periods respectively, than test cell 4 (without blind). In clear sky conditions, cell 3 (with blind) required 28% more auxiliary heat during the day period than cell 4 and 13% less at night. (day refer to the period of hours with insolation above  $0 \text{ W m}^{-2}$ ).

Analysis of measured and predicted parameters concerning the thermal performance of the blind-shaded fenestration are detailed in the following section.

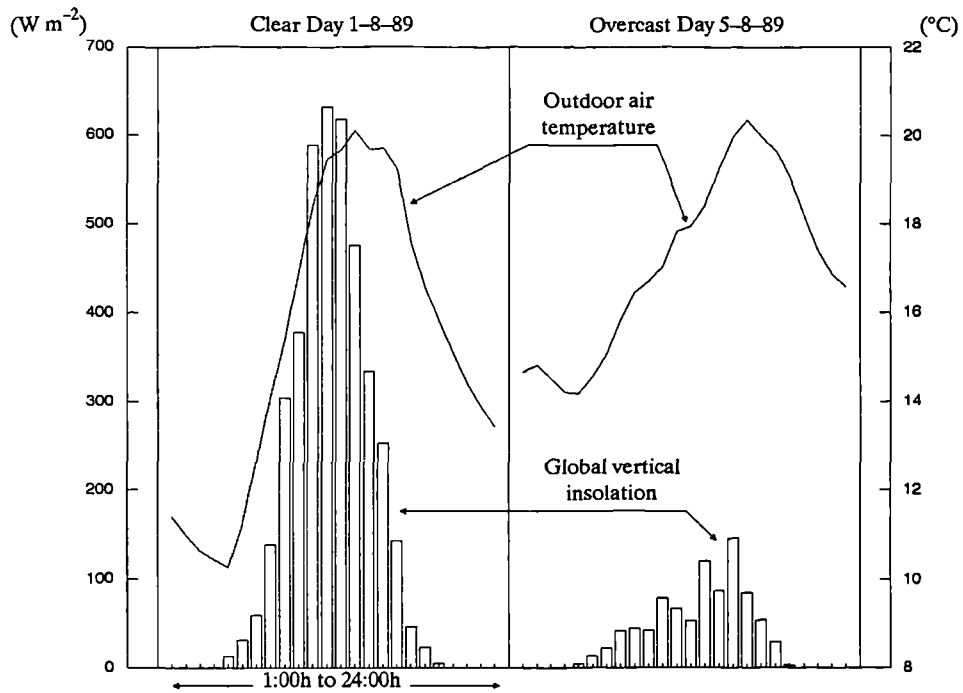


**Figure 7.24** Hourly measured global vertical insolation ( $W m^{-2}$ ) and outdoor air temperature ( $^{\circ}C$ ) for clear and overcast days.

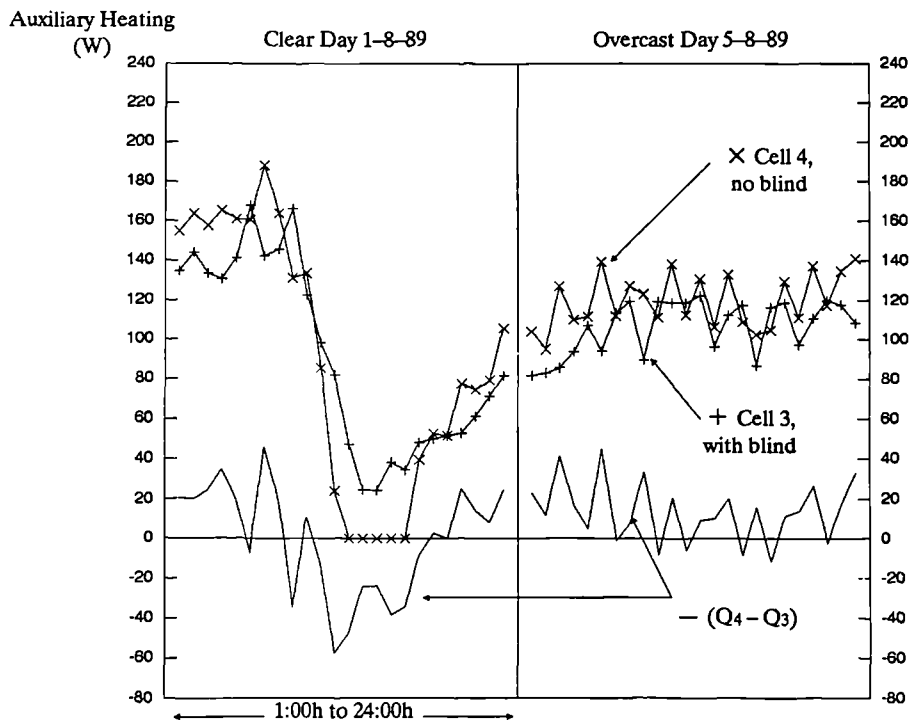


**Figure 7.25** Hourly heating requirements of cell 3 and cell 4 ( $Q_3$  and  $Q_4$ ) measured for clear and overcast days. Note that the auxiliary heating of cell 4 is modified for the  $1.1^{\circ}C$  difference in setpoint temperature (see section 7.4.2 for details).

## 7.5 Comparison Between Measured and Simulated Results by “ESP” and “CURTAIN” Models

---

The model “Curtain.Bas” developed by the author in chapter 5 (see section 5.6) is validated in this section against measured parameters obtained from the experiment (i.e. the temperatures of the fenestration layers). It was necessary to modify the program for this particular task as discussed below. The “ESP” program was also used to simulate the temperatures of the fenestration layers as well as the heating requirements of each test cell. Appendix G describes the ESP model in brief. For detailed description of the model, see Clarke et. al. (1990). Other literature is also available (e.g. Clarke & Forrest 1978; Bridges et. al. 1981; Clarke 1982; Sluce 1982; Littler 1983; Gough 1984; Clarke 1985; and a number of ESRU occasional papers from the University of Strathclyde) which describe the ESP system in general terms, as well as commercial application of the system.

### 7.5.1 Input Variables to the Models

#### *Fenestration & climate definition for the “Curtain” Model*

The program “Curtain.bas” was rewritten to simulate the heat transfer through (a) coated double glazing with blind and (b) without the blind. For the latter, the heat balance equations were arranged to yield the three dimensional matrix form of Table (7.12).

The program was also modified to read the hourly ambient temperature of each test cell from the climate input file. Thus the climate file consist of hourly data in the following order:– global horizontal insolation, diffuse horizontal insolation, outdoor air temperature, wind speed, wind direction and ambient temperatures of the two test cells. Simulation runs were conducted for the period from day 210 to 228 Julian inclusive.

#### *Test Cell, TF-Wall & the “Blind-Glazing” Definition in “ESP”*

The test cell zones geometry and construction data were input to ESP in the form of ASCII data files, these are listed and explained in Appendix (G). The geometry files are (*sroom.geo*, *troom.geo* and *wroom.geo*) and the construction data files are (*sroom.con*, *troom3.con*, *troom4.con* and *wroom.con*). Each fenestration was described as (i) a window in files that begin with the letter “w”, and (ii) transparent multi-layer construction. The latter should, in theory, produce better results. (see discussion below)

The following points were taken into account when defining the UK timber-frame wall components in ESP:

- To provide realistic interpretation of the TF-wall components in the ESP model, the studding (timber frame) area was calculated and defined as a separate surface, so was the wooden window frame. (see the figures given in Appendix G for each geometry file).

**Table 7.12** Matrix form of heat balance equations for the double glazing system in *cell 4*. (see section 5.5.3 of chapter 5 for explanation of the terms used and details on the calculation procedure.)

$$\begin{bmatrix} 1 & h_0 & 0 \\ 0 & h_0 + h_1 & -h_1 \\ 0 & -h_1 & h_1 + h_2 + h_3 \end{bmatrix} \times \begin{bmatrix} q_{rci} \\ T_{go} \\ T_{gi} \end{bmatrix} = \begin{bmatrix} G_v (\alpha'_{go} + \alpha'_{gi}) + h_0 T_o \\ G_v \alpha'_{go} + h_0 T_o \\ G_v \alpha'_{gi} + T_i (h_2 + h_3) \end{bmatrix}$$

- In heat transfer calculations through glazing, ESP default algorithm treats glazing as resistance only, between indoor and outdoor air temperature nodes, with an approximate treatment of longwave radiation exchanges. For this the program requires direct and total transmittance of the glazing for five angles of incidence (0°, 40°, 55°, 70° and 80°) and the U-value of the glazing. These were included in the construction file *wroom.con* which apply for both cell 3 and 4. However for cell 3, a blind control file, *wroom3.blm*, was created, with the above requirements modified.
- The direct and total transmittances of the fenestration (with and without the blind) for the required five angles of incidence were modeled using the “Curtain” program. Note that solar properties of transparent layers can be determine by the *ESPwin* module, however this module is only capable of analysing single and double glazing and further it cannot directly account for the low emissivity coating on the outer surface of the inner pane of a double glazed window, hence not used. U-values were averaged from the “Curtain” program results for the period of the experiment.
- The low emissivity window components were also described as transparent multi-layered construction, so that simulation will account for conduction, convection heat transfer, Infra-red radiation exchanges between the glazing/blind and other surfaces in the cell as well as transmitted solar radiation to the cell. For this the program requires the direct transmittance of the composite fenestration, and the absorptance of each layer in the fenestration, again for the five angles of incidence. These were modeled with the “Curtain” model, and given in the files *troom4.tmc* and *troom3.tmc*. The glazing was given as layers with an air-gap in the zone construction files *troom3.con* and *troom4.con*.
- Since ESP cannot directly account for the low emissivity coating on the outer surface of the inner pane of the fenestration, this has been taken into consideration by modelling the air gap resistance by the “Curtain” program, which yielded a value of  $0.232 \text{ m}^2 \text{ }^\circ\text{C W}^{-1}$  for cell 4. The air gap resistance for the fenestration of cell 3 was  $0.42 \text{ m}^2 \text{ }^\circ\text{C W}^{-1}$  which also account for the air space between the blind and the glazing.

### *Test Configuration & Climate Definition in ESP*

An operation file to instruct the *ESPbps* program of the extra casual gains and infiltration air change rate of each zone was created (*troom.opr*). Casual gains were set to zero, hence no casual gains existed in the cell, and air change rate was set to  $0.1 \text{ h}^{-1}$  (this value was chosen from Figure 7.10 which correspond to pressure difference of 40 Pa for air-tight cell). Casual gains and air change rate in the service room operation file (*sroom.opr*) were set to zero. Similar to the experiment configuration, set-point temperatures of  $30.6^\circ\text{C}$  and  $31.7^\circ\text{C}$  for test cells 3 and 4 respectively, were defined in a configuration control file (*blindx.cfl*). Note that these values are the average temperatures of the cells for the steady-state period of the experiment. The climatic data collected for the period of experiment (plus 2 weeks before and 2 weeks after) were formatted to construct a climate file (*glasgow.clm*) using *ESPclm*.

Finally, two configuration files for the period of experiment were created (*blindx1.cfg* and *blindx2.cfg*). Each configuration file was used to simulate the energy performance of both test cells. The difference is that the first considers each fenestration as transparent multi-layer construction while the second considers the fenestration as window with blind control for cell 3. The simulation runs were conducted, each with 6 days start-up period (determined by the program).

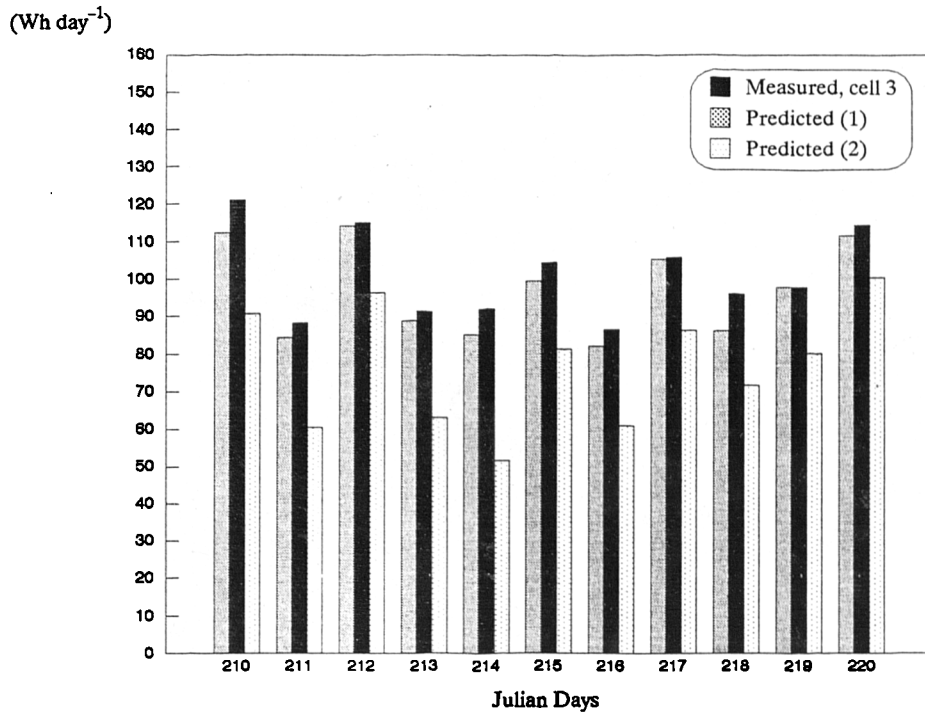


**Figure 7.26** Measured and predicted heating requirement of *cell 3*. Predicted values are from the two “ESP” simulation runs; with the fenestration described as (1) transparent multi-layered construction, and (2) default window with blind control. (see section 7.5.1).

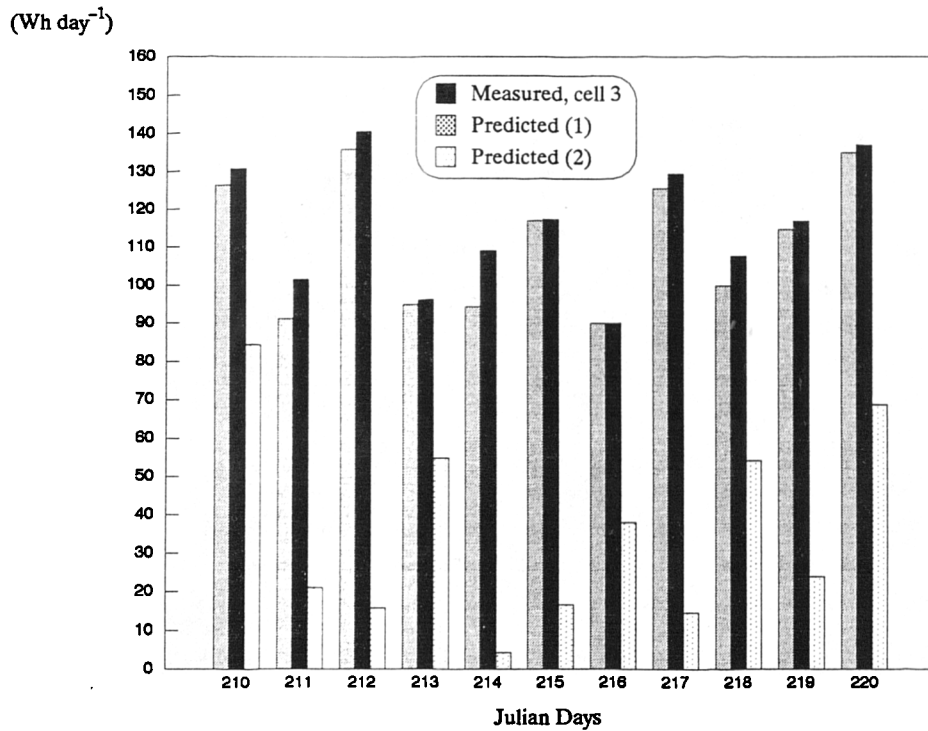


**Figure 7.27** Measured and predicted heating requirement of *cell 4*. Predicted values are from the two “ESP” simulation runs; with the fenestration described as (1) transparent multi-layered construction, and (2) default window with blind control.

## 7.5.2 Results and Discussion

### *Results for the Steady-state Period*

The first simulation run using ESP, in which the fenestration was considered as transparent multi-layer construction, produced better results than the default window treatment in the second simulation run. Figures 7.26 & 7.27 compare the measured and predicted average daily auxiliary heating of cells 3 & 4 for the period from 210 to 220 Julian. Over the whole period, the daily average heating of cell 3 was 4.1% and 24% underestimated by the first and second ESP runs respectively; while for cell 4, the auxiliary heating was underestimated by 4% and 68%. It is clear that the second ESP simulation run produced unacceptable results and based on the above figures, the ESP results discussed and analysed hereafter are from the first simulation run.

Figure 7.28 shows a comparison between the daily total energy balances at the air nodes of cell 3 and cell 4 (computed by ESP). The energy balance at the air node is divided into convective heat exchanges with (a) the cell side walls, roof and floor, (b) internal wall connecting to the service room, and (c) the passive solar component. The contributions of heat exchanges are also shown in pie charts on the same figure. From Fig.7.28, the total energy balance of cell 3 is 12.8% lower than that of cell 4. This is the same percentage reduction in measured auxiliary heating of the cells.

Energy balances of the passive solar components (TF-wall and fenestration) of cell 3 and cell 4 are shown in Figure 7.29. It is apparent that the presence of the blind on the fenestration of cell 3 reduces the total energy loss of the combined wall/fenestration by about 34% and the major reduction being through the fenestration.

### *Results for the Period of Free Floating Mode*

Hourly energy balances at the air nodes of cell 3 and cell 4 for the free floating mode (from 222 to 228 Julian, where no heating was supplied to the cells) are shown in Figure 7.30. A comparison between the measured and ESP predicted ambient temperatures of cell 3 and cell 4 are shown in Figure 7.31.

Shortwave fluxes transmitted through the fenestration of the Passys test cell undergoes a complex process of absorption and longwave heat exchanges, by the internal surfaces of the test cell. The net convective energy balance at the air node of the cell is therefore influenced by the magnitude of the transmitted solar radiation. (Note that transmitted solar fluxes through the fenestration of cell 3 and 4 are discussed later in the section of clear and overcast day results). Thus from Figure 7.30, the higher shortwave fluxes transmitted through the glazing of cell 4, as compared with cell 3, produced lower net energy loss at the air node due to the cell components (side walls, roof and floor).

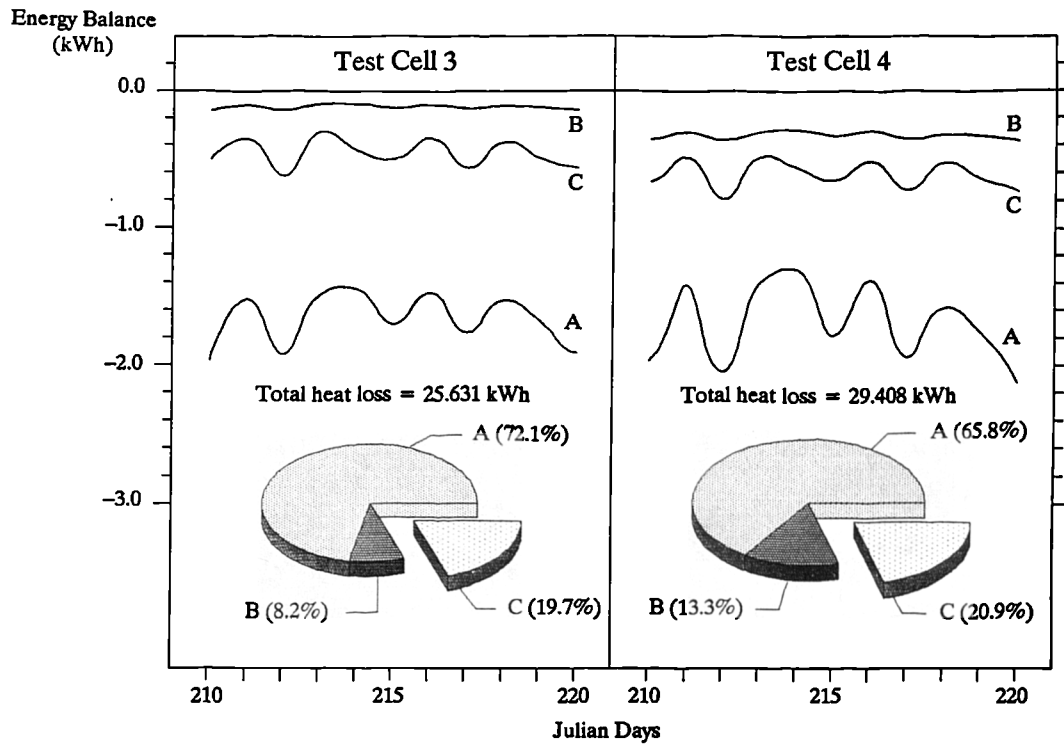


**Figure 7.28** Daily totals of the net energy balance at the air nodes of cells 3 & 4, calculated by the “ESP” model for the period from 210 to 220 Julian. The energy balance at air node is a combination of convective exchanges with (A) the cell side walls, roof and floor, (B) internal wall connecting to the service room, and (C) the passive solar component, i.e. the timber-frame wall.

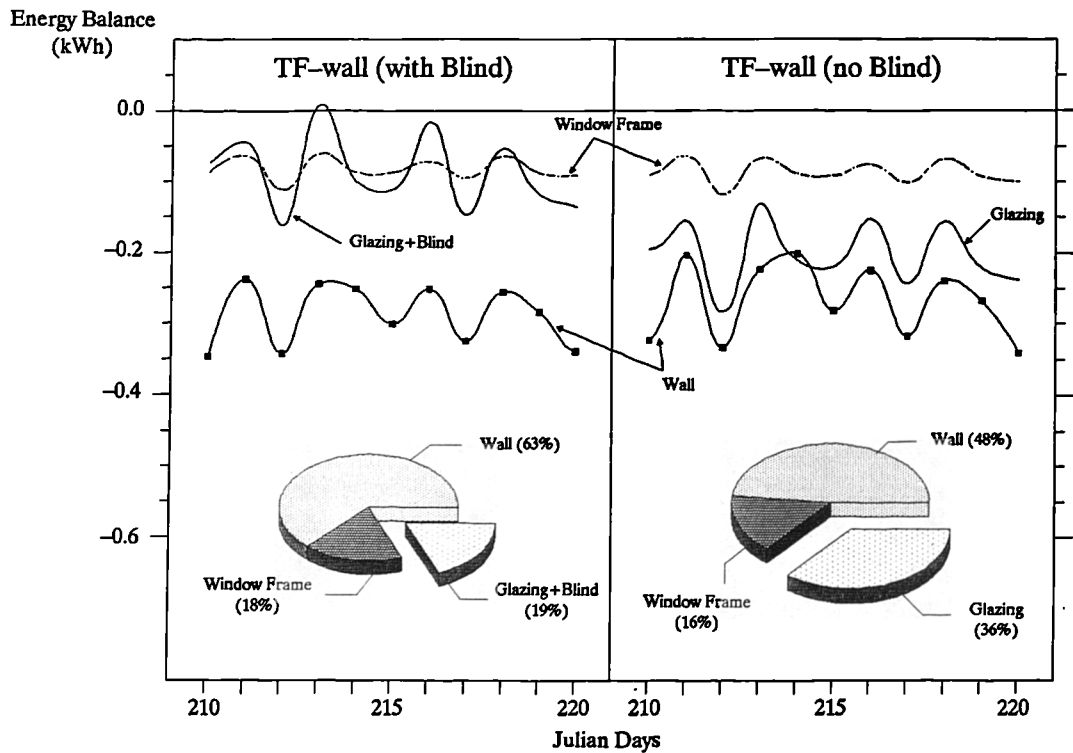


**Figure 7.29** A breakdown of the daily total net energy balance at the air nodes of cells 3 & 4, due to convective exchanges with the timber-frame wall components. Calculated by the “ESP” model for the period from 210 to 220 Julian.

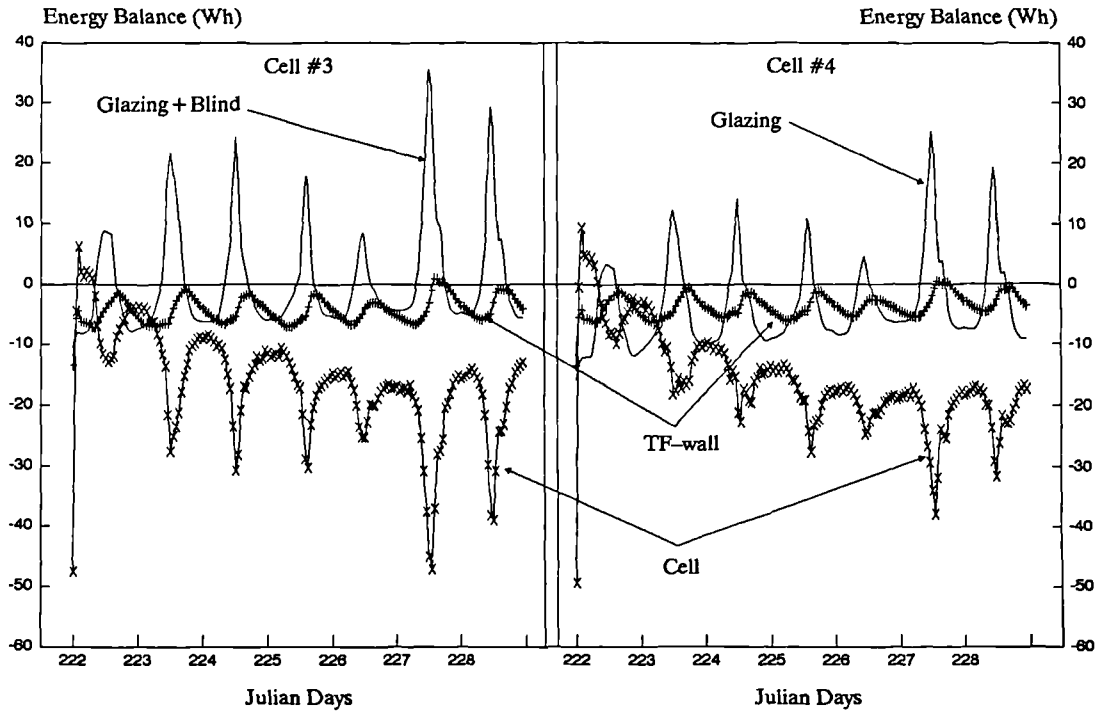


**Figure 7.30** Instantaneous energy balance at the air nodes of cells 3 & 4, due to convective exchanges with the test cell components (side walls, roof and floor), timber-frame wall components, and fenestration. Calculated by the “ESP” model for the free floating period of the experiment.

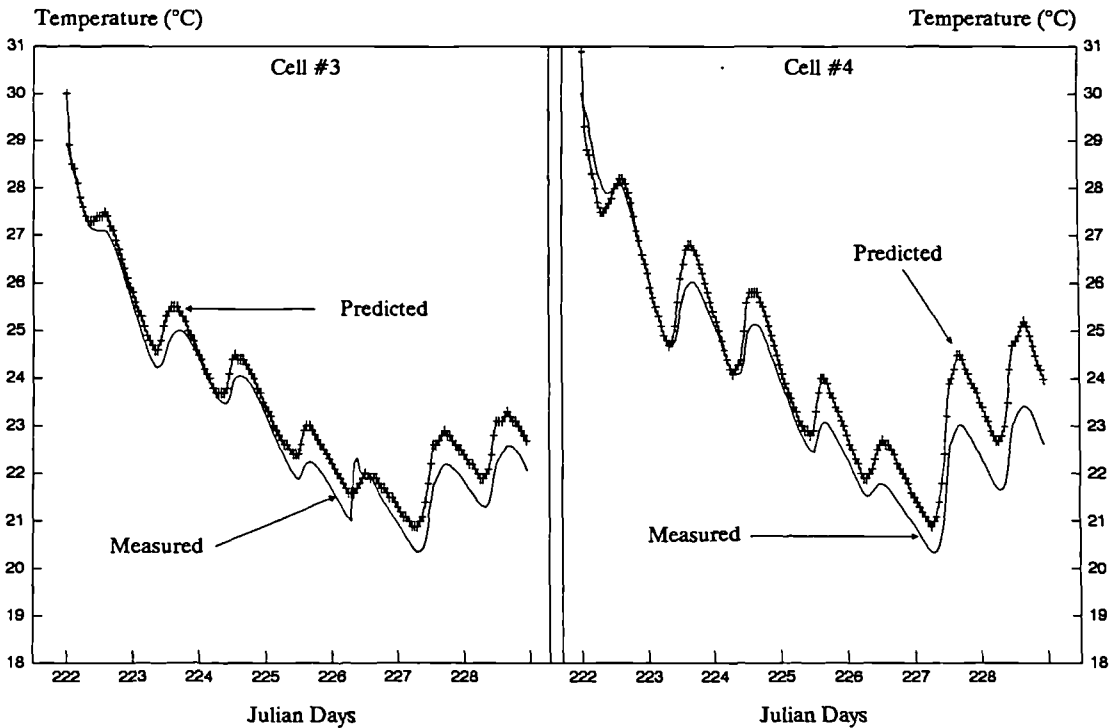


**Figure 7.31** Ambient temperature of cell 3 and cell 4 for the free floating period of the experiment, (August 10th to August 17th 1989). The predicted values are computed by the “ESP” program.

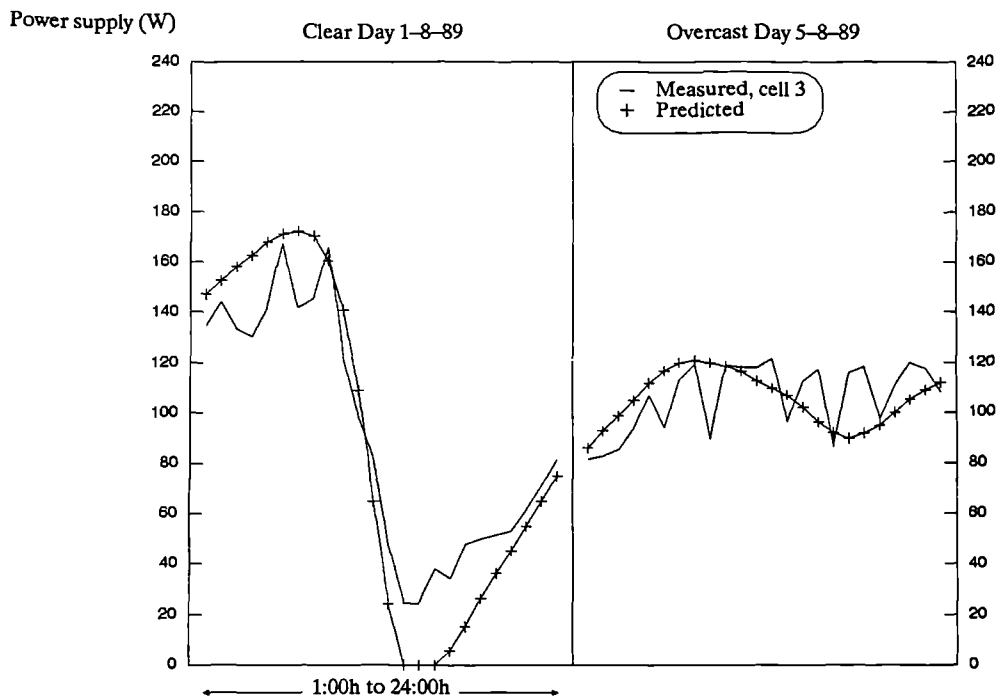


**Figure 7.32** Measured and predicted heating requirement of *cell 3* for clear and overcast days. Predicted values are from a simulation run using the “ESP” model.

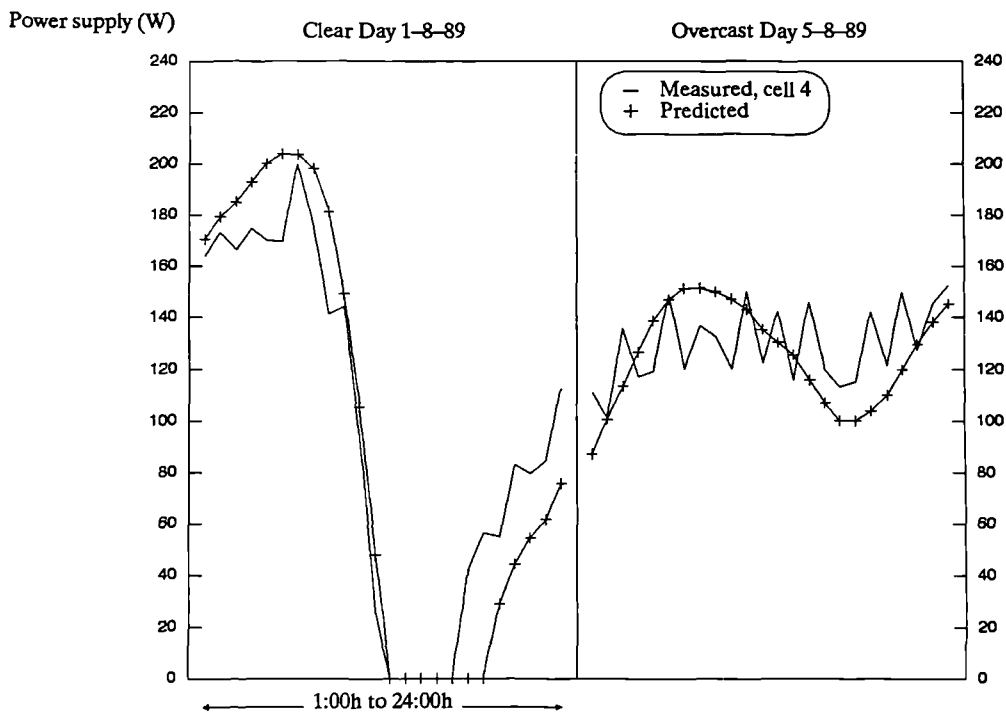


**Figure 7.33** Measured and predicted heating requirement of *cell 4* for clear and overcast days. Predicted values are from a simulation run using the “ESP” model.

The net energy balance at the air node due to heat exchanges with the opaque components of the TF-wall in cell 3 and cell 4 indicated that the wall has a time lag of 4 to 5 hours. (see the energy flow of the TF-walls in Figure 7.30). In comparison, the energy balance due to heat exchanges with the cell components indicated an energy flow which is almost instantaneous.

Figure 7.30 shows that net energy balance at the air node due to heat exchanges with the fenestration in cell 3 was lower than that of cell 4. The reason for this is that convective heat losses from the fenestration of cell 3 (glazing with blind) to the air node were lower in magnitude than from the fenestration of cell 4 (glazing only), and the reverse was true for heat gains.

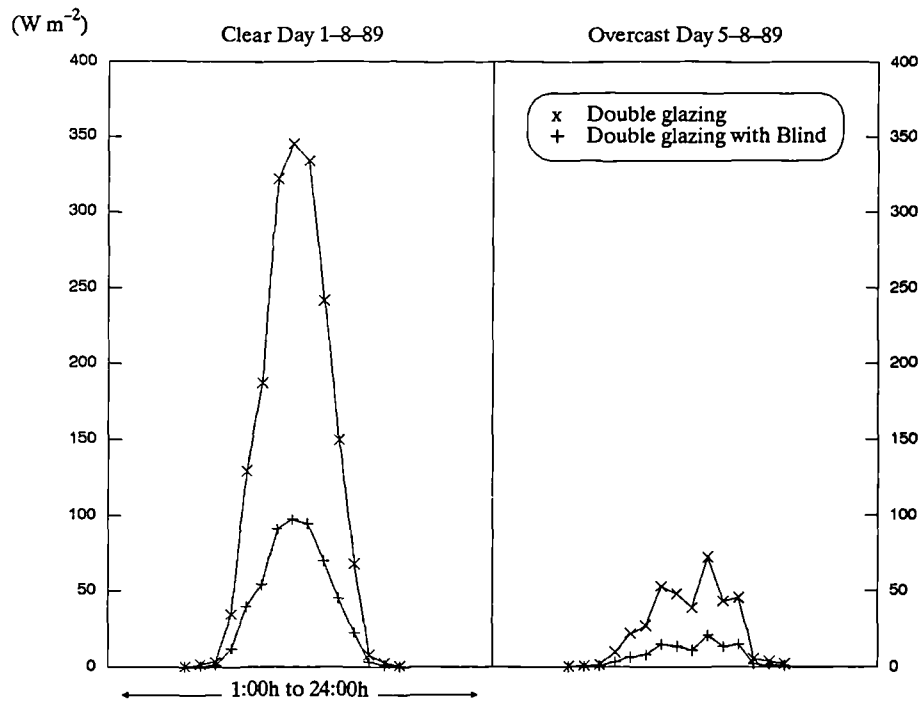
Comparison between the measured and ESP predicted ambient temperatures of the test cells (see Fig.7.31) show that predicted values have calculated standard errors of 1.1% and 2.2% on average for cell 3 and cell 4 respectively.

### *Results for Clear and Overcast Days*

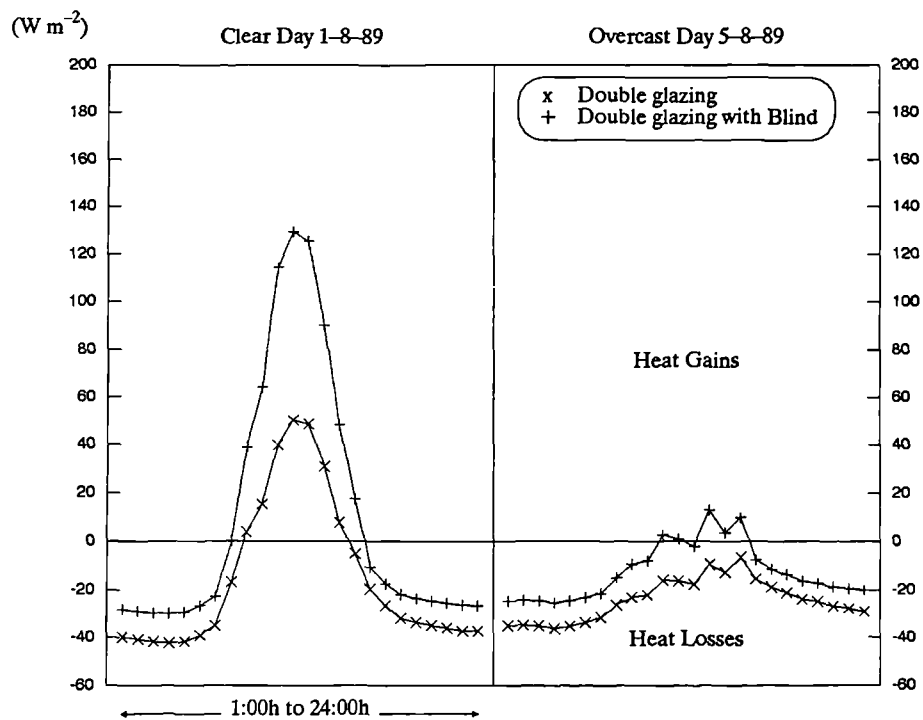
Comparisons between the measured and ESP predicted auxiliary heating of cell 3 for the clear and overcast days chosen previously in section 7.4.2 are shown in Figure (7.32). The same comparison but for cell 4 is given in Figure (7.33). From these figures, it is apparent that predicted hourly values follow a smoother path than the measured values, but consistent with their flow. Figure 7.32 shows that the total auxiliary heating of cell 3 is underestimated by 3% and 0.6% for the clear and overcast days respectively. Figure 7.33 shows that the total auxiliary heating of cell 4 is underestimated by 1.2% and 2.8% for the clear and overcast days respectively.

Figure 7.34 shows a comparison between the shortwave radiation fluxes transmitted through the fenestration of cell 3 and cell 4, for both clear and overcast days, calculated by the "Curtain" program. In either case (clear or overcast day) the total transmitted shortwave radiation per day, through the fenestration, is reduced by 70% due to the presence of the *blind*. (Note that the global insolation incident on the fenestration for both days were given previously in Figure 7.24).

Figure 7.35 compares the combined convective-longwave heat fluxes from the fenestration of cell 3 and cell 4, computed by the "Curtain" program, for both days. While shortwave radiation fluxes are reduced due to the blind, the convective-longwave heat fluxes are increased. The magnitude of convective-longwave heat flux increase, as calculated by the "Curtain" program, depends on the heat transfer coefficients at the surfaces of each layer in the fenestration. These are fully discussed in section 5.6.3 of chapter 5. The increase in heat gains of the fenestration of cell 3 is contributed to the inward-flow fraction of absorbed insolation as shown in Figure (7.36), and the reduction in heat loss is contributed to the fenestration U-value as shown in Figure (7.37).



**Figure 7.34** Shortwave radiation flux (solar) transmitted through the fenestration of *cell 3* and *cell 4*. Computed by the “Curtain” program for clear and overcast days



**Figure 7.35** Combined convective-longwave heat flux through the fenestration of *cell 3* and *cell 4*. Computed by the “Curtain” program for clear and overcast days.

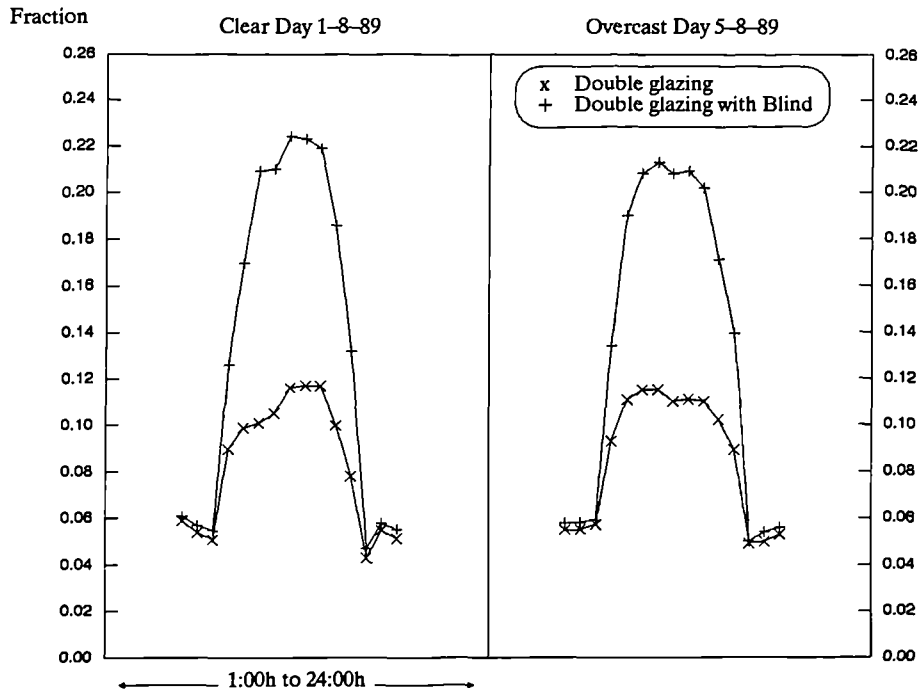


**Figure 7.36** Inward-flow fraction ( $N_i$ ) of absorbed insolation in the fenestration of *cell 3* and *cell 4* for clear and overcast days. Computed by the “Curtain” program.

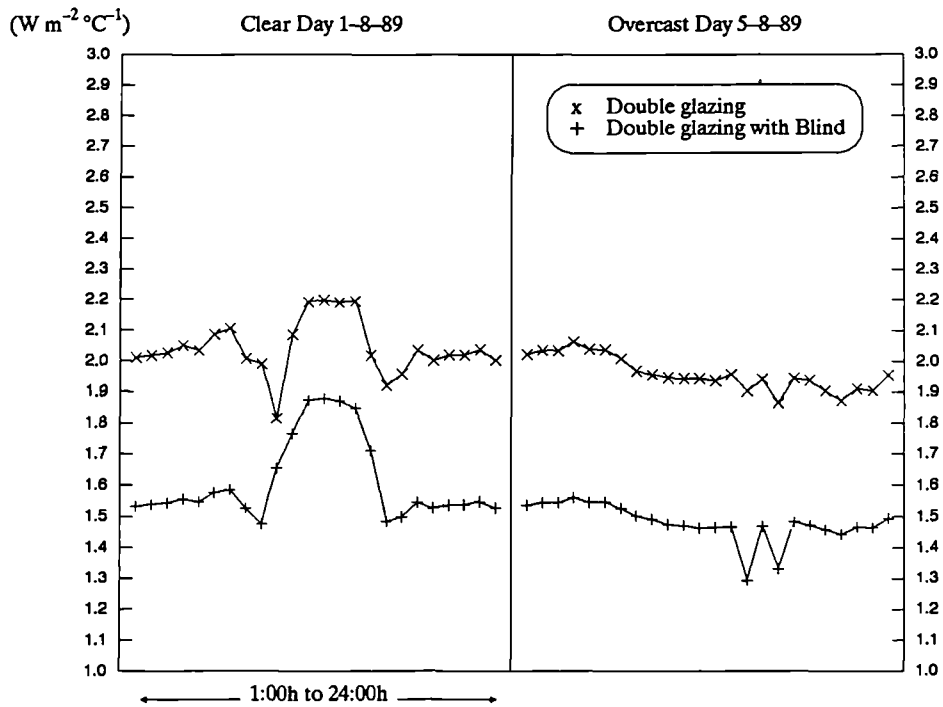


**Figure 7.37** U-value of the fenestration in *cell 3* and *cell 4* for clear and overcast days. Computed by the “Curtain” program.

**Table 7.13** Standard deviation and relative error percentages in the simulated temperatures of the fenestration layers in *cell 3* and *cell 4* for the stated periods. †

Analysis period	CURTAIN model					ESP model ‡			
	T <sub>b3</sub>	T <sub>go3</sub>	T <sub>go4</sub>	T <sub>gi3</sub>	T <sub>gi4</sub>	T <sub>b3</sub>	T <sub>go3</sub>	T <sub>go4</sub>	T <sub>gi4</sub>
29-7 to 16-8 (all data)	1.8 6.4%	1.1 5.9%	1.4 12.0%	2.2 8.8%	1.7 6.7%	2.0 7.3%	1.7 9.5%	1.9 10.1%	2.6 9.5%
29-7 to 8-8 (steady-state)	1.7 5.5%	1.0 5.1%	0.9 11.3%	2.2 8.3%	0.9 3.5%	1.6 5.3%	1.5 8.0%	1.4 7.1%	1.5 5.1%
9-8 to 16-8 (free floating)	2.0 8.0%	1.2 7.0%	1.1 15.0%	2.6 11.4%	1.1 5.0%	1.8 7.5%	1.8 10.7%	1.7 9.6%	1.7 7.3%
1-8 (clear day)	2.1 6.5%	1.3 6.5%	1.4 7.0%	2.8 9.5%	1.1 3.7%	5.2 17.0%	2.2 11.0%	2.2 10.6%	2.4 8.1%
5-8 (overcast day)	0.9 3.1%	0.6 2.8%	0.4 2.1%	1.2 5.1%	0.5 2.0%	1.3 4.7%	0.6 3.1%	0.6 2.8%	0.5 1.7%

† The standard deviation is calculated for the difference between measured and calculated parameters. Error percentage is calculated by dividing the standard deviation over the average of simulated parameters.

‡ The ESP results are taken from the first run, where the fenestration was considered as transparent multi-layered construction.

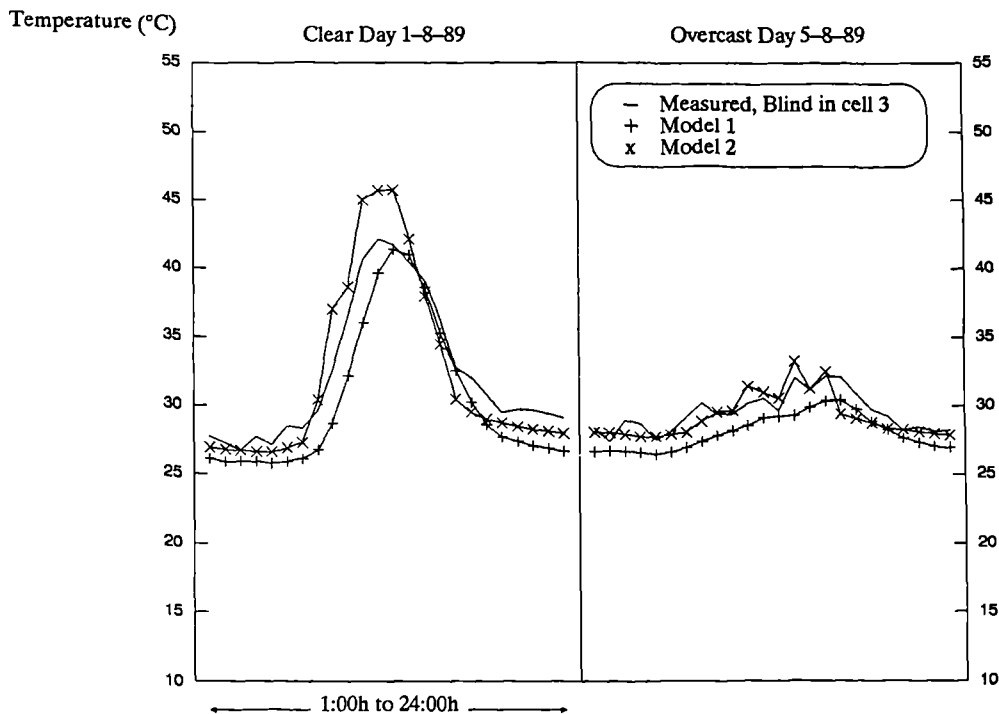


**Figure 7.38** Measured and predicted temperature of the *Passys Blind* in *cell 3* for a clear and overcast days. Model 2 refers to results from the “Curtain” program, and model 1 refers to results from the “ESP” simulation run. Note that the ESP predicted values are for the inner layer of the fenestration which include both properties of the glass and the blind (see section 7.5.1 for details).

The “Curtain” program results also include the temperature of fenestration layers in cell 3 and cell 4. These are compared with measured values and with simulated values by the ESP program for the whole period of experiment.

Error analysis in predicted temperatures for the whole period of experiment, the steady-state period, the free floating period and for the clear and overcast days are shown in Table 7.13. In general predicted temperatures by both programs are within acceptable range of accuracy.

Figures 7.38 shows the measured temperature of the Passys blind compared with calculated values by the “Curtain” and by ESP programs for the clear and overcast days. Comparison between measured and predicted temperatures of the inner pane of the glazing in cell 3 and cell 4 are shown in Figure 7.39 and Figure 7.40 respectively, for clear and overcast days. And Figures 7.41 and 7.42 show the measured and predicted temperatures of the outer glass pane in cell 3 and cell 4 respectively, again for both clear and overcast days.

From Figures 7.39 and 7.40, the effect of the blind on the temperature of the inner glass is apparent. In the absence of solar radiation, the blind in cell 3 acts as a barrier between the cell ambient temperature and the temperature of the outer glass, thus the temperature of the inner glass is lower than that of cell 4. In the presence of solar radiation, the temperature of the inner glass in cell 3 is higher than that of cell 4 due to extra absorption of solar radiation reflected off the blind surface. The same phenomena apply to the outer glass, as can be seen from Figures 7.41 and 7.42.

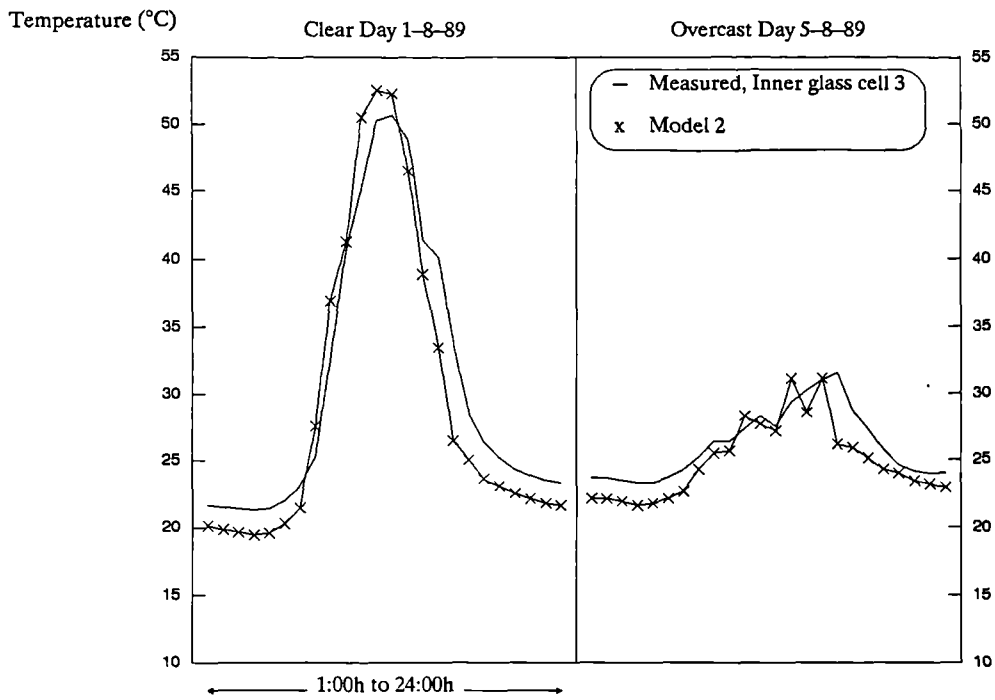


**Figure 7.39** Measured and predicted temperature of the *inner glass panel* in *cell 3*, for a clear and overcast days. Model 2 refers to results from the “Curtain” program.

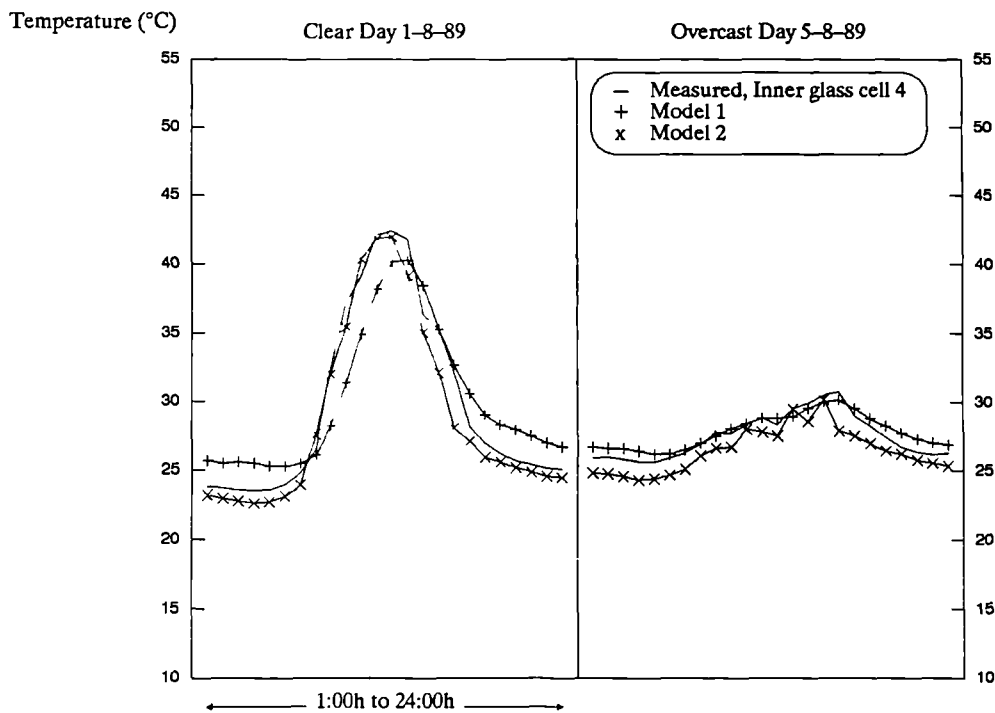


**Figure 7.40** Measured and predicted temperature of the *inner glass panel* in *cell 4*, for a clear and overcast days. Model 1 refers to results from the “ESP” simulation run and model 2 refers to results from the “Curtain” program.

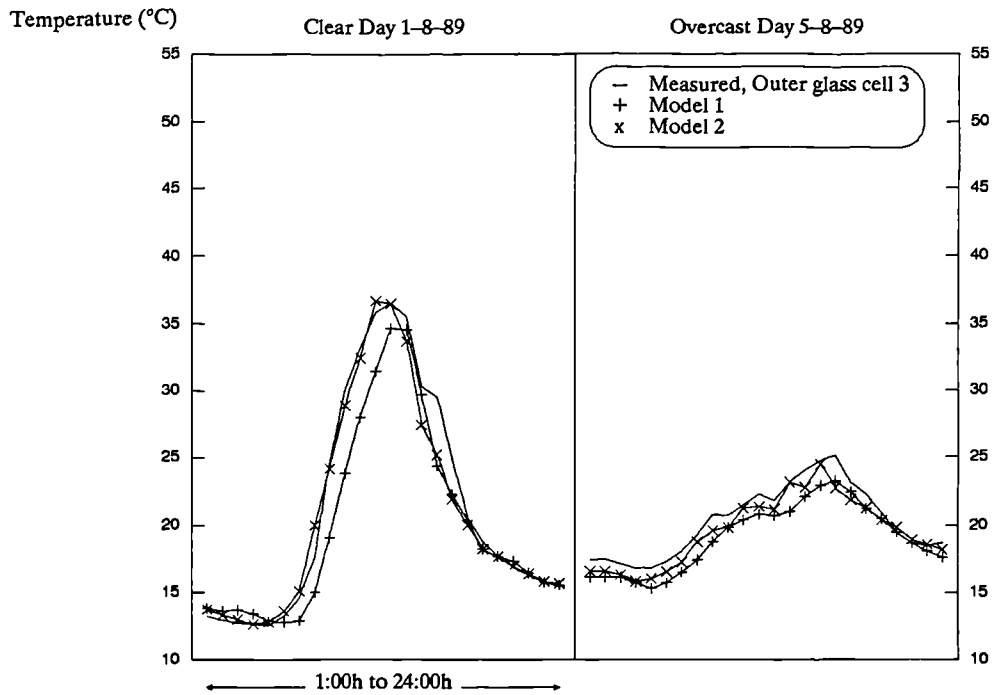


**Figure 7.41** Measured and predicted temperature of the *outer glass panel* in *cell 3*, for a clear and overcast days. Model 1 refers to results from the “ESP” simulation run and model 2 refers to results from the “Curtain” program.

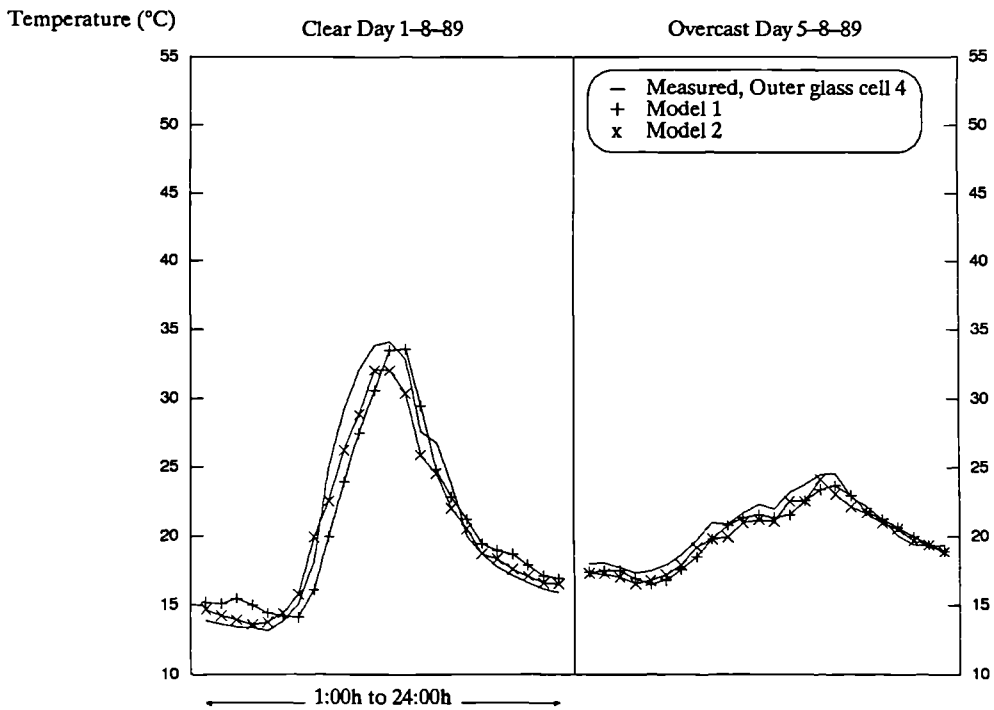


**Figure 7.42** Measured and predicted temperature of the *outer glass panel* in *cell 4*, for a clear and overcast days. Model 1 refers to results from the “ESP” simulation run and model 2 refers to results from the “Curtain” program.

## 7.6 Conclusions

---

The main steady-state characteristics of the test cells, one fitted with glazing and the *Passys* blind and the other with glazing only, have been derived from the experiment conducted in this chapter with accuracy of better than 10%. From the results it may be inferred that the heat transmission coefficient of the blind shaded fenestration is about  $1.1 \text{ (W K}^{-1}\text{)}$  lower than the unshaded glazing. The unshaded fenestration has a vertical solar aperture which is  $0.17 \text{ (m}^2\text{)}$  greater than the blind shaded fenestration.

Thus the closed window blind (in cell 3) can reduce the daily average heating requirement for the whole cell by 11% as compared with the identical cell without the blind (cell 4). Also the closed window blind can reduce solar heat gain to cell (3) by up to 34% as compared with cell (4).

New values of the UK wall characteristics in cell 4 ( $\hat{U}_4$  and  $\hat{A}_4$ ) have been determined which are quite different from those derived from previous calibration experiment. The difference is believed to be due to air leakage from the cell fenestration at the calibration experiment.

The outcome of study in this chapter also provided confidence in computer modeling of the test cell energy performance. The simulation results of the "Curtain" program, have shown good agreement with measured temperatures of the fenestration layers.

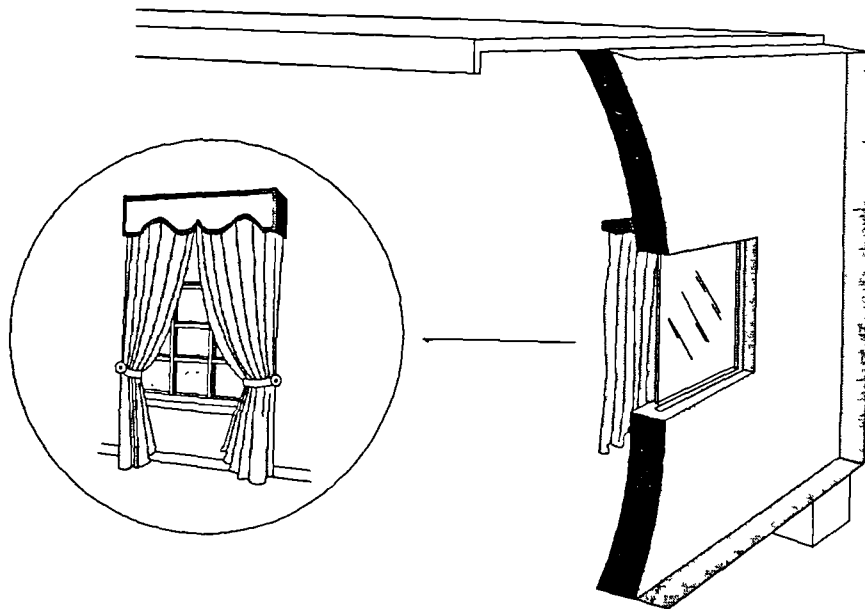
The ESP simulation results have also shown good agreements with measured parameters like the fenestration temperatures and auxiliary heating of the cells. However, future upgrading of the model should cover the best way of including (or defining) fabric shading devices with glazing; and probably reducing the task of preparing the huge amount of data files required for the simulation.

## 7.7 References

---

- Baker P. (1989) Private communications. Energy Studies Unit, Strathclyde University, Glasgow, Scotland.
- Bridges A., Clarke J. & Sussock H. (1981) "Computer Graphics for Building Energy Analysis", *Advanced Engineering Software*, v3 (2).
- Clarke J. (1982) "Computer Modelling of Passive Solar Architecture", *Proc. Passive Solar Architecture Conf.*, Cannes, Dec. 1982.
- Clarke J. (1985) Energy Simulation in Building Design. Adam Hilger Ltd., Bristol, UK.
- Clarke J. & Forrest I. (1978) "Validation of ESP Against Test Houses", *ABACUS Occasional Paper*.
- Clarke J., Hand J. & Strachan P. (1990) "ESP : A Building and Plant Energy Simulation System", version 6, *ESRU Manual U90/1*, Energy Simulation Research Unit, University of Strathclyde, Glasgow, UK.
- Cools C. & Gicquel R. (Eds) (1988) "The Project Passys", EMP, Sophia Antipolis, France.
- Dijk van. H. (1990) "The Parameter Identification Method MRQT", version 4.0, *User Guide*, TNO Institute of Applied Physics, Delft, The Netherland.
- Gough M. (1984) "ESP : Comparison with Monitored Direct Gain Test Cells", *BRE Report*, IEA Task 8, Building Research Establishment, Garston, England.
- Guy A. (1991) "Passys Test Components : Timber-Frame Wall, Common Description", *Internal Report*, Revision Oct. 1991, Pilkington Glass Ltd., UK.
- Knorr K. (1986) "Determination of the Thermal and Solar Properties of Metalized Shade, Type Versol", Report No. 326.207, TNO Institute of Applied Physics, Delft, Holland.
- Littler J. (1983) "Review of Some Promising Simulation Models for Passive Solar Design", *Sun at Work in Britain*, 16, June 1983.
- Strachan P., Baker P., Twidell J., Clarke J., Guy A. & Pinney A. (1988) "UK Participation in the Passys Project", *Euroforum Conference*, Saarbrucken, Sep. 1988.
- Wouters P. & Vandaele L. (Eds) (1990) "The Passys Test Cell", Subgroup Instrumentation final report Part 1, *Passys Document 114-89-PASSYS-INS-033*, BBRI, Brussels, Belgium.

# Chapter 8



## 8. TEST SITE EXPERIMENTS WITH A DOMESTIC CURTAIN

### 8.1 Introduction

---

Curtains are probably the most used form of indoor window coverings. They provide privacy, glare control, and aesthetic value. Curtains can also reduce summer heat gains and winter heat losses through fenestration, thus saving energy and improving comfort levels within living spaces. Designers must be able to assess the contribution that different curtain types and configurations will make to energy savings and comfort levels. These are better determined experimentally but the time and cost involved and the diversity of curtain fabric types give precedence to simulation models and simple design tools. Chapter 5 of this thesis provided the theoretical bases to determine the effectiveness of curtains in reducing heat gains and heat losses through windows.

Initially, the aim of the work of this chapter was to conduct side-by-side experiments on the three domestic curtains described in chapter 5 using the “Passys” test site facilities at Strathclyde University campus. (These facilities; i.e. the test cells, instrumentation, data acquisition and the south walls; have been described in section 7.2 of the previous chapter). However due to a tight time schedule, of the Passys project, experiments were confined to a single curtain fabric, (82% Dralon, 18% Nylon, light cream colour), fitted on a double glazed window. Unlike the experiments conducted on the previous chapter, one test cell was available for the curtain experiments (cell 2). The test cell was fitted with the “reference wall” (prefabricated concrete, with 100mm rigid foam insulation, incorporating a window with 1.2m<sup>2</sup> of double glazing with wooden frame).

From the experimental work of this chapter, the thermal performance characteristics of the “reference wall”, with and without the curtain, were determined. The main characteristics of this component are the heat loss coefficient ( $\hat{U}$ ) and the solar aperture ( $\hat{A}$ ).

The test methodology described in the previous chapter was used for this study. Results from this experiment are analysed over the whole period of experiment and for typical clear and overcast days. Comparisons between measured and predicted results by the “ESP” and the “CURTAIN” models are also presented.

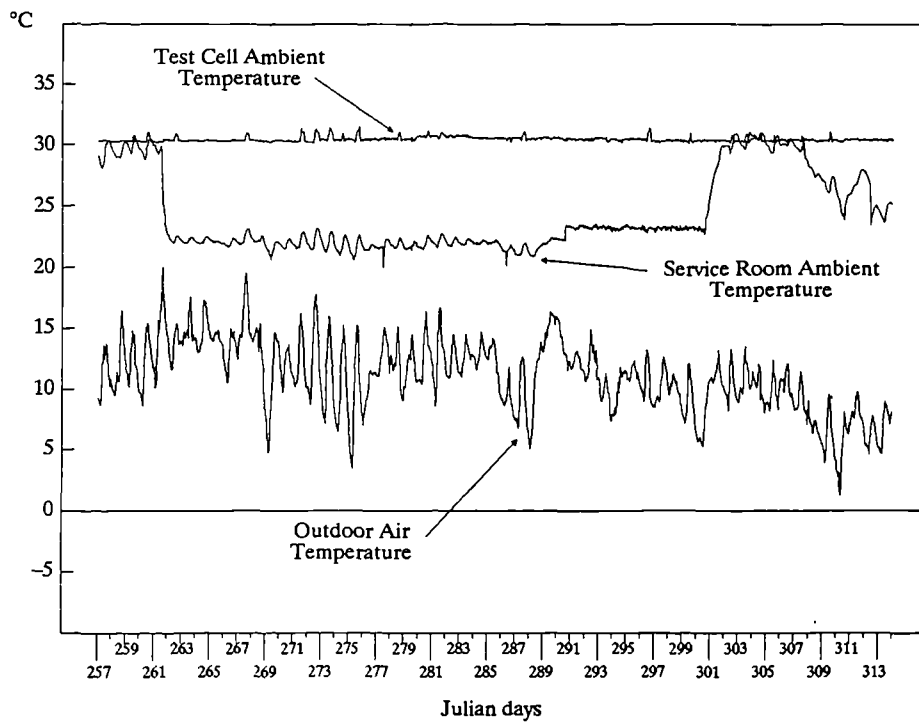


**Figure 8.1** Hourly ambient temperatures measured for the period from 257 to 313 Julian. The test cell temperature is taken as the average of air temperatures at 7 locations in the test room, while the service room temperature is taken from one sensor at the centre of the room.

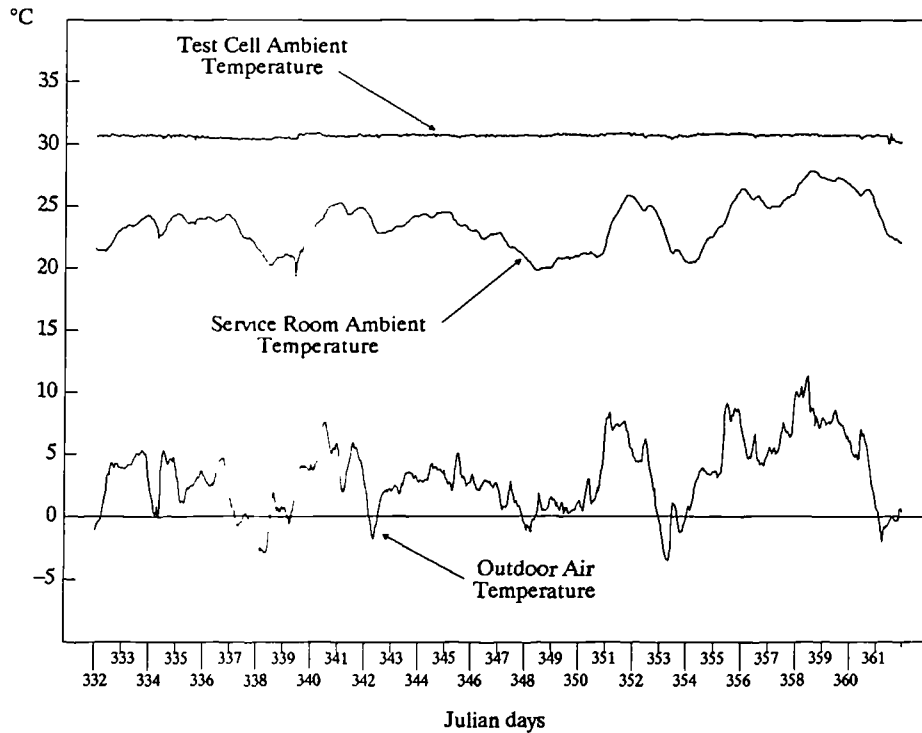


**Figure 8.2** Hourly ambient temperatures measured for the period from 332 to 361 Julian inclusive. The curtain was fitted throughout this period.

### 8.3 Analysis of Captured Data Sets

---

Climatic and cell data for the period from September 14<sup>th</sup> to November 9<sup>th</sup> (257 to 313 Julian) 1989 were obtained from calibration experiments conducted by the Passys project. The data are used to determine the performance characteristics of the test cell without curtain (see section 8.3.1 below). All climatic and cell data for the period of the curtain experiment (332 to 361 Julian) were valid. However, due to random errors, the fenestration temperature data were valid for the first week only, i.e. from Nov.28<sup>th</sup> to Dec.4<sup>th</sup> 1989.

Figure 8.1 shows the hourly outdoor air temperature and the ambient temperatures of the test room and the service room of cell 2 for the period 257–313 Julian. Figure 8.2 shows the hourly outdoor air temperature and the ambient temperatures of the test room and the service room of cell 2 for the period of the curtain experiment (332–361 Julian). The ambient temperature of the test room in Figures 8.1 and 8.2 is an average of seven readings taken at various positions within the cell as given in Table 7.10 of the previous chapter. The effective setpoint temperature of the cell was found to be 30.1°C for both periods.

From the first period (Fig.8.1), the outdoor air temperature swings ranged from a minimum of 1.7°C to a maximum of 11.7°C with an average of 5.2°C for the whole period. In comparison the minimum and maximum outdoor temperature swings from the second period (Fig.8.2) were 1.3°C and 6.1°C respectively with an average of 3.7°C for the whole period. From these results it can be inferred that the first period encountered more clear sky conditions than the second. This is more clearly shown in Figures (8.3 & 8.4). These figures give insolation data (24h averages of global, diffuse horizontal and global vertical insolation) recorded at the test site for the periods of the calibration and the curtain experiments respectively.

Daily total solar energy, incident on the test cell window, ranged from 38 to 5168 (Wh m<sup>-2</sup>) in the period of the calibration experiment with an average of 1797 (Wh m<sup>-2</sup>) over the whole period. In comparison, the daily total solar energy incident on the test cell window in the period of the curtain experiment ranged from 11 to 1985 (Wh m<sup>-2</sup>) with an average of 523 (Wh m<sup>-2</sup>) over the whole period.

Hourly wind speed and wind direction rose for the period of the calibration experiment are shown in Figure 8.5. The average wind speed for the whole period was 2.87 (m s<sup>-1</sup>). The wind direction was dominantly west and south-west oriented. 77% of the recorded wind directions were in the range of 165° to 285°, 73% of which have corresponding wind speeds in the range of 0 to 4 (m s<sup>-1</sup>).

Figure 8.6 shows the hourly wind speed and wind direction rose for the period of the curtain experiment (332–361 Julian). The average wind speed for the whole period was 2.6 (m s<sup>-1</sup>). Wind direction data show variable orientation, however 22% of recorded wind directions were in the range of 30° to 45°.

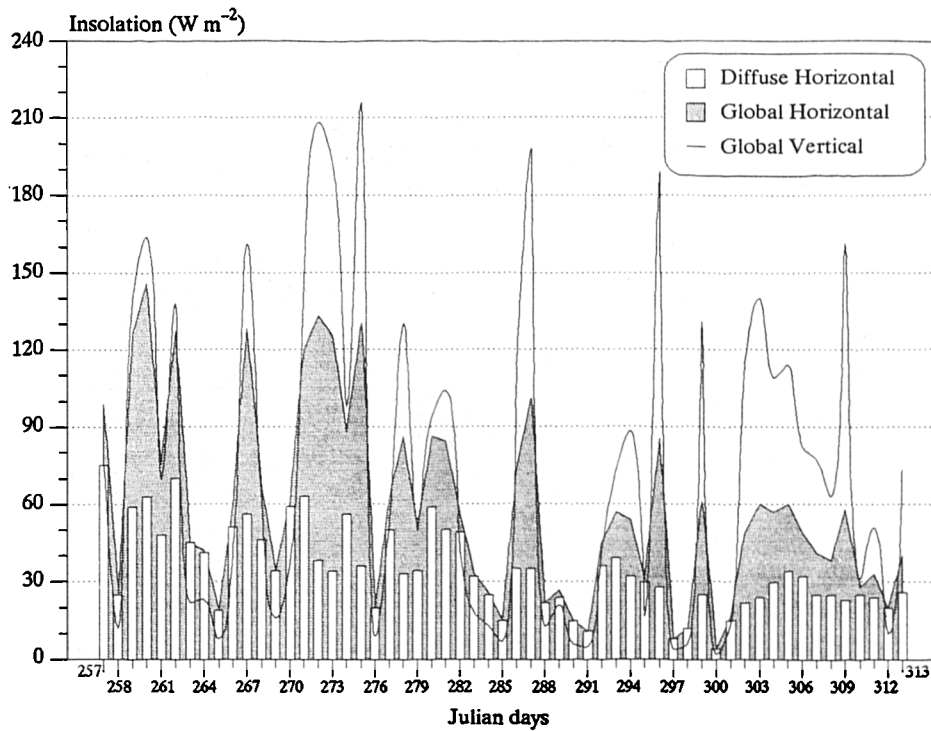


**Figure 8.3** Average daily insolation (global horizontal, diffuse horizontal and global insolation on south facing vertical surface) measured at the *Passys* test site for the period from 257 to 313 Julian.

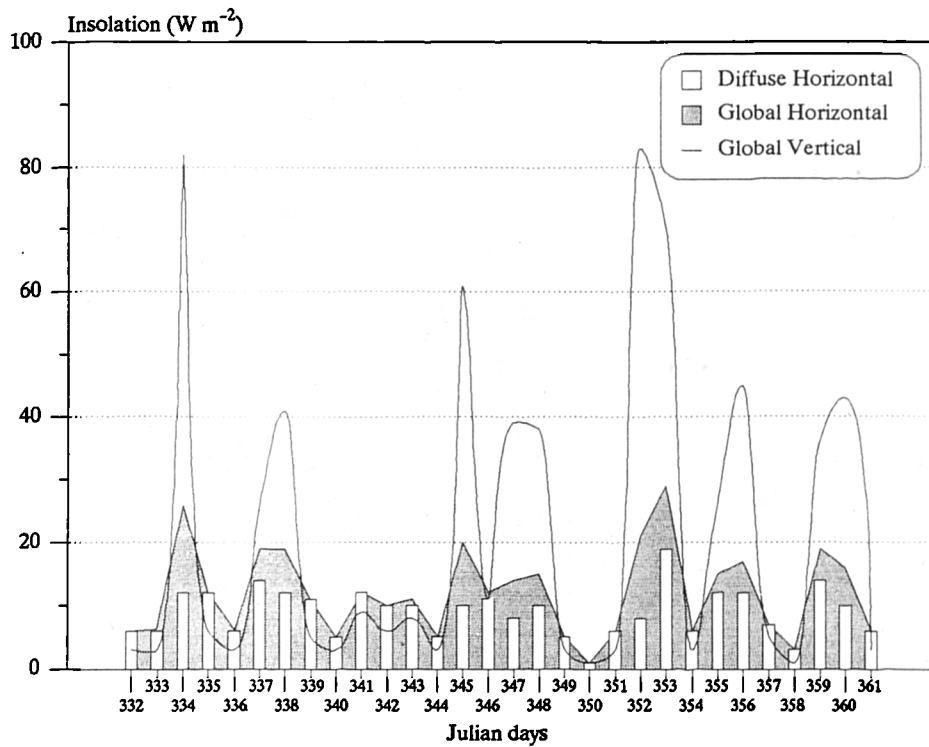


**Figure 8.4** Average daily insolation (global horizontal, diffuse horizontal and global insolation on south facing vertical surface) measured at the test site for the period from 332 to 361 Julian.

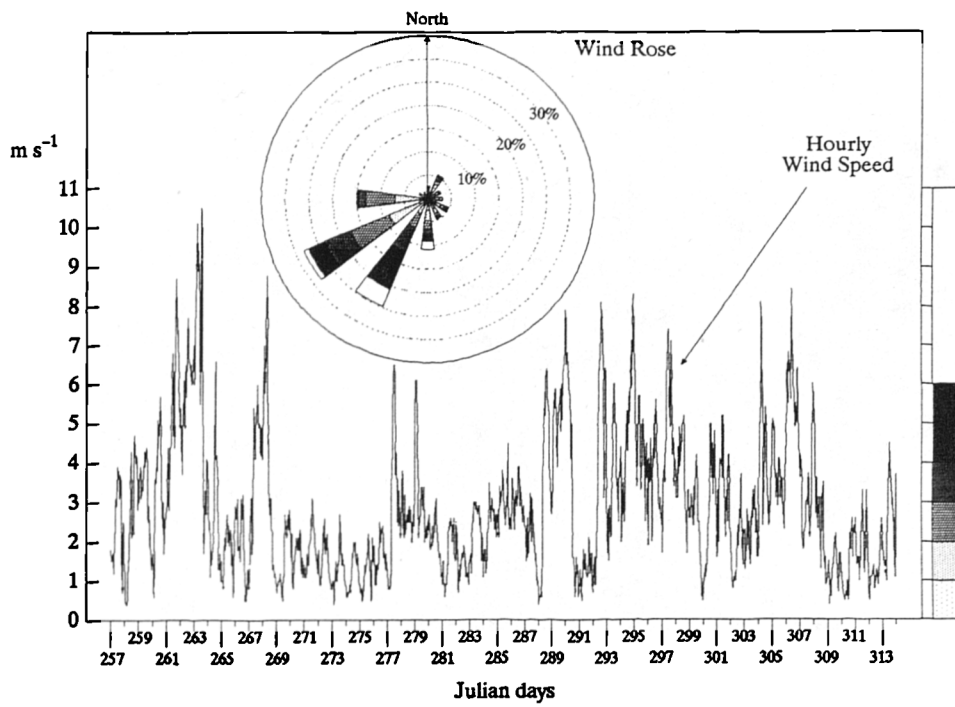


**Figure 8.5** Wind speed and direction measured at the *Passys* test site for the period from 257 to 313 Julian. Wind rose represents wind direction frequency with 30° bins, (i.e. -15° to 15°, 15° to 45°, etc).

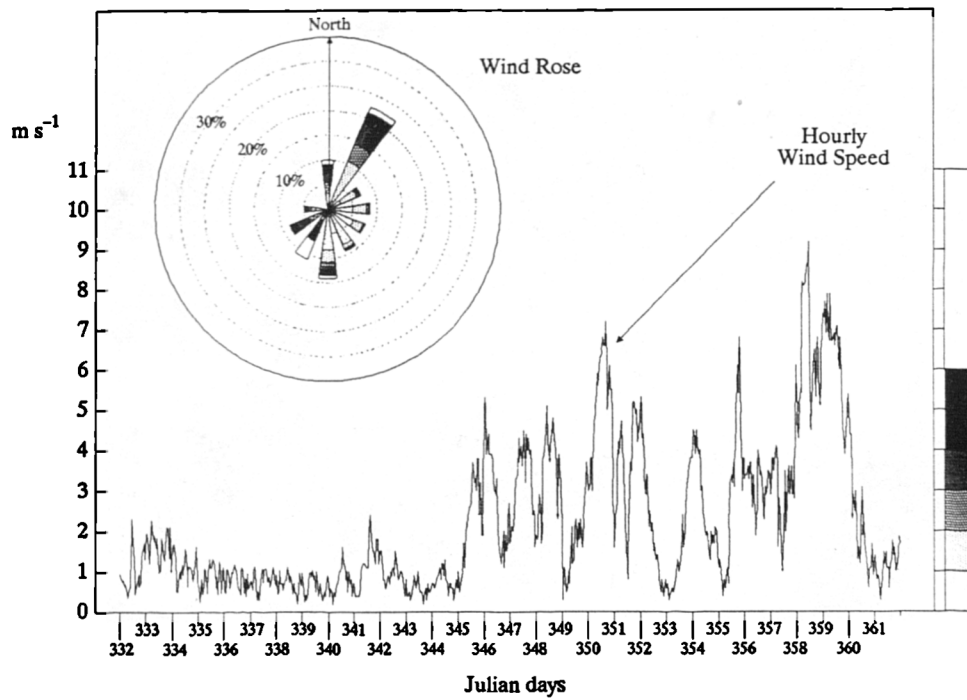


**Figure 8.6** Wind speed and direction measured at the test site for the period from 332 to 361 Julian inclusive. (curtain was fitted throughout this period)

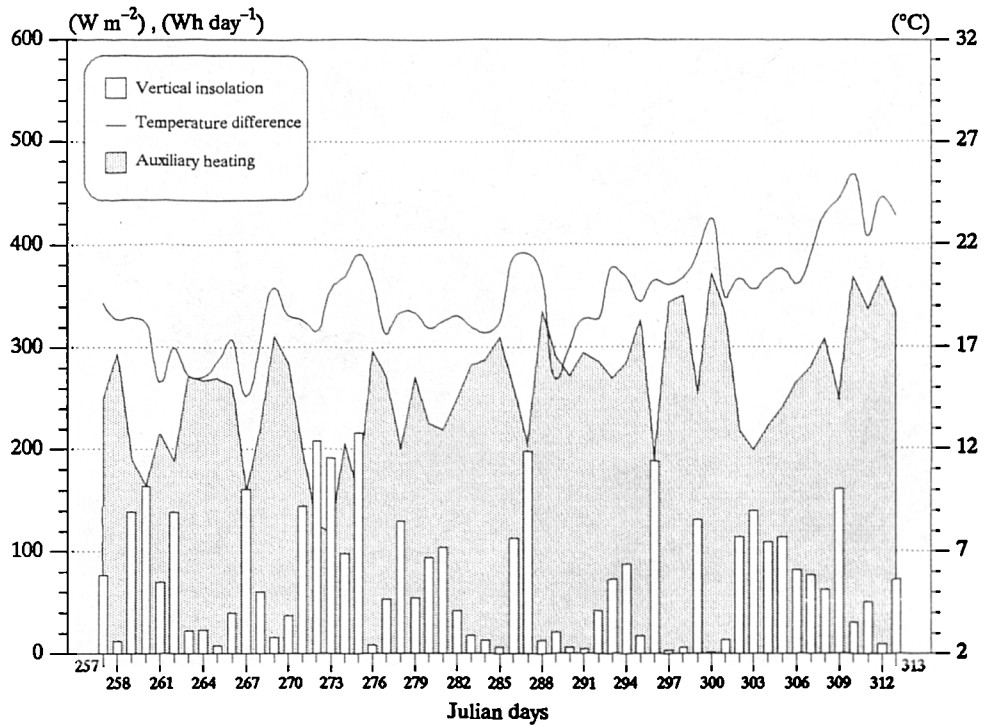


**Figure 8.7** Average data (over 24h) of global vertical insolation ( $W m^{-2}$ ), auxiliary heating of the cell (Wh per day), and the difference between the cell ambient and outdoor air temperatures ( $^{\circ}C$ ). Measured at the *Passys* test site for the period from 257 to 313 Julian.

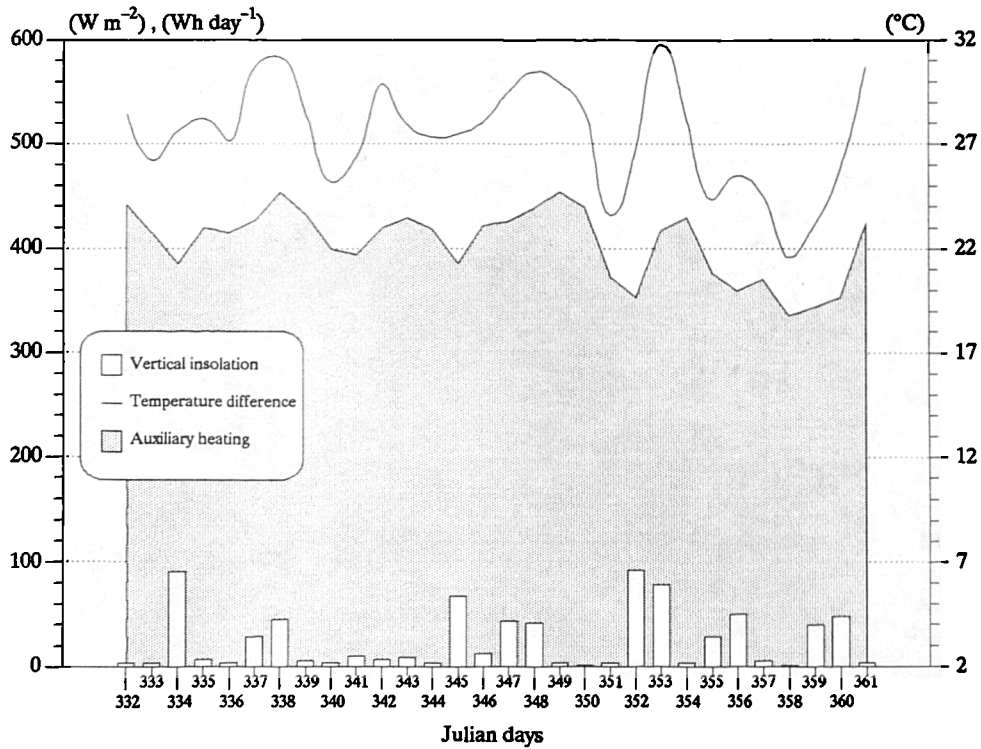


**Figure 8.8** Average data (over 24h) of global vertical insolation ( $W m^{-2}$ ), auxiliary heating of the cell (Wh per day), and the difference between the cell ambient and outdoor air temperatures ( $^{\circ}C$ ). Measured at the test site for the period from 332 to 361 Julian with the curtain fitted.

Figures 8.7 and 8.8 show the daily average auxiliary heating of the test cell ( $\text{Wh day}^{-1}$ ) measured for the periods of calibration and curtain experiments respectively. The figures also show daily average global vertical insolation and the difference between the cell ambient and outdoor air temperatures (24h averages).

Daily total auxiliary heating of the test cell ranged from 2.84 to 8.92 (kWh) in the period of the calibration experiment (cell without curtain) with an average of 6.24 (kWh) over the whole period. In comparison, the daily total auxiliary heating of the test cell with curtain (for the period from 332 to 361 Julian) ranged from 8.07 to 10.9 (kWh) with an average of 9.72 (kWh) over the whole period.

### 8.3.1 Steady-state Performance Characteristics of the Passys Test Cell (With and Without Curtain)

The steady state model discussed in section 7.3.2 of the previous chapter has been used to derive the performance characteristics of the test cell, namely the heat loss coefficients,  $\hat{U}_{2c}$  of test cell 2 with the curtain installed and  $\hat{U}_2$  ( $\text{W } ^\circ\text{C}^{-1}$ ) for the test cell without curtain; and the solar apertures,  $\hat{A}_{2c}$  and  $\hat{A}_2$  ( $\text{m}^{-2}$ ) related to the vertical global insolation  $G_v$ . The steady-state energy balance for each case is given in the linear relation between the measured response of the test cell ( $Q/\Delta T$ ) and the climatic correlation ( $G_v/\Delta T$ ) as given in Eq.8.1 and Eq.8.2.

$$(Q_{2c}/\Delta T_{2c}) = \hat{U}_{2c} - \hat{A}_{2c} G_v/\Delta T_{2c} \quad \{8.1\}$$

$$(Q_2/\Delta T_2) = \hat{U}_2 - \hat{A}_2 G_v/\Delta T_2 \quad \{8.2\}$$

where  $\Delta T$  is the difference between the ambient temperature of the test cell and the outdoor air temperature with the subscripts 2c and 2, respectively, denote properties of test cell 2 fitted with the curtain and test cell 2 without curtain; and the auxiliary heat input to the cell,  $Q$ , is modified for any difference in temperature between the test room and the service room,  $\Delta T_{\text{int}}$ , using the following equation:

$$Q = Q_{\text{aux}} - \hat{U}_{\text{int}} \Delta T_{\text{int}} \quad \{8.3\}$$

where  $Q_{\text{aux}}$  is the measured auxiliary heating of the cell; and  $\hat{U}_{\text{int}}$  the constant cell to service room heat loss coefficient ( $\hat{U}_{\text{int}} = 2.9 \text{ W}^\circ\text{C}^{-1}$ ) was determined from calibration experiments using the *opaque calibration wall* (see section 7.3.3 of the previous chapter). Note that the parameters of Eq.8.1 and Eq.8.2 are 24h averages.

The heat loss coefficients and solar apertures were derived by a linear regression analysis using Lotus-123<sup>®</sup> software. Regression analysis over 30 and 57 average daily values (for the periods of the experiment with and without curtain respectively) were performed. The data were then assorted, by excluding the data with maximum residual, and further regressions were performed. Results are listed in Table 8.1 and plotted in Figure 8.9 for both cases.

**Table 8.1** Steady-state characteristics of test cell 2. †

	with Curtain	no Curtain
Heat loss coefficient, $\bar{U}$ ( $\text{W } ^\circ\text{C}^{-1}$ )	14.52	15.80
Standard error	0.24	0.74
Solar aperture, $\hat{A}$ ( $\text{m}^2$ )	0.57	0.81
Standard error	0.05	0.03
Correlation R value	0.93	0.97

† In both cases the cell was fitted with double glazing window in the Reference wall. Regression with the curtain fitted is based on 21 average daily parameters. For the case with no curtain on, the regression is based on 51 parameters.

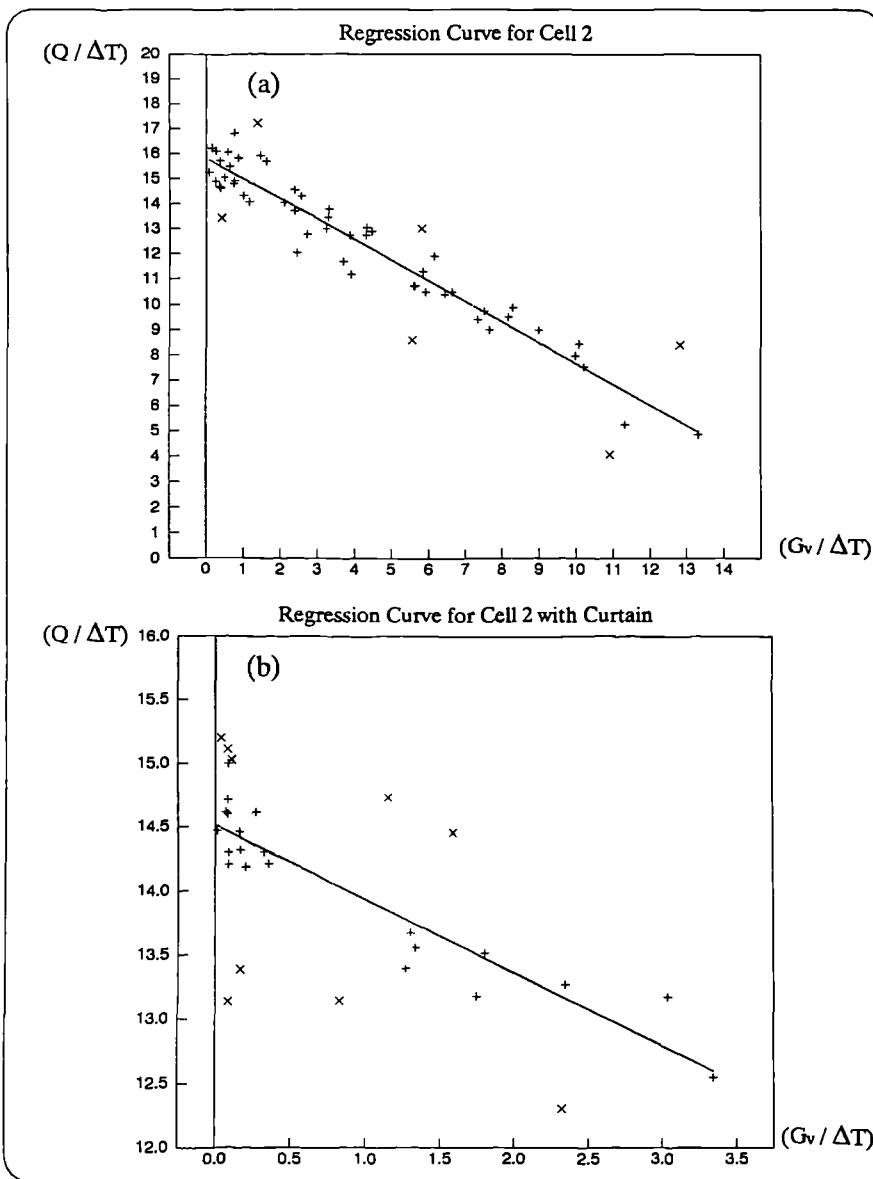


**Figure 8.9** Regression curves for (a) cell 2 fitted with glazing only, and (b) cell 2 fitted with glazing and the curtain. The average daily parameters marked "x" have large residual values.

The regression results (Table 8.1) show that the heat loss coefficient and solar aperture of the test cell, fitted with the curtain, are respectively 8% and 29.6% less than those of the test cell without curtain.

Figure 8.10 shows a comparison between the measured and calculated auxiliary heating requirement of test cell 2 without curtain using the correlation coefficients given in Table 8.1. The measured and calculated heating requirement of the test cell fitted with the curtain are compared in Figure 8.11. Note that calculated values in Figures 8.10 & 8.11 include heat flows between the test room and the service room in both cases.

The calculated average daily heating of the test cell with no curtain fitted (Fig.8.10), gave a standard error of 8% over the period from 257 to 313 Julian. In comparison, the calculated auxiliary heating of test cell 2 fitted with curtain had a standard error percentage of 4% over the period from 332 to 361 Julian.

Analysis of measured and predicted parameters concerning the thermal performance of the curtain-shaded fenestration for clear and overcast days (334 and 336 Julian respectively) are detailed later in section 8.4. The two days chosen for the analysis were based on the solar data shown in Figure 8.4 and on the fact that measured fenestration temperatures were only valid for the first week of the curtain experiment.

### 8.3.2 Test Cell Parameters Identification: (MRQT program)

The Passys recommended program "MRQT" was used to determine the transmission coefficients and solar apertures of the test cell with and without the curtain. The program performs iterative solution of a pre-defined dynamic thermal model of the test cell components. The model used with this program is called "LUMPA" (abbreviation for lumped parameters of the Passys test cell). The model consists of series of resistances and capacitances, similar to the nodal diagram shown in Figure 7.11 of the previous chapter. Full description of the model and the MRQT program are found in Dijk (1990). The program had been used with data from the blind experiment (see chapter 7), and result were reasonable but not as expected from such a sophisticated program.

The LUMPA thermal model handles 30 different parameters concerning the test cell and the passive solar components, but not all can be identified by the MRQT program. MRQT can only identify a maximum of 10 parameters. However, the user can freeze certain parameters so as to simplify or change the actual thermal network. The user can also change the maximum number of iterations that can be performed by the program.

Several MRQT simulation runs have been performed by the author, on hourly data from the experiments conducted on cell 2 with and without curtain, in an attempt to identify the test cell and reference wall performance characteristics.

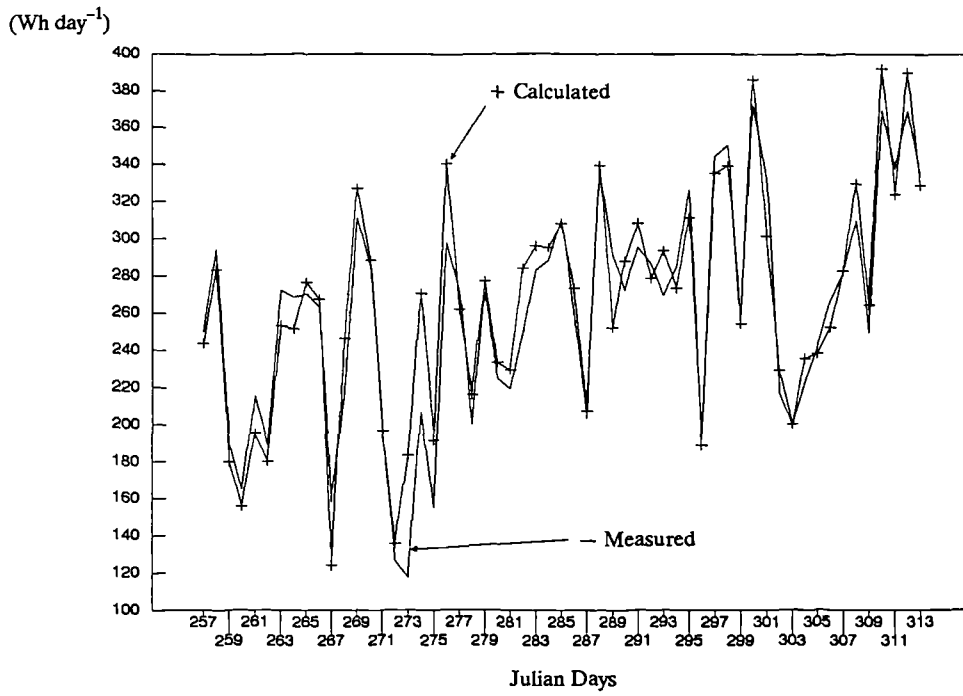


**Figure 8.10** Daily average heating requirements of *test cell 2* without curtain. A comparison between the measured and calculated values using the regression coefficients derived from the calibration experiment (see Table 8.1).

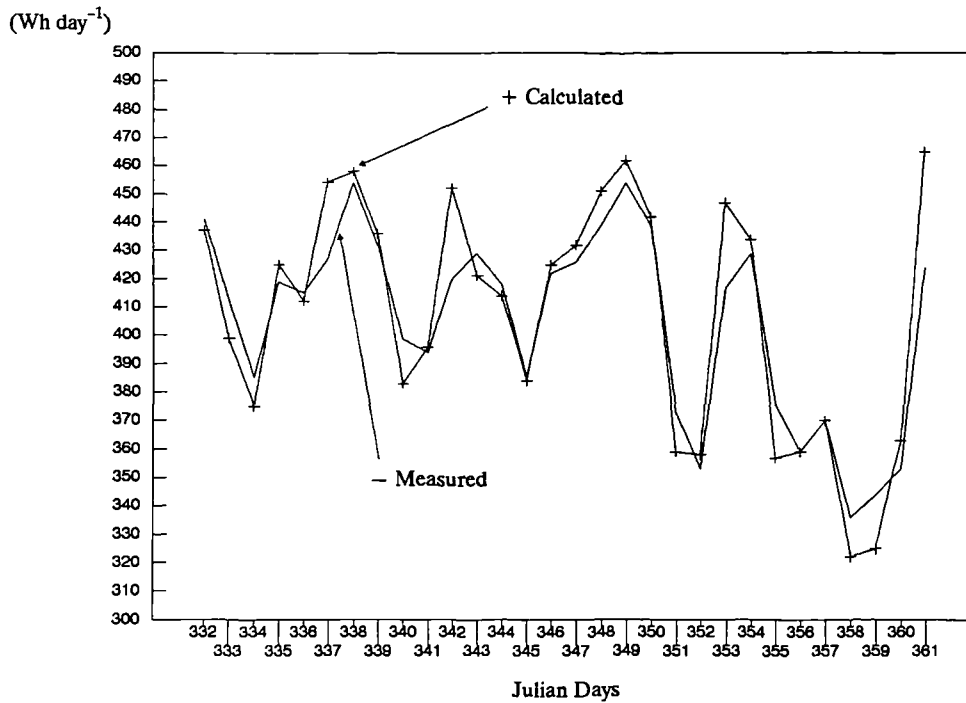


**Figure 8.11** Daily average heating requirements of *test cell 2* with the curtain installed. A comparison between the measured and calculated values using the regression coefficients derived from the calibration experiment (see Table 8.1).

Table 8.2 lists the heat transmission coefficients and solar apertures from 3 runs with variable conditions (see notes in Table 8.2). It is clear that the program produced unacceptable results with maximum iterations. Thus the following conclusions are drawn :

- In brief, the program reads hourly measured temperatures and vertical insolation, and initially identifies the parameters of the cell components (i.e. the first time step is a steady-state calculation), then a process of iterative corrections on these properties take place until calculated cell ambient temperatures mach the measured values. The presence of erroneous measured data will strongly influence the output of the program.
- The initial parameter values of the thermal network (i.e. input to LUMPA model) should be realistic. This reduces computational time and, if low number of iterations is chosen, it may produce good results. For example, results from the second case in Table 8.2 give test cell heat loss coefficients and solar apertures which are identical to the regression coefficients derived in Table 8.1.
- The program lacks obvious error handling routines to check for the validity of identified parameters.

**Table 8.2** Test cell parameters identified by the "MRQT" program with "LUMPA" v1.3 model of the cell.

Parameter	with Curtain	no Curtain
Case 1 †		
$\hat{U}_{tc}$	5.56*	5.56*
$\hat{U}_{int}$	2.91*	2.91*
$\hat{U}_{psc}$	8.32 (3%)	11.39 (2%)
$\hat{A}_{psc}$	-0.19 (30%)	1.13 (3%)
Case 2 ‡		
$\hat{U}_{tc}$	5.56*	5.56*
$\hat{U}_{int}$	2.91*	2.91*
$\hat{U}_{psc}$	9.00 (1%)	10.00 (2%)
$\hat{A}_{psc}$	0.57 (9%)	0.81 (3%)
Case 3 ¶		
$\hat{U}_{tc}$	21.46 (49%)	8.68 (38%)
$\hat{U}_{int}$	17.53 (15%)	1.45 (20%)
$\hat{U}_{psc}$	-15.90 (66%)	8.25 (39%)
$\hat{A}_{psc}$	0.21 (19%)	1.02 (5%)

Values in brackets are the error percentages of identified parameters estimates.  $\hat{U}_{tc}$ ,  $\hat{U}_{int}$ , and  $\hat{U}_{psc}$  are the heat loss coefficients ( $W^{\circ}C^{-1}$ ) of the test room components (side walls, roof and floor), the internal north wall, and the reference wall (passive solar component) respectively;  $\hat{A}_{psc}$  is the solar aperture ( $m^2$ ) of the reference wall.

\* Theoretical values (see Table 7.7 of the previous chapter). These were frozen during identification.

† Initial values of capacitances and conductances of the passive solar component were taken from Table 7.7 of the previous chapter (calculated by the author). Maximum number of iterations was set to 40.

‡ Initial values of capacitances and conductances of the passive solar component were calculated so that the total test cell heat loss coefficient would match those derived from the regression analysis. Maximum number of iterations = 2.

¶ 10 parameters were chosen for identification, with the maximum number of iterations set to 100.

## 8.4 Comparison Between Measured and Simulated Results by “ESP” and “CURTAIN” Models

---

The model “Curtain.Bas” developed by the author in chapter 5 (see section 5.6) is validated in this section against measured parameters obtained from the experiment (i.e. the temperatures of the fenestration layers). The “ESP” program was also used to simulate the temperatures of the fenestration layers as well as the heating requirements of the test cell with and without curtain.

### 8.4.1 Input Variables to the Models

#### *Fenestration & Climate Definition for the “Curtain” Model*

The program “Curtain.bas” was modified in the previous chapter to allow for the simulation of heat transfer through glazing alone and glazing with a internal blind. This modified version was also applied to the data of experiment conducted in present chapter.

The climate input file prepared for the “Curtain” model consist of hourly data in the following order:– global horizontal insolation, diffuse horizontal insolation, outdoor air temperature, wind speed, wind direction and ambient temperature of the test cell. Simulation runs were conducted for the periods from day 257 to 313 Julian and from day 332 to 361 Julian inclusive.

#### *Test Cell, Reference Wall & the Curtain Definition in “ESP”*

The test cell zones geometry and construction data were input to ESP in the form of ASCII data files, these are listed in Appendix (G). The geometry files are (*sroom.geo*, *troom2.geo* and *wroom2.geo*) and the construction data files are (*sroom.con*, *troom2.con*, *troom2c.con* and *wroom2.con*). File names that begin with the letter “w” refer to the condition of default definition of the fenestration as a window, and others refer to transparent multi-layered construction definition.

The following points were considered in defining the reference-wall components:

- To provide realistic interpretation of the reference wall components in the ESP model, the wooden window frame area was calculated and defined as a separate surface. (see the figures given with the geometry files in Appendix G).
- The glazing in cell 2 was described as default window. For this the program requires direct and total transmittance of the glazing for five angles of incidence (0°, 40°, 55°, 70° and 80°) and the U-value of the glazing. These were included in the construction file *wroom2.con*. For cell 2 with curtain fitted, a blind control file, *wroom2.blm*, was created, with the above requirements modified. The U-values, direct and total transmittances of the fenestration (with and without the curtain) for the required five angles of incidence were modeled using the “Curtain” program.

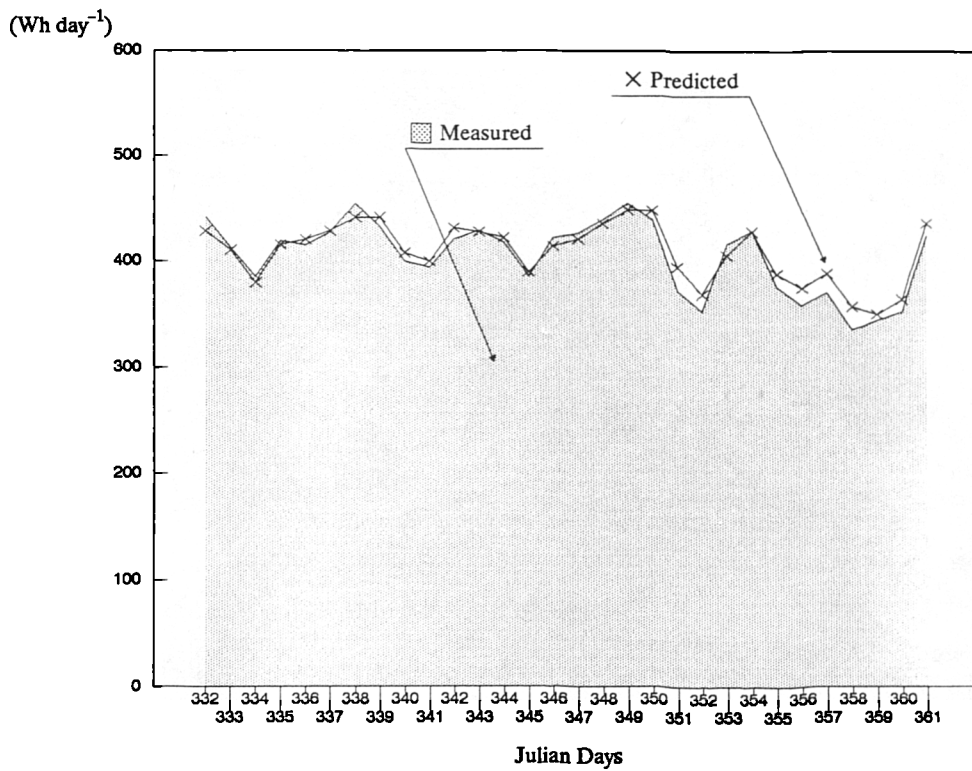


**Figure 8.12** Measured and predicted average daily heating requirements of *test cell 2* fitted with the curtain. Predicted values are computed by the ESP program for the period from Nov.28th to Dec.27th 1989.

- The fenestration (double glazing with and without curtain) were also described as transparent multi-layered constructions. For this the program requires the direct transmittance of the composite fenestration, and the absorptance of each layer in the fenestration, again for the five angles of incidence. These were modeled with the “Curtain” program, and given in the files *troom2.tmc* and *troom2c.tmc*. The glazing was given as two layers with an air-gap in the zone construction files *troom2.con* and *troom2c.con*. Air gap resistance was modeled by the “Curtain” program, and yielded a value of  $0.178 \text{ m}^2 \text{ }^\circ\text{C W}^{-1}$  for the double glazing unit, and  $0.23 \text{ m}^2 \text{ }^\circ\text{C W}^{-1}$  for the double glazing with the curtain.

### *Test Configuration & Climate Definition in ESP*

An operation file to instruct the ESP*bps* program of the extra casual gains and infiltration air change rate of each zone was created (*troom2.opr*). Casual gains were set to zero, hence no casual gains existed in the cell, and air change rate was set to  $0.25 \text{ h}^{-1}$ . Casual gains and air change rate in the service room operation file (*sroom.opr*) were set to zero.

Similar to the experiment configuration, a set-point temperature of  $30.65^\circ\text{C}$  for the test cell was defined in the configuration control file (*curtnx.cfl*). Note that this value is the average temperature of the cell for the period of the experiment. The climate data collected for the period of experiment (plus 2 weeks before and 2 weeks after) were formatted and appended to the climate file (*glasgow.clm*) using ESP*clm*.

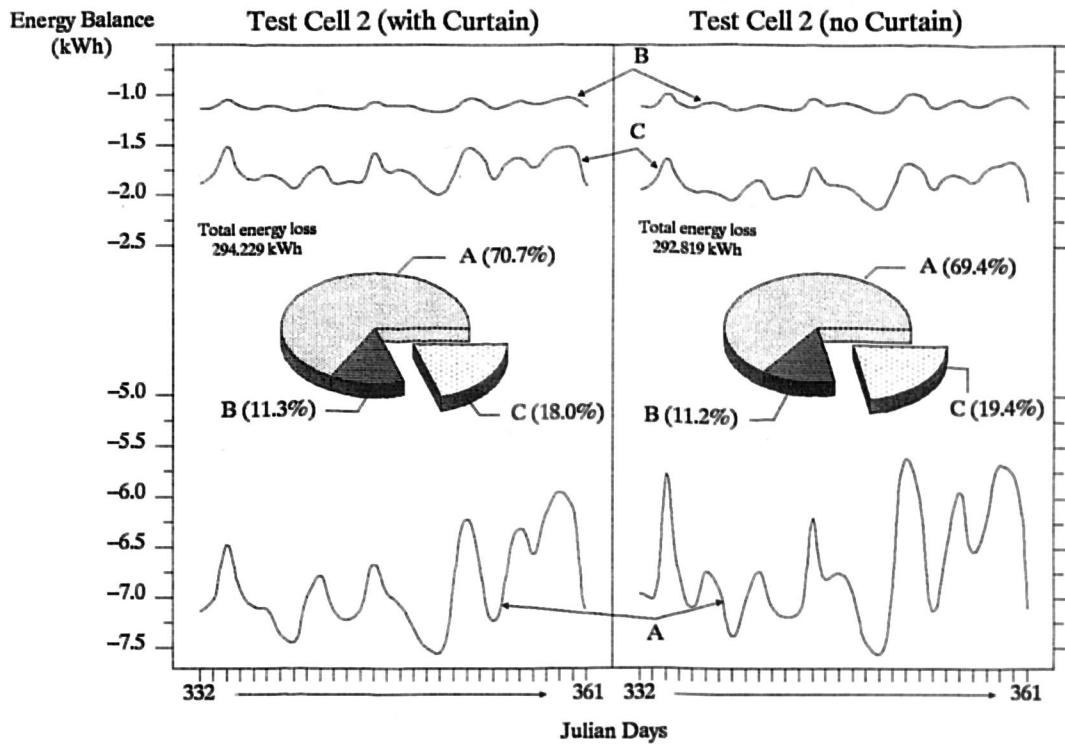
Finally, three configuration files were created (*curtnx1.cfg*, *curtnx2.cfg* and *curtnx3.cfg*). The first configuration file considers the fenestration (glazing with and without curtain) as transparent multi-layer constructions. The second considers the fenestration as window, with blind control for test cell 2 (curtain fitted). Both configuration files were used to simulate the energy performance of the test cell for the period from Nov.28<sup>th</sup> to Dec.27<sup>th</sup>. The third configuration file was used to simulate the energy performance of test cell 2 without curtain, considering the glazing as window and as multi-layered construction, for the period from Sep.14<sup>th</sup> to Nov.27<sup>th</sup>. The simulation runs were conducted, each with 6 days start-up period (determined by the program).

## 8.4.2 Results and Discussion

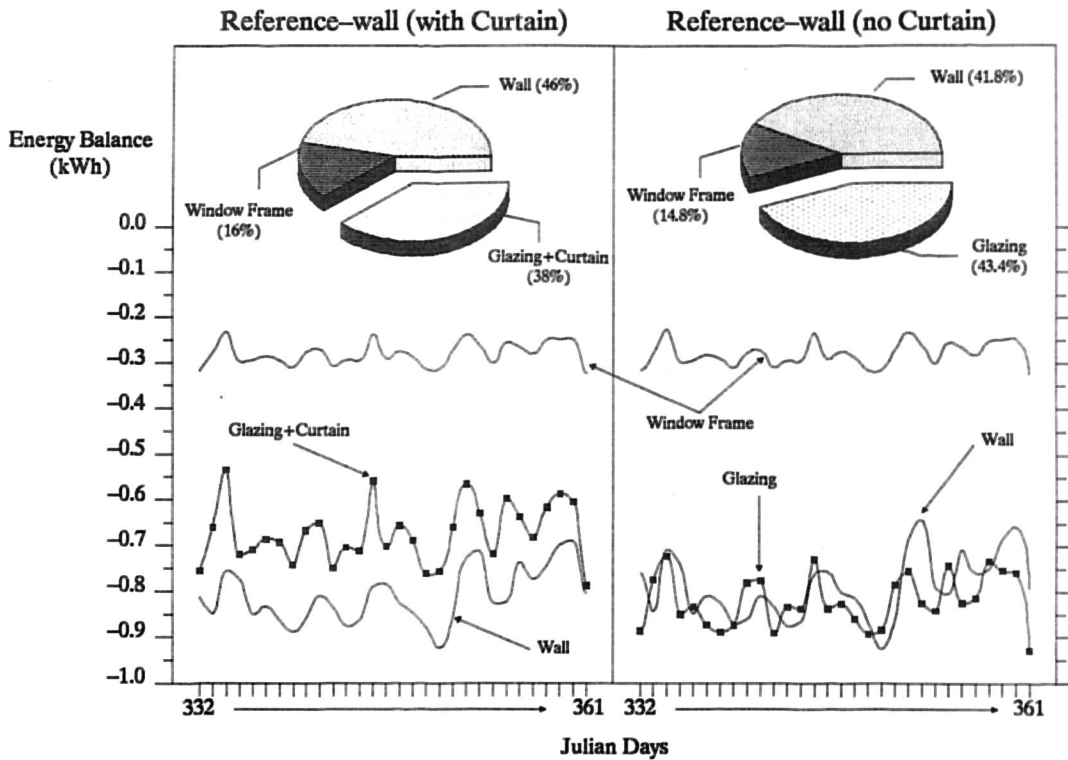
### *Effects of the Curtain on the Test Cell Energy Balance*

Simulation runs using ESP, in which the fenestration was considered as transparent multi-layered construction, as expected, produced better results than simulations with the default window treatment. Thus the ESP results discussed and analysed hereafter are from the first simulation run.

Figure 8.12 shows a comparison between measured and calculated average daily auxiliary heating of test cell 2 fitted with the curtain. The simulated values have a calculated standard error of 2.4% over the whole period (332–361 Julian).



**Figure 8.13** Daily total energy balance at the air node of cells 2 (with and without curtain), calculated by the “ESP” model for the period from 332 to 361 Julian. The energy balance at air node is a combination of convective exchanges with (A) the cell side walls, roof and floor, (B) internal wall connecting to the service room, and (C) the passive solar component, i.e. the Reference-wall.



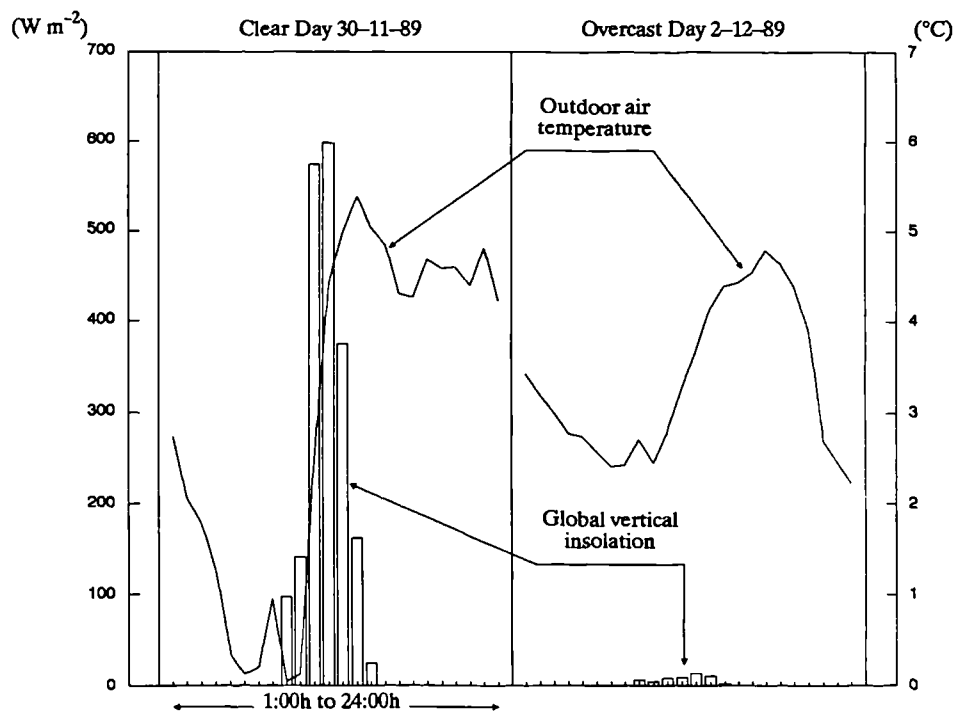
**Figure 8.14** A breakdown of the daily total energy balance at the air node of cell 2, due to convective exchanges with the Reference-wall components. Calculated by the “ESP” model for the period from 332 to 361 Julian.

Figure 8.13 shows a comparison between the daily total energy balances at the air node of test cell 2 (computed by ESP) with and without curtain, for the duration of the curtain experiment. The energy balance at the air node is divided into convective heat exchanges with (a) the cell side walls, roof and floor; (b) internal wall connecting to the service room; and (c) the passive solar component. The contributions of heat exchanges for the whole period are also shown as pie charts on Figure 8.13.

Energy balances of the passive solar component (“reference” wall, window frame and glazing) of cell 2 with and without curtain are shown in Figure 8.14 for the simulation period, 332–361 Julian. The presence of the curtain on the fenestration reduces the total energy loss of the combined wall–fenestration by about 6.6% over the whole period. This is primarily due to an 18% reduced heat losses through the curtain–shaded fenestration.

### *Comparative Analysis for Clear and Overcast Days*

The following comparative analysis and results of measured and simulated parameters relate to clear and overcast sky conditions. Two days were chosen, 334 and 336 Julian, for the reasons explained in section 8.3.1. Hourly global vertical insolation for the clear and overcast days are shown in Figure 8.15. This figure also shows the hourly outdoor air temperature variations for both days.



**Figure 8.15** Hourly measured global vertical insolation ( $\text{W m}^{-2}$ ) and outdoor air temperature ( $^{\circ}\text{C}$ ) for clear and overcast days from the curtain experiment.

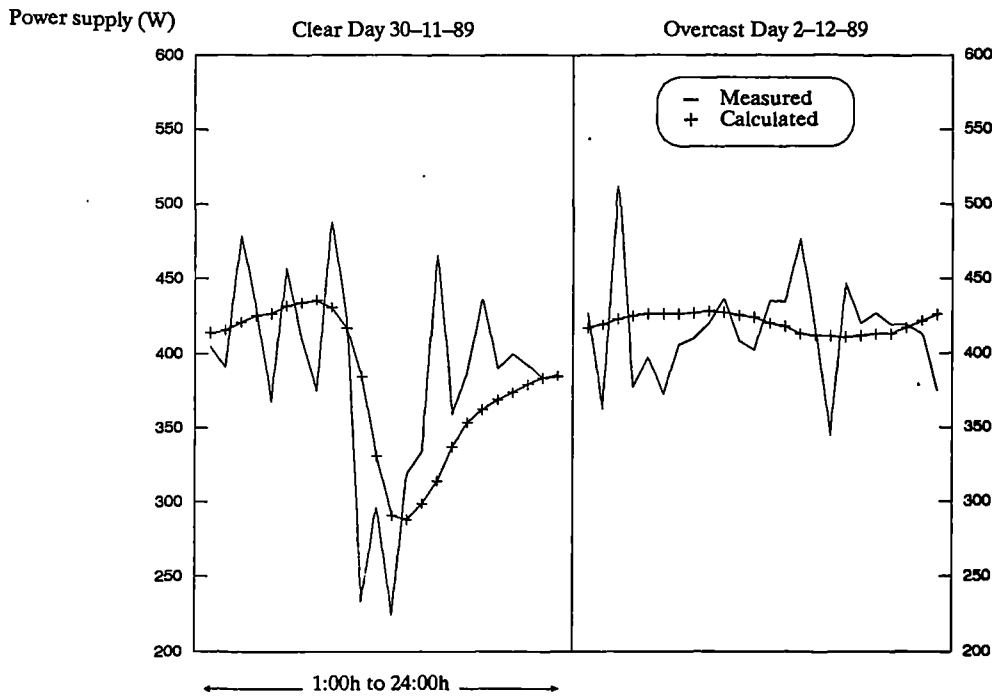


**Figure 8.16** Comparison between measured and predicted hourly heating requirements of *test cell 2* (with the curtain installed) for clear and overcast days. Calculated data are from the ESP simulation results.

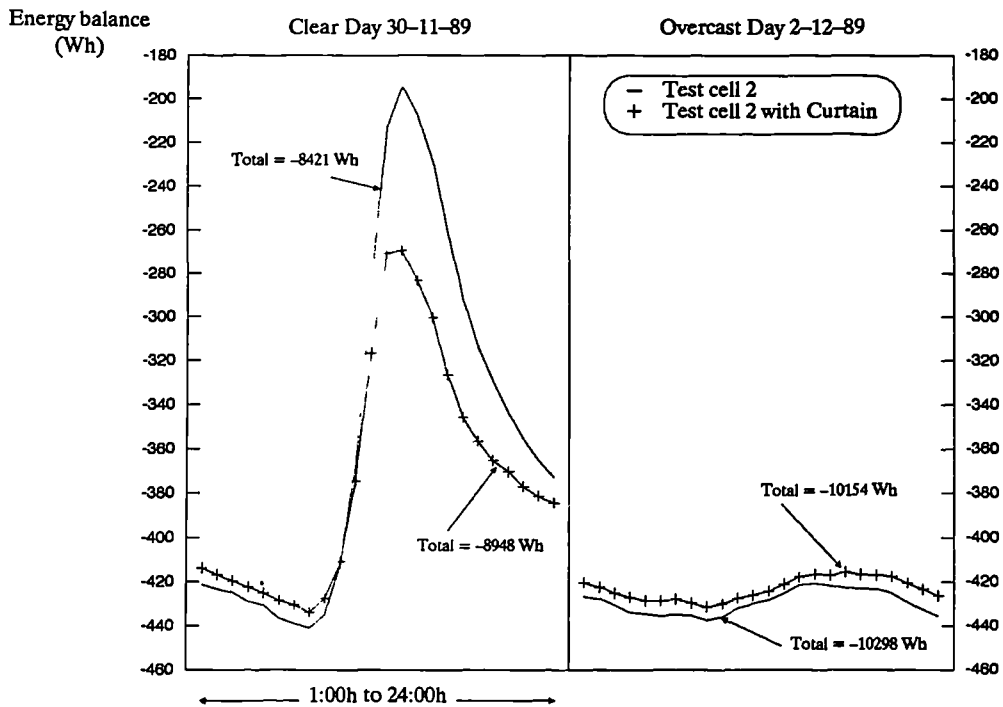


**Figure 8.17** Energy balance at the air node of *test cell 2* (with and without curtain). Computed by the "ESP" program for clear and overcast days.

Figure 8.16 shows a comparison between the measured and ESP simulated auxiliary heating of test cell 2 fitted with the curtain for clear and overcast days. From this figure, it is apparent that predicted hourly values follow a smoother path than the measured values. However, the total auxiliary heating for the clear day was underestimated by 1.4%. For the overcast day, the simulated auxiliary heating was overestimated by 1.3%.

The curtain experiment was conducted on a single test cell; thus direct comparison between the test cell performances, with and without curtain, from measured data was not possible. However, in view of the above comparisons, it is possible to study the performances of the test cell with and without the curtain, from the ESP simulations with very good accuracy.

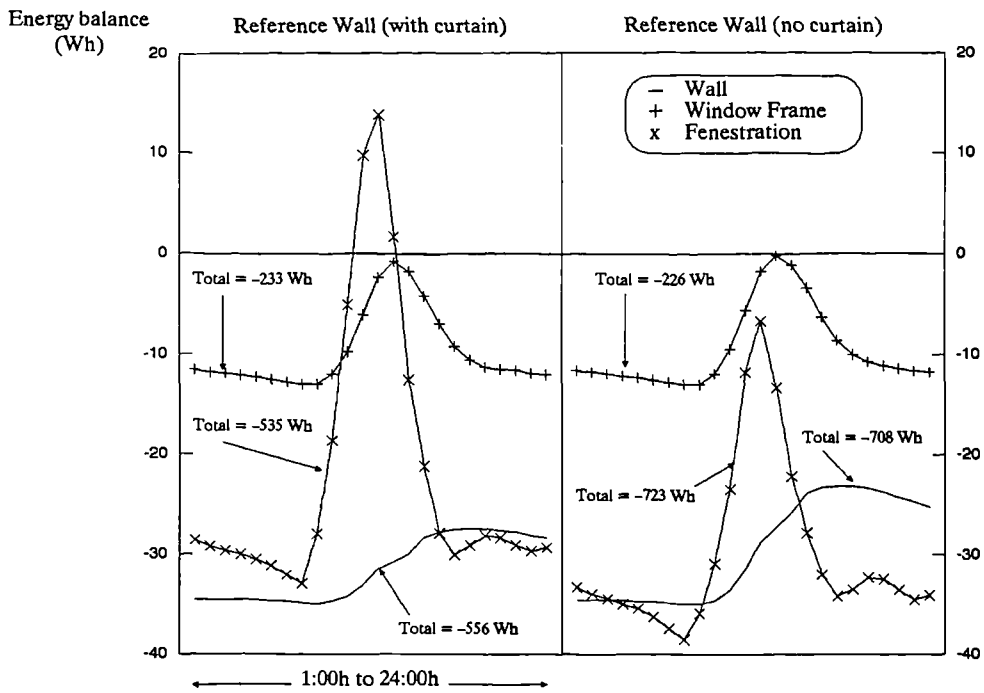
Figure 8.17 shows the air node energy balances of the test cell with and without the curtain as computed by the ESP program for both clear and overcast days. The results indicate that the curtain has increased the total heat loss of the test cell by 6.2% on the clear day, and reduced the test cell heat loss by 1.5% on the overcast day.

Figures 8.18 and 8.19 show the net energy balances of the reference wall components (with and without curtain), for clear and overcast days respectively. From the overcast day results (Fig.8.19), the reference wall, with the curtain fitted, has a reduced net heat loss which is 6.1% lower than the reference wall without curtain. From the clear day results (Fig.8.18), reduction in the net heat loss of the reference wall with curtain was 8.1%.

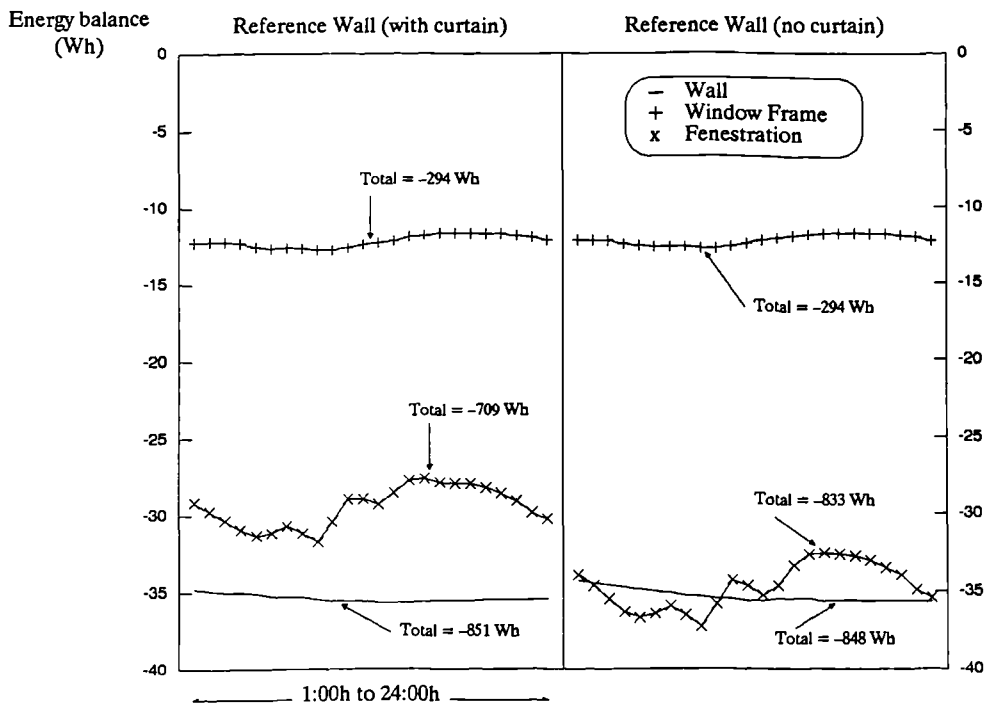
Shortwave fluxes transmitted through the fenestration of the test cell undergoes a complex process of absorption and longwave heat exchanges, by the internal surfaces of the test cell. The net convective energy balance at the cell air node is therefore influenced by the magnitude of the transmitted solar radiation. Figure 8.20 shows a comparison between the shortwave radiation fluxes transmitted through the fenestration of cell 2 with and without curtain, for both clear and overcast days, computed by the "Curtain" program. In either case (clear day or overcast day) the total transmitted shortwave radiation, through the fenestration, is reduced by 65% due to the presence of the curtain.

Figure 8.21 compares the combined convective-longwave heat fluxes from the fenestration of cell 2 with and without curtain, computed by the "Curtain" program, for both days. While shortwave radiation fluxes are reduced due to the curtain (Fig.8.20), the convective-longwave heat fluxes are increased (Fig.8.21).

The magnitude of increase in the convective-longwave heat flux, as calculated by the "Curtain" program, depends on the heat transfer coefficients at the surfaces of each layer in the fenestration. These are fully discussed in section 5.6.3 of chapter 5. The increase in heat gains of the fenestration in cell 2 with curtain is contributed to the inward-flow fraction of absorbed insolation as shown in Figure (8.22), and the reduction in heat loss is contributed to the fenestration U-value as shown in Figure (8.23).



**Figure 8.18** Energy balance at the air node of *test cell 2* (with and without curtain) due to convective heat exchanges with the reference wall components. Computed by the "ESP" program for a *clear day* (November 30th 1989).



**Figure 8.19** Energy balance at the air node of *test cell 2* (with and without curtain) due to convective heat exchanges with the reference wall components. Computed by the "ESP" program for an *overcast day* (December 2nd 1989).

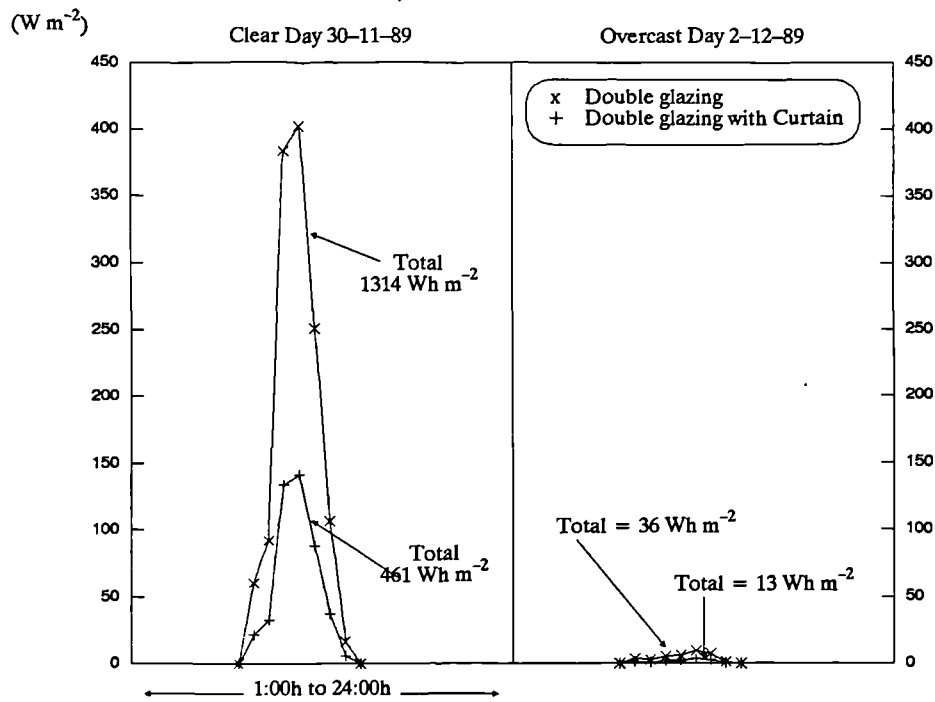


**Figure 8.20** Shortwave radiation flux (solar) transmitted through the fenestration of *test cell 2* (with and without curtain). Computed by the “Curtain” program for clear and overcast days.

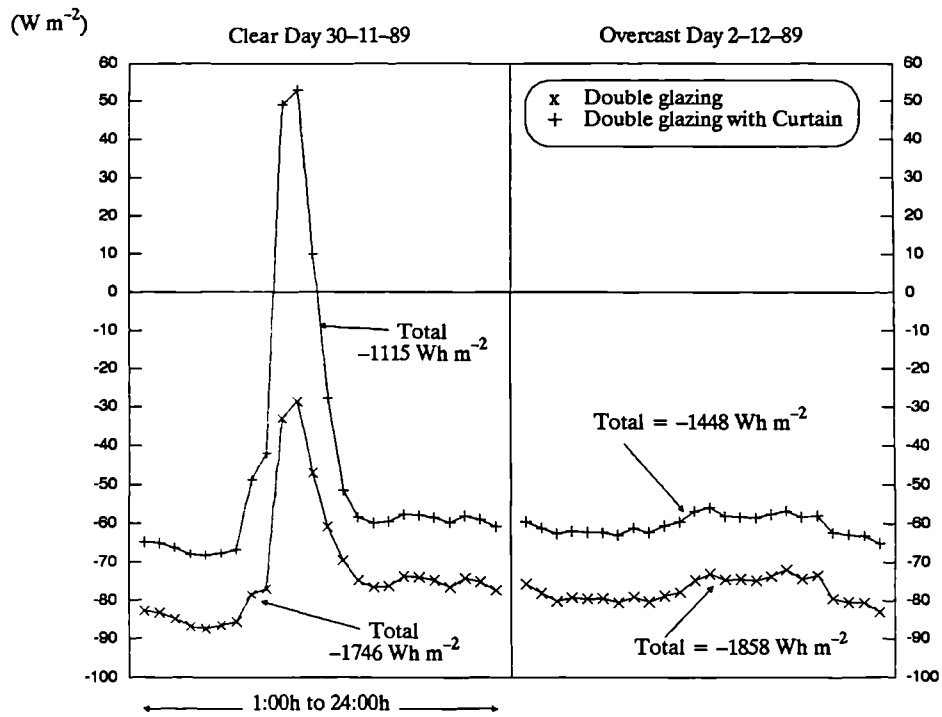


**Figure 8.21** Combined convective-longwave heat flux through the fenestration of *test cell 2* (with and without curtain). Computed by the “Curtain” program for clear and overcast days.

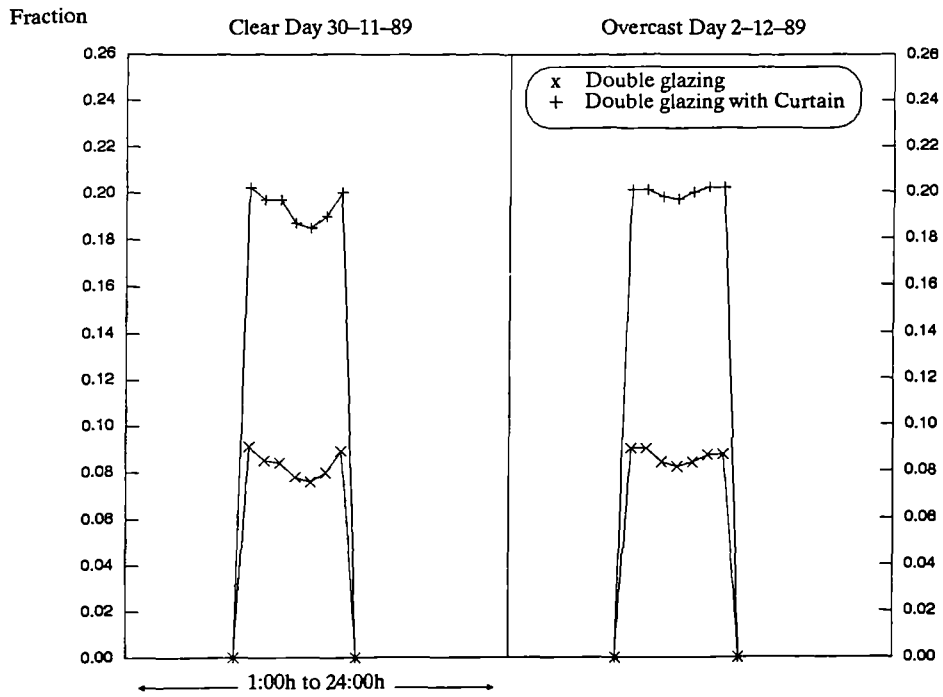


**Figure 8.22** Inward-flow fraction ( $N_i$ ) of absorbed insolation in the fenestration of *test cell 2* (with and without curtain). Computed by the “Curtain” program for clear and overcast days.

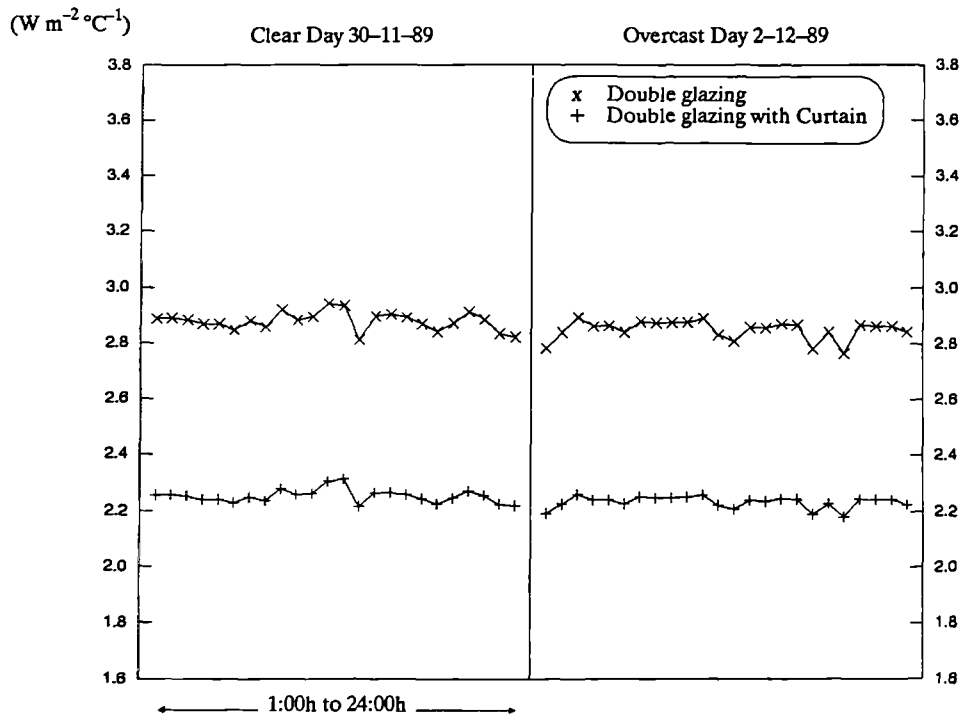


**Figure 8.23** U-value of the fenestration in *test cell 2* (with and without curtain). Computed by the “Curtain” program for clear and overcast days.

The “Curtain” program results also include the temperature of fenestration layers in cell 2 (with and without the curtain). These are compared with measured values and with simulated values by the ESP program for the whole period of experiment.

Figures 8.24 shows the measured temperature of the curtain compared with calculated values by the “Curtain” and by ESP programs for the clear and overcast days. Comparison between measured and predicted temperatures of the inner pane of the glazing in cell 2 with and without curtain are shown in Figure 8.25 and Figure 8.26 respectively, for clear and overcast days. Figures 8.27 and 8.28 show the measured and predicted temperatures of the outer glass pane in cell 2 with and without curtain respectively, again for both clear and overcast days.

From Figures 8.25 and 8.26, the effect of the curtain on the temperature of the inner glass is apparent. In the absence of solar radiation, the curtain acts as a barrier between the cell ambient temperature and the temperature of the outer glass, thus the temperature of the inner glass is lower in the presence of the curtain. With high levels of solar radiation, the temperature of the inner glass with the curtain in place is higher than that with no curtain due to extra absorption of solar radiation reflected off the curtain surface. The same phenomena apply to the outer glass, as can be seen from Figures 8.27 and 8.28.

Error analysis on predicted temperatures for the clear and overcast days, are shown on corresponding figures. In general predicted temperatures by both programs are within acceptable range of accuracy.

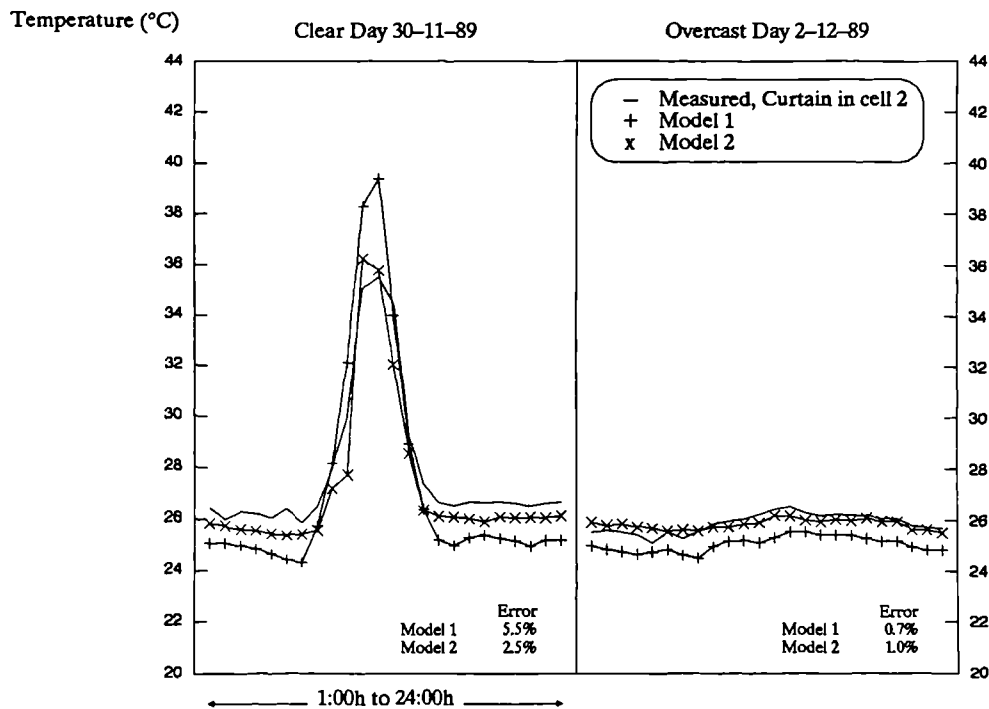


**Figure 8.24** Measured and predicted temperature of the curtain, installed in *cell 2*, for a clear and overcast days. Model 2 refers to results from the “Curtain” program, and model 1 refers to results from “ESP” simulation run. Note that the ESP predicted values are for the inner layer of the fenestration which include both properties of the glass and the curtain.

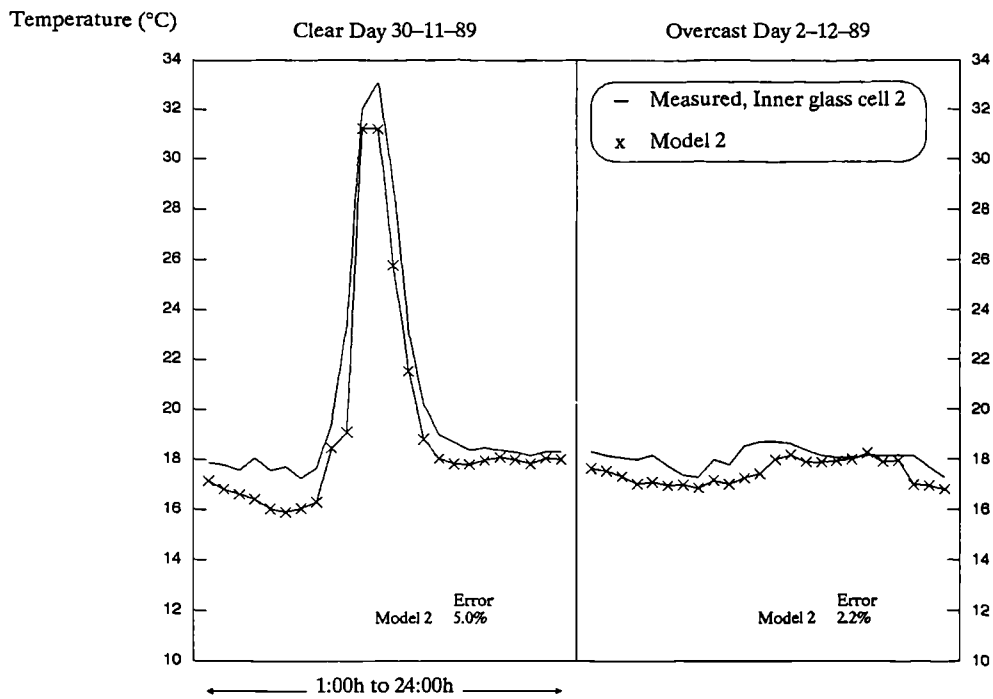


**Figure 8.25** Measured and predicted temperature of the *inner glass panel* in *cell 2* with the curtain installed, for a clear and overcast days. Model 2 refers to results from the “Curtain” program.

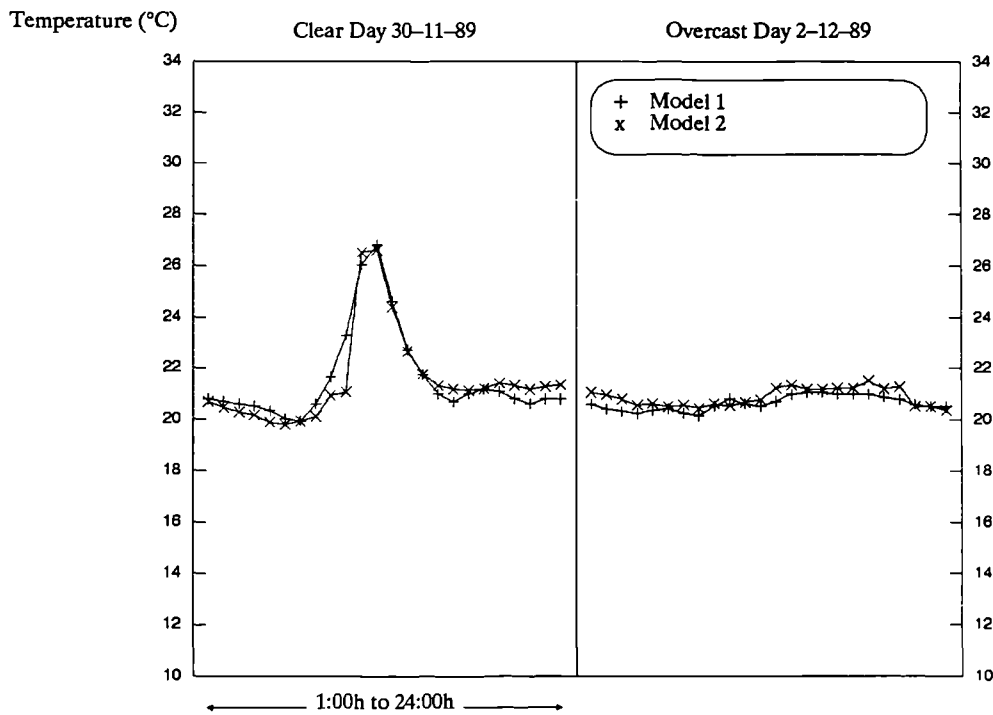


**Figure 8.26** Predicted temperature of the *inner glass panel* in *cell 2* without curtain, for a clear and overcast days. Model 1 refers to results from “ESP” simulation run and model 2 refers to results from the “Curtain” program.

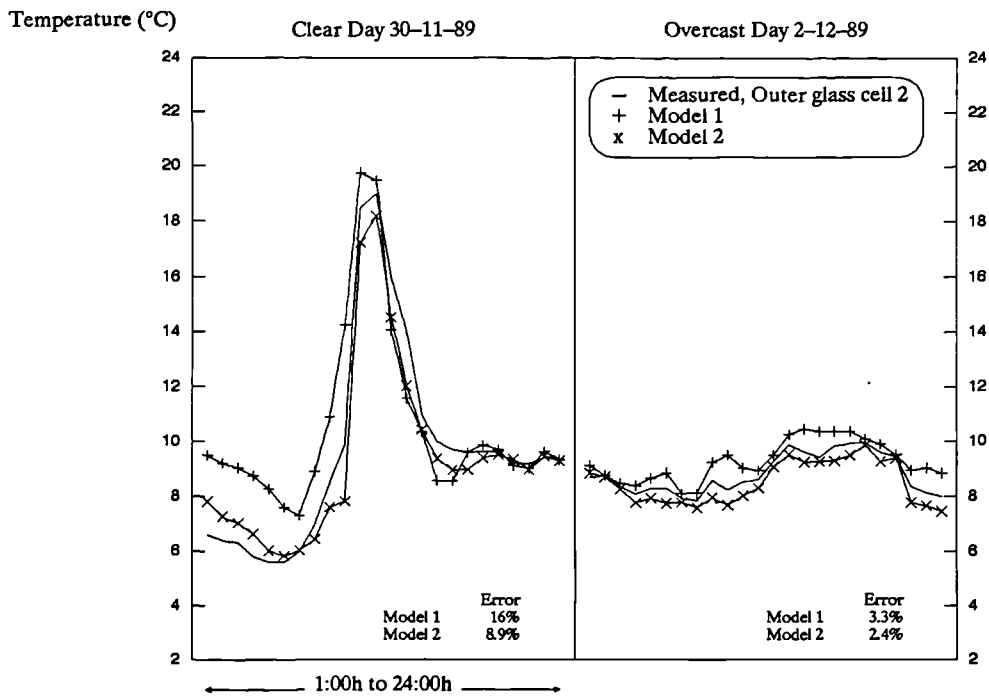


**Figure 8.27** Measured and predicted temperature of the *outer glass panel* in *cell 2* with the curtain installed, for a clear and overcast days. Model 1 refers to results from “ESP” simulation run and model 2 refers to results from the “Curtain” program.

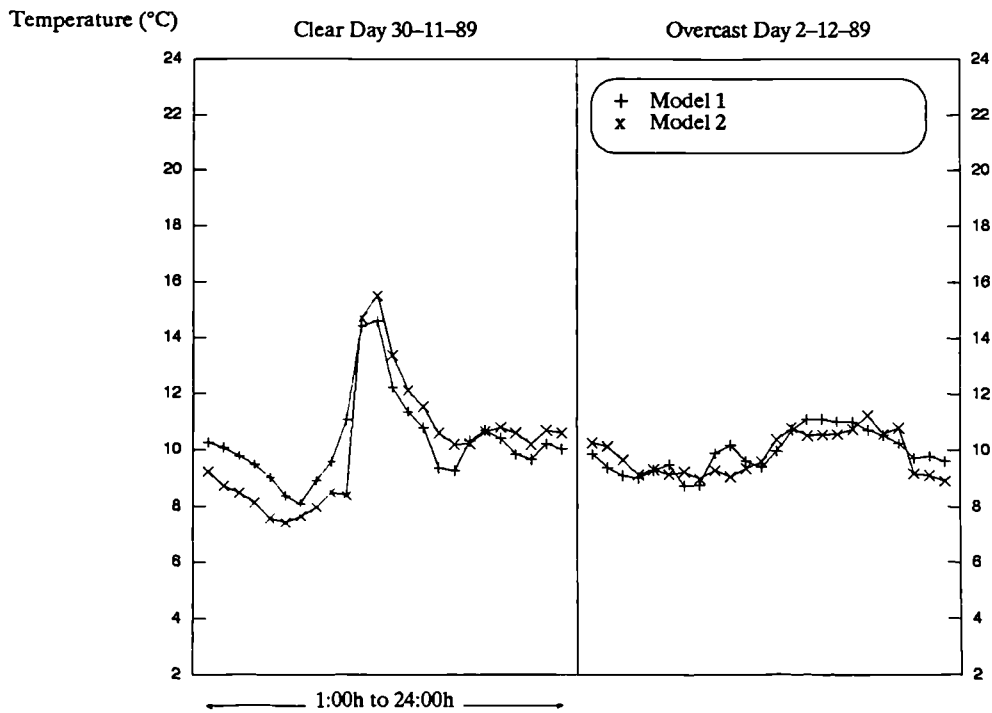


**Figure 8.28** Predicted temperature of the *outer glass panel* in *cell 2* without curtain, for a clear and overcast days. Model 1 refers to results from “ESP” simulation run and model 2 refers to results from the “Curtain” program.

## 8.5 Conclusions

---

The main steady-state characteristics of the test cell, (i) fitted with glazing unit in the “reference” wall and (ii) with the domestic curtain (82% Dralon, 18% Nylon, light cream colour) fitted flat onto the inside of the double glazing unit, have been derived from the experiments conducted in this chapter with accuracy of better than 8%.

The curtain-shaded window in cell 2 can reduce the daily average heating requirement for the whole cell by 8% as compared with unshaded window. Also the curtain can reduce solar heat gains to the test cell by up to 30%.

Comparing these results with the “blind”-shaded fenestration from the previous chapter (11% and 34% reductions in heat losses and heat gains respectively) it is apparent that the thermal performance of the Passys blind is better than the curtain's.

The outcome of the study in this chapter also provided confidence in computer modeling of the test cell energy performance. The simulation results of the “Curtain” program, have shown good agreement with measured temperatures of the fenestration layers. The “ESP” simulation results have also shown good agreements with measured parameters like the fenestration temperatures and auxiliary heating of the cell.

The “MRQT” program failed to identify acceptable test cell performance characteristics with the data sets obtained from the curtain experiment. Some reservations about the program were given in section 8.3.2. The main disadvantages of the program are (i) it lacks error handling routines to check the validity of identified parameters and (ii) because the program main priority is to derive a calculated cell temperature close or equal to the measured, the existence of erroneous or out-of-range input data will strongly influence the identified parameters.

## 8.6 References

---

- Baker P. (1990) Unpublished Results from experiments conducted on test cell 2 in 1990, Energy Studies Unit, Strathclyde University, Glasgow, Scotland.
- Baker P., Clarke J., Guy A., Owens P., Pearson K., Strachan P. & Twidell J. (1992) "Passys II Final Report of the UK Consortium", Draft report submitted to DG XII of the European Commission and the Energy Technology Support Unit, Jan. 1992.
- Clarke J., Hand J. & Strachan P. (1990) "ESP : A Building and Plant Energy Simulation System", version 6, *ESRU Manual U90/1*, Energy Simulation Research Unit, University of Strathclyde, Glasgow, UK.
- Cools C. & Gicquel R. (Eds) (1988) "The Project Passys", EMP, Sophia Antipolis, France.
- Dijk van. H. (1990) "The Parameter Identification Method MRQT", version 4.0, *User Guide*, TNO Institute of Applied Physics, Delft, The Netherland.
- Strachan P., Baker P., Twidell J., Clarke J., Guy A. & Pinney A. (1988) "UK Participation in the Passys Project", *Euroforum Conference*, Saarbrucken, Sep. 1988.
- Wouters P. & Vandaele L. (Eds) (1990) "The Passys Test Cell", Subgroup Instrumentation final report Part 1, *Passys Document 114-89-PASSYS-INS-033*, BBRI, Brussels, Belgium.

# Chapter 9

## 9. CONCLUSIONS

The aims and objectives set out at the introductory chapter of this thesis have been achieved. The data presented and the methods described provide architects and designers with powerful tools to produce better designs of energy efficient buildings. Design principles and choice of materials to adapt buildings to climate can be evaluated for their thermal characteristics by the different energy analysis techniques (models) discussed in this thesis. The main objective of defining a Climate Reference Year for use with energy simulation programs has been accomplished. Although the amount of climatic data available are limited, these have been used to the best of my effort in constructing the Climate Reference Year. Results should prove extremely valuable for energy simulation in building design; and provide the basis for future updates of the reference year, taking into account more data available.

The nature of the Riyadh climate and the resultant climate reference year made it also possible to develop procedures for predicting hourly climatic variable (i.e. insolation and temperature) with a high degree of accuracy. Thus by discussing and presenting these studies, a better description of the region's climate has been achieved. These may assist designers and architects to determine the comfort conditions most suited to this region in particular and for hot-arid climatic regions in general. The CRY may also be useful in other fields of research like active solar systems. Another area covered in this thesis, (measurement and instruments), have resulted in a valuable reference for engineers and should introduce designers and architects to the knowledge of the accuracy and use of instruments for both indoor and field measurements.

The study have also examined various properties associated with the curtain fabric and the curtain-glass fenestration, as means of solar control (shading). Of prime importance are the solar properties (curtain reflectance, transmittance and absorptance) which significantly influence the solar heat gain through fenestration. Interior shading devices, because of their position, have advantages over external devices in that they are protected against the weather and are easy to get at for control and maintenance. They can reduce heat gain and heat loss through windows; but in general they are less effective than external shades in minimizing solar heat gains because a proportion of the heat they absorb is released to the room. In reducing heat loss, if the device does not effectively trap air between itself and the window, the insulative value is minimal. However, if it is installed to provide an air-tight enclosure and its material is selected with proper solar properties, an interior shading device can improve the energy performance of a window.

The "Curtain" model developed and described in this thesis computes the fenestration temperatures and energy flows associated with curtain shaded single or double glazed windows exposed to real climatic conditions. This tool may be used on its own for the assessment of the energy performance of different interior shading devices and may also be incorporated in a dynamic simulation model.

A set of measurements of the implications of different indoor window coverings on passive building performance have been carried out in test rooms (cells) fitted with real building components. The tests were organised in such a way as to provide (a) the specific parameters required to characterise the shaded-fenestration in simple energy calculation procedures; namely the heat transmission coefficient  $\hat{U}$  and the solar aperture  $\hat{A}$ , and (b) confidence in the computer programs “Curtain” and “ESP” through validation. Key points in the test methodologies applied in the course of this work are:

- steady-state operation of the test cell with thermostatically controlled heaters yields accurate measurements of the characteristic performance of passive solar components. For different components (unshaded window and shaded window), the performance characteristics can be determined by experiments on (1) two test cell subjected to identical external and internal conditions; or (2) a single cell fitted in tern with the components at different periods. The former is generally preferred.
- in terms of data analysis, a 24 hour integration time is sufficient to average-out the transient effects of accumulated energy within the test cell components. (all such effects are therefore assumed to be linear with change in temperature). With the regression techniques described in this thesis, performance parameters can be achieved with acceptable degree of accuracy (8–10%).
- The parameter identification technique (MRQT) should, in theory, provide the performance characteristics of passive solar components from measurement with the test cell operated in steady-state or free-floating modes. However, the program did not produce satisfactory results.

Result from the tests conducted show that the curtain-shaded window can reduce the daily average heat transmission coefficient by 8% as compared with unshaded window. Also the curtain can reduce the solar aperture of the fenestration by 29%. Comparing these results with the “blind”-shaded fenestration, 11% and 34% reductions in heat transmission and solar aperture respectively, it is apparent that the thermal performance of the Passys blind is better than the curtain’s.

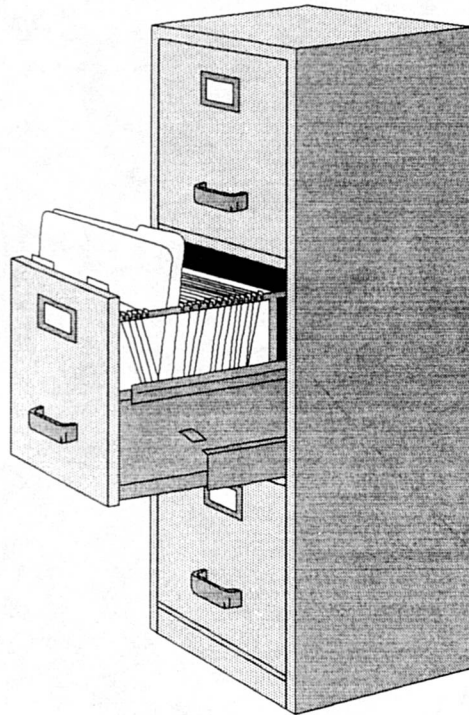
Clearly the parameters measured in these tests relate only to the particular samples of interior shading devices tested (i.e. the Passys blind and the domestic curtain), operating under the conditions of the tests. Variables which might lead to different results for other types of textile-based interior shading devices, or for the same samples in different conditions include:

- **Fabric type** : the amount of solar radiation reflected back out by the interior shading device will depend on the reflectivity of the fabric, which could vary over a wide range, with corresponding large effects. The effect of the interior shading device on heat transmission will depend on the fabric emissivity. This is unlikely to change for different “untreated” curtains, but low emissivity coated fabrics (such as the Passys blind) are now available on the market, giving reduced heat flow through the fenestration.
- **Geometric configuration** : For a curtain the parameters which describe the geometry are the density of the weave “openness” and the way in which the curtain is hung (its “fullness” and spacing from the glazing).

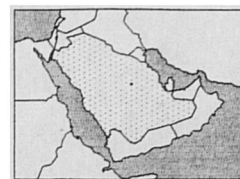
The outcome of the experimental studies have also provided confidence in computer modeling of the energy performance of passive solar components. The simulation results of the “Curtain” program, have shown good agreement with measured temperatures of the fenestration layers. The “ESP” simulation results have also shown good agreements with measured parameters like the fenestration temperatures and auxiliary heating of the cell. For accurate simulations using ESP, it has been necessary to incorporate results from the “Curtain” program into ESP data files. Thus, future upgrading of the ESP model should cover the best way of including (or defining) fabric shading devices with glazing; and probably reducing the task of preparing the huge amount of data files required for the simulation.

The theoretical and practical studies in this thesis have bridged a gap in the field of passive energy systems related to textile-based fabrics (curtains and blinds). The fact that curtains and blinds are quite common features in living spaces, for one reason or the other, the energy benefits alone would make them cost effective. However, peoples behaviour, when it comes to curtain installation and management, play a major role in the effectiveness of such devices. It is hoped that the study would also provide incentives for the rational use and installation of interior shading devices.

# Appendices



## Appendix A



---

# Climatic Data (Riyadh, Saudi Arabia)

---

The following tables represent daily climatic data of:

- Ambient temperature, (°C)
- Relative humidity, (%)
- Wind speed, ( $\text{m s}^{-1}$ )
- Wind direction, (°)
- Ground surface temperature, (°C)
- Rain fall, (mm)

The first four climatic parameters are derived from the Climate Reference Year file prepared by the author in chapter 3. The original source for raw climatic data is the King Abdulaziz City for Science and Technology (KACST). The source data represent extracts from the data acquisition system of the photovoltaic power site in the Solar Village, (Latitude  $24.54^\circ$  and Longitude  $46.24^\circ$ ) for the years 1984 to 1986. Supplementary data sheets containing daily data for 1985 and 1986 were also obtained from the same source. The ground surface temperature and rain fall climatic parameters are reproduced from these data sheets.

For more details on processing and developing the Climate Reference Year of Riyadh see the discussion of chapter 3.

**Table A.1** Meteorological data from Riyadh's Climate Reference Year. (JANUARY)

Day	Ambient Temp. (C°)			Relative Humidity (%)			Wind Speed (m/s)			Wind Dir. (deg)	Ground Temp. (C°)	Rain Fall (mm)
	A	H	L	A	H	L	A	H	L	A	A	T
1	9.6	15.1	4.6	42	69	23	2.4	4.4	0.7	153	12.5	0.4
2	12.3	20.3	4.6	37	50	26	2.4	3.8	1.3	153	13.5	0.2
3	14.3	20.4	8.3	37	49	29	3.7	6.8	1.1	178	15.0	0.0
4	12.0	18.2	6.9	33	50	21	3.6	6.1	1.1	222	14.0	0.0
5	10.5	16.8	4.2	57	73	44	1.9	2.9	0.8	305	13.5	0.2
6	12.0	19.8	5.5	59	76	41	1.8	3.8	0.7	289	13.0	0.3
7	13.4	21.6	6.2	53	78	33	1.9	3.2	0.7	238	13.0	0.6
8	15.2	22.5	7.9	43	56	30	1.8	3.7	0.5	196	13.0	0.0
9	16.0	23.3	8.3	39	50	28	2.0	4.2	0.5	196	13.0	0.0
10	16.8	24.6	9.1	39	52	22	2.2	4.1	0.5	171	13.0	0.0
11	14.2	20.5	7.9	41	51	30	2.6	5.1	0.5	171	14.0	0.0
12	14.1	20.0	8.8	41	56	30	3.1	6.2	1.3	153	15.5	0.0
13	11.6	17.2	5.9	47	63	35	2.7	4.7	0.8	178	15.0	0.0
14	13.8	20.9	6.0	51	77	35	2.1	3.9	0.7	115	14.5	0.0
15	17.7	23.8	11.9	42	69	25	3.4	6.5	1.1	134	16.0	0.1
16	14.9	20.6	9.1	48	63	35	2.8	5.1	1.0	178	16.0	0.0
17	15.0	22.0	10.0	52	72	39	3.6	7.0	0.9	184	15.0	0.0
18	13.8	19.7	7.5	49	65	35	3.5	6.6	1.1	133	15.5	0.0
19	14.3	22.4	6.0	47	65	35	2.5	5.3	0.5	171	17.0	0.3
20	10.4	14.9	6.2	52	58	45	4.4	7.2	2.0	248	15.5	0.2
21	8.0	13.9	2.6	44	62	30	2.6	4.6	1.0	178	14.5	0.0
22	9.7	17.6	0.3	41	51	30	2.1	3.7	1.0	204	15.0	0.0
23	11.3	17.4	6.1	44	60	30	2.6	5.6	0.9	222	15.5	0.0
24	10.6	16.3	4.9	47	63	35	2.9	5.1	1.6	184	13.5	0.2
25	12.2	18.5	4.8	44	59	40	3.5	6.1	1.3	184	13.5	5.2
26	13.1	17.3	9.4	52	72	39	2.3	5.4	0.5	184	13.5	0.8
27	13.7	20.0	7.5	72	87	56	2.3	3.7	0.8	184	14.0	0.0
28	14.6	19.2	9.5	87	99	75	3.5	6.7	1.1	200	13.5	1.5
29	14.6	21.3	8.6	84	99	60	3.9	7.2	1.3	133	15.0	0.1
30	11.4	15.4	7.3	85	96	71	3.4	6.5	0.8	305	15.5	4.4
31	11.1	15.9	6.8	82	99	60	2.8	5.3	1.0	204	17.0	0.5
Avg.	13	19.3	6.9	51	67	38	2.8	5.2	0.9	192	14.5	0.5

A = Average of 24 hourly values  
T = Daily total values  
H = Maximum hourly values  
L = Minimum hourly values

**Table A.2** Meteorological data from Riyadh's Climate Reference Year. (FEBRUARY)

Day	Ambient Temp. (C°)			Relative Humidity (%)			Wind Speed (m/s)			Wind Dir. (deg)	Ground Temp. (C°)	Rain Fall (mm)
	A	H	L	A	H	L	A	H	L	A	A	T
1	11.0	16.5	6.1	54	88	31	2.8	5.7	0.9	153	18.0	0.2
2	10.5	17.0	3.8	48	62	37	2.4	4.7	1.4	264	15.5	0.0
3	12.3	19.4	4.7	47	64	35	2.1	4.5	1.0	133	15.5	0.0
4	15.4	22.4	8.0	48	72	35	3.1	6.2	0.9	220	15.0	0.0
5	16.8	23.6	9.6	43	56	30	3.0	6.4	0.8	115	16.5	0.0
6	19.0	25.8	13.6	46	64	35	3.4	6.1	1.3	178	17.0	0.5
7	15.2	20.6	9.9	53	80	35	4.3	7.8	1.8	273	14.5	0.1
8	16.7	23.0	9.4	45	65	30	2.9	5.3	1.0	184	14.5	0.2
9	18.8	25.0	14.3	39	57	14	3.7	6.8	1.4	153	15.5	0.0
10	14.7	20.0	9.0	43	59	30	3.7	6.8	1.2	196	15.5	0.0
11	14.6	20.7	8.4	45	60	35	2.0	3.4	0.5	222	14.5	1.6
12	16.0	23.1	8.9	40	51	30	1.7	3.4	0.5	238	14.5	0.0
13	16.9	23.3	10.0	42	54	30	3.5	5.9	1.4	238	14.5	0.0
14	19.2	25.6	13.1	33	61	10	3.4	6.5	1.3	153	16.0	0.0
15	16.5	21.7	11.9	37	51	20	3.2	5.0	1.1	178	16.5	0.1
16	14.1	19.8	8.3	43	62	29	2.5	3.8	1.3	222	16.5	0.0
17	14.8	20.7	8.6	47	63	35	3.9	7.0	1.7	133	15.5	0.0
18	15.4	20.8	10.4	45	60	34	4.0	6.7	1.2	196	16.0	0.1
19	12.9	19.0	6.7	50	72	39	3.7	7.0	2.0	222	15.0	0.0
20	13.0	19.5	6.1	41	54	30	1.9	3.6	0.7	178	15.5	0.0
21	15.2	22.2	7.7	35	51	15	2.4	4.9	0.7	133	16.0	0.0
22	17.6	24.2	10.2	41	53	28	2.6	5.1	0.8	184	16.5	8.3
23	19.2	26.1	12.0	42	59	26	3.0	4.7	1.1	222	16.0	0.0
24	19.1	26.5	12.3	41	51	30	3.4	5.6	1.4	220	16.5	0.2
25	16.8	22.1	12.0	47	63	35	3.8	6.1	1.1	153	17.5	0.2
26	15.3	20.7	9.4	52	72	39	3.3	5.5	1.6	196	19.5	0.0
27	15.9	22.2	8.9	45	65	29	3.3	5.2	1.4	248	18.0	0.0
28	16.4	21.1	11.5	48	72	35	3.7	7.8	1.0	289	17.0	0.1
Avg.	15.7	21.9	9.5	44	62	30	3.1	5.6	1.2	196	16.0	0.4

A = Average of 24 hourly values  
 T = Daily total values  
 H = Maximum hourly values  
 L = Minimum hourly values

**Table A.3** Meteorological data from Riyadh's Climate Reference Year. (MARCH)

Day	Ambient Temp. (C°)			Relative Humidity (%)			Wind Speed (m/s)			Wind Dir. (deg)	Ground Temp. (C°)	Rain Fall (mm)
	A	H	L	A	H	L	A	H	L	A	A	T
1	14.0	19.0	10.3	44	62	32	3.2	5.8	1.1	238	17.5	0.7
2	13.0	18.2	7.8	55	75	33	2.4	4.3	1.0	184	17.0	4.1
3	14.5	20.2	8.5	59	70	51	2.9	4.6	1.4	273	17.0	0.3
4	16.0	21.6	10.1	44	58	32	2.6	4.2	0.9	184	16.5	1.3
5	16.4	21.0	12.0	50	70	32	3.2	6.6	1.6	204	16.0	6.6
6	18.0	22.6	13.7	54	73	31	2.8	5.1	0.5	220	16.0	0.4
7	19.5	24.8	14.3	46	66	32	4.1	7.2	1.8	196	18.5	0.7
8	20.3	26.2	13.4	36	50	26	3.4	5.6	1.2	196	17.5	0.0
9	23.5	30.1	15.7	32	41	24	3.7	7.2	1.4	204	18.0	0.0
10	25.4	30.9	20.7	28	41	12	3.5	7.2	1.6	222	19.5	0.0
11	21.0	27.0	14.4	31	38	23	3.4	5.3	1.6	159	20.0	0.1
12	21.9	28.0	14.9	32	41	24	2.3	4.9	0.7	184	19.5	0.0
13	23.6	29.5	17.3	31	38	24	2.9	6.0	0.5	115	21.5	0.3
14	21.5	27.6	15.1	31	37	23	4.4	7.1	1.4	134	22.5	0.0
15	21.0	26.5	15.7	29	40	20	3.8	5.5	1.4	133	24.5	0.0
16	18.5	23.2	13.3	33	42	24	3.5	5.9	1.6	196	22.0	0.0
17	18.5	23.8	12.2	31	38	23	2.8	6.2	0.5	204	24.0	0.0
18	20.7	27.7	14.1	29	42	15	3.5	6.2	1.1	115	23.0	0.0
19	18.9	24.7	12.2	26	38	10	4.4	7.8	1.3	178	22.0	0.0
20	21.2	28.0	13.6	41	51	33	2.7	5.3	1.2	248	23.5	0.3
21	19.6	27.1	13.1	39	54	28	2.9	4.8	1.2	184	23.0	0.4
22	19.6	24.9	14.7	38	50	28	2.5	4.3	0.9	184	24.5	0.0
23	20.2	26.2	13.8	36	53	26	3.0	5.2	1.1	115	25.5	0.0
24	21.6	26.6	16.7	40	58	31	3.9	7.8	1.7	196	26.0	8.4
25	22.0	28.2	15.2	34	42	24	3.9	7.0	1.7	200	26.0	0.1
26	19.0	25.1	12.6	45	58	33	4.6	8.0	1.8	264	25.0	0.1
27	21.4	28.2	14.4	42	53	32	2.4	4.8	0.5	159	24.0	0.3
28	20.2	26.5	13.7	41	63	31	2.4	5.1	1.1	184	23.5	0.0
29	20.8	26.1	14.9	36	53	26	3.3	8.2	1.6	115	23.5	0.0
30	22.8	29.0	16.5	35	50	23	3.7	7.0	2.0	178	26.5	0.0
31	24.1	30.5	18.0	38	50	28	4.1	7.0	2.0	178	27.5	0.0
Avg.	20.0	25.8	14.0	38	51	27	3.3	6.0	1.3	185	21.6	0.8

A = Average of 24 hourly values  
T = Daily total values  
H = Maximum hourly values  
L = Minimum hourly values

**Table A.4** Meteorological data from Riyadh's Climate Reference Year. (APRIL)

Day	Ambient Temp. (C°)			Relative Humidity (%)			Wind Speed (m/s)			Wind Dir. (deg)	Ground Temp. (C°)	Rain Fall (mm)
	A	H	L	A	H	L	A	H	L	A	A	T
1	22.5	29.0	15.3	25	31	18	3.3	6.5	0.9	200	27.0	0.0
2	22.9	29.1	16.1	28	34	24	2.7	6.9	0.5	153	29.0	0.0
3	22.0	27.3	16.2	30	37	23	3.4	6.4	1.4	204	26.0	0.0
4	20.8	25.0	16.3	35	49	24	3.9	7.5	2.3	305	25.5	2.9
5	21.6	26.6	16.5	44	54	30	3.1	7.2	1.2	196	23.0	1.6
6	22.3	27.8	16.1	47	57	31	2.5	5.9	0.5	196	22.0	1.9
7	22.9	28.3	17.7	40	52	26	3.3	6.7	1.3	159	22.5	3.3
8	24.8	30.9	18.0	30	43	21	2.8	6.5	1.0	178	24.0	0.0
9	24.5	30.8	17.7	30	37	23	3.0	6.5	1.1	222	25.5	0.1
10	24.2	30.4	17.2	39	54	22	2.6	5.1	0.7	171	23.5	0.3
11	25.8	32.7	18.7	34	49	25	2.2	5.6	0.7	196	23.5	0.0
12	25.1	30.2	19.7	28	39	21	2.9	7.1	1.0	159	27.0	0.0
13	25.4	31.3	21.0	31	41	24	2.8	4.4	1.1	153	26.0	0.7
14	23.2	29.0	15.9	31	43	23	2.2	4.7	0.5	133	29.0	0.0
15	22.8	27.4	17.6	25	31	18	2.0	4.5	0.8	153	30.0	0.0
16	23.0	27.7	18.0	30	36	25	2.7	5.4	1.1	196	26.0	0.0
17	25.1	32.2	18.8	30	39	20	3.0	4.8	1.4	222	27.5	5.9
18	26.8	33.7	21.6	35	50	25	2.7	6.0	0.8	204	30.5	0.1
19	23.5	29.6	17.5	40	54	27	3.1	7.6	0.9	222	29.0	5.6
20	19.6	24.2	15.3	45	50	37	2.5	5.4	1.0	196	29.0	5.2
21	21.8	28.1	14.5	37	50	27	3.4	6.8	1.1	222	26.5	0.8
22	25.4	32.0	17.6	30	43	20	2.9	5.3	0.9	196	26.5	0.0
23	26.6	33.5	19.1	36	49	27	2.2	3.8	0.9	238	37.0	1.3
24	25.3	31.6	18.7	33	48	20	3.8	7.0	1.3	193	33.0	7.1
25	24.8	30.8	17.8	35	51	25	3.4	6.9	1.2	222	32.0	3.8
26	25.0	30.9	20.7	31	43	22	3.1	6.2	1.0	171	31.0	2.3
27	23.8	30.6	16.7	33	48	23	3.0	6.7	1.2	124	31.5	0.0
28	21.4	28.4	15.0	26	33	20	2.7	4.8	1.2	238	26.0	6.8
29	22.1	29.5	15.8	27	38	20	3.3	7.9	0.5	171	27.5	6.8
30	26.6	33.5	18.8	35	46	22	2.9	7.2	1.0	196	29.5	0.0
Avg.	23.7	29.7	17.5	33	44	24	2.9	6.1	1.0	193	27.5	1.9

A = Average of 24 hourly values  
T = Daily total values  
H = Maximum hourly values  
L = Minimum hourly values

**Table A.5** Meteorological data from Riyadh's Climate Reference Year. (MAY)

Day	Ambient Temp. (C°)			Relative Humidity (%)			Wind Speed (m/s)			Wind Dir. (deg)	Ground Temp. (C°)	Rain Fall (mm)
	A	H	L	A	H	L	A	H	L	A	A	T
1	26.8	35.1	21.5	28	39	20	2.9	6.2	0.9	196	28.5	6.8
2	28.2	36.0	22.2	34	47	20	3.1	6.9	0.9	153	31.5	0.0
3	27.5	33.8	21.6	24	29	21	4.2	8.4	1.8	153	32.0	0.2
4	25.7	33.3	18.1	28	36	20	4.5	7.5	1.3	238	32.0	0.0
5	24.6	30.5	17.5	24	34	16	3.2	6.4	1.6	184	31.0	0.0
6	27.1	33.8	19.9	28	38	16	3.0	6.8	0.9	222	28.5	0.1
7	26.9	32.6	20.5	30	43	21	3.5	6.2	1.6	238	29.0	0.0
8	28.6	35.7	20.7	26	36	18	2.6	4.0	1.1	153	31.5	0.3
9	29.8	36.3	22.2	23	29	17	2.8	6.9	0.5	196	34.0	0.8
10	30.2	35.8	23.8	24	35	10	3.6	7.3	1.4	171	30.5	0.0
11	29.3	35.6	22.4	27	32	20	2.7	6.8	1.0	153	32.0	0.0
12	27.7	34.0	20.8	27	35	21	2.2	5.8	0.7	171	32.0	0.5
13	27.8	34.0	20.2	23	28	18	3.0	5.5	0.9	196	33.0	0.0
14	28.7	35.8	20.8	24	29	18	2.8	6.9	0.8	133	32.5	0.1
15	29.4	35.6	23.5	22	31	16	2.7	5.0	1.0	133	33.5	0.0
16	27.9	34.5	20.5	19	24	14	3.1	5.9	1.1	204	33.0	0.0
17	28.7	36.4	19.8	17	21	13	3.2	5.0	1.1	238	34.5	0.0
18	30.1	38.2	21.4	19	29	10	3.1	4.9	1.6	200	34.5	0.0
19	30.4	38.5	23.2	18	25	7	2.2	4.1	0.5	200	35.5	1.3
20	31.7	39.3	25.3	22	27	17	3.1	5.0	1.6	133	35.5	3.3
21	32.2	39.2	26.6	17	25	13	2.5	4.0	1.1	178	37.0	0.0
22	31.2	38.2	23.5	20	26	15	2.4	4.4	0.9	153	37.5	0.0
23	30.5	36.8	22.7	19	28	14	3.1	4.7	1.6	264	38.0	0.0
24	31.9	38.7	24.6	21	30	16	3.2	6.7	1.1	204	37.0	0.0
25	31.8	38.8	23.5	18	22	13	2.7	5.6	0.8	184	37.5	0.0
26	31.7	39.6	22.7	23	30	17	2.8	5.3	1.1	133	39.0	0.0
27	34.1	40.7	27.0	22	28	17	2.8	6.5	0.8	115	38.5	0.0
28	35.1	41.6	28.5	22	33	16	4.0	7.0	2.0	204	39.0	0.0
29	34.6	41.6	26.8	19	28	14	2.5	6.0	0.5	196	39.0	0.0
30	34.0	40.7	27.3	18	26	12	4.0	7.0	2.5	273	39.0	0.0
31	30.8	37.1	24.3	20	26	15	4.1	7.0	2.5	289	39.0	0.0
Avg.	29.8	36.7	22.7	23	31	16	3.1	6.0	1.2	189	34.4	0.4

A = Average of 24 hourly values  
T = Daily total values  
H = Maximum hourly values  
L = Minimum hourly values

**Table A.6** Meteorological data from Riyadh's Climate Reference Year. (JUNE)

Day	Ambient Temp. (C°)			Relative Humidity (%)			Wind Speed (m/s)			Wind Dir. (deg)	Ground Temp. (C°)	Rain Fall (mm)
	A	H	L	A	H	L	A	H	L	A	A	T
1	30.2	37.3	21.9	18	29	10	2.9	4.8	1.6	14	38.5	0.0
2	32.8	39.7	24.8	16	20	12	3.2	4.8	1.6	344	38.5	0.0
3	33.0	40.2	25.7	15	21	12	3.6	6.2	1.4	331	38.0	0.0
4	31.8	38.3	24.3	16	23	12	3.9	7.0	1.9	335	38.5	0.0
5	33.0	40.3	24.8	14	18	10	3.1	4.6	1.8	355	39.0	0.0
6	34.4	41.4	27.0	15	21	12	3.8	7.0	2.0	350	38.5	1.1
7	33.4	40.8	25.0	17	27	12	3.8	6.3	1.2	324	39.0	0.0
8	32.4	39.7	24.2	15	21	10	3.3	4.9	1.2	310	40.0	0.0
9	32.4	39.3	23.7	13	18	5	2.4	5.3	0.5	350	39.5	0.0
10	32.3	39.1	23.8	14	19	10	3.1	6.5	1.0	319	39.5	0.0
11	32.4	38.5	25.6	15	20	12	4.7	7.9	1.8	310	39.5	0.0
12	32.3	39.5	23.3	13	18	10	3.7	8.5	1.1	313	40.0	0.0
13	33.3	39.5	26.6	14	18	10	3.7	7.3	1.1	347	39.5	0.0
14	31.5	37.5	25.1	11	20	4	4.7	7.6	1.8	344	39.0	0.0
15	30.9	37.3	24.1	12	18	7	4.6	7.7	1.4	331	39.0	0.0
16	31.8	38.3	24.5	14	20	9	4.1	6.8	1.2	344	40.0	0.0
17	31.9	38.4	24.9	15	21	12	3.6	7.6	1.0	7	39.5	0.0
18	31.5	38.5	24.0	15	20	11	3.5	7.5	0.8	356	40.0	0.0
19	32.3	39.3	24.4	16	23	13	3.1	6.3	0.8	356	39.0	0.0
20	32.3	39.2	24.4	14	18	10	3.2	6.6	0.5	356	38.5	0.0
21	31.6	38.6	23.0	12	18	5	3.3	6.5	1.0	344	38.0	0.0
22	30.8	37.8	22.8	14	18	9	3.7	7.4	1.3	331	39.0	0.0
23	31.0	38.7	22.5	14	19	9	3.9	6.1	1.4	313	38.0	0.0
24	32.5	39.8	24.0	14	18	10	4.4	7.8	1.7	347	38.5	0.0
25	31.5	38.7	23.3	15	21	12	3.5	4.8	1.2	344	36.5	0.0
26	31.6	38.2	24.1	17	23	13	4.1	6.8	1.3	331	37.0	0.0
27	32.2	38.7	24.9	15	21	9	4.0	7.0	1.6	335	37.0	6.6
28	32.2	38.6	25.3	16	23	12	4.9	7.8	1.8	305	37.5	6.9
29	32.1	38.6	24.7	14	19	9	5.1	8.8	1.8	350	37.5	1.1
30	32.1	38.3	25.6	14	18	10	5.8	9.8	1.8	310	37.0	1.1
Avg.	32.1	38.9	24.4	15	20	10	3.8	6.8	1.4	314	38.6	0.6

A = Average of 24 hourly values  
T = Daily total values  
H = Maximum hourly values  
L = Minimum. hourly values

**Table A.8** Meteorological data from Riyadh's Climate Reference Year. (AUGUST)

Day	Ambient Temp. (C°)			Relative Humidity (%)			Wind Speed (m/s)			Wind Dir. (deg)	Ground Temp. (C°)	Rain Fall (mm)
	A	H	L	A	H	L	A	H	L	A	A	T
1	34.6	42.0	26.6	13	23	6	2.1	3.9	0.7	331	38.5	0.0
2	35.0	42.2	27.0	14	23	7	4.6	8.3	1.2	350	36.0	0.0
3	34.5	40.7	29.5	11	14	8	5.1	8.6	1.2	45	37.0	0.0
4	33.8	40.8	26.4	11	16	6	4.2	7.2	1.2	344	37.5	0.0
5	33.6	40.6	25.3	15	21	9	2.4	5.0	1.0	344	38.0	0.0
6	33.1	40.5	24.5	11	16	4	2.7	5.6	0.8	319	38.0	0.3
7	33.2	41.1	24.0	17	27	8	2.5	4.8	1.0	347	38.0	0.0
8	33.5	40.8	25.3	15	23	8	3.1	4.6	1.8	304	38.0	0.0
9	33.9	41.0	25.6	13	18	8	3.7	7.0	2.1	305	37.0	0.0
10	33.6	40.1	26.4	13	21	3	3.8	6.2	1.4	344	37.0	0.0
11	33.2	39.7	26.1	15	20	9	3.6	5.7	1.2	344	37.5	0.2
12	32.6	39.3	25.9	15	21	10	3.7	7.0	1.1	331	37.5	2.0
13	32.1	39.5	23.4	15	21	10	3.0	5.7	1.0	95	37.0	1.5
14	32.8	39.6	24.6	17	26	10	3.0	5.5	1.0	355	37.5	3.6
15	33.4	40.3	25.5	13	24	6	3.6	6.0	1.2	350	37.0	0.5
16	32.6	40.2	23.5	13	19	8	3.4	6.9	1.2	324	37.0	0.4
17	32.8	40.1	24.3	14	21	8	3.6	6.6	1.6	355	37.0	1.1
18	33.0	40.0	25.6	14	23	6	4.5	9.5	1.4	344	37.0	1.7
19	33.0	40.1	25.6	13	20	6	4.6	8.1	1.3	350	37.0	0.6
20	32.8	40.0	25.1	16	19	12	4.5	8.4	1.2	355	37.0	1.1
21	32.2	40.1	22.5	12	20	6	4.7	10.7	1.2	344	37.0	7.6
22	33.1	40.5	24.4	12	18	7	3.4	7.6	0.8	335	37.5	1.4
23	33.4	40.0	25.5	13	19	7	2.6	5.1	0.7	7	37.5	1.4
24	33.4	40.2	25.1	14	23	8	3.4	6.6	1.6	350	37.5	2.4
25	33.3	40.5	24.4	12	17	8	3.2	4.6	1.8	324	38.5	1.8
26	33.8	40.8	25.7	17	25	10	2.2	4.4	0.5	355	39.0	1.0
27	34.1	40.6	26.4	14	18	9	2.1	4.1	0.5	344	37.5	0.0
28	33.2	39.6	25.8	16	21	13	2.6	4.7	1.0	350	38.0	1.0
29	33.1	39.9	26.0	15	21	9	2.2	4.1	0.5	356	38.0	0.0
30	33.3	41.0	24.7	21	26	15	2.7	5.2	1.0	356	37.5	0.0
31	32.4	39.2	23.6	21	29	14	2.9	5.4	0.9	356	37.5	0.0
Avg.	33.3	40.4	25.3	14	21	8	3.3	6.2	1.1	313	37.5	1.0

A = Average of 24 hourly values

T = Daily total values

H = Maximum hourly values

L = Minimum. hourly values

**Table A.9** Meteorological data from Riyadh's Climate Reference Year. (SEPTEMBER)

Day	Ambient Temp. (C°)			Relative Humidity (%)			Wind Speed (m/s)			Wind Dir. (deg)	Ground Temp. (C°)	Rain Fall (mm)
	A	H	L	A	H	L	A	H	L	A	A	T
1	32.1	39.0	24.1	17	24	11	2.6	4.3	0.9	95	37.0	0.0
2	32.3	39.1	23.8	17	22	13	2.2	3.8	1.0	7	37.0	0.0
3	32.0	38.3	25.0	18	22	15	3.4	7.5	0.9	19	37.0	0.0
4	30.8	37.0	23.3	17	23	12	4.0	8.3	0.9	95	36.5	0.0
5	31.1	38.1	22.4	14	17	10	3.6	6.6	0.5	61	36.0	0.0
6	32.8	39.0	26.1	15	18	10	3.4	6.6	1.3	45	36.0	4.9
7	33.0	39.6	25.9	13	18	9	3.1	5.5	1.1	60	35.5	0.0
8	32.5	39.3	25.7	11	15	8	3.1	5.6	1.1	21	36.0	0.0
9	31.9	39.2	23.0	12	16	9	3.3	6.6	1.6	14	35.5	0.0
10	32.2	38.8	23.8	14	18	9	3.8	6.8	1.2	7	35.5	0.0
11	32.9	38.9	26.3	14	18	11	2.9	6.2	0.7	19	35.5	0.0
12	32.0	38.6	25.0	14	19	11	2.8	4.6	1.1	95	35.0	0.0
13	31.4	38.0	23.7	15	19	11	2.7	4.7	1.0	324	34.5	0.0
14	30.9	37.8	23.3	16	21	11	2.3	4.1	0.5	14	34.5	0.0
15	30.4	37.3	23.5	17	24	12	2.5	4.5	0.5	264	34.5	0.9
16	30.0	36.7	21.6	17	22	13	2.3	4.1	1.0	19	34.5	0.0
17	30.8	36.9	24.1	19	25	14	3.4	6.1	1.3	134	33.5	0.0
18	30.2	37.2	22.7	16	22	11	3.3	6.8	1.1	273	33.5	0.0
19	29.8	36.6	21.8	13	18	9	2.7	4.4	1.1	45	33.0	0.0
20	30.2	36.7	23.1	16	18	13	2.3	4.1	0.5	331	30.0	0.0
21	30.0	37.3	21.5	17	21	12	2.5	4.4	1.0	14	32.0	0.0
22	30.3	37.4	22.6	17	22	12	2.2	4.1	0.5	19	32.5	0.0
23	29.0	35.9	20.3	18	22	14	3.6	8.3	1.3	14	32.5	0.0
24	29.0	36.2	20.8	17	22	12	3.3	6.8	1.1	7	31.0	0.0
25	29.2	37.3	19.7	16	19	11	2.7	4.8	0.9	19	31.5	0.0
26	29.7	37.6	20.4	14	19	9	2.8	5.2	1.1	95	31.0	0.0
27	29.7	37.4	20.0	15	19	11	3.1	6.2	0.7	273	31.5	0.0
28	29.7	37.0	20.7	15	18	13	2.5	4.4	0.5	7	31.0	0.0
29	30.4	37.1	23.0	17	21	13	2.3	4.7	1.0	19	31.0	0.0
30	31.2	37.6	24.3	18	24	11	3.6	7.7	1.0	273	31.0	0.0
Avg.	30.9	37.8	23.1	16	20	11	2.9	5.6	0.9	89	33.9	0.2

A = Average of 24 hourly values  
T = Daily total values  
H = Maximum hourly values  
L = Minimum hourly values

**Table A.10** Meteorological data from Riyadh's Climate Reference Year. (OCTOBER)

Day	Ambient Temp. (C°)			Relative Humidity (%)			Wind Speed (m/s)			Wind Dir. (deg)	Ground Temp. (C°)	Rain Fall (mm)
	A	H	L	A	H	L	A	H	L	A	A	T
1	31.4	37.8	24.8	17	24	11	3.0	5.9	0.5	95	30.5	0.0
2	30.0	36.4	23.2	17	23	13	2.6	5.3	0.5	171	30.5	0.0
3	29.7	36.0	22.8	18	22	15	2.5	5.6	0.7	171	30.5	0.0
4	29.4	36.2	21.8	17	23	12	2.2	4.1	0.7	95	30.5	0.0
5	28.6	36.3	20.3	21	26	15	2.0	4.3	0.5	95	30.5	0.0
6	27.9	35.1	19.4	22	28	15	2.5	4.8	1.0	273	29.5	0.0
7	28.0	35.6	18.8	20	28	14	2.2	3.7	1.0	95	29.5	0.0
8	28.6	35.6	20.3	16	23	12	2.1	4.1	0.5	159	29.5	0.0
9	29.0	36.3	20.7	19	25	14	2.1	4.1	0.5	184	29.5	0.0
10	29.1	35.7	22.5	21	28	14	2.5	4.4	1.0	115	30.5	0.0
11	28.8	35.4	21.3	21	26	16	2.6	4.5	0.9	178	29.5	0.0
12	28.0	35.0	19.5	21	29	16	2.6	4.1	1.1	178	29.5	1.3
13	27.1	34.3	19.0	23	29	17	2.7	3.9	1.6	200	29.5	0.0
14	26.7	33.7	18.5	24	32	17	2.3	4.0	1.0	153	29.5	0.0
15	27.8	33.9	20.6	22	30	15	2.6	4.8	0.5	204	29.5	0.0
16	28.0	34.4	21.2	21	27	16	2.8	5.8	0.7	238	29.5	0.0
17	27.1	33.8	19.6	20	26	15	2.5	5.2	0.7	238	28.5	0.0
18	26.4	33.6	17.8	20	27	14	2.7	4.9	0.5	153	28.5	0.0
19	25.7	30.4	21.3	21	28	14	3.6	6.8	1.0	178	28.5	0.0
20	22.2	27.8	17.0	24	27	20	3.4	6.1	1.0	222	27.5	0.0
21	21.7	27.5	16.1	25	32	19	2.9	5.5	0.5	133	27.5	0.0
22	22.1	29.0	15.2	24	30	17	2.5	4.6	1.0	196	25.5	0.0
23	22.4	30.3	14.0	24	29	18	1.9	3.0	0.8	273	25.5	0.0
24	22.8	29.6	15.6	23	30	17	1.9	3.1	0.5	171	25.5	0.0
25	22.8	30.1	15.2	24	30	17	2.0	3.5	0.7	171	25.5	0.0
26	22.7	29.6	14.8	22	29	15	2.1	2.9	1.0	305	25.5	0.0
27	22.1	29.1	14.9	23	29	17	2.4	4.7	1.0	153	24.5	0.0
28	20.9	28.1	12.5	23	28	19	2.2	4.1	0.5	134	24.5	0.0
29	20.9	27.6	13.2	26	32	19	2.2	4.1	0.5	171	23.5	0.0
30	21.4	27.7	14.7	23	31	14	2.4	4.6	0.5	95	23.5	0.0
31	21.9	28.2	14.7	25	32	19	2.5	4.4	1.0	95	23.5	0.0
Avg.	25.8	32.6	18.4	22	28	16	2.5	4.5	0.8	171	27.9	0.0

A = Average of 24 hourly values

T = Daily total values

H = Maximum hourly values

L = Minimum. hourly values

**Table A.11** Meteorological data from Riyadh's Climate Reference Year. (NOVEMBER)

Day	Ambient Temp. (C°)			Relative Humidity (%)			Wind Speed (m/s)			Wind Dir. (deg)	Ground Temp. (C°)	Rain Fall (mm)
	A	H	L	A	H	L	A	H	L	A	A	T
1	22.6	29.0	15.8	41	60	27	2.9	5.8	1.0	95	23.5	0.0
2	23.4	29.1	17.4	44	58	30	3.3	7.3	0.5	134	24.5	0.0
3	22.6	28.5	17.3	46	56	38	3.0	6.1	0.7	273	24.5	0.0
4	20.8	26.7	14.2	39	54	29	2.5	4.9	0.7	95	24.5	0.0
5	20.2	25.0	14.5	40	52	27	2.9	5.8	0.5	273	24.5	0.0
6	22.7	28.1	17.0	43	58	29	3.6	7.9	0.5	153	23.5	0.0
7	23.8	28.7	18.7	42	61	29	3.4	6.5	1.0	178	23.5	0.0
8	23.6	28.3	19.3	34	47	24	3.2	6.2	0.9	222	24.5	0.0
9	22.1	27.5	17.5	47	69	31	3.4	7.3	1.0	305	24.5	0.0
10	19.3	24.7	13.9	50	67	34	3.0	5.2	1.0	289	25.5	1.7
11	19.6	26.1	13.3	52	63	45	3.3	5.3	1.6	238	25.5	0.0
12	17.9	24.0	13.7	45	62	33	3.8	6.4	1.6	196	25.5	0.3
13	14.6	19.9	9.0	46	60	33	3.2	5.1	0.9	273	25.5	0.3
14	15.7	22.2	9.5	49	67	33	2.7	4.5	1.0	133	23.5	0.0
15	18.8	24.8	12.8	48	70	33	3.0	6.3	0.7	305	22.5	0.2
16	19.4	25.3	13.7	39	56	27	2.7	5.4	0.7	204	21.5	0.0
17	19.0	24.5	14.7	32	42	25	3.0	5.4	1.0	153	24.5	0.0
18	20.0	26.2	13.9	31	43	20	3.3	6.8	1.0	264	22.5	0.0
19	18.5	23.7	13.5	31	45	20	3.3	5.5	0.5	133	22.5	0.0
20	17.5	22.7	12.2	35	42	27	3.1	5.8	0.7	220	21.5	0.0
21	19.5	26.3	13.3	32	45	20	2.5	5.1	0.5	115	21.5	0.0
22	18.9	24.0	13.9	33	44	25	2.8	5.0	0.7	178	22.5	0.0
23	19.2	24.4	14.7	33	47	23	2.5	4.8	0.5	273	22.5	0.0
24	18.0	23.1	13.3	34	45	27	3.1	6.2	0.5	184	22.5	0.0
25	18.1	23.1	12.9	34	43	26	3.2	6.8	0.5	153	21.5	0.0
26	18.1	23.4	12.7	33	45	24	3.7	7.5	0.5	196	21.5	0.0
27	19.6	25.1	14.3	30	39	21	3.1	6.1	0.7	222	21.5	0.0
28	20.5	26.6	14.4	31	46	23	3.0	5.5	0.7	238	21.5	0.0
29	21.6	27.6	15.7	42	53	32	2.8	7.2	0.5	95	21.5	0.0
30	18.1	24.3	12.5	37	50	23	1.9	3.4	1.0	134	20.5	0.0
Avg.	19.8	25.4	14.3	39	53	28	3.0	5.9	0.8	197	23.2	0.1

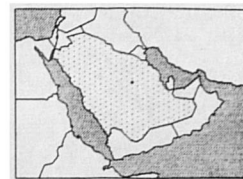
A = Average of 24 hourly values  
T = Daily total values  
H = Maximum hourly values  
L = Minimum. hourly values

**Table A.12** Meteorological data from Riyadh's Climate Reference Year. (DECEMBER)

Day	Ambient Temp. (C°)			Relative Humidity (%)			Wind Speed (m/s)			Wind Dir. (deg)	Ground Temp. (C°)	Rain Fall (mm)
	A	H	L	A	H	L	A	H	L	A	A	T
1	14.9	17.1	12.0	35	49	22	3.0	5.7	0.9	134	21.5	0.0
2	13.5	18.3	9.1	35	42	27	3.3	6.1	0.8	134	21.5	0.0
3	12.8	16.7	9.7	36	42	28	2.8	5.4	0.5	134	20.5	0.0
4	9.8	13.6	6.2	37	50	25	2.9	5.0	0.7	273	20.5	3.9
5	10.3	15.6	4.9	54	67	39	3.9	6.4	1.2	222	14.5	0.3
6	13.8	20.6	7.5	56	70	39	3.0	4.6	1.8	222	12.5	0.0
7	11.1	16.2	6.4	49	67	31	2.7	4.4	0.8	273	12.5	0.0
8	12.2	18.3	6.4	38	52	27	2.3	4.3	0.5	171	12.5	0.0
9	11.3	14.8	8.1	37	44	28	2.4	4.2	0.5	273	13.5	0.0
10	11.0	14.9	7.4	43	58	25	2.5	4.6	0.7	222	13.5	0.0
11	11.8	16.7	8.1	40	55	29	2.3	4.3	0.7	305	13.5	0.0
12	13.0	19.6	6.5	36	50	27	2.7	5.9	0.5	171	13.5	0.0
13	16.4	21.2	12.8	40	52	32	3.2	6.9	0.5	171	14.5	0.0
14	12.7	16.9	8.6	42	57	31	2.8	5.5	0.7	95	14.5	0.0
15	7.6	10.0	4.9	35	49	23	2.3	4.4	0.5	134	15.5	0.0
16	9.9	14.4	5.3	41	49	33	2.4	4.1	1.0	134	16.5	0.0
17	12.8	18.8	6.8	42	56	30	2.5	4.5	1.0	305	17.5	0.0
18	14.5	19.5	9.5	44	59	32	3.2	5.4	1.1	134	18.5	0.0
19	12.5	15.6	8.5	47	63	34	4.2	7.5	1.6	133	17.5	3.3
20	10.6	16.5	4.2	56	61	48	1.8	2.9	0.8	95	15.5	1.5
21	13.8	20.5	7.6	63	79	50	2.4	4.4	1.3	95	15.5	14.4
22	14.6	21.3	9.3	56	71	41	3.0	6.1	1.3	95	16.5	1.5
23	14.9	21.4	8.4	56	66	45	2.4	3.8	1.3	133	17.5	0.0
24	15.9	22.4	10.0	54	67	39	2.4	4.6	0.8	305	18.5	0.0
25	17.4	24.5	9.4	56	70	39	2.4	4.0	1.6	273	15.5	1.2
26	19.0	24.7	13.4	49	67	31	3.5	6.6	1.6	95	16.5	0.0
27	17.3	22.3	13.5	55	71	43	4.0	6.7	1.8	331	15.5	0.5
28	14.9	19.2	11.2	56	64	49	3.2	5.4	1.2	222	12.5	0.0
29	14.7	19.4	10.8	56	71	41	2.5	4.1	0.5	171	11.5	0.0
30	9.7	13.8	5.0	49	67	31	2.4	4.1	0.5	133	11.5	0.0
31	9.5	13.8	5.2	42	56	30	2.4	4.1	0.5	305	10.5	0.0
Avg.	13.0	18.0	8.3	46	59	34	2.8	5.0	0.9	190	15.5	0.9

A = Average of 24 hourly values  
T = Daily total values  
H = Maximum hourly values  
L = Minimum hourly values

## Appendix B



---

# Insolation Data (Riyadh, Saudi Arabia)

---

The following tables represent daily values of:

- Global horizontal insolation
- Diffuse horizontal insolation
- Direct normal insolation
- Ultra-violet insolation on horizontal surface
- Infra-red insolation on horizontal surface
- Extraterrestrial insolation
- Recorded and calculated maximum sunshine duration

The units are  $\text{Wh (m}^{-2} \text{d}^{-1})$  for daily total solar energy,  $\text{W m}^{-2}$  for hourly insolation and hours for sunshine duration. The original source for raw data (hourly values of global horizontal and direct normal insolation) is the King Abdulaziz City for Science and Technology (KACST). The source data represent extracts from the data acquisition system of the photovoltaic power site in the Solar Village, (Latitude  $24.54^\circ$  and Longitude  $46.24^\circ$ ) for the years 1984 to 1986. Supplementary data sheets containing daily data, including ultraviolet insolation, infrared irradiation and recorded sunshine hours, for 1985 and 1986 were also obtained from the same source.

The first three parameters are derived from the reference climate year file prepared by the author in chapter 3. The diffuse horizontal insolation, extraterrestrial insolation and maximum possible sunshine duration are calculated values, (see chapter 3). Recorded sunshine hours data, ultraviolet and infrared insolation data are averages for the years 1985 and 1986.

**Table B.1** Insolation data over Riyadh for the month of *JANUARY*.

Day	GLBH		DIFH		DIRN		UVH		IRH		EXTH	SUNH	
	T	H	T	H	T	H	T	H	T	H	T	act.	max.
1	4318	679	1542	230	3634	988	99	17	2470	245	6384	4.33	10.51
2	4106	662	1793	255	51	10	96	16	2825	276	6397	1.00	10.51
3	4043	646	1588	239	42	5	91	18	2998	297	6412	1.17	10.52
4	4307	678	1672	262	5075	942	98	16	2669	260	6426	0.33	10.53
5	4163	652	1329	181	6118	903	94	16	931	109	6442	0.17	10.53
6	4198	655	1491	237	5987	900	90	16	898	125	6460	3.83	10.54
7	4327	668	1397	226	7346	982	71	17	790	117	6479	5.00	10.55
8	4428	685	1416	257	5962	998	104	17	1058	120	6498	6.83	10.56
9	4349	671	1549	260	119	14	102	17	1200	135	6518	0.33	10.57
10	3935	619	1930	253	124	15	103	17	1418	159	6539	0.50	10.58
11	4392	676	1192	191	7867	973	105	17	2940	378	6561	9.17	10.59
12	4230	659	1442	260	4138	888	100	17	3708	367	6584	6.33	10.60
13	4359	679	1475	386	1982	731	102	17	3062	306	6608	0.50	10.61
14	4301	671	1649	311	6329	930	98	17	3094	302	6632	5.50	10.62
15	4276	659	1447	184	5888	902	96	16	3564	339	6659	6.00	10.63
16	3872	638	1765	291	5904	894	95	16	3175	304	6685	8.83	10.65
17	4445	679	1188	176	5995	897	97	16	3240	317	6713	5.17	10.66
18	4390	685	1253	163	5042	741	98	17	3758	393	6742	6.00	10.67
19	4548	698	1698	233	1225	476	106	17	3710	357	6772	2.50	10.69
20	4179	683	1690	245	1678	385	73	16	3168	307	6802	5.83	10.70
21	4578	700	898	126	6669	873	98	17	2676	263	6833	9.83	10.71
22	4117	629	1729	252	5224	746	98	18	3058	307	6865	9.67	10.73
23	4314	672	1826	248	2872	477	85	15	3367	326	6898	7.83	10.74
24	4220	659	1973	297	2194	387	86	15	3194	302	6932	7.33	10.76
25	3558	634	2379	415	2692	446	97	16	3427	326	6967	8.17	10.78
26	3535	574	1580	262	470	172	56	18	3830	380	7001	1.50	10.79
27	4328	676	1763	249	3526	649	94	16	3415	409	7037	7.50	10.81
28	2575	399	1476	220	54	5	23	8	3805	441	7073	0.50	10.82
29	3642	657	1778	303	470	194	61	19	3888	370	7110	1.17	10.84
30	4198	670	2193	374	126	30	88	19	3857	364	7149	0.50	10.86
31	3625	617	1455	273	95	18	58	18	4027	377	7188	0.33	10.88
Avg.	4124	653	1599	254	3384	567	89	17	2881	293	6721	4.3	10.7

GLBH = Global Horizontal, (0.3 – 2.8  $\mu\text{m}$ )  
DIFH = Diffuse Horizontal, (0.3 – 2.8  $\mu\text{m}$ )  
DIRN = Direct Normal, (0.3 – 2.8  $\mu\text{m}$ )  
T = Daily Total Insolation Energy ( $\text{Wh}/\text{m}^2$ )  
H = Maximum Insolation Power ( $\text{W}/\text{m}^2$ )

UVH = Ultra-Violet Horizontal, (0.29 – 0.39  $\mu\text{m}$ )  
IRH = Infra-Red Horizontal, (4 – 50  $\mu\text{m}$ )  
EXTH = Extraterrestrial, (Calculated, see chapter 3)  
SUNH = Recorded Bright Sunshine Hours (act.),  
and Calculated (max.), see chapter 3.

Table B.2 Insolation data over Riyadh for the month of *FEBRUARY*.

Day	GLBH		DIFH		DIRN		UVH		IRH		EXTH	SUNH	
	T	H	T	H	T	H	T	H	T	H	T	act.	max.
1	4453	661	2069	301	1105	256	96	19	3756	391	7226	4.50	10.89
2	5022	751	915	116	8291	1002	119	19	3072	339	7266	9.67	10.91
3	5019	744	880	127	7953	910	109	17	3168	305	7307	10.50	10.93
4	4785	745	1311	204	4858	816	107	18	3682	354	7347	9.00	10.95
5	4397	653	2246	332	1826	419	96	19	3895	372	7390	5.83	10.97
6	4569	725	2507	442	1091	533	104	20	4308	404	7431	0.33	10.99
7	4547	748	1459	274	4831	875	91	19	3785	354	7473	7.17	11.01
8	4508	709	2382	346	5113	688	112	18	3475	333	7516	6.50	11.03
9	4179	687	2666	447	275	123	87	21	4234	424	7561	0.17	11.05
10	4965	751	2008	258	6304	793	120	19	4224	449	7605	10.00	11.07
11	5216	779	1375	186	8286	912	127	20	3185	302	7648	10.67	11.09
12	5088	765	1979	282	4322	592	109	18	3468	333	7693	9.33	11.11
13	5277	783	3248	479	211	128	110	17	3564	331	7738	0.33	11.13
14	5287	772	3344	494	303	199	124	20	3698	346	7784	0.33	11.15
15	5215	780	1824	224	6178	841	119	19	3324	406	7830	8.83	11.17
16	5267	774	1392	190	7102	837	124	20	3264	312	7877	10.50	11.20
17	5091	779	1817	218	3800	670	110	19	3533	341	7922	9.17	11.22
18	5328	788	1580	253	5268	824	116	19	3658	344	7970	9.33	11.24
19	5612	815	856	120	9054	980	132	21	3038	307	8016	11.00	11.26
20	5593	814	1206	159	9706	1030	136	21	3062	294	8063	11.00	11.28
21	5595	815	1382	183	9769	1034	137	22	3211	315	8110	11.00	11.31
22	5690	827	1259	180	9015	1016	136	22	3406	331	8158	10.83	11.33
23	5112	769	2145	315	3723	716	120	22	4020	393	8206	7.83	11.35
24	5173	790	1895	258	5974	860	133	22	4039	409	8253	8.83	11.37
25	5098	701	2163	291	7063	876	143	22	3970	359	8301	10.33	11.40
26	5328	776	1997	278	7324	922	136	24	3581	362	8349	10.83	11.42
27	4980	721	1918	269	7332	877	140	22	4032	357	8397	10.67	11.44
28	2016	334	1693	255	1078	370	81	15	4447	395	8444	3.00	11.47
Avg.	4943	741	1840	267	5256	718	117	20	3646	356	7817	7.8	11.2

GLBH = Global Horizontal, (0.3 – 2.8  $\mu\text{m}$ )  
DIFH = Diffuse Horizontal, (0.3 – 2.8  $\mu\text{m}$ )  
DIRN = Direct Normal, (0.3 – 2.8  $\mu\text{m}$ )  
T = Daily Total Insolation Energy ( $\text{Wh}/\text{m}^2$ )  
H = Maximum Insolation Power ( $\text{W}/\text{m}^2$ )

UVH = Ultra-Violet Horizontal, (0.29 – 0.39  $\mu\text{m}$ )  
IRH = Infra-Red Horizontal, (4 – 50  $\mu\text{m}$ )  
EXTH = Extraterrestrial, (Calculated, see chapter 3)  
SUNH = Recorded Bright Sunshine Hours (act.),  
and Calculated (max.), see chapter 3.

**Table B.3** Insolation data over Riyadh for the month of *MARCH*.

Day	GLBH		DIFH		DIRN		UVH		IRH		EXTH	SUNH	
	T	H	T	H	T	H	T	H	T	H	T	act.	max.
1	5685	833	1084	156	6303	920	145	25	4598	404	8493	8.33	11.49
2	3915	648	1977	363	612	330	74	31	4565	405	8541	1.33	11.51
3	4723	690	2233	301	1635	503	103	32	4469	404	8588	4.33	11.54
4	5193	812	1911	314	2765	621	116	23	4325	404	8635	5.83	11.56
5	3406	553	1284	216	325	170	28	26	4325	382	8684	1.00	11.59
6	3962	547	1558	257	974	396	57	25	4459	390	8730	2.17	11.61
7	5455	750	2311	332	5086	765	134	27	4250	411	8778	8.67	11.63
8	6090	874	1469	205	8305	906	152	23	3830	367	8825	11.00	11.66
9	6135	868	1678	254	6451	829	147	23	4416	393	8872	10.67	11.68
10	6126	859	1935	270	6196	795	151	27	4644	408	8919	10.67	11.71
11	6151	883	1691	190	7687	911	157	24	4015	354	8966	10.83	11.73
12	6214	880	1701	233	7292	830	153	23	4133	357	9011	11.17	11.75
13	5754	828	2727	325	6304	793	150	23	4402	378	9057	10.33	11.78
14	5635	835	3040	431	4797	757	144	28	4702	430	9103	9.67	11.80
15	4582	669	2267	293	6492	825	159	24	4788	416	9148	10.67	11.83
16	5809	879	2291	301	6409	770	152	23	4147	357	9193	10.67	11.85
17	6042	858	2340	285	5886	718	146	22	4015	349	9238	10.83	11.88
18	5779	857	2714	374	4694	727	134	23	4152	411	9283	7.67	11.90
19	6340	904	1924	267	8369	916	165	24	3922	339	9327	11.33	11.93
20	5777	818	2190	308	8208	873	163	24	4010	349	9370	11.50	11.95
21	5069	898	1655	245	8083	870	162	24	4142	362	9414	11.33	11.98
22	4418	602	1953	288	7091	792	161	24	4339	393	9456	11.17	12.00
23	6137	877	2470	305	4092	542	141	21	4894	424	9498	9.83	12.02
24	6425	877	1926	243	5928	704	161	26	5143	456	9541	10.67	12.05
25	5972	870	2968	376	3742	566	143	25	4999	451	9582	9.33	12.07
26	6248	885	2402	306	5368	824	154	25	4217	359	9622	9.50	12.10
27	5771	837	2067	265	8943	894	174	26	3979	346	9664	12.00	12.12
28	6235	859	2341	270	7007	750	167	25	4524	396	9703	11.50	12.15
29	5845	822	3177	396	3564	470	145	23	4896	440	9743	10.17	12.17
30	6217	840	2779	337	3258	568	142	24	5261	456	9781	9.00	12.20
31	6638	909	2013	232	5912	762	176	26	5263	448	9820	9.83	12.22
Avg.	5605	810	2131	288	5412	713	141	25	4446	395	9180	9.1	11.9

GLBH = Global Horizontal, (0.3 – 2.8  $\mu\text{m}$ )  
DIFH = Diffuse Horizontal, (0.3 – 2.8  $\mu\text{m}$ )  
DIRN = Direct Normal, (0.3 – 2.8  $\mu\text{m}$ )  
T = Daily Total Insolation Energy ( $\text{Wh}/\text{m}^2$ )  
H = Maximum Insolation Power ( $\text{W}/\text{m}^2$ )

UVH = Ultra-Violet Horizontal, (0.29 – 0.39  $\mu\text{m}$ )  
IRH = Infra-Red Horizontal, (4 – 50  $\mu\text{m}$ )  
EXTH = Extraterrestrial, (Calculated, see chapter 3)  
SUNH = Recorded Bright Sunshine Hours (act.),  
and Calculated (max.), see chapter 3.

**Table B.4** Insolation data over Riyadh for the month of *APRIL*.

Day	GLBH		DIFH		DIRN		UVH		IRH		EXTH	SUNH	
	T	H	T	H	T	H	T	H	T	H	T	act.	max.
1	6642	907	1935	201	6307	735	170	25	4843	411	9858	11.00	12.25
2	6604	909	2019	238	4670	654	163	24	5702	471	9894	9.00	12.27
3	5488	826	2407	308	2617	540	121	28	5599	481	9931	5.67	12.29
4	3926	529	2498	354	106	23	55	11	5340	498	9967	0.33	12.32
5	5773	816	3074	416	3228	541	156	28	5258	432	10003	7.67	12.34
6	6290	867	2683	425	5338	909	171	30	5155	429	10038	9.17	12.37
7	5930	930	2524	334	3427	865	144	30	5136	427	10072	6.00	12.39
8	6304	827	2680	391	4909	762	167	32	5251	500	10105	10.17	12.41
9	5883	851	3035	362	4312	699	165	26	5419	440	10139	8.83	12.44
10	6831	927	1818	222	7893	841	179	25	4925	403	10171	11.67	12.46
11	5671	854	2282	307	7158	783	174	25	5107	419	10203	11.50	12.49
12	6492	898	2562	377	6370	759	168	24	5417	458	10234	11.50	12.51
13	5395	844	3160	456	2364	741	117	31	5330	529	10265	5.00	12.53
14	4199	593	2055	264	5828	822	171	30	5294	443	10295	9.83	12.56
15	4604	728	2364	436	5670	828	176	30	5436	445	10324	10.33	12.58
16	5506	775	3346	422	2043	422	144	22	5719	466	10353	7.00	12.60
17	6398	883	2944	478	5409	778	167	29	5736	469	10382	9.00	12.63
18	6326	851	3968	494	3713	811	150	31	5659	458	10409	6.00	12.65
19	5683	880	3252	498	3434	856	135	34	5338	458	10436	5.67	12.67
20	4588	632	2880	441	109	23	165	22	5114	413	10463	1.00	12.69
21	5949	856	3060	374	2638	527	138	36	5105	409	10488	5.50	12.72
22	7195	948	2611	269	6974	813	188	27	5074	408	10513	11.33	12.74
23	6852	930	3037	349	7510	784	188	26	5174	414	10537	11.67	12.76
24	5663	857	2744	362	3335	700	130	29	5376	453	10562	6.83	12.78
25	5460	849	3770	526	1129	275	117	31	5412	456	10584	4.33	12.80
26	6218	926	2775	316	3109	626	140	29	5568	447	10607	6.33	12.83
27	7072	936	2733	332	5046	559	171	25	5443	490	10629	11.50	12.85
28	7382	955	1881	202	8897	891	197	27	5040	409	10651	12.17	12.87
29	7165	951	2226	279	7421	902	193	28	5266	432	10672	10.17	12.89
30	7361	963	2406	313	6681	768	190	27	5410	432	10692	10.67	12.91
Avg.	6028	850	2691	358	4588	675	157	27	5322	447	10316	8.2	12.6

GLBH = Global Horizontal, (0.3 – 2.8  $\mu\text{m}$ )  
DIFH = Diffuse Horizontal, (0.3 – 2.8  $\mu\text{m}$ )  
DIRN = Direct Normal, (0.3 – 2.8  $\mu\text{m}$ )  
T = Daily Total Insolation Energy ( $\text{Wh}/\text{m}^2$ )  
H = Maximum Insolation Power ( $\text{W}/\text{m}^2$ )

UVH = Ultra-Violet Horizontal, (0.29 – 0.39  $\mu\text{m}$ )  
IRH = Infra-Red Horizontal, (4 – 50  $\mu\text{m}$ )  
EXTH = Extraterrestrial, (Calculated, see chapter 3)  
SUNH = Recorded Bright Sunshine Hours (act.),  
and Calculated (max.), see chapter 3.

**Table B.5** Insolation data over Riyadh for the month of *MAY*.

Day	GLBH		DIFH		DIRN		UVH		IRH		EXTH	SUNH	
	T	H	T	H	T	H	T	H	T	H	T	act.	max.
1	6794	925	3353	396	5067	726	175	28	5609	453	10711	8.50	12.93
2	7065	949	3264	398	4992	650	178	25	5952	468	10730	9.83	12.95
3	6174	884	3461	452	1841	484	105	25	6487	516	10749	4.17	12.97
4	5928	833	4100	568	6897	784	30	15	2230	406	10767	3.83	12.99
5	6935	875	3520	445	5558	678	196	28	5249	414	10784	10.83	13.01
6	7017	940	3847	421	4483	576	183	26	5352	430	10801	10.50	13.03
7	6361	905	4333	533	3297	574	170	28	5597	458	10818	9.00	13.05
8	7066	915	3741	448	4902	673	193	30	5969	490	10833	8.83	13.07
9	6742	954	3753	440	2756	608	162	28	6204	508	10849	6.50	13.09
10	7040	949	3706	476	3958	640	189	35	5892	477	10863	9.00	13.11
11	6591	887	3776	441	3768	590	182	31	6005	500	10877	8.67	13.12
12	7288	973	3273	419	6780	706	209	33	5498	456	10891	12.17	13.14
13	7359	955	3289	446	6788	735	210	28	5472	430	10904	12.00	13.16
14	6979	930	3602	437	5020	613	197	28	5534	542	10917	10.33	13.18
15	7789	986	3615	426	5905	663	213	29	5035	391	10929	11.50	13.19
16	7594	969	3405	391	6266	667	213	29	4207	391	10941	11.67	13.21
17	7565	961	3542	433	5984	648	210	28	2467	227	10952	11.67	13.22
18	7804	981	3044	385	7260	778	224	30	2378	206	10963	11.67	13.24
19	7817	973	2976	391	7566	759	227	31	2393	216	10973	12.50	13.26
20	7852	995	2978	344	7204	724	225	30	2503	214	10983	12.50	13.27
21	7684	989	3064	381	6408	694	217	29	2419	208	10993	12.33	13.29
22	7339	985	3261	363	5826	662	216	29	1260	141	11001	11.83	13.30
23	6993	928	4111	479	4570	507	200	27	4166	400	11010	11.33	13.31
24	7611	963	3470	364	6695	685	224	30	2590	523	11018	12.50	13.33
25	7393	968	3249	334	7016	706	224	30	5933	469	11026	12.67	13.34
26	7015	959	3577	412	6552	674	220	30	5623	471	11034	12.50	13.35
27	7809	982	3164	330	6679	692	225	30	5414	430	11041	12.33	13.37
28	7704	980	3483	398	5280	685	220	30	5846	482	11047	9.33	13.38
29	7812	976	3361	360	6535	681	225	30	5633	443	11054	12.00	13.39
30	7221	913	4072	456	5790	632	217	29	5695	451	11059	12.00	13.40
31	7372	939	3912	414	4848	586	207	28	5688	443	11065	11.00	13.41
Avg.	7217	946	3526	419	5564	661	196	29	4719	408	10922	10.5	13.2

GLBH = Global Horizontal, (0.3 – 2.8  $\mu\text{m}$ )DIFH = Diffuse Horizontal, (0.3 – 2.8  $\mu\text{m}$ )DIRN = Direct Normal, (0.3 – 2.8  $\mu\text{m}$ )T = Daily Total Insolation Energy ( $\text{Wh/m}^2$ )H = Maximum Insolation Power ( $\text{W/m}^2$ )UVH = Ultra-Violet Horizontal, (0.29 – 0.39  $\mu\text{m}$ )IRH = Infra-Red Horizontal, (4 – 50  $\mu\text{m}$ )

EXTH = Extraterrestrial, (Calculated, see chapter 3)

SUNH = Recorded Bright Sunshine Hours (act.),  
and Calculated (max.), see chapter 3.

**Table B.6** Insolation data over Riyadh for the month of *JUNE*.

Day	GLBH		DIFH		DIRN		UVH		IRH		EXTH	SUNH	
	T	H	T	H	T	H	T	H	T	H	T	act.	max.
1	7778	966	3241	358	5554	617	217	31	5599	448	11070	11.50	13.42
2	7554	974	2936	337	7304	844	227	31	5784	477	11075	11.83	13.43
3	8044	974	2451	340	7692	800	221	29	5784	495	11079	12.50	13.44
4	7855	977	2420	314	6917	766	222	30	5702	495	11083	11.00	13.45
5	7557	971	3200	376	4837	685	213	29	5779	516	11087	9.50	13.46
6	7857	987	3003	364	6266	720	222	30	5760	477	11091	11.83	13.47
7	7751	984	3068	361	5469	711	235	30	5638	474	11094	10.83	13.47
8	7585	946	3378	350	6175	702	222	29	4584	466	11097	11.83	13.48
9	7924	978	2701	312	7574	797	234	30	5765	464	11099	12.33	13.49
10	8196	1003	2081	291	8465	864	232	31	5822	471	11102	12.67	13.49
11	8128	1007	2368	325	7608	798	232	31	6000	456	11104	12.83	13.50
12	7802	985	3219	382	6857	724	230	30	6094	461	11105	12.33	13.50
13	7452	945	3702	407	6736	747	226	30	6182	482	11106	12.00	13.51
14	7606	948	3377	376	6478	730	223	30	6247	495	11108	12.00	13.51
15	8003	984	2468	324	7542	804	229	31	6202	468	11108	12.67	13.51
16	8034	992	2501	327	7942	825	227	31	5748	451	11109	12.67	13.52
17	8107	1002	2154	317	9206	910	231	32	5645	474	11109	13.00	13.52
18	8159	1013	2184	324	8743	871	241	31	5520	422	11109	13.00	13.52
19	8189	1003	2036	307	8485	858	208	31	6007	457	11108	12.83	13.52
20	7987	988	2199	319	7428	790	227	30	5748	451	11108	12.50	13.52
21	8022	991	2191	309	8047	825	222	31	5818	448	11107	12.83	13.52
22	7896	978	2563	326	8503	854	221	31	5575	427	11106	12.83	13.52
23	8015	993	2459	341	7966	873	227	32	5748	430	11104	12.33	13.52
24	7878	971	2793	347	7871	827	222	31	5818	442	11102	12.50	13.52
25	8008	991	2322	307	7823	829	221	31	5575	443	11100	12.67	13.52
26	8099	1005	2267	323	6767	763	220	31	5830	448	11098	12.17	13.52
27	8007	990	2562	324	7196	791	216	31	5849	448	11096	12.33	13.52
28	7888	983	2928	354	6442	719	228	31	5762	443	11093	12.17	13.51
29	7961	985	2438	333	7083	848	217	31	5599	445	11089	11.83	13.51
30	7698	978	3024	384	4996	721	227	30	5784	456	11086	9.50	13.50
Avg.	7901	983	2674	339	7199	787	225	31	5766	461	11098	12.1	13.5

GLBH = Global Horizontal, (0.3 – 2.8  $\mu\text{m}$ )  
DIFH = Diffuse Horizontal, (0.3 – 2.8  $\mu\text{m}$ )  
DIRN = Direct Normal, (0.3 – 2.8  $\mu\text{m}$ )  
T = Daily Total Insolation Energy ( $\text{Wh}/\text{m}^2$ )  
H = Maximum Insolation Power ( $\text{W}/\text{m}^2$ )

UVH = Ultra-Violet Horizontal, (0.29 – 0.39  $\mu\text{m}$ )  
IRH = Infra-Red Horizontal, (4 – 50  $\mu\text{m}$ )  
EXTH = Extraterrestrial, (Calculated, see chapter 3)  
SUNH = Recorded Bright Sunshine Hours (act.),  
and Calculated (max.), see chapter 3.

Table B.7 Insolation data over Riyadh for the month of *JULY*.

Day	GLBH		DIFH		DIRN		UVH		IRH		EXTH	SUNH	
	T	H	T	H	T	H	T	H	T	H	T	act.	max.
1	7777	955	2921	375	5969	752	201	29	5206	453	11082	10.83	13.50
2	8087	993	2440	320	8021	849	225	31	5114	497	11078	11.67	13.49
3	7938	990	2810	374	7824	811	233	31	5582	440	11074	12.50	13.49
4	7807	981	2635	347	8008	807	233	30	5686	448	11069	12.67	13.48
5	7716	977	2974	355	7639	763	228	30	5846	466	11065	12.83	13.48
6	7953	986	2414	300	8931	874	240	31	5695	451	11059	13.00	13.47
7	8184	1006	2043	293	9641	919	243	32	5537	474	11054	13.00	13.46
8	8090	996	2216	309	8726	857	238	32	5760	453	11048	13.00	13.45
9	7672	961	3207	372	5467	680	208	28	6257	500	11042	10.83	13.44
10	7752	960	3326	339	4906	606	209	29	6192	484	11035	9.67	13.44
11	7792	976	2823	312	5861	657	212	29	6084	482	11029	11.83	13.43
12	7602	974	3227	332	6990	759	227	30	6058	471	11021	11.83	13.42
13	7729	961	3057	355	7865	797	231	30	5964	469	11014	12.50	13.41
14	7518	945	3665	433	6309	722	220	30	6108	497	11006	12.33	13.39
15	7950	979	2663	289	7282	755	232	31	6000	479	10998	12.50	13.38
16	7728	978	2814	349	7052	817	230	31	6094	479	10989	11.67	13.37
17	7957	991	2407	252	6348	746	226	31	6182	479	10981	11.17	13.36
18	7840	975	2545	281	6091	714	223	31	6247	500	10972	11.67	13.35
19	8017	991	2121	248	7140	757	229	31	6202	482	10962	12.33	13.33
20	7964	982	2191	259	6938	733	228	31	6204	487	10952	12.33	13.32
21	7904	982	2305	258	6827	739	227	30	6108	479	10942	12.17	13.31
22	7966	989	2159	261	7380	794	231	31	6060	500	10931	11.67	13.29
23	7792	977	2687	286	5824	665	217	30	6305	487	10920	11.67	13.28
24	7429	977	3204	340	3321	534	196	30	6610	508	10908	9.00	13.26
25	7661	964	2806	303	5176	650	210	29	6408	497	10896	10.50	13.25
26	7271	960	2657	277	3994	586	188	28	6478	505	10884	8.67	13.23
27	7408	907	3067	354	4025	566	198	31	6523	536	10872	9.00	13.22
28	7649	966	2604	297	5671	690	215	30	6257	590	10858	11.33	13.20
29	7629	965	2813	294	7253	793	232	32	5954	464	10845	11.83	13.18
30	7459	951	3270	369	5494	675	237	29	6550	587	10830	11.00	13.17
31	7246	930	3593	434	4066	517	196	31	6223	505	10816	9.33	13.15
Avg.	7758	972	2763	322	6517	729	221	30	6048	489	10975	11.5	13.4

GLBH = Global Horizontal, (0.3 – 2.8  $\mu\text{m}$ )  
DIFH = Diffuse Horizontal, (0.3 – 2.8  $\mu\text{m}$ )  
DIRN = Direct Normal, (0.3 – 2.8  $\mu\text{m}$ )  
T = Daily Total Insolation Energy ( $\text{Wh/m}^2$ )  
H = Maximum Insolation Power ( $\text{W/m}^2$ )

UVH = Ultra-Violet Horizontal, (0.29 – 0.39  $\mu\text{m}$ )  
IRH = Infra-Red Horizontal, (4 – 50  $\mu\text{m}$ )  
EXTH = Extraterrestrial, (Calculated, see chapter 3)  
SUNH = Recorded Bright Sunshine Hours (act.),  
and Calculated (max.), see chapter 3.

**Table B.8** Insolation data over Riyadh for the month of *AUGUST*.

Day	GLBH		DIFH		DIRN		UVH		IRH		EXTH	SUNH	
	T	H	T	H	T	H	T	H	T	H	T	act.	max.
1	7223	905	3783	453	4552	522	199	27	6374	500	10801	10.33	13.13
2	7135	928	3778	405	4659	639	198	29	6607	609	10786	9.83	13.11
3	7060	902	4276	460	3437	530	187	28	6511	526	10770	10.17	13.10
4	7383	935	3246	337	6835	748	229	31	6158	516	10753	11.50	13.08
5	7486	949	3012	306	6975	721	225	31	6161	526	10736	11.83	13.06
6	7687	967	2609	268	7267	758	231	32	5563	466	10719	10.83	13.04
7	7614	960	2548	275	7088	712	229	31	5962	469	10701	11.17	13.02
8	7683	958	2315	243	7610	754	236	32	5899	466	10682	12.33	13.00
9	7380	940	2773	308	6289	666	220	30	6070	529	10664	12.00	12.98
10	7219	924	3433	375	5613	620	217	30	6094	477	10644	11.17	12.96
11	7311	943	2793	346	4819	623	211	30	6082	490	10625	10.17	12.94
12	7403	946	3211	339	5855	704	223	31	5561	458	10603	11.00	12.92
13	7581	961	2319	262	7597	748	233	32	5167	456	10583	11.67	12.90
14	7440	937	2503	278	6738	712	226	31	5897	466	10561	11.67	12.88
15	7435	937	2511	271	5493	593	213	29	6142	489	10539	11.33	12.86
16	7490	949	2376	263	6739	701	223	31	5990	495	10516	11.83	12.84
17	7543	950	2208	249	7101	714	226	31	5978	471	10493	12.17	12.81
18	7498	950	2339	274	6055	711	216	31	6115	487	10469	11.00	12.79
19	7518	948	2398	262	6156	662	219	30	6060	482	10445	11.67	12.77
20	7353	937	2435	287	6152	697	213	30	6151	490	10420	11.33	12.75
21	7281	938	2553	292	5529	707	208	30	6151	492	10394	10.33	12.73
22	7507	950	2671	303	6679	722	225	31	5635	455	10368	11.83	12.70
23	7182	943	2389	261	6193	768	207	30	3307	320	10342	11.00	12.68
24	7017	933	2331	307	5675	786	200	43	3041	281	10314	9.83	12.66
25	7316	947	2168	249	7622	828	218	31	2827	240	10286	12.00	12.64
26	7287	941	2104	251	7421	799	210	29	3535	471	10258	11.67	12.61
27	6943	916	2666	299	5142	665	196	41	6274	510	10229	10.50	12.59
28	7210	923	2279	250	7605	789	214	29	6010	491	10199	11.83	12.57
29	7074	914	2180	250	7065	769	209	29	6125	499	10170	10.83	12.54
30	7002	929	2775	314	4807	723	193	29	6204	576	10138	10.33	12.52
31	7064	930	2568	317	6288	760	203	30	5950	481	10107	11.50	12.50
Avg.	7333	938	2695	302	6228	705	215	31	5665	474	10494	11.2	12.8

GLBH = Global Horizontal, (0.3 – 2.8  $\mu\text{m}$ )  
DIFH = Diffuse Horizontal, (0.3 – 2.8  $\mu\text{m}$ )  
DIRN = Direct Normal, (0.3 – 2.8  $\mu\text{m}$ )  
T = Daily Total Insolation Energy ( $\text{Wh}/\text{m}^2$ )  
H = Maximum Insolation Power ( $\text{W}/\text{m}^2$ )

UVH = Ultra-Violet Horizontal, (0.29 – 0.39  $\mu\text{m}$ )  
IRH = Infra-Red Horizontal, (4 – 50  $\mu\text{m}$ )  
EXTH = Extraterrestrial, (Calculated, see chapter 3)  
SUNH = Recorded Bright Sunshine Hours (act.),  
and Calculated (max.), see chapter 3.

**Table B.9** Insolation data over Riyadh for the month of *SEPTEMBER*.

Day	GLBH		DIFH		DIRN		UVH		IRH		EXTH	SUNH	
	T	H	T	H	T	H	T	H	T	H	T	act.	max.
1	7048	915	2404	259	7746	818	217	30	5887	491	10075	11.67	12.47
2	7059	917	2324	248	6768	751	209	29	5606	477	10043	10.50	12.45
3	6485	877	2832	403	6702	784	193	30	6031	497	10010	11.33	12.43
4	6693	851	2961	364	7071	740	206	29	5962	570	9976	11.33	12.40
5	6956	919	2547	265	8016	834	211	30	5743	481	9942	11.83	12.38
6	6911	915	2571	251	7029	817	207	29	5525	458	9907	11.33	12.35
7	6764	913	2480	254	6894	805	200	29	5839	486	9872	11.00	12.33
8	6904	918	2318	245	7352	857	202	30	5705	471	9837	11.50	12.31
9	6852	915	2452	291	7453	791	206	30	5623	495	9800	11.67	12.28
10	6220	836	3212	394	6518	799	204	31	5693	471	9764	10.17	12.26
11	6599	881	2804	313	7032	819	201	29	5678	475	9726	11.17	12.23
12	6609	900	2870	363	6583	762	202	29	5503	455	9688	11.33	12.21
13	6863	908	2299	254	7717	857	207	29	5398	521	9650	11.17	12.18
14	6668	898	2352	283	7627	787	205	29	5076	432	9611	9.33	12.16
15	6930	902	2202	287	7818	787	61	29	2959	430	9572	7.00	12.14
16	6638	884	2545	289	6533	731	200	29	5772	489	9531	11.00	12.11
17	6390	901	3186	364	2906	584	101	29	6086	516	9491	6.50	12.09
18	6354	888	2734	382	4320	623	186	31	5758	489	9451	9.50	12.06
19	6259	886	2285	307	6840	735	196	28	5126	435	9410	11.17	12.04
20	6587	903	1870	249	7596	809	194	29	5083	435	9368	9.67	12.01
21	6572	885	1940	250	7887	842	194	28	5045	432	9326	11.17	11.99
22	6603	893	1861	238	8487	869	195	28	4824	440	9283	10.33	11.96
23	6540	893	1767	231	7826	892	194	29	4855	526	9241	9.33	11.94
24	6427	864	1815	230	7842	837	193	28	5170	445	9198	10.83	11.91
25	6327	876	2005	319	7538	787	187	28	5515	480	9155	9.83	11.89
26	6388	878	2173	247	7067	803	181	28	4997	478	9110	10.00	11.86
27	6340	880	2133	321	8277	869	162	28	3682	521	9066	8.33	11.84
28	6313	876	3170	408	7882	866	188	27	5189	445	9022	10.83	11.82
29	5969	862	3142	412	7769	840	185	27	5160	443	8977	11.33	11.79
30	5959	875	2638	345	7359	821	180	27	5194	460	8932	11.00	11.77
Avg.	6574	890	2463	302	7149	797	189	29	5323	475	9534	10.4	12.1

GLBH = Global Horizontal, (0.3 – 2.8  $\mu\text{m}$ )  
DIFH = Diffuse Horizontal, (0.3 – 2.8  $\mu\text{m}$ )  
DIRN = Direct Normal, (0.3 – 2.8  $\mu\text{m}$ )  
T = Daily Total Insolation Energy ( $\text{Wh/m}^2$ )  
H = Maximum Insolation Power ( $\text{W/m}^2$ )

UVH = Ultra-Violet Horizontal, (0.29 – 0.39  $\mu\text{m}$ )  
IRH = Infra-Red Horizontal, (4 – 50  $\mu\text{m}$ )  
EXTH = Extraterrestrial, (Calculated, see chapter 3)  
SUNH = Recorded Bright Sunshine Hours (act.),  
and Calculated (max.), see chapter 3.

**Table B.10** Insolation data over Riyadh for the month of *OCTOBER*.

Day	GLBH		DIFH		DIRN		UVH		IRH		EXTH	SUNH	
	T	H	T	H	T	H	T	H	T	H	T	act.	max.
1	6094	862	1456	202	7247	811	177	26	4870	500	8886	8.67	11.74
2	5947	845	1663	213	6295	724	179	27	4646	427	8842	11.33	11.72
3	5661	815	3226	482	6909	779	176	26	4618	422	8795	11.33	11.69
4	6053	841	2186	456	7653	866	173	26	4560	419	8750	11.17	11.67
5	6037	869	2318	451	7208	831	161	24	4577	422	8704	11.17	11.65
6	5955	862	2631	504	6044	719	152	25	4099	411	8658	10.50	11.62
7	6065	867	1637	221	6672	828	168	25	4512	417	8612	11.00	11.60
8	6001	847	1659	195	6733	806	169	25	4567	422	8565	11.00	11.57
9	5932	847	2956	375	6577	765	166	25	4608	419	8519	11.00	11.55
10	5804	831	3039	396	1480	256	170	26	4764	430	8472	11.00	11.53
11	5830	832	2156	448	6320	859	170	24	4541	414	8426	10.67	11.50
12	5726	831	2203	323	7351	845	157	25	4738	437	8379	10.17	11.48
13	5649	818	1837	253	7082	841	165	25	4634	422	8331	10.83	11.46
14	5521	807	2548	359	7121	832	166	25	4627	437	8285	10.83	11.43
15	5505	801	1808	258	7305	861	166	25	4536	417	8238	11.00	11.41
16	5584	811	1680	229	7585	853	164	25	4519	417	8191	10.67	11.39
17	5589	811	1688	225	6668	797	163	25	4457	409	8145	10.83	11.36
18	5530	814	1518	177	7223	846	161	24	4440	411	8099	10.83	11.34
19	5436	797	1646	320	6052	789	157	24	4438	406	8053	10.83	11.32
20	4810	706	1141	157	7672	865	158	24	4471	409	8007	11.00	11.30
21	5016	747	1181	187	7183	876	136	21	4282	393	7961	9.33	11.27
22	4882	737	1849	285	4688	816	152	24	4010	370	7915	10.50	11.25
23	5203	795	1794	271	4832	768	145	23	4123	380	7869	10.00	11.23
24	5041	753	2158	271	2712	499	147	23	4248	393	7824	10.50	11.21
25	4928	742	1965	236	2961	469	145	22	4284	401	7780	10.33	11.19
26	5021	746	1690	210	4286	603	146	23	4147	385	7735	10.50	11.16
27	5153	764	1601	203	5107	676	151	23	4022	372	7691	10.83	11.14
28	5178	767	1618	189	5456	714	150	23	4087	393	7646	10.83	11.12
29	5420	793	1053	148	8296	928	145	23	4123	380	7603	10.50	11.10
30	5317	780	942	146	8581	959	141	22	4080	380	7560	10.67	11.08
31	5189	767	996	161	8408	934	138	23	4190	388	7516	10.50	11.06
Avg.	5519	803	1866	276	6313	775	159	24	4413	410	8195	10.7	11.4

GLBH = Global Horizontal, (0.3 – 2.8  $\mu\text{m}$ )  
DIFH = Diffuse Horizontal, (0.3 – 2.8  $\mu\text{m}$ )  
DIRN = Direct Normal, (0.3 – 2.8  $\mu\text{m}$ )  
T = Daily Total Insolation Energy ( $\text{Wh}/\text{m}^2$ )  
H = Maximum Insolation Power ( $\text{W}/\text{m}^2$ )

UVH = Ultra-Violet Horizontal, (0.29 – 0.39  $\mu\text{m}$ )  
IRH = Infra-Red Horizontal, (4 – 50  $\mu\text{m}$ )  
EXTH = Extraterrestrial, (Calculated, see chapter 3)  
SUNH = Recorded Bright Sunshine Hours (act.),  
and Calculated (max.), see chapter 3.

**Table B.11** Insolation data over Riyadh for the month of *NOVEMBER*.

Day	GLBH		DIFH		DIRN		UVH		IRH		EXTH	SUNH	
	T	H	T	H	T	H	T	H	T	H	T	act.	max.
1	5196	774	977	144	8350	930	138	24	4183	411	7475	10.33	11.04
2	4085	561	978	144	8035	900	133	25	4301	414	7432	9.67	11.02
3	4312	648	1159	180	6909	852	130	22	4238	393	7392	10.33	11.00
4	4697	678	2050	296	3712	616	131	21	4255	396	7350	10.33	10.98
5	4787	707	1375	189	5883	714	95	26	4555	424	7309	3.83	10.96
6	3584	575	1827	283	3409	622	126	21	4200	398	7269	9.00	10.94
7	3935	626	1537	214	4045	719	108	22	4512	424	7230	6.17	10.92
8	4504	719	1136	151	6150	826	125	20	4579	440	7192	7.33	10.90
9	4773	704	1456	186	5673	713	131	20	4562	434	7153	10.17	10.89
10	4761	715	1269	200	5968	822	117	26	4781	456	7116	6.67	10.87
11	4528	691	1790	213	3467	555	99	16	4692	445	7079	8.33	10.85
12	4464	704	1616	197	3933	642	114	20	4630	432	7043	10.17	10.83
13	3513	573	1378	185	4304	639	105	22	4522	434	7007	5.83	10.82
14	4579	699	896	130	7230	855	121	20	4126	395	6973	8.83	10.80
15	4295	680	917	152	8279	918	88	22	4188	398	6938	5.00	10.78
16	4467	684	1057	148	6524	782	114	18	3456	388	6904	9.00	10.77
17	4036	656	1398	194	3860	675	1	0	782	398	6872	0.00	10.75
18	4088	647	1324	181	3865	688	116	21	4154	395	6840	3.00	10.74
19	4387	685	1173	149	5416	733	95	19	4253	405	6810	5.50	10.72
20	3710	644	1609	232	2460	511	115	19	4042	395	6779	10.17	10.71
21	4196	682	1490	192	3598	669	114	18	4171	405	6750	10.33	10.69
22	4112	672	1338	203	4683	773	117	19	4226	408	6720	10.33	10.68
23	4276	669	1446	219	3796	675	120	19	4202	413	6694	10.33	10.67
24	4326	687	1313	172	4674	751	119	19	4186	403	6666	10.33	10.65
25	4161	634	1498	202	3918	673	117	19	4090	395	6641	10.17	10.64
26	4017	644	1052	138	5828	785	119	19	4039	390	6616	10.33	10.63
27	3323	509	938	137	6421	811	111	20	4104	448	6590	6.00	10.62
28	3897	605	1388	210	4540	718	109	19	4056	392	6568	0.17	10.61
29	3925	628	1505	225	3170	555	114	18	3991	390	6545	0.17	10.59
30	4116	648	1104	145	5332	691	107	18	3547	445	6524	6.00	10.58
Avg.	4235	658	1333	187	5114	727	112	20	4121	412	6949	7.5	10.8

GLBH = Global Horizontal, (0.3 – 2.8  $\mu\text{m}$ )  
DIFH = Diffuse Horizontal, (0.3 – 2.8  $\mu\text{m}$ )  
DIRN = Direct Normal, (0.3 – 2.8  $\mu\text{m}$ )  
T = Daily Total Insolation Energy ( $\text{Wh/m}^2$ )  
H = Maximum Insolation Power ( $\text{W/m}^2$ )

UVH = Ultra-Violet Horizontal, (0.29 – 0.39  $\mu\text{m}$ )  
IRH = Infra-Red Horizontal, (4 – 50  $\mu\text{m}$ )  
EXTH = Extraterrestrial, (Calculated, see chapter 3)  
SUNH = Recorded Bright Sunshine Hours (act.),  
and Calculated (max.), see chapter 3.

Table B.12 Insolation data over Riyadh for the month of *DECEMBER*.

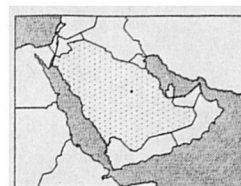
Day	GLBH		DIFH		DIRN		UVH		IRH		EXTH	SUNH	
	T	H	T	H	T	H	T	H	T	H	T	act.	max.
1	3570	643	1405	207	2168	675	109	21	4044	395	6503	7.33	10.57
2	2731	396	1006	157	40	5	96	16	4092	402	6484	1.33	10.56
3	3646	562	1688	224	42	5	55	17	4339	423	6466	0.83	10.56
4	2591	397	977	129	30	3	97	18	4020	406	6448	1.83	10.55
5	2198	397	889	123	33	3	99	18	2880	286	6432	0.17	10.54
6	3994	646	2039	283	1204	768	106	18	2794	363	6416	7.83	10.53
7	4150	651	1627	280	5186	1002	109	18	3043	294	6401	3.00	10.52
8	3264	500	1289	226	2949	933	106	18	3132	302	6388	10.17	10.52
9	3157	468	1221	267	5027	879	107	18	3173	312	6376	9.33	10.51
10	2296	376	1131	152	3600	650	105	18	3070	296	6364	10.17	10.51
11	2138	343	1183	204	1087	472	96	18	3180	326	6354	9.67	10.50
12	3331	638	1465	271	3548	908	105	18	3286	322	6346	10.17	10.50
13	3765	607	1901	302	875	401	104	17	3463	338	6337	10.17	10.49
14	2989	449	1683	321	3126	816	99	18	3449	341	6330	10.00	10.49
15	2604	402	1527	223	1153	378	104	20	3607	353	6323	9.50	10.48
16	1163	229	770	143	35	5	107	17	3773	376	6319	10.17	10.48
17	3798	594	1354	231	3072	776	103	17	3804	389	6315	9.83	10.48
18	3685	621	1491	221	2699	726	78	19	4303	424	6312	4.33	10.48
19	3815	606	1481	249	2868	725	23	9	3984	404	6310	0.33	10.48
20	3316	522	1276	180	2042	527	55	10	3720	375	6309	0.17	10.48
21	4059	639	657	91	6416	886	24	13	4056	457	6309	0.00	10.48
22	3992	629	897	118	5583	746	73	17	4181	411	6311	3.83	10.48
23	3909	625	1099	159	6613	863	90	15	4272	421	6314	7.83	10.48
24	4021	639	996	142	7384	933	55	16	4411	438	6317	2.50	10.48
25	3958	641	1167	148	7405	917	17	4	4010	439	6321	0.00	10.48
26	4044	638	791	128	7106	893	71	18	4082	408	6328	4.50	10.48
27	4000	635	1035	172	7294	890	91	16	3264	318	6335	8.00	10.49
28	3806	659	1651	234	5335	757	94	16	2731	323	6341	1.67	10.49
29	2577	384	1186	332	5037	788	98	17	2570	250	6351	6.33	10.49
30	4116	642	1279	353	5804	911	98	17	2585	345	6361	0.17	10.50
31	3251	530	2320	340	1650	299	96	16	2323	229	6371	3.83	10.50
Avg.	3353	539	1306	213	3433	630	86	16	3537	360	6361	5.3	10.5

GLBH = Global Horizontal, (0.3 – 2.8  $\mu\text{m}$ )DIFH = Diffuse Horizontal, (0.3 – 2.8  $\mu\text{m}$ )DIRN = Direct Normal, (0.3 – 2.8  $\mu\text{m}$ )T = Daily Total Insolation Energy ( $\text{Wh/m}^2$ )H = Maximum Insolation Power ( $\text{W/m}^2$ )UVH = Ultra-Violet Horizontal, (0.29 – 0.39  $\mu\text{m}$ )IRH = Infra-Red Horizontal, (4 – 50  $\mu\text{m}$ )

EXTH = Extraterrestrial, (Calculated, see chapter 3)

SUNH = Recorded Bright Sunshine Hours (act.),  
and Calculated (max.), see chapter 3.

## Appendix C



---

# Sol–Air Temperature Data (Calculated) Riyadh, Saudi Arabia

---

The monthly means of hourly sol–air temperature given in this appendix were computed for a flat roof and walls of 8 compass orientations. The calculation procedure is based on the following assumptions:

- Ground surface albedo = 0.2
- Surface emissivity of wall or roof = 0.9
- Wall absorptivity = 0.4
- Roof absorptivity = 0.6
- External wall surface resistance =  $0.06 \text{ (m}^2\text{C W}^{-1}\text{)}$
- External roof surface resistance =  $0.04 \text{ (m}^2\text{C W}^{-1}\text{)}$

These assumptions are appropriate for typical light to medium coloured building surfaces. Hourly global horizontal insolation, direct normal insolation and temperature data from the Climate Reference Year of Riyadh are used with the above assumptions in calculating the sol–air temperatures. (see section 2.4.1 of chapter 2 for more details).

The sol–air temperature can be used with Eq.2.7 for the estimation of building heating and cooling loads. (see the examples given in chapter 2).

**Table C.1** Sol-air temperatures of a flat roof and walls of stated orientations in Riyadh, for the month of *JANUARY*.

Time	Air temp. (°C)	Wall Orientation								Roof	
		N	NW	W	SW	S	SE	E	NE	Horizontal	
01:00	10.5	10.5	10.5	10.5	10.5	10.5	10.5	10.5	10.5	10.5	7.1
02:00	9.9	9.9	9.9	9.9	9.9	9.9	9.9	9.9	9.9	9.9	6.5
03:00	9.1	9.1	9.1	9.1	9.1	9.1	9.1	9.1	9.1	9.1	5.8
04:00	8.4	8.4	8.4	8.4	8.4	8.4	8.4	8.4	8.4	8.4	5.0
05:00	7.0	7.0	7.0	7.0	7.0	7.0	7.0	7.0	7.0	7.0	3.5
06:00	7.0	7.0	7.0	7.0	7.0	7.0	7.0	7.0	7.0	7.0	3.5
07:00	8.4	8.6	8.6	8.6	8.6	8.7	8.7	8.7	8.6	8.6	5.3
08:00	9.0	10.1	10.1	10.1	10.1	11.0	11.6	11.3	10.3	10.3	7.8
09:00	11.0	13.6	13.7	13.6	13.6	16.5	17.7	16.5	13.6	13.6	13.9
10:00	13.3	17.3	17.3	17.2	18.4	22.1	22.8	20.1	17.1	17.1	20.1
11:00	15.2	19.3	19.2	19.0	23.1	27.1	26.2	21.0	19.1	19.1	24.8
12:00	16.4	21.1	20.9	21.4	27.3	29.4	26.3	20.8	21.0	21.0	27.4
13:00	17.9	22.9	22.7	26.4	31.7	31.6	26.2	22.7	22.9	22.9	29.6
14:00	18.7	24.1	23.9	29.2	32.6	30.7	24.9	24.0	24.2	24.2	29.0
15:00	19.2	23.8	24.4	29.6	31.4	28.7	23.8	23.8	23.9	23.9	26.5
16:00	18.6	22.0	23.3	26.6	27.2	24.7	22.0	22.0	22.0	22.0	22.3
17:00	18.0	19.5	20.4	21.8	21.9	20.5	19.5	19.5	19.5	19.5	17.6
18:00	15.9	16.1	16.2	16.4	16.4	16.2	16.1	16.1	16.1	16.1	13.1
19:00	14.7	14.7	14.7	14.7	14.7	14.7	14.7	14.7	14.7	14.7	11.5
20:00	14.1	14.1	14.1	14.1	14.1	14.1	14.1	14.1	14.1	14.1	10.8
21:00	13.3	13.3	13.3	13.3	13.3	13.3	13.3	13.3	13.3	13.3	10.0
22:00	12.6	12.6	12.6	12.6	12.6	12.6	12.6	12.6	12.6	12.6	9.3
23:00	12.0	12.0	12.0	12.0	12.0	12.0	12.0	12.0	12.0	12.0	8.7
24:00	11.3	11.3	11.3	11.3	11.3	11.3	11.3	11.3	11.3	11.3	8.0
Avg	13.0	14.5	14.6	15.4	16.3	16.5	15.7	14.9	14.5	14.5	13.6

**Table C.2** Sol-air temperatures for a flat roof and walls of stated orientations in Riyadh, for the month of *FEBRUARY*.

Time	Air temp. (°C)	Wall Orientation								Roof	
		N	NW	W	SW	S	SE	E	NE	Horizontal	
01:00	13.2	13.2	13.2	13.2	13.2	13.2	13.2	13.2	13.2	13.2	9.9
02:00	12.4	12.4	12.4	12.4	12.4	12.4	12.4	12.4	12.4	12.4	9.2
03:00	11.7	11.7	11.7	11.7	11.7	11.7	11.7	11.7	11.7	11.7	8.4
04:00	11.0	11.0	11.0	11.0	11.0	11.0	11.0	11.0	11.0	11.0	7.7
05:00	9.6	9.6	9.6	9.6	9.6	9.6	9.6	9.6	9.6	9.6	6.2
06:00	9.6	9.6	9.6	9.6	9.6	9.6	9.6	9.6	9.6	9.6	6.2
07:00	11.1	11.3	11.3	11.3	11.3	11.9	12.8	12.9	12.0		8.4
08:00	12.0	12.9	12.9	12.9	12.9	15.4	18.0	17.7	14.5		12.3
09:00	13.9	15.7	15.8	15.8	15.7	21.0	24.1	22.2	16.6		19.0
10:00	15.9	18.9	18.9	18.8	20.1	25.9	27.5	23.9	18.8		25.4
11:00	17.4	21.5	21.5	21.4	25.5	29.6	28.8	23.6	21.4		30.3
12:00	18.9	23.6	23.4	24.6	30.5	32.3	28.7	23.3	23.5		33.4
13:00	20.5	25.9	25.6	30.2	34.6	33.7	28.0	25.7	25.9		34.8
14:00	21.4	26.8	27.0	34.3	37.4	34.0	26.8	26.8	27.0		34.5
15:00	21.9	26.7	29.0	35.9	37.3	32.4	26.6	26.8	26.8		31.7
16:00	21.3	25.2	28.8	34.0	34.0	28.9	25.2	25.2	25.2		27.1
17:00	20.9	23.2	26.5	29.7	29.1	25.0	23.2	23.2	23.2		22.3
18:00	18.9	19.4	20.2	20.7	20.5	19.6	19.4	19.4	19.4		16.7
19:00	17.7	17.7	17.7	17.7	17.7	17.7	17.7	17.7	17.7		14.6
20:00	16.9	16.9	16.9	16.9	16.9	16.9	16.9	16.9	16.9		13.8
21:00	16.3	16.3	16.3	16.3	16.3	16.3	16.3	16.3	16.3		13.1
22:00	15.6	15.6	15.6	15.6	15.6	15.6	15.6	15.6	15.6		12.4
23:00	14.7	14.7	14.7	14.7	14.7	14.7	14.7	14.7	14.7		11.5
24:00	14.0	14.0	14.0	14.0	14.0	14.0	14.0	14.0	14.0		10.8
<b>Avg</b>	<b>15.7</b>	<b>17.2</b>	<b>17.7</b>	<b>18.8</b>	<b>19.7</b>	<b>19.7</b>	<b>18.8</b>	<b>18.1</b>	<b>17.4</b>		<b>17.5</b>

**Table C.3** Sol-air temperatures for a flat roof and walls of stated orientations in Riyadh, for the month of *MARCH*.

Time	Air temp. (°C)	Wall Orientation								Roof	
		N	NW	W	SW	S	SE	E	NE	Horizontal	
01:00	17.3	17.3	17.3	17.3	17.3	17.3	17.3	17.3	17.3	17.3	14.2
02:00	16.7	16.7	16.7	16.7	16.7	16.7	16.7	16.7	16.7	16.7	13.5
03:00	16.0	16.0	16.0	16.0	16.0	16.0	16.0	16.0	16.0	16.0	12.8
04:00	15.3	15.3	15.3	15.3	15.3	15.3	15.3	15.3	15.3	15.3	12.1
05:00	14.1	14.1	14.1	14.1	14.1	14.1	14.1	14.1	14.1	14.1	10.8
06:00	14.1	14.1	14.1	14.1	14.1	14.1	14.1	14.1	14.1	14.1	10.9
07:00	15.5	16.0	16.0	16.0	16.0	16.4	17.9	18.3	17.3	17.3	13.7
08:00	16.7	17.9	17.9	17.9	17.9	19.7	23.4	23.9	20.8	20.8	18.6
09:00	18.7	20.8	20.9	20.9	20.8	24.4	28.5	28.0	23.3	23.3	25.4
10:00	20.6	23.5	23.6	23.5	23.5	28.7	31.4	29.3	23.9	23.9	31.5
11:00	22.0	25.8	25.9	25.7	28.0	31.9	32.1	28.4	25.7	25.7	35.9
12:00	23.1	28.0	27.8	28.6	32.9	34.2	31.6	27.7	27.9	27.9	38.8
13:00	24.5	30.1	29.8	34.2	37.2	35.7	30.8	30.0	30.2	30.2	40.2
14:00	25.2	30.7	32.3	38.3	39.8	35.7	30.6	30.9	31.1	31.1	39.8
15:00	25.6	30.8	34.6	40.0	40.0	34.4	30.8	31.0	31.0	31.0	37.2
16:00	25.2	29.4	34.3	38.6	37.5	31.6	29.5	29.5	29.5	29.5	32.6
17:00	24.7	27.6	31.6	34.1	32.7	28.3	27.6	27.6	27.6	27.6	27.6
18:00	23.8	24.8	26.0	26.6	26.0	24.8	24.7	24.7	24.7	24.7	22.6
19:00	22.0	22.2	22.3	22.4	22.3	22.2	22.2	22.2	22.2	22.2	19.4
20:00	20.8	20.8	20.8	20.8	20.8	20.8	20.8	20.8	20.8	20.8	17.8
21:00	20.2	20.2	20.2	20.2	20.2	20.2	20.2	20.2	20.2	20.2	17.2
22:00	19.5	19.5	19.5	19.5	19.5	19.5	19.5	19.5	19.5	19.5	16.5
23:00	18.9	18.9	18.9	18.9	18.9	18.9	18.9	18.9	18.9	18.9	15.8
24:00	18.2	18.2	18.2	18.2	18.2	18.2	18.2	18.2	18.2	18.2	15.1
Avg	19.9	21.6	22.3	23.2	23.6	23.3	23.0	22.6	21.9	21.9	22.5

**Table C.4** Sol-air temperatures for a flat roof and walls of stated orientations in Riyadh, for the month of *APRIL*.

Time	Air temp. (°C)	Wall Orientation								Roof	
		N	NW	W	SW	S	SE	E	NE	Horizontal	
01:00	20.7	20.7	20.7	20.7	20.7	20.7	20.7	20.7	20.7	20.7	17.7
02:00	19.9	19.9	19.9	19.9	19.9	19.9	19.9	19.9	19.9	19.9	16.9
03:00	19.2	19.2	19.2	19.2	19.2	19.2	19.2	19.2	19.2	19.2	16.1
04:00	17.7	17.7	17.7	17.7	17.7	17.7	17.7	17.7	17.7	17.7	14.6
05:00	17.7	17.7	17.7	17.7	17.7	17.7	17.7	17.7	17.7	17.7	14.6
06:00	19.1	19.5	19.4	19.4	19.4	19.4	19.8	20.0	19.9	19.9	16.6
07:00	19.6	20.8	20.6	20.6	20.6	20.7	22.8	23.8	23.0	23.0	19.2
08:00	21.0	23.0	23.0	23.1	23.0	23.4	27.3	28.8	26.8	26.8	24.5
09:00	22.9	25.9	26.1	26.1	26.0	27.2	31.5	32.5	29.5	29.5	30.9
10:00	24.7	28.6	28.8	28.7	28.6	30.8	34.0	33.9	30.6	30.6	36.6
11:00	26.2	30.7	30.8	30.7	30.9	33.4	34.4	33.1	30.8	30.8	39.7
12:00	27.4	33.0	32.9	33.1	35.0	35.7	34.6	32.8	32.9	32.9	42.5
13:00	28.8	34.4	34.6	37.7	38.9	37.2	34.3	34.4	34.5	34.5	44.8
14:00	29.0	34.3	36.9	40.4	40.2	36.5	34.4	34.7	34.7	34.7	43.2
15:00	29.2	33.8	38.2	41.5	40.1	35.1	33.9	34.2	34.0	34.0	40.2
16:00	28.6	32.4	37.0	39.3	37.5	32.7	32.5	32.6	32.5	32.5	35.5
17:00	28.3	31.1	34.5	35.8	34.1	30.9	30.9	30.9	30.9	30.9	31.1
18:00	27.7	29.1	30.4	30.7	29.9	28.7	28.7	28.7	28.7	28.7	27.0
19:00	25.8	26.1	26.2	26.2	26.1	26.0	26.0	26.0	26.0	26.0	23.5
20:00	24.7	24.7	24.7	24.7	24.7	24.7	24.7	24.7	24.7	24.7	21.8
21:00	23.8	23.8	23.8	23.8	23.8	23.8	23.8	23.8	23.8	23.8	20.9
22:00	23.1	23.1	23.1	23.1	23.1	23.1	23.1	23.1	23.1	23.1	20.2
23:00	22.4	22.4	22.4	22.4	22.4	22.4	22.4	22.4	22.4	22.4	19.4
24:00	21.7	21.7	21.7	21.7	21.7	21.7	21.7	21.7	21.7	21.7	18.7
<b>Avg</b>	<b>23.7</b>	<b>25.6</b>	<b>26.3</b>	<b>26.8</b>	<b>26.7</b>	<b>26.2</b>	<b>26.5</b>	<b>26.6</b>	<b>26.1</b>	<b>26.1</b>	<b>26.5</b>

**Table C.5** Sol-air temperatures for a flat roof and walls of stated orientations in Riyadh, for the month of *MAY*.

Time	Air temp. (°C)	Wall Orientation								Roof	
		N	NW	W	SW	S	SE	E	NE	Horizontal	
01:00	26.2	26.2	26.2	26.2	26.2	26.2	26.2	26.2	26.2	26.2	23.5
02:00	25.5	25.5	25.5	25.5	25.5	25.5	25.5	25.5	25.5	25.5	22.7
03:00	24.5	24.5	24.5	24.5	24.5	24.5	24.5	24.5	24.5	24.5	21.6
04:00	22.9	22.9	22.9	22.9	22.9	22.9	22.9	22.9	22.9	22.9	20.0
05:00	22.8	22.8	22.8	22.8	22.8	22.8	22.8	22.8	22.8	22.8	19.8
06:00	24.2	25.1	24.8	24.8	24.8	24.8	25.3	25.9	25.8	25.8	22.5
07:00	25.1	27.8	26.8	26.8	26.8	26.8	29.4	31.5	30.9	30.9	26.7
08:00	27.0	30.8	30.0	30.1	30.1	29.9	34.6	37.5	35.9	35.9	33.5
09:00	29.3	33.8	33.7	33.9	33.7	33.6	38.9	41.4	39.1	39.1	40.9
10:00	31.1	36.4	36.7	36.8	36.6	37.0	41.2	42.7	40.3	40.3	46.8
11:00	32.7	38.9	39.1	39.1	38.9	40.1	42.1	42.3	40.4	40.4	51.7
12:00	34.1	40.8	40.8	40.9	41.8	42.1	41.6	40.7	40.8	40.8	54.2
13:00	35.7	42.4	44.1	45.9	45.7	43.4	42.5	42.6	42.6	42.6	55.3
14:00	36.4	43.0	47.0	49.4	47.8	43.4	43.2	43.5	43.3	43.3	54.2
15:00	36.6	42.8	47.9	49.9	47.4	42.5	42.8	43.0	42.7	42.7	50.5
16:00	35.8	41.6	46.7	48.2	45.2	40.6	40.8	40.9	40.7	40.7	45.7
17:00	35.1	40.0	43.4	44.1	41.7	38.8	38.9	38.9	38.9	38.9	40.8
18:00	34.2	36.9	38.5	38.6	37.3	36.1	36.1	36.1	36.1	36.1	35.6
19:00	32.1	33.0	33.3	33.3	33.0	32.8	32.8	32.8	32.8	32.8	30.9
20:00	30.7	30.7	30.7	30.7	30.7	30.7	30.7	30.7	30.7	30.7	28.2
21:00	29.9	29.9	29.9	29.9	29.9	29.9	29.9	29.9	29.9	29.9	27.4
22:00	29.0	29.0	29.0	29.0	29.0	29.0	29.0	29.0	29.0	29.0	26.4
23:00	28.1	28.1	28.1	28.1	28.1	28.1	28.1	28.1	28.1	28.1	25.4
24:00	27.2	27.2	27.2	27.2	27.2	27.2	27.2	27.2	27.2	27.2	24.5
Avg	29.8	32.5	33.3	33.7	33.2	32.4	33.2	33.6	33.2	33.2	34.5

**Table C.6** Sol-air temperatures for a flat roof and walls of stated orientations in Riyadh, for the month of *JUNE*.

Time	Air temp. (°C)	Wall Orientation								Roof	
		N	NW	W	SW	S	SE	E	NE	Horizontal	
01:00	28.4	28.4	28.4	28.4	28.4	28.4	28.4	28.4	28.4	28.4	25.8
02:00	27.4	27.4	27.4	27.4	27.4	27.4	27.4	27.4	27.4	27.4	24.7
03:00	26.5	26.5	26.5	26.5	26.5	26.5	26.5	26.5	26.5	26.5	23.8
04:00	24.5	24.5	24.5	24.5	24.5	24.5	24.5	24.5	24.5	24.5	21.7
05:00	24.5	24.5	24.5	24.5	24.5	24.5	24.5	24.5	24.5	24.5	21.7
06:00	26.0	27.4	26.7	26.7	26.7	26.7	27.5	28.6	28.5	28.5	24.7
07:00	26.9	30.3	28.4	28.4	28.4	28.4	31.8	35.2	34.6	34.6	29.3
08:00	29.4	33.5	31.6	31.7	31.7	31.6	37.0	41.3	39.8	39.8	36.9
09:00	32.1	36.2	35.1	35.2	35.1	35.0	40.8	44.6	42.6	42.6	44.6
10:00	33.8	37.8	37.6	37.7	37.6	37.5	42.3	44.8	42.9	42.9	50.5
11:00	35.1	39.4	39.5	39.5	39.5	39.7	42.2	43.2	41.9	41.9	54.8
12:00	36.1	41.0	41.1	41.5	41.6	41.4	41.1	41.0	41.0	41.0	57.3
13:00	38.0	43.3	46.4	47.9	46.6	43.4	43.4	43.5	43.4	43.4	59.0
14:00	38.6	44.9	50.3	52.3	49.5	44.4	44.7	44.9	44.6	44.6	57.8
15:00	38.9	45.7	52.7	54.8	50.5	44.3	44.7	44.8	44.5	44.5	55.2
16:00	38.0	45.5	51.2	52.5	48.5	43.6	43.9	43.9	43.7	43.7	50.1
17:00	37.6	43.8	47.6	48.1	45.0	41.9	42.0	42.0	41.9	41.9	44.7
18:00	37.0	41.4	44.6	44.6	41.5	39.3	39.3	39.3	39.3	39.3	39.6
19:00	34.8	36.2	36.8	36.7	36.0	35.7	35.7	35.7	35.7	35.7	34.2
20:00	33.3	33.3	33.3	33.3	33.3	33.3	33.3	33.3	33.3	33.3	31.1
21:00	32.4	32.4	32.4	32.4	32.4	32.4	32.4	32.4	32.4	32.4	30.0
22:00	31.4	31.4	31.4	31.4	31.4	31.4	31.4	31.4	31.4	31.4	29.0
23:00	30.4	30.4	30.4	30.4	30.4	30.4	30.4	30.4	30.4	30.4	27.9
24:00	29.5	29.5	29.5	29.5	29.5	29.5	29.5	29.5	29.5	29.5	26.9
<b>Avg</b>	<b>32.1</b>	<b>34.8</b>	<b>35.7</b>	<b>36.1</b>	<b>35.3</b>	<b>34.2</b>	<b>35.2</b>	<b>35.9</b>	<b>35.5</b>	<b>35.5</b>	<b>37.6</b>

**Table C.7** Sol-air temperatures for a flat roof and walls of stated orientations in Riyadh, for the month of *JULY*.

Time	Air temp. (°C)	Wall Orientation								Roof
		N	NW	W	SW	S	SE	E	NE	Horizontal
01:00	31.1	31.1	31.1	31.1	31.1	31.1	31.1	31.1	31.1	28.6
02:00	30.1	30.1	30.1	30.1	30.1	30.1	30.1	30.1	30.1	27.5
03:00	29.2	29.2	29.2	29.2	29.2	29.2	29.2	29.2	29.2	26.6
04:00	27.2	27.2	27.2	27.2	27.2	27.2	27.2	27.2	27.2	24.5
05:00	27.3	27.3	27.3	27.3	27.3	27.3	27.3	27.3	27.3	24.6
06:00	28.8	29.9	29.4	29.4	29.4	29.4	30.1	30.8	30.8	27.5
07:00	29.3	32.0	30.7	30.7	30.7	30.7	33.6	36.1	35.5	31.1
08:00	31.7	35.2	34.0	34.1	34.0	33.9	38.8	42.2	40.7	38.5
09:00	34.9	38.8	38.3	38.5	38.4	38.2	43.7	46.6	44.5	47.0
10:00	36.8	41.1	41.2	41.4	41.2	41.3	45.7	47.4	45.4	53.1
11:00	38.1	43.3	43.3	43.4	43.3	44.0	45.9	46.3	44.9	57.5
12:00	39.1	44.8	44.9	45.5	45.9	45.7	45.0	44.8	44.9	60.1
13:00	40.8	47.0	49.7	51.5	50.6	47.5	47.0	47.2	47.1	61.8
14:00	41.3	47.9	53.3	55.7	53.1	47.8	48.0	48.3	48.0	60.9
15:00	41.4	48.4	55.2	57.6	53.7	47.4	47.7	48.0	47.6	58.0
16:00	40.4	47.6	53.6	55.2	51.1	45.9	46.1	46.2	46.0	52.5
17:00	40.0	46.1	50.1	50.8	47.6	44.3	44.3	44.4	44.3	47.3
18:00	39.4	43.4	45.8	45.9	43.6	41.8	41.8	41.8	41.8	42.2
19:00	37.2	38.6	39.1	39.1	38.4	38.1	38.1	38.1	38.1	36.8
20:00	35.8	35.8	35.8	35.8	35.8	35.8	35.8	35.8	35.8	33.7
21:00	34.7	34.7	34.7	34.7	34.7	34.7	34.7	34.7	34.7	32.5
22:00	33.9	33.9	33.9	33.9	33.9	33.9	33.9	33.9	33.9	31.6
23:00	32.9	32.9	32.9	32.9	32.9	32.9	32.9	32.9	32.9	30.6
24:00	31.9	31.9	31.9	31.9	31.9	31.9	31.9	31.9	31.9	29.6
Avg	34.7	37.4	38.4	38.9	38.1	37.1	37.9	38.4	38.1	40.2

**Table C.8** Sol-air temperatures for a flat roof and walls of stated orientations in Riyadh, for the month of *AUGUST*.

Time	Air temp. (°C)	Wall Orientation								Roof	
		N	NW	W	SW	S	SE	E	NE	Horizontal	
01:00	29.6	29.6	29.6	29.6	29.6	29.6	29.6	29.6	29.6	29.6	27.0
02:00	28.5	28.5	28.5	28.5	28.5	28.5	28.5	28.5	28.5	28.5	25.8
03:00	27.4	27.4	27.4	27.4	27.4	27.4	27.4	27.4	27.4	27.4	24.7
04:00	25.5	25.5	25.5	25.5	25.5	25.5	25.5	25.5	25.5	25.5	22.7
05:00	25.4	25.4	25.4	25.4	25.4	25.4	25.4	25.4	25.4	25.4	22.6
06:00	26.9	27.7	27.5	27.5	27.5	27.5	28.0	28.4	28.3	28.3	25.3
07:00	27.4	29.1	28.7	28.7	28.7	28.7	31.7	33.4	32.3	32.3	28.4
08:00	29.6	32.1	32.0	32.1	32.0	32.2	37.6	39.9	37.5	37.5	35.5
09:00	33.3	36.7	36.9	37.0	36.8	37.8	43.3	45.0	41.7	41.7	44.5
10:00	35.6	40.0	40.3	40.4	40.1	42.1	46.1	46.5	43.0	43.0	51.1
11:00	36.9	42.2	42.3	42.3	42.2	44.9	46.5	45.4	42.5	42.5	55.6
12:00	38.0	43.9	43.8	44.4	46.4	46.8	45.5	43.8	43.9	43.9	58.3
13:00	39.6	45.8	47.0	50.3	51.0	48.5	45.8	46.0	46.1	46.1	60.0
14:00	40.1	46.5	50.5	54.4	53.4	48.3	46.6	47.0	46.9	46.9	58.8
15:00	40.3	46.2	52.4	56.0	53.6	47.1	46.5	46.8	46.6	46.6	55.7
16:00	39.4	44.8	51.6	54.4	51.2	44.6	44.6	44.7	44.6	44.6	50.5
17:00	39.0	43.8	49.2	50.9	47.7	42.7	42.8	42.8	42.8	42.8	45.3
18:00	38.2	41.1	43.4	43.9	42.2	40.3	40.3	40.3	40.3	40.3	40.1
19:00	36.1	37.0	37.4	37.4	37.1	36.8	36.8	36.8	36.8	36.8	35.3
20:00	34.6	34.6	34.6	34.6	34.6	34.6	34.6	34.6	34.6	34.6	32.4
21:00	33.6	33.6	33.6	33.6	33.6	33.6	33.6	33.6	33.6	33.6	31.3
22:00	32.5	32.5	32.5	32.5	32.5	32.5	32.5	32.5	32.5	32.5	30.2
23:00	31.4	31.4	31.4	31.4	31.4	31.4	31.4	31.4	31.4	31.4	29.0
24:00	30.5	30.5	30.5	30.5	30.5	30.5	30.5	30.5	30.5	30.5	28.0
<b>Avg</b>	<b>33.3</b>	<b>35.7</b>	<b>36.8</b>	<b>37.4</b>	<b>37.0</b>	<b>36.1</b>	<b>36.7</b>	<b>36.9</b>	<b>36.3</b>	<b>36.3</b>	<b>38.3</b>

**Table C.9** Sol-air temperatures for a flat roof and walls of stated orientations in Riyadh, for the month of *SEPTEMBER*.

Time	Air temp. (°C)	Wall Orientation								Roof	
		N	NW	W	SW	S	SE	E	NE	Horizontal	
01:00	27.0	27.0	27.0	27.0	27.0	27.0	27.0	27.0	27.0	27.0	24.3
02:00	26.1	26.1	26.1	26.1	26.1	26.1	26.1	26.1	26.1	26.1	23.4
03:00	25.1	25.1	25.1	25.1	25.1	25.1	25.1	25.1	25.1	25.1	22.3
04:00	23.2	23.2	23.2	23.2	23.2	23.2	23.2	23.2	23.2	23.2	20.3
05:00	23.1	23.1	23.1	23.1	23.1	23.1	23.1	23.1	23.1	23.1	20.2
06:00	24.7	25.1	25.1	25.1	25.1	25.1	25.8	26.2	25.9		22.7
07:00	25.0	26.1	26.1	26.1	26.1	26.6	30.7	32.2	30.0		25.3
08:00	27.0	29.0	29.1	29.1	29.1	31.1	37.5	39.0	34.6		32.3
09:00	30.9	33.8	34.0	34.0	33.8	37.5	43.7	44.0	38.2		41.3
10:00	34.0	37.8	38.0	37.9	37.7	42.9	47.2	45.8	39.6		49.0
11:00	35.4	39.9	40.0	39.8	41.0	46.1	47.5	44.2	39.7		53.6
12:00	36.3	41.2	41.1	41.1	45.8	47.8	45.8	41.1	41.1		56.0
13:00	37.3	42.5	42.3	46.8	50.2	48.8	43.6	42.4	42.7		56.7
14:00	37.6	42.5	44.4	50.8	52.3	47.8	42.4	42.7	42.8		54.8
15:00	37.7	41.9	46.8	53.0	52.6	45.9	42.0	42.2	42.2		51.3
16:00	37.0	40.5	47.0	52.2	50.4	42.8	40.6	40.7	40.6		46.0
17:00	36.5	39.0	44.6	47.6	45.6	39.6	39.0	39.0	39.0		40.3
18:00	35.0	36.2	37.9	38.6	37.8	36.0	36.0	36.0	36.0		34.7
19:00	33.1	33.5	33.6	33.7	33.6	33.4	33.4	33.4	33.4		31.4
20:00	31.9	31.9	31.9	31.9	31.9	31.9	31.9	31.9	31.9		29.5
21:00	30.9	30.9	30.9	30.9	30.9	30.9	30.9	30.9	30.9		28.5
22:00	29.9	29.9	29.9	29.9	29.9	29.9	29.9	29.9	29.9		27.4
23:00	29.0	29.0	29.0	29.0	29.0	29.0	29.0	29.0	29.0		26.4
24:00	28.0	28.0	28.0	28.0	28.0	28.0	28.0	28.0	28.0		25.4
Avg	30.9	32.6	33.5	34.6	34.8	34.4	34.6	34.3	33.3		35.1

**Table C.10** Sol-air temperatures for a flat roof and walls of stated orientations in Riyadh, for the month of *OCTOBER*.

Time	Air temp. (°C)	Wall Orientation								Roof
		N	NW	W	SW	S	SE	E	NE	Horizontal
01:00	22.7	22.7	22.7	22.7	22.7	22.7	22.7	22.7	22.7	19.8
02:00	22.0	22.0	22.0	22.0	22.0	22.0	22.0	22.0	22.0	19.0
03:00	21.0	21.0	21.0	21.0	21.0	21.0	21.0	21.0	21.0	18.0
04:00	20.1	20.1	20.1	20.1	20.1	20.1	20.1	20.1	20.1	17.1
05:00	18.5	18.5	18.5	18.5	18.5	18.5	18.5	18.5	18.5	15.4
06:00	18.6	18.6	18.6	18.6	18.6	18.6	18.6	18.6	18.6	15.5
07:00	20.0	21.1	21.1	21.1	21.1	22.2	24.9	25.4	23.4	19.2
08:00	21.7	24.1	24.1	24.1	24.1	27.4	32.4	32.6	27.7	25.5
09:00	25.2	28.7	28.8	28.8	28.7	34.1	39.1	37.9	31.3	34.0
10:00	28.5	32.8	33.0	32.8	32.7	39.9	43.4	40.4	33.0	41.3
11:00	30.0	34.7	34.8	34.5	37.2	43.1	43.9	39.0	34.4	45.5
12:00	30.9	35.6	35.4	35.2	41.4	44.8	42.4	35.8	35.3	47.5
13:00	32.1	36.6	36.3	39.9	45.5	45.7	40.2	36.3	36.6	48.3
14:00	32.5	36.4	36.3	43.5	47.3	44.4	36.9	36.4	36.6	46.2
15:00	32.5	35.8	37.9	45.3	47.2	42.2	35.7	35.8	35.9	42.7
16:00	31.7	34.1	37.9	44.0	44.2	38.5	34.1	34.1	34.1	37.4
17:00	31.0	32.4	35.4	38.2	37.7	34.0	32.4	32.4	32.4	31.9
18:00	28.9	29.3	29.6	29.7	29.6	29.4	29.3	29.3	29.3	27.1
19:00	27.6	27.6	27.6	27.6	27.6	27.6	27.6	27.6	27.6	24.9
20:00	26.7	26.7	26.7	26.7	26.7	26.7	26.7	26.7	26.7	24.0
21:00	25.8	25.8	25.8	25.8	25.8	25.8	25.8	25.8	25.8	23.0
22:00	25.0	25.0	25.0	25.0	25.0	25.0	25.0	25.0	25.0	22.2
23:00	24.1	24.1	24.1	24.1	24.1	24.1	24.1	24.1	24.1	21.3
24:00	23.3	23.3	23.3	23.3	23.3	23.3	23.3	23.3	23.3	20.4
Avg	25.9	27.4	27.8	28.9	29.7	30.0	29.6	28.8	27.7	28.6

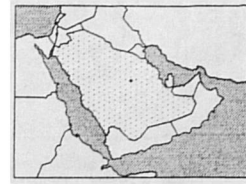
**Table C.11** Sol-air temperatures for a flat roof and walls of stated orientations in Riyadh, for the month of *NOVEMBER*.

Time	Air temp. (°C)	Wall Orientation								Roof
		N	NW	W	SW	S	SE	E	NE	Horizontal
01:00	17.5	17.5	17.5	17.5	17.5	17.5	17.5	17.5	17.5	14.4
02:00	16.8	16.8	16.8	16.8	16.8	16.8	16.8	16.8	16.8	13.7
03:00	16.3	16.3	16.3	16.3	16.3	16.3	16.3	16.3	16.3	13.1
04:00	15.7	15.7	15.7	15.7	15.7	15.7	15.7	15.7	15.7	12.5
05:00	14.5	14.5	14.5	14.5	14.5	14.5	14.5	14.5	14.5	11.2
06:00	14.4	14.4	14.4	14.4	14.4	14.4	14.4	14.4	14.4	11.2
07:00	15.9	16.5	16.5	16.5	16.5	17.5	18.9	18.9	17.5	14.0
08:00	16.8	18.5	18.5	18.5	18.5	21.5	24.3	23.7	20.1	17.8
09:00	18.6	21.6	21.6	21.6	21.5	26.7	29.8	28.0	22.4	23.9
10:00	20.4	24.3	24.4	24.3	25.2	31.6	33.7	30.1	24.2	29.6
11:00	21.8	26.1	26.1	25.9	29.6	35.2	35.2	29.7	25.9	33.7
12:00	23.0	27.5	27.3	27.1	33.9	37.4	34.7	27.6	27.3	36.0
13:00	24.4	28.7	28.4	31.4	37.7	38.4	33.2	28.4	28.6	36.9
14:00	25.1	28.5	28.4	34.7	39.5	37.7	30.4	28.5	28.6	35.5
15:00	25.4	28.0	28.5	36.0	38.9	35.3	28.0	28.0	28.1	32.2
16:00	24.7	26.5	28.4	33.9	35.0	31.1	26.5	26.5	26.5	27.4
17:00	24.0	24.8	25.8	27.3	27.4	25.9	24.8	24.8	24.8	22.8
18:00	22.2	22.4	22.5	22.5	22.5	22.5	22.4	22.4	22.4	19.6
19:00	21.1	21.1	21.1	21.1	21.1	21.1	21.1	21.1	21.1	18.1
20:00	20.5	20.5	20.5	20.5	20.5	20.5	20.5	20.5	20.5	17.4
21:00	19.9	19.9	19.9	19.9	19.9	19.9	19.9	19.9	19.9	16.8
22:00	19.2	19.2	19.2	19.2	19.2	19.2	19.2	19.2	19.2	16.2
23:00	18.6	18.6	18.6	18.6	18.6	18.6	18.6	18.6	18.6	15.5
24:00	18.0	18.0	18.0	18.0	18.0	18.0	18.0	18.0	18.0	14.9
Avg	19.8	21.1	21.2	22.2	23.3	23.9	23.1	22.0	21.2	21.0

**Table C.12** Sol-air temperatures for a flat roof and walls of stated orientations in Riyadh, for the month of *DECEMBER*.

Time	Air temp. (°C)	Wall Orientation								Roof
		N	NW	W	SW	S	SE	E	NE	Horizontal
01:00	11.2	11.2	11.2	11.2	11.2	11.2	11.2	11.2	11.2	7.9
02:00	10.6	10.6	10.6	10.6	10.6	10.6	10.6	10.6	10.6	7.3
03:00	10.1	10.1	10.1	10.1	10.1	10.1	10.1	10.1	10.1	6.7
04:00	9.6	9.6	9.6	9.6	9.6	9.6	9.6	9.6	9.6	6.2
05:00	8.5	8.5	8.5	8.5	8.5	8.5	8.5	8.5	8.5	5.2
06:00	8.6	8.6	8.6	8.6	8.6	8.6	8.6	8.6	8.6	5.2
07:00	9.9	10.3	10.3	10.3	10.3	10.7	11.1	11.0	10.5	7.3
08:00	10.6	11.8	11.8	11.8	11.8	13.6	14.9	14.3	12.3	10.1
09:00	12.0	14.4	14.4	14.4	14.4	18.2	19.8	18.2	14.4	15.1
10:00	13.6	17.0	17.0	16.9	18.2	22.3	23.1	20.3	16.9	19.7
11:00	14.8	18.3	18.3	18.1	21.8	25.7	25.1	20.4	18.1	23.0
12:00	15.8	19.7	19.5	19.6	25.5	27.9	25.2	19.4	19.6	25.2
13:00	17.0	21.1	20.9	23.7	28.8	29.2	24.7	20.9	21.0	26.6
14:00	17.7	21.2	21.1	26.4	30.3	28.8	22.8	21.2	21.3	25.7
15:00	18.0	20.7	20.9	27.6	30.2	27.2	20.7	20.7	20.7	23.1
16:00	17.3	19.2	20.7	25.6	26.8	23.6	19.2	19.2	19.2	18.9
17:00	16.7	17.4	18.2	19.8	19.9	18.6	17.4	17.4	17.4	14.8
18:00	15.0	15.1	15.1	15.2	15.2	15.1	15.1	15.1	15.1	12.0
19:00	14.0	14.0	14.0	14.0	14.0	14.0	14.0	14.0	14.0	10.7
20:00	13.5	13.5	13.5	13.5	13.5	13.5	13.5	13.5	13.5	10.2
21:00	12.9	12.9	12.9	12.9	12.9	12.9	12.9	12.9	12.9	9.6
22:00	12.4	12.4	12.4	12.4	12.4	12.4	12.4	12.4	12.4	9.1
23:00	11.9	11.9	11.9	11.9	11.9	11.9	11.9	11.9	11.9	8.7
24:00	11.4	11.4	11.4	11.4	11.4	11.4	11.4	11.4	11.4	8.1
Avg	13.0	14.2	14.3	15.2	16.2	16.5	15.6	14.7	14.2	13.2

## Appendix D



---

# Solar Heat Gain Flux Through Standard Glass (Riyadh, Saudi Arabia)

---

The following tables give monthly means of hourly solar heat gain flux ( $\text{W m}^{-2}$ ) through a standard 3mm clear glass in the climate of Riyadh. The data are derived from the QREF.BAS program output, developed by the author in chapter 4. The calculations are based on the following conditions:

- Negligible thermal resistance across the glass
- Negligible thermal storage within the glass
- Indoor air temperature is held constant at 21°C
- Room internal surfaces are considered as a black body at 21°C
- Glass emissivity = 0.9
- Ground albedo = 0.2

The computed data takes into account wind speed and direction, outdoor air temperature, and the direct and diffuse insolation incident on the glazing surface from the Climate Reference Year of Riyadh. (see section 4.4.2 in chapter 4 for detailed discussion on the calculation procedure, and chapter 2 for examples on using the data).

**Table D.1** Total solar heat gain through a standard 3mm clear glass ( $\text{W m}^{-2}$ ), for the stated month and surface orientations.

<i>JANUARY</i> Time	Vertical Orientation								Horizontal
	N	NW	W	SW	S	SE	E	NE	
06:00	0	0	0	0	0	0	0	0	0
07:00	6	7	7	6	9	12	12	7	10
08:00	41	46	44	38	74	108	94	43	70
09:00	107	116	106	97	216	277	216	97	212
10:00	153	157	144	167	341	375	248	140	345
11:00	157	154	144	279	462	423	187	147	449
12:00	178	169	167	409	503	365	163	171	499
13:00	194	179	285	537	535	280	179	194	517
14:00	213	192	398	560	470	204	205	226	456
15:00	187	175	420	514	372	168	194	213	341
16:00	134	159	330	362	235	127	147	154	214
17:00	55	85	151	153	91	55	56	57	90
18:00	8	8	8	8	8	8	8	8	13
19:00	0	0	0	0	0	0	0	0	0
<b>Total</b>	<b>1433</b>	<b>1447</b>	<b>2204</b>	<b>3130</b>	<b>3316</b>	<b>2402</b>	<b>1709</b>	<b>1457</b>	<b>3216</b>

**Table D.2** Total solar heat gain through a standard 3mm clear glass ( $\text{W m}^{-2}$ ), for the stated month and surface orientations.

<i>FEBRUARY</i> Time	Vertical Orientation								Horizontal
	N	NW	W	SW	S	SE	E	NE	
06:00	0	0	0	0	0	0	0	0	0
07:00	8	9	9	8	25	70	74	33	17
08:00	32	37	36	31	121	245	226	75	117
09:00	63	66	64	61	258	398	316	71	288
10:00	107	109	105	122	373	445	283	104	451
11:00	148	147	144	263	456	422	189	145	568
12:00	171	168	177	423	504	342	165	169	626
13:00	198	191	329	536	497	240	192	199	611
14:00	207	195	488	630	477	194	206	219	556
15:00	188	229	564	634	393	177	205	216	429
16:00	149	263	530	533	271	148	179	180	272
17:00	87	208	358	331	137	89	98	96	136
18:00	17	17	17	17	17	17	17	17	29
19:00	0	0	0	0	0	0	0	0	0
<b>Total</b>	<b>1375</b>	<b>1639</b>	<b>2821</b>	<b>3589</b>	<b>3529</b>	<b>2787</b>	<b>2150</b>	<b>1524</b>	<b>4100</b>

**Table D.3** Total solar heat gain through a standard 3mm clear glass ( $\text{W m}^{-2}$ ), for the stated month and surface orientations.

<i>MARCH</i> Time	Vertical Orientation							Horizontal	
	N	NW	W	SW	S	SE	E	NE	
06:00	0	0	0	0	0	0	0	0	0
07:00	19	22	24	20	26	96	115	71	41
08:00	45	52	53	47	94	270	292	147	172
09:00	78	82	82	77	191	381	360	138	347
10:00	106	108	106	105	282	405	311	109	500
11:00	136	136	135	181	351	360	197	135	611
12:00	169	167	173	330	390	273	167	168	667
13:00	198	195	324	459	394	205	196	199	660
14:00	204	225	487	553	370	199	208	213	613
15:00	194	306	573	570	302	193	217	217	494
16:00	161	347	568	509	212	171	204	194	335
17:00	105	272	395	326	117	115	132	122	173
18:00	33	33	33	33	33	33	33	33	55
19:00	7	7	7	7	7	7	7	7	11
<b>Total</b>	1455	1952	2960	3217	2769	2708	2439	1753	4679

**Table D.4** Total solar heat gain through a standard 3mm clear glass ( $\text{W m}^{-2}$ ), for the stated month and surface orientations.

<i>APRIL</i> Time	Vertical Orientation							Horizontal	
	N	NW	W	SW	S	SE	E	NE	
06:00	13	12	13	12	11	24	35	30	18
07:00	39	42	48	43	37	124	176	136	82
08:00	72	80	85	77	76	246	316	222	220
09:00	110	115	117	112	134	322	365	230	383
10:00	143	144	144	143	195	335	332	188	529
11:00	162	162	162	164	233	277	224	163	582
12:00	203	203	203	248	274	236	202	203	636
13:00	203	205	296	347	277	202	203	203	670
14:00	195	256	410	402	242	194	198	198	595
15:00	171	323	474	415	192	175	187	182	477
16:00	140	328	442	351	143	154	172	158	321
17:00	96	251	316	231	93	107	118	105	170
18:00	47	105	119	83	40	42	43	41	64
19:00	9	9	9	9	9	9	9	9	16
<b>Total</b>	1603	2235	2838	2637	1956	2447	2580	2068	4763

**Table D.5** Total solar heat gain through a standard 3mm clear glass ( $\text{W m}^{-2}$ ), for the stated month and surface orientations.

MAY Time	Vertical Orientation								Horizontal
	N	NW	W	SW	S	SE	E	NE	
06:00	34	24	27	26	23	43	72	68	37
07:00	86	69	83	77	63	164	271	237	139
08:00	120	116	129	121	108	285	424	349	317
09:00	157	161	167	161	156	347	460	361	500
10:00	196	198	199	197	201	345	410	306	651
11:00	230	230	229	229	242	305	310	249	765
12:00	247	247	247	256	263	254	247	247	798
13:00	250	273	334	325	261	249	249	249	777
14:00	244	359	460	392	247	244	246	245	709
15:00	218	410	501	390	215	223	231	223	557
16:00	194	429	506	358	180	202	215	193	415
17:00	165	342	381	253	139	163	172	148	256
18:00	97	175	183	116	72	80	81	73	115
19:00	24	24	24	24	24	24	24	24	40
<b>Total</b>	<b>2262</b>	<b>3057</b>	<b>3470</b>	<b>2925</b>	<b>2194</b>	<b>2928</b>	<b>3412</b>	<b>2972</b>	<b>6076</b>

**Table D.6** Total solar heat gain through a standard 3mm clear glass ( $\text{W m}^{-2}$ ), for the stated month and surface orientations.

JUNE Time	Vertical Orientation								Horizontal
	N	NW	W	SW	S	SE	E	NE	
06:00	49	26	32	32	26	55	109	107	43
07:00	105	58	71	68	55	181	345	314	161
08:00	118	86	96	92	83	279	477	410	352
09:00	118	109	112	110	107	305	475	386	533
10:00	136	136	137	136	136	276	388	298	690
11:00	161	161	161	161	162	213	246	201	793
12:00	181	181	182	184	183	181	181	181	841
13:00	195	254	312	264	196	196	195	195	831
14:00	216	395	486	364	215	216	217	215	758
15:00	212	505	599	409	198	207	212	202	640
16:00	245	525	592	391	210	238	248	220	483
17:00	210	415	444	275	162	192	198	167	295
18:00	157	315	319	165	89	105	105	89	139
19:00	31	31	31	31	31	31	31	31	52
<b>Total</b>	<b>2134</b>	<b>3197</b>	<b>3574</b>	<b>2682</b>	<b>1853</b>	<b>2675</b>	<b>3427</b>	<b>3016</b>	<b>6611</b>

**Table D.7** Total solar heat gain through a standard 3mm clear glass ( $\text{W m}^{-2}$ ), for the stated month and surface orientations.

<i>JULY</i> Time	Vertical Orientation								Horizontal
	N	NW	W	SW	S	SE	E	NE	
06:00	39	25	29	28	24	48	88	84	40
07:00	81	53	63	60	50	159	283	251	141
08:00	102	87	95	91	83	263	419	349	322
09:00	127	125	129	126	123	311	444	350	512
10:00	156	157	158	157	158	291	372	278	662
11:00	190	191	191	191	196	243	257	211	772
12:00	211	212	215	222	219	212	211	211	824
13:00	227	278	349	312	231	227	227	227	817
14:00	236	407	513	404	236	238	239	237	760
15:00	228	510	615	443	220	231	239	227	639
16:00	232	526	605	405	204	232	244	216	470
17:00	206	422	458	288	161	191	199	168	291
18:00	141	263	268	154	92	103	103	93	145
19:00	33	33	33	33	33	33	33	33	55
<b>Total</b>	<b>2209</b>	<b>3289</b>	<b>3721</b>	<b>2914</b>	<b>2030</b>	<b>2782</b>	<b>3358</b>	<b>2935</b>	<b>6450</b>

**Table D.8** Total solar heat gain through a standard 3mm clear glass ( $\text{W m}^{-2}$ ), for the stated month and surface orientations.

<i>AUGUST</i> Time	Vertical Orientation								Horizontal
	N	NW	W	SW	S	SE	E	NE	
06:00	26	23	25	24	22	44	64	57	35
07:00	55	56	66	59	50	171	254	202	117
08:00	88	97	105	97	89	309	415	303	293
09:00	128	134	137	132	143	376	450	300	482
10:00	165	167	168	166	204	371	387	233	636
11:00	194	195	195	195	255	315	269	196	749
12:00	213	213	216	262	282	240	213	213	802
13:00	226	239	349	381	284	226	226	226	799
14:00	232	339	511	471	266	234	238	236	727
15:00	216	436	601	499	228	227	239	230	598
16:00	188	479	621	464	186	210	231	207	437
17:00	154	422	511	346	138	166	183	154	256
18:00	96	207	229	151	75	81	82	77	120
19:00	27	27	27	27	27	27	27	27	46
<b>Total</b>	<b>2008</b>	<b>3034</b>	<b>3761</b>	<b>3274</b>	<b>2249</b>	<b>2997</b>	<b>3278</b>	<b>2661</b>	<b>6097</b>

**Table D.9** Total solar heat gain through a standard 3mm clear glass ( $\text{W m}^{-2}$ ), for the stated month and surface orientations.

SEPTEMBER Time	Vertical Orientation								Horizontal
	N	NW	W	SW	S	SE	E	NE	
06:00	17	17	18	17	17	35	46	38	27
07:00	42	53	61	50	49	236	305	202	89
08:00	77	92	98	83	120	426	496	286	266
09:00	108	118	119	109	211	500	513	244	455
10:00	140	143	142	139	301	497	434	168	619
11:00	159	159	158	171	365	429	278	158	738
12:00	173	173	172	300	396	306	173	173	789
13:00	184	183	297	450	391	202	184	185	774
14:00	175	204	476	545	343	174	179	180	686
15:00	155	299	592	579	265	157	171	170	544
16:00	130	376	627	542	181	141	167	156	369
17:00	92	325	478	374	103	108	129	113	176
18:00	40	110	137	102	39	40	41	40	64
19:00	11	11	11	11	11	11	11	11	18
Total	1503	2263	3386	3472	2792	3262	3127	2124	5614

**Table D.10** Total solar heat gain through a standard 3mm clear glass ( $\text{W m}^{-2}$ ), for the stated month and surface orientations.

OCTOBER Time	Vertical Orientation								Horizontal
	N	NW	W	SW	S	SE	E	NE	
06:00	0	0	0	0	0	0	0	0	1
07:00	40	49	52	43	68	204	228	129	64
08:00	92	115	116	93	196	450	457	215	212
09:00	135	154	148	129	325	567	510	190	395
10:00	161	169	161	153	423	580	445	156	543
11:00	170	171	166	219	486	522	298	165	643
12:00	166	164	161	361	516	410	164	163	689
13:00	161	156	238	496	504	257	156	160	667
14:00	146	139	399	571	446	146	144	150	574
15:00	125	158	501	585	355	119	132	138	437
16:00	92	210	508	519	238	91	112	113	261
17:00	55	166	310	283	101	59	75	71	97
18:00	18	18	17	17	18	18	18	18	29
19:00	0	0	0	0	0	0	0	0	0
Total	1361	1669	2777	3469	3676	3423	2739	1668	4612

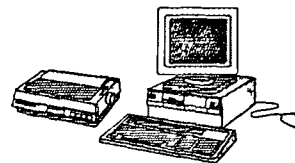
**Table D.11** Total solar heat gain through a standard 3mm clear glass ( $\text{W m}^{-2}$ ), for the stated month and surface orientations.

<i>NOVEMBER</i> Time	Vertical Orientation								Horizontal
	N	NW	W	SW	S	SE	E	NE	
06:00	0	0	0	0	0	0	0	0	0
07:00	25	29	29	25	57	123	124	59	39
08:00	67	82	79	64	175	317	289	107	126
09:00	120	138	126	109	314	465	376	120	278
10:00	156	165	150	152	437	536	368	141	424
11:00	164	164	152	255	518	520	260	152	521
12:00	166	160	152	396	554	435	155	158	562
13:00	157	147	213	504	539	296	145	155	538
14:00	132	120	346	568	485	154	125	137	458
15:00	106	97	417	551	382	94	107	119	323
16:00	75	112	380	435	246	68	86	93	168
17:00	32	63	139	142	71	32	38	38	50
18:00	7	7	7	7	7	7	7	7	12
19:00	0	0	0	0	0	0	0	0	0
<b>Total</b>	<b>1207</b>	<b>1284</b>	<b>2190</b>	<b>3208</b>	<b>3785</b>	<b>3047</b>	<b>2080</b>	<b>1286</b>	<b>3499</b>

**Table D.12** Total solar heat gain through a standard 3mm clear glass ( $\text{W m}^{-2}$ ), for the stated month and surface orientations.

<i>DECEMBER</i> Time	Vertical Orientation								Horizontal
	N	NW	W	SW	S	SE	E	NE	
06:00	0	0	0	0	0	0	0	0	0
07:00	14	15	15	14	27	45	43	20	22
08:00	46	51	49	43	115	176	151	53	85
09:00	95	103	96	88	243	320	244	88	212
10:00	133	137	127	150	340	382	248	123	323
11:00	135	134	125	244	429	403	180	126	398
12:00	149	142	136	364	473	354	136	142	443
13:00	154	144	214	454	475	263	142	152	443
14:00	143	129	321	508	439	159	134	148	382
15:00	113	99	381	509	364	99	114	128	267
16:00	78	100	343	402	242	71	88	96	139
17:00	26	50	123	130	69	26	28	28	40
18:00	3	3	3	3	3	3	3	3	6
19:00	0	0	0	0	0	0	0	0	0
<b>Total</b>	<b>1089</b>	<b>1107</b>	<b>1933</b>	<b>2909</b>	<b>3219</b>	<b>2301</b>	<b>1511</b>	<b>1107</b>	<b>2760</b>

## Appendix E



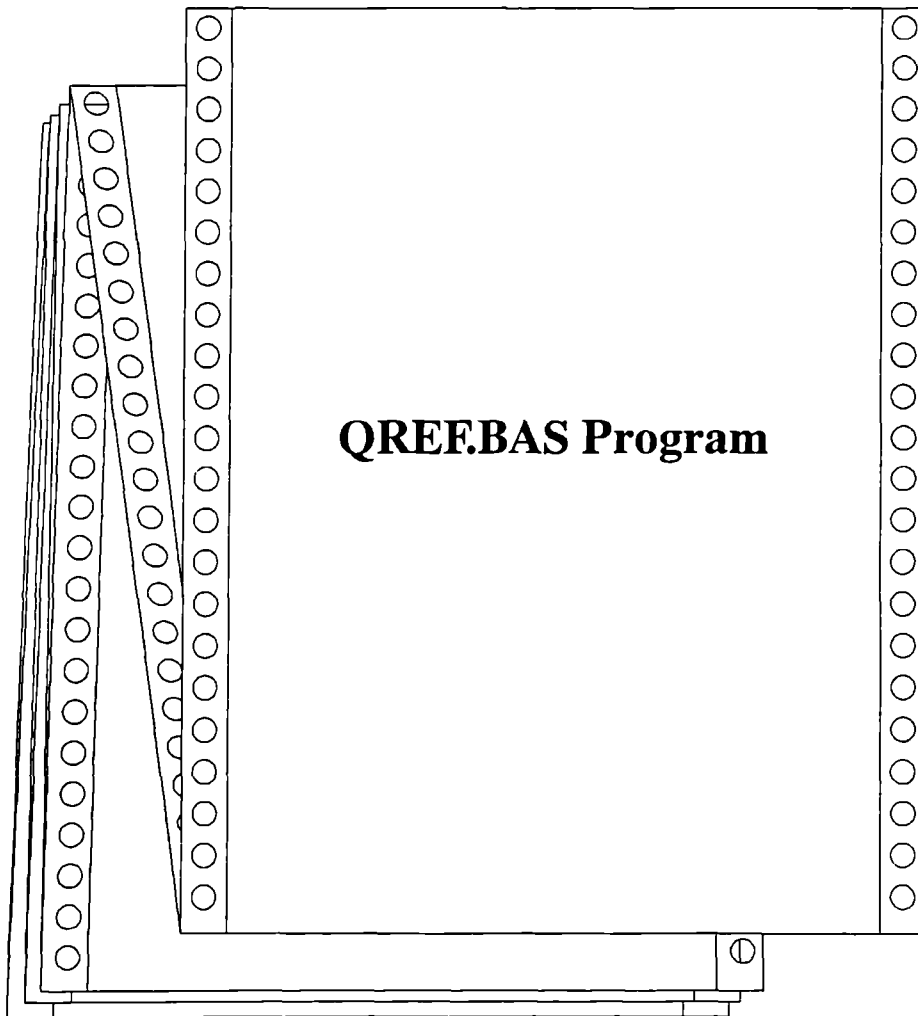
---

# Computer Programs (Code Listing)

---

The following programs are written in GW-Basic code by the author for specific tasks in various chapters:

- QREF.BAS : computes the hourly solar heat gain flux through a 3mm clear glass of various orientations using the climatic data of Riyadh. Description and flow charts of the program are given in chapter 4, and the program output is tabulated in Appendix D. The program can be modified for use as a subroutine in a dynamic thermal model of energy simulation.
- CURTAIN.BAS : Computes the transmitted solar flux and the convective-longwave heat fluxes through a curtain shaded window system. The window can be of a single or double glazing of any type and thickness. The program considers three types of curtain fitting; sealed, normal, and loose which allow for air circulation between the room and the space between curtain and glass. The program output results to a library file in ASCII format with basic or comprehensive data sets for analysis. (see also chapter 5 of this thesis for more details).
- DTCLM.BAS : analyses and processes the output data of the  $\Delta T$ -Logger. Description and a flow chart of the program main routines are given in chapter 6. The program may be of help to  $\Delta T$ -Logger users.



SOLAR HEAT GAIN THROUGH A 3mm GLASS  
File: QREF.BAS/JOUDAH1990

SOLAR HEAT GAIN THROUGH A 3mm GLASS  
File: QREF.BAS/JOUDAH1990

Page 2/4

Page 1/4

```

Shortwave, longwave and convective heat gain through a 3mm clear glass. Calculated for vertical
glazing with 8 orientations from North to North-East (AZ = -180 to 135 step 45 deg.), and for a
Horizontal Skylight.
-----
Initialise Constants
10  slc
    PI = 3.1415927#
    RAD = PI / 180
    LAT = 24.54 * RAD
    LONG = 46.24
    FLONG = -4.96
    GF = 0.1
    S = 5.6697E-08
    K = 273.15
    TI = 21 + K
    FIS = "riyadh clim"
    FS = "qref"
    AB(0) = 0.01154
    AB(1) = 0.77674
    AB(2) = -3.94657
    AB(3) = 8.57881
    AB(4) = -8.38135
    AB(5) = 3.01188
    TR(0) = -0.00885
    TR(1) = 2.71235
    TR(2) = -0.62062
    TR(3) = -7.07329
    TR(4) = 9.759949
    TR(5) = -3.89922
-----
Program main routine.
-----
for N = 1 to 9
  AZ = RAD * (45 * (N - 1) - 180)
  FOS = FS + slc * (-N)
  open FIS for input as #1
  open FOS for output as #2
  print "Processing data for " + FOS
  for DAY = 1 to 365
    locate N * 2, 1
    print "day: ";
    locate N * 2, 7
    print DAY
    DEC = 23.45 * RAD * sin(2 * PI * (DAY + 284) / 365)
    E = 2 * PI * (DAY - 81) / 364
    EQT = (FLONG + 9.87 * sin(2 * E) - 7.53 * cos(E) - 1.5 * sin(E)) / 60
    'Conversion factor from degree to radian
    'Latitude of Solar Village in Riyadh.
    'Longitude (deg). Standard Longitude = 45 deg. East.
    'Long. correction factor = Sid. - Loc. * 4 minutes per deg.
    'Ground factor = (0.5 * 0.2) = view factor * ground reflectance
    'Stefan-Boltzmann constant.
    'Celsius to Kelvin conversion.
    'Indoor air temperature & average temp. of room surfaces
    'Input climate file name.
    'Prefix for Output file(s) name(s).
    'Polynomial coefficients for glass absorptance
    'Polynomial coefficients for glass transmittance
    'cos angle of incidence on vertical surface
    'beam horizontal insolation
    'if not horizontal
    'calculate solar flux incident on vertical surface
    'calculate absorbed flux & transmitted flux (tau_alfa)
    'Solar heat gain through the glass
    'next hour glass temp.
    'input from climate file
    'initial estimate of glass temp.
    'external surface h.t.c.
    'internal surface h.t.c.
    'inward-flow fraction of absorbed solar flux.
    'hour angle
    'cos zenith angle
    'cos angle of incidence on vertical surface
    'beam horizontal insolation
    'if not horizontal
    'calculate solar flux incident on vertical surface
    'calculate absorbed flux & transmitted flux (tau_alfa)
    'Solar heat gain through the glass
    'next hour glass temp.
    print #2, using "###" "GAIN";
  next H
  print #2,
  next DAY
close
next N
print
print "Processing completed .... Bye!"
end
-----

```

```

for H = 1 to 24
  locate N * 2, 16
  print "hour: ";
  locate N * 2, 23
  print H
  input #1, DN, GH, DFH, T, WS, WD, RH
  T = T + K
  if DAY = 1 and H = 1 then TG = T
  gosub 1230
  490  gosub 1450
  510  HO = HV + HR
  520  gosub 1500
  530  gosub 1590
  540  HI = HV + HR
  550  if GH = 0 goto 730
  560  NI = HI / (HI + HO)
  570  HA = (12 - H + EQT) * PI / 12
  580  K1 = sin(DEC) * sin(LAT)
  590  K2 = cos(DEC) * cos(LAT) * cos(HA)
  600  COZE = K1 + K2
  610  K1 = cos(DEC) * sin(LAT) * cos(AZ) * cos(HA)
  620  K2 = sin(AZ) * sin(HA) * cos(DEC) -
  630  K3 = sin(DEC) * cos(LAT) * cos(AZ)
  640  COIN = K1 + K2 - K3
  650  DH = GH - DFH
  660  if N < > 9 goto 710
  670  DIRIN = DH
  680  DIFIN = DFH
  690  COIN = COZE
  700  goto 720
  710  gosub 860
  720  gosub 990
  730  GAIN = TAU + ALFA * NI
  740  TG = (ALFA + HO * T + HI * TI) / (HO + HI)
  750  TAU = 0
  760  ALFA = 0
  770  print #2, using "###" "GAIN";
  next H
  print #2,
  next DAY
close
next N
print
print "Processing completed .... Bye!"
end
-----

```

SOLAR HEAT GAIN THROUGH A 3mm GLASS  
File: QREF.BAS/JOUDAH 1990

```

1280 if abs(DS) > 180 then DS = 360 - abs(DS)
      if abs(DS) > 90 goto 1300
      if WS > 2 then VS = 0.25 * WS else VS = 0.5
      goto 1310
1300 VS = 0.3 + 0.05 * WS
1310 HV = 18.6 * VS ^ .605
      goto 1430
1340 if WS < 4.888 goto 1390
      A = 0
      B = 0.5
      C = 0.78
      goto 1420
1390 A = 0.99
      B = 0.21
      C = -1
1420 HV = 5.678 * (A + B * (WS / 0.3048) ^ C)
1430 return

Subroutine to calculate External Radiative h.t.c.
1450 TS = 0.05532 * T ^ 1.5
      if N = 9 then TE = TS
      else TE = (.5 * (TS ^ 4 + T ^ 4)) ^ .25
1470 HR = 0.9 * S * (TG ^ 2 + TE ^ 2) * (TG + TE)
1480 return

Subroutine to calculate Internal Convective h.t.c.
1500 if N = 9 goto 1540
      A = 1.5
      B = 1.23
      goto 1560
1540 A = 1.4
      B = 1.63
1560 HV = ((A * abs(TG - TI) ^ .25) ^ 6 + (B * abs(TG - TI) ^ (1/3)) ^ 6) ^ (1/6)
1570 return

Subroutine to calculate Internal Radiative h.t.c.
1590 HR = 0.9 * S * (TG ^ 2 + TI ^ 2) * (TG + TI)
1600 return

```

SOLAR HEAT GAIN THROUGH A 3mm GLASS  
File: QREF.BAS/JOUDAH 1990

```

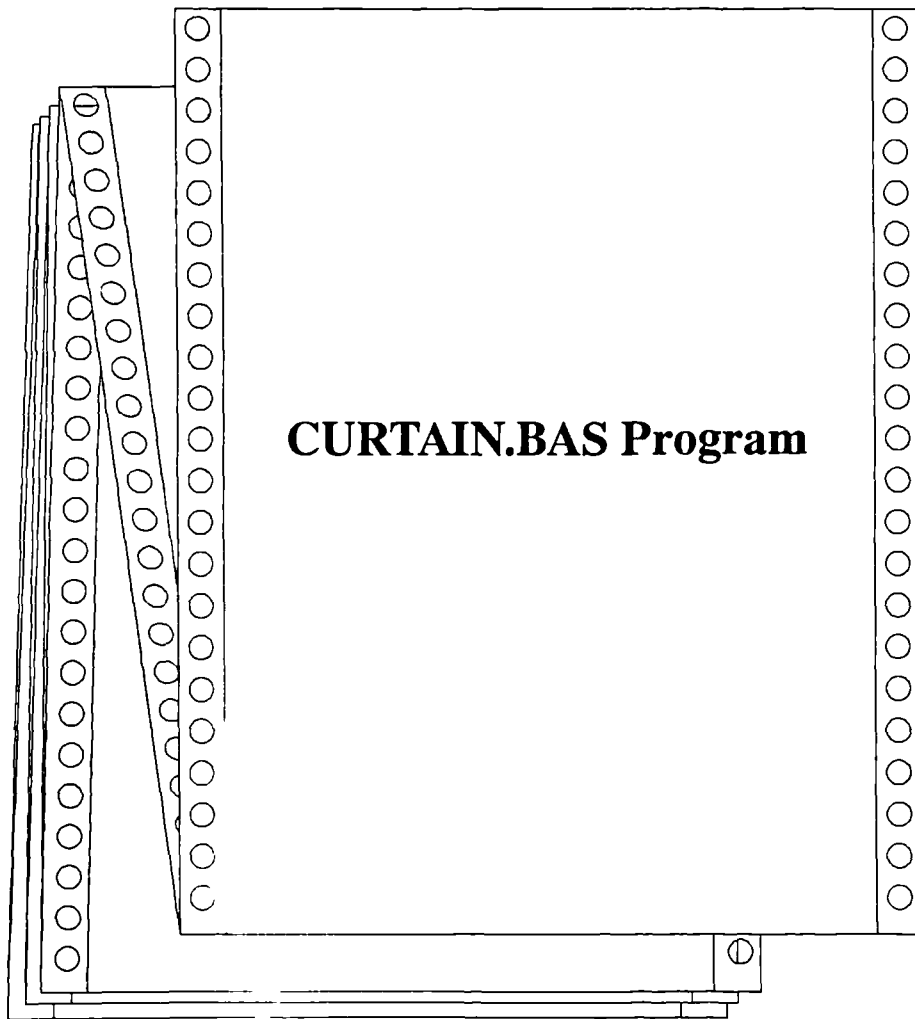
Subroutine to calculate Direct & diffuse insolation on vertical surfaces
860 if DH > 0 goto 890
870 SF = 0.5
      goto 940
890 K1 = 1 - (DFH / GH) ^ 2
      K2 = (sin(PI/4)) ^ 3
      K3 = (sin(atan(COZE / sqrt(1 - COZE * COZE))) + PI/2) ^ 3
      K4 = (COIN) ^ 2
930 SF = 0.5 * (1 + K1 * K2) * (1 + K1 * K3 * K4)
940 DIRIN = COIN * DN
      if DIRIN < 0 then DIRIN = 0
960 DIFIN = SF * DFH + GF * GH
      if DIFIN < 0 then DIFIN = 0
980 return

Subroutine to calculate the Transmitted and absorbed solar flux
990 if COIN <= 0 goto 1130
      for I = 0 to 5
          Y(I) = TR(I)
      next I
      gosub 1170
1050 TAU = DIRIN * X + DIFIN * 0.799016
      for I = 0 to 5
          Y(I) = AB(I)
      next I
      gosub 1170
1100 ALFA = DIRIN * X + DIFIN * 0.0543595
      goto 1150
1130 TAU = DIFIN * 0.799016
1140 ALFA = DIFIN * 0.0543595
1150 return

Subroutine to solve the polynomial equation for glass Tau & Alfa.
1170 X = 0
      for I = 0 to 5
          X = X + Y(I) * (COIN ^ I)
      next I
1210 return

Subroutine to calculate the External Convective h.t.c.
1230 if N = 9 goto 1340
      DS = (AZ / RAD) + 180 - WD

```



To calculate the transmitted solar flux and the convective/longwave heat fluxes through a curtain fenestration. Applicable for single or double glazed windows (of any glass type and thickness) shaded with an indoor fabric curtain.

Initialise constants and define mathematical functions

```

10  PI = 3.1415927#
    RAD = PI/180
    S = 5.6697E-08
    KLVN = 273.15
    RNDX = 1.526
    def fnckl(X, Y) = exp(-X/(sqrt(1-(sin(Y)/RNDX)^2)))
    def fntau(X, Y) = X*(1-Y)^2/(1-Y^2+X^2)
    def fnalfa(X, Y) = 1-Y-(X*(1-Y)^2/(1-Y*X))
    def fnacos(X) = (PI/2)-atn(X/sqrt(1-X*X))
    def fnasin(X) = atn(X/sqrt(1-X*X))
    def fnhv(X, Y) = ((1.5*abs(X-Y)^25)^6 + (1.23*abs(X-Y)^(1/3))^6)^(1/6)
    def fnbr(X, Y) = EPS*S*(X^2+Y^2)*(X+Y)
    'Degree to Radians conversion factor
    'Stefan-Boltzmann constant
    'Celsius to Kelvin conversion.
    'Refractive index of glass
    'Transmittance
    'Absorptance
    'Inverse cosine X
    'Radiative h.c. with X, Y temperatures.

```

Assign input strings (from subroutine 1320) to program variables, and calculate constant terms

```

30  gosub 1320
40  GZ = val(A$(0))
    LAT = val(A$(1))*RAD
    FLONG = val(A$(2))
    GF = 5*val(A$(3))
    AZIMUTH = val(A$(4)):AZ = AZIMUTH*RAD
    SDAY = INT(val(A$(5)):LDAY = val(A$(6))
    TSH = val(A$(9))
    RSH = val(A$(10))
    SEPSO = val(A$(11))
    SEPSI = val(A$(12))
    GNT = val(A$(14))
    GEPSO = val(A$(15)):GEPSI = val(A$(16))
    FOS = A$(7)
    FIS = A$(17)
    SAVO = val(A$(13))
    TI = val(A$(21)) + KLVN
    A = val(A$(8))
    if A = 1 then H7 = 2.4 else if A = 3 then H7 = 9.6 else H7 = 4.8
    K3 = (sin(PI/4))^3
    RPN = ((RNDX-1)/(RNDX+1))^2
    KL1 = log(((1-RPN)^2 + sqrt((1-RPN)^4 + 4*GNT^2*RPN^2))/(2*GNT))
    if GZ = 1 then 180
    GCGNT = val(A$(18))
    GGEPSO = val(A$(19)):GGEPSI = val(A$(20))
    KL2 = log(((1-RPN)^2 + sqrt((1-RPN)^4 + 4*GGNT^2*RPN^2))/(2*GGNT))
    crase A$, B$

```

180

Define arrays, open climate file and position to start day

```

200 if GZ = 2 then N = 5 else N = 4
    dim A(N, N+N), C(N)
    open FIS$ for input as #1
    if SDAY = 1 then 250
    print: print "Please Wait ...."
    for DAY = 1 to SDAY-1
        for H = 1 to 24
            input #1, X, X, X, X, X, X
            next H
        next DAY
    'Input climatic data in the dummy variable X

```

Program main routine

```

250 cls: print "***** CURTAIN Program v1.10 *****"
    print "Energy Performance Simulation of Curtain Fenestration"
    locate 5, 5
    print "Processing Day ...."
    locate 7, 5
    print "Processing Hour ..."
    for DAY = SDAY to LDAY
        locate 5, 25
        print DAY
        DEC = 23.45*RAD*sin(2*PI*(DAY+284)/365)
        E = 2*PI*(DAY-81)/364
        EQT = (FLONG*4 + 9.87*sin(2*E) - 7.53*cos(E) - 1.5*sin(E))/60
        for H = 1 to 24
            input #1, GH, DFH, T0, WS, WD, X, T0 = T0 + KLVN
            locate 7, 25: print " "
            locate 7, 25
            print H
            if DAY = SDAY and H = 1 then 380 else 390
            TEMPF = (T0-TI)/N
            X(1) = T0
            for I = 2 to N
                X(I) = X(I-1)-TEMPF
            next I
            Calculate h.t.c at the fenestration surfaces: convective, radiative or combined
            DS = AZIMUTH + 180 - WD
            if abs(DS) > 180 then DS = 360-abs(DS)
            if WS > 2 then VS = .25*WS else VS = .5
            if abs(DS) > 90 then VS = .3 + .05*WS
            'if Lecward
            'wind direction relevant to window surface
            'wind speed at window surface if windward
            'if Lecward

```

```

EPS = GEPSO
TSKY = .05532 * T0 ^ 1.5
TE = (.5 * (TSKY ^ 4 + T0 ^ 4)) ^ .25
H0 = 18.6 * VS ^ .605 + fahr(X(2), TE)
if GZ = 2 then 510
EPS = 1 / ((1 / GEPSI) + (1 / SEPSO) - 1)
H3 = fahr(X(2), X(4))
EPS = SEPSI
H6 = fahr(X(4), TI)
H2 = fahr(X(2), X(3))
H4 = fahr(X(4), X(3))
H5 = fahr(X(4), TI)
goto 580
EPS = 1 / ((1 / GEPSI) + (1 / GGEPSO) - 1)
H1 = fahr(X(2), X(3)) + fahr(X(2), X(3))
EPS = 1 / ((1 / GGEPSI) + (1 / SEPSO) - 1)
H3 = fahr(X(3), X(5))
EPS = SEPSI
H6 = fahr(X(5), TI)
H2 = fahr(X(3), X(4))
H4 = fahr(X(5), X(4))
H5 = fahr(X(5), TI)

-----
Calculate incident solar angle, then branch control to calculate incident direct and diffuse
insolation, and the fenestration transmittance & absorptance.
580 if GH <= 1 goto 660
HA = (12 - H + EOT) * PI / 12
COZE = sin(DEC) * sin(LAT) + cos(DEC) * cos(LAT) * cos(HA)
if sign(COZE) = -1 goto 660
K1 = cos(DEC) * sin(LAT) * cos(AZ) * cos(HA)
K2 = sin(AZ) * sin(HA) * cos(DEC)
COIN = K1 + K2 - (sin(DEC) * cos(LAT) * cos(AZ))
ANGI = fncos(COIN)
goto 770
gosub 860
goto 670
TAUF = 0: ALF1 = 0
ALF2 = 0: ALF3 = 0
NI = 0: GV = 0
' Fenestration transmittance, and outer glass absorptance
' Inner glass & curtain absorptances
' Inward convective/radiative flow fraction & incident insolation

Assign variables for the constant vector of heat balance matrix, branch to subroutine 1120 to
compute the fenestration U-value, Ni, qrci, and the temperatures of curtain, air gap & glass
pane(s), then print results.
670 if SAVO = 1 then 710
GVV = 0: TOX = 2: TIX = 1
gosub 1120

```

```

U = X(1)
if GH < 1 then 710
GVV = 1: TOX = 1: TIX = 1
gosub 1120
NI = X(1)
GVV = GV: TOX = T0: TIX = TI
' Assign to calculate qrci & fenestration temperatures
SGAIN = TAUF * GV
' Transmitted shortwave through the fenestration
' to print results
' Repeat for next hour
' Repeat for next day
next DAY
close
print ""
end
-----
Subroutine to calculate the direct & diffuse insolation incident upon the window
770 if GH < DFH then GH = DFH
DH = GH - DFH
if DH > 0 then 800
SF = .5
goto 820
K1 = 1 - (DFH / GH) ^ 2
SF = 5 * (1 + K1 * K2) * (1 + K1 * (sin(fncos(COZE))) ^ 3 * (COIN) ^ 2)
DIRIN = DH * COIN / COZE
if DIRIN < 0 then DIRIN = 0
DIFIN = SF * DFH + GF * GH
GV = DIRIN + DIFIN
return
' isotropic sky condition
' for the anisotropic sky condition formula next
' Direct incident solar radiation
' Diffuse incident solar radiation
' Total incident solar radiation

-----
Subroutine to calculate the fenestration solar transmittance & the absorptance of each layer at
incident angle ANGI. The transmittance and absorptance of glass are computed by the Fresnel
equations for monochromatic radiation using the equivalent normal-incidence KL value. The
curtain transmittance and absorptance are assumed constant at all angles of incidence.
860 if ANGI / RAD > 85 then ANGI = 85 * RAD
if ANGI > 0 then 890
RPL = RPN: RPD = RPN
ANGR = 0
' Glass specular reflectance for parallel & perpendicular polarisation
' Glass angle of refraction at normal incidence
goto 920
SINR = sin(ANGI) / RNDX
ANGR = fncsin(SINR)
RPL = (sin(ANGI - ANGR) ^ 2 / (sin(ANGI + ANGR) ^ 2)
RPD = (tan(ANGI - ANGR) ^ 2 / (tan(ANGI + ANGR) ^ 2)
EKL = fnckl(KL1, ANGI)
TAU = .5 * (fnciu(EKL, RPL) + fnciu(EKL, RPD))
ALFA = .5 * (fncifa(EKL, RPL) + fncifa(EKL, RPD))
' Snell's law
' Glass angle of refraction
' Fraction of incident flux transmitted (Bouguer-Lambert's law)

-----
Assign variables for the constant vector of heat balance matrix, branch to subroutine 1120 to
compute the fenestration U-value, Ni, qrci, and the temperatures of curtain, air gap & glass
pane(s), then print results.
710
730
740
750
760
-----
Subroutine to calculate the direct & diffuse insolation incident upon the window
770
800
820
-----
Subroutine to calculate the fenestration solar transmittance & the absorptance of each layer at
incident angle ANGI. The transmittance and absorptance of glass are computed by the Fresnel
equations for monochromatic radiation using the equivalent normal-incidence KL value. The
curtain transmittance and absorptance are assumed constant at all angles of incidence.
860
890
920

```

```

940 if GZ = 2 then 980
    ROW = 1 - TAU - ALFA
    ASH = 1 - TSH - RSH
    TAU = TAU * TSH / (1 - ROW * RSH)
    ALF1 = ALFA * (1 + (TAU * RSH) / (1 - ROW * RSH))
    ALF2 = TAU * ASH / (1 - ROW * RSH)
    goto 1070
980 EKL = fneck(KL, ANGI)
    TAU2 = .5 * (fntau(EKL, RPL) + fntau(EKL, RPD))
    ALFA2 = .5 * (fnalfa(EKL, RPL) + fnalfa(EKL, RPD))
    TU1 = TAU
    AF1 = ALFA
    RO1 = 1 - TAU - ALFA
    TU2 = TAU2
    AF2 = ALFA2
    RO2 = 1 - TAU2 - ALFA2
    TU3 = TSH
    RO3 = RSH
    AF3 = 1 - TSH - RSH
    TAU = TU1 * TU2 * TU3
    ROW = RO1 + RO2 * TU1 ^ 2
    ALF1 = AF1 + TU1 * RO2 * AF1
    ALF2 = AF2 * TU1
    ALF3 = TU1 * TU2 * AF3
    X = TU1 * RO1 * RO2
    Y = RO3 * TU1 * TU2
1030 TAU = TAU + TU2 * TU3 * X + TU3 * RO2 * Y
    ROW = ROW + TU1 * RO2 * X + TU1 * TU2 * Y
    ALF1 = ALF1 + AF1 * RO2 * X + AF1 * TU2 * Y
    ALF2 = ALF2 + AF2 * X + AF2 * Y
    ALF3 = ALF3 + TU2 * AF3 * X + AF3 * RO2 * Y
    X1 = RO2 * X + TU2 * Y
    Y1 = TU2 * X + RO2 * Y
    X = RO1 * X1
    Y = RO3 * Y1
    Z = TAU + ROW + ALF1 + ALF2 + ALF3
    if Z < .999 then 1030
1070 return
Subroutine to solve the heat balance equations of the fenestration as follows:
Define the Matrix of coefficients [a] and the constant vector [c]
1120 A(1,1) = 1
    A(1,2) = H0
    C(2) = H0 * T0X + ALF1 * GVV
    if GZ = 2 then 1170
    'Common coefficients for single or double glazing with curtain
    'Single glazing with curtain
    'Properties of the inner glass pane
    'Double glazing with curtain
    'Complete loop at 001 variance

```

```

1140 A(2,2) = H0 + H2 + H3
    A(2,3) = -H2
    A(2,4) = -H3
    A(3,2) = -H3
    A(3,3) = -H4
    A(3,4) = H3 + H4 + H5 + H6
    A(4,2) = H2
    A(4,3) = -H2 - H4 - H7
    A(4,4) = H4
    C(1) = H0 * T0X + GVV * (ALF1 + ALF2)
    C(3) = TIX * (H5 + H6) + ALF2 * GVV
    C(4) = -H7 * TIX
    goto 1200
    'for single glazing and curtain
1170 A(2,2) = H0 + H1
    A(2,3) = -H1
    A(3,2) = -H1
    A(3,3) = H1 + H2 + H3
    A(3,4) = -H2
    A(3,5) = -H3
    A(4,3) = -H3
    A(4,4) = -H4
    A(4,5) = H3 + H4 + H5 + H6
    A(5,3) = H2
    A(5,4) = -H2 - H4 - H7
    A(5,5) = H4
    C(1) = H0 * T0X + GVV * (ALF1 + ALF2 + ALF3)
    C(3) = ALF2 * GVV
    C(4) = TIX * (H5 + H6) + ALF3 * GVV
    C(5) = -H7 * TIX
    'for double glazing and curtain
    Align the coefficient matrix with an identity matrix
1200 for I = 1 to N
    for J = N + 1 to N + N
        A(I,J) = 0
    next J
    A(I,I + N) = 1
next I
Perform Matrix inversion (Gauss-Jordan method)
for K = 1 to N
    gosub 1270
    DUMMY = A(K,K)
    for J = 1 to N + N
        A(K,J) = A(K,J) / DUMMY
    next J
    for I = 1 to N
        'for partial pivoting

```

```

1240      if I = K then 1240
          DUMMY = A(I,K)
          for J = 1 to N + N
              A(I,J) = A(I,J) - DUMMY * A(K,J)
          next J
      next I
      next K

      'The matrix inverse [a]-1 are a(k, n + j) where k & j from 1 to n, thus the solution for [x] unknown
      vector [s] = [c] * [a]-1.
      for K = 1 to N
          X(K) = 0
      next K
      for K = 1 to N
          for J = 1 to N
              X(K) = X(K) + A(K, N + J) * C(J)
          next J
          A(K, J) = 0
      next K
      return
      'end of matrix solution & return to program main routine

      Subroutine for partial pivoting in the Gauss-Jordan inversion method, to avoid division by zero
      and to eliminate round-off error
1270      JJ = K
          Y = abs(A(K,K))
          for I = K + 1 to N
              YP = abs(A(I,K))
              if Y - YP > = 0 then 1290
                  Y = YP
                  JJ = I
          next I
1290      if JJ - K = 0 then 1310
          for J = K to N + N
              X = A(JJ,J)
              A(JJ,J) = A(K,J)
              A(K,J) = X
          next J
          return

      Subroutine for string input in the array a$(21) by the user via the terminal. Array b$(21) stores
      questions to print on screen. Both arrays will be deleted in the program main routine at a later
      stage to free memory blocks.
1320      cls
          dim a$(21), b$(21)
          on error goto 2130
          open "Curtain.In" for input as #1
1330      'To print information page about the program
          'Open error trapping routine

```

```

1340      if eof(1) then 1370
          A$ = input$(1, #1)
          if asc(A$) = 13 goto 1340
          print A$;
          goto 1340
          locate 22, 75
1370      A$ = inkey$
          if len(A$) = 0 then 1370
          if asc(A$) < > 32 then 1370
          close
          for I = 5 to 22
              locate I, 1
              print space$(79)
          next I
          DG$ = chr$(248)
          locate 5, 4
          print " Input data as prompted; press Enter to accept defaults."
          print " Program defaults are given as (d = value)."
          locate 10, 5
1420      input "Glazing type, 1-single 2-double (d = 1)"; A$
          A = 1
          if A$ < > "" and val(A$) < > 1 and val(A$) < > 2 then 2170
          if val(A$) = 2 then A$(0) = "2" else A$(0) = "1"
          gosub 1590 'for input and editing of 14 or 17 array variables, depending on the type of glazing
          cls
          locate 5, 1
          input " Output file name (d = Curtain.Res)"; A$(7)
          if A$(7) = "" then A$(7) = "Curtain.Res"
          locate 6, 1
1490      input " Save Option 1-Basic 2-Comprehensive (d = 1)"; A$
          A = 0
          if A$ < > "" and val(A$) < > 1 and val(A$) < > 2 then 2170
          if val(A$) = 2 then A$(13) = "2" else A$(13) = "1"
          locate 7, 1
          print space$(79)
          A = A + 1
          locate 7, 1
          input " Climate file name"; A$(17)
          open A$(17) for input as #1
          locate 8, 1
1530      print " Room Control Temperature" + DG$ + "C (d = 21)";
          input A$(21)
          if A$(21) = "" then A$(21) = "21"
          on error goto 0
          close
          return
          'Terminate error trapping routine
          'to program main routine

```

Subroutine to input and allow modification of variables in the string array a\$. First define the variables of b\$ array.

```

1590 B$(1) = "Site and Date Information"
B$(2) = " 2 Latitude Angle 0-80" + DG$
B$(3) = " 3 Longitude Difference" + DG$ + " (d=0)"
B$(4) = " 4 Ground Albedo <1 (d=.2)"
B$(5) = " 5 Surface Azimuth" + DG$ + " (d=0)"
B$(6) = " 6 Start Day (Julian)"
B$(7) = " 7 Last Day (Julian)"
B$(8) = "Curtain Properties"
B$(9) = " 9 Fitting Type 1, 2 or 3 (d=2)"
B$(10) = "10 Transmittance <1"
B$(11) = "11 Reflectance <1"
B$(12) = "12 Ext. Emissivity <1 (d=.9)"
B$(13) = "13 Int. Emissivity <1 (d=.9)"
B$(14) = "Glass Properties"
B$(15) = "15 Transmittance <1 (d=.78)"
B$(16) = "16 Ext. Emissivity <1 (d=.84)"
B$(17) = "17 Int. Emissivity <1 (d=.84)"
if val(A$(0)) = 1 then 1720
B$(14) = "Outer Glass Pane"
B$(18) = "Inner Glass Pane"
B$(19) = "19 Transmittance <1 (d=.78)"
B$(20) = "20 Ext. Emissivity <1 (d=.84)"
B$(21) = "21 Int. Emissivity <1 (d=.84)"
N = 21

```

```

1720 goto 1740
N = 17

```

\*i.e. Single glazing with curtain

Start terminal input of string variables representing: site information & dates of simulation, curtain properties, and glazing properties.

```

1740 cls: print B$(1)
for J = 2 to N
    if J = 8 or J = 14 or J = 18 then 1760
    locate J, 1: print string$(38, 250)
next J
locate 2, 1
for J = 2 to N
    print B$(J)
next J
if IDIT = 1 goto 1810
for J = 1 to N-1
    if J = 7 or J = 13 or J = 17 then 1800
    locate J + 1, 40: input A$(J)
    gosub 1890
next J

```

\*If edit mode is ON

\*Processing for input mode

\*To check for errors in user input strings

Subroutine to account for characters occupying columns 40 and 50 of raw L on the screen

```

1810 IDIT = 1
for J = 1 to N-1
    if J = 7 or J = 13 or J = 17 then 1820
    locate J + 1, 39: print " = "; val(A$(J))
next J
print: input " Line# Change or (N)ext"; L$
L = val(L$)
if L < 2 or L > N then 1860
gosub 1870
A$(L-1) = AA$
J = L-1
gosub 1890
if IRR = 1 then 1840
goto 1740
return

```

Subroutine to account for characters occupying columns 40 and 50 of raw L on the screen

```

1870 locate L, 40
input "", A$
AA$ = ""
for KK = 40 to 50
    AA$ = AA$ + chr$(screen(L, KK))
next KK
return

```

Subroutine for error trapping, and to assign default values if input string is null

```

1890 IRR = 0
if A$(J) = "" then 2030
A = val(A$(J))
if J = 1 and (A < 0 or A > 80) then 2110
if J = 2 and (A < -15 or A > 15) then 2110
if J = 3 and (A <= 0 or A >= 1) then 2110
if J = 4 and (A < -180 or A > 180) then 2110
if J = 5 and (A < 1 or A > 365) then 2110
if J = 6 and (A < 1 or A > 365 or A < val(A$(5))) then 2110
if J = 8 and A < 1 and A > 2 and A < > 3 then 2110
if J > 8 and (A <= 0 or A >= 1) then 2110
if J = 9 and IDIT = 1 and A + val(A$(10)) >= .99 then 2110
if J = 10 and A + val(A$(9)) >= .99 then 2110
goto 2120
2030 if J = 1 or J = 5 or J = 6 or J = 9 or J = 10 then 2110
if J = 2 or J = 4 then A$(J) = "0"
if J = 3 then A$(J) = "2"
if J = 8 then A$(J) = "2"
if J = 11 or J = 12 then A$(J) = ".9"

```

\*Initialise error flag

\*to assign default values

\*Convert input string to value for error trapping

\*These do not accept default values

```

if J = 14 or J = 18 then A$(J) = ".78"
if J = 15 or J = 16 or J = 19 or J = 20 then A$(J) = ".84"
goto 2120
beep
locate J + 1, 40
print space$(10)
J = J - 1
IRR = 1
return

-----
Error handling routine
-----
2130 beep
if err = 53 and err1 = 1330 then resume 1390 'Execute program without displaying information page
if err = 53 and err1 = 1540 then print "File not found..." 'Climate file not found
if A < 5 then resume 1530
print "Time Out --- program aborted."
end
beep
print " ERROR... reprint 1, 2 or Enter" 'Apply for glazing type and save option input
if A = 0 then 2190
locate 10, 5: print space$(70)
goto 1420
locate 6, 1: print space$(70)
goto 1490

-----
Subroutine to print results of one hour processing
-----
2200 print #2, using "###.###"; T0 - KLVN;
for K = 2 to N
    print #2, using "###.###"; X(K) - KLVN;
next K
print #2, using "###.###"; TI - KLVN;
print #2, using "###.###"; X(1); SGAIN;
if SA VO = 1 then 2290
print #2, using "###.###"; U; NI;
if GZ = 2 then 2270
print #2, using "###.###"; TAUF; ALF1; ALF2;
print #2, using "###.###"; H0; H2; H3; H4; H5; H6; H7;
goto 2290
print #2, using "###.###"; TAUF; ALF1; ALF2; ALF3;
print #2, using "###.###"; H0; H1; H2; H3; H4; H5; H6; H7;
print #2,
return
'To program main routine for next hour calculation
-----

```

```

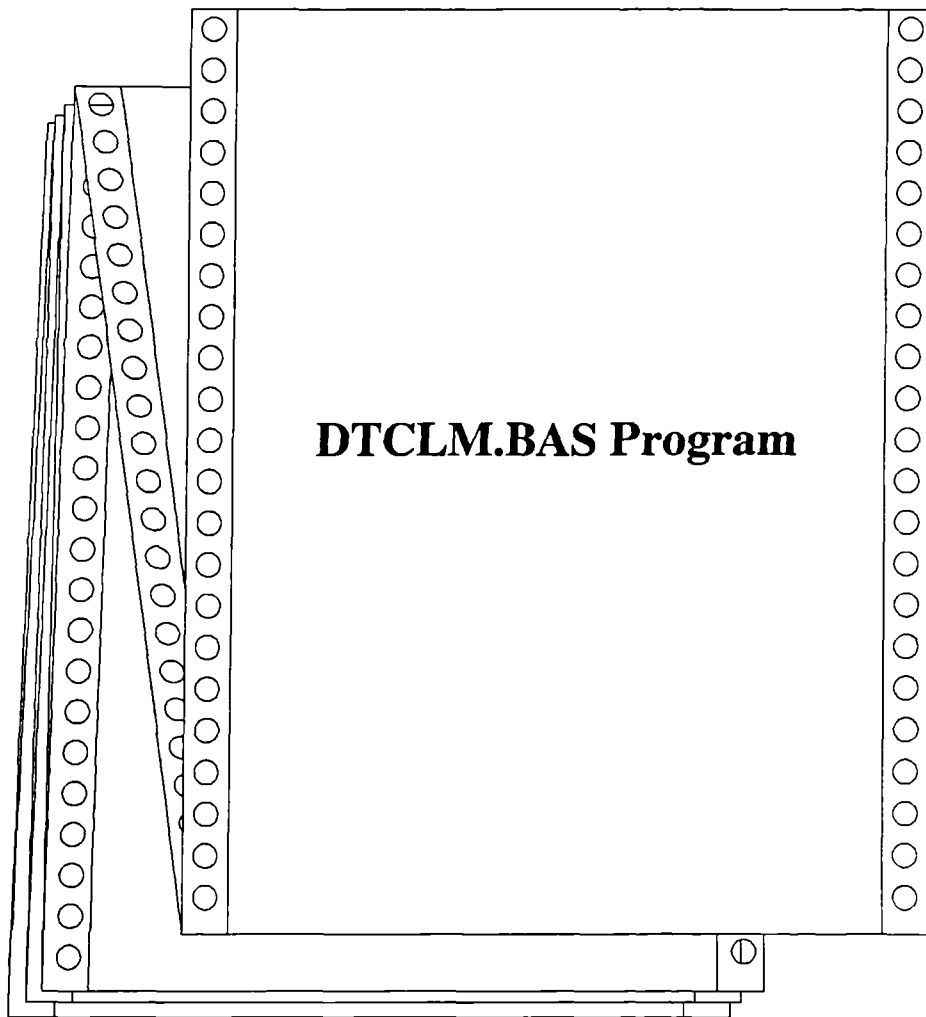
-----
Contents of the supplementary information File: CURTAIN.INF / JOUDAH 1990
-----
CURTAIN
-----
This program calculates the instantaneous rate of heat gain/loss through curtain shaded windows of single or double glazing. The input variables consist of three parts:

(1) Site information: Latitude, longitude difference and ground albedo.
(2) Hourly climatic variables: Global horiz insolation, diffuse horiz insolation, outdoor air temperature, wind speed and wind direction.
(3) Fenestration properties: Solar transmittance of glazing layer(s) at normal incidence, curtain transmittance & reflectance, emissivity of each surface for each layer, and the type of curtain fitting.

Two output save options are available: 1-Basic; reports the transmitted solar flux, convective/longwave heat flux to indoor space, & temperature of each layer in the fenestration; 2-Comprehensive; as the basic option plus the surface heat transfer coefficients, U-value and composite solar properties of the fenestration.

Press Space Bar to continue ...
-----

```



DATA PROCESSING PROGRAM  
File: DTCLM.BAS/JOUDAH1988

Page 1/20

DATA PROCESSING PROGRAM  
File: DTCLM.BAS/JOUDAH1988

Page 2/20

```

5' define & switch soft-key trapping On for program protection.
10 key 15, chr$(&H44) + chr$(70):
key 16, chr$(&H44) + chr$(70)
20 key(15) ON: key(16) ON
30 on key(15) gosub 1040:
on key(16) gosub 1040:
if BRK = -9 goto 100

-----
Initialise Constants and Array Dimensions
50 color 4,3 : cls
60 dim C(60), Z(22,15), ZOO(23), CV(15), CV$(15)
70 TONES$ = "T255 O1 L10 ABCDEF L1 G P62 O3 L15 FED L20 ABC":
TONE1$ = "T255 O1 L10 AAA L1 G P62 O3 L12 A L8 B":
TONE2$ = "T255 O1 L12 A L8 B":
TONE3$ = "T255 O1 L12 A L8 B L4 C":
goto 3630

-----
Inkey Subroutine
80 Z$ = inkey$:
if len(Z$) = 0
goto 80
else Z% = asc(Z$)
return

-----
Start Execution after Menu and open Error Trapping, and Merge with other
Programs to Free Memory by Deleting Part(s) of the Main Program
100 cls : print "Please Wait ..."
110 on error goto 1060
120 BRK = -9:
chain merge "DELPL", 10, all, delete 3620-4750
130 if SVE = 0
then chain merge "DELPL1", 10, all, delete 3420-3610
140 if SVE = 1
then chain merge "DELPL2", 10, all, delete 3300-3410

-----
Display Instructions to User
150 play TONE1$:
if NNS$ = "" then NNS$ = "B:"
160 if (NDS$ = "C:")
goto 260
170 if (NDS$ = "A:")
goto 210
180 if (NNS$ = "B:") and (SVE <> 0)
goto 190
else goto 200
190 cls : locate 8,5 : print "Remove Program Disk .....Then":
locate 10,5 : print "INSERT ...DATA DISK IN DRIVE [ A: ]":
locate 11,12 : print "...A FORMATTED DISK IN DRIVE [ B: ]":
goto 220
200 cls : locate 8,5 : print "Remove Program Disk .....Then":
locate 10,5 : print "INSERT ...DATA DISK IN DRIVE [ A: ]":
goto 220
210 cls : locate 10,5 : print "INSERT ...DATA DISK IN DRIVE [ A: ]":
locate 22,5 : print "Press [ RET ] When Ready ...": MG = 0
220

```

DATA PROCESSING PROGRAM  
File: DTCLM.BAS/JOUDAH1988

Page 3/20

```

450 print: print DLS: color 1,7: play TONE1$:
for FL = 1 to 9:
locate 22,1: print SPL$:
locate 22,1: print "*** READ ABOVE INFORMATION *":
next FL:
locate 22,30:
print "..... PRESS [RET] to CONTINUE ....": play TONE2$:
gosub 80:
if Z% < > 13
goto 460

-----
Arrange Screen for Channel Numbers Input
480 color 7,1: cls
490 print DDL$: print "Channel number "; chr$(4); " .....Label": print DLS
500 for K = 1 to C:
print using "#"; K:
next K: print DDL$: print
print "Choose Channel Number(s) from the ABOVE TABLE "
print "[SPACE BAR] -- next Channel Number [RET] ----- next Line":
print "[On BEEP] --- Ready for Input [ESC] ----- Reinput":
S = 0: play TONE$: color 1,7: locate 21,1:
print "Input Channel Number(s) For...;: color 7,1:
gosub 1560

-----
Start Analysis Menu
540 color 0,3: cls
550 color 2,1: play TONE1$:
for FR = 7 to 13:
locate FR,22: print FR$:
next FR
color 0,7: locate 9,27: print "0 "; locate 11,27: print "1 "
locate 9,31: print "RESTART CHANNEL INPUT "
locate 11,31: print "START ANALYSIS "
gosub 80:
if Z% < > 48 and Z% < > 49
if Z% = 48
goto 570
if Z% = 48
goto 480
585 analysis headings
590 color 22,0: cls
600 play TTONES: print chr$(178); chr$(177); chr$(176): color 6,0:
locate 15: print "DATA ANALYSIS IN PROGRESS ...":
print DLS: color 7,0:
if SVE < > 1 then 620
locate 11,26: color 2,0: print "Wait ... or go get busy ...!"
615 erase channel labels & units array; and re-define local constants
620 if SVE = 0 or KTB = 1
then ERASE ABS
630 FR1$ = string$(240, 177): FR2$ = string$(80, 177):
FR3$ = string$(240, 176): FL$ = string$(40, 177):
FL1$ = string$(40, 176): YP$ = chr$(253): YD$ = chr$(248)
639 ' to be executed if hard disk is being used
640 if PRD = 1
then chain merge "DELPL3", 10, all, delete 120-630

```

DATA PROCESSING PROGRAM  
File: DTCLM.BAS/JOUDAH1988

Page 4/20

```

-----
Input TI (Logging Intervals) from Data File
660 gosub 2000:
close #1:
open "#1, FF$:
665 ' to be executed if hard disk is being used
670 if PRD = 1
then chain merge "DELPL4", 10, all, delete 1230-2070

-----
Read Row Data from Disk & Save in Array
680 LF% = lof(1) / 128:
BI = val(HHS): DT$ = DD$ + "/" + MM$ + " " + HH$ + DMH$ + " "
locate 23,50: print "Job -- Completed ...":
gosub 690
LC% = 100 * (loc(1)) / LF%:
locate 23,72: print LC%: "%":
return
P = 0: locate 1,45: print SP$:
locate 1,45: print "Reading From ", FF$: " File":
gosub 685
input #1, N$:
if len(N$) < > 17
goto 700
705 ' search for starting date string at the first execution of this routine
710 E = E + 1: if E < > 1
goto 740
if N$ = DT$:
E = 0:
goto 700
if P < > 0
goto 760
DT$ = left$(N$, 5): DD$ = left$(DT$, 2):
MM$ = right$(DT$, 2): DDD = val(DD$): MMM = val(MM$)
755 ' input number of values on each interval; open loop for data input, & detect invalid data
760 P = P + 1: input #1, CHN$:
C(P) = val(CHN$):
for I = 1 to C(P)
input #1, A1$(I):
if A1$(I) = "" goto 770
if A1$(I) < > "&" and A1$(I) < > "#" and A1$(I) < > "*"
and A1$(I) < > "$" goto 800
XXX = 1: ZZZ = 1
if ZZZ = 0 goto 820
ZZZ = 0: goto 770
815 assign (*) flag for invalid values and store values in AAS array
820 if XXX = 1 then A1$(I) = ""
830 AA$(P, I) = A1$(I): XXX = 0
840 next I
850 if P < > TI goto 700

-----
Controlling Path to Calculation Subroutines
870 ZO = 0: locate 1,45: print SP$:
locate 1,45: print "Analysing...":
for II = 1 to S:

```

DATA PROCESSING PROGRAM  
File: DTCLM.BAS/JOUDAH 1988

Page 5/20

DATA PROCESSING PROGRAM  
File: DTCLM.BAS/JOUDAH 1988

Page 6/20

```

locate 1,60 : print II :
if Z(U,0) = 0 goto 900
ZO = ZO + 1
ON II gosub 2090, 2120, 2150, 2170, 2220, 2260, 2300, 2330, 2360, 2390,
2410, 2430, 2450, 2470, 2490, 2510, 2530, 2550, 2570, 2590, 2610
next II
-----
Controlling Path to Output Subroutines
910 if SVE = 0
    goto 960
if KTB = 0
    goto 940
930 locate 1,45 : print SP$: locate 1,45 : print "Writing to "; NF1$, " File" :
    gosub 3530 :
    if KTB = 1
        goto 950
940 locate 1,45 : print SP$: locate 1,45 : print "Writing to "; NF$, " File" :
    gosub 3430
    if SVE = 1
        goto 970
960 gosub 3310
970 if BOBO = -1
    goto 1020
980 B1 = B1 + 1 :
    if B1 = 24 then B1 = 0
990 goto 690
-----
Execute for EOF values
1000 if (P = 0) or (P = 1)
    goto 1020
1010 BOBO = -1 :
    P = P - 1 : TT = P :
    RESUME 850
-----
Instruct & Draw Attention to End Program Execution
1020 close #1 : color 18,0 : locate 23,1 : print SPL$:
    locate 23,1 : print "END OF FILE....." :
    SND = SND + 1 : SOUND 1970,5 : SOUND 750,4 :
    Z$ = inkey$ :
    if len(Z$) = 0 and SND < 11
        goto 1030
    else
        for I = 1 to 2 :
            SOUND 1800,3 : SOUND 1750,2 : SOUND 1800,3 :
            SOUND 800,3 : SOUND 750,2 : SOUND 800,3 :
            SOUND 1000,3 : SOUND 1050,2 : SOUND 1000,3 :
        next I
1040 color 0,3 : goto 1100
-----
Error Trapping Routines
1040 if (err = 53) and (err = 280) goto 1120
1070 if (err = 53) and (err = 300) goto 1190
1080 if err = 71 goto 1150
1090 if err = 62 goto 1000
-----
DATA PROCESSING PROGRAM
File: DTCLM.BAS/JOUDAH 1988
-----
Terminate Execution
1100 cls : SYSTEM
-----
ERROR Messages
1120 for MG = 1 to 3 :
    locate 20,1 : print SPL$: locate 20,3 :
    print " Oh Oh,if Diskette Contains no [DATA] files " : play "L3 G" :
    next MG :
    locate 22,3 : print " Press [ RET ] to LIST files ..." :
    gosub 80 :
    if Z% < > 13
        goto 1130
1140 HES$ = " " : MES$ = " " : FH$ = " " :
    RESUME 270
1150 for MG = 1 to 3 :
    locate 20,1 : print SPL$: locate 20,3 :
    print " ERROR ... Disk Drive NOT READY " : play "L3 G" :
    next MG :
    locate 22,3 : print " Press [ RET ] When Ready ..." :
    gosub 80 :
    if Z% < > 13 goto 1160
1170 locate 1,1 : print SPL$:
    next I :
    if (err = 280) then
        locate 1,1
    RESUME
1180 if T < = 4 then
    for MG = 1 to 3 :
        locate 20,1 : print SPL$: locate 20,3 :
        print " ERROR IN FILE NAME ... TRY AGAIN" : play "L3 G" :
    next MG
1200 RESUME 1210
1210 T = T + 1 : if T < > 6
    goto 290
1220 color 7,0 : play TONEZ$: locate 11,1 :
    print " Sorry... I Am Going to Sleep *** Good Night ****" :
    goto 1100
-----
Subroutine to Input User Defined Starting Date
1240 color 7,1 : locate 11,1 : print SPL$: locate 11,3 :
    INPUT "Enter The Start Day .... DD "; Q$:
    Q = len(Q$) :
    if Q = 2 goto 1260
    BEEP : goto 1240
    O1$ = left$(Q$, 1) : O2$ = right$(Q$, 1) :
    O1 = asc(O1$) : O2 = asc(O2$) :
    if O1 > = 48 and O1 < = 57 and O2 > = 48 and O2 < = 57
        goto 1270
    else goto 1250
    QQ = val(Q$) :
    if QQ > = 1 and QQ < = 31
        goto 1280
    else goto 1250

```

Page 8/20

DATA PROCESSING PROGRAM  
File: DTCLM.BAS/JOUDAH1988

```

1430 input #1, CHN$:
C = val(CHN$):
if P > 1 goto 1450
dim A$(C), V$(C), ABS(2,C), AA$(60,C)
for I = 1 to C
input #1, A$(I):
if A$(I) = "" goto 1460
DES = "": M = 0:
for W = 1 to 8:
MES = left$(A$(I), 1):
A$(I) = right$(A$(I), 8 - W):
if MES = "" and M = 0 goto 1490
DES = DES + MES:
M = I
next W:
ABS(P, I) = DES:
next I
1495 display labels & units on screen
print DDL$:
if P = 1
then print "Channel Number"; chr$(4); " "; HS; " ....."; DLS
else print HS; " ....."; DLS
for K = 1 to C:
if P < > 1 goto 1530
print using "#"; K; K; print chr$(4);:
print using "\ "; ABS(P, K);: print " ";:
goto 1540
print " ";: print using "\ "; ABS(P, K);
next K:
return

```

Subroutine for Channels Input, print Questions on Screen and  
Direct Program to Numbers Input Subroutine

```

1560 locate 21,35 : print "Wind Direction & Ref. "; gosub 1780
1570 locate 21,35 : print "Wind Speed (Puls) "; gosub 1780
1580 locate 21,35 : print "Wind Speed (Volt) "; gosub 1780
1590 locate 21,35 : print "Dry & Wet Bulb Temperature "; gosub 1780
1600 locate 21,35 : print "Diffuse SRH, CF = (10^3/5.32)"; gosub 1780
1610 locate 21,35 : print "Global SRH.1 CF = (10^3/5.62)"; gosub 1780
1620 locate 21,35 : print "Global SRH.2 CF = (00)"; gosub 1780
1630 locate 21,35 : print "Global SRH.3 CF = (000)"; gosub 1780
1640 locate 21,35 : print "Global SRV.1 CF = (10^3/4.46)"; gosub 1780
1650 locate 21,35 : print "Thermocouples in Cell #1 "; gosub 1780
1660 locate 21,35 : print "Thermocouples in Serv-R #1 "; gosub 1780
1670 locate 21,35 : print "Thermocouples in Cell #2 "; gosub 1780
1680 locate 21,35 : print "Thermocouples in Serv-R #2 "; gosub 1780
1690 locate 21,35 : print "Thermocouples in Cell #3 "; gosub 1780
1700 locate 21,35 : print "Thermocouples in Serv-R #3 "; gosub 1780
1710 locate 21,35 : print "Thermocouples in Cell #4 "; gosub 1780
1720 locate 21,35 : print "Thermocouples in Serv-R #4 "; gosub 1780
1730 locate 21,35 : print "Power meter in Cell #1 "; gosub 1780
1740 locate 21,35 : print "Power meter in Cell #2 "; gosub 1780
1750 locate 21,35 : print "Power meter in Cell #3 "; gosub 1780
1760 locate 21,35 : print "Power meter in Cell #4 "; gosub 1780
return

```

Page 7/20

DATA PROCESSING PROGRAM  
File: DTCLM.BAS/JOUDAH1988

```

1280 locate 12,1 : print SPL$: locate 12,3 :
INPUT "Enter The Start Month .. MM ", L$:
Q = len(L$):
if Q = 2 goto 1300
BEEP : goto 1280
Q1$ = left$(L$, 1): Q2$ = right$(L$, 1):
Q1 = asc(Q1$): Q2 = asc(Q2$):
if Q1 > = 48 and Q1 < = 57 and Q2 > = 48 and Q2 < = 57
goto 1310
else goto 1290
LL = val(L$):
if LL > = 1 and LL < = 12
goto 1320
else goto 1290
locate 13,1 : print SPL$ locate 13,3
INPUT "Enter The Start Hour .. HH ", P$:
Q = len(P$):
if Q = 2 goto 1340
BEEP : goto 1320
Q1$ = left$(P$, 1): Q2$ = right$(P$, 1):
Q1 = asc(Q1$): Q2 = asc(Q2$):
if Q1 > = 48 and Q1 < = 57 and Q2 > = 48 and Q2 < = 57
goto 1350
else goto 1330
PP = val(P$):
if PP > = 0 and PP < = 23
goto 1360
else goto 1330
if ((QQ = DD and LL = MM and PP > = HH)
OR (QQ > DD and LL > = MM)
OR (QQ < = DD and LL > MM)
goto 1380
else goto 1370
locate 11,1 : print SPL$: SPL$: SPL$:
for MG = 1 to 6:
locate 12,3 : print "ERROR IN INPUT DATE": play TONE1$:
next MG:
goto 1240
if (QQ = DE and LL = ME and PP < HE)
OR (QQ < > DE and LL < ME)
OR (QQ < DD and LL < = ME)
goto 1400
else goto 1390
locate 11,1 : print SPL$: SPL$: SPL$:
for MG = 1 to 6:
locate 12,3 :
print "ERROR: Input Date Past Finishing Date": play TONE1$:
next MG : goto 1240
DDL$ = Q$: MMS = L$: HHS = P$:
return
Subroutine to Input and Display Labels and Units from File
1420 input #1, NS:
if left$(NS, 5) < > H$ goto 1420

```

```

2070      return
21 Subroutines to Assign Results to Variables
2090      gosub 2640:
if TA = 0 then WDIR = -999 else WDIR = CINT(SWD/TA)
ZOO(ZO) = WDIR: WDIR1 = WDIR:
if WDIR1 < 0 then WDIR1 = 0
return
2110      gosub 2760:
if TA = 0 then WSP = -999 else WSP = CINT((WSP/TA) * 100) / 100
ZOO(ZO) = WSP: WSP1 = CINT(WSP * 10):
if WSP1 < 0 then WSP1 = 0
return
2130      gosub 2830:
if TA = 0 then WSPV = -999
else WSPV = CINT((WSPV/TA) * 100) / 100
ZOO(ZO) = WSPV:
return
2160      gosub 2900:
if TAA = 0 then RH = -999 else RH = INT(RH/TAA)
ZOO(ZO) = RH: RH1 = RH: ZO = ZO + 1:
if RH1 < 0 then RH1 = 0
2180      if TA = 0 then TT = -999 else TT = CINT((TT/TA) * 100) / 100
ZOO(ZO) = TT: TT1 = CINT(TT * 10):
if TT1 = -999 then TT1 = 0
return
2210      CFT = 10 ^ 3 / 5.32:
return
2220      gosub 3010
if TA = 0 then DIF = 999 else DIF = CINT(SOL/TA)
ZOO(ZO) = DIF: DIF1 = DIF:
if DIF1 < 0 then DIF1 = 0
return
2250      CFT = 10 ^ 3 / 5.62:
gosub 3010
2270      if TA = 0 then GSH = -999 else GSH = CINT(SOL/TA)
ZOO(ZO) = GSH: GSH1 = GSH:
if GSH1 < 0 then GSH1 = 0
return
2290      CFT = 1: gosub 3010
2300      if TA = 0 then GSH1 = -999 else GSH1 = CINT(SOL/TA)
ZOO(ZO) = GSH1:
return
2330      CFT = 1: gosub 3010
2340      if TA = 0 then GSH2 = -999 else GSH2 = CINT(SOL/TA)
ZOO(ZO) = GSH2:
return
2360      CFT = 10 ^ 3 / 4.46:
gosub 3010
2370      if TA = 0 then GSV = -999 else GSV = CINT(SOL/TA)
ZOO(ZO) = GSV:
return
2390      gosub 3090:
if TA = 0 then T1 = -999 else T1 = CINT((TEM/TA) * 100) / 100
ZOO(ZO) = T1:
return
2400

```

Numbers Input Subroutine, to Read and Save Numbers from keyboard

```

1770 ' draw attention for next line input
1780      S = S + 1:
      gosub 1940:
      if S then play TONE1$:
      return
1785 ' read numbers by INKEY input
1790      YY = UU: X1 = 0: locate V,YY: print "*"
1800      N$ = "":
for J = 1 to 2
      locate V,UU
      Z$ = inkey$:
      if len(Z$) = 0
      goto 1820
      else Z% = asc(Z$)
      if Z% < > 27 goto 1850
      Y = 1: goto 1930
      if Z% = 13 goto 1910
      if Z% = 32 and J > 1 goto 1920
      if Z% > 47 and Z% < 58 goto 1890
      UU = YY: goto 1800
      print Z$: N$ = N$ + Z$:
      UU = UU + 1:
next J:
goto 1920
1900      print chr$(7): goto 1790
1910      X = val(N$): X1 = 1: goto 1930
1920      X = val(N$)
return
1935 ' save input numbers in array Z(S,U)
1940      U = 0: UU = 7: Y = 0:
      locate 22,1: print SPL$
      U = U + 1: V = 22: UU = UU + 4:
      locate V + 1,UU: print " = " :
      gosub 1790:
      locate V + 1,YY: print " " :
      if Y = 1 goto 1940
      Z(S,U) = X:
      if X1 = 0 goto 1950
      if U = 1 and Z(S,1) = 0
      then Z(S,0) = 0
      else Z(S,0) = U
      return
Subroutine to Define TI (Logging Intervals) value
2000      for UU = 1 to 2
2010          input #1, N$:
      if len(N$) < > 17 goto 2010
      HES = left$(N$, 8): M$ = right$(HES, 2):
      U = val(M$)
2030      if U = 0 then U = 24
2040      HES = left$(N$, 11): M$ = right$(HES, 2):
      Y = val(M$)
      C1(UU) = U * 60 + Y:
      next UU
2060      TI = 60 / (C1(2) - C1(1))

```

DATA PROCESSING PROGRAM  
File: DTCLM.BAS/JOUDAH 1988

Page 11/20

```

2410 gosub 3090 :
2420 if TA = 0 then TS1 = -999 else TS1 = CINT((TEM / TA) * 100) / 100
2430 ZOO(ZO) = TS1 :
2440 return
2450 if TA = 0 then T2 = -999 else T2 = CINT((TEM / TA) * 100) / 100
2460 ZOO(ZO) = T2 :
2470 return
2480 if TA = 0 then TS2 = -999 else TS2 = CINT((TEM / TA) * 100) / 100
2490 ZOO(ZO) = TS2 :
2500 return
2510 if TA = 0 then T3 = -999 else T3 = CINT((TEM / TA) * 100) / 100
2520 ZOO(ZO) = T3 :
2530 return
2540 if TA = 0 then TS3 = -999 else TS3 = CINT((TEM / TA) * 100) / 100
2550 ZOO(ZO) = TS3 :
2560 return
2570 if TA = 0 then T4 = -999 else T4 = CINT((TEM / TA) * 100) / 100
2580 ZOO(ZO) = T4 :
2590 return
2600 if TA = 0 then TS4 = -999 else TS4 = CINT((TEM / TA) * 100) / 100
2610 ZOO(ZO) = TS4 :
2620 return
2630 if TA = 0 then TM1 = -999 else TM1 = CINT(TMM)
2640 ZOO(ZO) = TM1 :
2650 return
2660 if TA = 0 then TM2 = -999 else TM2 = CINT(TMM)
2670 ZOO(ZO) = TM2 :
2680 return
2690 if TA = 0 then TM3 = -999 else TM3 = CINT(TMM)
2700 ZOO(ZO) = TM3 :
2710 return
2720 if TA = 0 then TM4 = -999 else TM4 = CINT(TMM)
2730 ZOO(ZO) = TM4 :
2740 return

```

Algorithm to Calculate Wind Direction

```

2640 SWD = 0 : NWD = 0 : SDC = 0 : TA = 0 :
2650 for LL = 1 to TI :
2660 gosub 3250 :
2670 TA = TA + 1 : W = 0 : W = W + 1
2680 if CV$(1) = "" or CV$(1) = "" or sgn(val(CV$(1))) = -1
2690 OR CV$(2) = "" or CV$(2) = "" or sgn(val(CV$(2))) = -1
2700 then goto 2670
2710 CV(1) = val(CV$(1)) : CV(2) = val(CV$(2)) :
2720 goto 2680
2730 W = W - 1
2740 if W = 0
2750 then TA = TA - 1
2760 else goto 2690
2770 goto 2740

```

DATA PROCESSING PROGRAM  
File: DTCLM.BAS/JOUDAH 1988

Page 12/20

```

2690 if LL < > 1 goto 2710
2700 SWD = CV(1) * 358 / CV(2) : SDC = SWD : goto 2740
2710 NWD = CV(1) * 358 / CV(2)
2720 if (SDC - NWD) > 180 then NWD = NWD + 360 :
2730 if (SDC - NWD) < -180 then NWD = NWD - 360
2740 SWD = SWD + NWD : SDC = SWD / TA :
2750 if SDC > 360 then SWD = (SDC - 360) * TA :
2760 if SDC < 0 then SWD = (SDC + 360) * TA
2770 next LL :
2780 return

```

Algorithm to Calculate Wind Speed (Puls Counting)

```

2760 WSP = 0 : WS = 0 : TA = TI :
2770 for LL = 1 to TI :
2780 gosub 3250 :
2790 W = 0 : W = W + 1
2800 if CV$(1) = "" or CV$(1) = "" or sgn(val(CV$(1))) = -1
2810 goto 2790
2820 WS = val(CV$(1)) : WSP = WSP + WS :
2830 goto 2800
2840 W = W - 1
2850 if W = 0 then TA = TA - 1
2860 next LL :
2870 return

```

Algorithm to Calculate Wind Speed (Voltage Sensor)

```

2830 WSPV = 0 : WSV = 0 : TA = TI :
2840 for LL = 1 to TI :
2850 gosub 3250 :
2860 W = 0 : W = W + 1
2870 if CV$(1) = "" or CV$(1) = "" or sgn(val(CV$(1))) = -1
2880 goto 2860
2890 WSV = val(CV$(1)) : WSPV = WSPV + WSV :
2900 goto 2870
2910 W = W - 1
2920 if W = 0 then TA = TA - 1
2930 next LL :
2940 return

```

Algorithm to Calculate Outdoor Air Temperature, and Define DBT & WBT for Relative Humidity Algorithm

```

2900 RH = 0 : TT = 0 : TA = TI : TAA = TI :
2910 for LL = 1 to TI :
2920 gosub 3250 :
2930 FH = 0 : W(1) = 0 : W(2) = 0 :
2940 for X = 1 to 2 :
2950 W(X) = W(X) + 1
2960 if CV$(X) = "" or CV$(X) = "" or sgn(val(CV$(X))) = -1
2970 then goto 2930
2980 CV(X) = val(CV$(X)) + 273.16 : goto 2940
2990 W(X) = W(X) - 1
3000 next X :
3010 if W(1) < > 0 and W(2) < > 0
3020 then gosub 2970
3030 else TAA = TAA - 1

```

```

3180 if CV$(1) = "" or CV$(1) = "" goto 3210
3190 CV(1) = val(CV$(1))
    then TM = 1
    else TM = 0
3200 TMM = TMM + TM:
    goto 3220
3210 W = W - 1
3220 if W = 0 then TA = TA - 1
3230 next LL:
    return

Subroutine to Obtain Row values from Z(s,u) Array for use in Calculation Algorithms
3250 for U = 1 to Z(II,0)
3260 U1 = Z(II,U)
3270 CV$(U) = AA$(LL,U1)
3280 next U
3290 return

Subroutine to Display Results On Screen
3300 ' headings
3310 color 0,1: locate 2,1: print FR1$,FR1$,FR2$,FR3$:
    locate 12,1: print FR1$,FL1$,FL2$,FR2$:
    for I = 17 to 22:
        locate I,1: print FL$,FL1$:
    next I
    color 0,3: locate 3,9: print "DAY.",DDD:
    locate 3,9: print "HOUR.",B1:
    locate 5,9: print "METEOROLOGICAL DATA.."
    locate 7,9: print "Gh": locate 7,18: print "to":
    locate 7,27: print "Gulf": locate 7,36: print "WS":
    locate 7,45: print "WD": locate 7,54: print "RH":
    locate 7,63: print "Gv":
    locate 8,9: print "W/m",YPS,"": locate 8,18: print "YD$,°C":
    locate 8,27: print "W/m",YPS,"": locate 8,36: print "m/s":
    locate 8,45: print "deg": locate 8,54: print "%":
    locate 8,63: print "W/m",YPS,""
    locate 13,29: print "INDOOR DATA..": locate 15,41: print "CELL #1":
    locate 15,51: print "CELL #2": locate 15,61: print "CELL #3":
    locate 15,71: print "CELL #4"
    locate 17,2: print "Average Test Room Temp. (": YD$,°C)":
    locate 19,2: print "Average Service Room Temp. (": YD$,°C)":
    locate 21,2: print "Heating Period (min)"
3369 ' results
3370 color 0,7: locate 10,9: print GSH:
    locate 10,18: print TT: locate 10,27: print DIF:
    locate 10,36: print WSP: locate 10,45: print WDIR:
    locate 10,54: print RH: locate 10,63: print GSV
    locate 17,41: print T1: locate 17,51: print T2:
    locate 17,61: print T3: locate 17,71: print T4
    locate 19,41: print TS1: locate 19,51: print TS2:
    locate 19,61: print TS3: locate 19,71: print TS4
    locate 21,41: print TM1: locate 21,51: print TM2:
    locate 21,61: print TM3: locate 21,71: print TM4
3410 color 7,0:
    return
    
```

```

2950 if W(T) < > 0
    then TT = TT + (CV(1) - 273.16)
    else TA = TA - 1
    RH = RH + FH:
    next LL:
    return

Algorithm to Calculate Relative Humidity
2970 DB = CV(1): WB = CV(2):
    PD = 28.59051 - 8.2 * log(DB) / log(10) + 0.0024804 * DB - 3142.31/DB
    PW = 28.59051 - 8.2 * log(WB) / log(10) + 0.0024804 * WB - 3142.31/WB
    PD = 1000 * 10 ^ PD: PW = 1000 * 10 ^ PW:
    FH = (PW - 1013.25 * 0.000666 * (DB - WB)) * 100 / PD:
    return

Algorithm to Calculate Solar Radiation
3010 SOL = 0: GS = 0: TA = TI
    for LL = 1 to TI:
        gosub 3250:
        W = 0: W = W + 1
        if CV$(1) = "" or CV$(1) = "" goto 3050
        GS = val(CV$(1)) * CFT:
        if sign(GS) = -1 then GS = 0
        SOL = SOL + GS: goto 3060
        W = W - 1
        if W = 0 then TA = TA - 1
    next LL:
    return

Algorithm to Calculate Average Ambient Air Temperature
3090 TEM = 0: TA = TI:
    for LL = 1 to TI:
        gosub 3250:
        T = 0: W = 0:
        for X = 1 to U:
            W = W + 1
            if CV$(X) = "" or CV$(X) = "" goto 3120
            CV(X) = val(CV$(X)):
            T = T + CV(X): goto 3130
            W = W - 1
        next X:
        if W = 0
            goto 3140
        else goto 3150
        TA = TA - 1:
        goto 3160
        T = T / W: TEM = TEM + T
    next LL:
    return

Algorithm to Calculate Heating Load Periods in Test Cells
3170 TMM = 0: TM = 0: TA = TI:
    for LL = 1 to TI:
        gosub 3250:
        W = 0: W = W + 1
    
```

DATA PROCESSING PROGRAM  
File: DTCLM.BAS/JOUDAH1988

Page 15/20

```

Subroutine to write results on [*DAF] file
3430 open NF$ for append AS #2
3440 print #2, COT$, ; print #2, using "#", DDD; ;
print #2, ", "; print #2, using "#", MMM; ;
print #2, "@ "; print #2, using "#", B1; ;
print #2, " : 00 hour"; COT$, ;
for I = 1 to ZO
if ZOO(I) = INT(ZOO(I)) goto 3470
print #2, using "#", ZOO(I); ; print #2, ", "; ;
goto 3480
next I;
print #2;
if B1 = 23 then print #2, COT$, PDL$, COT$
close #2
return

```

```

Subroutine to write results on [*ESP] file
3530 open NF1$ for append AS #3
3540 if E <> T1 goto 3570
3550 if B1 = 0 goto 3580
3560 write #3, " ", DDD, MMM; ;
for I = 1 to B1; ;
write #3, 0, 0, 0, 0, 0; ;
next I;
if B1 <> 0 goto 3590
3570 write #3, " ", DDD, MMM
3580 write #3, DIF1, T1, GSHH, WSP1, WD1R1, RH1
3600 close #3
3610 return

```

```

Title Page
3630 FR1$ = string$(80, 178) : FR2$ = string$(70, 177) :
SP$ = string$(48, 32) : FR3$ = string$(60, 176)
3640 locate 2,1 :
for FR = 1 to 15 :
print FR1$ :
next FR
for FR = 4 to 14 :
locate FR,6 : print FR2$ :
next FR
for FR = 6 to 12 :
locate FR,11 : print FR3$ :
next FR
for FR = 8 to 10 :
locate FR,17 : print SP$ :
next FR
3680 play TONE$ : color 1,3 : locate 9,27 :
print "DATA ANALYSIS PROGRAM"
3690 color 0,3 : play TONES$ :
locate 18,1 : print "Version 1.10" : locate 18,65 : print date$
3700 locate 19,1 : print "By: N. JOUDAH" :
locate 21,27 : print "Press Any key to Continue .."
3710 locate 19,65 : print time$ : Z$ = inkey$ :
if len(Z$) = 0 goto 3710

```

DATA PROCESSING PROGRAM  
File: DTCLM.BAS/JOUDAH1988

Page 16/20

```

MENU FACILITIES
Initialise Local Constants
3730 FR1$ = string$(31, 177) : FR2$ = string$(52, 177) :
FR3$ = string$(35, 177) : FL$ = chr$(176) :
FL1$ = chr$(178) : AR$ = chr$(26) :
SPL$ = string$(80, 32) : DLS = string$(80, 45) :
DDL$ = string$(80, 61) : SP$ = string$(35, 32) :
COT$ = chr$(34) : PDL$ = string$(78, 45)

Main Menu
3740 color 4,3 : cls
3750 play TONE$ :
for FR = 4 to 16 :
locate FR,24 :
print FR1$ :
next FR
color 1,7 : locate 6,31 : print "0" :
locate 8,31 : print "1" : locate 10,31 : print "2" :
locate 12,31 : print "3" : locate 14,31 : print "4" :
locate 6,35 : print "HELP" :
locate 10,35 : print "SAVE" : locate 12,35 : print "SYSTEM I/O" :
locate 14,35 : print "CHECK / RUN"
color 7,1 :
for MG = 1 to 5 :
locate 20,1 : print SPL$ : locate 21,24 : print space$(56)
locate 20,1 : print " Choose Item By Number... Default System
[MS-DOS In Double Disk Drive PC]" : locate 21,24 :
print " ... DEFAULT SAVE [NON .. Screen Display Only ]" :
next MG
gosub 80 :
if Z% << > > 48 and Z% <> 49 and Z% <> 50
and Z% <> 51 and Z% <> 52
then goto 3810
if Z% = 48 then 3860
3820 if Z% = 49 then 4130
3830 if Z% = 50 then 4290
3840 if Z% = 51 then 4470
3850 if Z% = 52 then 4590

Information pages
3860 cls : play TONE1$
3870 PG = 0 : color 7,1 : cls : locate 2,30 :
print " DATA ANALYSIS PROGRAM" : print : print DLS :
locate 4,66 : print " Summary" : print
3880 print " * This version is designed to execute under GW-BASIC or BASICA in Double
Disk or Hard Disk PC. Instruction(s) shown frequently on screen are to help following
the program procedures." : print
3890 print " * The program analyses data that is read from a specified [ DATA] sequential disk
file. In particular, it compute defined values of Meteorological &/or Thermal condi-
tions related to raw values obtained from DT-Logger." : print
3910 print " * A User Specified analysis version, independent from the default format, may
be completed in Summer-90." : print
3920 print " * A list of the program plus detailed explanation of all sections is available (Ask
N.Joudah)." :
goto 4060

```

DATA PROCESSING PROGRAM  
File: DTCLM.BAS/JOUDAH 1988

```

4180 if Z% = 48 then NN$ = "B:"
4190 if Z% = 49 then NN$ = "C:"
4200 if Z% = 50 then NN$ = "C:"
4210 if Z% < > 50 goto 4280

System Input for Hard Disk PC
4220 color 0,1 : cls
4230 PRD = 1 : play TONE1$:
for FR = 7 to 13:
locate FR,22 : print FR$:
next FR
4240 color 1,7 : locate 9,25 : print "0" : locate 11,25 : print "1"
4250 locate 9,29 : print "Data Disk In Drive (A. )" :
locate 11,29 : print "Data File In Drive (C. )" :
gosub 80 :
if Z% < > 48 and Z% < > 49 goto 4260
if Z% = 48
then ND$ = "A."
else if Z% = 49
then ND$ = "C."
goto 3740

```

Save and Display Options

```

4280 color 0,3 : cls
4290 play TONE1$:
for FR = 6 to 14 :
locate FR,14 : print FR$:
next FR
4310 color 0,7 : locate 8,20 : print "0" :
locate 10,20 : print "1" : locate 12,20 : print "2"
4320 locate 8,24 : print "Display Results On Screen.... Only" :
locate 10,24 : print "Save Results On Disk File(s). Only" :
locate 12,24 : print "Save and Display ....." :
gosub 80 :
if Z% < > 48 and Z% < > 49 and Z% < > 50
goto 4330
4340 if Z% = 48 then SVE = 0
4350 if Z% = 49 then SVE = 1
4360 if Z% = 50 then SVE = 2
4370 if SVE = 0 goto 3740

```

Save Format Options

```

4380 color 0,1 : cls
4390 play TONE1$:
for FR = 6 to 14 :
locate FR,14 : print FR$:
next FR
4400 color 0,3 : locate 8,20 : print "0" :
locate 10,20 : print "1" : locate 12,20 : print "2"
4410 locate 8,24 : print "Save Results On [DAF] File. Only" :
locate 10,24 : print "Save Met. Data On [ESP] File Only" :
locate 12,24 : print "Save On Both File Formats...." :
gosub 80 :
if Z% < > 48 and Z% < > 49 and Z% < > 50 goto 4330
if Z% = 48 then KTB = 0

```

DATA PROCESSING PROGRAM  
File: DTCLM.BAS/JOUDAH 1988

```

3930 color 7,1 : cls : locate 2,30 :
print " DATA ANALYSIS PROGRAM " : print : print DL$:
locate 4,54 : print " System Input/Output " : print
print "** The program is set to operate in a Double Disk PC. If [System] Menu is executed
you optionally can alter the program system to operate in Hard Disk PC.
if the program is operating in drive [C:], you need to specify if the Data File (input
source for analysis) is stored in the same drive or on a floppy disk in drive [A:] : print
print "** In Double Disk PC, drive [A:] is used to execute the program and to read data
from [DATA] file disk. If results are to be saved (see next page for Save details) a
formatted disk is required to hold output files from drive [B:] : print
print "** In Hard Disk PC, drive [A:] or [C:] can be used to execute the program and/or
input data. Thus, output file(s) (if requested) are saved in Drive [C:] :
goto 4060
3990 color 7,1 : cls : locate 2,30 :
print " DATA ANALYSIS PROGRAM " : print : print DL$:
locate 4,61 : print " Save Options " : print
4000 print "** Program is set to display 19 values of Passys related results. If [Save] menu is
executed you optionally can alter the program to save results on special file format(s).
: print
4010 print "** [ESP] format is designed to hold (6) Meteorological Data, for later use with
Environmental System Performance program (ESP) : print
4020 print "** [*DAP] format is designed to hold all results (Hourly & Daily averaged) for
later use in Tabular or/and Graphical Output. : print
print "** See next page for Output details. :
goto 4060
4030 color 7,1 : cls : locate 2,30 :
print " DATA ANALYSIS PROGRAM " : print : print DL$:
locate 4,59 : print " Output Options " : print
for I = 1 to 4 :
print :
next I
4050 print "** This facility is not fully implemented. " : print :
goto 4060
4060 PG = PG + 1 : color 1,7 : locate 21,1 : print SPL$: locate 21,1 :
print " [RET] -- next Page ... [ESC] -- Exit to Main Menu ... " :
gosub 80 :
if Z% < > 13 and Z% < > 27 goto 4070
4080 if Z% = 13 and PG = 1 goto 3930
4090 if Z% = 13 and PG = 2 goto 3990
4100 if Z% = 13 and PG = 3 goto 4030
4110 if Z% = 13 and PG = 3 goto 3870
4120 if Z% = 27 goto 3740

```

System I/O Menu

```

4130 color 2,1 : cls
4140 PRD = 0 : play TONE1$:
for FR = 6 to 14 :
locate FR,14 : print FR$:
next FR
4150 color 1,7 : locate 8,17 : print "0" :
locate 10,17 : print "1" : locate 12,17 : print "2"
4160 locate 8,21 : print " DOUBLE DISK PC ... Program In Drive (A. ) " :
locate 10,21 : print " HARD DISK PC .... Program In Drive (A. ) " :
locate 12,21 : print " HARD DISK PC .... Program In Drive (C. ) " :
gosub 80 :
if Z% < > 48 and Z% < > 49 and Z% < > 50 goto 4170

```

DATA PROCESSING PROGRAM  
File: DTCLM.BAS/JOUDAH1988

```

else if KTB = 1
  then print "[.ESP] File."
if TG = 0 goto 4720
print: print " * OUTPUT Results to Line printer ... ";
if TG = 1
  then print "(TABLES)."
  else if TG = 2
    then print "(GRAPHS)."
color 0,7: locate 21,1: print SPL$:locate 21,1:
print "[RET] --> Confirmed ... [ESC] --> Exit to Alter ..."
gosub 80:
if Z% <> 13 and Z% <> 27 goto 4730
if Z% = 13 goto 100
goto 3740

```

File: DELPL.BAS/JOUDAH1988

120 \* .....

File: DELPL1.BAS/JOUDAH1988

130 \* .....

File: DELPL2.BAS/JOUDAH1988

140 \* .....

File: DELPL3.BAS/JOUDAH1988

640 \* .....

File: DELPL4.BAS/JOUDAH1988

660 \* .....

670 \* .....

DATA PROCESSING PROGRAM  
File: DTCLM.BAS/JOUDAH1988

```

4440 if Z% = 49 then KTB = 1
4450 if Z% = 50 then KTB = 2
4460 goto 3740

```

Output Options

```

4470 cls: play TONE1$:
4480 if SVE <> 0 goto 4520
4490 locate 10,4: print "No Output Performed Without SAVED Results";
locate 11,4: print "Define Save Option First ....."; color 1,7:
locate 21,1: print SPL$:
locate 21,1: print "[RET] -- Exit to Main Menu ..."
4500 gosub 80:
if Z% <> 13 goto 4500
4510 goto 3740
4520 color 0,1:
for FR = 9 to 17:
  locate FR,24: print FR1$:
next FR:
color 0,3: locate 11,29: print "0";
color 13,29: print "1"; locate 15,29: print "2"
4530 locate 11,33: print "No Output .....";
locate 13,33: print "Tabular Output ";
locate 15,33: print "Graphics Output "; color 7,1:
locate 7,29: print "Output to Line printer"
4540 gosub 80:
if (Z% <> 48 and Z% <> 49 and Z% <> 50) goto 4540
4550 if Z% = 48 then TG = 0
4560 if Z% = 49 then TG = 1
4570 if Z% = 50 then TG = 2
4580 goto 3740

```

Check List

```

4590 color 0,3: cls: play TONE1$:
4600 if SVE <> 0 goto 4620
4610 TG = 0: KTB = 0
4620 locate 2,34: print "CHECK LIST "; print:
print DL$: color 0,7: locate 4,60:
if NN$ = "" or NN$ = "B:"
  then print " Double Disk PC"
else print " Hard Disk PC"
4630 color 0,3: print: print " * Program is executed from drive ";
if PRD = 0
  then print "[A:]"
else print "[C:]"
4640 print: print " * Data Source File ([.DAT] file) on ";
if ND$ = "" or ND$ = "A:"
  then print "a FLOPPY DISK."
else print "HARD DISK."
4650 if SVE = 1 goto 4670
4660 print: print " * DISPLAY Results on Screen. ";
if SVE = 0 goto 4700
4670 print: print " * SAVE Results in ";
if KTB <> 2 goto 4690
4680 print "[.DAF] and [.ESP] files. "; goto 4700
4690 if KTB = 0
  then print "[.DAF] File."

```

## Appendix F



---

# Error Analysis and Instrumentation Data Sheets

---

Both the climatic data analysis and the practical part of this research required the knowledge of the accuracy and use of instruments for both indoor and field measurements. Chapter 6 of this thesis provided a review of various instruments. This appendix fulfills the following objectives:

- Outline the sources of error in experimentation and discuss the statistical method of error analysis used in this thesis.
- Provide a quick and specific reference to instruments used in the experimentation of this thesis. This is presented in data sheets which include: manufacturer or supplier address in the UK; description with illustrations; output type; range; accuracy; and performance evaluation of each instrument. The sensing mechanism of these instruments was discussed in the main text of chapter 6. Definitions and terminology associated with instruments, and statements of error and accuracy are included in the glossary section (Appendix H).

Errors can be systematic or random. Systematic errors arise from faults or changes in conditions which could be corrected or allowed for. Errors caused by chance are referred to as Random errors. Random errors are those that are left after the systematic ones have been accounted for. Accuracy in experimental work comes from eliminating sources of systematic errors. Table (E.1) provides a checklist example of different error categories. Measurement errors can be divided into such categories as; *equipment error*, *interference error* and *personal mistakes* (ASHRAE 1985).

### *Equipment Errors*

These can arise from a quality defect in the instrument or in its original design, or from improper selection, poor maintenance and adjustment, or inadequate calibration. Equipment errors include inaccuracies from calibration, linearity, hysteresis, zero drift and sensitivity changes.

### *Interference Errors*

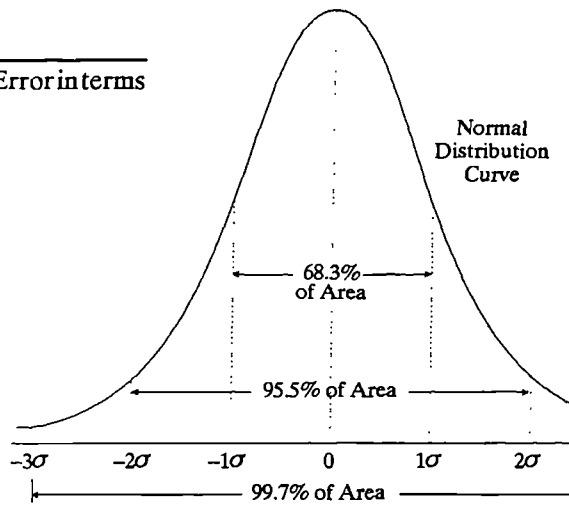
These are caused by unwanted disturbances usually superimposed on input or low level signals. Examples include noise, ripple, switching, transients and line transients.

**Table F.1** Errors in Measurements: Checklist. (after Tuve and Domholdt 1966)

Category of Error	Items to be Examined and Checked
Instrument selection.....	Range sensitivity and scale length, scale graduation, precision or accuracy (quality, resolution or least count, damping, response or time constant (record and full identification)
Instrument condition.....	Leveling, zero setting, friction, pen or pointer drag, hysteresis, wear and backlash, yielding of supports, capillarity.
Instrument calibration.....	Calibration before and after use, accuracy at calibration points, amplification and linearity, repeatability, zero drift, damping.
Environment.....	Temperature heat transfer and radiation, humidity, air motion, ambient or barometric pressure, vibration, local gravity, leakage, grounding or short-circuiting, "noise," accessibility and convenience of setup.
Observational.....	Parallax, accidental scale-reading errors, inaccurate estimates of average reading, poor timing or nonsimultaneous reading, inaccurate interpolation, inaccurate conversion of units, pure mistakes.
Test planning.....	Nonequilibrium conditions, inadequate control of variables, non-representative samples, poor scheduling, nontypical conditions.

**Figure F.1**

Probability Curve of Deviation of Error in terms of Standard Deviation  $\sigma$ .



Deviation from Mean $\epsilon/\sigma$	Probability of Occurrence within the deviation. %
0.00	0.00
0.50	38.29
1.00	68.26
1.50	86.64
2.00	95.45
2.50	98.76
3.00	99.73
3.50	99.95
4.00	99.99

**Table F.2** Probability of occurrence of errors or events according to the normal probability curve in Figure (F.1),  $\epsilon/\sigma$  = deviation of error  $\epsilon$  measured in terms of standard deviation  $\sigma$  (after ASHRAE chp.13 1985).

### *Personal Mistakes*

Inaccurate mental average of a non-steady indicator, defective or illegible recording of readings, inaccurate interpolations and incorrect conversion of units are personal mistakes.

The study of random error in experimentation requires an understanding of statistics and probability. There are several statistical methods for analysis of errors and inaccuracies covered in various literatures (e.g. see Ambrosius, et. al. 1966; Barford, 1967; and Schenck, 1968). The only one considered here is based on examination of deviation from the arithmetic average, using the normal probability curve (Figure F.1). This method is used in all error analysis of this thesis.

In order to judge the reliability of an experiment the measurements should be repeated, preferably many times. From (n) measurements of (x) the best estimate of the true value is the mean,  $\bar{x}$  :

$$\bar{x} = n^{-1} \sum_{i=1}^n x_i \quad \{\text{F.1}\}$$

The best estimate of the variance is the Root Mean Square (RMS) deviation,  $\sqrt{S_x^2}$ , thus

$$S_x^2 = \sum_{i=1}^n [(x_i - \bar{x})^2 / (n-1)] \quad \{\text{F.2}\}$$

and the standard deviation  $\sigma$  is

$$\sigma = \sqrt{(S_x^2)} \quad \{\text{F.3}\}$$

Figure (F.1) is a graphical statement of the deviation of all values from the mean. It is the normal error function (also called the normal frequency or Gaussian probability curve) on which three common measures of central tendency (the mean, the mode and the median) all coincide. The mean is the arithmetic average, the mode is the value that occurs most frequently, and the median is the middle value.

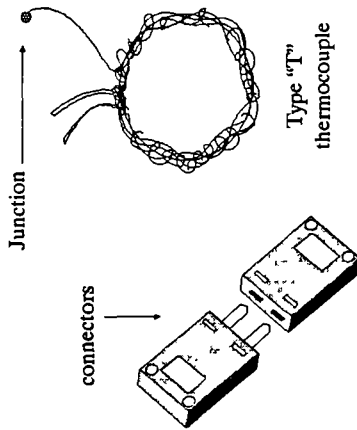
The usefulness of this distribution curve is apparent, because of certain conventional practices and available tables. For instance, 68.26% of all readings should lie within ( $\pm\sigma$ ) of the average, and 99.73% should lie within ( $\pm 3\sigma$ ), where  $\sigma$  is the standard deviation or RMS error. Other percentage selections can be made, and results obtained with the aid of Table (F.2).

The data sheets follow :

Thermocouple Type (T) and Connections

Manufacturer / Supplier

R.S. COMPONENTS Ltd.  
 P.O.Box 99, Corby, Northants,  
 NN17 9RS, United Kingdom  
 Tel: (0536) 201234  
 Fax: (0536) 201501



Description

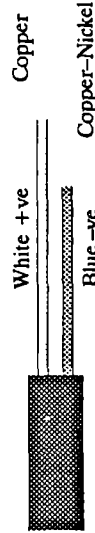
A welded junction copper/constantan type "T" thermocouple for the measurement of temperature in confined spaces. The twisted pair thermocouple wires are individually insulated with P.T.F.E. Plus type "T" flat pair extension cable and connectors (plug & socket) suitable for use with the thermocouple without inducing spurious EMF's.

Specifications

Range: Thermocouple = -50 to 200°C; Connectors = -40 to 220°C;  
 and Extension cable = -10 to 105°C.  
 Wire size: Thermocouple = 1/0.2mm diameter; Extension = 7/0.2mm diameter; Connectors are suitable for 0.5mm<sup>2</sup> max. wire size.  
 Insulation : Polytetrafluoroethylene (PTFE) for thermocouple wires;  
 P.V.C. for extension cable and the connectors body material is glass-filled polyester.

Comments

- The hot junction tip is welded in an argon atmosphere to eliminate any oxidising of the junction.
- Calibration is to the international reference standards under BS 4937 part 5 (1973), with accuracy of ±1°C.
- Type "T" thermocouple requires a reference junction compensation at 0°C. In most modern recording instruments this is fitted as standard, and EMF converted to °C temperature output.
- An external cold junction can be used with ordinary voltmeter. Table (F.3), after RS Data Handbook 1983 #4973, show the relationship between EMF (absolute mV) output and temperature °C. This relationship can be obtained mathematically as discussed in section 6.2.1 (see chapter 6 of this thesis).
- Ordinary copper wires should never be used for connection to measuring instruments, as the error will be equal to the difference in temperature between the connecting point of the thermocouple and the instrument (or external reference junction).
- It is important to maintain the same polarity when using connectors and extension cables with thermocouples. If the polarity is reversed, the error is equal to twice the temperature difference between the connecting point of the thermocouple and the recording instrument.
- Thermocouple and extension cable wire identification :



Data Sheet DSI continued

Table F.3 Type "T" thermocouple reference table (with reference junction at 0°C).

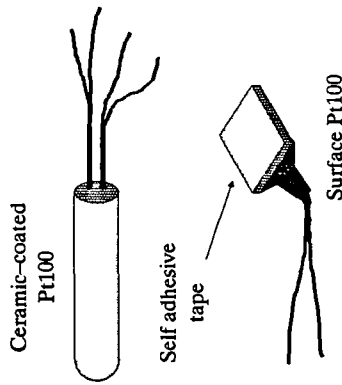
°C	Thermoelectric Voltage "EMF" (mV)										
	0	1	2	3	4	5	6	7	8	9	10
-60	-2.152	-2.185	-2.218	-2.250	-2.283	-2.315	-2.348	-2.380	-2.412	-2.444	-2.475
-50	-1.819	-1.853	-1.886	-1.920	-1.953	-1.987	-2.020	-2.053	-2.087	-2.120	-2.152
-40	-1.475	-1.510	-1.544	-1.579	-1.614	-1.648	-1.682	-1.717	-1.751	-1.785	-1.819
-30	-1.121	-1.157	-1.192	-1.228	-1.263	-1.299	-1.334	-1.370	-1.405	-1.440	-1.475
-20	-0.757	-0.794	-0.830	-0.867	-0.903	-0.940	-0.976	-1.013	-1.049	-1.085	-1.121
-10	-0.383	-0.421	-0.458	-0.496	-0.534	-0.571	-0.608	-0.646	-0.683	-0.720	-0.757
0	0.000	-0.039	-0.077	-0.116	-0.154	0.193	-0.231	0.269	-0.307	-0.345	-0.383
0	0.000	0.039	0.078	0.117	0.156	0.195	0.234	0.273	0.312	0.351	0.391
10	0.391	0.430	0.470	0.510	0.549	0.589	0.629	0.669	0.709	0.749	0.789
20	0.789	0.830	0.870	0.911	0.951	0.992	1.032	1.073	1.114	1.155	1.196
30	1.196	1.237	1.279	1.320	1.361	1.403	1.444	1.486	1.528	1.569	1.611
40	1.611	1.653	1.695	1.738	1.780	1.822	1.865	1.907	1.950	1.992	2.035
50	2.035	2.078	2.121	2.164	2.207	2.250	2.294	2.337	2.380	2.424	2.467
60	2.467	2.511	2.555	2.599	2.643	2.687	2.731	2.775	2.819	2.864	2.908
70	2.908	2.953	2.997	3.042	3.087	3.131	3.176	3.221	3.266	3.312	3.357
80	3.357	3.402	3.447	3.493	3.538	3.584	3.630	3.676	3.721	3.767	3.813
90	3.813	3.859	3.906	3.952	3.998	4.044	4.091	4.137	4.184	4.231	4.277
100	4.277	4.324	4.371	4.418	4.465	4.512	4.559	4.607	4.654	4.701	4.749

Data Sheet DS2

Platinum Resistance Temperature Sensors (Pt100)

**Manufacturer / Supplier**

LABFACILITY Ltd.  
 26 Tudor Road, Hampton,  
 Middx, TW12 2NQ. U.K.  
 Agents for Scotland  
 Industrial & Biological  
 Electronics, 12 Royal Terrace,  
 Glasgow, G3 7NY.



**Description**

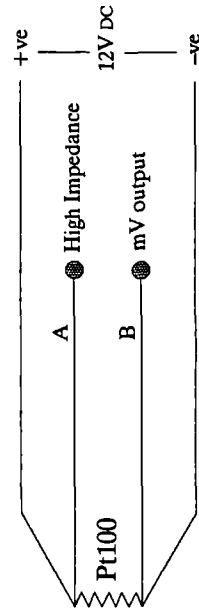
A 13mm platinum element (PT100) embodied in a 15mm long ceramic sonde with two leads and four PTFE insulated wire connection, for ambient air temperature measurements. Plus a 4mm<sup>2</sup> Pt100 film with ceramic coating and four PTFE insulated wires; designed for surface temperature measurements.

**Specifications**

Range : -50 to 50°C.  
 Platinum resistance : 100Ω at 0°C constant to within ±0.1%.  
 Accuracy : ±0.2°C.  
 Response time : between 0.6 to 0.03 sec.  
 Self heating : less than 0.015°C.  
 Stability : better than 0.05%.

**Comments**

- Resistance-Temperature characteristics (see Table F.4), and tolerance (see Figure 6.1 in chapter 6 of this thesis) are to international standards for class A, 100Ω element under BS 1904:1964 & DIN 43760.
- Unlike thermocouples, the platinum resistance thermometers do not require cold junction.
- For ambient air temperature and surface temperature measurements, the sensors must be shielded from radiation.
- Voltage supply is 12V DC with recommended maximum current of 3mA. Typical 4-wire bridge circuit is illustrated below.
- The 4-wire connection obtain maximum accuracy and compensate for any resistance introduced by connecting cables. (because the measuring parameter is potential difference across wires carrying extremely low current. The resistance of cables A B does not cause an error)



Data Sheet DS2 continued

**Table F.4** Resistance / Temperature Relationship.

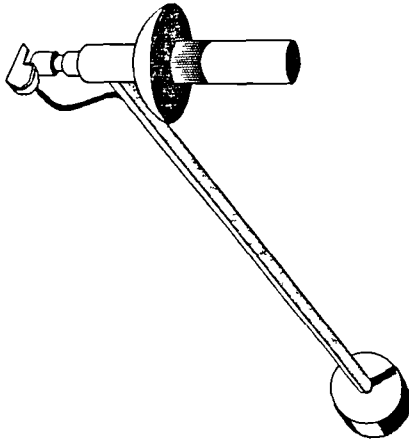
°C	Resistance / Temperature Relationship.		W/°C
	W DIN/43760	W BS/1904	
-100	60.25	60.28	0.405
-90	64.30	64.32	0.403
-80	68.33	68.34	0.400
-70	72.33	72.35	0.400
-60	76.33	76.34	0.398
-50	80.31	80.32	0.396
-40	84.27	84.29	0.395
-30	88.22	88.23	0.394
-20	92.16	92.16	0.393
-10	96.09	96.09	0.391
0	100.00	100.00	0.390
10	103.90	103.90	0.389
20	107.79	107.79	0.388
30	111.67	111.67	0.387
40	115.54	115.54	0.386
50	119.40	119.40	0.384
60	123.24	123.24	0.383
70	127.07	127.07	0.382
80	130.89	130.89	0.381
90	134.70	134.70	0.380
100	138.50	138.50	0.379

### Aspirated Thermometer (R.M. Young 43405)

#### Manufacturer / Supplier

R.M. YOUNG Co. 2801 Aero  
Park Drive, Traverse City, MI  
49684, U.S.A.

Sales & Maintenance  
Bureau Technique Wintgens  
S.A. Rue Neuve, 7-9 B-4700,  
Eupen, Belgium.



#### Description

A platinum resistance thermometer with aspirated temperature and radiation shield. A motor driven fan draws air at constant speed past the platinum sensor.

#### Specifications

Range : -20 to 65°C  
Sensor resistance : 100Ω at 0°C constant to within ±0.06%.  
Accuracy : ±0.1°C.  
Response time : less than 30 sec.  
Fan rating : 3m/s air velocity at the sensor;  
Power supply : 220V AC.

### Data Sheet DS3

#### Comments

- The instrument is quite expensive compared with ones made in the UK. (e.g about 3-4 times more expensive than Vector Instruments).
- It can detect automatically if there is an air flow through the system.
- The long distance between the fan and the sensor eliminates any influence of IR radiation from the fan body on temperature measurements.
- Recommended height for mounting the instrument is 2m above ground.

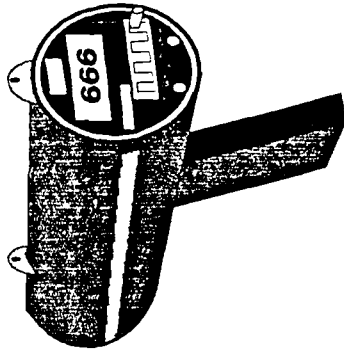
Infrared Digital Thermometer (Infratrace 801)

Data Sheet DS4

Manufacturer / Supplier

KANE-MAY Ltd.  
Burrowfield, Welwyn  
Garden City, Hertfordshire,  
United Kingdom

Tel: (0707) 331051



Description

Hand-held instrument providing non-contact measurement of either temperature or thermal radiation, with audio signal and visual display. Additional linear analogue output is also provided for use with remote recorders.

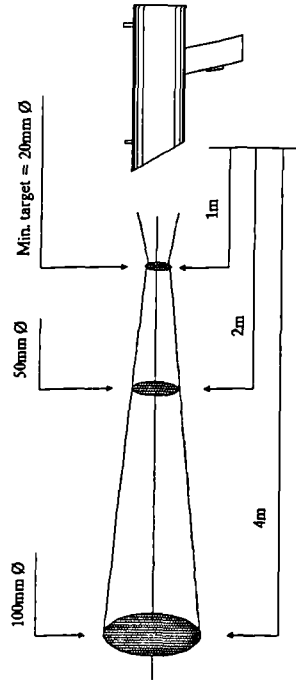
Specifications

Range : Temperature = 0–800°C, IR Radiation = 316–1999 W(m<sup>-2</sup>).  
Spectral range : 8–14 μm.  
Output (analogue) : 1 mV per W(m<sup>-2</sup>), 1 mV per °C.  
Field of view : 1.5°, 20mm target size at 1m minimum distance.  
Resolution : 1°C, 1W(m<sup>-2</sup>)  
Accuracy : ±0.7% of reading (18°–28°C), ±0.4% of full scale.  
Repeatability : better than ±3 °C

Comments

- The instrument measures the thermal radiation being emitted by a minimum target size of 20mm diameter at 1 meter distance, and a distance-target size ratio of 40:1 at greater distances as illustrated below.

Spot size depends on distance to target (1:40)

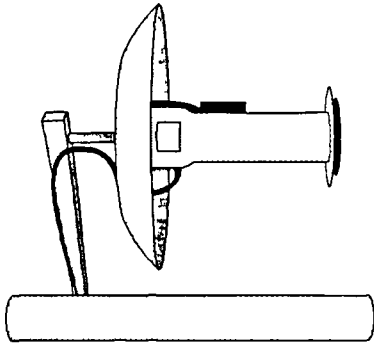


- On shiny surfaces like glass, polished metal, water, etc., the instrument should be held at a right angle to the surface because IR radiation can be reflected off the surface.
- Emissivity control switch is provided; it has no effect on IR radiation measurement, but it is used for correction purposes in temperature measurements.
- The user should know the emissivity ( $\epsilon$ ) of the target surface for accurate surface temperature readings.
- When measuring the surface temperature of an ordinary soda-lime glass, the Infratrace 801 may be used with  $\epsilon$  set to 0.95. Any heat source behind the glass plate will have minimal influence on the reading, hence glass absorbs radiation  $> 2.5\mu\text{m}$ .

Data Sheet DS5

Aspirated Psychrometer (H 301)

**Manufacturer / Supplier**



**VECTOR INSTRUMENTS.**  
 113 March Road, Rhyl, Clwyd.  
 LL182AB, United Kingdom  
 Tel: (0745) 50700  
 Fax: (0745) 344206

**Description**

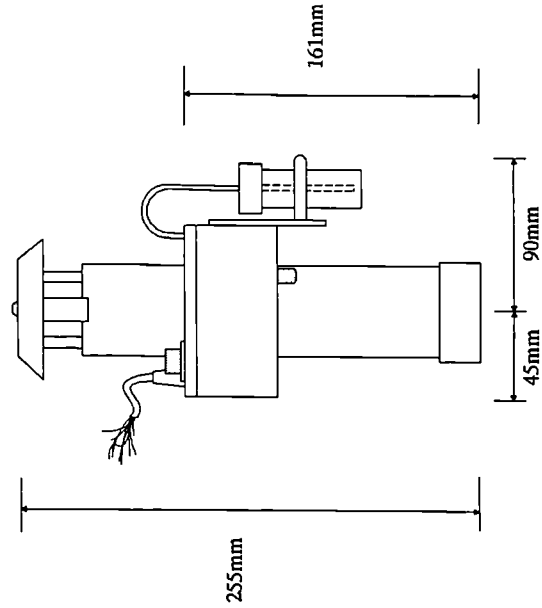
An aspirated sensor using wet and dry bulb method for the measurement of air temperature and relative humidity. It incorporates shielding against thermal radiation and supplied with a 50ml water reservoir. Sensing elements are made of platinum in stainless steel cylindrical sheathing (4-wire PT100).

**Specifications**

Range : -20°C to 65°C.  
 Accuracy : 0.2°C.  
 Response time : 50 seconds.  
 Sensor resistance : 100Ω at 0°C.  
 Loop resistance : 0.8Ω per 5m cable.  
 Fan rating : 40m<sup>3</sup>/hour (equivalent to 18 m/s air velocity);  
 Motor life : 12000 hours at 12V DC.

**Comments**

- Relative humidity is calculated from the dry and wet bulb temperature readings, (see section 6.3.2 in chapter 6 of this thesis).
- The fan motor has a separate cable to avoid interference on the low-level transducer signal.
- Recommended height for mounting the instrument is 1.5m above ground.
- Periodical checkup is needed to refill the reservoir (50ml capacity for 1day, or 500ml capacity for 7days), and to clean the wick and ensure its contact with the sensor. Failing to do so results in serious errors in the wet bulb temperature measurement.
- Installation and dimensions of the H301 psychrometer:

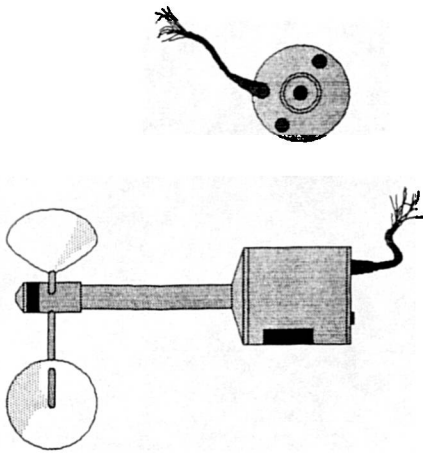


**Cup Anemometers (A100M & A100H)**

Data Sheet DS6

**Manufacturer / Supplier**

**VECTOR INSTRUMENTS,**  
 113 March Road, Rhyl, Clwyd.  
 LL182AB, United Kingdom  
 Tel: (0745) 50700  
 Fax: (0745) 344206



**Description**

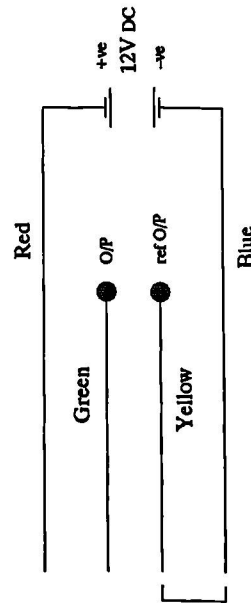
Two 3-cup anemometers for the instantaneous measurement of wind speed. The A100H anemometer is a photoelectric tachogenerator producing linear analogue output with wind speed. The A100M model is a modified version to make use of slotted opto-switch for pulse output. Both instruments share the same external mechanical parts and require 12V DC voltage supply.

**Specifications**

Range : 0.5 to 75 m/s.  
 Threshold = 0.15 m/s.  
 Accuracy : 2%, 0.1m/s.  
 Linearity : 2%.  
 Output : 0-11V with 30mV max. ripple for A100H model; and 0.1-12V square wave with 12V supply for A100M model.

**Comments**

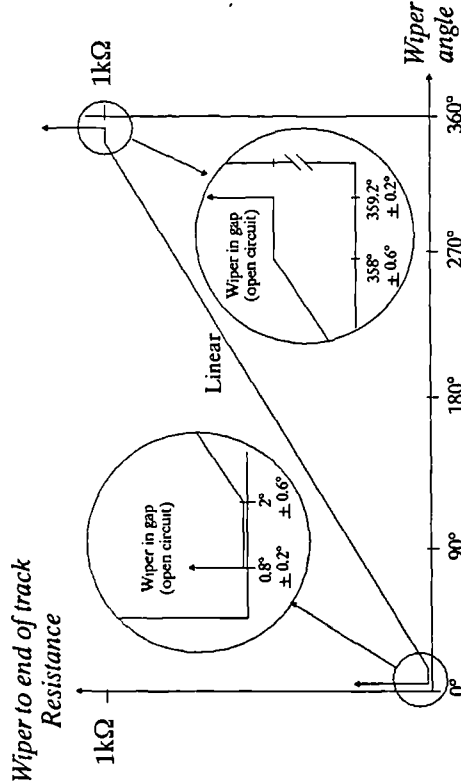
- The rotor in both instruments is attached by patented gravity sensitive fastener for rapid fitting and release (will not release unless the anemometer is inverted).
- Calibration is 104 mV per m/s for the A100H anemometer, and 10 pulses per m/s for the A100M anemometer. The instruments should be calibrated against a standard instrument annually.
- Instrument life is 10<sup>8</sup> revolutions, (equivalent to 10 years typical exposure).
- Meteorological standard height of the instrument is 10m above ground level.
- Connection circuit diagram of the instruments:



Data Sheet DS7

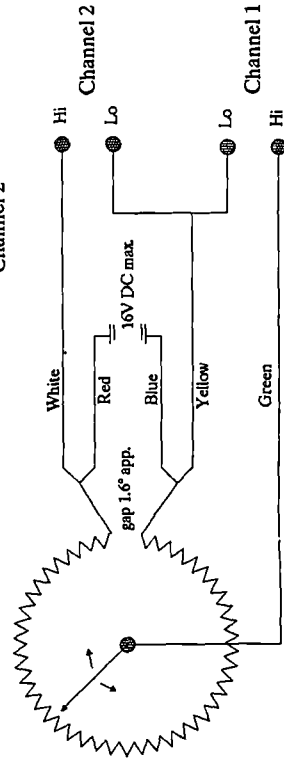
**Comments**

- Instrument life is equivalent to ten years typical exposure.
- For accurate results, the instrument should be aligned to north and mounted 10m above the ground.
- Wiper-resistance relationship :



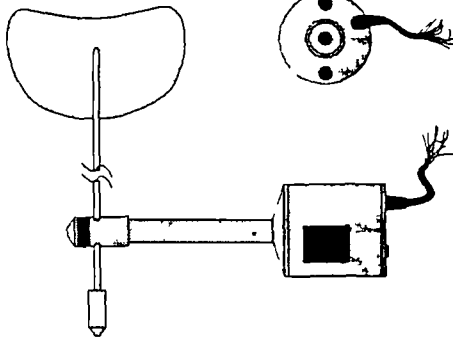
**Termination :**

$$\text{Angle} = \frac{\text{Channel 1}}{\text{Channel 2}} * 357.5$$



Potentiometer Windvane (W200P)

**Manufacturer / Supplier**



**VECTOR INSTRUMENTS.**  
 113 March Road, Rhyl, Clwyd.  
 LL18 2AB. United Kingdom

Tel: (0745) 50700  
 Fax: (0745) 344206

**Description**

The W200P wind vane incorporates a 357° micro-torque wire-wound potentiometer, with the gap at north filled with insulating material to insure smooth operation over the full 360° wind direction range. It requires voltage supply (16V max.) and comes with 5-wire 3m cable.

**Specifications**

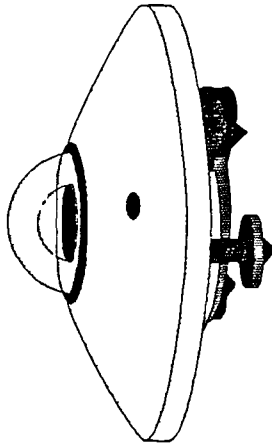
**Range :** 360° mechanical angle, 357.5° ± 0.9° electrical angle with a gap of 1.6° ± 0.4° at north (wiper open circuit).  
**Threshold :** 0.6 m/s.  
**Accuracy :** ± 2° in steady winds over 5m/s.  
**Resolution :** 0.3° continuous except at the north open circuit.  
**Linearity :** 0.5% of full output range.  
**Repeatability :** ± 0.5°.

Data Sheet DS8

Solarimeter (CM-11)

**Manufacturer / Supplier**

**KIPP & ZONEN.**  
 Mercuriusweg 1, P.O.Box 507,  
 Delft, Holland.  
  
**Sales & Maintenance :**  
**ENRAF-NONIUS Ltd.**  
 Highview house, 165/7 Station  
 Rd., Middx. HA8 7JU. U.K.  
 Tel: (081) 952 1643



**Description**

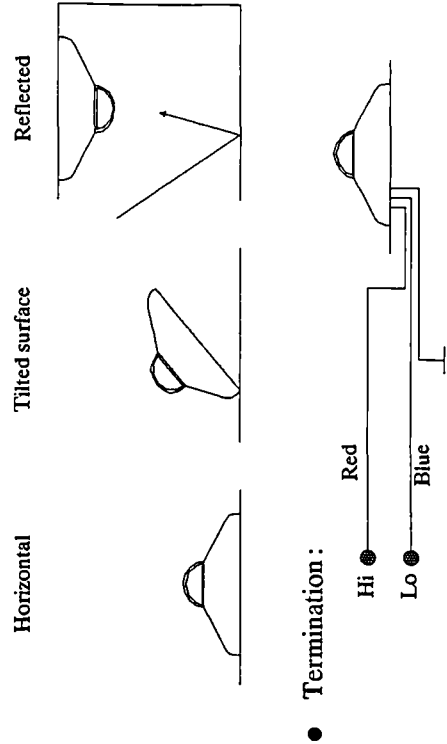
An instrument for measuring global insolation on a flat surface received from a whole hemisphere. It is supplied with leveling screws and a screen to shield the body of the instrument from radiation. The sensor is a 100 junction mol-thermopile imprinted on a ceramic substrate, and covered with inner and outer glass domes.

**Specifications**

Range : 0-2000 W(m<sup>-2</sup>).  
 Spectral range : 0.305-2.8 μm.  
 Sensitivity : 4.5-6 μV/W(m<sup>-2</sup>), constant to within ±1% over the temperature range of -10° to 40°C.  
 Nonlinearity : 0% for 0-500 W(m<sup>-2</sup>), 0.7% at 1000 W(m<sup>-2</sup>).  
 Time constant : 5 sec. (1/e, 63% response), 24 sec. (98% response).  
 Stability : ±0.5% sensitivity change per year.

**Comments**

- The CM-11 solarimeter is a first class pyranometer according to the WMO classification.
- Calibration is referred to the World Radiometry Reference (WRR). Each instrument is provided with a calibration factor of the type [X\*mV/W(m<sup>-2</sup>)].
- Additional heat flows in the sensor (not caused by radiation), are compensated for by a second substrate.
- Heat convection in the inner dome is negligible hence the temperature difference across the sensor does not exceed 3°C. Thus the sensitivity of the solarimeter does not decrease more than 0.5% when used in a tilted position.
- CM-11 solarimeter exhibits very low angle dependence (cosine and azimuth response 3%), so it can measure solar radiation on inclined surfaces. (see the installation possibilities illustrated below).



**Albedometer (DRA/2)**

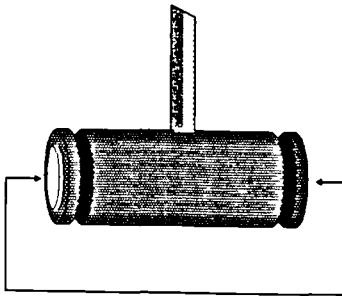
**Data Sheet DS9**

**Manufacturer / Supplier**

DIDCOT Instrument Co. Ltd.  
 Station Road, Abingdon,  
 Oxon, OX14 3LD.  
 United Kingdom

Tel: (0235) 22345  
 Fax: (0235) 553471

Two silicon based solarimeters



**Description**

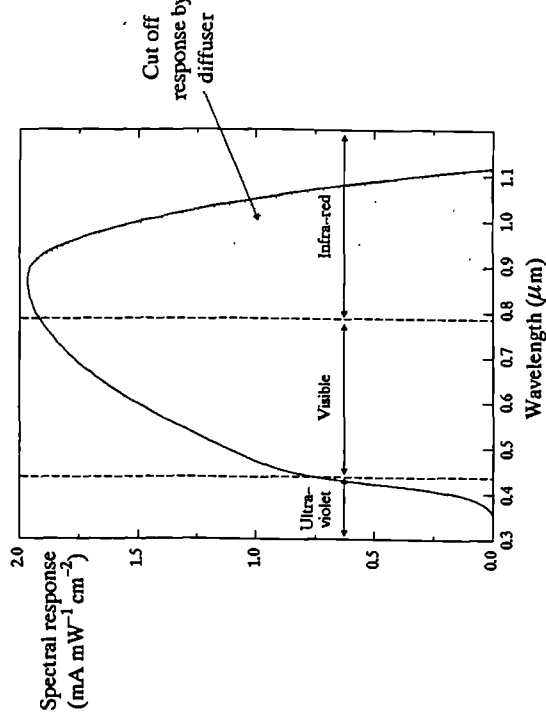
The DRA/2 albedometer is based on two identical silicon photocell solarimeters. It may be used to measure total incident solar radiation and short wave radiation balance, as a difference between the two opposite directions.

**Specifications**

Spectral range : 0.4-0.9  $\mu\text{m}$ .  
 Sensitivity : upper sensor  $15.8 \mu\text{V/W}(\text{m}^{-2})$ , and  $14.85 \mu\text{V/W}(\text{m}^{-2})$  for the lower sensor.  
 Accuracy :  $\pm 5\%$ .  
 Linearity :  $\pm 5\%$ .  
 Response time : less than 1s (90% response).  
 Internal resistance : approx.  $18\Omega$  at  $20^\circ\text{C}$  for both sensors.

**Comments**

- Each sensor is covered with a white plastic diffuser to enhance its cosine response. (see section 6.5.2 in chapter 6 of this thesis)
- The plastic diffuser reduces the spectral response of silicon cells from  $0.4-1.1\mu\text{m}$  to  $0.4-0.9\mu\text{m}$  as illustrated in the graph below.
- Despite the lower accuracy and spectral response, this albedometer has a faster response time than a thermopile based albedometer, and cost about 1/5th the price of thermopile based one.



• **Output Polarity**

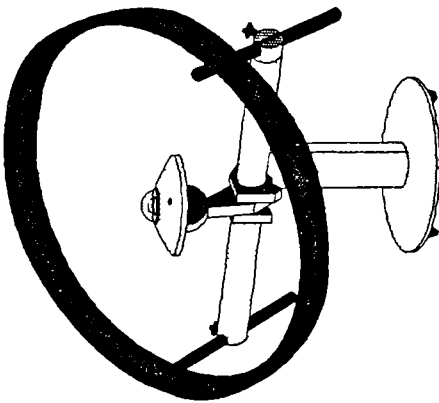
- Red ● +ve
  - Black ● -ve
  - Yellow ● +ve
  - Blue ● -ve
- Upper sensor
- Lower sensor

Data Sheet DS10

Solarimeter with Shadow Ring (CM 11/121)

**Manufacturer / Supplier**

**KIPP & ZONEN.**  
 Mercuriusweg 1, P.O.Box 507,  
 Delft, Holland.  
 Sales & Maintenance  
 ENRAF-NONIUS Ltd.  
 Highview house, 165/7 Station  
 Rd., Middx. HA8 7JU. U.K.  
 Tel: (081) 952 1643



**Description**

The instrument is a CM 11 solarimeter mounted in an adjustable shadow ring attachment (CM 121). It is suited for the measurement of diffuse insolation on a flat surface. It comes with sights for north-south alignment of the shadowring.

**Specifications**

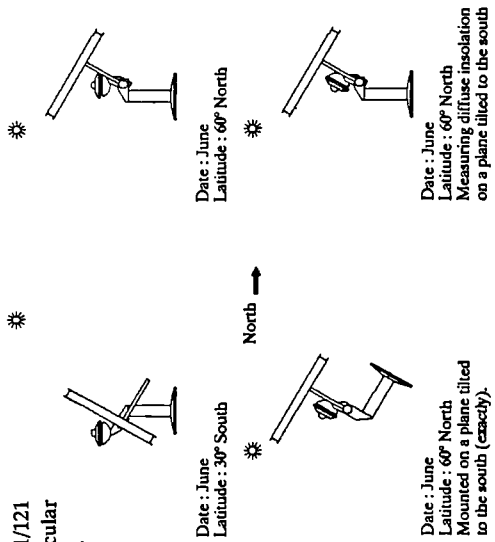
**Material :** Anodized Aluminium.  
**Ring width :** 55mm.  
**Ring outer diameter :** 620mm.  
**Ring width/radius Ratio :** 0.185  
**View angle (apparent width of the ring as seen from the solarimeter) :** 10.6° constant to within ±2%.  
**Solarimeter :** see data sheet DS8.

**Comments**

- The measured data should be corrected by a correction factor which varies between 1.00 and 1.15 depending on date and latitude.
- A list of correction factors for all latitudes (only valid for a solarimeter in a horizontal position), is provided in the Table (F.5). Theoretical derivation of these factors is discussed in section 6.5.2 (see chapter 6 of this thesis).
- The last row in Table F.5 represents the sliding bar setting in (mm), to adjust the shadowring position at the shown date intervals. The formula used for the figures in this row is:  

$$L = R \tan(\delta)$$
 where  $\delta$  is the declination of the sun, R is the ring radius (297mm). (see the illustrations below).
- The CM-11/121 can be mounted on any surface within ±1° horizontal. It can be mounted on a tilted plane also, if the plane faces south or north within ±0.25°.

Setup of CM11/121 for some particular situations.



Data Sheet DS10 continued

**Table F.5** Kipp & Zonen CM12 shadowing correction factors for uniform sky conditions (view angle = 10.6°)

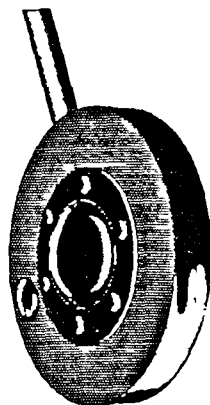
Date Interval	January			February			March			April			May			June											
	1	17	26	2	8	15	21	26	3	9	14	19	3	8	14	19	25	2	9	16	26	2	9	16	26	11	
90	1	1	1	1	1	1	1	1	1	1	1	1	1	1	1	1	1	1	1	1	1	1	1	1	1	1	
85	1	1	1	1	1	1	1	1	1	1	1	1	1	1	1	1	1	1	1	1	1	1	1	1	1	1	1
80	1	1	1	1	1	1	1	1	1	1	1	1	1	1	1	1	1	1	1	1	1	1	1	1	1	1	1
75	1	1	1	1	1	1	1	1	1	1	1	1	1	1	1	1	1	1	1	1	1	1	1	1	1	1	1
70	1	1	1	1	1	1	1	1	1	1	1	1	1	1	1	1	1	1	1	1	1	1	1	1	1	1	1
65	1	1	1	1	1	1	1	1	1	1	1	1	1	1	1	1	1	1	1	1	1	1	1	1	1	1	1
60	1.01	1.01	1.01	1.01	1.01	1.01	1.01	1.01	1.01	1.01	1.01	1.01	1.01	1.01	1.01	1.01	1.01	1.01	1.01	1.01	1.01	1.01	1.01	1.01	1.01	1.01	1.01
55	1.01	1.02	1.02	1.02	1.03	1.03	1.03	1.04	1.04	1.05	1.05	1.06	1.06	1.07	1.07	1.08	1.08	1.09	1.10	1.11	1.11	1.12	1.12	1.13	1.13	1.14	1.14
50	1.02	1.02	1.03	1.03	1.04	1.04	1.04	1.05	1.05	1.06	1.06	1.07	1.07	1.08	1.08	1.09	1.10	1.11	1.11	1.12	1.12	1.13	1.13	1.14	1.14	1.14	1.14
45	1.03	1.03	1.04	1.04	1.05	1.05	1.06	1.06	1.07	1.07	1.08	1.08	1.09	1.09	1.10	1.11	1.11	1.12	1.12	1.13	1.13	1.14	1.14	1.14	1.14	1.14	1.14
40	1.04	1.04	1.05	1.05	1.06	1.06	1.07	1.07	1.08	1.08	1.09	1.09	1.10	1.11	1.11	1.12	1.12	1.13	1.13	1.14	1.14	1.14	1.14	1.14	1.14	1.14	1.14
35	1.05	1.05	1.06	1.06	1.07	1.07	1.08	1.08	1.09	1.09	1.10	1.11	1.11	1.12	1.12	1.13	1.13	1.14	1.14	1.14	1.14	1.14	1.14	1.14	1.14	1.14	1.14
30	1.06	1.06	1.07	1.07	1.08	1.08	1.09	1.09	1.10	1.11	1.11	1.12	1.12	1.13	1.13	1.14	1.14	1.14	1.14	1.14	1.14	1.14	1.14	1.14	1.14	1.14	1.14
25	1.07	1.07	1.08	1.08	1.09	1.09	1.10	1.11	1.11	1.12	1.12	1.13	1.13	1.14	1.14	1.14	1.14	1.14	1.14	1.14	1.14	1.14	1.14	1.14	1.14	1.14	1.14
20	1.08	1.08	1.08	1.09	1.09	1.10	1.11	1.11	1.12	1.12	1.13	1.13	1.14	1.14	1.14	1.14	1.14	1.14	1.14	1.14	1.14	1.14	1.14	1.14	1.14	1.14	1.14
15	1.08	1.09	1.09	1.10	1.11	1.11	1.12	1.12	1.13	1.13	1.14	1.14	1.14	1.14	1.14	1.14	1.14	1.14	1.14	1.14	1.14	1.14	1.14	1.14	1.14	1.14	1.14
10	1.09	1.10	1.11	1.11	1.12	1.12	1.13	1.13	1.14	1.14	1.14	1.14	1.14	1.14	1.14	1.14	1.14	1.14	1.14	1.14	1.14	1.14	1.14	1.14	1.14	1.14	1.14
5	1.10	1.11	1.11	1.12	1.12	1.13	1.13	1.14	1.14	1.14	1.14	1.14	1.14	1.14	1.14	1.14	1.14	1.14	1.14	1.14	1.14	1.14	1.14	1.14	1.14	1.14	1.14
0	1.11	1.12	1.12	1.13	1.13	1.14	1.14	1.14	1.14	1.14	1.14	1.14	1.14	1.14	1.14	1.14	1.14	1.14	1.14	1.14	1.14	1.14	1.14	1.14	1.14	1.14	1.14
5	1.12	1.12	1.13	1.13	1.13	1.13	1.13	1.13	1.13	1.13	1.13	1.13	1.13	1.13	1.13	1.13	1.13	1.13	1.13	1.13	1.13	1.13	1.13	1.13	1.13	1.13	1.13
10	1.12	1.13	1.13	1.13	1.13	1.13	1.13	1.13	1.13	1.13	1.13	1.13	1.13	1.13	1.13	1.13	1.13	1.13	1.13	1.13	1.13	1.13	1.13	1.13	1.13	1.13	1.13
15	1.13	1.13	1.13	1.13	1.13	1.13	1.13	1.13	1.13	1.13	1.13	1.13	1.13	1.13	1.13	1.13	1.13	1.13	1.13	1.13	1.13	1.13	1.13	1.13	1.13	1.13	1.13
20	1.13	1.13	1.14	1.14	1.14	1.14	1.14	1.14	1.14	1.14	1.14	1.14	1.14	1.14	1.14	1.14	1.14	1.14	1.14	1.14	1.14	1.14	1.14	1.14	1.14	1.14	1.14
25	1.14	1.14	1.14	1.14	1.14	1.14	1.14	1.14	1.14	1.14	1.14	1.14	1.14	1.14	1.14	1.14	1.14	1.14	1.14	1.14	1.14	1.14	1.14	1.14	1.14	1.14	1.14
30	1.14	1.14	1.14	1.14	1.14	1.14	1.14	1.14	1.14	1.14	1.14	1.14	1.14	1.14	1.14	1.14	1.14	1.14	1.14	1.14	1.14	1.14	1.14	1.14	1.14	1.14	1.14
35	1.14	1.14	1.14	1.14	1.14	1.14	1.14	1.14	1.14	1.14	1.14	1.14	1.14	1.14	1.14	1.14	1.14	1.14	1.14	1.14	1.14	1.14	1.14	1.14	1.14	1.14	1.14
40	1.14	1.14	1.14	1.14	1.14	1.14	1.14	1.14	1.14	1.14	1.14	1.14	1.14	1.14	1.14	1.14	1.14	1.14	1.14	1.14	1.14	1.14	1.14	1.14	1.14	1.14	1.14
45	1.14	1.14	1.14	1.14	1.14	1.14	1.14	1.14	1.14	1.14	1.14	1.14	1.14	1.14	1.14	1.14	1.14	1.14	1.14	1.14	1.14	1.14	1.14	1.14	1.14	1.14	1.14
50	1.14	1.14	1.14	1.14	1.14	1.14	1.14	1.14	1.14	1.14	1.14	1.14	1.14	1.14	1.14	1.14	1.14	1.14	1.14	1.14	1.14	1.14	1.14	1.14	1.14	1.14	1.14
55	1.14	1.14	1.14	1.14	1.14	1.14	1.14	1.14	1.14	1.14	1.14	1.14	1.14	1.14	1.14	1.14	1.14	1.14	1.14	1.14	1.14	1.14	1.14	1.14	1.14	1.14	1.14
60	1.14	1.14	1.14	1.14	1.14	1.14	1.14	1.14	1.14	1.14	1.14	1.14	1.14	1.14	1.14	1.14	1.14	1.14	1.14	1.14	1.14	1.14	1.14	1.14	1.14	1.14	1.14
65	1.14	1.13	1.13	1.13	1.12	1.11	1.10	1.10	1.09	1.08	1.08	1.07	1.06	1.05	1.04	1.04	1.03	1.03	1.03	1.03	1.03	1.03	1.03	1.03	1.03	1.03	1.03
70	1.15	1.14	1.13	1.12	1.11	1.10	1.09	1.08	1.07	1.06	1.05	1.04	1.03	1.03	1.02	1.01	1.01	1.01	1.01	1.01	1.01	1.01	1.01	1.01	1.01	1.01	1.01
75	1.15	1.14	1.13	1.12	1.11	1.10	1.09	1.08	1.07	1.06	1.05	1.04	1.03	1.03	1.02	1.01	1.01	1.01	1.01	1.01	1.01	1.01	1.01	1.01	1.01	1.01	1.01
80	1.16	1.14	1.13	1.12	1.11	1.09	1.08	1.07	1.05	1.04	1.03	1.02	1.01	1.01	1.01	1.01	1.01	1.01	1.01	1.01	1.01	1.01	1.01	1.01	1.01	1.01	1.01
85	1.16	1.15	1.13	1.12	1.11	1.09	1.08	1.07	1.05	1.04	1.03	1.02	1.01	1.01	1.01	1.01	1.01	1.01	1.01	1.01	1.01	1.01	1.01	1.01	1.01	1.01	1.01
90	1.16	1.15	1.13	1.12	1.11	1.10	1.08	1.07	1.05	1.04	1.03	1.02	1.01	1.01	1.01	1.01	1.01	1.01	1.01	1.01	1.01	1.01	1.01	1.01	1.01	1.01	1.01
Date Interval	12	27	18	10	4	29	23	17	12	7	1	26	21	16	11	5	31	25	19	13	6	29	19	3	19	3	
	December	December	November	November	October	September	September	September	September	September	August	August	August	August	August	July	July	July	July	July							
	-24	-22	-20	-18	-16	-14	-12	-10	-8	-6	-4	0	0	2	4	6	8	10	12	14	16	18	20	22	24	24	
	132	120	108	97	85	74	63	53	42	31	21	10	0	10	21	31	42	53	63	74	85	97	108	120	132		

## Data Sheet DS11

## Data Sheet DS11

### Manufacturer / Supplier

DIDCOT Instrument Co. Ltd.  
Station Road, Abingdon,  
Oxon, OX14 3LD,  
United Kingdom  
Tel: (0235) 22345  
Fax: (0235) 553471



### Description

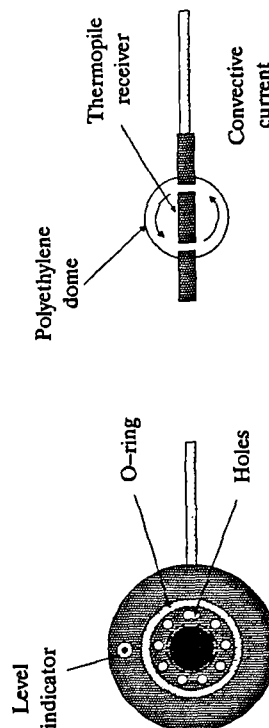
The DRN/301 net radiometer measures the earth/sky total radiation balance (shortwave and longwave). It is based on multi-element thermopile. The junctions are arranged with upper and lower radiation receivers (blackened copper disks), and covered with polyethylene domes. A large silica gel drier tube is attached to the sensor steam. A colour-change indicator shows the level of humidity present in the instrument enclosure.

### Specifications

Spectral range : 0.3–80  $\mu\text{m}$ . (i.e. short and long wave)  
Sensitivity : 9.71  $\mu\text{V/W}(\text{m}^{-2})$ .  
Accuracy :  $\pm 5\%$ .  
Response time : 15 sec. (90% response).  
Internal resistance : approx. 9.5  $\Omega$  at 20°C.

### Comments

- The output level and polarity of the instrument indicates radiation level differential and direction.
- Although the response time of the instrument is 15 seconds for 90% change, a 1 to 1.5 minutes allowance is required for steady state reading.
- An adapter can be fitted to one side of the DRN/301 for use as a single sensor instrument "pyr radiometer". (see section 6.5.4 of this thesis).
- The holes in the sensor head (see the diagrams below) serve two purposes; first to ensure free movement of air as the silica gel dries out all moisture from the sensor head; secondly to ensure equilibrium of the air temperature under both domes, as difference in temperature would affect the sensor reading.
- The instrument is restricted for use in a horizontal position due to the presence of these holes, as for example in a vertical position, the convection currents would extremely upset the sensor reading. (see section 5.4 in chapter 5 of this thesis for more details).



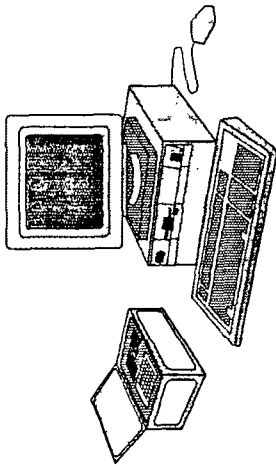
Data Sheet DS12

Delta-T Logger (DL2)

Manufacturer / Supplier

DELTA-T DEVICES Ltd.  
128 Low Road, Burwell,  
Cambridge, CB5 0EJ.  
United Kingdom

Tel: (0638) 742922  
Fax: (0638) 743155



Description

The Delta Logger ( $\Delta T$ ) is a device for receiving and storing readings from sensors. Up to 64 input channels are available for input. The logger can accept input in the form of voltage, resistance, counts, frequencies or digital levels. It can be configured manually or via a personal computer. Recorded data are stored in the logger's memory (128KByte RAM) and can be output to the logger's display (LCD), a printer or a computer for storage on disks.

Specifications

Power supply : switchable 7-15V DC external supply or 6 internal AA size batteries. Plus internal 3V Lithium cell backup.  
Input channels : 60 differential or single-ended analogue channels, 2 counters, and two output relays.  
Recording frequency : 1sec. to 24 hours programmable.  
Analogue range : 1 $\mu$ V to 2V, with auto-ranging option.

Comments

- The  $\Delta T$ -Logger has an on-board cold-junction thermistor for use with thermocouples. Linearisation tables resident in the logger's PROM enables conversion to engineering units.
- The logger has an RS232 interface for computer or printer connection, and plug-in connectors with screw terminals for sensors.
- All channels can be independently programmed for sensor type, sampling intervals, valid reading range, engineering units, and data compression.
- An IBM PC or PC-compatible with a serial interface and MS-DOS version 2 or above plus a GW-BASIC compiler are required to run the logger.
- The menu-driven LCS software (supplied with the instrument) can be used to define and download the logging configuration to the logger, as well as retrieving stored data from the logger to the computer.
- If no computer is available the logger can be instructed manually (pressing keys on the logger's top panel), and will operate with a limited default configuration resident in the logger's PROM.
- The effect of manual or computer (user-configured) instructions on the status of the Logger are summarised in the following diagram (see Figure F.2).

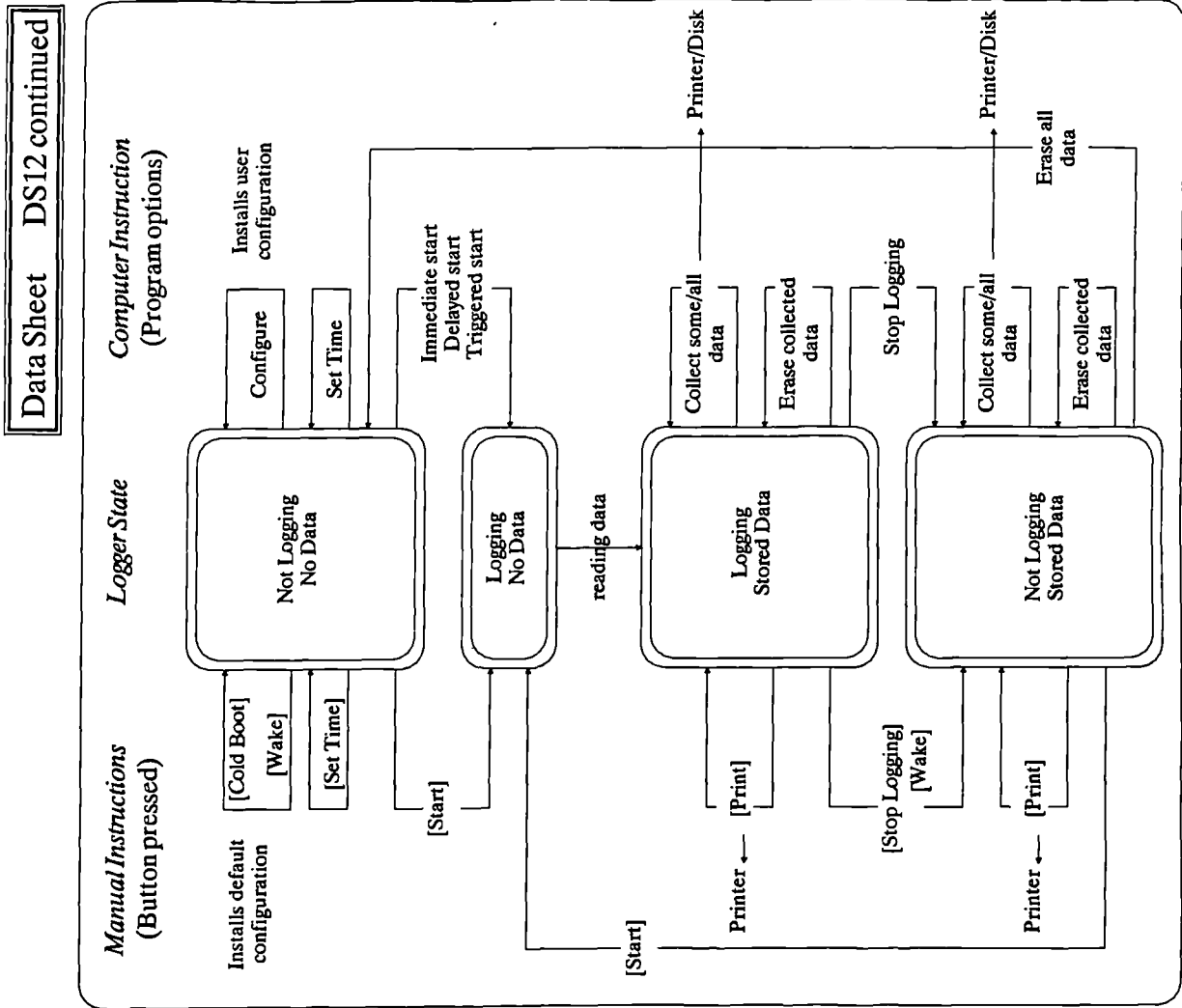


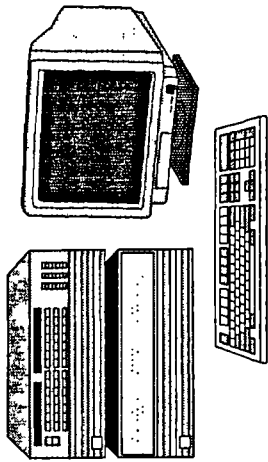
Figure F.2 Diagram of the states of the logger with manual and computer instructions.

## HP Data Acquisition System

### Manufacturer / Supplier

HEWLETT PACKARD Ltd.  
Nine Mile Ride, Eastham-  
stead, Wokingham, Berkshire  
RG11 3LL, England, U.K.

Sales & Maintenance  
South Queensferry, West  
Lothian EH30 9TG, Scotland.  
Tel: (0734) 696622  
Fax: (0734) 699609



### Description

A system for on-line logging and analysis of the Passys project experimentation variables. It comprises three main components; (1) data acquisition system type HP-3852A, (2) micro "16" set type HP-2456A, and (3) terminal microcomputer type HP-45851AU. The system operated with a software provided by the French group of Passys project. In the second phase of Passys an Italian software was used.

### Specifications

Input channels : 7x20 channels relay multiplexers  
Data input : Integrating Voltmeter for measuring DC or AC voltage, and 2-or-4 wire  $\Omega$  resistance.  
Data output : 40MB hard disk; 710KB floppy disk; 1/4" cartridge tape backup; screen; and printer.  
Recording frequency : programmable.

## Data Sheet DS13

### Comments

A brief description of the system components follows.

- HP2456A : Micro "16" set comprising a 2426E processor, 8 channel multiplexer 12040C, and 12009A interface.
- HP9134L : 40MB Winchester hard disk drive.
- HP9144A : 1/4" cartridge tape drive for data backup. It uses 16 or 67MB preformatted cartridges.
- HP45851AU : Personal computer model HP150-II, includes 12" green CRT, 256KB RAM, Interfaces RS232, Keyboard.
- HP9123D : Dual 3.5" floppy disk drive with 710KB format.
- HP2225DU : ThinkJet printer with serial interface.
- HP3852A : Data Acquisition/Control unit with processor, front panel keyboard, displays HP-IB interface, real-time clock, 11KB Memory, alarms, and 8 slots for modules.
- HP3853A : Extension chassis with 10 slots for modules, control cable, and two 3-wire analogue signal cables.
- HP44701A : 5.5 digit integrating voltmeter for measuring DC or AC voltage, and 2-or-4 wire ohms resistance (built in current source) with guard terminal.
- HP44705A : 20 channel relay multiplexer switches high, low, and guard on all 20 channels. 2 and 4 wire  $\Omega$ .
- HP44725A : 16 channel general purpose switch.
- HP44727A : 4 channel voltage Digital Analogue Converter.

The above components are correlated in the data control and the data acquisition system diagrams illustrated below. (see Figures F.3 & F.4)

Data Sheet DS13 continued

Figure F.4 Data Acquisition System

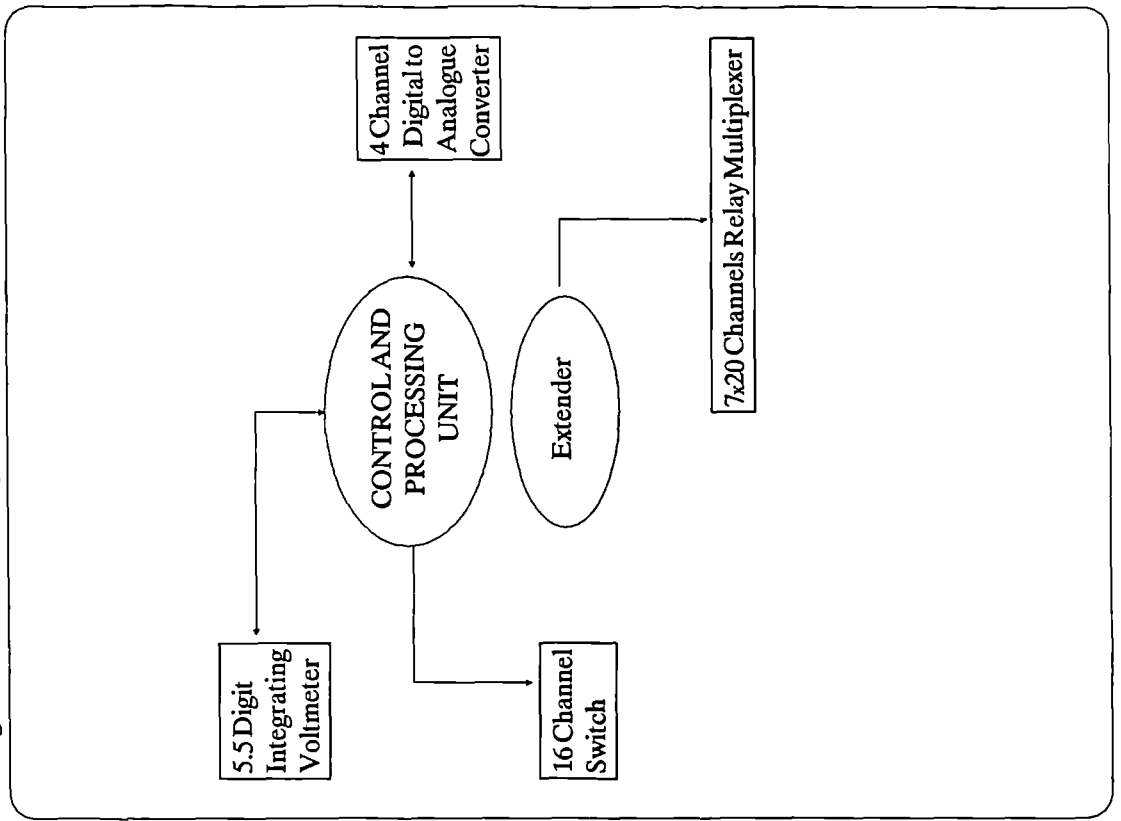
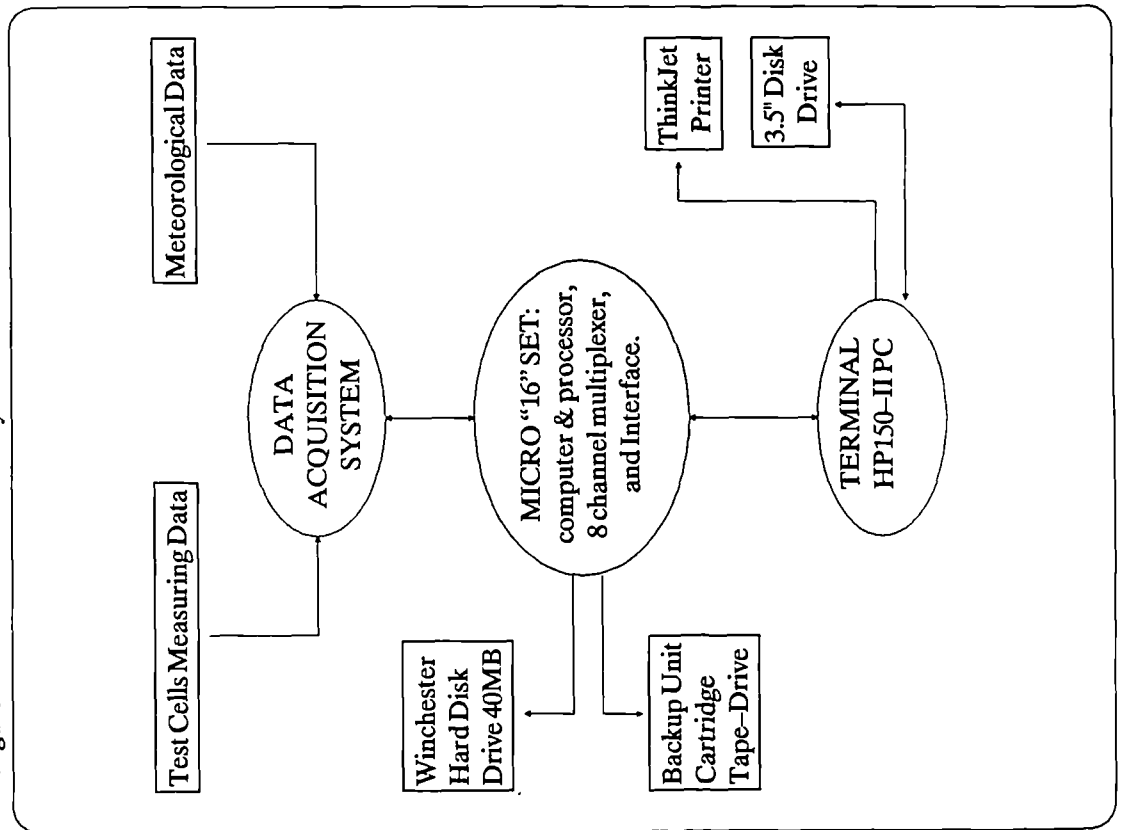
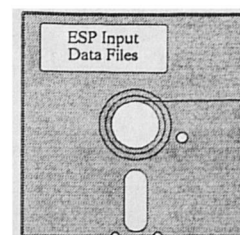


Figure F.3 Data Control System



## Appendix G




---

# “ESP” Input Data Files: for Energy Performance Simulation of the UK “Passys” Test Cells

---

The dynamic program “ESP” was used in chapter 7 and chapter 8 for simulating the energy performances of test cells 2, 3 & 4 (at the UK Passys site, Glasgow) fitted with various passive solar components. This appendix briefly describes the important modules of the “ESP” program and lists the files required to describe the test cells and configuration controls for the “ESP” model to perform the simulations.

### *A Brief Description of the “ESP” Model*

Environmental Systems Performance, “ESP”, is a transient energy simulation software capable of modeling the energy and mass flows within buildings and the energy flows within plant systems. Any building, defined as a collection of interlocking polyhedral zones, specified in terms of geometry, construction and usage profiles, can be associated with a plant system consisting of a distributed network of plant components. The combined system can then be subjected to simulation processing under dynamic control.

Figure G.1 shows the connections between the various program and database modules which comprise ESP. The three main modules *imp*, *bps*, and *res* can be used to investigate performance and, by iteration, to assess the consequence of any change to the building or plant control. The various databases are used to reduce the input task and the utility modules exist to allow the subsystems they address to be treated in great detail; but only if this can be justified by the design objectives.

Input to ESP consists of *geometry*, *construction* and *operational* details for building zones, miscellaneous thermal parameters for plant components, and *configurational* and *control* information for the combined network. The ESP software is not user friendly. However, the user manual is extensive and divided into a number of distinct sections corresponding to separate program modules (covering theory, operation and validity). Description of the modules used by the author follows:

**ESPimp** Allows the interactive definition of the combined building/plant network to be subjected to some weather influence and simulated over time. All items, as input, are processed through legality and within acceptable range checks before being located in an output file for transfer to the simulation engine ESPbps. Other facilities include a range of interactive editing commands and automatic access to construction, casual gain profile and plant component databases.

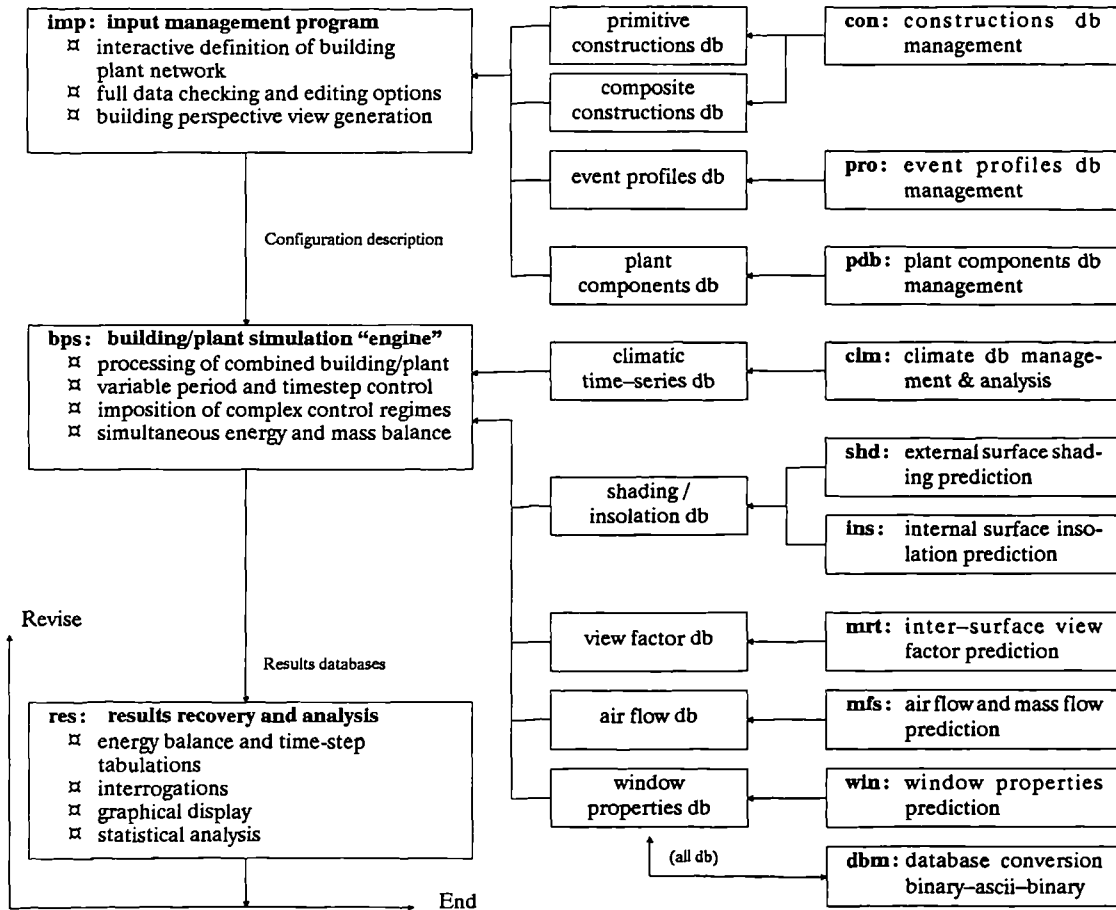


Figure G.1 Program modules of the "ESP" software (series 6, 1990).

ESPbps	The central simulation engine which simulates energy flow by a heat balance matrix inversion technique of implicit enumeration. The technique is unconditionally stable for all computational time-increments and operates in conjunction with hourly values of various climatological parameters recovered from the climatological database. As the model steps through the user defined time increments, it continuously predicts the environmental and energy status of the simulated building. This is done by placing nodes at many points of interest for each node performing a heat balance between all interacting regions (over time and space dimensions), and then simultaneously solving the resulting set of equations at each time step.
ESPres	The output program which operates on the simulation results located in the results database by ESPbps. A variety of output facilities are available: visualisation, result interrogation; graphical display; statistical analysis and tabulations.
ESPwin	Performs a spectral analysis of a multi layered window system to determine overall transmission, reflection and absorption. However, this module is only capable of analysing single and double transparent layers.
ESPclm	Manages the climatological database allowing prediction, modification and analysis of the hourly time series values of the various climatic parameters retained in a climate reference year. Hourly data of six climatic variables should be formatted in columns with the following sequence: <ul style="list-style-type: none"> <li>- Diffuse horizontal insolation (<math>\text{W m}^{-2}</math>);</li> <li>- Outdoor dry bulb temperature (<math>10^{-1} \text{ }^{\circ}\text{C}</math>);</li> <li>- Direct normal or Global horizontal insolation (<math>\text{W m}^{-2}</math>);</li> <li>- Wind speed (<math>10^{-1} \text{ m s}^{-1}</math>);</li> <li>- Wind direction (degrees from North);</li> <li>- Relative humidity (%).</li> </ul>

ESPclm accepts Direct Normal insolation values as default input, but with a special flag indicating that input data is Global Horizontal insolation, the later will be invoked.

### *The Input Data Files*

Each test cells was divided into two zones; (i) test room and (ii) service room. (see chapter 7 for detailed description of these zones). Chapter 7 also provide the procedures and justification for producing the input files. (see section 7.5.1).

The data input to ESP, describing the Passys test cells and the configuration of the blind and curtain experiments, consisted of 8 file types: *geometry*, *construction*, *operation*, *utility*, *blind control*, *transparent multi-construction*, *system configuration* and *configuration control*. In order to read and understand the contents of these files, Tables G.1–G.8 describe the fields of the records on each file type.

**Table G.1** Contents of a zone *geometry* file (\*.GEO).

Record	Description of fields
1	Zone shape type ( <i>REC</i> or <i>GEN</i> )
2 for <i>REC</i>	<i>x, y</i> & <i>z</i> coordinate of bottom left-hand corner, length, height and angle of orientation.
2/1 for <i>GEN</i>	Total number of vertices comprising zone, number of bounding surfaces and axes rotation angle.
2/2 for <i>GEN</i>	<i>x, y</i> & <i>z</i> coordinates of each vertex in any convenient order.
2/3 for <i>GEN</i>	For the first surface: the number of vertices and then an anti-clockwise description of each as seen from outside the zone. (see the wire-frame drawings of each zone shown on file lists)
2/4 for <i>GEN</i>	Repeat 2/3 for surface 2 ....
2/n for <i>GEN</i>	and continue until last surface.
3	Number of windows in each surface.
4/1 →	For first surface with windows, the <i>x'</i> & <i>z'</i> coordinates of bottom left-hand corner, width and height for each window in turn.
4/2	Repeat for next surface with windows .....
4/?	and continue until last window surface.
5	Number of doors in each surface.
6/1 →	For first surface with doors, the <i>x'</i> coordinate of bottom left-hand corner, width and height for each door in turn.
6/2	Repeat for next surface with doors .....
6/?	and continue until last door surface.
7	Default insolation scheme: number of internal surfaces to receive direct radiation [1, 2 or all(3)], surface 1 number (for 1 or 2 receiving), surface 2 number (for 2 receiving) and surface with windows receiving [0 (no surface) or receiving surface 1 or 2].

**Table G.2** Contents of a zone *construction* file (\*.CON).

Record	Description of fields
1/1 →	For each surface in turn, the construction is defined in terms of the total number of homogeneous elements (including air gaps) and, separately, the number of air gaps.
1/n	Repeating 1/1 for each surface in turn.
2/1 →	The position (an integer count from outside) and overall thermal resistance of each air gap in first construction with air gaps.
2/n	Repeating 2/1 for all construction with air gaps.
3/1 →	For each element in surface 1: conductivity, density, specific heat and thickness; outside to inside order. For air gaps, only thickness is held, all other properties being set to zero.
3/n	Repeat 3/1 for all other constructions.
4/1 →	Window thermophysical properties for each window in turn in first surface with windows. Properties include shortwave direct transmittance and total transmittance for each of 5 angles of incidence (0°, 40°, 55°, 70° & 80°). The window U-value is also held.
4/n	Repeat 4/1 for all other surfaces with windows.
5/1 →	Thermal transmittance value (U-value) for each door in first surface with doors.
5/n	Repeat 5/1 for all other surfaces with doors.
6	Internal surface emissivity for each construction, then external surface emissivity.
7	Internal surface solar absorptivity for each construction, then external surface solar absorptivity.

**Table G.3** Contents of a zone *operation* file (\*.OPR).

Record	Description of fields
1	Zone character descriptor.
2	Control index (0 = no active thermostatic control on zone air flows), lower and upper temperatures. (0,0,0 is the default for zone air flow scheme).
3	Number of distinct intervals within a typical weekday .....
4/1 →	then for each interval, the start time, finish time, infiltration air change rate, zone-coupled air change rate and coupled zone definition.
4/n	repeat for next interval.
5 & 6	As 3 & 4 but for a typical Saturday.
7 & 8	As 3 & 4 but for a typical Sunday.
9	Number of distinct intervals within a typical weekday for default casual heat gain scheme (if 0 skip to 11).
10/1 →	then for each interval: the gain type, the start time, sensible heat gain, latent heat gain, radiant component and convective component.
10/n	repeat for next interval.
11 & 12	As 9 & 10 but for a typical Saturday.
13 & 14	As 9 & 10 but for a typical Sunday.

**Table G.4** Contents of a zone *utilities* file (\*.UTL).

Record	Description of fields
1	Zone air flow file flag.
1A	Air flow file name if flag = 1.
2	Zone casual gains file flag.
2A	Casual gains file name if flag = 1.
3	Zone view factor file flag.
3A	View factor file name if flag = 1.
4	Zone shading/insolation file flag.
4A	Shading/insolation file name if flag = 1.
5	Zone convection coefficient file flag.
5A	Convection coefficient file name if flag = 1.
6	Zone blind/shutter file flag.
6A	Blind/shutter file name if flag = 1.
7	Zone transparent multi-layered construction file flag.
7A	Transparent multi-layered construction file name if flag = 1.
8	Zone casual gain control file flag.
8A	Casual gain control file name if flag = 1.

**Table G.5** Contents of a zone *blind/shutter* file (\*.BLN).

Record	Description of fields
1	Number of distinct control intervals during a day. Also the surface number of the radiation sensor (if one exists).
2	Start and finish hours for the first interval.
3 *	For first interval: replacement window properties (shortwave direct and total transmittance for 5 angles of incidence and U-value) plus a control index and activation point for first period.
4 →	Repeat records 2 and 3 for each additional control interval.
* Note that the window properties may define a window arrangement which has a blind or shutter in place. In this case the zone construction file will point to the uncovered window case. Conversely, the role of the two zone files can be reversed.	

**Table G.6** Contents of a zone *transparent multi-layered construction* file (\*.TMC).

Record	Description of fields
1	Total number of multi-layered constructions in zone.
2	For each construction: an index stating whether or not it is transparent (0 opaque; 1 transparent).
3	Number of elements (including air gap) of the first transparent multi-layer construction (TMC).
4	For first TMC: direct transmittance at 5 angles of incidence; followed by the absorbance for each element for the 5 angles of incidence – outside to inside – in turn.
5	Control flag. If flag is zero then records 3 to 5 are repeated for each TMC. If flag is 1 then other records are required as in blind/shutter file.

**Table G.7** Contents of the *system configuration* file (\*.CFG).

Record	Description of fields
1	Configuration type (1, 2 or 3) defining a building only, plant only or building/plant simulation.
2	Site latitude and longitude difference.
3	Site exposure type and ground reflectivity. Site exposure types determine the appropriate surroundings, sky and ground view factors (8 types are available, the chosen type 2 represents an urban site).
4	* Building (this record may be omitted)
5	Title of building configuration.
6	Number of zones.
7	For first zone: code number.
8, 9 & 10	For first zone: operation, geometry and construction file names.
11	For first zone: utilities file index.
12	For first zone: utilities file name if the record 11 index is 1.
13 → I	Repeat records 7 through 12 for each additional zone in turn.
I + 1	Total number of zone bounding surfaces in building configuration.
I + 2 → J	For each bounding surface: zone number, surface number, connection type (0-5), supplementary data (2 items).
J + 1	Air flow simulation index. (0 indicate that no building air flow simulation).

**Table G.8** Contents of the *configuration control* file (\*.CTL).

Record	Description of fields
1	Identifying character string for overall control.
2	* Building
3	Identifying character string for building control regime.
4	Number of control functions.
For each control function cycle to record 12 .....	
5	* Control Function
6	Sensor location (3 data items).
7	Actuator location (3 data items).
8	Number of control day types.
For each day type cycle to record 12 .....	
9	Start and finish dates of validity (Julian day numbers, January 1st = day 1).
10	Number of distinct control periods.
For each control period cycle to record 12 .....	
11	Controller type, control law, period start time.
12	Number of data items associated with the control law, then data values.
13	List of associated control functions for each zone in system configuration.

The two files listed below are executable shell scripts to perform the simulations automatically. Note that *Blindx.Run* file includes two simulation runs, and *Curtain.Run* file includes three simulation runs (see text in chapters 7 & 8 for more details).

The climate file *glasgow.clm* was constructed from measured data at the Passys site. It includes climatic variables for the periods of both the blind and the curtain experiment. Specific data for the analysis conducted in chapters 7 & 8 were obtained from the simulation result library files *\*.res*.

The following pages list the ESP input files. Note that the system configuration files are listed first so that it is easy to understand the inter-relationship between the rest of the files.

File: <i>BLINDX.RUN</i>	File: <i>CURTAINX.RUN</i>
<pre> bps &lt; &lt; blind -6   glasgow.clm   w   n   1   blindx1.cfg   n   3   blindx1.res   23      7   18      8   1   4   s   y   blindx.ctl   y   &gt;   -   1   blindx2.cfg   n   3   blindx2.res   23      7   18      8   1   3   s   y   blindx.ctl   y   &gt;   -   f blind </pre>	<pre> bps &lt; &lt; curtain -6   glasgow.clm   w   n   1   curtnx1.cfg   n   3   curtnx1.res   28      11   27      12   1   4   s   y   curtnx.ctl   y   &gt;   -   1   curtnx2.cfg   n   3   curtnx2.res   28      11   27      12   1   3   s   y   curtnx.ctl   y   &gt;   -   1   curtnx3.cfg   n   3   curtnx3.res   14      9   27      11   1   2   s   y   curtnx.ctl   y   &gt;   -   f curtain </pre>

```

File: BLINDX1. CFG
1
55.9 -4.15
2 0.2
configuration as tmc
4
1
sroom.opr
sroom.geo
sroom.con
0
2
troom.opr
troom.geo
troom4.con
1
troom4.utl
3
sroom.opr
sroom.geo
sroom.con
0
4
troom.opr
troom.geo
troom3.con
1
troom3.utl
38
1 1 3 2 4
1 2 0 0 0
1 3 0 0 0
1 4 0 0 0
1 5 0 0 0
1 6 0 0 0
2 1 0 0 0
2 2 0 0 0
2 3 0 0 0
2 4 3 1 1
2 5 0 0 0
2 6 0 0 0
2 7 0 0 0
2 8 0 0 0
2 9 0 0 0
2 10 0 0 0
2 11 0 0 0
2 12 0 0 0
2 13 0 0 0
3 1 3 4 4
3 2 0 0 0
3 3 0 0 0
3 4 0 0 0
3 5 0 0 0
3 6 0 0 0
4 1 0 0 0
4 2 0 0 0
4 3 0 0 0
4 4 3 3 1
4 5 0 0 0
4 6 0 0 0
4 7 0 0 0
4 8 0 0 0
4 9 0 0 0
4 10 0 0 0
4 11 0 0 0
4 12 0 0 0
4 13 0 0 0
0
    
```

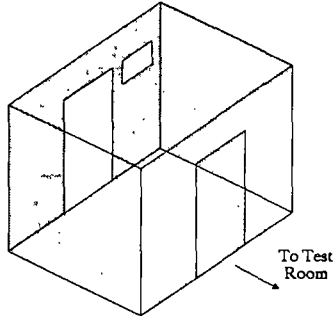
```

File: BLINDX2. CFG
1
55.9 -4.15
2 0.2
configuration as window with blind
4
1
sroom.opr
sroom.geo
sroom.con
0
2
troom.opr
wtroom.geo
wtroom.con
0
3
sroom.opr
sroom.geo
sroom.con
0
4
troom.opr
wtroom.geo
wtroom.con
1
wtroom3.utl
36
1 1 3 2 4
1 2 0 0 0
1 3 0 0 0
1 4 0 0 0
1 5 0 0 0
1 6 0 0 0
2 1 0 0 0
2 2 0 0 0
2 3 0 0 0
2 4 3 1 1
2 5 0 0 0
2 6 0 0 0
2 7 0 0 0
2 8 0 0 0
2 9 0 0 0
2 10 0 0 0
2 11 0 0 0
2 12 0 0 0
3 1 3 4 4
3 2 0 0 0
3 3 0 0 0
3 4 0 0 0
3 5 0 0 0
3 6 0 0 0
4 1 0 0 0
4 2 0 0 0
4 3 0 0 0
4 4 3 3 1
4 5 0 0 0
4 6 0 0 0
4 7 0 0 0
4 8 0 0 0
4 9 0 0 0
4 10 0 0 0
4 11 0 0 0
4 12 0 0 0
0
    
```

File: CURTNX1. CFG						File: CURTNX2. CFG						File: CURTNX3. CFG					
1						1						1					
55.9 -4.15						55.9 -4.15						55.9 -4.15					
2 0.2						2 0.2						2 0.2					
configuration as tmc						config as window with blind						config for both (no curtain)					
4						4						4					
1						1						1					
sroom.opr						sroom.opr						sroom.opr					
sroom.geo						sroom.geo						sroom.geo					
sroom.con						sroom.con						sroom.con					
0						0						0					
2						2						2					
troom2.opr						troom2.opr						troom2.opr					
troom2.geo						wtroom2.geo						troom2.geo					
troom2.con						wtroom2.con						troom2.con					
1						0						1					
troom2.utl						3						troom2.utl					
3						sroom.opr						3					
sroom.opr						sroom.geo						sroom.opr					
sroom.geo						sroom.con						sroom.geo					
sroom.con						0						sroom.con					
0						4						0					
4						troom2.opr						4					
troom2.opr						wtroom2.geo						troom2.opr					
troom2.geo						wtroom2.con						wtroom2.geo					
troom2c.con						1						wtroom2.con					
1						wtroom2.utl						0					
troom2c.utl						34						35					
36						1 1 3 2 4						1 1 3 2 4					
1	1	3	2	4		1	2	0	0	0		1	1	3	2	4	
1	2	0	0	0		1	3	0	0	0		1	2	0	0	0	
1	3	0	0	0		1	4	0	0	0		1	3	0	0	0	
1	4	0	0	0		1	5	0	0	0		1	4	0	0	0	
1	5	0	0	0		1	6	0	0	0		1	5	0	0	0	
1	6	0	0	0		2	1	0	0	0		1	6	0	0	0	
2	1	0	0	0		2	2	0	0	0		2	1	0	0	0	
2	2	0	0	0		2	3	0	0	0		2	2	0	0	0	
2	3	0	0	0		2	4	3	1	1		2	3	0	0	0	
2	4	3	1	1		2	5	0	0	0		2	4	3	1	1	
2	5	0	0	0		2	6	0	0	0		2	5	0	0	0	
2	6	0	0	0		2	7	0	0	0		2	6	0	0	0	
2	7	0	0	0		2	8	0	0	0		2	7	0	0	0	
2	8	0	0	0		2	9	0	0	0		2	8	0	0	0	
2	9	0	0	0		2	10	0	0	0		2	9	0	0	0	
2	10	0	0	0		2	11	0	0	0		2	10	0	0	0	
2	11	0	0	0		3	1	3	4	4		2	11	0	0	0	
2	12	0	0	0		3	2	0	0	0		2	12	0	0	0	
3	1	3	4	4		3	3	0	0	0		3	1	3	4	4	
3	2	0	0	0		3	4	0	0	0		3	2	0	0	0	
3	3	0	0	0		3	5	0	0	0		3	3	0	0	0	
3	4	0	0	0		3	6	0	0	0		3	4	0	0	0	
3	5	0	0	0		4	1	0	0	0		3	5	0	0	0	
3	6	0	0	0		4	2	0	0	0		3	6	0	0	0	
4	1	0	0	0		4	3	0	0	0		4	1	0	0	0	
4	2	0	0	0		4	4	3	3	1		4	2	0	0	0	
4	3	0	0	0		4	5	0	0	0		4	3	0	0	0	
4	4	3	3	1		4	6	0	0	0		4	4	3	3	1	
4	5	0	0	0		4	7	0	0	0		4	5	0	0	0	
4	6	0	0	0		4	8	0	0	0		4	6	0	0	0	
4	7	0	0	0		4	9	0	0	0		4	7	0	0	0	
4	8	0	0	0		4	10	0	0	0		4	8	0	0	0	
4	9	0	0	0		4	11	0	0	0		4	9	0	0	0	
4	10	0	0	0		0						4	10	0	0	0	
4	11	0	0	0								4	11	0	0	0	
4	12	0	0	0								0					
0																	

*File: SROOM.GEO*

REC	-0.408	5.474	-0.268	
	3.584	2.404	3.286	0.0
	0	0	1	0
	0.200	1.600	0.600	0.4
	1	0	1	0
	1.287	1.010		2.00
	1.287	1.010		2.00
3	0	0	0	

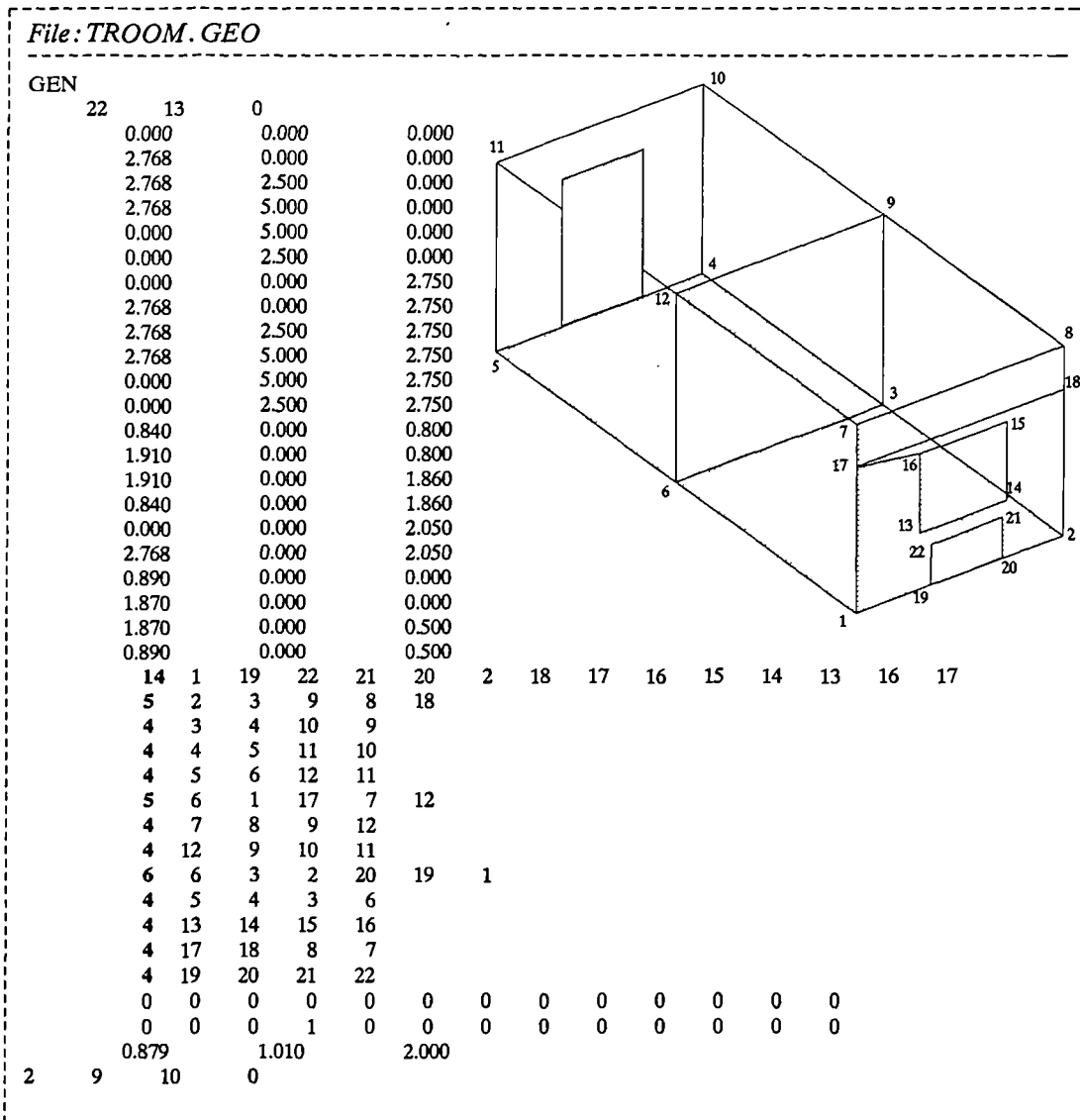


*File: SROOM.OPR*

service	room				
0	0	0			
	1				
	0	24	0	0	0
	1				
	0	24	0	0	0
	1				
	0	24	0	0	0
0					
0					
0					

*File: SROOM.CON*

6	0				
4	0				
4	0				
4	0				
4	0				
4	0				
	50.00	7800.0	502.0	0.0020	
	0.150	800.0	2093.0	0.0080	
	0.040	33.0	850.0	0.4000	
	0.150	800.0	2093.0	0.0130	
	0.040	105.0	1800.0	0.0400	
	0.150	800.0	2093.0	0.0130	
	<b>50.00</b>	<b>7800.0</b>	<b>502.0</b>	<b>0.0015</b>	
	<b>0.150</b>	<b>800.0</b>	<b>2093.0</b>	<b>0.0130</b>	
	<b>0.040</b>	<b>105.0</b>	<b>1800.0</b>	<b>0.0800</b>	
	<b>0.150</b>	<b>800.0</b>	<b>2093.0</b>	<b>0.0130</b>	
	50.00	7800.0	502.0	0.0015	
	0.150	800.0	2093.0	0.0130	
	0.040	105.0	1800.0	0.0800	
	0.150	800.0	2093.0	0.0130	
	<b>50.00</b>	<b>7800.0</b>	<b>502.0</b>	<b>0.0015</b>	
	<b>0.150</b>	<b>800.0</b>	<b>2093.0</b>	<b>0.0130</b>	
	<b>0.040</b>	<b>105.0</b>	<b>1800.0</b>	<b>0.0800</b>	
	<b>0.150</b>	<b>800.0</b>	<b>2093.0</b>	<b>0.0130</b>	
	50.00	7800.0	502.0	0.0015	
	0.150	800.0	2093.0	0.0260	
	0.040	105.0	1800.0	0.0800	
	0.150	800.0	2093.0	0.0130	
	<b>0.150</b>	<b>800.0</b>	<b>2093.0</b>	<b>0.0080</b>	
	<b>0.035</b>	<b>33.0</b>	<b>850.0</b>	<b>0.0500</b>	
	<b>0.150</b>	<b>800.0</b>	<b>2093.0</b>	<b>0.0210</b>	
	<b>0.850</b>	<b>2000.0</b>	<b>837.0</b>	<b>0.0030</b>	
	0.71	0.69	0.64	0.47	0.22
	0.77	0.75	0.71	0.54	0.27
	1.20				3.10
	2.10				
	0.91	0.91	0.91	0.91	0.91
	0.89	0.25	0.25	0.25	0.90
	0.65	0.65	0.65	0.65	0.65
	0.65	0.40	0.40	0.45	0.85



*File: TROOM.OPR*

test	room				
0	0	0			
	1				
0	24	0.1	0	0	0
	1				
0	24	0.1	0	0	0
	1				
0	24	0.1	0	0	0
0					
0					
0					



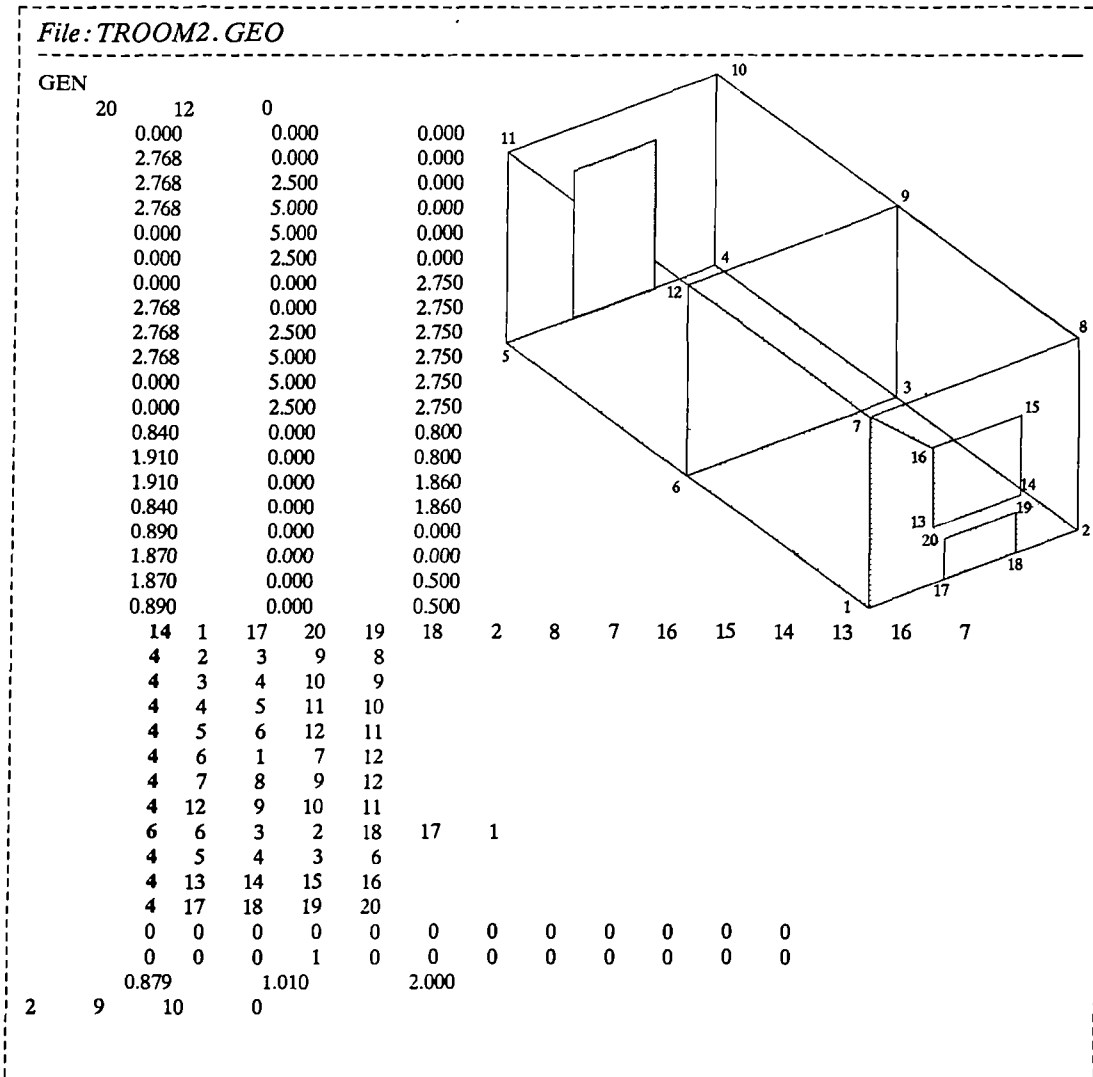
50.00	7800.0	502.0	0.0015									
0.150	800.0	2093.0	0.0130									
0.040	105.0	1800.0	0.0800									
0.150	800.0	2093.0	0.0130									
0.040	33.0	850.0	0.4000									
0.150	800.0	2093.0	0.0080									
50.00	7800.0	502.0	0.0020									
0.150	800.0	2093.0	0.0130									
0.040	105.0	1800.0	0.0400									
0.150	800.0	2093.0	0.0130									
0.040	33.0	850.0	0.4000									
0.150	800.0	2093.0	0.0080									
50.00	7800.0	502.0	0.0020									
50.00	7800.0	502.0	0.0015									
0.150	800.0	2093.0	0.0130									
0.040	105.0	1800.0	0.0800									
0.150	800.0	2093.0	0.0130									
0.040	33.0	850.0	0.4000									
0.150	800.0	2093.0	0.0080									
50.00	7800.0	502.0	0.0020									
50.00	7800.0	502.0	0.0015									
0.150	800.0	2093.0	0.0260									
0.040	105.0	1800.0	0.0800									
0.150	800.0	2093.0	0.0130									
0.040	33.0	850.0	0.2600									
0.150	800.0	2093.0	0.0080									
50.00	7800.0	502.0	0.0020									
50.00	7800.0	502.0	0.0015									
0.150	800.0	2093.0	0.0260									
0.040	105.0	1800.0	0.0800									
0.150	800.0	2093.0	0.0130									
0.040	33.0	850.0	0.2600									
0.150	800.0	2093.0	0.0080									
50.00	7800.0	502.0	0.0020									
0.150	560.0	2500.0	0.0300									
0.035	33.0	850.0	0.3000									
0.150	800.0	2093.0	0.0190									
50.00	7800.0	502.0	0.0020									
0.150	560.0	2500.0	0.0300									
0.035	33.0	850.0	0.3000									
0.150	800.0	2093.0	0.0190									
50.00	7800.0	502.0	0.0020									
1.050	3500.0	837.0	0.0060									
0.000	0.0	0.0	0.0120									
1.050	3500.0	837.0	0.0060									
0.650	1810.0	800.0	0.1000									
0.150	560.0	2500.0	0.0100									
0.110	600.0	1210.0	0.1000									
0.160	950.0	840.0	0.0120									
0.160	800.0	2093.0	0.0500									
1.20												
0.89	0.89	0.89	0.89	0.89	0.89	0.89	0.89	0.89	0.89	0.76	0.89	0.89
0.93	0.25	0.25	0.91	0.25	0.25	0.25	0.25	0.90	0.90	0.82	0.93	0.89
0.65	0.65	0.65	0.65	0.65	0.65	0.65	0.65	0.65	0.65	0.31	0.65	0.65
0.70	0.40	0.40	0.65	0.40	0.40	0.45	0.45	0.85	0.85	0.35	0.70	0.65

*File: TROOM4. CON*

4	0											
7	0											
7	0											
6	0											
7	0											
7	0											
7	0											
4	0											
4	0											
3	1											
4	0											
1	0											
2	0.232											
	0.650	1810.0		800.0		0.1000						
	0.150	560.0		2500.0		0.0100						
	0.040	13.6		840.0		0.1000						
	0.160	950.0		840.0		0.0120						
	1.050	3500.0		837.0		0.0060						
	0.000	0.0		0.0		0.0120						
	1.050	3500.0		837.0		0.0060						
	<b>0.650</b>	<b>1810.0</b>		<b>800.0</b>		<b>0.1000</b>						
	<b>0.150</b>	<b>560.0</b>		<b>2500.0</b>		<b>0.0100</b>						
	<b>0.110</b>	<b>600.0</b>		<b>1210.0</b>		<b>0.1000</b>						
	<b>0.160</b>	<b>950.0</b>		<b>840.0</b>		<b>0.0120</b>						
	0.160	800.0		2093.0		0.0500						
	1.20											
0.89	0.89	0.89	0.89	0.89	0.89	0.89	0.89	0.89	0.89	0.82	0.89	0.89
0.93	0.25	0.25	0.91	0.25	0.25	0.25	0.25	0.90	0.90	0.82	0.93	0.89
0.65	0.65	0.65	0.65	0.65	0.65	0.65	0.65	0.65	0.65	0.35	0.65	0.65
0.70	0.40	0.40	0.65	0.40	0.40	0.45	0.45	0.85	0.85	0.35	0.70	0.65

*File: WTROOM. CON*

4	0											
7	0											
7	0											
6	0											
7	0											
7	0											
7	0											
4	0											
4	0											
4	0											
1	0											
	0.6500	1810.0		800.0		0.1000						
	0.1500	560.0		2500.0		0.0100						
	0.0400	13.6		840.0		0.1000						
	0.1600	950.0		840.0		0.0120						
	0.6500	1810.0		800.0		0.1000						
	0.1500	560.0		2500.0		0.0100						
	0.1100	600.0		1210.0		0.1000						
	0.1600	950.0		840.0		0.0120						
	<b>0.1600</b>	<b>800.0</b>		<b>2093.0</b>		<b>0.0500</b>						
	0.588	0.557	0.499	0.344	0.155							
	0.703	0.682	0.625	0.463	0.240	2.00						
	1.20											
0.89	0.89	0.89	0.89	0.89	0.89	0.89	0.89	0.89	0.89	0.89	0.89	
0.93	0.25	0.25	0.91	0.25	0.25	0.25	0.25	0.90	0.90	0.93	0.89	
0.65	0.65	0.65	0.65	0.65	0.65	0.65	0.65	0.65	0.65	0.65	0.65	
0.70	0.40	0.40	0.65	0.40	0.40	0.45	0.45	0.85	0.85	0.70	0.65	



*File: TROOM2.OPR*

test	room2					
0	0	0				
	1					
0	24	0.3	0	0	0	
	1					
0	24	0.3	0	0	0	
	1					
0	24	0.3	0	0	0	
0						
0						
0						



50.00	7800.0	502.0	0.0015								
0.150	800.0	2093.0	0.0130								
0.040	105.0	1800.0	0.0800								
0.150	800.0	2093.0	0.0130								
0.040	33.0	850.0	0.4000								
0.150	800.0	2093.0	0.0080								
50.00	7800.0	502.0	0.0020								
0.150	800.0	2093.0	0.0130								
0.040	105.0	1800.0	0.0400								
0.150	800.0	2093.0	0.0130								
0.040	33.0	850.0	0.4000								
0.150	800.0	2093.0	0.0080								
50.00	7800.0	502.0	0.0020								
50.00	7800.0	502.0	0.0015								
0.150	800.0	2093.0	0.0130								
0.040	105.0	1800.0	0.0800								
0.150	800.0	2093.0	0.0130								
0.040	33.0	850.0	0.4000								
0.150	800.0	2093.0	0.0080								
50.00	7800.0	502.0	0.0020								
50.00	7800.0	502.0	0.0015								
0.150	800.0	2093.0	0.0130								
0.040	105.0	1800.0	0.0800								
0.150	800.0	2093.0	0.0130								
0.040	33.0	850.0	0.4000								
0.150	800.0	2093.0	0.0080								
50.00	7800.0	502.0	0.0020								
50.00	7800.0	502.0	0.0015								
0.150	800.0	2093.0	0.0260								
0.040	105.0	1800.0	0.0800								
0.150	800.0	2093.0	0.0130								
0.040	33.0	850.0	0.2600								
0.150	800.0	2093.0	0.0080								
50.00	7800.0	502.0	0.0020								
50.00	7800.0	502.0	0.0015								
0.150	800.0	2093.0	0.0260								
0.040	105.0	1800.0	0.0800								
0.150	800.0	2093.0	0.0130								
0.040	33.0	850.0	0.2600								
0.150	800.0	2093.0	0.0080								
50.00	7800.0	502.0	0.0020								
0.150	560.0	2500.0	0.0300								
0.035	33.0	850.0	0.3000								
0.150	800.0	2093.0	0.0190								
50.00	7800.0	502.0	0.0020								
0.150	560.0	2500.0	0.0300								
0.035	33.0	850.0	0.3000								
0.150	800.0	2093.0	0.0190								
50.00	7800.0	502.0	0.0020								
1.050	3500.0	837.0	0.0040								
0.000	0.0	0.0	0.0120								
1.050	3500.0	837.0	0.0040								
0.160	800.0	2093.0	0.0500								
1.20											
0.90	0.89	0.89	0.89	0.89	0.89	0.89	0.89	0.89	0.89	0.90	0.91
0.90	0.25	0.25	0.90	0.25	0.25	0.25	0.25	0.90	0.90	0.82	0.91
0.65	0.65	0.65	0.65	0.65	0.65	0.65	0.65	0.65	0.65	0.13	0.70
0.65	0.40	0.40	0.65	0.40	0.40	0.45	0.45	0.85	0.85	0.15	0.70

*File: TROOM2.CON*

3	0										
7	0										
7	0										
6	0										
7	0										
7	0										
7	0										
4	0										
4	0										
3	1										
1	0										
2	0.178										
	0.175	2400.0		880.0		0.0800					
	0.030	30.0		1200.0		0.1000					
	0.175	2400.0		880.0		0.1200					
	↓ →	.		.		.					
	1.050	3500.0		837.0		0.0040					
	0.000	0.0		0.0		0.0120					
	1.050	3500.0		837.0		0.0040					
	0.160	800.0		2093.0		0.0500					
	1.20										
0.90	0.89	0.89	0.89	0.89	0.89	0.89	0.89	0.89	0.89	0.82	0.91
0.90	0.25	0.25	0.90	0.25	0.25	0.25	0.25	0.90	0.90	0.82	0.91
0.65	0.65	0.65	0.65	0.65	0.65	0.65	0.65	0.65	0.65	0.09	0.70
0.65	0.40	0.40	0.65	0.40	0.40	0.45	0.45	0.85	0.85	0.12	0.70

Same as in file TROOM2C.CON

*File: WTROOM2.CON*

3	0										
7	0										
7	0										
6	0										
7	0										
7	0										
7	0										
4	0										
4	0										
1	0										
	0.175	2400.0		880.0		0.0800					
	0.030	30.0		1200.0		0.1000					
	0.175	2400.0		880.0		0.1200					
	↓ →	.		.		.					
	0.1600	800.0		2093.0		0.0500					
	0.680	0.650	0.600	0.440	0.200						
	0.750	0.730	0.690	0.520	0.270	3.00					
	1.20										
0.90	0.89	0.89	0.89	0.89	0.89	0.89	0.89	0.89	0.89	0.91	
0.90	0.25	0.25	0.90	0.25	0.25	0.25	0.25	0.90	0.90	0.91	
0.65	0.65	0.65	0.65	0.65	0.65	0.65	0.65	0.65	0.65	0.70	
0.65	0.40	0.40	0.65	0.40	0.40	0.45	0.45	0.85	0.85	0.70	

Same as in file TROOM2C.CON

*File: TROOM3. UTL*

```

0
0
0
0
0
0
1
troom3.tmc
0
    
```

*File: TROOM4. UTL*

```

0
0
0
0
0
0
1
troom4.tmc
0
    
```

*File: WTROOM3. UTL*

```

0
0
0
0
0
1
wtroom3.blm
0
0
    
```

*File: TROOM3. TMC*

```

13
0 0 0 0 0 0 0 0 0 0 0 1 0 0
3
0.162    0.154    0.142    0.107    0.056
0.193    0.207    0.218    0.225    0.211
0.000    0.000    0.000    0.000    0.000
0.178    0.170    0.165    0.136    0.082
0
    
```

*File: TROOM4. TMC*

```

13
0 0 0 0 0 0 0 0 0 0 0 1 0 0
3
0.588    0.557    0.499    0.344    0.155
0.156    0.170    0.184    0.202    0.203
0.000    0.000    0.000    0.000    0.000
0.193    0.150    0.151    0.132    0.091
0
    
```

*File: WTROOM3. BLN*

```

1    0
0    24
0.162    0.154    0.142    0.107    0.056    0
0.268    0.274    0.263    0.198    0.094
1.50
0    -99
    
```

*File: TROOM2C. UTL*

```

0
0
0
0
0
0
1
troom2c.tmc
0
    
```

*File: TROOM2. UTL*

```

0
0
0
0
0
0
1
troom2.tmc
0
    
```

*File: WTROOM2. UTL*

```

0
0
0
0
0
1
wtroom2.bin
0
0
    
```

*File: TROOM2C. TMC*

```

12
0 0 0 0 0 0 0 0 0 0 1 0
3
0.237 0.230 0.216 0.172 0.092
0.213 0.221 0.237 0.235 0.202
0.000 0.000 0.000 0.000 0.000
0.195 0.194 0.188 0.157 0.092
0
    
```

*File: TROOM2. TMC*

```

12
0 0 0 0 0 0 0 0 0 0 1 0
3
0.676 0.652 0.604 0.441 0.202
0.113 0.124 0.134 0.148 0.154
0.000 0.000 0.000 0.000 0.000
0.088 0.094 0.097 0.088 0.063
0
    
```

*File: WTROOM2. BLN*

```

1 0
0 24
0.237 0.230 0.216 0.172 0.092 0
0.431 0.424 0.409 0.339 0.199
2.30
0 -99
    
```

*File: BLINDX.CTL*

blind exp.  
 \*Building  
 temp. setpoint  
 4

\*Control function  
 1 0 0  
 1 0 0  
 1 365  
 1 1  
 0 1 0  
 6.0  
 10.00 0.00 10.00 0.00 30.00 30.00

\*Control function  
 2 0 0  
 2 0 0  
 2 221  
 1 1  
 0 1 0  
 6.0  
 10.00 0.00 10.00 0.00 31.70 31.70  
 222 365  
 1 1  
 0 2 0  
 0

\*Control function  
 3 0 0  
 3 0 0  
 1 365  
 1 1  
 0 1 0  
 6.0  
 10.00 0.00 10.00 0.00 30.00 30.00

\*Control function  
 4 0 0  
 4 0 0  
 2 221  
 1 1  
 0 1 0  
 6.0  
 10.00 0.00 10.00 0.00 30.60 30.60  
 222 365  
 1 1  
 0 2 0  
 0

1 2 3 4

*File: CURTNX.CTL*

curtain exp.  
 \*Building  
 temp. setpoint  
 4

\*Control function  
 1 0 0  
 1 0 0  
 1 365  
 1 1  
 0 1 0  
 6.0  
 10.00 0.00 10.00 0.00 25.00 25.00

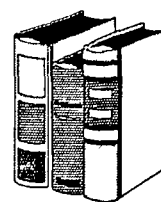
\*Control function  
 2 0 0  
 2 0 0  
 2 331  
 1 1  
 0 1 0  
 6.0  
 10.00 0.00 10.00 0.00 30.65 30.65  
 332 365  
 1 1  
 0 1 0  
 6.0  
 10.00 0.00 10.00 0.00 30.50 30.50

\*Control function  
 3 0 0  
 3 0 0  
 1 365  
 1 1  
 0 1 0  
 6.0  
 10.00 0.00 10.00 0.00 25.00 25.00

\*Control function  
 4 0 0  
 4 0 0  
 2 331  
 1 1  
 0 1 0  
 6.0  
 10.00 0.00 10.00 0.00 30.65 30.65  
 332 365  
 1 1  
 0 1 0  
 6.0  
 10.00 0.00 10.00 0.00 30.50 30.50

1 2 3 4

## Appendix H




---

# Glossary

---

**Accuracy** : The capability of an instrument to indicate the true value of measured quantity. This is often confused with inaccuracy, which is the departure from the true value into which all causes of error are lumped including hysteresis, nonlinearity, drift and temperature effect.

**Acrylic** : A synthetic long-chain polymer made primarily of acrylonitrile, a liquid derivative of natural gas and air. Other ingredients are coal, petroleum, and limestone. Used for drapery curtains and upholstery in blend of other materials like cotton, wool and acetate.

**AMR** : Acronym for the Annual Mean Range, which is the difference between the highest mean monthly maximum temperature and the lowest mean monthly minimum temperature.

**AMT** : Acronym for the Annual Mean Temperature, which is the average of the highest mean monthly maximum and the lowest mean monthly minimum.

**ASCII** : Acronym for American Standard Code for Information Interchange. It is a standardised 8-bit code used by most computers for interfacing.

**ASHRAE** : Acronym for American Society of Heating, Refrigerating and Air-conditioning Engineers.

**BASIC** : Acronym for Beginner's All-purpose Symbolic Instruction Code. It is a computer programming language.

**Brocade** : An embossed appearance is created in brocade fabrics. Elaborated patterns

often of flowers and figures, stand out from the background. Brocades are made from a wide range of fibres. Fabrics are used for upholstery, draperies etc.

**Casement drapery** : A term used to refer to a wide variety of curtain fabrics that are used alone at the window.

**Cosine Law** : An ideal black "Lambertian surface" absorbs incident radiation in proportion to the cosine of the incident angle measured from the normal to the surface.

**Diaphanous sheers** : Transparent or translucent finely woven curtains used for daytime privacy and to diffuse glare.

**Dralon** : Trade name of acrylic fibre.

**ESP** : Acronym for Environmental System Performance, an energy simulation program.

**ESU** : Acronym for the Energy Studies Unit.

**Fenestration** : A term used to signify an opening in a building to admit insolation through a transparent media. This could be a single glazing window, multiple glazing, or a combination of glazing and shading device(s).

**Filament** : A variety of fibre having an extreme length, not readily measured.

**Films** : Synthetic polymers extruded in the form of sheets rather than as fibres. These are not considered to be true textiles. They are sometimes laminated to textiles and therefore may be part of the structure of some textile products.

**Hysteresis** : The summation of all effects, under constant environmental conditions, that causes output of an instrument to assume different values at a given stimulus point when that point is approached first with increasing stimulus and then with decreasing stimulus. It is usually measured as a percent of full scale when input varies over the full increasing and decreasing range.

**Insolation** : The total amount of solar radiation –direct, diffuse and reflected– incident on a surface.

**Insulation** : Materials or systems used to prevent/reduce loss or gain of heat.

**Mali, Malimo** : A fabric formation technique in which fibres or yarns are held together by stitching through the materials.

**Man-made fibres** : Fibres created through technology either from natural materials or from chemicals.

**Marquisette** : A popular type of fine light-weight curtain fabrics made with the Leno weave technique. (refer to Tortora 1987 cited in chapter 6 for more details).

**MS-DOS** : Acronym for Microsoft Disk Operating System.

**Ninon** : Tightly woven sheer. The finish is crisp yet not stiff. Sometimes called french voile, french tregal, or triple voile.

**Noise** : Any unwanted electrical disturbance or spurious signal that modifies the transmission, measurement or recording of desired data.

**Nylon** : A long-chain polymer fibre derived from petroleum, natural gas (carbon), air (nitrogen and oxygen), and water. The fibre-forming substances–polymides are dry spun and stretched after cooling. Because of its sensitivity to sunlight, nylon is used in draperies and curtains only in blends.

**PASSYS** : A CEC research project : Passive Solar Components and System testing.

**Plain weave** : The simplest of textile weaves which account for over half of all the decorative fabric base constructions. Among the best known of the plain weave, standard fabrics are; the open weave, sheer and chiffon.

Variations of the plain weave include the basket weave, rib variation and seersucker.

**Pleated fabric blinds** : Factory-made treatment of heat-set polyester fabric that can have a metallised backing to reflect heat outward as a shading device or direct heat inward.

**Polyester** : Made of coal, air, water, and petroleum, polyester is a complex ester that forms a long-chain synthetic polymer. Usually used for curtain fabrics in blends of various fibres.

**Polymer** : A compound formed by the reaction of simple molecules having functional groups that permit their combination to proceed to high molecular weights under suitable conditions. Polymers may be formed by polymerisation (addition polymer) or polycondensation.

**Precision** : The repeatability of measurements of the same quantity under the same conditions. Not a measure of absolute accuracy. The precision of a measurement is used in this thesis to describe the relative tightness of the distribution of measurement of a quantity about their mean value. Therefore, precision of a measurement is associated more with its repeatability than its accuracy. It is given in terms of deviation from a mean value.

**Reliability** : The probability that an instrument's repeatability and accuracy will continue to fall within specified limits.

**Repeatability, Reproducibility** : See Precision.

**Satin** : A type of weave which produces a smooth lustrous fabric surface. Application depend on the fibre and type of yarn used. Also may be a base weave for other fabrics such as brocade.

**Selectivity** : Maximum error in sensitivity due to instrument's departure from its assumed input response.

**Shading Mask** : The projection on a horizontal plane of the section of the sky which are obscured by any object from an observer at the centre of the diagram.

**Sheer** : A term that includes many types of diaphanous fabrics.

**Skylight** : A clear or translucent panel set into a roof to admit sunlight into a building.

**Threshold** : The smallest stimulus or signal that results in a detectable output.

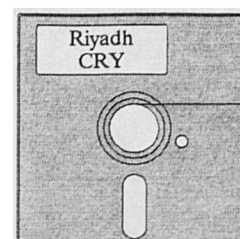
**Time Constant** : The time required for an exponential quantity to change by an amount equal to 0.632 times the total change required to reach steady state for first-order systems.  $0.632 = 1 - (1/e)$ .

**Velveteen** : A type of pile fabrics which cut and stand up densely on the surface.

**Vinyl** : A liquid solution made of vinyl alcohol, usually hydrochloric or polyvinyl chloride (PVC). It usually is not extruded or spun into fibre form but extruded as a film or coated textile that is flowed onto a net, woven or non-woven fabrics. Commonly used in roller shades.

**Zero Shift** : Drift in zero indication of an instrument without any change in measured variable.

## Appendix I




---

# Contents of Supplementary Floppy Disk

---

The floppy disk supplied with this thesis (see binding pocket) contains an archive of the following files:

- “RIYADH . CRY” representing 6\*8760 spread sheet of climatic data in ASCII format (Climate Reference Year). The climatic variables in six columns are: (1) global horizontal insolation, (2) diffuse horizontal insolation, (3) dry bulb temperature, (4) wind speed, (5) wind direction, and (6) relative humidity.
- “MKESP . BAS” represents a basic program to make the Climate Reference Year of Riyadh in the format required by the “ESP” software.
- “RIYADH-D . MET” represents daily meteorological data for Riyadh, Saudi Arabia, as given in Appendix A.
- “RIYADH-D . SOL” represents calculated and measured daily Insolation data for Riyadh, Saudi Arabia, as given in Appendix B.

The archive file is named “RIYADH . ZIP”. To extract the above files, the user should perform the following steps:

- Copy the contents of the floppy disk to your Hard Disk in any directory of your choice. For example you may use the following commands from [C: > prompt]
 

```
MD C:\CRY
CD C:\CRY
COPY A:\*.*
```
- then extract the files by the following command from your C: drive
 

```
PKUNZIP RIYADH
```

## Appendix J



# Index

## A

- Absorptance, solar
  - calculation for different glass types 117-8
  - of selected building materials 16a
  - test cell surfaces 151a
- Accuracy 260
  - instruments, see Instrumentation data sheets
  - measured solar properties of flat curtains 110
  - test room thermostatic control 160, 177
  - test room auxiliary heat measurements 159, 176
- Adiabatic wall, see Opaque calibration wall
- Air change rate
  - of the Passys test cell 158a
  - recommended rates for building zones 18a
  - see also Infiltration heat loss
- Air speed and direction measurements 134-5, 134a
  - see also Anemometers, Windvanes
- Albedometer 138, 138a, 244
  - for measuring curtain solar properties 108
- Aluminum coated polyester films 96a
- Analysis of captured data sets 160, 177
- Anemometers 134, 241
- Annual heating & cooling requirements 26-32
  - see also Degree day, Variable degree day
- Annual mean range 260, see also Mahoney tables
- Applied films 96, 260
- Architecture 2, see also Building design
- Architectural projections 90-1
- Aspirated psychrometer 240
- Aspirated thermometer 238
- Awnings 91

## B

- Base temperature 26-9, 32
  - see also Degree day, Variable degree day
- Bioclimatic chart 11, 11a
- Blind, see Passys blind, Venetian blinds
- Blind experiment, see Test site experiments
- Blind-glazing definition in "ESP" 164
- Bouger-Lambert law 68, 118
- Building design 2-3, 10-33
- Building heat gains 19-25, see also Heat gains
- Building heat losses 14-8

## C

- Calibration
  - of instruments, 128-41, 158, 176, 234-46
  - of the Passys test cells 157-8
  - experiments 158, 158a, 162, 177
  - wall, see Opaque calibration wall
- Campbell-Stokes sunshine recorder 141, 141a
- Cavity radiometer (standard) 140, 140a
- Classification
  - of curtain fabric 104
  - of pyranometers 137
  - of pyrhemometers 139a
- Climate definition
  - for the "Curtain" model 164, 182
  - in ESP model 165, 183, 250
- Climate diagnoses, see Mahoney tables
- Climate reference year 6, 38, 263
  - contents of CRY data floppy disk 263
  - data required to compile 44
  - data processing 45
  - development for Riyadh 44-8
  - results, remarks, & further analysis 48-62
  - selection procedure by various countries 39, 39a
- Climatic data, Riyadh 196-202
- Climatic design 2, 10
- Climatic stress, see Mahoney tables
- Computer programs see GW-Basic programs, ESP model, MRQT
- CRY, see Climate reference year
- Curtain experiment, see Test site experiments
- Curtain definition in "ESP" 182
- "Curtain" program (model) 115
  - components of heat gain/loss 115, 115a
  - heat balance equations 122-3
  - inward heat flow by convection and radiation 120
  - matrix solution 123
  - solar angles & incident solar radiation 116
  - shortwave transmission & absorption 117-9
  - see also GW-Basic programs
- Curtains 92, 102-24
  - arrangements for energy efficiency 92a
  - measurement of solar properties of flat 107-11
  - see also Internal shading devices

## D

- Data logging 142
- Degree day (DD)
  - calculation of 26, 26a, 27
  - cooling, Riyadh 27a
  - heating, Riyadh 27a
  - see also Base temperature
- Diffuse insolation
  - calculation of hourly, Riyadh 45, 56
  - data from "blind" experiment 160, 161a
  - data from "curtain" experiment 177, 178a
  - data for Riyadh, see Insolation data
  - estimation of daily 61, 61a
  - measurement, see Shadow ring
- Direct normal insolation
  - data for Riyadh 203-9
  - measurement, see Pyrheliometers
- "DTclm" program (model) 142
  - calculation subroutines 144
  - flow chart of main routines 142a
  - logging data input 143
  - see also GW-Basic programs
- DT-Logger 142, 247a

## E

- Efficiency of shading devices 89-93
- Emissivity, surface
  - blind fabrics 154a
  - curtain fabric 121
  - glass 71, 83, 121, 165, 217
  - selected building materials 16a
- Empirical correlations, see Regression analysis
- Energy conservation strategies 2
- Energy balance of the test cell 154, 154a
- Error analysis 234-5
- ESP model, description 249-52a
- ESP input data files 252-9
- Exterior shading devices 89-91
- External surface resistance 15, 15a, 210
  - see also Heat transfer at glazing surfaces
- Extraterrestrial insolation data for riyadh 51a, 203-9

## F

- Fenestration definition for "Curtain" model 164, 182
- Fins, see Shading design tools
- Folding ratio, see Fullness
- Forced convective heat transfer 77-9
- Free floating mode 158
  - ambient temperature of the test cells 166, 167-8
  - energy balance of the test cells 166, 167-8
- Free gains, estimation 25
- Frequency distribution 48a-50a, 52
- Fresnel's formula 68, 117
- Fullness 112-4
  - vs. solar properties of curtains 112, 112a-3a

## G

- Gaus-Jordan matrix inversion, see "Curtain" program
- Geometric configuration 112

- fullness vs. curtain solar properties 112-3
  - vs. U-value of fenestration 113-4
- Glazing energy processes 66-86
- Global insolation
  - calculation of hourly, Riyadh 45, 56-8a
  - data from "blind" experiment 160, 161a
  - data from "curtain" experiment 177, 178a
  - data for Riyadh, see Insolation data
  - estimation of daily 59-60
  - measurement, see Solarimeters
- Ground temperatures
  - estimation of 73
  - data for Riyadh 48, 196-202
- GW-Basic programs
  - "Curtain" code listing 224-7
  - "DTclm" code listing 228-33
  - "Qref" code listing 222-3

## H

- Heat-absorbing glass 94
- Heat emission from people and appliances 25a
  - see also Free gains estimation
- Heat gains
  - through exterior roofs & walls 19-22
  - through fenestration 23-4
  - see also Free gains estimation
- Heating cooling system (HCS) 153, 153a
- Heat-reflecting glass 95
- Heat transfer at glazing surfaces 70-
- Hot arid 3, 6, 10, 192
- Hourly solar heat gain through reference glazing in
  - Riyadh, see "Qref" program
- Human comfort, see Bioclimatic chart, Mahoney tables
- Humidity measurement 132a, 132-3
  - see also Relative humidity
- Hygrometers 132a, 133a

## I

- Infiltration heat loss
  - calculation 18, 156
  - measurement 156, 158
- Infrared radiometers 140, 239
  - see also Remote temperature sensors, Pyrheliometers, Pyrrometers
- Infrared radiation data for Riyadh 203-9
- Insolation data
  - for Riyadh 51a, 51-2, 203-9
  - processing 45-6
  - validity of raw 45a
  - variation during the day 56-8a
- Insolation measurement 136
- Instrumentation data sheets 236a-48
- Insulating shutters, see Shutters
- Insulation 16a, 261
  - see also Efficiency of shading devices
- Internal shading devices 91-3
- Internal surface resistance 15, 15a
  - see also Heat transfer at glazing surfaces
- Inward-flow fraction of absorbed insolation 80
  - in clear single glass 80-1
  - in curtain-shaded fenestration 115, 123
  - see also "Curtain" program, "Qref" program

Index of refraction 68

Isohel & iso-radiation maps, Saudi Arabia 42, 42a

Isohyetes map, Saudi Arabia 42a

Isotherm maps, Saudi Arabia 41a

## J

Junction

arrangements of hot & cold 137a

n-p, see Silicon solar cell

test cell and south wall 158, 158a

see also Thermocouple, Radiation sensors

## L

Lambert's law, see Bouger-Lambert law

Lining, liners 113-4, 114a

Load, building cooling/heating 26

Longwave radiation

balance between sky & building surface 20, 22

emittance, see emissivity

## M

Mahoney tables 12a, 13a, 11-3

Mashrabiya, see Sun screens

Maximum solar heat gain through glazing 80

see also "Qref" program

Measurement and instruments 128-41, 158, 176, 234-48

Model for averaged test cell behaviour 155-7

Modeling hourly heat transfer through curtain-shaded

windows, see "Curtain" program

"MRQT" program 148, 180-1

see also Parameter identification

## N

Natural convective heat transfer 75

Net radiometer 140, 246

Net radiometer, modified 141a

Neutral glass, see Heat-absorbing glass

Nomogram 55a

## O

Opaque calibration wall (OCW) 150, 158

heat loss coefficients & capacitances 156a

thermophysical characteristics 152, 156a

Openness factor 104

measuring instruments 104a

see also Classification of curtains

Overall heat transfer coefficient, see U-values

Overhangs, see shading design tools

## P

Parameters identification 154, 154a, 180-1

Passys blind, 154a

Passys project 2, 5, 149

Passys test site facilities 5, 7, 149

instrumentation and data acquisition 153

Passys test cell, see Test cell

south walls (PSC) 150, 152a, 152

see also Opaque calibration wall, Reference

wall, Timber frame wall, Heating cooling system

Photo-chromatic glass 95

Photoelectric sensors 137-8

Planting and shading 93, 93a

Polynomial coefficients

for calculating saturation vapour pressure 133a

of glass transmittance & absorptance factors 69a

of type "T" thermocouple 130a

Precipitation, see Rain fall, Isohyetes

Pre-design analysis 11

see also Bioclimatic chart, Mahoney tables

Pressurisation tests 156, 158, 158a

see also Infiltration heat loss, Air change rate

Processing DT-logger data, see DTclm Program

PRT (Pt100) 130

Psychrometers 132, 240

Pyranometers 137, 138a

Pyrgometers 140, 140a

Pyrheliometers 139

Pyrradiometers 140

see also Modified net radiometer

## Q

"Qref" program (model) 82

flow charts 82a-4a

initial glass temperature estimate 82

input climatic data 82

results 84-6

surface heat transfer coefficients 83

see also GW-Basic programs, Inward-flow

fraction of absorbed insolation, Solar heat gain

flux through standard glass (Riyadh)

## R

Radiation sensors 136

photoelectric 137

thermoelectric 136

Radiative heat transfer 71-5

at external surfaces 72

at internal surfaces 71

see also Sky temperature, Ground temperature

Rain fall, Riyadh, 43a, 196-202

Reference wall 8, 150, 155

components heat loss coefficients & capacitances 156a

construction 152a

definition in "ESP" 182

thermophysical characteristics 152

Regression analysis

diffuse insolation & extraterrestrial 61

global insolation & sunshine 58-60

insolation & cell power input 161, 180a

meteorological and surface wind speed 79

multivariate 157

sky temp & meteorological variables 74

Relationship between insolation & sunshine duration in Riyadh 58-61

Relative humidity

calculation of 47, 132

indicators 133

- see also Humidity, Psychrometers, Hygrometers
- Relative humidity data  
for Riyadh 43a, 49, 49a, 196–202  
processing 47, 47a
- Remote temperature sensors 131
- Resistance of unventilated cavities 15a
- Resistance thermometers 130  
characteristics & construction of 131  
specifications of 130, 130a
- Riyadh climate (an overview) 43  
see also Climate reference year
- Roller blinds (exterior) 90
- Roller shades (internal) 92
- Roof planting, see Planting and shading
- ## S
- Saudi Arabia  
background information 41  
climate of 41  
solar village 44
- Service room 149–50  
definition in “ESP” 254a  
north wall and partition door 150, 156a  
setpoint temperature 158, 176  
see also Test cell
- Shade tree effectiveness vs. orientation 93a
- Shading calculations, see Shading design tools
- Shading coefficient 24, 24a, 96a
- Shading design tools 87–8, 88a
- Shading mask 87–8, 87a, 261  
protractor 88a
- Shadow ring 138, 245a
- Shutters  
exterior 89–90, 90a  
insulating 92–3, 93a
- Silicon solar cell 137, 137a  
angular response of 138a  
spectral response 244
- Sketch design, see Pre–design
- Sky temperature estimation 73
- Snell’s law 68
- Sol–air temperature  
data calculated for riyadh 23a, 210–6  
excess 29a
- Solar characteristics  
of interior shading devices 101  
of glass 68
- Solar control devices, see External shading devices,  
Internal shading devices, Solar control glazing
- Solar control glazing 94–6
- Solar geometry 20–1, 20a, 87, 87a
- Solar heat gain  
factor 24, 24a  
flux through standard glass (Riyadh) 217–20
- Solarimeters 243, 245a  
see also Pyranometers
- Solar irradiation variations during the day 56
- Specific heat capacity of textile fabrics 105
- Steady–state characteristics of the test cells 154, 154a,  
158a, 160–1, 179, 180a
- Sun screens 89, 89a
- Sunshine data (calculated & measured) for Riyadh  
51a, 203–9
- Sunshine recorders 141
- see also Campbell–Stokes
- Surface albedo calculation 138
- Surface resistance, see Internal surface resistance,  
External surface resistance
- Surface temperature  
blind 170a  
curtain 187  
glazing 170–1, 188a, 188
- ## T
- Temperature data  
for Riyadh 43a, 48, 48a, 196–202  
processing 46  
validity of raw 45a
- Temperature measurement 129
- Temperature prediction (hourly) 54  
see also Nomogram
- Temperature–EMF relationship 129–30  
polynomial coefficients for type “T” 130a  
reference table 236
- Temperature–resistance relationship 130
- Temperature variation during the day 53, 54a
- Test cell 149, 149a  
air leakage & tightness 158, 158a  
definition in “ESP” 164, 182  
detailed drawings 150a  
performance with blind 183  
performance with curtain 163  
surfaces absorptance and emittance 150, 151a  
thermophysical properties 151a  
see also Passys test site facilities, Test site  
experiments
- Test configuration definition in ESP 165, 183, 352–3
- Test methodology 148–9, 154, 175  
see also MRQT program, Model for averaged test  
cell behaviour
- Test room, see Test cell
- Test site experiments  
a domestic curtain 175–81  
a window blind 148, 154–63  
comparison between measured & simulated  
results 164–71, 182–8  
experimental setup 108, 176  
instrumentation & monitoring details 154–8  
results for clear and overcast days 168, 184  
results for the free floating mode 166–8  
results for the steady–state period 160–2, 179–81
- TF–wall, see Timber frame wall
- Thermal characteristics of interior shading devices 101
- Thermal conductivity of textile fabrics 106
- Thermophysical properties  
of curtain fabrics 105  
of selected building materials 16a
- Thermocouples 129  
in series 130  
type “T” 236a  
see also Temperature–EMF relationship
- Thermoelectric sensors 136
- Thermopile 130, 136, 137a
- Thermostatic control 158
- Timber frame wall 7, 150, 155  
components heat loss coefficients & capacitances  
156a  
construction 152a

definition in "ESP" 164  
thermophysical characteristics 152  
Transmission heat loss (steady-state) 14-7

## U

U-values 14  
floors 15, 17, 17a  
single glazing under Riyadh climate (hourly) 86a  
test cell & service room 150  
typical wall & roof materials in Saudi Arabia 17  
windows (general) 16  
window with blind (hourly) 169  
window with curtain (hourly) 187a  
Ultraviolet radiation data for Riyadh 203-9  
Ultraviolet radiometers 140-1, 141a

## V

Validity of raw climatic data, Riyadh 45a-6a  
Variable degree day (VDD) 28-9  
see also Degree day, Annual heating & cooling  
requirements, Base temperature  
Variation of Riyadh climate through the day 53-7  
Venetian blinds 91  
Village, solar 44

## W

Wind direction data  
averaging algorithms 135, 135a  
for Riyadh 43a, 50, 196-202  
processing 47-8  
Wind speed data  
for Riyadh 43, 43a, 50, 50a, 196-202  
processing 47-8  
validity of raw 46a  
variations during the day 54  
Windvanes 134, 242